Kumulative Habilitation/Cumulative Habilitation

zur Erlangung der/for attainment of the
Venia Legendi

für das Fach Entwicklungsbiologie/
for the specialty Developmental Biology

mit dem Titel/entitled

Drosophila melanogaster as a model to study muscular dystrophies, stem cells and their niches

eingereicht an der/submitted to
Georg-August-Universität Göttingen, Deutschland /
Georg-August-University of Goettingen, Germany

von/by

Halyna R Shcherbata, PhD

Göttingen, 12.12.2011

Acknowledgments

This work would not have been possible without the essential and gracious support of many individuals.

First and foremost I offer my sincerest thanks to my parents, who have supported me throughout my life with love and patience and created an environment in which following the scientific researcher path seemed so natural. My husband, my shadow and my light, he encouraged, supported, understood, and loved me at every moment and on every side of the globe. My sister for an enormous amount of faith in me and an infinite amount of wise words. My older son, Roman for giving me so many reasons to be proud as a parent and for his absolute trust and friendship. My younger son, Marko for his unconditional love and ability to brighten the colors of my life.

I am deeply grateful to my teachers Hannele Ruohola-Baker, Daria V. Maksymiv, Yaroslava I. Chernik, Elena M. Belokon' and Heinrich Reichert for teaching me, challenging me with research questions that could keep me busy for the rest of my life, giving me the confidence to explore science and the guidance to avoid getting lost in my exploration.

I owe a great deal to the members of my lab, Andriy Yatsenko, Mariya Kucherenko, April Marrone, Annekatrin König and Ibrahim Ömer Cicek, my colleagues and students at Max Planck Institute of biophysical chemistry, Georg-August University, Lviv National University and University of Washington who have helped extend my involvement in the field of molecular developmental biology and who, through their own research, comments and questions have encouraged, supported and enlightened me.

Special thanks to Herbert Jäckle for honesty, support, and conversations that clarified my thinking on a career in science and other matters, Ernst Wimmer for encouraging me to write this work and my reviewers for their time and consideration.

Despite the geographical distance, my friends were always nearby. Thank you all for the good times and fond memories that I will always treasure.

Now I see our lives as a climbing test: positive phototaxis, negative geotaxis, and every few years – a new tube to assess our climbing ability. Despite all of the difficulties we all are trying to climb up, to be the winners and to do our best. We must not fear new challenges, be able to learn new things and start from the beginning. This work is dedicated to everyone who climbs up with me.

This Habilitation Thesis has two thematic core themes and is based on the following original articles:

I. Use of a *Drosophila* Model Towards Dissecting Muscular Dystrophy

1. Shcherbata, H.R., Yatsenko, A.S., Patterson, L., Sood, V.D., Nudel, U., Yaffe, D., Baker, D., and Ruohola-Baker, H. (2007). Dissecting muscle and neuronal disorders in a *Drosophila* model of muscular dystrophy. EMBO J *26*, 481-493.

2. Kucherenko, M.M., Marrone, A.K., Rishko, V.M., Magliarelli Hde, F., and Shcherbata*, H.R. (2011). Stress and muscular dystrophy: a genetic screen for dystroglycan and dystrophin interactors in *Drosophila* identifies cellular stress response components. Dev Biol *352*, 228-242.

3. Marrone, A.K., Kucherenko, M.M., Wiek, R., Gopfert, M.C., and Shcherbata*, H.R. (2011b). Hyperthermic seizures and aberrant cellular homeostasis in *Drosophila* dystrophic muscles. Sci Rep *1*.

4. Marrone, A.K., Kucherenko, M.M., Rishko, V.M., and Shcherbata*, H.R. (2011a). New Dystrophin/Dystroglycan interactors control neuron behavior in *Drosophila* eye. BMC Neurosci *12*, 93.

5. Yatsenko, A.S., Kucherenko, M.M., Pantoja, M., Fischer, K.A., Madeoy, J., Deng, W.M., Schneider, M., Baumgartner, S., Akey, J., Shcherbata*, H.R., *et al.* (2009). The conserved WW-domain binding sites in Dystroglycan C-terminus are essential but partially redundant for Dystroglycan function. BMC Dev Biol *9*, 18.

II. *Drosophila* Germline as a Model to Study Stem Cell Self-Renewal and Communication with the Niche

1. Shcherbata, H.R^.,Hatfield, S.D^., Fischer, K.A., Nakahara, K., Carthew, R.W., and Ruohola-Baker, H. (2005). Stem cell division is regulated by the microRNA pathway. Nature *435*, 974-978. ^-equal contribution

2. Shcherbata, H.R., Ward, E.J., Fischer, K.A., Yu, J.Y., Reynolds, S.H., Chen, C.H., Xu, P., Hay, B.A., and Ruohola-Baker, H. (2007). Stage-specific differences in the requirements for germline stem cell maintenance in the *Drosophila* ovary. Cell Stem Cell *1*, 698-709.

3. Konig, A., Yatsenko, A.S., Weiss, M., and Shcherbata*, H.R. (2011). Ecdysteroids affect *Drosophila* ovarian stem cell niche formation and early germline differentiation. EMBO J *30*, 1549-1562.

*-corresponding author

Zusammenfassung

Molekulargenetische Studien haben gezeigt, dass die Fruchtfliege *Drosophila melanogaster* ein ausgezeichneter Modellorganismus ist, um konservierte Mechanismen die mit Krankheiten beim Menschen assoziiert sind, zu studieren. Meine Forschung konzentriert sich auf den Dystroglycan-Dystrophin-Komplex, der bei der Entstehung von Muskeldystrophien und neurologischen Auffälligkeiten eine Rolle spielt. Dystroglycan- und Dystrophin-Mutanten führen bei *Drosophila* zu verringerter Mobilität, einer verkürzten Lebenszeit und altersabhängiger Muskeldegeneration. In Neuronen und Gliazellen von *Drosophila* wird der Dystroglycan-Dystropin-Komplex für die Steuerung der Wuchsrichtung der Photorezeptor-Axone benötigt. Ich habe ein *Drosophila*-Modell entwickelt, mit dessen Hilfe wichtige Erkenntnisse zur Entstehung von Muskeldystrophien bzw. zu Therapieansätzen dieser fatalen neuromuskulären Erkrankungen gewonnen werden können. Mit Hilfe dieses Modells haben wir verschiedene Screens zur Identifizierung von neuen Dystroglycan- und Dystrophin-Interaktionspartnern durchgeführt. Viele der Gene, die wir als Interaktionspartner identifiziert haben, spielen eine Rolle bei der zellulären Stressantwort. Entsprechend sind in Dystroglycan- bzw. Dystrophin-Mutanten die adaptiven Reaktionen gestört, was bedeutet, dass der Dystrophin-Dystroglycan-Komplex nicht nur für die Plastizität und Muskelhomeostase wichtig ist, sondern auch für die Stressantwort. Eine detaillierte Analyse der Interaktionspartner und der beteiligten Signalwege wird zu einem besseren Verständnis der Funktion des Dystrophin-

Dystroglycan-Komplexes und seiner Regulierung unter normalen bzw. unter Stressbedingungen führen und wichtige Erkentnisse zur Entstehung von Muskeldegeneration liefern.

Ein weiterer Fokus meiner Forschung ist die Funktion des miRNA Signalweges bei der Kontrolle der Selbsterneuerung von Stammzellen, wobei auch hier *Drosophila* - genauer gesagt *Drosophila*-Keimbahnstammzellen - als Modell verwendet wird. Neue Erkenntnisse wie zum Beispiel über Expressionsmuster, prognostizierte Targets von miRNA und Überexpressionsstudien weisen darauf hin, dass miRNAs eine entscheidende Rolle bei der Kontrolle der Genexpression in Stammzellen spielen. Für die Regulierung von Stammzellteilung, Selbsterneuerung, und Differenzierung sind miRNAs besonders interessante Kandidaten, da sie verschiedene mRNAs simultan steuern und daher Gruppen von Genen gezielt gemeinschaftlich regulieren können. Wir konnten weiterhin zeigen, dass der miRNA-Signalweg möglicherweise wichtig ist, um Stammzellen gegenüber Veränderungen des Millieus, die sonst den Zellzyklus am G1/S-Kontrollpunkt stoppen würden würden, unempfindlicher zu machen. Keimbahnstammzellen, denen die für die Biogenese von miRNAs erforderliche doppelsträngige RNaseIII dicer-1 (Dcr-1) fehlt, produzieren weniger differenzierte Zysten. Obwohl die für Dcr-1 mutierten Keimbahnzellen normale Stammzellmarker zeigen, haben sie eine gestörte Zellzykluskontrolle. Mit der Hilfe von Zellzyklusmarkern und genetischen Interaktionen konnten wir zeigen, dass Dcr-1 defiziente Keimbahnzellen den G1/S-Kontrollpunkt, der durch die Cyclin-abhängigen Kinaseinhibitor

Dacapo reguliert wird, zeitverzögert durchlaufen. Dies legt nahe, dass miRNAs wichtig sind damit Stammzellen den G1/S-Kontrollpunkt durchlaufen können. Darüber hinaus habe ich heraus gefunden, dass miRNAs nicht nur für die Kontrolle des Zellzyklus sondern auch für die Erhaltung der Keimbahnstammzellen benötigt werden. Dieser Mechanismus ist jedoch abhängig vom Entwicklungsstand - prä-adulte Keimbahnstammzellen haben eine Unempfindlichkeit, die im adulten Stadium verloren geht.

Weiterhin konnten wir zeigen, dass Steroidhormone die ersten Schritte der Differenzierung von Keimbahnstammzellen steuern. Bei Ecdyson-Mangel im Adultus wird das Differenzierungsprogramm von Stammzellen erst zeitverzögert angeschaltet, womit auch ein reduzierter TGF-β-Signalweg und erhöhte Mengen von Zelladhäsions- und Zytoskelettproteinen in somatischen Nischenzellen einher gehen. Wenn der Ecdyson-Signalweg dagegen während der Entwicklung der somatischen Stammzell-Nische gestört wird, werden vergrößerte funktionale Nischen gebildet, die in der Lage sind, zusätzliche Stammzellen zu beherbergen. Unsere weiteren Analysen haben gezeigt, dass bei der steroidabhängigen Regulierung der Stammzell-Nische miRNAs in einem positiven Feedback loop wirken und so Stärke und zeitliche Koordinierung der Hormonantwort steuern.

Zu verstehen, wie die Differenzierung von Stammzellen und die Bildung von somatischen Stammzell – Nischen steroidabhängig reguliert werden, ist – insbesonder im Hinblick auf die regenerative Medizin – von großer Bedeutung.

Summary

Molecular genetic studies showed that *Drosophila melanogaster* can serve as a valuable model system for conserved mechanisms underlying human disorders. My research topic is focused on the analysis of the Dystroglycan-Dystrophin complex (DGC), perturbation in which results in muscular dystrophies and brain abnormalities in humans. *Dystroglycan* and *Dystrophin* mutants in *Drosophila* show decreased mobility, shortened lifespan and age-dependent muscle degeneration. In the *Drosophila* brain, the Dystroglycan-Dystrophin complex is required in neurons and glial cells for proper photoreceptor axon path-finding. I have developed a *Drosophila* model for studying muscular dystrophies, which should provide new insights into the origin of muscular dystrophy and facilitate development of novel therapeutic strategies for treatment of these fatal neuromuscular diseases. Using this model we performed an array of genetic interaction screens that allowed finding novel Dystroglycan and Dystrophin interactors. Furthermore, many of the genes found in our muscle screen have been shown to be involved in cellular stress response. Our data concluded that the adaptive reactions in *Dystrophin* and *Dystroglycan* mutants are compromised and proposes that the DGC is not required solely for the plasticity and homeostasis of the muscles, but also plays a role in stress-response pathways. In-depth analysis of the interaction of discovered proteins and their pathways will ultimately help for a better understanding of DGC signaling and regulation under normal and stress conditions and provide new insights into the origin of muscle degeneration.

My scientific interests also include studying the role of the microRNA pathway in self-renewal control in stem cells. *Drosophila* germline stem cells (GSC) are used as a model system. Although direct evidence for a functional role for miRNAs in stem cell biology is just emerging, tantalizing hints based on expression patterns, predicted targets, and overexpression studies suggest their involvement as key regulators of gene expression. miRNAs are especially attractive candidates for regulating stem cell proliferation, self-renewal and cell fate decisions, as their ability to simultaneously regulate many targets provides a means for coordinated control of concerted gene action. We have shown that the miRNA pathway might be part of a mechanism that makes stem cells insensitive to environmental signals that normally stop the cell cycle at the G1/S transition. Analysis of GSCs mutant for dicer-1 (dcr-1), the double-stranded RNaseIII essential for miRNA biogenesis, revealed a marked reduction in the rate of germline cyst production. These dcr-1 mutant GSCs exhibit normal identity but are defective in cell cycle control. On the basis of cell cycle markers and genetic interactions, we conclude that dcr-1 mutant GSCs are delayed in the G1/S transition, which is dependent on the cyclin-dependent kinase inhibitor Dacapo, suggesting that miRNAs are required for stem cells to bypass the normal G1/S checkpoint. Later, using the same model system I have discovered that in addition to regulating the cell cycle, miRNAs are also required for *Drosophila* GSC maintenance. This requirement is temporal and depends on the developmental stage; pre-adult germline stem cells have robustness that is lost during adult stages.

Recently we also showed that in the germline steroid hormones regulate progression through the early steps of germ cell lineage. Upon ecdysone signaling deficit germline stem cell progeny delay to switch on a differentiation program. This differentiation impediment is associated with reduced TGF-β signaling in the germline and increased levels of cell adhesion complexes and cytoskeletal proteins in somatic escort cells. Additionally, when ecdysone signaling is perturbed during the process of somatic stem cell niche establishment enlarged functional niches able to host additional stem cells are formed. Our further analysis reveals that the steroid-dependent regulation of the stem cell niche involves miRNAs that act in a positive feedback to fine-tune the strength and timing of hormonal signaling required for the niche establishment.

The knowledge of steroid regulation of stem cells and their niche has great potential for further stem cell study in regenerative medicine. Our findings open the way for detailed analysis of the role of steroid hormones amd miRNAs in niche development and regulation of germline differentiation via adjacent soma.

I. USE OF A *DROSOPHILA* MODEL TOWARDS DISSECTING MUSCULAR DYSTROPHY

I.I. INTRODUCTION

Muscular dystrophies (MDs) are a group of inherited diseases that are characterized by progressive muscular degeneration and concomitant loss of muscular strength ultimately leading to skeletal muscle deterioration and cardiac and/or respiratory failure (Hayashi et al., 1998; Lim and Campbell, 1998). In addition MDs are often associated with brain defects. Based upon the clinical symptoms of these muscle diseases they are categorized into various subtypes and there are no current cures or preventions for MD. Duchenne Muscular Dystrophy (DMD) results from Dystrophin (Dys) deficiency in humans and in *mdx* mice, the highly studied mouse model for DMD. The dystrophin gene was identified and cloned in 1987 (Hoffman et al., 1987), it is remarkably large and complex (gene length 2.5 MB, 79 exons, cDNA 11 kb) and encodes a protein product Dystrophin with a molecular weight of 427 kDa (Hoffman et al, 1987: Koenig et al., 1987). The structure of the Dys gene is highly conserved during evolution, it encodes for multiple isoforms controlled by different internal promoters and the large size of the gene and protein product make transgenic therapies extremely difficult. Dys is expressed in skeletal and cardiac muscles and brain and consists of four structural domains, the N-terminal actin-binding domain, the spectrin-like rod domain, the cystein-rich domain, and the C-terminus with the Dystroglycan (Dg) interacting WW domain. Dys provides a link between the cytoskeletal actin and the ECM via the glycoprotein Dg, binding along with

several other transmembrane proteins (two syntrophins, two dystrobrevins, and four sarcoglycans) (Kanagawa and Toda, 2006; Sciandra et al., 2003) and assembling the Dystrophin Glycoprotein Complex (DGC).

The association between Dg and Dys is an integral part of the larger DGC. The interaction is mediated by the proline-rich motif of the Dg cytoplasmic tail and the WW domain of Dys. The proline-rich motif and the WW domain are small protein interaction modules often found in proteins involved in structural functions or cell signaling (Bork, Sudol, 1994; Andre, Springael, 1994; Hofmann, Bucher, 1995; Sudol et al., 1995). The WW domain contains about 38-40 amino acids and is defined by two highly conserved tryptophan residues that are spaced 20-22 amino acids apart, hence the WW domain, which has an antiparallel beta-sheet structure, is well suited for binding to ligands containing proline-rich domains with the PPxY core motif. In mammalian systems, Dg interacts with the WW domain of dystrophin via the non-phosphorylated PPPY motif. Phosphorylation of the terminal tyrosine in the PPxY motif abolishes the binding to the WW domain, suggesting that this posttranslational modification may represent a mechanism of regulation for dystrophin functions (Sotgia et al, 2001). The C-terminal portion of dystrophin and its interactions with other components of the DGC are particularly important for its function; deletions in this region give rise to a severe dystrophic phenotype in which the DGC fails to form (Rentschler et al., 1999, Jung et al., 1995, Koenig et al., 1987).

In mammalian systems, it has been shown that Dg and Dys function in a variety of developmental processes including embryogenesis, adhesion, branching epithelial morphogenesis, muscle differentiation, kidney and

neuronal development. However, determination of Dg's function is far from complete. Due to an early embryonic lethal phenotype, experimental tools for dissecting the DGC's functions have been largely limited to biochemical analyses.

In muscles the DGC is best envisioned as a mechanosignaling unit that has a dual role in muscle membrane stabilization: mechanical via anchoring the ECM to the cytoskeleton and non-mechanical as a signal-transducing module involved in cross talk between the internal and external environments of the muscle cell. The DGC helps muscles to withstand the rigors of contraction (cellular deformation and shortening) that requires specific activity of both the nervous and somatic systems, from excitation of myofibers at the neuromuscular junction (NMJ) to the ATP-regulated power-stroke of myosin. The myofiber contractile machinery must remain intimately connected with the sarcolemma and the basement membrane of the ECM, upon which muscles depend for survival and function.

The DGC also has become known as a scaffold responsible for the membrane localization of signaling proteins (Pilgram et al., 2010). For example, neuronal nitric oxide synthase (nNOS) signaling, which regulates many signaling pathways and is responsible for the direct regulation of a subset of myo-specific microRNAs, is coordinated by the DGC (Adams et al., 2008; Cacchiarelli et al., 2010). Recently various kinases, channels, and other enzymes have been shown to associate with the DGC, although only a few of these interactions have been confirmed *in vivo* (Adams et al., 2008; Pilgram et al., 2010).

Despite the vast data about the functional diversity of DGC components, the exact mechanism of how dystrophic muscle cells degenerate is still elusive. Muscle contraction induces mechanical stress leading to muscle injury; however, the specialized repair system is rapidly activated in healthy muscle, while in dystrophic muscles necrosis is triggered (Jaalouk and Lammerding, 2009). There are several potential pathogenic mechanisms implicated in the initiation of muscle decay associated with insufficiency of the DGC, including the mechanical fragility of the sarcolemma, high calcium influx, aberrant cytoskeleton rearrangements, increased energetic stress and abnormal metabolic control and inappropriate cell signalling (Vercherat et al., 2009; Wallace and McNally, 2009).

Due to the seriousness of DMD, affecting 1 out of every 3,500 males it is imperative from a human health standpoint to develop more rigorous therapies that could lead to prevention and/or a cure (Muir and Chamberlain, 2009). Within the past couple of years different animal models for DGC-associated muscular dystrophy have significantly contributed to understanding the pathogenesis of the disease, but still many questions about the mechanisms of these disorders remain unanswered.

To address the question what mechanisms contribute to dystrophic muscle degeneration and how it can be alleviated I decided to test if genetically tractable *Drosophila* can be used as a MD model.

I.II. DISCUSSION

- **Dissecting muscle and neuronal disorders in a *Drosophila* model of muscular dystrophy**

Previously the use of animal models in the studies of muscular dystrophy has been proven to be effective; some of the models have been generated by gene targeting (Watchko et al., 2002), others are naturally ocuring mutations such as the *mdx*-mouse, muscular dystrophy dog, cat, and hamster. Unfortunately, DGC regulations and controls are not yet fully understood, and there are no known successful therapeutics for MDs. Therefore, further studies in new model organisms with easy-to-manipulate genetics may possibly disclose the mode of regulation of Dg-Dys via discovery of the key regulatory components through suppressor screens. Furthermore, a thorough functional analysis of the DGC complex in different cell types in model organisms might present a unifying theme which may better reveal its molecular mechanism of function.

The fly genome encloses many highly conserved orthologues to human disease genes (Bier, 2005; Reiter et al., 2001), including neurological, cardiovascular, endocrine, and metabolic disease-genes. On top of the mentioned orthologues, the fly genome also contains nearly all components of the DGC (Deng and Ruohola-Baker, 2000; Deng et al., 2003; Greener and Roberts, 2000). We measured Dys-Dg binding constants using human and *Drosophila* proteins and found that the cross-species interaction are in the same range as within species interactions indicating that the Dys-Dg protein interface is highly conserved from humans to flies (Shcherbata et al., 2007).

These data suggest that insights from *Drosophila* should be transferable to humans.

Importantly, genetic and *RNAi*-induced mutants of both *Dg* and *Dys* genes show symptoms observed in MD: reduced mobility, muscle deterioration, shortened lifespan, and brain defects (Shcherbata et al., 2007). When Dg and Dys are specifically eliminated in mesoderm-derived tissues, age-dependent muscle degeneration was observed. This reveals the necessity of these proteins in muscle maintenance in adult flies. In addition, the DGC has both cell autonomous and non-cell autonomous function in the nervous system, as it is required for the neuron path finding process (Shcherbata et al., 2007). Based upon our data, the *Drosophila* is an excellent genetically tractable model to study MDs and neuronal abnormalities caused by defects in the DGC.

- **Stress and muscular dystrophy: a genetic screen for dystroglycan and dystrophin interactors in *Drosophila* identifies cellular stress response components**

Since the development of a *Drosophila* model for studying muscular dystrophies (Shcherbata et al., 2007), we have decided to use the genetic tractability of *Drosophila* to search for novel functions of the DGC, as well as components that may encompass its signaling and regulation. In our primary screen we looked at easily score-able, highly penetrant phenotype, an alteration in the posterior crossvein, and have found modifiers belonging to various functional groups. The genes we found were involved in muscle development, neuronal/cell migration and motor function, as well as

cytoskeletal and components of the TGF-β, EGFR and Notch pathways (Kucherenko et al., 2008).

Due to the fact that the primary screen was based solely on a crossvein phenotype, we then performed an *in vivo* genetic interaction screen in ageing dystrophic muscles and identified genes that have not been shown previously to have a role in development of MD and interact with Dystrophin and/or Dystroglycan (Kucherenko et al., 2011). The majority of them are phylogenetically conserved and implicated in human disorders, mainly tumors.

Importantly, we found that in *Drosophila* mutations in many of these interacting genes cause age-dependent morphological and heat induced physiological defects in muscles, which suggests their importance in the tissue.

Found interactors can be divided by function into main categories: proteins involved in communication between muscle and neuron, and interestingly, in mechanical and cellular stress response pathways (Kucherenko et al., 2011).

Due to the fact that the genes found in our screen have been previously associated with cellular adaptive responses to stress, we analyzed the difference in stress responsiveness of the normal and dystrophic muscle using different stress conditions. Even in wild type animals, muscle degeneration can be stimulated by stress (Kucherenko et al., 2011). Additionally, stress accelerates the commencing and severity of age-dependent MD in *Dys* and *Dg* mutants (Kucherenko et al., 2011). Normal and dystrophic muscles are similarly sensitive to elevated temperature and oxidative stress. Remarkably, lower temperature increased dystrophic muscle

damage analogous to what was seen in aged mutant animals. The effects of energetic stress had a large impact on the muscle maintenance only in *Dg* mutants with severe degeneration of the muscle far exceeding that observed in *Dys* mutants (Kucherenko et al., 2011).

Our data concluded that the adaptive reactions in *Dystrophin* and *Dystroglycan* mutants are compromised and proposes that the DGC is not required solely for the plasticity and homeostasis of the muscles, but also plays a role in stress-response pathways. Furthermore, many of the genes found in our muscle screen have been shown to be involved in cellular stress response. In-depth analysis of the interaction of discovered proteins and their pathways will ultimately help for a better understanding of DGC signaling and regulation under normal and stress conditions and provide new insights into the origin of muscle degeneration.

- **Hyperthermic seizures and aberrant cellular homeostasis in *Drosophila* dystrophic muscles**

Multiple metabolic disorders in vertebrates have been implicated in seizure activity; for example mitochondrial encephalopathy - the most common neuro-metabolic disorder - presents various symptoms including seizures (Tucker et al., 2010) and mice that are partially deficient for mitochondrial superoxide dismutase have an increased incidence of spontaneous seizures (Liang and Patel, 2004). The *mdx* mouse, a model for MD, have sustained oxidative stress in skeletal muscle (Dudley et al., 2006; Tidball and Wehling-Henricks, 2007; Whitehead et al., 2008). In *Drosophila*, it has been shown that *Dg* mutant larvae have an altered state of cellular homeostasis and are

sensitive to ambient temperature (Kucherenko et al., 2011). A continuous increase in mitochondrial oxidative metabolism, caused by a *Dg* hypomorphic mutation, causes a change in thermoregulatory behavior (Takeuchi et al., 2009). Under stress, *Dys* and *Dg* mutants have altered levels of ROS, which suggests that these proteins play a role in maintaining cellular homeostasis (Marrone et al., 2011b). Furthermore, as noted above it has been reported that suboptimal temperatures and energetic stress accelerate age-dependent muscular dystrophy in both, *Dys* and *Dg* mutants (Kucherenko et al., 2011).

As shown in our data, higher temperatures intensify mobility defects in DGC mutants and their interactors found in the screen (Kucherenko et al., 2011). We therefore decided to examine the reason behind this behavioral defect, which can originate from either muscle or neuron malfunction. We showed that *Drosophila Dys* mutants have muscle defects resulting in seizures that only occur when *Dys* is downregulated during development of muscles by electrophysiologically measuring the muscle activity on live dystrophic animals, implying a developmental requirement for Dys (Marrone et al., 2011b).

Since Dg is a binding partner of Dys, we initially believed that mutations Dg would phenocopy the dystrophic seizure phenotype. Surprisingly, *Dg* loss-of-function mutants exhibit no seizing activity. Even more, reduction of *Dg* can actually rescue dystrophic seizures, Since Dys and Dg are the key components of the DGC, integrity of which is crucial for proper muscle function and maintenance, we wanted to understand this discrepancy. It has been shown previously that Dg, but not Dys regulates localization of NMJ specific

proteins in *Drosophila* larval muscles; therefore we tested a mutant for one of these proteins, Coracle. Reduction of Cora similarly to Dg prevents dystrophic seizure occurrence, showing the importance of the NMJ composition in regulation of muscle activity. This reveals novel dynamics between two components of the DGC and their interaction.

Interestingly, found in our screen the Ca^{2+} binding protein, Calmodulin, which binds to dystrophin in mammals, also rescued hyperthermic seizures, implying that that Ca^{2+} levels are important for the dystrophic seizure activity. We assessed by which mechanism Ca^{2+} plays a role in the observed seizures via feeding *Dys* mutants various Ca^{2+} channel blockers [Nifedipine (dihydropyridine channel), 2-APB (inositol 1,4,5-triphosphate receptors, IP3R) and Ryanodine (Ryanodine receptors, RyR)]. Both 2-APB and Ryanodine treated flies showed a decrease in seizure activity, with Ryanodine having the most dramatic effect. This shows that Ca^{2+} released via IP3R and RyR activated channels plays a role in hyperthermic seizures.

Release of neurotransmitter at the NMJ results in depolarization of the muscle membrane causing release of Ca^{2+} from the SR required for muscle contraction. In the absence of Dg and Cora glutamate receptors are improperly localized causing insufficient muscle response. In contrast, Dys is involved in retrograde signaling, upon its deficiency the muscle does not signal back to the neuron that keeps activating muscle contraction.

Taken together, our data show that the DGC acts at the muscle side of the NMJ to regulate muscle cell homeostasis in response to neuronal signaling. The DGC acts at the muscle side of the NMJ to regulate muscle cell

homeostasis in response to neuronal signaling which implies that Dys is involved in muscle-neuron communication.

- **New Dystrophin/Dystroglycan interactors control neuron behavior in *Drosophila* eye**

We have previously performed a range of genetic screens using a *Drosophila* model for MD in order to find different DGC interactors targeting to explain the signaling role(s) in which the complex is involved (Kucherenko et al., 2011; Kucherenko et al., 2008; Shcherbata et al., 2007). The DGC is well known for its function in muscle tissue; however when Dys and Dg, the main components of DGC are affected, it also leads to mental retardation, cognitive impairment and muscle degeneration (Moore et al., 2002). In *Drosophila* Dys and Dg are expressed in the CNS, PNS and visual system and both proteins are required for proper photoreceptor axon guidance and rhabdomere elongation (Shcherbata et al., 2007; Zhan et al., 2010). Therefore we continued to analyze the DGC modifiers' function in the developing *Drosophila* nervous system in order to define the function of the DGC in the brain and nervous system.

Central and peripheral nervous system establishment depends on proper neuron migration and differentiation and the dynamic rearrangement of the actin cytoskeleton is crucial. The process not only requires the cell autonomous regulation of neuron motility, but also the interaction between the migrating cell and its underlying substrate. This interaction is often dependent on the signaling transduced via the ECM. In the *Drosophila* brain, the migration of R1-R6 growth cones into the lamina occurs in a similar

manner to brain layer formation, where glia cells that migrate from progenitor regions into the lamina provide a termination cue to innervating axons.

The DGC is one of the factors believed to be mediating of actin dynamics in growing axons and during neuronal cell morphogenesis. Our study found components that interact with Dys and/or Dg in both of these activities. Furthermore, the phenotypes seen with *Dys* and *Dg* mutants in the developing and adult eye are similar to the phenotypes caused by mutations of these components. The reasons for these defects are the extracellular matrix protein affinity abnormalities that influence neuronal communication and result in learning and memory defects.

In this research we identified new components implicated in the process of eye-neuron development. Moreover, we found that Nrk, Mbl, Cam and Capt genetically interact with Dys and/or Dg in visual system establishment. Our results suggest that in neurons the DGC is involved in the processes of actin cytoskeleton regulation since most of these proteins have been shown to affect actin organization, polymerization and recycling.

Based on our data, we were able to conclude that the DGC plays a role in signaling to cause cytoskeletal rearrangement and actin turnover in cones. Since many cases of MD are associated with mental retardation, we consider it is important to understand the role of the DGC in axon migration. Understanding this process could facilitate the finding of an adequate therapy for this aspect of the disease's physiology. Because the human brain continues to develop well after gestation, and there is evidence showing that

nerves uphold their plasticity throughout an individual's lifespan, therapies could be developed in order to reverse these defects after birth.

- **The conserved WW-domain binding sites in Dystroglycan C-terminus are essential but partially redundant for Dystroglycan function**

The DGC complex contains a variety of extracellular proteins, including laminin, agrin, and perlecan. The Dg protein plays a crucial role in the complex acting as an anchor between the actin cytoskeleton and the extracellular matrix. While the crystal structure of the human DGC complex has been resolved (Huang et al., 2000), the binding correspondence for the Dys-Dg interaction in human or *Drosophila* has not been analyzed. In order to determine the binding dissociation constants (Kd) for both the human and *Drosophila* complexes, we developed a fluorescence polarization assay (Shcherbata et al., 2007). We also tested whether human Dg can interrelate with *Drosophila* Dys and vice versa. Both these cross species interactions were in the same range as the within species interactions with binding affinities of 24μM and 3.7μM, respectively. We also found that more than half (34 residues) of Dg proline-rich conserved C-terminal regions in loss-of-function and overexpression studies can be deleted without significantly compromising the function of Dg in cellular polarity regulation in *Drosophila*. Particularly, the truncation eliminates the first WW domain binding motif at the very C-terminus of the protein thought to mediate interactions with Dystrophin, suggesting that the second, internal WW binding motif can also mediate this interaction and both WWbsI and

WWbsII can bind the Dystrophin protein *in vitro* (Shcherbata et al., 2007; Yatsenko et al., 2007).

Next, we tested whether both WW binding sites can function and are required *in vivo*. We generated transgenic mutants and found that while each WW binding site mutation yields to close to normal Dg function, the double WWbs mutation has lost Dg C-terminal activity. These data suggest that at least one WWbs is required for full Dg function *in vivo* and that the two sites may be partially redundant.

The functional idleness of the WW binding sites poses interesting questions: have both binding sites survived through evolution to protect organisms from the mutations in an essential complex or does each binding site have a specific function in different tissues and/or developmental stages. Only mutations in dystrophin are associated with known types of muscular dystrophies in vertebrates, but not in dystroglycan. In mice, mutations in dystroglycan are embryonic lethal, which suggests that dystroglycan is an essential gene and, perhaps the redundant dystrophin binding sites in dystroglycan provide an additional means for DGC regulation.

The comparative sequence analysis of *Drosophila* and human WW binding motifs, revealed very high conservation. However, each WWbs resides in a specific protein microenvironment, which may suggest that each site has specific binding partners. The previously performed by us genetic screens for modifiers of Dg and Dys (Kucherenko et al., 2011; Kucherenko et al., 2008; Marrone et al., 2011a) showed that the DGC interacts with components of different signaling pathways and components involved in cell/neuronal migration, cytoskeletal rearrangement and muscle development. This

suggests that the DGC might be a major hub that regulates transfer of extracellular information to the cytoskeleton. Therefore it will be important in the future to test if WW binding sites have specific and independent biological functions in different tissues. This kind of analysis is likely to provide insights into the specific functions of the DGC and serve as a basis for the development of novel therapeutic approaches for the treatment of muscular dystrophy.

II. *DROSOPHILA* GERMLINE AS A MODEL TO STUDY STEM CELL SELF-RENEWAL AND COMMUNICATION WITH THE NICHE

II.I. INTRODUCTION

The formation of embryonic and regeneration of adult tissues both depend on stem cells. Embryonic stem cells have the ability to become almost any cell type if placed in an appropriate context (Boiani and Scholer, 2005; Tiedemann et al., 2001). Adult stem cells on the other hand, have been identified to have only limited differentiation ability. Though the end products of these stem cells in tissue regeneration are different, they share some key characteristics that give them the "stemness" fingerprint. During cell division, stem cells divide asymmetrically to produce a new stem cell and a daughter that differentiates into one or multiple distinct lineages, and unlike other cell types, stem cells retain the ability to divide for the entire duration of the life of the organism. However, this division has to be carefully regulated; loss of tissue homeostasis and cancer result from too few or too many divisions respectively.

The cell type that the differentiated daughter cell will differentiate into depends on the environment it is in (Reya et al., 2001; Temple, 2001; Weigel and Jurgens, 2002; Yamashita et al., 2005). In some stem cells, the daughter cell differentiates rapidly to one lineage while for others, their daughter cells are semi-differentiated, retaining the ability to generate multiple cell types that can establish separate lineages. This is the case in the vertebrate hematopoietic system and neuronal precursors in the metazoan nervous systems.

Adult stem cells are usually found in microenvironments called niches and they also posses the ability to self-renew and produce a daughter cell that will differentiate (Eckfeldt et al., 2005; Fuchs et al., 2004). It has been recently shown that stem cell function is controlled by concerted actions of extrinsic signals from its regulatory niche and intrinsic factors including hyperdynamic plasticity of chromatin proteins (Boyer et al., 2005; Li and Xie, 2005; Meshorer et al., 2006; Williams and Fletcher, 2005; Xi and Xie, 2005). When removed from the niche, stem cells lose their stem cell character; however in most cases the stem cell niche is difficult to define (Watt and Hogan, 2000). *Drosophila* germ line stem cell niche in testes and ovary, mammalian hematopoietic, epithelial and neural stem cell niches, and plant shoot and root meristems are some of the best studied niches (Fuchs et al., 2004; Li and Xie, 2005; Stahl and Simon, 2005; Tumbar et al., 2004; Williams and Fletcher, 2005; Yamashita et al., 2005).

In the *Drosophila* ovary, 2-3 stem cells are found in a niche made up of somatic cells at the anterior tip of the germarium. In testes around 10-12 stem cells are found in a somatic niche called the hub that is located at the anterior end of the testes. Signaling from the niche is essential for GSC maintenance and the same signaling pathways are found to be critical for niche-GSC signaling in both, ovaries and testes (Decotto and Spradling, 2005; Watt and Hogan, 2000).

The proliferative rate of many adult stem cells *in vivo* is much slower compared to that of their progeny (Cheng, 2004; Weissman, 2000). In fact, without induction by environmental stress, many stem cells do not divide.

The pathways regulating long-term self-renewal and transitions through the cell cycle may be unique to or modulated differently in stem cells.

miRNAs (miRNAs) are especially attractive candidates for regulating stem cell proliferation, self-renewal and cell fate decisions, as their potential ability to simultaneously regulate many targets provides a means for coordinated control of concerted gene action. miRNAs are short 20–22 nucleotide RNA molecules that are negative regulators of gene expression in a variety of eukaryotic organisms (Alvarez-Garcia and Miska, 2005; Du and Zamore, 2005; Hammond, 2006). These RNA molecules are produced from larger transcripts that are processed to form hairpin precursors that serve as substrates for Drosha and Dicer, members of the RNase III enzyme family. Unlike humans, mice, or nematodes, *Drosophila* melanogaster has two Dicer enzymes that are encoded by separate genes (Lee et al., 2004). Dicer-1 (Dcr-1) is responsible for processing pre-miRNAs into mature miRNAs but it also can process long double-stranded RNA (dsRNA) into small-interfering RNAs (siRNAs). Dicer-2 (Dcr-2) makes siRNAs and does not contribute to mature miRNA production at detectable levels. Hundreds of miRNA genes have been found in all metazoans (Bartel and Chen, 2004) of which many are phylogenetically conserved. It has been shown, that miRNAs have a role in developmental timing, neuronal cell fate, cell death, cell proliferation, regulation of insulin secretion, hematopoietic cell fate and stem cell division (Ambros, 2004; Bartel and Chen, 2004; Cheng, 2004; Hatfield et al., 2005; Murchison and Hannon, 2004).

It has been suggested that small RNAs regulate stem cell character in plants and animals (Bernstein et al., 2003; Carmell et al., 2002; Schauer et al.,

2002; Williams and Fletcher, 2005). Furthermore, some miRNAs are differentially expressed in stem cells, suggesting a specialized role in stem cell regulation (Houbaviy et al., 2003; Murchison and Hannon, 2004; Rao, 2004; Suh et al., 2004). A stem cell-specific profile of miRNA expression is most likely the strategy used by stem cells to control miRNA-responsive genes rather than controlling the activity of the miRNA pathway machinery itself (Aboobaker et al., 2005; Biemar et al., 2005; Kloosterman et al., 2006). Altered expression levels or activation states of miRNA pathway components relative to what is present in other cell types – coupled with the expression of stem cell-specific proteins encoded by miRNA-responsive transcripts – could account for the prominent role of the miRNA pathway in the stem cells. However, the large number of distinct miRNA genes within each species studied, in addition to their expression in various combinations in different cell types, suggests that the miRNA pathway is active in most cell types. The effectiveness of RNA interference (RNAi) (Paddison et al., 2002; Paddison and Hannon, 2002) also suggests that the protein components of the miRNA pathway (such as Dicer and the Argonaute family proteins) are ubiquitously-expressed. Because some miRNA-responsive genes might require different degrees of regulation in different cells, transcriptional control of a stem cell-specific combination of miRNAs would provide the level of post-transcriptional control of targets needed for proper stem cell function.

II.II. DISCUSSION

Stem cell division is regulated by the microRNA pathway

One of the key characteristics of adult stem cells is their capacity to divide for long periods of time in an environment where most of the cells are quiescent. In this aspect, stem cells are comparable to cancer cells which are also able to elude cell cycle stop signals. This poses the critical question in stem cell and cancer biology: how is cell division regulated?

The proliferative rate of many adult stem cells *in vivo* is much slower compared to that of their progeny (Cheng, 2004). In fact, many stem cells do not divide until they are induced to do so. For example, muscle satellite cells spend most of their time in a seemingly quiescent stage, but can be induced to divide as a consequence of injury induced by exercise. While a complex array of extracellular signals and intracellular transduction pathways certainly participate in this distinct response, the cell cycle machinery, as a final step, must communicate with the specific regulatory cues and cell cycle regulators must play key roles in this process (D'Urso, 2001).

In *Drosophila*, the adult germ line stem cell (GSC) population undergoes slow cell division, the kinetics of which can be controlled by the environment. As we have shown, the miRNA pathway plays a role in the mechanism that makes stem cells insensitive to environmental signals that normally stop the cell cycle at the G1/S transition (Hatfield et al., 2005). After the analysis for Dicer-1, the double-stranded RNaseIII essential for miRNA biogenesis, of *Drosophila* GSCs mutant, it has been revealed that there is a marked reduction in the rate of germline cyst production. These *dcr-1* mutants are

defective in cell cycle control whilst exhibiting normal identity. Further analysis using cell cycle stage markers revealed that *dcr-1* deficient GSCs were delayed in the p21/p27/Dacapo-dependent G1/S transition concomitant with increased expression of CDK-inhibitor p21/27/Dacapo, suggesting miRNA stipulation for stem cells to bypass the normal G1/S checkpoint (Hatfield et al., 2005). Therefore, the inactivation of the mechanism that controls stem cell sensitivity to environmental signals that normally control cell cycle at the G1/S transition can be caused by the loss of the microRNA pathway (Shcherbata et al., 2006). Since miRNAs are also the novel class of genes involved in human tumorigenesis, it could be tempting to speculate the similarity of the role played by miRNAs in cancer cells.

The pathways regulating long-term self-renewal and transition through the cell cycle may be unique to or modulated differently in stem cells. For example, as it has been shown for cells in meiosis (Swan and Schupbach, 2005), some stem cells use a distinct set of cell cycle controllers (Wang and Lin, 2005). Several investigators have examined cell cycle protein expression in embryonic stem (ES) cells (Aladjem et al., 1998; Burdon et al., 2002; Prost et al., 1998). ES cells normally have a short G1-S transition, and cell-cycle control mechanisms operating in G1 after DNA damage are reduced or absent. Because of this, ES cells do not show growth arrest after irradiation and do not regulate their growth with the Ras/Raf/MEK pathway (Fluckiger et al., 2005). However, in the absence of DNA damage, the normal ES cell cycle requires the activities of p21 and ATP kinases (Jirmanova et al., 2005). The Cyclin Dependent Kinase Inhibitor (CKI) p21 has emerged as a key player linking environmental cues to the cell cycle machinery that also serves

as a gatekeeper for quiescent stem cells (Cheng, 2004; Cheng et al., 2000a; Cheng et al., 2000b; Ezoe et al., 2004; Walkley et al., 2005a; Walkley et al., 2005b).

An attractive hypothesis is that the timing of stem cell division in general is regulated by microRNA action on the cell cycle gate-keeper p21. The environmental regulation of *Drosophila* GSC division, such as nutrition dependent Insulin receptor (InR) activation in GSCs could act through microRNA dependent regulation of p21/p27/Dacapo. We were also able to show genetic evidence (Yu et al., 2009) that places miRNAs and Dap downstream of InR signaling in regulating cell division: cell division of *Dcr-1* or *dap* mutant GSCs does not respond to nutrition, and reduction of *dap* partially rescues the cell cycle defects of *InR* mutant GSCs. Thus, our results suggest that InR can regulate the *Drosophila* GSC cell cycle through miRNAs and Dap. When the conditions are unfavorable for division, the key microRNAs could be downregulated, resulting in an increase in p21/p27/Dacapo levels, which subsequently halts the cell cycle in G1/S. Furthermore, it will be interesting to test whether the timing of stem cell division in adult mammalian stem cells is similiarly regulated by microRNA based p21 control, and whether this process is environmentally controlled.

- **Stage-specific differences in the requirements for germline stem cell maintenance in the *Drosophila* ovary**

In this study we tried to uncover the role of miRNAs in *Drosophila* germline stem cell maintenance. What we have discovered is that miRNAs are not only responsible for stem cell division, but also stem cell maintenance. Also we found that younger germline stem cells are resilient to some perturbations that are detrimental to older germline stem cells.

Setting aside a stem cell population to replenish injured or lost tissue is one of the most fundamental processes a developing animal needs to accomplish. Currently not much is known about the processes involved in stem cell establishment during development, though it has been suggested that communication between stem cells and their environment is the key regulator of the homeostasis process (Gilboa and Lehmann, 2006; Ward et al., 2006). Mechanistic insight into how microRNAs control stem cell proliferation came from previous work in which Dicer-1, the RNase required for microRNA maturation was mutated in *Drosophila* germline stem cells (Hatfield et al., 2005). Further our findings report that in addition to regulating the cell cycle, microRNAs are also required for *Drosophila* GSC maintenance if the GSCs lack functional Dicer-1 only during adult life (Shcherbata et al., 2007). Loss of the *bantam* microRNA mimics the Dicer-1 maintenance defect in adult GSCs. Disruption of the TGF-β pathway, previously shown to be required for GSC maintenance, produced similar phenotypes as Dicer-1. Mad, a component of the receiving end of the TGF-β pathway, is required for adult GSC maintenance if the GSCs lose Mad during adult life, but is dispensable if the GSCs already lack Mad during pupal

development. These results suggest that GSC maintenance is governed by a robust, redundant mechanism during development; the adult requirement for either microRNAs or Mad activity for GSC maintenance is compensated if maintenance defects are encountered already during earlier developmental stages.

There are two important conclusions from this work. First, Dicer-1 and, more specifically, *bantam* microRNA are required for adult stem cell maintenance. Second, stem cells have a robust maintenance mechanism during development to protect the precious stem cell pool; if one of the maintenance pathways is defective during development, a compensatory pathway is activated.

The microRNA *bantam* has been previously found to simultaneously stimulate cell proliferation and prevent apoptosis (Brennecke et al., 2003). The Hippo-tumor-suppressor pathway has emerged as a key regulator for *bantam* expression in *Drosophila* imaginal discs (Nolo et al., 2006; Thompson and Cohen, 2006). This work (Shcherbata et al., 2007) builds perhaps a different view of potential *bantam* action in *Drosophila* GSCs, adding new possibilities to the repertoire of *bantam* functions. In this adult stem cell population *bantam* microRNA is essential for the stem cell niche-maintenance and acts independent of the Hippo-pathway. An array of questions remain to be answered for this new function of *bantam*: What biological process is defective in *bantam* mutant GSCs that results in their loss from the niche? What are the targets of *bantam* and the pathways that regulate its expression in GSC maintenance? In theory, the biological process and the targets of *bantam* in GSCs might be the same as those involved with

larval epithelial cell cycle control. However, cell cycle defects alone might not result in GSC loss since *dicer-1* mutant GSCs that are generated during larval/early pupal-stages, show adult GSC division defects but are maintained normally in the niche. Other possibilities exist: four components/pathways have been shown to be required for adult GSC niche-maintenance, TGF-β, microRNA, epigenetic control of chromatin and Notch-pathway. It will be important to dissect whether these pathways control *bantam* expression and/or whether *bantam* controls key regulators of these processes.

How might microRNAs influence adult stem cell maintenance? Interestingly, a group of molecules, when defective in GSCs, show the same phenotype as *dicer-1* in GSC maintenance, chromatin modification enzymes, such as ISWI and Stonewall (Maines et al., 2007; Xi and Xie, 2005). It will be interesting to explore whether Dicer-1, and specifically *bantam* acts through the chromatin remodeling machinery in the context of GSC maintenance. Importantly, stem cell chromatin modifications have recently been shown to be a critical factor in stemness.

The presented work reveals the robustness of stem cells. Developing organisms have a means of protecting their precious stem cells during many intricate developmental processes. What is then the nature of the protection in developing *Drosophila*, what is the compensatory pathway that protects the stem cells during developmental stages? One possibility is that the compensatory regulation is accomplished through hormonal pathways and the concept of the existence of such a pathway is novel and may in the future help reveal ways to rejuvenate failing stem cells. For example, ecdysone plays a key role in larval/pupal regulation of *Drosophila* (Hodin and Riddiford,

1998) and now we show the role for the ecdysone receptor pathway in the GSCs and their niches (Konig et al., 2011).

- **Ecdysteroids affect *Drosophila* ovarian stem cell niche formation and early germline differentiation**

Adult stem cells usually reside in the stem cell niche. The niche helps stem cells carry on self-renewing divisions through the lifetime of an organism in an environment where most of the other cells are quiescent. It includes both cellular and a non-cellular elements which can be divided into one of two main mechanistic types – physical contacts and diffusible factors (Walker et al., 2009). These close contacts include tight junctions, adherens junctions, gap junctions, the Notch signaling pathway, the basement membrane and extracellular matrix proteins. Diffusible factors, which are secreted by the niche and travel over varying distances from a cell source to instruct stem cells how to maintain the stem cell fate, often affect transcription. Stem cells must be anchored to the niche through cell to cell interactions so they will stay both close to niche factors that specify self-renewal and far from differentiation stimuli that induce differentiation

So far, the existence of a stem cell niche with specialized cells that both directly and indirectly participate in stem cell regulation has been demonstrated for mammalian adult stem cells in the hematopoietic, epidermal, neural, and intestinal systems. However the niches that are involved in maintenance of adult mammalian issues and cancers remain complex, poorly defined, and difficult to study *in vivo*.

We have been using a *Drosophila* ovarian stem cell niche, one of the best characterized niches, to show that misexpression of ecdysone signaling components during developmental stages leads to the formation of an enlarged germline stem cell niche that can facilitate more stem cells. Furthermore, ecdysone signaling is also involved in control of early germline differentiation. When ecdysone signaling is perturbed, the strength of TGF-β signaling in GSCs and their progeny is modified resulting in a differentiation delay. Moreover, soma specific disruption of ecdysone signaling affects germline differentiation cell non-autonomously. Ecdysteroids act in somatic ESCs and their daughters to regulate cell adhesion complexes and cytoskeletal proteins important for soma-germline communication.

It is clear that stem cell division and germline differentiation are regulated by systematic signaling depending on the general state of the organism. Hormones are great candidates for regulation since they act in a paracrine fashion and their levels are changing in response to ever-changing external and internal conditions. Steroid binding to nuclear receptors in vertebrates triggers a conformational switch accompanied by increased histone acetylation that permits transcriptional coactivators binding and the transcription initiation complex assembly (Collingwood et al., 1999; Privalsky, 2004).

Through the ability of co-factors in the targeted tissue we can achieve specificity to endocrine signaling. We have shown that Tai is a spatially restricted co-factor that interacts with the EcR/USP nuclear receptor complex to express appropriate responses to globally available hormone signals. It's positive regulation of ecdysone signaing can be improved by

Abrupt through direct binding of these two proteins that prevents Tai association with EcR/USP (Jang et al., 2009). Abrupt has been shown to be down regulated by JAK/STAT signaling (Jang et al., 2009). Furthermore, JAK/STAT signaling also controls the morphology and proliferation of ESCs as well as GSCs as well as plays a critical role in ovarian niche function (Decotto and Spradling, 2005). It is possible that JAK/STAT signaling interacts with ecdysone pathway components in ECs to further modulate cell-type specific responses to global endocrine signaling. A combination of factors that are regulated by different signaling pathway factors and are spatially and timely restricted builds a network that ensures the specificity of systemic signaling.

Cooperation between two stem cell types, germline and somatic (escort) stem cells, is required for the progression of oogenesis within the germarium. In *Drosophila* reciprocal signals between germline and escort (in female) or somatic cyst (in male) cells can inhibit reversion to the stem cell state (Brawley and Matunis, 2004; Kai and Spradling, 2004) and restrict germ cell proliferation and cyst growth (Matunis et al., 1997). Thus, the necessity of two stem cell types that share the same niche (GSC and ESC) can explain the non-autonomous ecdysone effect to coordinate their division and progeny differentiation. This coordination is most likely achieved via adhesive cues, since disruption of ecdysone signaling affects turnover of adhesion complexes and cytoskeletal proteins in somatic escort cells: mutant cells exhibited abnormal accumulation of DE-Cadherin, β-catenin/Armadillo and Adducin.

Cell adhesion plays a crucial role in *Drosophila* stem cells; GSCs are recruited to and maintained in their niches via cell adhesion (Song et al., 2002). Two

III. REFERENCES

Aboobaker, A.A., Tomancak, P., Patel, N., Rubin, G.M., and Lai, E.C. (2005). Drosophila microRNAs exhibit diverse spatial expression patterns during embryonic development. Proc Natl Acad Sci U S A *102*, 18017-18022.

Adams, M.E., Tesch, Y., Percival, J.M., Albrecht, D.E., Conhaim, J.I., Anderson, K., and Froehner, S.C. (2008). Differential targeting of nNOS and AQP4 to dystrophin-deficient sarcolemma by membrane-directed alpha-dystrobrevin. Journal of cell science *121*, 48-54.

Aladjem, M.I., Spike, B.T., Rodewald, L.W., Hope, T.J., Klemm, M., Jaenisch, R., and Wahl, G.M. (1998). ES cells do not activate p53-dependent stress responses and undergo p53-independent apoptosis in response to DNA damage. Curr Biol *8*, 145-155.

Alvarez-Garcia, I., and Miska, E.A. (2005). MicroRNA functions in animal development and human disease. Development *132*, 4653-4662.

Ambros, V. (2004). The functions of animal microRNAs. Nature *431*, 350-355.

Bartel, D.P., and Chen, C.Z. (2004). Micromanagers of gene expression: the potentially widespread influence of metazoan microRNAs. Nat Rev Genet *5*, 396-400.

Bernstein, E., Kim, S.Y., Carmell, M.A., Murchison, E.P., Alcorn, H., Li, M.Z., Mills, A.A., Elledge, S.J., Anderson, K.V., and Hannon, G.J. (2003). Dicer is essential for mouse development. Nat Genet *35*, 215-217.

Biemar, F., Zinzen, R., Ronshaugen, M., Sementchenko, V., Manak, J.R., and Levine, M.S. (2005). Spatial regulation of microRNA gene expression in the Drosophila embryo. Proc Natl Acad Sci U S A *102*, 15907-15911.

Bier, E. (2005). Drosophila, the golden bug, emerges as a tool for human genetics. Nat Rev Genet *6*, 9-23.

Boiani, M., and Scholer, H.R. (2005). Regulatory networks in embryo-derived pluripotent stem cells. Nat Rev Mol Cell Biol *6*, 872-884.

Boyer, L.A., Lee, T.I., Cole, M.F., Johnstone, S.E., Levine, S.S., Zucker, J.P., Guenther, M.G., Kumar, R.M., Murray, H.L., Jenner, R.G*., et al.* (2005). Core transcriptional regulatory circuitry in human embryonic stem cells. Cell *122*, 947-956.

Brawley, C., and Matunis, E. (2004). Regeneration of male germline stem cells by spermatogonial dedifferentiation in vivo. Science *304*, 1331-1334.

Burdon, T., Smith, A., and Savatier, P. (2002). Signalling, cell cycle and pluripotency in embryonic stem cells. Trends Cell Biol *12*, 432-438.

Cacchiarelli, D., Martone, J., Girardi, E., Cesana, M., Incitti, T., Morlando, M., Nicoletti, C., Santini, T., Sthandier, O., Barberi, L.*, et al.* (2010). MicroRNAs involved in molecular circuitries relevant for the Duchenne muscular dystrophy pathogenesis are controlled by the dystrophin/nNOS pathway. Cell Metab *12*, 341-351.

Carmell, M.A., Xuan, Z., Zhang, M.Q., and Hannon, G.J. (2002). The Argonaute family: tentacles that reach into RNAi, developmental control, stem cell maintenance, and tumorigenesis. Genes Dev *16*, 2733-2742.

Cheng, T. (2004). Cell cycle inhibitors in normal and tumor stem cells. Oncogene *23*, 7256-7266.

Cheng, T., Rodrigues, N., Dombkowski, D., Stier, S., and Scadden, D.T. (2000a). Stem cell repopulation efficiency but not pool size is governed by p27(kip1). Nat Med *6*, 1235-1240.

Cheng, T., Rodrigues, N., Shen, H., Yang, Y., Dombkowski, D., Sykes, M., and Scadden, D.T. (2000b). Hematopoietic stem cell quiescence maintained by p21cip1/waf1. Science *287*, 1804-1808.

Collingwood, T.N., Urnov, F.D., and Wolffe, A.P. (1999). Nuclear receptors: coactivators, corepressors and chromatin remodeling in the control of transcription. J Mol Endocrinol *23*, 255-275.

D'Urso, G., Datta, S. (2001). Stem Cell Biology (New York, Cold Spring Harbor Laboratory Press).

Decotto, E., and Spradling, A.C. (2005). The Drosophila ovarian and testis stem cell niches: similar somatic stem cells and signals. Dev Cell *9*, 501-510.

Deng, W.M., and Ruohola-Baker, H. (2000). Laminin A is required for follicle cell-oocyte signaling that leads to establishment of the anterior-posterior axis in Drosophila. Curr Biol *10*, 683-686.

Deng, W.M., Schneider, M., Frock, R., Castillejo-Lopez, C., Gaman, E.A., Baumgartner, S., and Ruohola-Baker, H. (2003). Dystroglycan is required for polarizing the epithelial cells and the oocyte in Drosophila. Development *130*, 173-184.

Du, T., and Zamore, P.D. (2005). microPrimer: the biogenesis and function of microRNA. Development *132*, 4645-4652.

Dudley, R.W., Khairallah, M., Mohammed, S., Lands, L., Des Rosiers, C., and Petrof, B.J. (2006). Dynamic responses of the glutathione system to acute oxidative stress in dystrophic mouse (mdx) muscles. Am J Physiol Regul Integr Comp Physiol *291*, R704-710.

Eckfeldt, C.E., Mendenhall, E.M., and Verfaillie, C.M. (2005). The molecular repertoire of the 'almighty' stem cell. Nat Rev Mol Cell Biol *6*, 726-737.

Ezoe, S., Matsumura, I., Satoh, Y., Tanaka, H., and Kanakura, Y. (2004). Cell cycle regulation in hematopoietic stem/progenitor cells. Cell Cycle *3*, 314-318.

Fluckiger, A.C., Marcy, G., Marchand, M., Negre, D., Cosset, F.L., Mitalipov, S., Wolf, D., Savatier, P., and Dehay, C. (2005). Cell-cycle features of primate embryonic stem cells. Stem Cells.

Fuchs, E., Tumbar, T., and Guasch, G. (2004). Socializing with the neighbors: stem cells and their niche. Cell *116*, 769-778.

Greener, M.J., and Roberts, R.G. (2000). Conservation of components of the dystrophin complex in Drosophila. FEBS Lett *482*, 13-18.

Hammond, S.M. (2006). MicroRNAs as oncogenes. Curr Opin Genet Dev *16*, 4-9.

Hatfield, S.D., Shcherbata, H.R., Fischer, K.A., Nakahara, K., Carthew, R.W., and Ruohola-Baker, H. (2005). Stem cell division is regulated by the microRNA pathway. Nature *435*, 974-978.

Hayashi, Y.K., Chou, F.L., Engvall, E., Ogawa, M., Matsuda, C., Hirabayashi, S., Yokochi, K., Ziober, B.L., Kramer, R.H., Kaufman, S.J., *et al.* (1998). Mutations in the integrin alpha7 gene cause congenital myopathy. NatGenet *19*, 94-97.

Hodin, J., and Riddiford, L.M. (1998). The ecdysone receptor and ultraspiracle regulate the timing and progression of ovarian morphogenesis during Drosophila metamorphosis. Dev Genes Evol *208*, 304-317.

Houbaviy, H.B., Murray, M.F., and Sharp, P.A. (2003). Embryonic stem cell-specific MicroRNAs. Dev Cell *5*, 351-358.

Hsu, H.J., and Drummond-Barbosa, D. (2009). Insulin levels control female germline stem cell maintenance via the niche in Drosophila. Proc Natl Acad Sci U S A *106*, 1117-1121.

Huang, X., Poy, F., Zhang, R., Joachimiak, A., Sudol, M., and Eck, M.J. (2000). Structure of a WW domain containing fragment of dystrophin in complex with beta-dystroglycan. Nat Struct Biol *7*, 634-638.

Jaalouk, D.E., and Lammerding, J. (2009). Mechanotransduction gone awry. Nat Rev Mol Cell Biol *10*, 63-73.

Jang, A.C., Chang, Y.C., Bai, J., and Montell, D. (2009). Border-cell migration requires integration of spatial and temporal signals by the BTB protein Abrupt. Nat Cell Biol *11*, 569-579.

Jirmanova, L., Bulavin, D.V., and Fornace, A.J., Jr. (2005). Inhibition of the ATR/Chk1 Pathway Induces a p38-Dependent S-phase Delay in Mouse Embryonic Stem Cells. Cell Cycle *4*.

Kai, T., and Spradling, A. (2004). Differentiating germ cells can revert into functional stem cells in Drosophila melanogaster ovaries. Nature *428*, 564-569.

Kanagawa, M., and Toda, T. (2006). The genetic and molecular basis of muscular dystrophy: roles of cell-matrix linkage in the pathogenesis. JHumGenet *51*, 915-926.

Kloosterman, W.P., Wienholds, E., de Bruijn, E., Kauppinen, S., and Plasterk, R.H. (2006). In situ detection of miRNAs in animal embryos using LNA-modified oligonucleotide probes. Nat Methods *3*, 27-29.

Konig, A., Yatsenko, A.S., Weiss, M., and Shcherbata, H.R. (2011). Ecdysteroids affect Drosophila ovarian stem cell niche formation and early germline differentiation. EMBO J *30*, 1549-1562.

Kucherenko, M.M., Marrone, A.K., Rishko, V.M., Magliarelli Hde, F., and Shcherbata, H.R. (2011). Stress and muscular dystrophy: a genetic screen for dystroglycan and dystrophin interactors in Drosophila identifies cellular stress response components. Dev Biol *352*, 228-242.

Kucherenko, M.M., Pantoja, M., Yatsenko, A.S., Shcherbata, H.R., Fischer, K.A., Maksymiv, D.V., Chernyk, Y.I., and Ruohola-Baker, H. (2008). Genetic modifier screens reveal new components that interact with the Drosophila dystroglycan-dystrophin complex. PLoS One *3*, e2418.

Leatherman, J.L., and Dinardo, S. (2010). Germline self-renewal requires cyst stem cells and stat regulates niche adhesion in Drosophila testes. Nat Cell Biol *12*, 806-811.

Lee, Y.S., Nakahara, K., Pham, J.W., Kim, K., He, Z., Sontheimer, E.J., and Carthew, R.W. (2004). Distinct roles for Drosophila Dicer-1 and Dicer-2 in the siRNA/miRNA silencing pathways. Cell *117*, 69-81.

Li, L., and Xie, T. (2005). Stem cell niche: structure and function. Annu Rev Cell Dev Biol *21*, 605-631.

Liang, L.P., and Patel, M. (2004). Mitochondrial oxidative stress and increased seizure susceptibility in Sod2(-/+) mice. Free Radic Biol Med *36*, 542-554.

Lim, L.E., and Campbell, K.P. (1998). The sarcoglycan complex in limb-girdle muscular dystrophy. CurrOpinNeurol *11*, 443-452.

Maines, J.Z., Park, J.K., Williams, M., and McKearin, D.M. (2007). Stonewalling Drosophila stem cell differentiation by epigenetic controls. Development *134*, 1471-1479.

Marrone, A.K., Kucherenko, M.M., Rishko, V.M., and Shcherbata, H.R. (2011a). New Dystrophin/Dystroglycan interactors control neuron behavior in Drosophila eye. BMC Neurosci *12*, 93.

Marrone, A.K., Kucherenko, M.M., Wiek, R., Gopfert, M.C., and Shcherbata, H.R. (2011b). Hyperthermic seizures and aberrant cellular homeostasis in Drosophila dystrophic muscles. Sci Rep *1*.

Matunis, E., Tran, J., Gonczy, P., Caldwell, K., and DiNardo, S. (1997). punt and schnurri regulate a somatically derived signal that restricts proliferation of committed progenitors in the germline. Development *124*, 4383-4391.

Meshorer, E., Yellajoshula, D., George, E., Scambler, P.J., Brown, D.T., and Misteli, T. (2006). Hyperdynamic plasticity of chromatin proteins in pluripotent embryonic stem cells. Dev Cell *10*, 105-116.

Moore, S.A., Saito, F., Chen, J., Michele, D.E., Henry, M.D., Messing, A., Cohn, R.D., Ross-Barta, S.E., Westra, S., Williamson, R.A*., et al.* (2002). Deletion of brain dystroglycan recapitulates aspects of congenital muscular dystrophy. Nature *418*, 422-425.

Muir, L.A., and Chamberlain, J.S. (2009). Emerging strategies for cell and gene therapy of the muscular dystrophies. ExpertRevMolMed *11*, e18.

Murchison, E.P., and Hannon, G.J. (2004). miRNAs on the move: miRNA biogenesis and the RNAi machinery. Curr Opin Cell Biol *16*, 223-229.

Nolo, R., Morrison, C.M., Tao, C., Zhang, X., and Halder, G. (2006). The bantam microRNA is a target of the hippo tumor-suppressor pathway. Curr Biol *16*, 1895-1904.

Paddison, P.J., Caudy, A.A., and Hannon, G.J. (2002). Stable suppression of gene expression by RNAi in mammalian cells. Proc Natl Acad Sci U S A *99*, 1443-1448.

Paddison, P.J., and Hannon, G.J. (2002). RNA interference: the new somatic cell genetics? Cancer Cell *2*, 17-23.

Pilgram, G.S., Potikanond, S., Baines, R.A., Fradkin, L.G., and Noordermeer, J.N. (2010). The roles of the dystrophin-associated glycoprotein complex at the synapse. Mol Neurobiol *41*, 1-21.

Privalsky, M.L. (2004). The role of corepressors in transcriptional regulation by nuclear hormone receptors. Annu Rev Physiol *66*, 315-360.

Prost, S., Bellamy, C.O., Clarke, A.R., Wyllie, A.H., and Harrison, D.J. (1998). p53-independent DNA repair and cell cycle arrest in embryonic stem cells. FEBS Lett *425*, 499-504.

Rao, M. (2004). Conserved and divergent paths that regulate self-renewal in mouse and human embryonic stem cells. Dev Biol *275*, 269-286.

Reiter, L.T., Potocki, L., Chien, S., Gribskov, M., and Bier, E. (2001). A systematic analysis of human disease-associated gene sequences in Drosophila melanogaster. Genome Res *11*, 1114-1125.

Reya, T., Morrison, S.J., Clarke, M.F., and Weissman, I.L. (2001). Stem cells, cancer, and cancer stem cells. Nature *414*, 105-111.

Schauer, S.E., Jacobsen, S.E., Meinke, D.W., and Ray, A. (2002). DICER-LIKE1: blind men and elephants in Arabidopsis development. Trends Plant Sci *7*, 487-491.

Sciandra, F., Bozzi, M., Bianchi, M., Pavoni, E., Giardina, B., and Brancaccio, A. (2003). Dystroglycan and muscular dystrophies related to the dystrophin-glycoprotein complex. AnnIstSuperSanita *39*, 173-181.

Shcherbata, H.R., Ward, E.J., Fischer, K.A., Yu, J.Y., Reynolds, S.H., Chen, C.H., Xu, P., Hay, B.A., and Ruohola-Baker, H. (2007a). Stage-specific differences in the requirements for germline stem cell maintenance in the Drosophila ovary. Cell Stem Cell *1*, 698-709.

Shcherbata, H.R., Yatsenko, A.S., Patterson, L., Sood, V.D., Nudel, U., Yaffe, D., Baker, D., and Ruohola-Baker, H. (2007b). Dissecting muscle and neuronal disorders in a Drosophila model of muscular dystrophy. EMBO J *26*, 481-493.

Song, X., Zhu, C.H., Doan, C., and Xie, T. (2002). Germline stem cells anchored by adherens junctions in the Drosophila ovary niches. Science *296*, 1855-1857.

Stahl, Y., and Simon, R. (2005). Plant stem cell niches. Int J Dev Biol *49*, 479-489.

Suh, M.R., Lee, Y., Kim, J.Y., Kim, S.K., Moon, S.H., Lee, J.Y., Cha, K.Y., Chung, H.M., Yoon, H.S., Moon, S.Y., *et al.* (2004). Human embryonic stem cells express a unique set of microRNAs. Dev Biol *270*, 488-498.

Swan, A., and Schupbach, T. (2005). Drosophila Female Meiosis and Embryonic Syncytial Mitosis Use Specialized Cks and CDC20 Proteins for Cyclin Destruction. Cell Cycle *4*.

Takeuchi, K., Nakano, Y., Kato, U., Kaneda, M., Aizu, M., Awano, W., Yonemura, S., Kiyonaka, S., Mori, Y., Yamamoto, D., *et al.* (2009). Changes in temperature preferences and energy homeostasis in dystroglycan mutants. Science *323*, 1740-1743.

Temple, S. (2001). Stem cell plasticity--building the brain of our dreams. Nat Rev Neurosci *2*, 513-520.

Thompson, B.J., and Cohen, S.M. (2006). The Hippo pathway regulates the bantam microRNA to control cell proliferation and apoptosis in Drosophila. Cell *126*, 767-774.

Tidball, J.G., and Wehling-Henricks, M. (2007). The role of free radicals in the pathophysiology of muscular dystrophy. J Appl Physiol *102*, 1677-1686.

Tiedemann, H., Asashima, M., Grunz, H., and Knochel, W. (2001). Pluripotent cells (stem cells) and their determination and differentiation in early vertebrate embryogenesis. Dev Growth Differ *43*, 469-502.

Tucker, E.J., Compton, A.G., and Thorburn, D.R. (2010). Recent advances in the genetics of mitochondrial encephalopathies. Curr Neurol Neurosci Rep *10*, 277-285.

Tumbar, T., Guasch, G., Greco, V., Blanpain, C., Lowry, W.E., Rendl, M., and Fuchs, E. (2004). Defining the epithelial stem cell niche in skin. Science *303*, 359-363.

Vercherat, C., Chung, T.K., Yalcin, S., Gulbagci, N., Gopinadhan, S., Ghaffari, S., and Taneja, R. (2009). Stra13 regulates oxidative stress mediated skeletal muscle degeneration. Hum Mol Genet *18*, 4304-4316.

Walkley, C.R., Fero, M.L., Chien, W.M., Purton, L.E., and McArthur, G.A. (2005a). Negative cell-cycle regulators cooperatively control self-renewal and differentiation of haematopoietic stem cells. Nat Cell Biol *7*, 172-178.

Walkley, C.R., McArthur, G.A., and Purton, L.E. (2005b). Cell division and hematopoietic stem cells: not always exhausting. Cell Cycle *4*, 893-896.

Wallace, G.Q., and McNally, E.M. (2009). Mechanisms of muscle degeneration, regeneration, and repair in the muscular dystrophies. Annu Rev Physiol *71*, 37-57.

Wang, Z., and Lin, H. (2005). The division of Drosophila germline stem cells and their precursors requires a specific cyclin. Curr Biol *15*, 328-333.

Watchko, J.F., O'Day, T.L., and Hoffman, E.P. (2002). Functional characteristics of dystrophic skeletal muscle: insights from animal models. J Appl Physiol *93*, 407-417.

Watt, F.M., and Hogan, B.L. (2000). Out of Eden: stem cells and their niches. Science *287*, 1427-1430.

Weigel, D., and Jurgens, G. (2002). Stem cells that make stems. Nature *415*, 751-754.

Weissman, I.L. (2000). Translating stem and progenitor cell biology to the clinic: barriers and opportunities. Science *287*, 1442-1446.

Whitehead, N.P., Pham, C., Gervasio, O.L., and Allen, D.G. (2008). N-Acetylcysteine ameliorates skeletal muscle pathophysiology in mdx mice. J Physiol *586*, 2003-2014.

Williams, L., and Fletcher, J.C. (2005). Stem cell regulation in the Arabidopsis shoot apical meristem. Curr Opin Plant Biol *8*, 582-586.

Xi, R., and Xie, T. (2005). Stem cell self-renewal controlled by chromatin remodeling factors. Science *310*, 1487-1489.

Yamashita, Y.M., Fuller, M.T., and Jones, D.L. (2005). Signaling in stem cell niches: lessons from the Drosophila germline. J Cell Sci *118*, 665-672.

Yatsenko, A.S., Gray, E.E., Shcherbata, H.R., Patterson, L.B., Sood, V.D., Kucherenko, M.M., Baker, D., and Ruohola-Baker, H. (2007). A putative Src homology 3 domain binding motif but not the C-terminal dystrophin WW domain binding motif is required for dystroglycan function in cellular polarity in Drosophila. J Biol Chem *282*, 15159-15169.

Yu, J.Y., Reynolds, S.H., Hatfield, S.D., Shcherbata, H.R., Fischer, K.A., Ward, E.J., Long, D., Ding, Y., and Ruohola-Baker, H. (2009). Dicer-1-dependent Dacapo suppression acts downstream of Insulin receptor in regulating cell division of Drosophila germline stem cells. Development *136*, 1497-1507.

Zhan, Y., Melian, N.Y., Pantoja, M., Haines, N., Ruohola-Baker, H., Bourque, C.W., Rao, Y., and Carbonetto, S. (2010). Dystroglycan and mitochondrial ribosomal protein l34 regulate differentiation in the Drosophila eye. PloS one *5*, e10488.

Appendix I. Relevant Selected Publications

The EMBO Journal (2007) 26, 481–493 | © 2007 European Molecular Biology Organization | All Rights Reserved 0261-4189/07
www.embojournal.org

THE EMBO JOURNAL

Dissecting muscle and neuronal disorders in a *Drosophila* model of muscular dystrophy

Halyna R Shcherbata[1], Andriy S Yatsenko[1,2], Larissa Patterson[1], Vanita D Sood[1], Uri Nudel[3], David Yaffe[3], David Baker[1] and Hannele Ruohola-Baker[1,*]

[1]Department of Biochemistry, Institute for Stem Cell and Regenerative Medicine, University of Washington, Seattle, WA, USA, [2]Ivan Franko National University in Lviv, Lviv, Ukraine and [3]Molecular Cell Biology, The Weizmann Institute of Science, Rehovot, Israel

Perturbation in the Dystroglycan (Dg)–Dystrophin (Dys) complex results in muscular dystrophies and brain abnormalities in human. Here we report that *Drosophila* is an excellent genetically tractable model to study muscular dystrophies and neuronal abnormalities caused by defects in this complex. Using a fluorescence polarization assay, we show a high conservation in Dg–Dys interaction between human and *Drosophila*. Genetic and RNAi-induced perturbations of *Dg* and *Dys* in *Drosophila* cause cell polarity and muscular dystrophy phenotypes: decreased mobility, age-dependent muscle degeneration and defective photoreceptor path-finding. Dg and Dys are required in targeting glial cells and neurons for correct neuronal migration. Importantly, we now report that Dg interacts with insulin receptor and Nck/Dock SH2/SH3-adaptor molecule in photoreceptor path-finding. This is the first demonstration of a genetic interaction between Dg and InR.
The EMBO Journal (2007) **26,** 481–493. doi:10.1038/sj.emboj.7601503; Published online 11 January 2007
Subject Categories: development; molecular biology of disease
Keywords: axon path-finding; Dystroglycan–Dystrophin complex; insulin receptor; muscular dystrophy; Nck/Dock

Introduction

The transmembrane protein Dystroglycan (Dg) is part of a complex that links the extracellular matrix (ECM) to cytoskeletal actin via the cytoplasmic protein Dystrophin (Dys). The Dys contains an actin binding domain on its N-terminus and the Dg interacting WW + EF hand-domain on its C-terminus (Hoffman *et al*, 1987; Koenig *et al*, 1987; Winder, 2001). These linkages are vital and disruption of any component or the interaction between them can cause muscular dystrophy and brain defects in humans (Campbell, 1995; Cohn and Campbell, 2000; Michele *et al*, 2002; Moore *et al*, 2002; Montanaro and Carbonetto, 2003; Cohn, 2005).

Mutations in Dystrophin glycoprotein complex (DGC) in vertebrates lead to muscle degeneration as well as phenotypes in many other cell types (Durbeej and Campbell, 2002; Cohn, 2005). For example, several muscular dystrophies exhibit neuronal migration disorders (Muntoni *et al*, 2002; Qu and Smith, 2004), showing that Dg interactions are essential for normal neuron migration. However, the mechanism of action and regulation of this complex are not fully understood in any cell type. Multiple proteins interacting with Dg have been identified through biochemical assays resulting in the hypothesis that Dg is involved in regulation of the actin cytoskeleton, signal transduction and cell morphology (Yang *et al*, 1995; Sotgia *et al*, 2001; Spence *et al*, 2002, 2004a, b).

It is now critical to analyze which of these biochemical interactions are required for Dg–Dys function and regulation and in which cell types do these interactions take place. Model organisms are essential for these functional studies and a few of such models exist and have been analyzed. For example, Dys is defective in Duchenne Muscular Dystrophy (DMD) patients as well as in mdx mice, the highly studied mouse model for DMD. However, in mdx mice, a compensating process limits muscular necrosis during most of the animal's life (Durbeej and Campbell, 2002; Michele *et al*, 2002; Moore *et al*, 2002). In addition, *Caenorhabditis elegans* and zebrafish have recently been used to model muscular dystrophies (Gieseler *et al*, 2000; Parsons *et al*, 2002; Bassett and Currie, 2003).

Dys is a 427 kDa rod-shaped protein that is defective in DMD. The huge gene encodes for three full-length dystrophin isoforms and four shorter, truncated products, controlled by different internal promoters. The complex structure of the gene is highly conserved during evolution. Similarly to the mammalian dystrophin gene, the fly gene encodes three full-length dystrophin-like products (DLPs) and three truncated products consisting of the C-terminal and cysteine-rich domains with various extensions into the spectrin-like repeats domain of DLP. Like the human gene products, the *Drosophila* gene products are expressed in a tissue-specific manner (Neuman *et al*, 2001, 2005; Figure 1A).

We now report that *Drosophila Dg* and *Dys* mutants develop age-dependent muscle degeneration and mobility defects, indicating that this easy to genetically manipulate organism serves as a remarkably good model for muscular dystrophy. Using this model, we demonstrate that Dg–Dys complex is required in brain in the photoreceptor neurons and in the targeting glial cells for proper axon path-finding, suggesting that ECM-based process regulated both from neuronal and glial side contribute to axon migration. Furthermore, the loss-of-function-mutant analysis and genetic interactions suggest that Dg and Dys act in similar axon path-finding processes as Insulin Receptor (InR) and the adaptor protein Nck/Dock.

Results

Dg and Dys are both required for cellular polarity in Drosophila

A gain of function screen for mutants defective in polarity in *Drosophila* oogenesis resulted in the finding of *Drosophila*

*Corresponding author. Department of Biochemistry, University of Washington, Box 357350, Seattle, WA 98195, USA.
Tel.: +1 206 543 1710; Fax: +1 206 685 1792;
E-mail: hannele@u.washington.edu

Received: 7 June 2006; accepted: 22 November 2006; published online: 11 January 2007

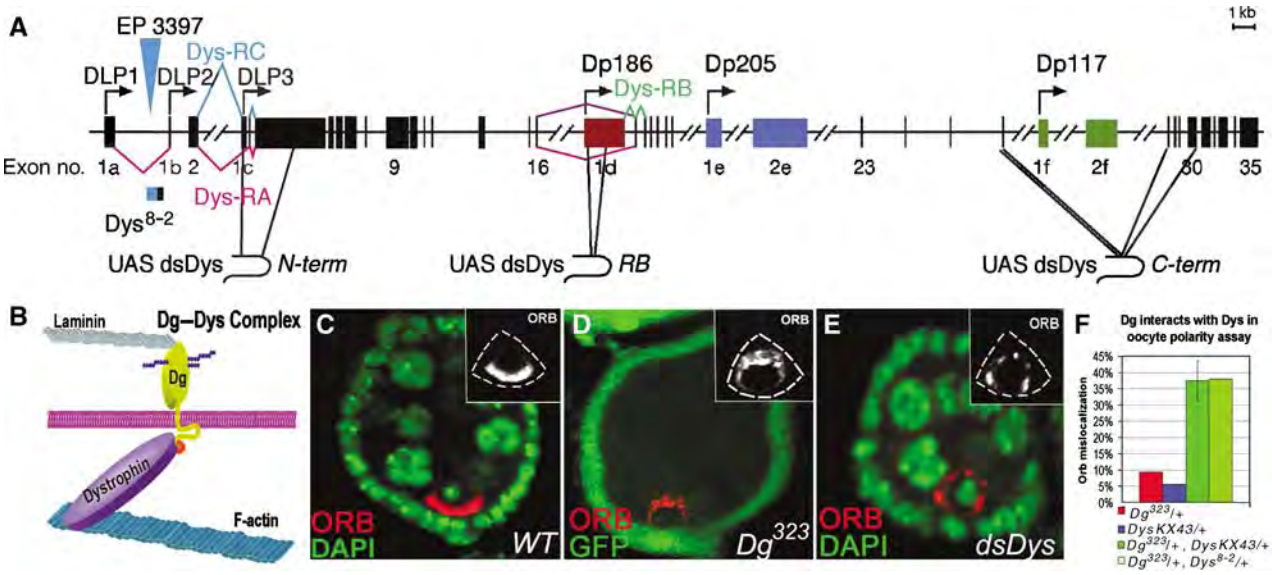

Figure 1 Dg and Dys interact *in vivo*, setting up the anterior–posterior polarity of the oocyte. (**A**) The *Drosophila Dys* gene structure. Bars represent exons, horizontal bold lines—introns, bent arrows—translation start sites. *Dys* genetic deletion *8-2* and *UAS RNAi Dys* constructs are shown. *UAS dsDys C-term* will affect all known Dys transcripts while *UAS dsDys RB* is specific for the short transcript RB and *UAS dsDys N-term* for the transcripts RA and RC (additional transcripts have recently been isolated (Neuman *et al*, 2005)). (**B**) A cartoon of *Drosophila* Dg–Dys complex is shown. The transmembrane protein Dg provides a link between Laminin in the extracellular matrix and Dys that is attached to the intracellular cytoskeleton. Dg C-terminal Dys-binding peptide shown in Figure 2C is marked in red. (**C–E**) The oocyte polarity marker Orb, which colocalizes with MTOC, is mislocalized in the oocytes of *Dg* mutants (D, *hsFLP; FRT42D* Dg^{323}*/FRT42D Ubi-GFP), Dys* mutant *(*$Dys^{8\text{-}2}$*/DysKX43;* Table I) and transgenic *dsDys* flies (E, *dsDys N-term/MatTub-GAl4;* Table I). Instead of being localized to the posterior of the developing oocyte at stages 4–6, Orb surrounds the oocyte in a circle or accumulates in a clump at one side of the oocyte. Red = Orb, Green = DAPI (C, E) or GFP (D). In the right top corners: mislocalization of MTOC in stage 6 oocytes marked by Orb. (**F**) A bar graph showing that Dg interacts with Dys in the oocyte polarity assay. Transheterozygous $Dg^{323}/+$*; DysKX43/+* and $Dg^{323}/+$*;* $Dys^{8\text{-}2}/+$ mutants show oocyte polarity defects with increased frequency in comparison to control $Dg^{323}/+$ or *Dys KX43/+* flies ($Dg^{323}/+$ 9.4%, $n = 117$; *Dys KX43/+* 5.5%, $n = 163$; $Dg^{323}/+$*; DysKX43/+* 37.4±6.1%, $n = 309$ and $Dg^{323}/+$*;* $Dys^{8\text{-}2}/+$ 37.9%, $n = 124$).

homologs of components in the Dg complex: *Drosophila* Dg, LamininA and Dys (Deng and Ruohola-Baker, 2000; Deng *et al*, 2003; Figure 1B). Further analysis revealed that the *Drosophila* genome has all the known components of the Dg complex (Greener and Roberts, 2000; Dekkers *et al*, 2004). While vertebrates have two closely related proteins, dystrophin and utrophin, encoded by two different genes, *Drosophila* has only one gene encoding *Dystrophin*. The expression of *Drosophila* Dys overlaps with Dg in adult and embryonic tissues (Supplementary Figures 1–3).

To test whether Dg and Dys act in the same cell types and interact genetically in *Drosophila*, we isolated a mutant allele for *Dystrophin* and generated *dsRNA* constructs (Figure 1A). We have analyzed the phenotypes associated with two *Dys* deletion mutants *(*$Dys^{8\text{-}2}$ and Dys^{e6}) and three different *dsRNA* constructs (Figure 1A; *dsDysN-term* targets the long, *dsDysRB* the short and *dsDysC-term* all *Dys* isoforms) and compared these to the phenotypes of previously isolated Dg mutants (Deng *et al*, 2003). A significant reduction of Dys was observed with all mutants analyzed (Supplementary Figure 3C–I, M and N; Supplementary Table I). Specifically, while the genetic loss-of-function mutant *(*$Dys^{8\text{-}2}$*/DysKX43)* showed a 149-fold reduction, N- and C-terminal *dsDys* constructs showed 6–18-fold reduction of the transcript DLP2 (Supplementary Table I).

Dg is required for cellular polarity: in *Dg* germline clones, the early oocyte polarity marker Orb fails to show the normal posterior localization in stage 4–6 oocytes (Deng *et al*, 2003; Table I; Figure 1C and D). This and the accompanied growth defect of the egg chamber can be partially rescued by germ line expression of full-length Dg protein (Yatsenko *et al*, 2006). To analyze whether Dys is also required in the germline for oocyte polarity, we examined Orb localization in *Dys* mutant ovaries ($Dys^{8\text{-}2}$*/DysKX43*, Dys^{e6}*/DysKX43* or *pUASPdsDys N-term/MatTub-Gal4*). Reduction of Dys function in the germline resulted in an Orb mislocalization phenotype reminiscent of the phenotype seen in *Dg* mutant; Orb surrounds the entire oocyte in a circle, or it accumulates in a clump at the sides of the oocyte (Figure 1E; Table I). Therefore, Dys, like Dg, is required in germ line for establishment of early oocyte polarity. We also analyzed Dys function in another cell type, follicle epithelial cells, and observed that reduction of *Dys* results in polarity defects in this cell type as well (Supplementary Figure 3J–L).

To test whether Dg and Dys act in the same process in the germ line, we tested to see if Dg and Dys showed genetic interactions in the oocyte polarity assay; the polarity of $Dg^{323}/+$*; DysKX43/+* and $Dg^{323}/+$*;* $Dys^{8\text{-}2}/+$ oocytes was analyzed. The double heterozygous animals showed significant polarity defects indistinguishable from the homozygous Dg^{323} or $Dys^{8\text{-}2}$*/DysKX43* mutants, suggesting that Dg and Dys interact in this process (Figure 1F). Thus, both Dg and Dys are required in the germ line and interact in the establishment of cellular polarity during oogenesis.

The Dys–Dg interaction is conserved from human to flies

While the crystal structure of the human Dys–Dg complex has been solved (Huang *et al*, 2000), the binding affinity for this interaction in human or *Drosophila* has not been ana-

Table I *Dg* and *Dys* mutations cause similar developmental phenotypes in *Drosophila*

	Control	Dg^{323}	$Dys^{8\text{-}2}$	Control		*RNAi mutants*		
	OR	$FRT42DDg^{323}$/ $FRT42DDg^{323}$	$Dys^{8\text{-}2}$/*Def KX43*	*UAS GFP*	*UAS dsDg*	*UAS dsDys*		
Phenotypes						*N-term*	*RB*	*C-term*
Oocyte polarity	10%, $n=50$	96%[a], $n=26$	41%[b], $n=69$	5%, $n=64$	—[c]	× *MatTub-Gal4* 49%, $n=324$	—[c]	—[c]
Mobility ($T_{1/2}$, days)	24, $n=114$	—	12, $n=108$	22, $n=91$	10, $n=79$	× *tubP-Gal4* 12, $n=74$	14, $n=95$	13, $n=83$
Muscle degeneration	3 days, 20(0)%[d], $n=10$	—	3 days, 35(0)%, $n=34$	17(0)%, $n=23$	24(8)%, $n=103$	× *tubP-Gal4 (3 days old)* 22(0)%, $n=103$	27(0)%, $n=30$	—
				24(0)%, $n=54$	62(48)%, $n=65$	× *tubP-Gal4 (12 days old)* 58(24)%, $n=113$	58(48)%, $n=36$	—
	12 days, 25(0)%, $n=57$		12 days, 66(22)%, $n=110$	18(0)%, $n=110$	32(8)%, $n=119$	× *24B-Gal4 (3 days old)* 21(4)%, $n=159$	—	25(4)%, $n=81$
				11(0)%, $n=47$	73(33)%, $n=108$	× *24B-Gal4 (20days old)* 69(57)%, $n=124$	—	—
Axon path-finding	11%, $n=18$	85%[e], $n=33$	67%, $n=27$	29%, $n=17$	74%, $n=19$	× *GMR Gal4* 74%, $n=32$	57%, $n=26$	61%, $n=36$
				29%, $n=67$	71%, $n=80$	× *repo-Gal4* 60%, $n=27$	55%, $n=18$	76%, $n=58$

n = number of analyzed egg chambers in polarity analysis, flies in mobility and longevity analyses, individual thoracic muscles in muscle degeneration or brain hemispheres in axon path-finding analyses.

[a]*hsFLP; FRT42D* Dg^{323}/*FRT42D Ubi-GFP* (only germ line clones analyzed).

[b]The frequency of oocyte polarity defects in an independent loss-of-function mutant Dys^{e6}/*DefKX43* is 40.5% ($n=84$).

[c]The construct that allows germline expression *(pUASp dsDg* or *dsDys)* does not yet exist.

[d]In parentheses is shown the percentage of extreme muscle degeneration phenotypes (loss of muscle fibers or vacuolization of muscle tissue). Independent indirect flight muscles were calculated.

[e]eyFLP, GMR-lacZ; FRT42D Dg^{323}/FRT42D l(2)cl-R11[1].

lyzed. We developed a fluorescence polarization assay to determine the binding dissociation constants (K_d) for both the human and *Drosophila* complexes (Figure 2). In this assay, human or *Drosophila* Dys (WW + EF hand domains) was titrated into buffer containing fluorescent-labeled Dg peptide. Human Dys binds human Dg peptide (HmWWbsI) with a K_d of 7.6±1.6 μM. While *Drosophila* Dys binds *Drosophila* Dg peptide (DmWWbsI) with a K_d of 16±4 μM (Figure 2A, B and D). To verify that we were measuring binding at the same interface elucidated by the crystal structure, we tested human Dys binding with a mutant Dg peptide in which the tyrosine of the PPPY motif (Tyr 892; Figure 2C) was mutated to a proline (HmWWbsI-P: KNMTPYRSPPPPVSP). This tyrosine contributes two hydrogen bonds to the binding interface and forms van der Waals contacts to a hydrophobic pocket on the dystrophin WW domain (Huang *et al*, 2000), all of which are expected to be lost upon mutation to proline. As expected, this titration showed reduced affinity (K_d 172±39 μM) indicating that the assay measures the correct interaction (Figure 2A and D).

In addition, we tested whether human Dg can interact with *Drosophila* Dys and vice versa. Both these cross species interactions were in the same range as the within species interactions with binding affinities of 24 and 3.7 μM, respectively (Figure 2D). The affinity measured for Dg–Dys interactions is in the expected range for previously analyzed WW-interactions (Kato *et al*, 2002). These data show that the Dys–Dg protein interface is highly conserved from humans to flies, suggesting that insights from *Drosophila* should be transferable to humans.

Dys and Dg mutants show mobility defects

Defects in the Dg complex in human cause muscular dystrophies, which are associated with muscle weakening and degeneration (Cohn and Campbell, 2000). To test whether the Dys–Dg complex plays a similar role in *Drosophila* muscle function, we first analyzed the mobility of the *Drosophila Dg* and *Dys* mutants by measuring their climbing capability (Benzer, 1967) using *dsDg* and *dsDys* constructs driven by *P-tub-Gal4* and the *Dys* loss-of-function mutant $Dys^{8\text{-}2}$/*DysKX43*. This rate of climbing decay in *Dg* and *Dys* mutants was significantly faster than in wild-type flies, suggesting that Dg and Dys might be required in the musculature (Figure 3A and B; Table I, $T_{1/2}$(mobility): control 22–24 days, $Dys^{8\text{-}2}$/*DysKX43* 12 days).

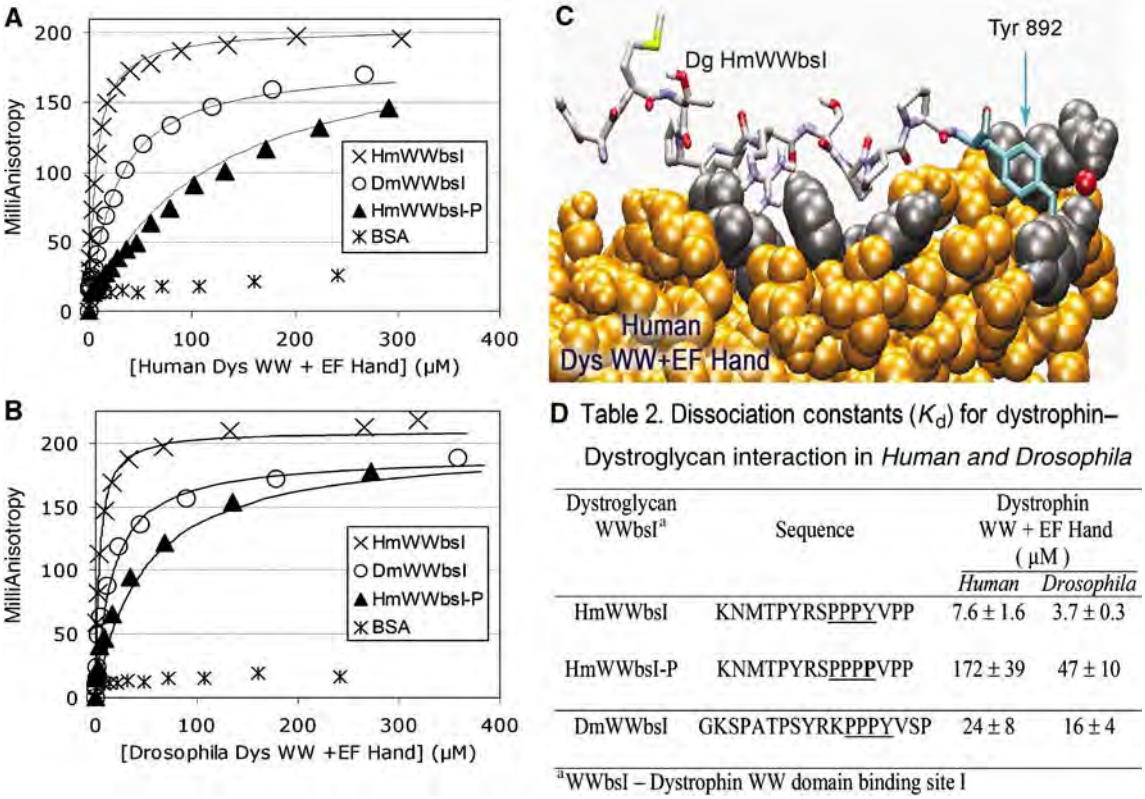

D Table 2. Dissociation constants (K_d) for dystrophin–Dystroglycan interaction in *Human and Drosophila*

Dystroglycan WWbsI[a]	Sequence	Dystrophin WW + EF Hand (μM)	
		Human	*Drosophila*
HmWWbsI	KNMTPYRSPPPYVPP	7.6 ± 1.6	3.7 ± 0.3
HmWWbsI-P	KNMTPYRSPPPPVPP	172 ± 39	47 ± 10
DmWWbsI	GKSPATPSYRKPPPYVSP	24 ± 8	16 ± 4

[a]WWbsI – Dystrophin WW domain binding site I

Figure 2 Dg and Dys interact *in vitro*; fluorescence polarization assay reveals that Dys binding to Dg is highly conserved from human to flies. (**A**) MilliAnisotropy values of human Dys WW + EF hand titrated into buffer containing fluorescently labeled Dg peptides show that human Dys can bind both human (HmWWbsI) and fly (DmWWbsI) Dg peptides. BSA titrated with 200 nM HmWWbsI peptide serves as a negative control. (**B**) MilliAnisotropy value of *Drosophila* Dys WW + EF hand titrated into buffer containing fluorescently labeled Dg peptides indicates that *Drosophila* Dys can also bind both *Drosophila* (DmWWbsI) and human (HmWWbsI) Dg peptides. BSA is used as the negative control. Binding affinity is reduced in both human and *Drosophila* models when the wild-type human peptide is substituted with a mutated peptide (HmWWbsI-P) in which the terminal tyrosine of the PPxY motif is mutated to a proline. (**C**) Space filling model of the interaction surface between human Dys WW + EF hand and human Dg peptide HmWWbsI. Human Dys residues that directly contact the HmWWbsI are colored gray. The tyrosine of the PPxY motif, mutated to proline in the HmWWbsI-P peptide is colored in cyan (arrow). (**D**) Dissociation constants of human and *Drosophila* Dys–Dg interaction. Data indicate that this interaction is highly conserved from fly to man: human Dg can interact with *Drosophila* Dys (WW + EF hand) and vice versa with similar K_d.

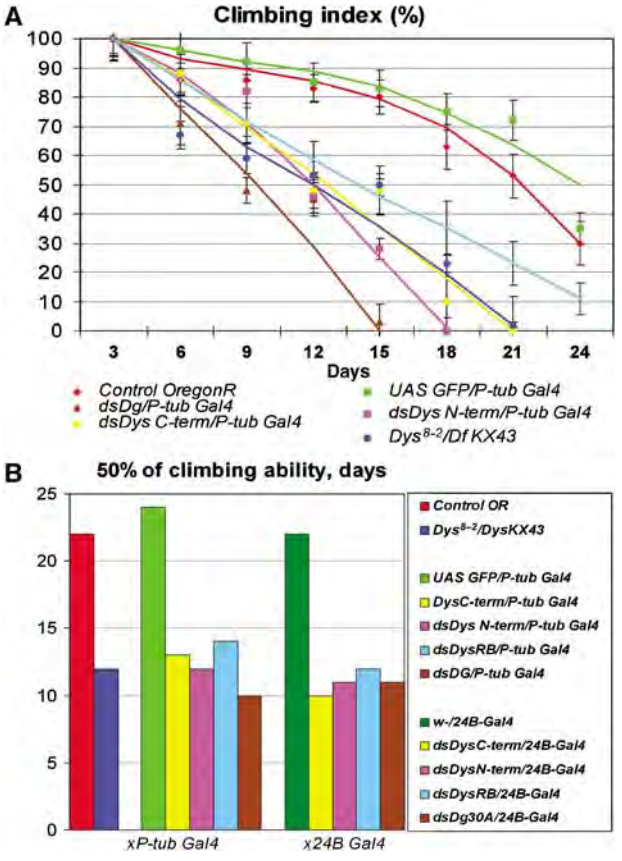

Figure 3 Mutations in *Dg* and *Dys* cause decreased mobility. (**A**) Dys and Dg function is required for normal locomotion. *Dys* and *Dg* mutants exhibit impaired climbing ability relative to control flies. They begin adult life with normal mobility, but the climbing decay rate is faster in mutants than in wild-type flies. This indicates that *Dg* and *Dys* defects cause age-dependent climbing disability. (**B**) A bar-graph showing that *Dys* mutant *8-2* and transgenic ubiquitous *Dg* and *Dys RNAi* animals (*dsDg* and *dsDys/P-tub Gal4*) and muscle-specific *dsDg* and *dsDys/24B-Gal4* mutants have lost 50% of their climbing ability in 10–14 days after eclosion in comparison to 22–24 days in control.

To test whether the climbing defects in DGC mutant animals were due to Dg and Dys function in muscle tissue, we analyzed mobility of *Dys* and *Dg* mutants using *dsDg* and *dsDys* constructs driven by mesodermal driver *24B-Gal4*. The speed of climbing decay in *dsDg* and *dsDys/24B Gal4* mutants was similar to what was observed for *dsDg* and *dsDys/P-tub Gal4* mutants (Figure 3B, $T_{1/2}$(mobility): control 22–24 days, *dsDg/P-tub-Gal4* 10 days, *dsDg/24B-Gal4* 11 days, *dsDysC-term/P-tub-Gal4* 13 days, *dsDysC-term/24B-Gal4* 10 days). These results indicate that Dg–Dys complex is required in the mesoderm.

Age dependent degeneration of Dys and Dg mutant muscles

To understand the cell biological basis for the observed mobility defects in *Dg* and *Dys* mutants, we analyzed their muscle morphology (*dsDg* and *dsDys/P-tub-Gal4, Dys^{8-2}/DysKX43)*. Histological analysis of the major thoracic muscles showed age-dependent muscle degeneration in *Dg* and *Dys* mutants, consistent with the mobility dysfunction in these mutants (Figure 4A–G; Table I). Confocal and light micrographs of histological sections revealed that the cellular appearance of muscle in *Dg* and *Dys* mutants was less organized than in control flies, numerous lesions within the muscular tissue were observed. In 12-day-old control flies the indirect flight muscles (IFM) have well structured muscle fibers with peripherally located nuclei (Figure 4A and D). Twelve days after eclosion, animals expressing *dsDg* and *dsDys* or Dys^{8-2}/*DysKX43* mutants show loss of muscle fiber organization, vacuolization (Figure 4B, C and G) and absence of some muscles (Figure 4F). These phenotypes became much more pronounced in older mutant flies; the frequency of muscle degeneration increased six-fold in the mutants (Dys^{8-2}/*DysKX43* or *dsDg* and *dsDys* crossed to *P-tub Gal4*) compared to the controls during a 9-day period (Figure 4H; Table I). Similar phenotypes have been observed before in *Drosophila parkin* and *pink1* mutants (Pesah *et al*, 2004; Yang *et al*, 2006).

To determine whether this age-dependent muscle degeneration phenotype is due to a requirement of Dg–Dys complex in muscle tissue, we used a mesoderm specific *24B-Gal4*-driver to express the *Dg* and *Dys RNAi* constructs. Severe muscle degeneration phenotypes, accompanied with extensive vacuolization of muscle tissue and muscle fiber loss were observed when the *Dg* and *Dys RNAi* were directed in the mesoderm (Figure 4H–K; Table I). We further showed that, similar to what was observed in ubiquitous *Dg* and *Dys RNAi* animals (*dsDg* and *dsDys/P-tub Gal4*), in muscle-specific *dsDg* and *dsDys/24B-Gal4* mutants the muscle deterioration process has an age-dependent character (Figure 4H–K; Table I). Taken together, these results suggest that, similar to human, Dg and Dys are required for muscle maintenance throughout the lifetime of *Drosophila*.

Dg and Dys are required for proper photoreceptor axon path-finding

Brain-selective deletion of Dg in mice is sufficient to cause congenital muscular dystrophy-like brain malformations, including disarray of cerebral cortical layering and aberrant migration of granule neuronal cells (Michele *et al*, 2002; Moore *et al*, 2002; Qu and Smith, 2004). Within the cortex, however, it is not clear whether the Dg–Dys complex is required in neurons, glia, or both for proper neuronal migrations. To better understand the function of the Dg complex in the brain, we analyzed potential brain defects in the *Drosophila Dg* and *Dys* mutants.

Dg is expressed in the *Drosophila* adult eye, brain, and the developing larval brain and visual system, especially in optic lobes and photoreceptors (Figure 5B; Supplementary Figure 4D). In the optic lobe, Dg is present both on photoreceptor axons (in the optic stalk, lamina plexus and medulla neuropil) and the Repo-expressing brain glial cells (Figure 5B). Dys shows similar expression patterns in the optic lobes.

To examine the role of Dg–Dys complex in the *Drosophila* brain, we analyzed frontal sections of adult heads from mutant *Dys* and *Dg* adult flies and observed abnormalities in the formation of retina: retinal photoreceptor cells were not elongated in *Dg* or *Dys* mutants (*eyFLP; Dg^{323}FRT 42D/FRT 42D l(2)cl-R11* 100%, Dys^{8-2}/*DysKX43* 88%, *dsDg30A* and *dsDg33A/P-tubGal4* 92%, *dsDysC-term/P-tubGal4* 100%, control *UAS GFP/P-tubGal4* 0%; Supplementary Figure 4), suggesting that the Dg–Dys complex is required in these photoreceptor sensory neurons.

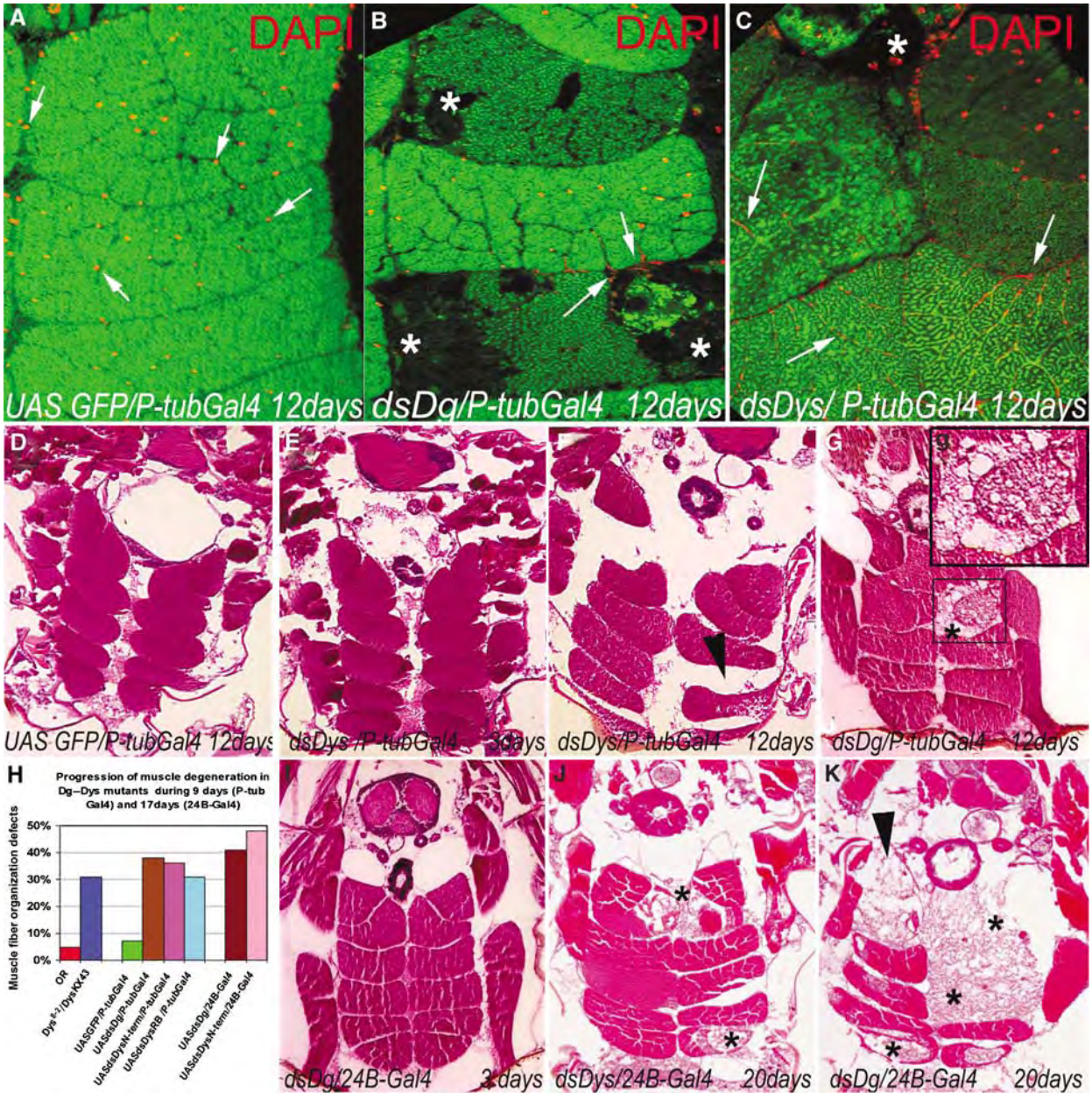

Figure 4 *Dg* and *Dys* mutants manifest age-dependent muscle degeneration. (**A–C**) Confocal analysis of histological transverse sections of IFM of 12 days old adult flies stained with a nuclear marker DAPI in red. (A) Control flies (*UASGFP/P-tub-Gal4)* show normal organization of the IFM and the muscle fibers are well structured with the nuclei located at the periphery (arrows). (B, C) *Dg* and *Dys* mutants (*dsDg30A* and *dsDysN-term/P-tub-Gal4)* show severe muscle degeneration: wasting and loss of muscle tissue, vacuolization (asterisks), the integrity of subsets of muscle cells is disrupted and the nuclei appear to be dispersed between fibers (arrows). (**D–G, I–K**) Light microscopy of histological transverse sections of IFMs stained with H&E. (D) Control (*UASGFP/P-tub-Gal4*, 12 days after eclosion). (E–G) *Dys* and *Dg* mutants (*dsDys N-term/P-tub-Gal4*, *dsDg30A/P-tub-Gal4*) exhibit mainly normal muscle architecture at 3 days after eclosion, but at 12 days in most of the cases the muscle degeneration progresses, the density of myofibrils per muscle decreases and some muscles are absent (arrowhead) or vacuolized (G, asterisk). (**H**) Bar graph represents increase in frequency of muscle fiber organization defects in 9 days in Dys^{8-2}*and Dg–Dys* transgenic animals (*dsDg* and *dsDys/P-tub-Gal4*) and in 17 days in flies with directed knockout of *Dg* and *Dys* in muscle (*dsDg* and *dsDys/24B-Gal4*), which suggest that muscle degeneration has an age-dependent character. Independent IFMs were calculated (Table I). (I–K) The mesoderm-specific RNAi-based reduction of *Dg* and *Dys* (*dsDys C-term* and *dsDg30A/24B-Gal4*) at 20 days after eclosion, but not at 3 days after eclosion (I) show obvious IFM muscle pathology: the loss of fiber density and vacuolization (asterisks).

The *Drosophila* compound eye consists of ~800 ommatidia, each containing eight different photoreceptor sensory neurons, R cell subtypes that project axons into one of two optic ganglia layers in the brain during late larval development. R1–R6 axons innervate the most superficial layer, the lamina, generating a smooth lamina plexus, whereas R7 and R8 project axons through the lamina into the deeper medulla layer (Figure 5A and D) (Perez and Steller, 1996; Tessier-Lavigne and Goodman, 1996; Clandinin and Zipursky, 2002; Ruan *et al*, 2002). The patterning of the R-cell subtypes in eye discs and the extension of their axons to the optic lobes of the developing brains occur by late third instar larvae, while the elongation of the retinal cell body takes place at pupal stage (Izaddoost *et al*, 2002).

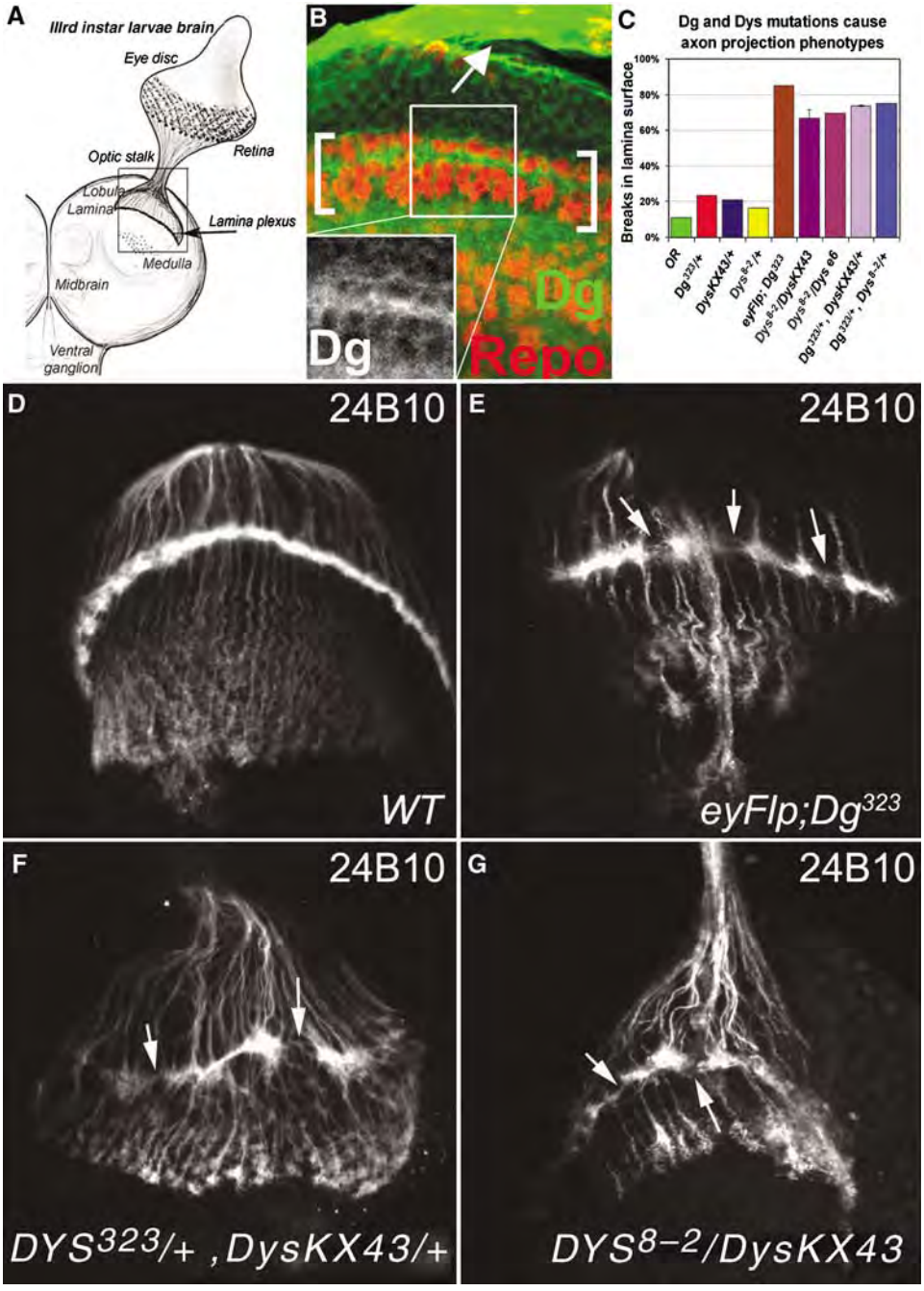

Figure 5 Dg–Dys complex is required for proper axon path-finding in *Drosophila* brain. (**A**) Schematic drawing of developing *Drosophila* third instar larval brain. Boxed area indicates the lamina plexus and the medulla. (**B**) Dg antibody staining shows that Dg protein is expressed in neurons and glia in larval *Drosophila* brain. High levels of Dg in larval *Drosophila* brain are detected on axons of photoreceptor sensory neurons in the optic stalk (yellow arrow) in addition to glial cells in the optic lobes. Red = Repo, Green = Dystroglycan. (**C**) A bar graph represents the frequency of axon path-finding defects caused by mutations in Dg–Dys complex. Both *Dg* and *Dys* loss-of-function mutants *(eyFLP; Dg^{323}FRT42D/FRT42D l(2)cl-R11* and *Dys^{8-2}/DysKX43*; Table I) as well as *Dg/Dys* transheterozygous mutants (*Dg^{323}/+; DysKX43/+*, 73.5±0.4% $n = 95$, s.d. is from three independent experiments) show photoreceptor axon projection phenotypes. (**D–G**) Photoreceptor axonal projection patterns in third-instar larvae visualized with 24B10 antibody, the lamina plexus is indicated with brackets. (D) Wild-type pattern of photoreceptor neuron projection in the lamina plexus. In *Dg* loss-of-function mutants (E, *eyFLP; Dg^{323}FRT 42D/FRT 42D l(2)cl-R11*), *Dg/Dys* transheterozygous mutants (F, *Dg^{323}/+; DysKX43/+*) and *Dys* loss-of-function mutants (G, *Dys^{8-2}/DysKX43*) photoreceptor axons are clumping at the lamina and stop irregularly making gaps in the normal termination zone of the lamina plexus (arrows).

To determine at which stage Dg is required in photoreceptor neuron development, we induced eye-specific mutant clones *(eyFLP; Dg^{323}FRT 42D/FRT 42D l(2)cl-R11)* and analyzed the developing neurons in late third instar larvae using a photoreceptor-specific monoclonal antibody 24B10. The patterning of the *Dg* mutant ommatidia was normal, suggesting that Dg is not required for the determination and differentiation of the R-cells. However, the axonal projections of these sensory neurons to the brain optic lobes were disturbed due to the lack of Dg, most of the axons

migrate to the correct termination zone in lamina, but formed abnormal patches in the lamina plexus. Similar axonal problems were observed in *Dys* mutants. In the normal wild-type brain the photoreceptor axons terminate in a stereotypic fashion producing a fan-like structure in the lamina plexus (Figure 5A, B and D). However, in 85% of *Dg* loss-of-function (*eyFLP; Dg^{323}FRT 42D/FRT 42D l(2)cl-R11*) and 67–75% of *Dys* loss-of-function (*$Dys^{8\text{-}2}$/DfKX43* and *Dys^{e6}/$Dys^{8\text{-}2}$*) mutant third-instar larvae optic lobes the lamina plexus is irregular; photoreceptor axons stop irregularly making gaps in the normal termination zone of the lamina plexus, deviate from the path and bundle aberrantly (Figure 5C, E and G; Table I).

Importantly, Dg and Dys proteins interact in controlling the photoreceptor axon path-finding since simultaneous reduction of the level of both genes (*Dg^{323}/+; DysKX43/+* and *Dg^{323}/+; $Dys^{8\text{-}2}$/+*) results in a high percentage of the axon projection phenotypes while reduction of each gene independently (*Dg^{323}/+*, *DysKX43/+ or $Dys^{8\text{-}2}$/+*) does not (Figure 5F and C).

Dg and Dys are required both in neurons and glia for regular lamina plexus formation

Photoreceptor axon guidance requires correct photoreceptor specification as well as proper function of brain glia and neurons; the axons extend along glial cells, stop in response to signals produced by marginal glial cells, and establish synaptic connections with lamina neurons (Perez and Steller, 1996; Tessier-Lavigne and Goodman, 1996; Poeck *et al*, 2001; Clandinin and Zipursky, 2002; Ruan *et al*, 2002). Previous studies demonstrate complex interactions between R-cell axons and laminal glial cells: R-cell axons induce the differentiation and migration of laminal glial cells (Perez and Steller, 1996), and conversely laminal glial cells present a stop signal for terminating R1–R6 axons within the lamina (Poeck *et al*, 2001).We tested whether axon path-finding defects in *Dg* or *Dys* mutants were caused by loss of Dg-complex function in extending neurons or supportive glial cells by using eye- and glia-specific drivers (*GMR-Gal4* and *repo-Gal4*).

We first showed that in the majority of *Dg* and *Dys RNAi* mutants driven by *P-tub-Gal4*, the photoreceptor axons exhibited targeting phenotypes similar to *Dg* clonal phenotypes, they bundled and/or terminated irregularly in the normal termination zone of the lamina plexus. When these *Dys* and *Dg* RNAi constructs were expressed in eye disks, photoreceptor axons similarly terminated irregularly in the lamina region of the brain and formed uneven lamina neuropil with gaps and abnormally densely packed regions (Figure 6A and B; Table I, *dsDg* and *dsDys/GMR-Gal4* 74 and 61%). When *Dys* and *Dg* RNAi constructs were expressed in all glial cells, including eye disk and lamina glia, but not neurons, axons of the photoreceptor sensory neurons also showed bundling and irregular termination (Figure 6A and C; Table I, *dsDg* and *dsDys/repo-Gal4* 71 and 76%). To test whether the obtained axon path-finding phenotype is specific to DGC function in neurons and glia, we knocked-down Dg and Dys in mesodermal tissue and observed no effect on the axon termination process above control samples (Figure 6A and D; *dsDg* and *dsDys/24B-Gal4*). To determine the potential effect of DGC mutations on the development of laminal glial cells, we stained the third-instar optic lobe using a monoclonal antibody that recognizes the glial-specific nuclear protein Repo (Perez and Steller, 1996; Poeck *et al*, 2001). In wild type (Figure 6E and G), differentiating glial cells migrate into the lamina forming two clearly separated layers of glial cells (i.e., epithelial and marginal glia), which in turn present a stop signal for terminating R1–R6 growth cones in the lamina (Poeck *et al*, 2001). In *Dg* and *Dys* mutants, although glial cells migrated correctly into the lamina, they appeared less organized lacking the clear separation of epithelial and marginal glial layers (Figure 6F and H). We also used the MARCM technique in order to generate marked photoreceptor neurons and/or glial cells mutant for *Dg^{323} (elav-Gal4 hsFLP;FRT42B tubGal80/FRT42BDg^{323};UAS GFP act<CD2<Gal4)*. The termination zone observed for mutant photoreceptors was irregular; clumping of axons at the lamina and lamina breaks were associated with the presence of *Dg* mutant glial cells as well as mutant photoreceptor axons (Supplementary Figure 5A and B). In contrast to the wild-type regular axon/glia/axon pattern, in *Dg* mutant lamina the gaps were occupied by mislocalized glial cells (Supplementary Figure 5B). These data suggest that Dg acts autonomously and non-autonomously for correct axon path-finding; Dg–Dys complex is required both in neurons and in glial cells for proper neuron axonal growth and targeting.

As discussed, several congenital muscular dystrophies exhibit neuronal migration disorders (Michele *et al*, 2002; Moore *et al*, 2002). The mediations of axon path-finding and neuronal migration require similar processes including supportive glial cells (Bloch-Gallego *et al*, 2005). In the vertebrate brain, Dg is required for granule neuron migration (Michele *et al*, 2002; Moore *et al*, 2002; Qu and Smith, 2004). It will be interesting to see in the future if similar to *Drosophila* axon path-finding, the Dg–Dys complex in vertebrates acts both in neurons and glial cells for this process. Indeed, Dg function has been demonstrated in a support cell type in peripheral nervous system, Schwann cells for neuronal connectivity (Saito *et al*, 2003).

Dg interacts with Nck/Dock SH2/SH3 adaptor protein and InR to regulate axon guidance in Drosophila brain

The phenotypes we have observed in Dg and Dys mutant photoreceptor axon path-finding are reminiscent of phenotypes observed before with Nck/Dock SH2/SH3 adaptor protein (Garrity *et al*, 1996) and InR (Song *et al*, 2003) mutants. To test whether Dock and InR might act in concert with Dg and Dys in this process, we analyzed whether they genetically interact with Dys and Dg. Importantly, Dg shows a strong interaction with InR and Dock, while Dys does not; *Dg*, *Dys*, *InR* and *Dock* heterozygous mutants (*Dg^{323}/+*, *DysKX43/+*, *$Dys^{8\text{-}2}$/+*, *$InR^{ex52.1}$/+*, *InR^{34}/+* *$Dock^{P1}$/+*, *$Dock^{P2}$/+*) and double heterozygous animals *Dys/InR* and *Dys/Dock* (*DysKX43/$InR^{ex52.1}$*, *DysKX43/InR^{34}*, *$Dys^{8\text{-}2}$/$InR^{ex52.1}$*, *$Dys^{8\text{-}2}$/InR^{34}*, *$Dock^{P1}$/+; DysKX43/+*, *$Dock^{P2}$/+; DysKX43/+*, *$Dock^{P1}$/+; $Dys^{8\text{-}2}$/+*, *$Dock^{P2}$/+; $Dys^{8\text{-}2}$/+*) mostly had regular termination zone in the lamina plexus, while *Dg^{323}/$Dock^{P1}$*, *Dg^{323}/$Dock^{P2}$*, *Dg^{323}/+; $InR^{ex52.1}$/+* and *Dg^{323}/+; InR^{34}/+* double transheterozygous mutants showed a significantly increased frequency of axon projection defects (Figure 7A). Previous genetic and biochemical work showed that InR can function as a guidance receptor for Dock. However, this InR function is independent of Chico, the *Drosophila* insulin receptor substrate homolog (Song *et al*,

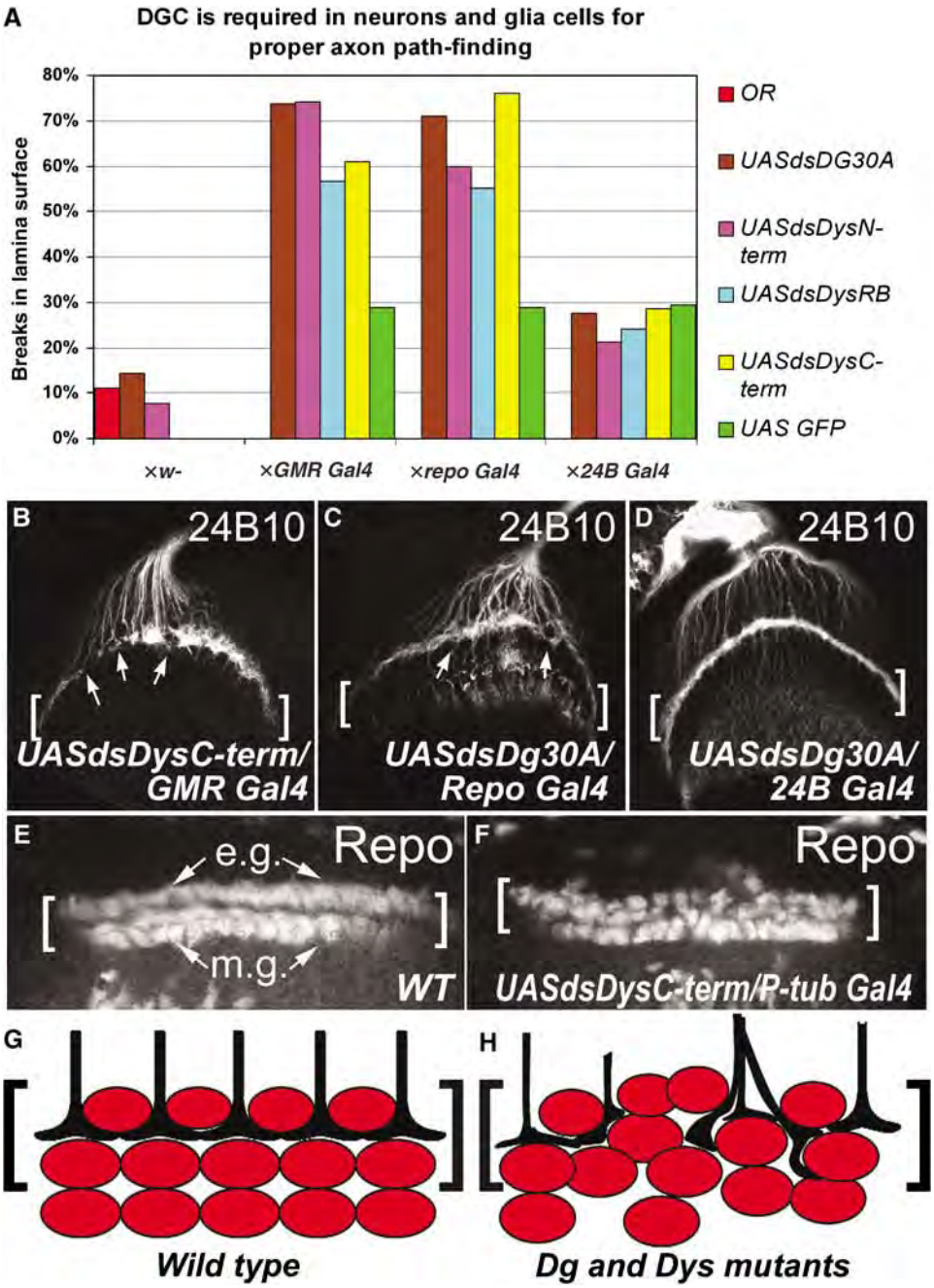

Figure 6 Dg–Dys complex is required in both neurons and glial cells for proper axon path-finding in *Drosophila*. (**A**) A bar graph represents the frequency of irregular and uneven lamina layer in *Dg* and *Dys* mutants. Analysis of axon path-finding phenotypes using photoreceptor *(GMR-Gal4)* and glia specific *(repo-Gal4)* drivers suggests that Dg–Dys complex is required in neurons and glial cells; lack of Dg–Dys complex in either cell type results in axonal mistargeting. Knocking out of DGC in the mesoderm *(24B-Gal4)* does not affect axon path-finding over control levels. (**B**) A representative image of the majority of preparations showing the clumping and uneven lamina plexus phenotype (indicated by arrows) in photoreceptor specific *Dg* and *Dys* mutants *(dsDg* and *dsDys/GMR-Gal4)*. (**C**) Similar phenotypes observed when *Dys* and *Dg* RNAi constructs were expressed in all glial cells, including eye disk and lamina glia, but not neurons *(dsDg* and *dsDys/Repo-Gal4)*. (**D**) Axons of photoreceptor sensory neurons in *dsDg* and *dsDys* crossed to a muscle-specific *24B-Gal4* driver showed regular lamina layer, indistinguishable from control (Figure 5D). (**E, F**) In wild-type (E) glial cells (marked with Repo) migrate from progenitor regions into the lamina where they are organized into two layers, the epithelial (e.g.) and marginal glia (m.g.), presenting a stop signal for the termination of R1–R6 growth cones at the lamina plexus (brackets). (F) In DGC mutants, although glial cells migrated correctly into the lamina, they appeared less organized. (**G**) In wild-type *Drosophila* brain the termination zone is organized stereotypically: each axon terminates between glial cells resulting in a regular axon/glia/axon pattern. (**H**) In *Dg* or *Dys* mutants the termination zone is disorganized: glial cells are irregularly positioned and photoreceptor axons bundle causing gaps and densely packed regions in the lamina.

2003). Similarly, while Dg interacts with InR, it does not interact with the substrate protein Chico. Double heterozygous $Dg^{323}/chico^{1}$ R-cell projection patterns were indistinguishable from wild-type (Figure 7A). These observations demonstrate that InR and the adaptor protein Nck/Dock can genetically interact with Dg but not Dys. Furthermore, since previous work has revealed that InR and Dock show genetic interactions in this process (Song *et al*, 2003), these data

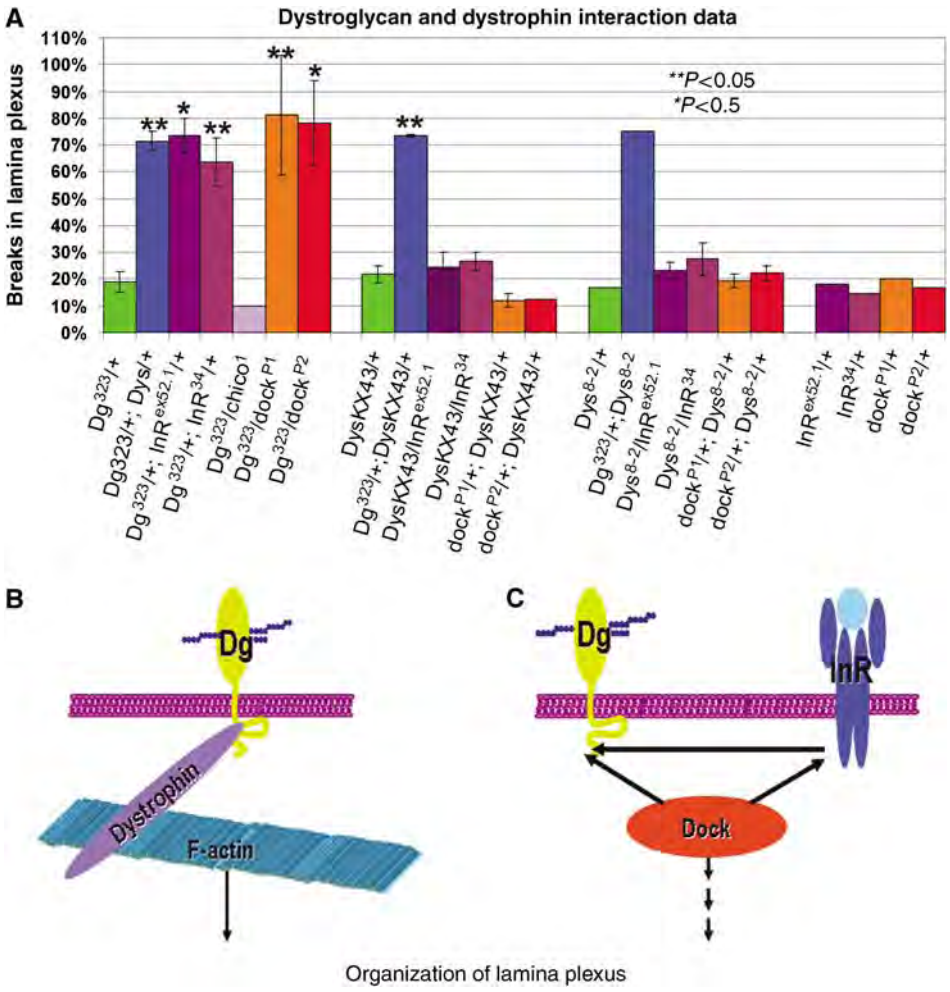

Figure 7 Dg interacts with Dock and InR pathways to regulate axon guidance in *Drosophila* brain. (**A**) A bar graph showing that Dg but not Dys interacts with Dock and InR pathways. The $Dg^{323}/+$, $DysKX43/+$, $Dock^{P1}/+$; $DysKX43/+$ and $DysKX43/InR^{ex52.1}$ animals mostly displayed normal projection patterns, while $Dg^{323}/Dock^{P1}$ and $Dg^{323}/+$; $InR^{ex52.1}/+$ double transheterozygous mutants showed increased frequency of axon mistargeting (**$P<0.05$, *$P<0.5$ value calculated from two to four independent experiments). Similar results were obtained by using independent alleles for InR, Dock or Dys (InR^{34}, $dock^{2}$, Dys^{8-2}). Dg interacts with tyrosine kinase protein InR, but not with its substrate protein Chico. (**B**) Model showing that Dg connects to actin cytoskeleton through Dys during axon guidance, Dg interaction with Dock and/or InR could abolish Dg–Dys binding allowing cytoskeletal rearrangements (**C**). In this case, Dg might participate in Dock and InR mediated signal transduction.

suggest that Dg, InR and Dock interact in axon path-finding (Figure 7B and C).

Discussion

The fly genome contains many highly conserved orthologues to human disease genes (Reiter *et al*, 2001; Bier, 2005), including neurological, cardiovascular, endocrine and metabolic disease-genes. Among these, nearly all components of the Dg–Dys complex, which is involved in muscular dystrophies, are present in flies (Deng and Ruohola-Baker, 2000; Greener and Roberts, 2000; Deng *et al*, 2003). We now show that Dys and Dg interact genetically and biochemically and are required in the same cell types in *Drosophila*. A fluorescence polarization assay revealed that the Dg–Dys binding interface is highly conserved in humans and *Drosophila* (Figure 2). Both proteins are required for oocyte cellular polarity and interact in this process (Figure 1). Futhermore, mutants of both *Dg* and *Dys* genes show symptoms observed in muscular dystrophy. Reduction of Dg and Dys proteins results in age-dependent mobility defects (Figure 3). Eliminating Dg and Dys specifically in mesoderm derived tissues reveals that these proteins are required for muscle maintenance in adult flies: age-dependent muscle degeneration was observed in mutant tissues (Figure 4). Dg–Dys complex is also required for neuron path-finding and has both cell autonomous and non-cell autonomous functions for this process (Figures 5 and 6). Further, we have now shown that in neuronal path-finding process Dg interacts with InR and an SH2/SH3-domain adapter molecule Nck/Dock (Figure 7).

Drosophila as a muscular dystrophy model

Animal models have been used efficiently in muscular dystrophy studies. Some of the models are naturally occurring mutations (mdx-mouse, muscular dystrophy dog, cat and hamster), others have been generated by gene targeting (Watchko *et al*, 2002). However, the regulation and the control of Dg–Dys complex are not understood, and no successful therapeutics exist yet for muscular dystrophies

(however, systemic delivery-studies using adeno-associated viral vectors show promise (Gregorevic *et al*, 2004)). Studies in new model organisms with easy-to-manipulate genetics might reveal the mode of regulation of the complex by identifying key regulatory components through suppressor screens. In addition, careful functional analysis of the complex in different cell types in model organisms might result in a unifying theme that will reveal its molecular mechanism of function. Such recently developed models for muscular dystrophy exist in *C. elegans* and zebrafish (Gieseler *et al*, 2000; Parsons *et al*, 2002; Bassett and Currie, 2003). In *C. elegans Dys* mutant, the transporter *snf-6* that normally participates in eliminating acetylcholine from the cholinergic synapses, is not properly localized, resulting in an increased acetylcholine concentration at the neuromuscular junction and muscle wasting (Kim *et al*, 2004). The function of Dys in neuromuscular junctions has also been recently addressed in *Drosophila* (van der Plas *et al*, 2006). These results bring up the possibility that muscular dystrophies in humans might also at least partly be attributed to the altered kinetics of acetylcholine transmission through neuromuscular junctions.

We have now shown that *Drosophila melanogaster* acts as a remarkably good model for age-dependent progression of muscular dystrophy. Dg and Dys reduction in *Drosophila* show age-dependent muscle degeneration and lack of climbing ability. It is tempting to speculate that the common denominator between different defects observed in *Dg–Dys* mutants in *Drosophila* and *C. elegans* is defective cellular polarity. The defects observed in *C. elegans* could be due to a defect in polarization of a cell, which will generate a neuromuscular junction that leads to miss-targeted *snf-6*. Similarly, we have shown that *Drosophila* Dg–Dys complex is required for cellular polarity in the oocyte. In addition, neural defects observed are plausibly due to polarity defects in the growing axon.

Dg–Dys complex in axon path-finding

Similar to neuronal defects observed in human muscular dystrophy patients, neuronal defects were also found in *Drosophila Dg* and *Dys* mutant brains. In vertebrate brains, Dg affects neuronal migration (Montanaro and Carbonetto, 2003; Qu and Smith, 2004) possibly through interaction of neurons with their glial guides. The neuronal migration and process outgrowth have been shown to require supportive input from glial cells and involve the formation of adhesion junctions along the length of the soma. Also, the outgrowth of the leading process involves rapid extension and contraction over the length of the glial fiber (Rivas and Hatten, 1995; Shaham, 2005). Disruption of the cytoskeletal organization within the neuron, either of actin filaments (Rivas and Hatten, 1995) or microtubule interactions (Vallee *et al*, 2000), has been shown to inhibit glial-mediated neuronal migration. The glial function in this process is less well studied.

Drosophila photoreceptor path-finding provides an excellent system for genetic dissection of neuronal outgrowth and target recognition (Dickson, 2002). During the formation of the nervous system, newly born neurons send out axons to find their targets. Each axon is led by a growth cone that responds to extracellular axon guidance cues and chooses between different extracellular substrates upon which to migrate. Recent work has also identified a variety of intracellular signaling pathways by which these cues induce cytoskeletal rearrangements (Guan *et al*, 1996; Rao, 2005), but the proteins connecting signals from cell surface receptors to actin cytoskeleton have not been clearly determined. Dg is a good candidate for linking receptor signaling to the remodeling of the actin cytoskeleton and thereby polarizing the growth cone. We have now shown that perturbation of Dg–Dys complex causes phenotypes that resemble Nck/Dock-Pak-Trio axon path-finding phenotypes (Figure 5) (Rao, 2005), suggesting that Dg may be one of the key players in Nck/Dock signaling pathway for axon guidance and target recognition in *Drosophila*.

Interestingly, Insulin receptor-tyrosine kinase (InR) mutants also show similar phenotypes to those of Nck/Dock signaling in photoreceptor axon path-finding and these two proteins show genetic and biochemical interactions (Song *et al*, 2003). These data have led to speculations of mammalian InR acting in conjunction with Nck/Dock pathway in learning, memory and eating behavior (Dickson, 2003; Song *et al*, 2003). Our data now add Dg–Dys complex to this pathway; similar to what is seen in the case of Dg and Dys photoreceptor mutants, InR mutants show no obvious defects in patterning of the photoreceptors. However, the guidance of photoreceptor cell axons from the retina to the brain is aberrant (Song *et al*, 2003; Figures 5 and 6). Furthermore, genetic and biochemical evidence suggests that InR function in axon guidance involves the Dock-Pak pathway rather than the PI3K-Akt/PKB pathway. Independently, biochemical interaction between Nck/Dock and Dg has been reported (Sotgia *et al*, 2001) supporting the hypothesis that InR, Dg and Nck/Dock interaction regulates Dg–Dys complex. Furthermore, we have now shown that Dg interacts genetically with InR and Dock in photoreceptor axon path-finding. Since Dys interacts with Dg but not with InR and Dock, it is tempting to speculate that Dg can selectively interact with either Dys or InR and Dock (Figure 7). One possibility is that the tyrosine kinase activity of InR could regulate the Dg–Dys interaction by tyrosine phosphorylation in the Dg–Dys binding interphase (Figure 2). This tyrosine phosphorylation could prohibit the Dg–Dys interaction and thereby result in rearrangements in the actin cytoskeleton. Alternatively, other components observed in Dg–Dys complex might be involved in this regulation (Zhan *et al*, 2005). However, it is also possible that potential polarity defects in the Dg mutant axons result in defective InR membrane localization. Interestingly, in another cell type, the *Drosophila* oocyte, InR, Dg and Dys also show similar phenotypes (Deng *et al*, 2003; LaFever and Drummond-Barbosa, 2005; Figure 1). In addition, insulin-like growth factors (IGF) and InR are important in maintaining muscle mass in vertebrates (Singleton and Feldman, 2001). Further connection of InR to Dg–Dys complex comes from experiments showing that muscle specific expression of IGF counters muscle decline in mdx-mice (Barton *et al*, 2002; Shavlakadze *et al*, 2004; Dobrowolny *et al*, 2005). The work presented in this study is the first demonstration of genetic interaction between Dg and InR. Future biochemical studies should unravel the molecular mechanism of this interaction.

Furthermore, we have now shown that Dg–Dys complex is required both in neural and in targeting glial cells for correct neuronal axon path-finding in *Drosophila* brain. These data reveal that Dg–Dys complex also has a non-cell autonomous

effect on axon path-finding and suggest that Dg–Dys-controlled ECM both from neuron and glial cells regulate neuronal axon path-finding. Further experiments are required to reveal whether long-range Laminin fibers are involved in this process, as has been shown in epithelial planar polarity (Bateman *et al*, 2001; Deng *et al*, 2003), or whether glial processes are observed in close proximity to the neural growth cone (Georges-Labouesse *et al*, 1998). Interestingly, similar phenotypes are observed with Integrin mutants (Tanaka and Sabry, 1995; Campos, 2005; Curtin *et al*, 2005), suggesting that, as in planar polarity (Bateman *et al*, 2001; Deng *et al*, 2003), Integrin and Dg–Dys complex might act in concert to regulate the process of ECM organization that will regulate the cytoskeleton of the cells involved.

Taken together, the phenotypes caused by *Drosophila Dg* and *Dys* mutations are remarkably similar to phenotypes observed in human muscular dystrophy patients, and therefore suggest that functional dissection of Dg–Dys complex in *Drosophila* should provide new insights into the origin and potential treatment of these fatal neuromuscular diseases. As a proof of principle, using *Drosophila* as a model we have now identified InR as a signaling pathway that genetically interacts with Dg. Future studies are directed to unravel the molecular mechanism of Dg and InR–Dock interactions in invertebrates as well as vertebrates.

Materials and methods

Fly stocks

FRT42D Dg^{323}*/Cyo* and *FRT42B* Dg^{323}*/CyO (Dg* null allele), *UASdsDg* (*dsDg30A* and *dsDg33A* (Deng *et al*, 2003), *Df(3R)Dl-X43* (referred as *DysKX43*), EP(3)3397*(Dys)* (Bloomington Stock Center), the deletion mutant $Dys^{8\text{-}2}$ in *Dys* gene that was generated by inducing transposition of the EP(3)3397 P-element insertion (http://engels.genetics.wisc.edu//Pelements/index.html), Dys^{e6} deletion mutant (van der Plas *et al*, 2006), three *dsRNA* constructs were created to knock out the different Dys transcripts: *UASdsDysN-term (dsDys N-term)* knocks out the three long forms (DLPs), *UASdsDysRB (dsDys RB)* the short form (Dp186), and *UASdsDysC-term (dsDys C-term)* targets the common C-terminus, thereby knocking down all transcripts (see Supplementary Materials and Methods), *yw;FRT82BpM88C* InR^{34}*/TM6, FRT82B* $InR^{ex52.1}$*/TM6* (gifts from B Edgar), $dock^{P1}$*FRT40A/CyOGFP, yw;eyFlpgl-lacZ;Trio*^{1}*FRT80B/TM6, yw;eyFlpgl-lacZ;* Pak^{14}*FRT82B/TM6* (gifts from N Harden), *hsFLP; FRT42DUbi-GFP/Cyo* and *eyFLPGMR-lacZ; FRT42D l(2)cl-*$R11^{1}$*/CyO, Gal4-elav hsFLP; FRT42B tubGal80/CyO*^{3}*; act-GFP* and *P-tub-Gal4* (ubiquitous expression), *w;MatTub-Gal4/CyO* (germline expression), *GMR-Gal4* (eye expression), w^{-}*;;24B-Gal4* (mesoderm, muscle expression), w^{-}*;;repo-Gal4/TM3,Sb* (glial expression) from Bloomington Stock Center.

Supplementary data

Supplementary data are available at *The EMBO Journal* Online (http://www.embojournal.org).

Acknowledgements

We thank Drs Leslie Pick and Paul Garrity for reagents and advice, Alex Whitworth for help with mobility assay, Glenda Froelick for help with histological sections, Volodymyr Shcherbatyy for injections to produce the transgenic lines, Christian Walker-Richards and Luis Tulloch for generating $Dys^{8\text{-}2}$ deletion line, Merle Gilbert for help with initial experiments, Greg Martin for confocal microscopy instructions, Junlin Qi for help with qRT–PCR, Arul Subramanian and Amir Sapir for helping in the preparation of the *RNAi* flies, Michael Eck and Florence Poy for the human Dystrophin clone, Martina Schneider and Ellen Ward for help with embryonic analysis, and Mario Pantoja for critical reading. This work was supported by an AHA fellowship for HRS, CRDF for ASY, HRS and HR-B, CIHR for VDS, MDA, AFM grants and The Israel Science Foundation for UN and DY, MDA for HR-B and by the grants from the National Institute of Health for DB and HR-B.

References

Barton ER, Morris L, Musaro A, Rosenthal N, Sweeney HL (2002) Muscle-specific expression of insulin-like growth factor I counters muscle decline in mdx mice. *J Cell Biol* **157:** 137–148

Bassett DI, Currie PD (2003) The zebrafish as a model for muscular dystrophy and congenital myopathy. *Hum Mol Genet* **12** (Spec No 2)**:** R265–R270

Bateman J, Reddy RS, Saito H, Van Vactor D (2001) The receptor tyrosine phosphatase Dlar and integrins organize actin filaments in the *Drosophila* follicular epithelium. *Curr Biol* **11:** 1317–1327

Benzer S (1967) Behavioral mutants of *Drosophila* isolated by countercurrent distribution. *Proc Natl Acad Sci USA* **58:** 1112–1119

Bier E (2005) *Drosophila*, the golden bug, emerges as a tool for human genetics. *Nat Rev Genet* **6:** 9–23

Bloch-Gallego E, Causeret F, Ezan F, Backer S, Hidalgo-Sanchez M (2005) Development of precerebellar nuclei: instructive factors and intracellular mediators in neuronal migration, survival and axon pathfinding. *Brain Res Brain Res Rev* **49:** 253–266

Campbell KP (1995) Three muscular dystrophies: loss of cytoskeleton-extracellular matrix linkage. *Cell* **80:** 675–679

Campos LS (2005) Beta1 integrins and neural stem cells: making sense of the extracellular environment. *Bioessays* **27:** 698–707

Clandinin TR, Zipursky SL (2002) Making connections in the fly visual system. *Neuron* **35:** 827–841

Cohn RD (2005) Dystroglycan: important player in skeletal muscle and beyond. *Neuromuscul Disord* **15:** 207–217

Cohn RD, Campbell KP (2000) Molecular basis of muscular dystrophies. *Muscle Nerve* **23:** 1456–1471

Curtin KD, Meinertzhagen IA, Wyman RJ (2005) Basigin (EMMPRIN/CD147) interacts with integrin to affect cellular architecture. *J Cell Sci* **118:** 2649–2660

Dekkers LC, van der Plas MC, van Loenen PB, den Dunnen JT, van Ommen GJ, Fradkin LG, Noordermeer JN (2004) Embryonic expression patterns of the *Drosophila* dystrophin-associated glycoprotein complex orthologs. *Gene Expr Patterns* **4:** 153–159

Deng WM, Ruohola-Baker H (2000) Laminin A is required for follicle cell-oocyte signaling that leads to establishment of the anterior–posterior axis in *Drosophila*. *Curr Biol* **10:** 683–686

Deng WM, Schneider M, Frock R, Castillejo-Lopez C, Gaman EA, Baumgartner S, Ruohola-Baker H (2003) Dystroglycan is required for polarizing the epithelial cells and the oocyte in *Drosophila*. *Development* **130:** 173–184

Dickson BJ (2002) Molecular mechanisms of axon guidance. *Science* **298:** 1959–1964

Dickson BJ (2003) Development. Wiring the brain with insulin. *Science* **300:** 440–441

Dobrowolny G, Giacinti C, Pelosi L, Nicoletti C, Winn N, Barberi L, Molinaro M, Rosenthal N, Musaro A (2005) Muscle expression of a local Igf-1 isoform protects motor neurons in an ALS mouse model. *J Cell Biol* **168:** 193–199

Durbeej M, Campbell KP (2002) Muscular dystrophies involving the dystrophin–glycoprotein complex: an overview of current mouse models. *Curr Opin Genet Dev* **12:** 349–361

Garrity PA, Rao Y, Salecker I, McGlade J, Pawson T, Zipursky SL (1996) *Drosophila* photoreceptor axon guidance and targeting requires the dreadlocks SH2/SH3 adapter protein. *Cell* **85:** 639–650

Georges-Labouesse E, Mark M, Messaddeq N, Gansmuller A (1998) Essential role of alpha 6 integrins in cortical and retinal lamination. *Curr Biol* **8:** 983–986

Gieseler K, Grisoni K, Segalat L (2000) Genetic suppression of phenotypes arising from mutations in dystrophin-related genes in *Caenorhabditis elegans*. *Curr Biol* **10:** 1092–1097

Greener MJ, Roberts RG (2000) Conservation of components of the dystrophin complex in *Drosophila*. *FEBS Lett* **482:** 13–18

Gregorevic P, Blankinship MJ, Allen JM, Crawford RW, Meuse L, Miller DG, Russell DW, Chamberlain JS (2004) Systemic delivery of genes to striated muscles using adeno-associated viral vectors. *Nat Med* **10:** 828–834

Guan B, Hartmann B, Kho YH, Gorczyca M, Budnik V (1996) The *Drosophila* tumor suppressor gene, dlg, is involved in structural plasticity at a glutamatergic synapse. *Curr Biol* **6:** 695–706

Hoffman EP, Brown Jr RH, Kunkel LM (1987) Dystrophin: the protein product of the Duchenne muscular dystrophy locus. *Cell* **51:** 919–928

Huang X, Poy F, Zhang R, Joachimiak A, Sudol M, Eck MJ (2000) Structure of a WW domain containing fragment of dystrophin in complex with beta-dystroglycan. *Nat Struct Biol* **7:** 634–638

Izaddoost S, Nam SC, Bhat MA, Bellen HJ, Choi KW (2002) *Drosophila* crumbs is a positional cue in photoreceptor adherens junctions and rhabdomeres. *Nature* **416:** 178–183

Kato Y, Ito M, Kawai K, Nagata K, Tanokura M (2002) Determinants of ligand specificity in groups I and IV WW domains as studied by surface plasmon resonance and model building. *J Biol Chem* **277:** 10173–10177

Kim H, Rogers MJ, Richmond JE, McIntire SL (2004) SNF-6 is an acetylcholine transporter interacting with the dystrophin complex in *Caenorhabditis elegans*. *Nature* **430:** 891–896

Koenig M, Hoffman EP, Bertelson CJ, Monaco AP, Feener C, Kunkel LM (1987) Complete cloning of the Duchenne muscular dystrophy (DMD) cDNA and preliminary genomic organization of the DMD gene in normal and affected individuals. *Cell* **50:** 509–517

LaFever L, Drummond-Barbosa D (2005) Direct control of germline stem cell division and cyst growth by neural insulin in *Drosophila*. *Science* **309:** 1071–1073

Michele DE, Barresi R, Kanagawa M, Saito F, Cohn RD, Satz JS, Dollar J, Nishino I, Kelley RI, Somer H, Straub V, Mathews KD, Moore SA, Campbell KP (2002) Post-translational disruption of dystroglycan–ligand interactions in congenital muscular dystrophies. *Nature* **418:** 417–422

Montanaro F, Carbonetto S (2003) Targeting dystroglycan in the brain. *Neuron* **37:** 193–196

Moore SA, Saito F, Chen J, Michele DE, Henry MD, Messing A, Cohn RD, Ross-Barta SE, Westra S, Williamson RA, Hoshi T, Campbell KP (2002) Deletion of brain dystroglycan recapitulates aspects of congenital muscular dystrophy. *Nature* **418:** 422–425

Muntoni F, Brockington M, Blake DJ, Torelli S, Brown SC (2002) Defective glycosylation in muscular dystrophy. *Lancet* **360:** 1419–1421

Neuman S, Kaban A, Volk T, Yaffe D, Nudel U (2001) The dystrophin/utrophin homologues in *Drosophila* and in sea urchin. *Gene* **263:** 17–29

Neuman S, Kovalio M, Yaffe D, Nudel U (2005) The *Drosophila* homologue of the dystrophin gene—introns containing promoters are major contributors to the large size of the gene. *FEBS Lett* **579:** 5365–5371

Parsons MJ, Campos I, Hirst EM, Stemple DL (2002) Removal of dystroglycan causes severe muscular dystrophy in zebrafish embryos. *Development* **129:** 3505–3512

Perez SE, Steller H (1996) Migration of glial cells into retinal axon target field in *Drosophila melanogaster*. *J Neurobiol* **30:** 359–373

Pesah Y, Pham T, Burgess H, Middlebrooks B, Verstreken P, Zhou Y, Harding M, Bellen H, Mardon G (2004) *Drosophila* parkin mutants have decreased mass and cell size and increased sensitivity to oxygen radical stress. *Development* **131:** 2183–2194

Poeck B, Fischer S, Gunning D, Zipursky SL, Salecker I (2001) Glial cells mediate target layer selection of retinal axons in the developing visual system of *Drosophila*. *Neuron* **29:** 99–113

Qu Q, Smith FI (2004) Alpha-dystroglycan interactions affect cerebellar granule neuron migration. *J Neurosci Res* **76:** 771–782

Rao Y (2005) Dissecting Nck/Dock signaling pathways in *Drosophila* visual system. *Int J Biol Sci* **1:** 80–86

Reiter LT, Potocki L, Chien S, Gribskov M, Bier E (2001) A systematic analysis of human disease-associated gene sequences in *Drosophila melanogaster*. *Genome Res* **11:** 1114–1125

Rivas RJ, Hatten ME (1995) Motility and cytoskeletal organization of migrating cerebellar granule neurons. *J Neurosci* **15:** 981–989

Ruan W, Long H, Vuong DH, Rao Y (2002) Bifocal is a downstream target of the Ste20-like serine/threonine kinase misshapen in regulating photoreceptor growth cone targeting in *Drosophila*. *Neuron* **36:** 831–842

Saito F, Moore SA, Barresi R, Henry MD, Messing A, Ross-Barta SE, Cohn RD, Williamson RA, Sluka KA, Sherman DL, Brophy PJ, Schmelzer JD, Low PA, Wrabetz L, Feltri ML, Campbell KP (2003) Unique role of dystroglycan in peripheral nerve myelination, nodal structure, and sodium channel stabilization. *Neuron* **38:** 747–758

Shaham S (2005) Glia–neuron interactions in nervous system function and development. *Curr Top Dev Biol* **69:** 39–66

Shavlakadze T, White J, Hoh JF, Rosenthal N, Grounds MD (2004) Targeted expression of insulin-like growth factor-I reduces early myofiber necrosis in dystrophic mdx mice. *Mol Ther* **10:** 829–843

Singleton JR, Feldman EL (2001) Insulin-like growth factor-I in muscle metabolism and myotherapies. *Neurobiol Dis* **8:** 541–554

Song J, Wu L, Chen Z, Kohanski RA, Pick L (2003) Axons guided by insulin receptor in *Drosophila* visual system. *Science* **300:** 502–505

Sotgia F, Lee H, Bedford MT, Petrucci T, Sudol M, Lisanti MP (2001) Tyrosine phosphorylation of beta-dystroglycan at its WW domain binding motif, PPxY, recruits SH2 domain containing proteins. *Biochemistry* **40:** 14585–14592

Spence HJ, Chen YJ, Batchelor CL, Higginson JR, Suila H, Carpen O, Winder SJ (2004a) Ezrin-dependent regulation of the actin cytoskeleton by beta-dystroglycan. *Hum Mol Genet* **13:** 1657–1668

Spence HJ, Chen YJ, Winder SJ (2002) Muscular dystrophies, the cytoskeleton and cell adhesion. *Bioessays* **24:** 542–552

Spence HJ, Dhillon AS, James M, Winder SJ (2004b) Dystroglycan, a scaffold for the ERK-MAP kinase cascade. *EMBO Rep* **5:** 484–489

Tanaka E, Sabry J (1995) Making the connection: cytoskeletal rearrangements during growth cone guidance. *Cell* **83:** 171–176

Tessier-Lavigne M, Goodman CS (1996) The molecular biology of axon guidance. *Science* **274:** 1123–1133

Vallee RB, Faulkner NE, Tai CY (2000) The role of cytoplasmic dynein in the human brain developmental disease lissencephaly. *Biochim Biophys Acta* **1496:** 89–98

van der Plas MC, Pilgram GS, Plomp JJ, de Jong A, Fradkin LG, Noordermeer JN (2006) Dystrophin is required for appropriate retrograde control of neurotransmitter release at the *Drosophila* neuromuscular junction. *J Neurosci* **26:** 333–344

Watchko JF, O'Day TL, Hoffman EP (2002) Functional characteristics of dystrophic skeletal muscle: insights from animal models. *J Appl Physiol* **93:** 407–417

Winder SJ (2001) The complexities of dystroglycan. *Trends Biochem Sci* **26:** 118–124

Yang B, Jung D, Motto D, Meyer J, Koretzky G, Campbell KP (1995) SH3 domain-mediated interaction of dystroglycan and Grb2. *J Biol Chem* **270:** 11711–11714

Yang Y, Gehrke S, Imai Y, Huang Z, Ouyang Y, Wang JW, Yang L, Beal MF, Vogel H, Lu B (2006) Mitochondrial pathology and muscle and dopaminergic neuron degeneration caused by inactivation of *Drosophila* Pink1 is rescued by Parkin. *Proc Natl Acad Sci USA* **103:** 10793–10798

Yatsenko AS, Gray EE, Shcherbata HR, Patterson LB, Sood VD, Kucherenko MM, Baker D, Ruohola-Baker H (2006) A putative SH3-domain binding motif but not the C-terminal Dystrophin WW-domain binding motif is required for Dystroglycan function in cellular polarity in *Drosophila*. *J Biol Chem* (submitted)

Zhan Y, Tremblay MR, Melian N, Carbonetto S (2005) Evidence that dystroglycan is associated with dynamin and regulates endocytosis. *J Biol Chem* **280:** 18015–18024

Supplementary Information

Materials and Methods

Generation of *pUASTdsDys* Transgenic Animals. Three *dsRNA* constructs were created to knock out the different *Dystrophin* transcripts. *UASdsDysN-term (dsDys N-term)* knocks out the three long forms (DLPs), *UASdsDysRB (dsDys RB)* the short form (Dp186), and *UASdsDysC-term (dsDys C-term)* targets the common C-terminus, thereby knocking down all transcripts.

The 825 bp *dsRNAi* region for the *dsDys N-term* construct begins in the first common exon (exon 3). A 500bp loop separates the two complementary strands. The PCR primers used were: 5' fragment, sense: AG[GAATTC]ATGAAAGACAGCACATACAGAAG (EcoRI), 5' fragment, antisense: GAGAGATCTATGGGATATACGATCTTCGACACTG, 3' fragment, sense: GAGAGATCTGCCAGCACTGTCTGAAGTATAAAG, 3' fragment, antisense: GC[TCTAGA]ATGAAAGACAGCACATACAGAAG (XbaI).

The 965 bp *dsRNAi* for *UAS dsDys RB* construct begins with the initiator ATG of the Dp186 transcript and includes a 520 bp loop. The PCR primers used were: 5' fragment, sense: AG[GAATTC]ATGACTGCCAAACCACCGCCTCCA (EcoRI), 5' fragment, antisense: GCTGGTACCTTCTGCGCATGCGCAGCTCC, 3' fragment, sense: GCGGTACCTCCTCCAGGGATTGTCGCGAGT, 3' fragment, antisense: AA[TCTAGA]ATGACTGCCAAACCACCGCCTCCAATC (XbaI).

The 1145 bp ds region for *UAS dsDys C-term* construct begins in exon 26 and has a 640 bp loop. The PCR primers used were: 5' fragment, sense: CCG[CTCGAG]CATGGCCGAGGAGCAGAGCCGTGAGCTA (XhoI), 5' fragment, antisense: CGTGGAATTCGAGCCCGTTCCGCCGTA, 3' fragment, sense: AGGAATTCTGGCGGGGTACCTGAATGCAATCGT, 3' fragment, antisense: AAA[TCTAGA]CAGTGGAACAATCTCCTCGATAG (XbaI).

Each pair of PCR products (5' and 3' fragments) and the vector pUAST were cut with the appropriate restriction enzymes, mixed, ligated and then cloned into *E.coli* HB101. The constructs were injected into embryos to obtain stable transformant lines. Two independent transgenic lines for each construct were chosen and analyzed: *UASTdsDys [dsDys N-term (tg3,4), dsDys C-term (tg5,6) and dsDys RB (tg1,2*)]. The ovarian expression of Dys protein

was highly reduced in *Dys*$^{8-2}$*/KX43* as well as *dsDys/P-TubGal4* backgrounds (Supplementary Figure 3).

Generation of *pUASPdsDysN-term* Transgenic Animals. To create a *UASdsDysN-term* construct for over expression in the germline, the region cloned between the EcoRI and Xba I sites of *UASTdsDysN-term* was excised and cloned into pBS(KS+) to generate the intermediate plasmid pBS-*dsDysN-term*. This plasmid was then digested with KpnI and XbaI to remove the *dsDysN-term* insert from pBS(KS+). The fragment was then ligated with pUASP to create *UASPdsDysN-term*. This construct was injected into embryos to obtain stable transformant lines. Four independent transgenic lines were chosen and analyzed: *UASP dsDys N-term (Dys.N18, Dys.N23, Dys.N35 and Dys.N3)*.

Plasmid Construction For In Vitro Analysis and Protein Expression. The WW-EF hand region of *Drosophila* Dystrophin (2840-3109 aa) was amplified using PCR and cloned between the *NdeI* and *XhoI* restriction sites of the His-Tag expression vector pET-15b (Novagen). *Drosophila* Dys WW+EF hand protein was expressed in *E.coli* strain BL21(DE3) after induction by IPTG. Cell pellets were collected and lysed by French Press. Protein was purified using Ni-NTA (QIAGEN) affinity chromatography. Protein was concentrated using an Amicon Ultra Centrifugal Device (Millipore) and imidazole removed by dialysis. Purified Dys WW+EF Hand protein was stored in 50 mM MOPS pH 6.5, 150 mM NaCl, 400mM Na_2SO_4, 10 mM DTT. The Dys WW+EF hand of human Dystrophin (Huang et al., 2000) was expressed as a GST-fusion protein and purified by glutathione affinity chromatography. 500 U of thrombin (Amersham) were loaded onto the glutathione column with Dys WW+EF hand bound, the column sealed and incubated overnight at 4°C to cleave the GST from the Dys WW+EF hand. The Dys WW+EF hand was washed off the column, concentrated and the buffer exchanged during concentration to the same storage buffer used for the *Drosophila* Dys WW+EF hand.

Fluorescence Polarization Experiments. Three Dg WWbsI (Dystrophin WW binding site I) peptides were synthesized and N-terminally tagged with tetramethylrhodamine by Invitrogen Evoquest Services (sequences DmWWbsI GKSPATPSYRKPPPYVSP; HmWWbsI KNMPTYRSPPPYVPP; HmWWbsI-P KNMPTYRSPPPPVPP). All peptides were over 95% pure based upon HPLC and mass spectrometry analysis. Fluorescence polarization experiments were performed at 25°C using a Wallac 1420 Victor3 (PerkinElmer). Dg peptide (200nM) was incubated with increasing concentrations of Dys protein in storage buffer (50

mM MOPS pH 6.5, 150 mM NaCl, 400mM Na_2SO_4, 10 mM DTT) to a final volume of 250 μl. Anisotropy values were measured at an excitation wavelength of 531nm and an emission wavelength of 595nm. Binding dissociation constants (Kd) were determined by plotting milliAnisotrophy against the concentration of Dys WW+EF hand and fitting the data to the equilibrium binding equation

$$\frac{WDg}{Dg} = \frac{Dg + W + K_d - \sqrt{Dg^2 - 2 \bullet Dg \bullet W + W^2 + 2 \bullet W \bullet K_d + K_d^2}}{2 \bullet Dg}$$

where Dg is the total concentration of Dystroglycan peptide, *W* is the total concentration of Dystrophin protein, *W*Dg is the concentration of Dg-Dys complex, and *Kd* is the apparent dissociation constant for the complex.

Loss-of-function mosaic analysis. To obtain germline clones, flies were heat-shocked third instar larvae and early pupae for 2 hours on 2 consecutive days. Once they emerged as adults, they were placed in vials with fresh yeast paste for 4-5 days before dissection. To analyze mutant clones in eye discs wandering third instar larvae were collected. For MARCM analysis first instar larvae were heat-shocked for 2 hours and dissected as third instar larvae.

Interaction analysis. To study the interaction of Dystroglycan and Dystrophin with Dock and InR pathways we crossed *Dg^{323}* and *DysKX43* flies to *Dock, InR, Pak* and *Trio* mutants and analyzed larval brains of transheterozygous flies.

Staining Procedures. The *Drosophila* ovaries, larval brains and imaginal disc were dissected rapidly in PBS and fixed in 4% paraformaldehyde for 10'. The antibody staining procedure was the same as described previously (Shcherbata et al., 2004).

Histological sections of muscle and brain were prepared from wax-embedded material. Flies were fixed in Carnoy's solution (6:3:1 ethanol:chlorophorm:acetic acid), dehydrated, and infiltrated with paraffin. Frontal sections were cut at 7μm thickness, deparafinized in xylene (2 X 4'), rehydrated in ethanol (100% EtOH 2 X 4', 95% EtOH 1 X 3', 70%EtOH 1 X 2', H_2O 1X1') and stained with hematoxyline (7') and eosin (2') (H&E staining). Sections were dehydrated mounted in Vectashield and analyzed using light microscopy. For immunostainings of paraffin-embedded adult brains, sections were deparafinized in xylene (2 times for 4 minutes), rehydrated in ethanol (100% EtOH 2 X 4', 95% EtOH 1 X 3', 70%EtOH 1 X 2', H_2O 1'), rinsed for 15' in PBT (PBS/0.2% Triton X-100) and blocked in PBTB (PBT, 0.2% BSA, 5% NGS) for one hour at room temperature. The sections were incubated with primary antibodies overnight at 4^oC. The next day they were rinsed with PBT 4 X 10',

blocked in PBTB for one hour at room temperature and incubated in secondary antibodies overnight at 4^{o}C. The next day they were rinsed with PBT 4 X 15', stained with DAPI (1µg/ml in PBT 10') washed for 2 X 5' with PBT. They were then mounted onto slides in 70% glycerol, 2% NPG, 1X PBS and analyzed using a two-photon laser-scanning microscope (Leica TCS SP/MP).

The following antibodies were used: rabbit anti-Dg (1:3000;(Deng et al., 2003), anti-Dys CO_2H (1:3000, (van der Plas et al., 2006)), anti-ß-HSpectrin (Thomas et al., 1998); mouse anti-Orb, anti-Repo, anti-24B10 (1:20, 1:50, 1:50 respectively, Developmental Studies Hybridoma Bank), Alexa 488, 568, or 633 goat anti-mouse, Alexa 488, 568, or 633 goat anti-rabbit (1:500, Molecular Probes).

Behavioral Assays. Climbing (mobility) assays were performed by using a countercurrent apparatus developed initially for phototaxis experiments (Benzer, 1967). Twenty to thirty flies were placed into the first chamber, tapped to the bottom, then given 30 sec to climb a distance of 10 cm. Flies that successfully climbed 10 cm in 30 sec were then shifted to a new chamber, and successful flies were given another opportunity to climb the 10-cm distance. This procedure was repeated a total of five times. Then, the number of flies in each chamber was counted. The climbing index was calculated as the sum of the number of flies in each chamber multiplied by the number of the chamber and divided by five times the number of flies in the assay (Greene et al., 2003).

Estimation of Dys protein levels

To calculate the efficacy of dsRNA Dys constructs the relative amounts of Dys protein were calculated using ImageJ software. The *Drosophila* ovarioles from wild type and dsRNA mutants were immunostained with Dys-CO_2H antibody (van der Plas et al., 2006), which is specific to long (DLP1, DLP2) and short (RB) Dys isoforms. The brightness of germline staining was used as a background level and was subtracted from the brightness of follicle cell epithelial staining to obtain the value that represents Dys expression level (brightness/per pixel$\pm$SD). To calculate relative amount of Dys protein in Dys *RNAi* mutants versus wild type, the brightness of wild type staining was assumed as 100% and decreased expression in mutants was estimated with respect to that.

RNA preparation and real-time PCR

To determine the effects of expression of the *Dys RNAi* transgene on the expression levels of the *dystrophin* isoforms we performed quantitative reverse transcription (RT)-PCR on total

RNA derived from whole animal using primer pairs specific for DLP2, which is mainly expressed in muscles (van der Plas et al., 2006). Total RNAs were extracted from flies with RNeasy Mini kit (Qiagen), followed by DNase treatment with the RNase-Free Dnase set (Qiagen). Reverse transcription was done with Omniscript RT kit (Qiagen). Dys DLP2 was was tested together with RP49 serving as loading control by real-time PCR assays using SyberGreen master mix (Applied Biosystems) performed on the New Opticon I system (M. J. Research, Inc.). The reactions were incubated in a 96 well plate at 95 ^{o}C for 10 min, followed by 40 cycles of 94^{o}C for 15 s and 54^{o}C for 30 s and 72^{o}C for 30 s. All reactions were run in triplicate, except that RT minus controls were run in duplicate. The threshold cycle (CT) is defined as the fractional cycle number at which the fluorescence passes the fixed threshold. Primers used were as follows: DLP2 forward, CGTAAAGACTTGAAACGCGTCG; DLP2 reverse, TGGATTCCATGGCGTGGT; RP49 forward, ATGACCATCCGCCCAGCA; and RP49 reverse, TTGGGGTTGGTGAGGCGGAC.

References:

Benzer, S. (1967) Behavioral mutants of Drosophila isolated by countercurrent distribution. *Proc Natl Acad Sci U S A*, **58**, 1112-1119.

Deng, W.M., Schneider, M., Frock, R., Castillejo-Lopez, C., Gaman, E.A., Baumgartner, S. and Ruohola-Baker, H. (2003) Dystroglycan is required for polarizing the epithelial cells and the oocyte in Drosophila. *Development*, **130**, 173-184.

Greene, J.C., Whitworth, A.J., Kuo, I., Andrews, L.A., Feany, M.B. and Pallanck, L.J. (2003) Mitochondrial pathology and apoptotic muscle degeneration in Drosophila parkin mutants. *Proc Natl Acad Sci U S A*, **100**, 4078-4083.

Shcherbata, H.R., Althauser, C., Findley, S.D. and Ruohola-Baker, H. (2004) The mitotic-to-endocycle switch in Drosophila follicle cells is executed by Notch-dependent regulation of G1/S, G2/M and M/G1 cell-cycle transitions. *Development*, **131**, 3169-3181.

Thomas, G.H., Zarnescu, D.C., Juedes, A.E., Bales, M.A., Londergan, A., Korte, C.C. and Kiehart, D.P. (1998) Drosophila betaHeavy-spectrin is essential for development and contributes to specific cell fates in the eye. *Development*, **125**, 2125-2134.

van der Plas, M.C., Pilgram, G.S., Plomp, J.J., de Jong, A., Fradkin, L.G. and Noordermeer, J.N. (2006) Dystrophin is required for appropriate retrograde control of neurotransmitter release at the Drosophila neuromuscular junction. *J Neurosci*, **26**, 333-344.

Supplementary Table 1. Dys RNAi mutants show decrease in Dys mRNA levels

Genotype	DLP2 Average C_T	RP49 Average C_T	Δ C_T DLP2-RP49[a]	ΔΔ C_T ΔC_T- $\Delta C_{T,\ control}$[b]	Average DLP2 relative to control[c]	DLP2 mRNA fold reduction relative to control[d]
Control TM3/P-tubGal4	25.21±0.28	20.96±0.15	4.25±0.32	0.00±0.32	1	1
dsDysN-term(tg4) /P-tubGal4	26.68±0.25	19.67±0.13	7.01±0.28	2.76±0.28	0.15±0.04	6.92±1.88
dsDysRB(tg2)/ P-tubGal4	26.35±0.06	20.52±0.24	5.84±0.25	1.59±0.25	0.34±0.08	3.05±0.72
dsDysC-term(tg6)/ P-tubGal4	26.73±0.47	18.42±0.05	8.30±0.47	4.05±0.47	0.06±0.03	17.51±7.85
dsDysC-term(tg5)/ P-tubGal4	26.13±0.22	19.34±0.17	6.79±0.28	2.54±0.28	0.17±0.05	5.93±1.59
Dys^{8-2}/DysKX43	26.15±0.40	14.78±0.05	11.41±0.41	7.15±0.41	0.01±0.01	148.5±57.7

a. The **Δ C_T** value is determined by subtracting the average RP49 C_T value from the average DLP2 or Dp186 C_T value. The standard deviation of the difference is calculated from the standard deviations of the DLP2 and RP49 values using the following formula: $\mathbf{s=\sqrt{s1^2+s2^2}}$, where: **s = std dev**.

b. The calculation of **ΔΔ C_T** involves subtraction by the **Δ C_T** calibrator value. This is subtraction of an arbitrary constant, so the standard deviation of **ΔΔ C_T** is the same as the standard deviation of the **Δ C_T** value.

c. The range given for DLP2 relative to Control is determined by evaluating the expression: $\mathbf{2^{-\Delta\Delta CT}}$ with **ΔΔ C_T + s** and **ΔΔ C_T – s**, where s = the standard deviation of the **ΔΔ C_T** value.

d. The fold reduction given for DLP2 relative to Control is determined by evaluating the expression: $\mathbf{2^{\Delta\Delta CT}}$ with **ΔΔ C_T + s** and **ΔΔ C_T – s**, where s = the standard deviation of the **ΔΔ C_T** value.

Supplementary Figure Legends

Supplementary Figure 1. Dystroglycan expression in *Drosophila* embryo.

(A-H) Dystroglycan is expressed in ectoderm and its derivatives: salivary glands, foregut **(A,A'),** central nervous system (brain, **B**, ventral neural cord, **C**) and peripheral nervous system **(D)**, Malpighian tubules **(G)**, and tracheal system **(H)**.

(E-H). Dystroglycan is also expressed in some of the mesodermal derived tissues: cells of heart **(E)**, aorta **(F)**, and gut **(F-H)**.

(I-L) In *Dg* loss-of-function mutant *(Dg^{323}/Dg^{323})* Dystroglycan staining is diminished in the ectoderm **(I,I')**, central nervous system **(J,J')**, heart **(K,K')** and gut **(L,L').**

Red=Dystroglycan, Green=Crumbs in **(A)**, Armadillo in **(B-H)** or DAPI in **(I-L)**,

Supplementary Figure 2. Dystrophin expression in *Drosophila* embryo.

(A-D) Dystrophin, like Dystroglycan, is expressed in *Drosophila* heart **(A,A', B,B')** and gut **(D,D')**. In Dystrophin loss-of-function mutant (*Dys^{8-2}/DysKX43)* Dystrophin staining is highly reduced **(C,C', E).**

Red=Dystrophin C-term, Green= DAPI.

Supplementary Figure 3. Dystroglycan and Dystrophin expression in *Drosophila* ovaries.

(A) Dystroglycan is present in the germline and in the follicle cells, especially on the basal side of follicle cells membrane (Deng et al., 2003). **(B)** *Dystrophin* in situ pattern. **(C,C')** Dystrophin antibody staining in wild type ovaries is similar to the Dg expression pattern. **(D-I)** Dys staining is reduced in the *Dys* loss-of function mutant (*Dys^{8-2}/DysKX43,* **D,D', F,F')** and in *Dys* RNAi mutants (*dsDysC-term*, **G,G',** *dsDysN-term*, **H,H',** *dsDysRB*, **I,I)**.

Red=Dg or Dys, Green=Armadillo, Blue=DAPI.

(J-L) Loss of *Dg* or *Dys* in the follicle cells (**K,L** *dsDys30A* and *dsDys C-term/P-tubGAL4*) disturbs the apical-basal polarity; the apical marker ß-Heavy-Spectrin is disrupted and/or expanded to the basal side (yellow arrows).

Green=ß-Heavy-Spectrin, Red=DAPI.

(M) The quantitative analysis of Dys protein level reduction in *Dys RNAi* mutants and the *Dys* loss-of function *Dys^{8-2}/DysKX43* mutant (immunohistochemistry using antibody against Dys

C-terminus, the common region for all isoforms). The bar graph shows that knocking out the long form of Dys by expressing *dsDys N-term/P-tub-Gal4* reduces expression of the Dys protein 2.9 folds, knocking out the short form of Dys by expressing *dsDys RB/P-tub-Gal4* reduces the expression of Dys protein 2.1 fold, knocking out all Dys isoforms by of Dys *dsDys C-term/P-tub-Gal4* reduces the expression of Dys protein 4.8 fold. The *Dys* loss-of function Dys^{8-2}*/DysKX43* mutant has a 3.8 fold reduction of Dys protein levels in comparison to the control *TM3/P-tub-Gal4.*

(L) Quantative RT-PCR data showing that the relative amounts of Dys long form mRNA (DLP2) are significantly decreased in the *Dys RNAi* mutants *dsDys N-term/P-tub-Gal4* (6 fold reduction), *dsDys RB/P-tub-Gal4* (3 fold reduction), *and dsDys C-term/P-tub-Gal4* (from 16 to 6 fold reduction). The *Dys* loss-of function Dys^{8-2}*/DysKX43* mutant has a 148 fold reduction of DLP2 Dys mRNA.

Supplementary Figure 4. Dg-Dys complex is required for normal retina development.

(A) Frontal histological sections of adult wild type *Drosophila* brain. Retina cells are elongated.

(B, C) In *Dg* and *Dys* mutants (dsDys C-term/P-tubGal4, *eyFLP GMR-lacZ; FRT42D* Dg^{323}*/FRT42D l(2)cl-R11*^{1}*)* retinal cells fail to elongate during development (black arrows).

(D) Dg is expressed in the membranes of retinal cells and in optic lobes.

Supplementary Figure 5. Dg acts in neuronal and glial cells for normal photoreceptor axon connectivity.

(A-B) *Dg* single-mutant photoreceptor neurons were generated by using the MARCM method with *hsFLP* to promote mitotic recombination and with labeled cells marked by *Gal4* expression of *UAS GFP (Gal4-elav hsFLP; FRT42B tubGal80/ FRT42BDg*^{323}*; UAS GFP act<CD2<Gal4),* photoreceptor cells are marked with 24B10 antibody **(A-A'')**, glial cells are marked with Repo antibody **(B-B''')**. Gaps in the termination zone are associated with the presence of *Dg* mutant mutant photoreceptor axons **(A)** as well as *Dg* mutant glial cells **(B)**.

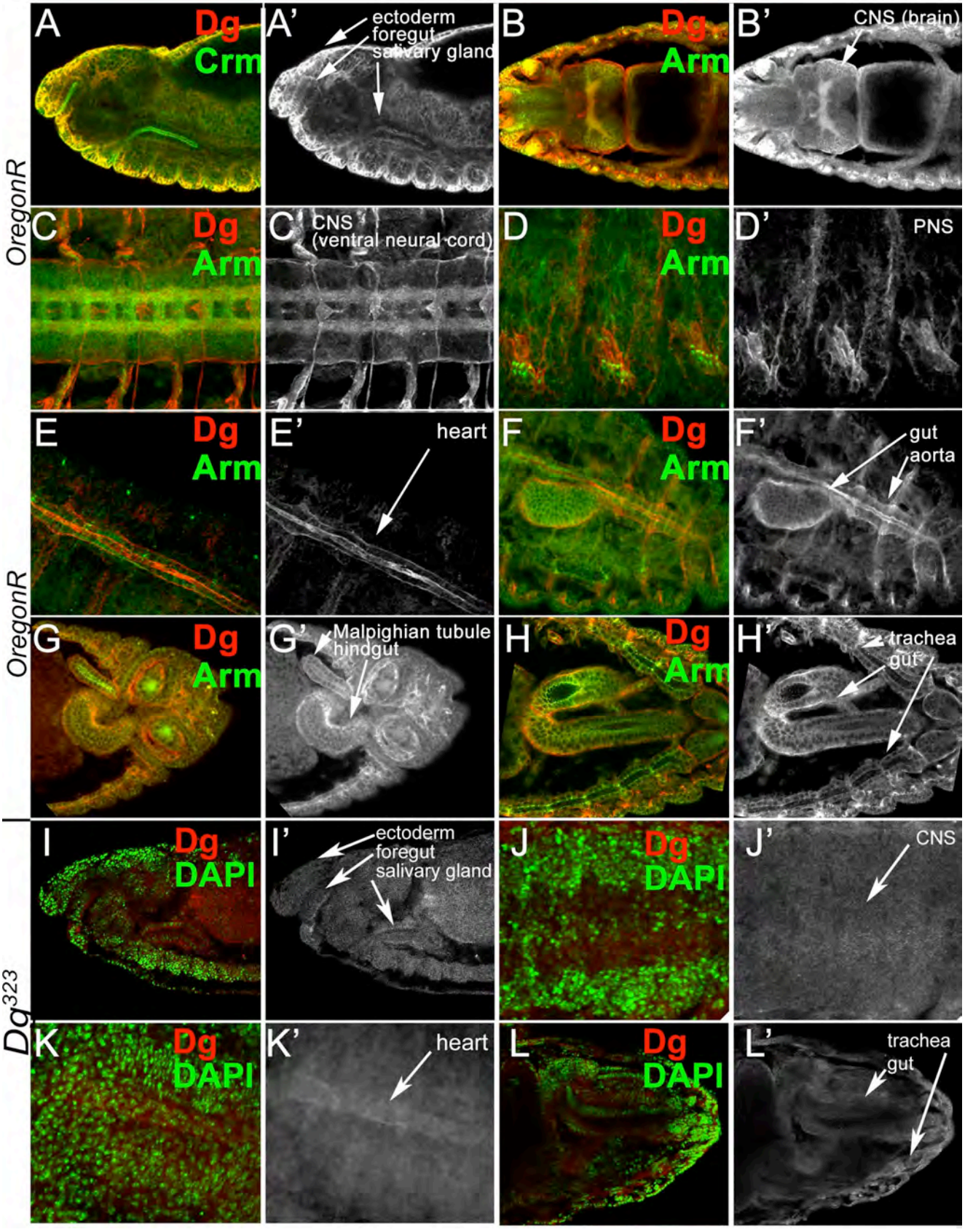

Supplementary Figure1

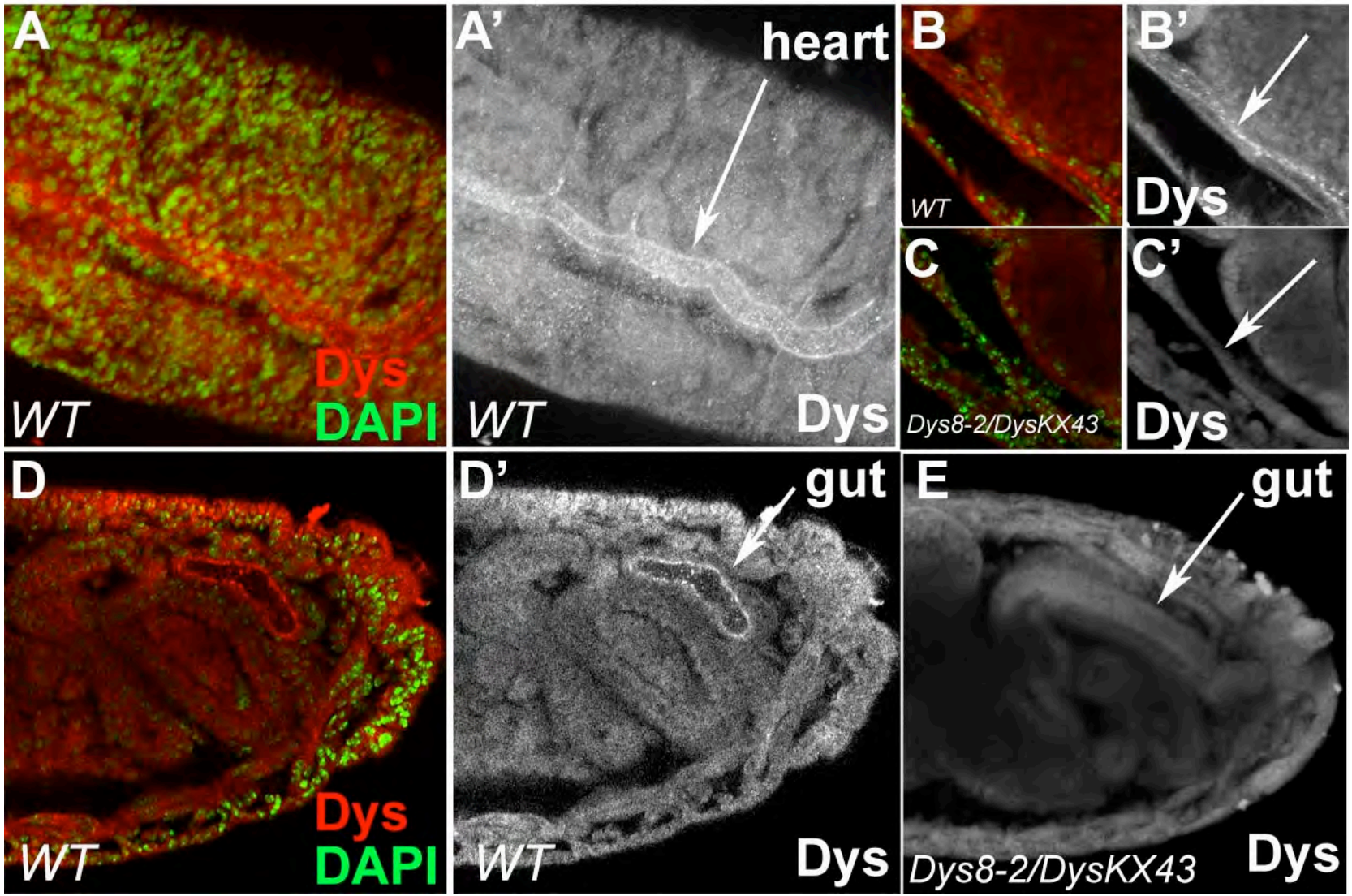

Supplementary Figure 2

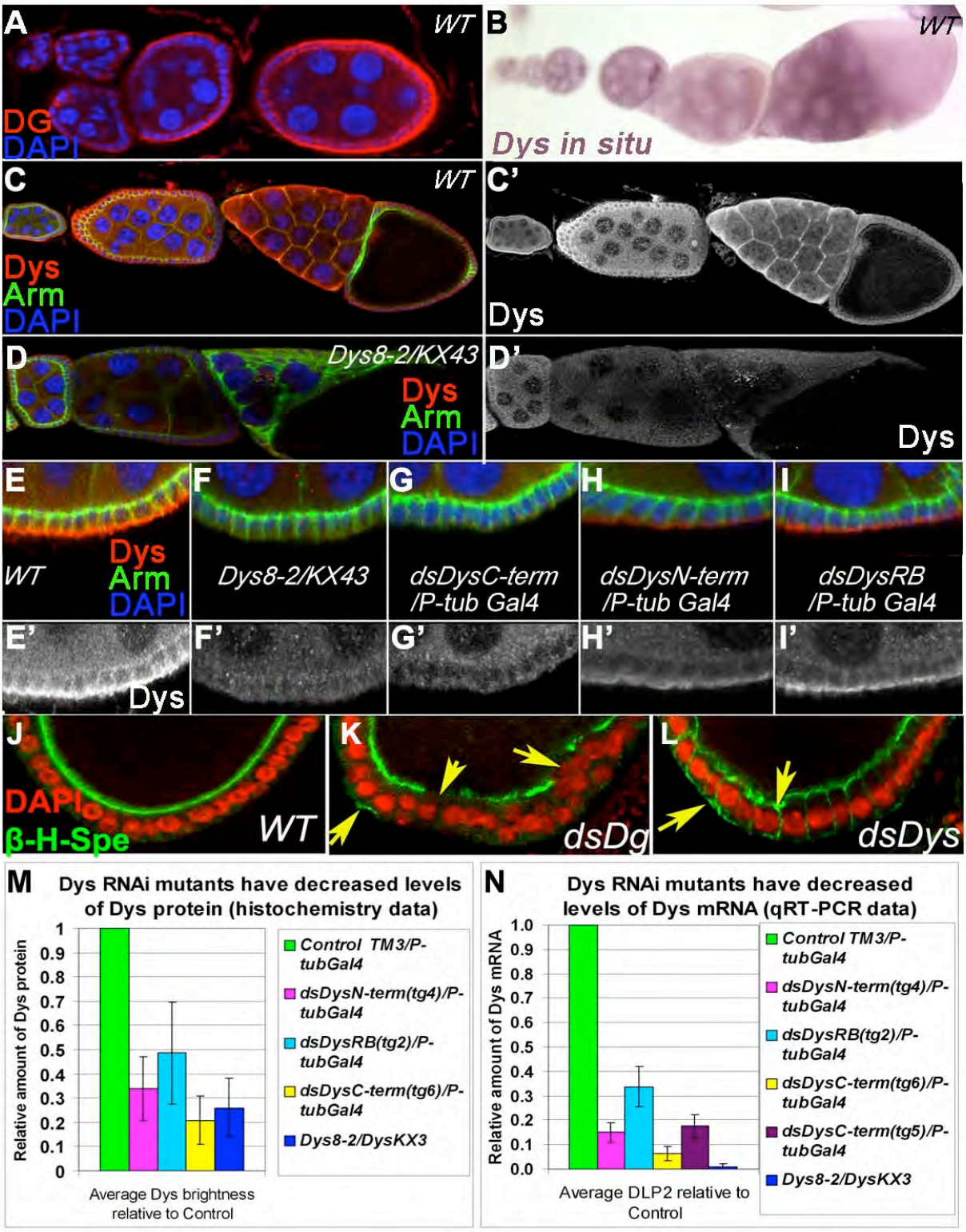

Supplementary Figure 3

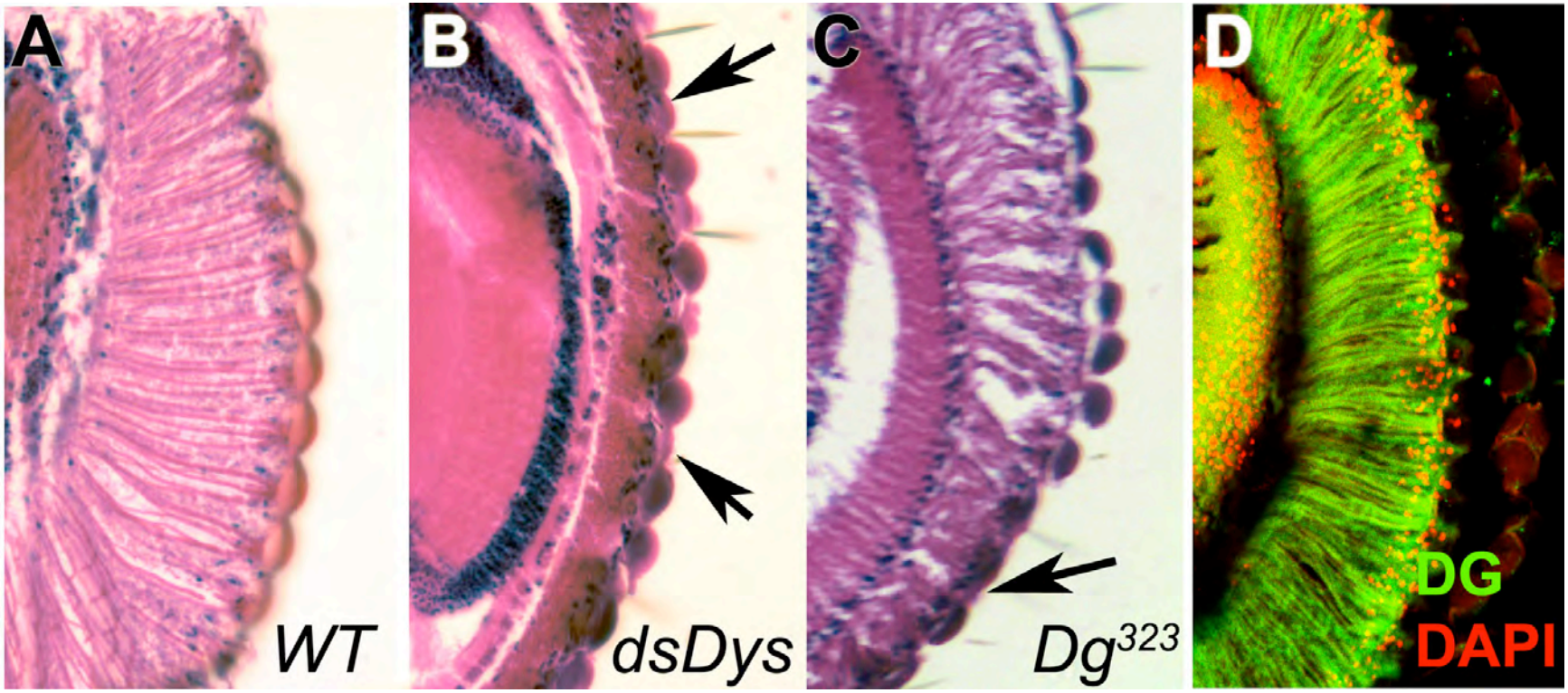

Supplementary Figure 4

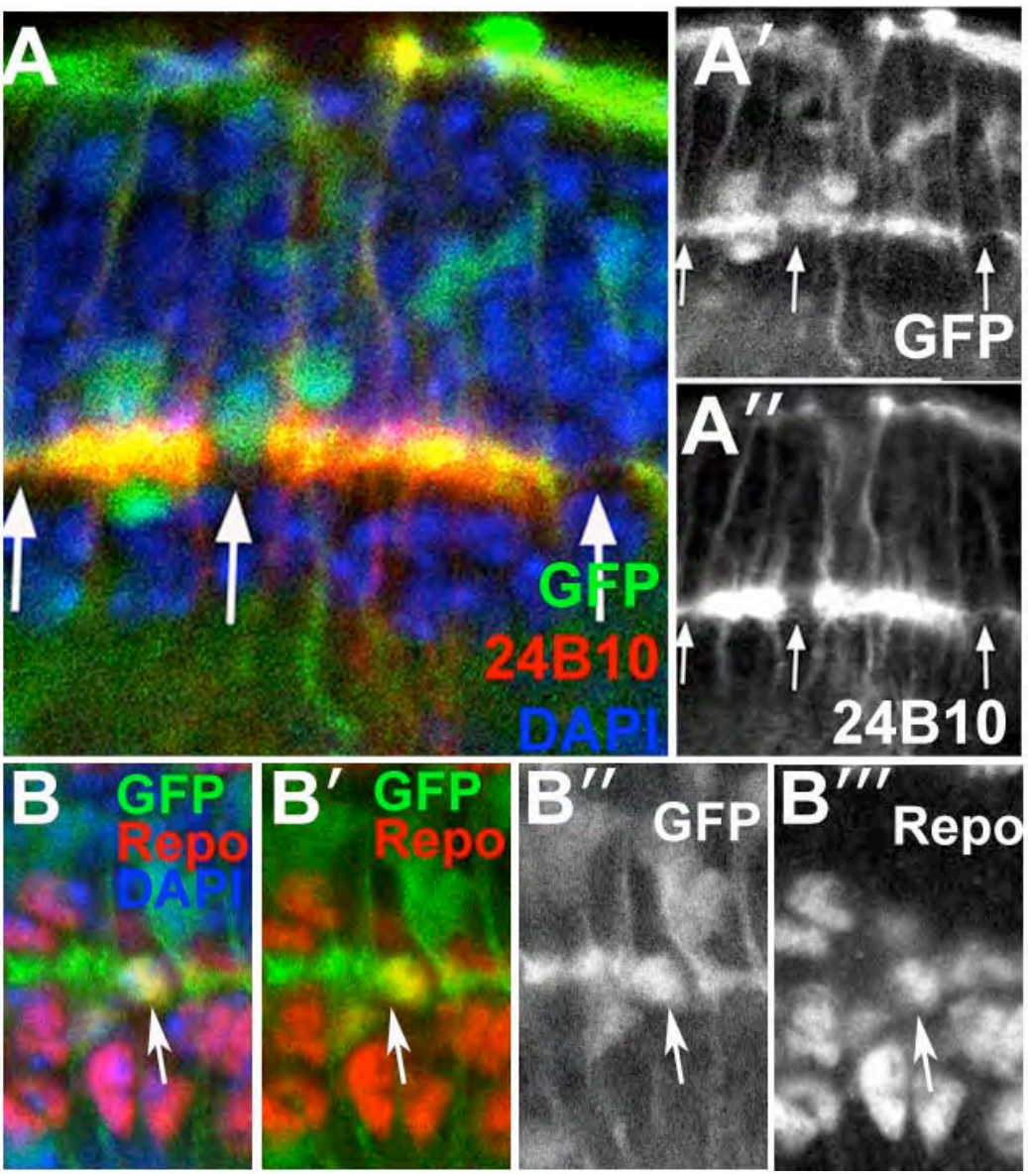

Supplementary Figure 5

Developmental Biology 352 (2011) 228–242

Contents lists available at ScienceDirect

Developmental Biology

journal homepage: www.elsevier.com/developmentalbiology

Stress and muscular dystrophy: A genetic screen for Dystroglycan and Dystrophin interactors in *Drosophila* identifies cellular stress response components

Mariya M. Kucherenko [a], April K. Marrone [a], Valentyna M. Rishko [a,b], Helena de Fatima Magliarelli [a], Halyna R. Shcherbata [a,*]

[a] Max Planck Institute for biophysical chemistry, Am Fassberg 11, 37077, Goettingen, Germany
[b] Ivan Franko National University of Lviv, Department of Genetics and Biotechnology, Hrushevsky 4, 75005, Ukraine

ARTICLE INFO

Article history:
Received for publication 12 August 2010
Revised 11 January 2011
Accepted 12 January 2011
Available online 21 January 2011

Keywords:
Muscular dystrophy
Stress
Drosophila
Dystrophin
Dystroglycan
Genetic screen

ABSTRACT

In Drosophila, like in humans, Dystrophin Glycoprotein Complex (DGC) deficiencies cause a life span shortening disease, associated with muscle dysfunction. We performed the first in vivo genetic interaction screen in ageing dystrophic muscles and identified genes that have not been shown before to have a role in the development of muscular dystrophy and interact with dystrophin and/or dystroglycan. Mutations in many of the found interacting genes cause age-dependent morphological and heat-induced physiological defects in muscles, suggesting their importance in the tissue. Majority of them is phylogenetically conserved and implicated in human disorders, mainly tumors and myopathies. Functionally they can be divided into three main categories: proteins involved in communication between muscle and neuron, and interestingly, in mechanical and cellular stress response pathways. Our data show that stress induces muscle degeneration and accelerates age-dependent muscular dystrophy. Dystrophic muscles are already compromised; and as a consequence they are less adaptive and more sensitive to energetic stress and to changes in the ambient temperature. However, only dystroglycan, but not dystrophin deficiency causes extreme myodegeneration induced by energetic stress suggesting that dystroglycan might be a component of the low-energy pathway and act as a transducer of energetic stress in normal and dystrophic muscles.

Introduction

Stress accelerates ageing and worsens pre-existing health conditions. Different tissues in the organism respond to unfavorable conditions via various mechanisms and have different thresholds of how much stress they can resist before damage becomes irreversible. Muscles are highly sensitive as well as quite resilient to stress and the signaling pathways involved in adaptive responses in normal muscles are comprehensively described (Palomero and Jackson, 2010). Normally muscles can withstand numerous rough situations induced by mechanical stress; however, dystrophic muscle cells that are present in Muscular Dystrophy (MD) patients are easily damaged and do not properly regenerate causing muscle tissue loss. Not only mechanical stress, but also other environmental stresses may affect muscle tissue welfare. It is not clear whether dystrophic cells just have an unstable membrane that is breaking upon stress or the signaling pathways that are required for proper cell homeostasis are disrupted causing necrotic processes to overtake the normal muscle regeneration.

Muscle degeneration is a hallmark of Muscular Dystrophies, a group of genetically inherited fatal diseases that are characterized by concomitant loss of muscular strength that ultimately leads to skeletal muscle deterioration and cardiac and/or respiratory failure (Batchelor and Winder, 2006; Durbeej and Campbell, 2002; Ervasti, 2003). MDs are mostly related to deficiencies in the Dystrophin Glycoprotein Complex (DGC), a membrane-associated multiprotein complex classically consisting of dystrophin, the dystroglycans (α and β), the sarcoglycans (α, β, γ and δ), sarcospan, the syntrophins (α1, β1, β2, γ1-, γ2) and α-dystrobrevin (Durbeej and Campbell, 2002).

In vertebrates the main component of the complex, Dystrophin (Dys) is expressed in skeletal and cardiac muscles and brain and consists of four structural domains, the N-terminal actin-binding domain, the spectrin-like rod domain, the cystein-rich domain, and the C-terminus with the Dystroglycan (Dg) interacting WW domain. Dg is the transmembrane anchor of the complex; it binds to the extracellular matrix (ECM) component laminin-2 at its N-terminal end and to the cytoskeleton via Dystrophin at its C-terminal end, providing a crucial link between the extracellular matrix and cytoskeletal network (Davies and Nowak, 2006).

In muscles the DGC is best envisioned as a mechanosignaling unit that has a dual role in muscle membrane stabilization: mechanical via anchoring the ECM to the cytoskeleton and non-mechanical as a signal-transducing module involved in cross talk between the internal and external environments of the muscle cell. The binding between the two main components of the DGC, Dg and Dys is mediated by the

* Corresponding author.
E-mail address: halyna.shcherbata@mpibpc.mpg.de (H.R. Shcherbata).

0012-1606/$ – see front matter © 2011 Elsevier Inc. All rights reserved.
doi:10.1016/j.ydbio.2011.01.013

proline-rich motif of the Dg cytoplasmic tail and the WW domain of Dys, and the phosphorylation of Dg might act as a molecular switch between WW or SH3, and SH2 domains during cellular adhesion in the process of out–in signaling (Moore and Winder, 2010; Yatsenko et al., 2009). When Dg interaction with laminin is prevented, apoptosis is activated and the pro-cell survival signaling, PI3K/AKT is inhibited (Langenbach and Rando, 2002). Dg is also thought to modulate the MEK/ERK pathway and *c-jun* activity (Spence et al., 2004; Zhou et al., 2007) and recently it has been found in the nucleus of different cells, suggesting unknown nuclear functions (Fuentes-Mera et al., 2006).

The DGC helps muscles to withstand the rigors of contraction (cellular deformation and shortening) that requires the specific activity of both the nervous and somatic systems, from excitation of myofibers at the neuromuscular junction (NMJ) to the ATP-regulated power-stroke of myosin. The myofiber contractile machinery must remain intimately connected with the sarcolemma and the basement membrane of the ECM, upon which muscles depend for survival and function. This interaction is arbitrated primarily by the DGC complex and integrin receptors. α7 integrin is a muscle-expressed integrin that, like Dg connects laminin to the cytoskeleton contributing to the overall integrity of the sarcolemma (Burkin et al., 2001; Cote et al., 2002). Interestingly, increased amounts of α7 integrin are found in DMD patients and *mdx* mice, indicating that enhanced α7 integrin expression is a mechanism by which muscle can compensate for the loss of dystrophin, additionally upregulation of integrin α7 in the mdx background can ameliorate some aspects of muscular dystrophy (Burkin et al., 2001; Cote et al., 2002; Liu et al., 2008). Facts that integrins can compensate in mediating cell-extracellular matrix attachment but cannot fully rescue the dystrophic phenotype suggest that the DGC has additional roles in muscles than just being a structural link between the cell cytoskeleton and laminin in the basal lamina.

The DGC also has become known as a scaffold responsible for the membrane localization of signaling proteins (Pilgram et al., 2010). For example, neuronal nitric oxide synthase (nNOS) signaling, which regulates many signaling pathways and is responsible for the direct regulation of a subset of myo-specific microRNAs, is coordinated by the DGC (Adams et al., 2008; Cacchiarelli et al., 2010). Recently various kinases, channels, and other enzymes have been shown to associate with the DGC, although only a few of these interactions have been confirmed *in vivo* (Adams et al., 2008; Pilgram et al., 2010).

Despite the vast data about the functional diversity of DGC components, the exact mechanism of how dystrophic muscle cells degenerate is still elusive. Muscle contraction induces mechanical stress leading to muscle injury; however, the specialized repair system is rapidly activated in healthy muscle, while in dystrophic muscles necrosis is triggered (Jaalouk and Lammerding, 2009). There are several potential pathogenic mechanisms implicated in the initiation of muscle decay associated with insufficiency of the DGC, including the mechanical fragility of the sarcolemma, high calcium influx, aberrant cytoskeleton rearrangements, increased energetic stress and abnormal metabolic control and inappropriate cell signalling (Constantin et al., 2006; Vercherat et al., 2009; Wallace and McNally, 2009).

To address the question on what mechanisms contribute to dystrophic muscle degeneration we used a previously established genetically tractable *Drosophila* MD model (Shcherbata et al., 2007). First we show that in *Drosophila,* similarly to human, *Dystrophin* and *Dystroglycan* are localized in striated muscles and required for muscle maintenance. Second, we carried out the first *in vivo* genetic screen in the musculature of adult flies exhibiting muscular dystrophy and found new genetic components that are involved in the DGC signaling and regulation. The novelty of this work is that modifiers that have been examined have not been implicated in prior works to have muscle function and/or interact with the DGC. Third, we established that many of these genes are required for muscle integrity and physiological response to heat-induced stress. Most of them have human homologues that have been associated with different disorders and potentially can be used as easier drug targets for muscular dystrophy treatment. Finally, we found that unfavorable factors such as high temperature and oxidative stress cause myodegeneration regardless of the genetic background; in addition, in dystrophic muscle the damage is significantly amplified in response to low temperature, energetic stress and ageing. This shows that the adaptive reactions in *Dys* and *Dg* mutants are somewhat different and suggests that the DGC is not only required for muscle homeostasis and plasticity, but also plays a role in stress-response pathways. *Dys* and *Dg* mutants had rather distinctive response to different stresses, which shows that they not only act together as components of one complex, but also might interact with different partners to ensure proper perpetuation of muscle functioning.

Materials and methods

Fly strains and genetic screen

To identify heterozygous genetic interaction in muscles, loss-of-function *DysDf*, Dg^{O86} (Christoforou et al., 2008) and Dg^{323} (Deng et al., 2003) mutant females were crossed to males carrying the mutation of interest. The progeny heterozygous for *Dys* or *Dg* and the screened allele were collected for muscle analysis. Heterozygotes, in which one allele of each recessive gene that function in unrelated pathways is mutant, would show no phenotype. However, if the genes act in the same pathway, then mutations in two steps should enhance each other and cause a phenotype. To identify dominant suppressors/enhancers of the muscle degeneration phenotype, virgin females $Dys^{N\text{-}RNAi}$:*act-Gal4* and Dg^{RNAi}:*tub-Gal4* (Kucherenko et al., 2008) that have 2.5 and 6 fold mRNA downregulation, respectively (Supplementary Tables 1, 2) were crossed to males carrying the screened mutation. Alleles used for the screen were obtained from DGRC and BDSC. All crosses were kept at 25 °C. Flies with the correct genotype were aged for three weeks at 25 °C and subsequently analyzed for muscle degeneration. The data were statistically compared using the χ^2 test and p was calculated based on the critical value.

Other alleles used in this study are: Dg^{O55} (Christoforou et al., 2008), $CG7845^{EMS\text{-}Mod4}$ (Kucherenko et al., 2008), $SP1070^{Uif\text{-}E(br)155}$ and $SP1070^{Uif\text{-}2B7}$ (Zhang and Ward, 2009), *tub-Gal4* and *MHC-Gal4* enhancer trap lines (BDRC), all RNAi lines are from VDRC. For control crosses either *OregonR* or w^{1118} flies were used.

Histology

For analysis of indirect flight muscle (IFM) morphology 10 μm paraffin-embedded sections were cut from fly thoraxes. In order to prepare *Drosophila* muscle sections, the fly bodies were immobilized in collars in the required orientation and fixed in Carnoy fixative solution (6:3:1 = Ethanol:Chloroform:Acetic acid) at 4 °C overnight. Tissue dehydration and embedding in paraffin were performed as described previously (Kucherenko et al., 2010). Histological sections were prepared using a Hyrax M25 (Zeiss) microtome and stained with hematoxylin and eosin (H&E) or aniline blue (0.12 %). All chemicals for these procedures were obtained from Sigma Aldrich. Muscle analysis was done using a light microscope (Zeiss). The frequency of muscle degeneration was quantified as a ratio of degenerated muscles to the total number of analyzed muscles. The analyzed IFM sections were located at a position 200–250 μm to the posterior of the fly thorax.

To prepare *Drosophila* muscle cryosections flies were located in collars and immediately frozen in TissueTek® O.C.T. (Sacura) at about −40 °C. Frozen muscles were sectioned on a cryo-microtom Leica CM3050S (between −15 and −18 °C) with a section thickness of 15 μm. Fixation was carried out in 4% formaldehyde (Polyscience, Inc.) for 10 min at room temperature.

Lipid droplets were detected with oil red O stain on cryosections (Kucherenko et al., 2010). After tissue fixation, slides were washed with water twice for 5 min, equilibrated in propylene glycol for 10 min and stained for 3 h in oil red O stain at room temperature. Samples were washed 2 times for 5 min in propylene glycol and 30 min in 1× PBS. Nuclei were visualized with DAPI. Samples were mounted in 30% glycerol in 1× PBS.

Immunohistochemistry

Immunostaining was performed according to the previously described procedures (Shcherbata et al., 2007). After immunostaining tissue was mounted onto slides in 70% glycerol, 3% NPG, 1xPBS and analysed using a confocal microscope (Leica TCS SP5). The following antibodies were used: rabbit anti-Dg (Deng et al., 2003) and anti-Dys (Schneider et al., 2006) 1:500, rat anti-Kettin (1:200; Babraham Institute), Alexa 568 goat anti-rabbit, Alexa 488 goat anti-rat (1:500, Molecular Probes). Nuclei were visualized with DAPI.

Analysis of muscle degeneration in response to stress

Temperature, sugar-free food (energetic stress), Paraquat-containing food (oxidative stress) and ageing were used as stress conditions. Flies age and incubation time on stress conditions for different experimental groups are shown in Supplementary Table 5.

Energetic stress

All flies were kept on a standard corn-molasses medium with yeast, agar, propionic acid and nipagin. For energetic stress experiments animals were transferred to plates containing sugar-free food (2.12% agar–agar in dH_2O with 0.2 ml of yeast paste). The control plates contained medium with 2.12% agar–agar and 2.5% sugar in an apple juice:dH_2O solution (1:3) and 0.2 ml of yeast paste (apple juice plates).

Temperature conditions

For temperature condition experiments wild type and mutant flies hatched at 25 °C, then incubated at 18 °C or 33 °C on apple juice plates. The control animals were left at 25 °C for the same period of time.

Oxidative stress

Paraquat (N,N′-dimethyl-4,4′-bipyridinium dichloride) in apple juice medium was used to catalyze the formation of superoxide radicals, a major form of reactive oxygen species (Bus and Gibson, 1984). Wild type and mutant flies were hatched in normal food at 25 °C conditions and transferred as adults to 2.5 mM Paraquat-containing medium. The control experiment used same age animals on apple juice plates.

Data analysis

The muscle degeneration was counted as the percentage of muscles with signs of degeneration from total muscle number. Experiments were repeated at least 2 times for each genotype and 50–200 muscles were scored in each experiment. The “extreme” muscle degeneration (EMD, cases where all the muscle was deteriorated or substituted with non-muscle tissue) was included in percentage of total muscle degeneration but was treated as a separate group in statistical analysis. For statistics the One-Way ANOVA with post Dunnett's tests (Version SPSS 16.0) were used. For analysis of wild type muscle response to stress conditions the data for genotypes (*OregonR* and w^{1118}) within each of “experimental conditions” group were compared to each other and after data were proven not to be different they were treated as an individual data set. Data from “25 °C and normal food” conditions group were used as control. For analysis of dystrophic muscles response to stress conditions the data for genotypes within each of “experimental conditions” group (*DysDf* and $Dg^{O86/DgO55}$) were compared to control (*OregonR*), and then each genotype from every “experimental conditions” group was compared to the respective genotype from control group (25 °C and normal food). Taking into account the age of animals used in analysis all experiments were divided into experimental groups, which were compared to different controls. In each evaluation the total muscle degeneration and EMD were compared separately.

Climbing assay

The climbing assay was performed and the climbing index was calculated as described previously (Shcherbata et al., 2007). The climbing test was performed 3 times using 20–30 7–10 day old animals each trial.

Temperature-sensitive activity

This method was adapted from Montana and Littleton (2004). Flies were placed into a preheated vial at a temperature of 39 ± 1 °C. Temperature-sensitive behavioral defects were scored in 30 s intervals. The analysis was done with at least 5 repetitions for each genotype and each repetition contained an independent set of 6–18 flies that were 2–5 days old. For the data analysis the mobility index, which equals the minus logarithm of the absolute value of the slope (the slope equals change in ordinate divided by change in abscises) was calculated. The mean value and standard error of 3–5 trials were calculated and the Student's one-tailed *t*-test was used.

RNA preparation and real-time PCR

To determine the effect of the *Dg RNAi* transgene on the *Dg* expression levels quantitative reverse transcription (RT-qPCR) was performed on total RNA derived from whole adult animals. RNAs were extracted from flies with the RNeasy Mini kit (Qiagen), followed by reverse transcription using the High Capacity cDNA Reverse Transcription kit (Applied Biosystems) following the manufacturer's protocols. Dg was tested with RpL32 as an endogenous control for q-PCR using Fast SYBR® Green master mix on a Step One Plus 96 well system (Applied Systems). The reactions were incubated at 95 °C for 10 min, followed by 40 cycles of 95 °C for 15 s and 54 °C for 30 s. All reactions were run in triplicate with appropriate blank controls. The threshold cycle (C_T) is defined as the fractional cycle number at which the fluorescence passes the fixed threshold. Primers were used as follows: RpL32 forward—AAGATGACCATCCGCCCAGC; RpL32 reverse—GTCGATACCCTTGGGCTTGC; Dg forward—ACTCAAGGACGAGAAGCCGC; Dg reverse—ATGGTGGTGGCACATAATCG; Dys forward—GTTGCAGACACTGACCGACG; Dys reverse—CGAGGGCTCTATGTTGGAGC. The ΔC_T value was determined by subtracting the average RpL32 C_T value from the average Dg C_T value. The $\Delta\Delta C_T$ value was calculated by subtracting the ΔC_T of the control sample (*tubGal4/+*) from the ΔC_T of the suspect sample (Dg^{RNAi}*:tubGal4/+*). The relative amount of mRNA was then determined using the expression $2^{-\Delta\Delta CT}$. Errors were determined starting with the standard deviation of the raw C_T values and performing appropriate regression analysis.

Metabolic rates

The production of CO_2 is correlated with oxygen consumption and reflects the metabolic rate. The respirometers were 1000 µl micropipette tips with a 50 µl capillary glued to the tip end. A piece of foam was placed into the pipette to keep flies from falling through to the end of the tip. Five flies were placed into the container and another piece of foam was fitted to the top portion of the tip. Soda lime, a CO_2 absorbent (Wako Chemicals, Japan) was added to the container and the top was sealed with parafilm and then dipped into liquid paraffin to seal the container. The containers were inserted tip down into a solution of eosin for color in a closed container at 25 °C and allowed to equilibrate for 15 min. The movement of the liquid up the capillary

was monitored over the next hour and the production of CO_2 was calculated per fly (on average 1 fly weighs 0.80 ± 0.11 mg ($n = 180$)). All flies were measured at the same time and a respirometer without flies was also measured to correct for variations in ambient temperature and pressure. Three to ten independent assays were performed for each genotype in each condition. The mean value and standard error of the replicates was calculated and the Student's *t*-test was performed to check for significant differences.

Homology prediction and interaction network

All homology predictions for candidate genes were made using NCBI BLAST (http://blast.ncbi.nlm.nih.gov/Blast.cgi) and STRING version 8.2 (www.string-db.org). The network for the DGC interactors was built by integrating obtained genetic interaction results to publically available interaction data. STRING version 8.2 (www.string-db.org) was used as the interaction data resource. The DGC-interacting members were classified into functional groups based on information obtained from FlyBase (http://flybase.org/) for *Drosophila* and the function of their orthologs. The association with disorders was identified using the GeneCard Human Gene Database version 3 (http://genecards.bioinformatics.nl).

Results

Like in vertebrates, Drosophila Dystroglycan and Dystrophin are expressed in adult muscles and their deficiencies cause age-dependent muscle degeneration

Adult *Drosophila* multi-fiber muscles structurally resemble the vertebrate striated muscles with a highly conserved basic patterning consisting of actin (Z-band) and myosin (M-band) containing myofibrils (Miller, 1950). We analyzed the tissue specific expression of Dys and Dg in several types of these multinucleated muscle cells: indirect flight muscles (IFM, Figs. 1A–H), leg (Figs. 1I–L), ovarian, gut and heart muscles (Supplementary Fig. 1). Consistent with Dg being a transmembrane protein, in *Drosophila* it is localized in the muscle sarcolemma (Figs. 1A, E, I, Supplementary Fig. 1). A punctate staining is seen in the regions that coincide with Z-bands, which resemble costameric regions of myofibril connections in vertebrates (Supplementary Figs. S1G, O, T). The presence of Dg in these bands suggests that it might connect *Drosophila* myofibrils to the extracellular matrix. In *Dg* loss-of-function mutant Dg^{O55}/Dg^{O86}, Dystroglycan staining is diminished (Figs. 1C, G, K, Supplementary Fig. 1). Dys is a cytoplasmic protein that connects to Dg via its N-terminus and to cortical actin via its C-terminal end. In *Drosophila*, the Dys protein is present in the muscle cytoplasm, and transverse sections show that Dys is enriched in close proximity to the sarcolemma where Dg is located (Figs. 1B, F, J, Supplementary Fig. 1). Dystrophin staining is no longer detected in *DysDf* loss-of-function mutant (Figs. 1D, H, L, Supplementary Fig. 1). These data show the similarity of Dys and Dg localization in *Drosophila* and invertebrate adult muscles (Cote et al., 2002; Ervasti, 2003) implying that in different species these proteins may have analogous roles.

Previously it has been shown that the *Dys* hypomorph and *Dys* and *Dg RNAi* mutants exhibit age-dependant muscle weakening and loss, climbing defects and reduced lifespan (Shcherbata et al., 2007; Taghli-Lamallem et al., 2008), now we confirmed the appearance of age-dependent MD in *Dg* and *Dys* loss-of-function mutants (Supplementary Fig. 2). *Dystrophin* mutants showed plenty of mildly degenerated muscles, while the extreme muscle degeneration phenotype was frequently seen in *Dys* and *Dg* old mutant flies (Supplementary Fig. 2). Mostly, myofibrils on the periphery of the muscle were extensively damaged (Supplementary Fig. 2H), the more central parts appeared to

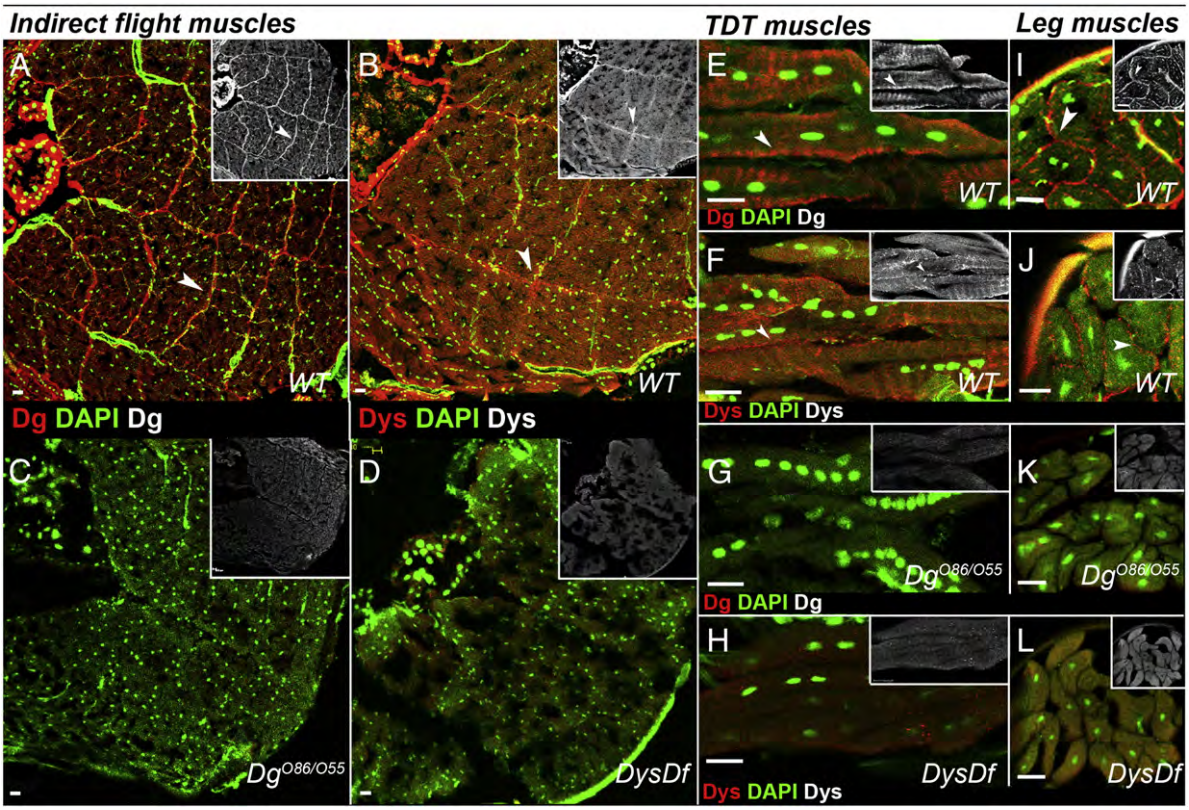

Fig. 1. *Drosophila* DCG is localized to the sarcolemma. Transverse sections of *Drosophila* IFM and leg muscles and longitudinal sections of trochanter (TDT) muscles stained with anti-Dg (A, E, I) and anti-Dys antibodies (B, F, J) (Dg, Dys—red and in separate channel, DAPI—green). Dystroglycan is localized to the muscle membrane and Dystrophin staining is seen in the cytoplasm with significant enrichment close to the membrane (indicated by arrowheads). Antibody staining is no longer seen in *Dg* (C, G, K) and *Dys* (D, H, L) mutant muscles.

be less vulnerable. Since distal myofibrils are subjected to greater levels of mechanical stress and one function of the DGC is to provide mechanical reinforcement to the sarcolemma, loss of Dys and Dg compromises sarcolemma integrity causing focal muscle deterioration. The healthy muscle cell actively regulates its metabolism, determined by substrate availability and energetic requirements. However, when muscle cell performance is jeopardized, metabolism regulation is disabled resulting in replacement of muscle by fatty and fibrous tissue. Since the prime source of energy during muscle contraction is fatty acids, we tested if *Dys* and *Dg* deficiencies lead to improper consumption of fat. We detected lipid droplets in *Dys* and *Dg* deficient muscles; however the amounts of intramuscular fat were not obviously different in control and mutant muscles (Supplementary Figs. 2L–M). Also they contained no extra quantities of collagen visualized by aniline blue staining (data not shown), instead, zones of abnormal muscle tissue showed signs of necrosis marked by pale H&E staining (Supplementary Fig. 2I).

Genetic modifier screen for components that interact with Dys and Dg in muscles

The *Drosophila* MD model provides a unique possibility to screen for DGC interactors that are not necessarily biochemically linked but act transiently by testing for a trans-heterozygous interaction. Previously performed large-scale primary screens identified modulators of a wing-vein phenotype in *Dys* and *Dg* mutants (Kucherenko et al., 2008). Now we carried out the secondary screen to analyze if these modulators would specifically modify Dys/Dg age-dependent muscular dystrophy.

When *Dys* and *Dg* are reduced by one copy (*DysDf/+*, $Dg^{323}/+$ and $Dg^{O86}/+$), no obvious changes in muscle morphology are observed (Supplementary Table 3, Figs. 2A–B, F–G), therefore these mutants were used to identify trans-heterozygous interactions. Importantly, *Dys*/*Dg* trans-heterozygotes showed a genetic interaction, the occurrence of degenerated muscles significantly increased ($DysDf/Dg^{O55}$ 17.7%, n = 69, $DysDf/Dg^{O86}$ 19%, n = 97, $DysDf/Dg^{323}$ 18%, n = 44, Figs. 2A–B, F, Supplementary Figs. 2H, J). Flies lacking one copy of the gene-candidate in the *Dys* and/or *Dg* heterozygous background were aged for three weeks and the frequency of degenerated muscles was quantified (Figs. 2A–B, F, H–J, Supplementary Tables 3 and 4). In addition, $Dys^{N\text{-}RNAi}$*:act-Gal4* and Dg^{RNAi}*:tub-Gal4* mutants showed a moderate muscle degeneration (Figs. 2C–D, Supplementary Table 3), which made them suitable for identifying dominant suppressors or enhancers (Figs. 2C–D, K–L, Supplementary Table 3). To confirm or disprove found interactions we used multiple alleles of the same gene; to avoid an additive effect control crosses to the w^{1118} line were made (Fig. 2E, Supplementary Tables 3 and 4). Some differences were noticed when different alleles were analyzed due to the diverse nature of mutations that can cause possible incongruent effects on protein structure and function, in turn causing a different pattern of interaction. In total we found 16 modifiers of *Dys* and/or *Dg*-dependent muscle degeneration (Supplementary Table 3) that have been sorted into five groups: (1) signal transduction and/or (2) cytoskeleton organization, (3) regulation of gene expression, (4) metabolism, and (5) genes with unknown function (Fig. 3A). Most interestingly many genes from these different groups could be labeled as the stress response genes that control cell adaptation to mechanical and cellular stress and factors involved in neuro-muscle communications (Fig. 3B).

We identified *Cam (Calmodulin), capt (capulet)* and *Lis-1 (Lissencephaly-1)* as Dys-interacting components (Fig. 3A). Reduction of *Cam* and *capt* by one copy showed heterozygous interaction with *DysDf* and $Dys^{N\text{-}RNAi}$*:act-Gal4* resulting in an increased frequency of muscle degeneration. Reduction of *Lis-1* also led to a heterozygous interaction with *DysDf* (~10–27%), and increased the Dg^{O86} phenotype, but since *Lis-1* heterozygotes also show some muscle degeneration, the *Dg*/*Lis-1* phenotype (~5–8%) was considered as additive (Fig. 2B, Supplementary Table 3).

Fkbp13, Pgk (Phosphoglycerate kinase), SP2353 and *vimar (visceral mesoderm armadillo repeats)* mutants showed strong interaction as trans-heterozygotes with *Dg*, but not *Dys* and were considered as Dg interacting components, *vimar* also strongly enhances the Dg^{RNAi}*:tub-Gal4* muscle degeneration phenotype (Fig. 2D, Supplementary Table 3).

Nine other DGC modifiers, *Nrk (Neuronal receptor kinase), Fhos, ßν-Integrin, robo (roundabout), chif (chiffon), mbl (muscleblind), Rack1 (Receptor of activated protein kinase C 1), CG7845* and *CG34400* interacted with both *Dys* and *Dg*. They increased the frequency of muscle degeneration of *Dys* and *Dg* loss-of-function heterozygous mutants and, mostly, enhanced *Dys* and *Dg RNAi* phenotypes (Fig. 3A, Supplementary Table 3). Intriguingly, reduction of *robo* by one copy suppresses muscle degeneration in $Dys^{N\text{-}RNAi}$*:act-Gal4* and Dg^{RNAi}*:tub-Gal4* mutants (Figs. 2C–D, Table S2). It has been shown that *D. melanogaster* cardiac lumen formation is dependent on interactions between the Slit/Robo pathway and Dg (Medioni et al., 2008) and the loss of Dys leads to an age-dependent disruption of the myocardium myofibrillar organization and alterations in cardiac performance (Taghli-Lamallem et al., 2008). Further studies of the DGC and Slit/Robo interactions are valuable since muscular dystrophies in humans cause progressive cardiomyocyte degeneration and fibrosis.

Since many genes that showed interaction with the DGC are not well characterized, we first examined if they are evolutionarily conserved and have homologs implicated in human diseases. Computational analysis of protein identity showed that all of the found genes have vertebrate homologs and many of them have a high degree of protein similarity and identity (Fig. 3C, Table 1). Data analysis showed that most of the vertebrate homologs could be classified by their association with two disorders: muscular dystrophies and/or tumors (Table 1). These findings are interesting due to the fact that the DGC is implicated not only in MD development, but also Dg is downregulated in a wide variety of tumors, with low levels of expression correlating with a poor prognosis (Muschler et al., 2002). Most tumor cells, like muscles, require a large amount of glucose and are likely to be subjected to energetic stress. Logically, both proteins involved in metabolic processes, Pgk and Vimar showed interactions with Dg only, suggesting that the low-energy pathway may play a role in tumor progression and muscle maintenance via Dg. This evidence provides good reason to study in more detail the effect of energy metabolism on dystrophic muscles.

Novel genes found in the DGC modifier screen have specific roles in muscle function

Next, we tested if mutations in found genes would affect muscle maintenance (Fig. 3, Table 1). Two of the genes found to interact with Dys, *Cam* and *capt* did not show considerable muscle degeneration when downregulated via *RNAi* driven by *tub-Gal4*, suggesting that both proteins may affect muscle only via Dys. Mutations in another Dys interactor *Lis-1*, both DGC-interacting genes that regulate gene expression: *mbl* and *chif*, a formin homology protein *Fhos*, and a transmembrane protein *CG34400* showed a significant frequency of defects in ageing muscles (Table 1, Figs. 4A, D–F). Consistent with the *Nrk* gene being expressed specifically in the nervous system (Oishi et al., 1997), downregulation of *Nrk* in motor neurons, but not in muscles, affected muscle maintenance (Table 1, Figs. 4A, G). The DGC-interacting mutants with unknown function: *CG7845, vimar, SP2353, Fkbp13* and non-DGC-interacting mutants: *nAcRalpha* and *SP1070* also showed significant muscle deterioration (Table 1, Figs. 3A, H–N).

Since it has been shown that high temperature stress causes behavioral dysfunction and noticeably exaggerates muscle electrical responses (Benshalom and Dagan, 1981; Montana and Littleton, 2004), we also tested if dystrophic muscle function is affected by heating flies (~39 °C) and calculated their mobility index. The high temperature induced mobility defects seen with *Dys* mutants are much more severe than those seen with *Dg* mutants, nonetheless both

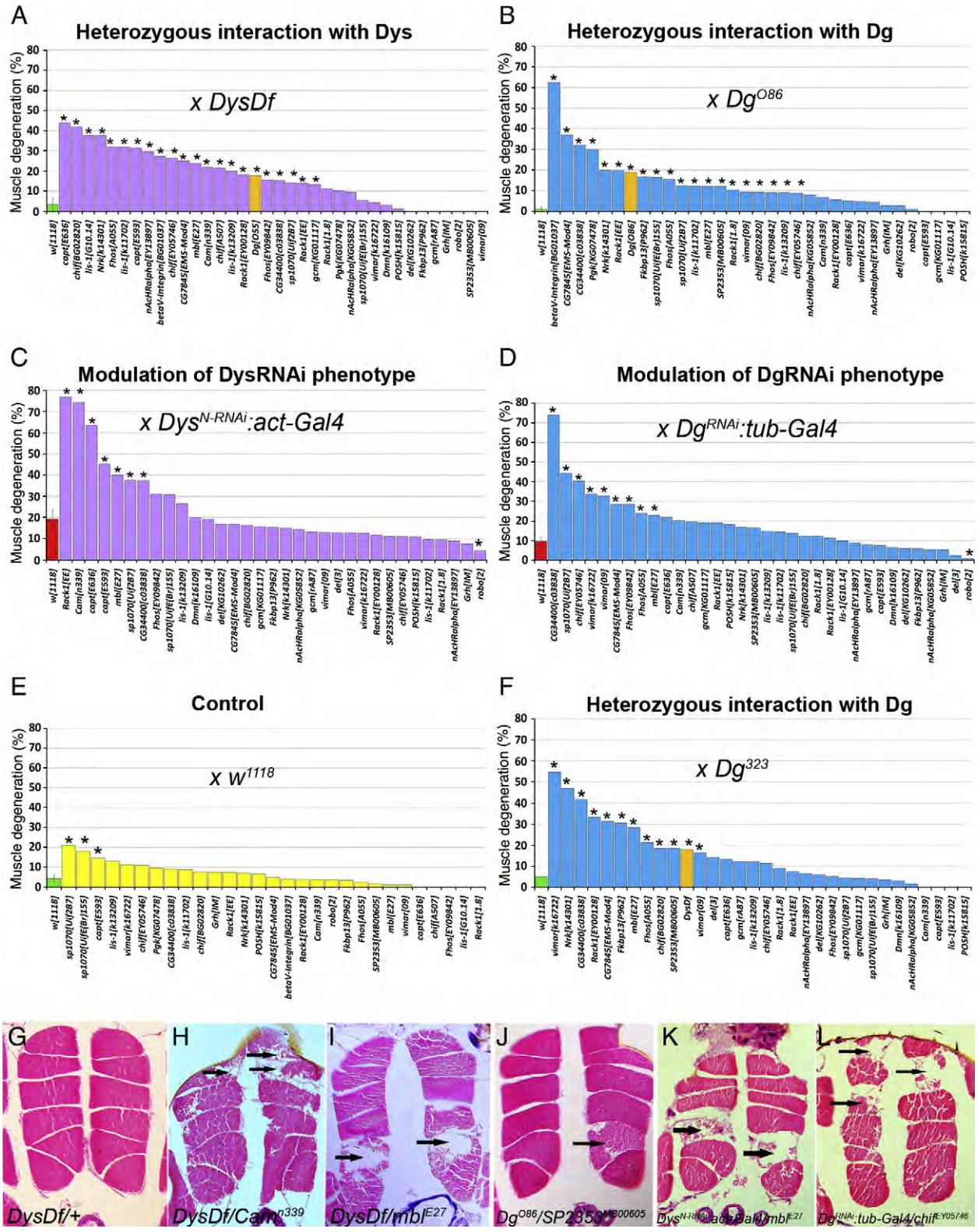

Fig. 2. In the genetic screen for components that genetically interact with *Dys* and *Dg* in muscle maintenance the frequency of muscle degeneration resulting from heterozygous interaction between *DysDf* (A), Dg^{O86} (B), Dg^{323} (F) and screened alleles was measured. (C, D) Modulation of $Dys^{N\text{-}RNAi}$*:act-Gal4* and Dg^{RNAi}*:tub-Gal4* muscle degeneration phenotype by one copy reduction of screened components. (E) The frequency of muscle degeneration phenotype by one copy reduction of screened components. Statistics were done using the χ^2-test with one degree of freedom and Yates's correction. Asterisks indicate statistically significant ($p \leq 0.05$) heterozygous interactions (A, B, F), enhancement or suppression of *Dys* and *Dg* RNAi phenotype (C, D), and dominant muscle degeneration phenotype in screened alleles (C). (H–L) Exemplary IFMs showing muscle degeneration from 3 weeks old animals lacking Dys or Dg and one copy of screened alleles in comparison to *DysDf/+* flies (G).

had a lower mobility index than wild type (Fig. 4B). In addition, under high temperature stress the majority of the screened mutants also have significantly reduced mobility indices (Table 1, Fig. 3B), suggesting their possible involvement in muscle stress responsive pathways. Since many of these genes have not been studied previously in *Drosophila*, further experiments are planned.

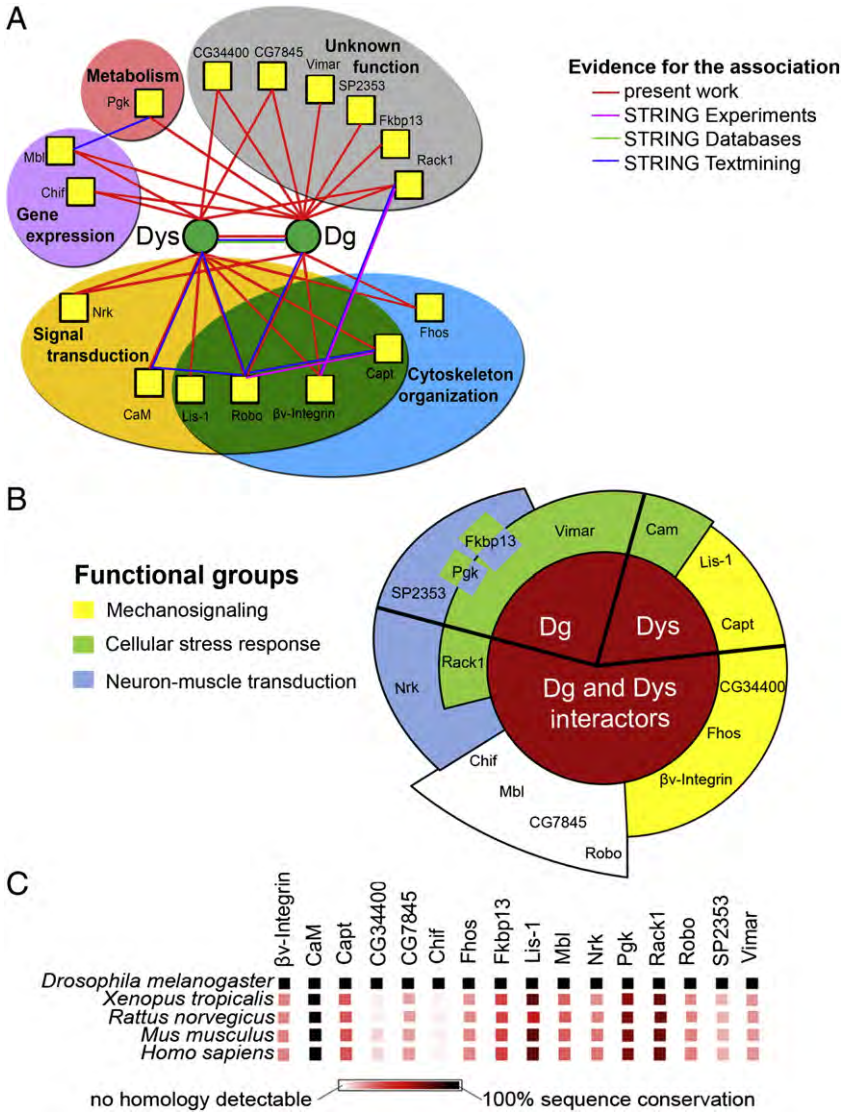

Fig. 3. DGC-interacting components. (A) An interaction network for the DGC. Proteins are shown as nodes and the relationship as edges (edge color indicates evidence for interaction). (B) Proportion of interacting factors divided into functional groups. (C) Homology of DGC-interacting components with vertebrates.

Drosophila muscles are susceptible to stress

Many genes found in our muscle screen have been shown previously to be involved in cellular adaptive responses. For example, *βν-integrin*, *Fhos*, *capt* and *CG34400* encode for proteins that bind to actin and control muscle cell cytoskeleton rearrangement in response to mechanical stress (Boehm et al., 2005; Gasteier et al., 2005; Mburu et al., 2003; Medina et al., 2008; Perkins et al., 2010). Mechanical stress is translated by the cell into biochemical signals such as changes in intracellular calcium levels leading to activation of diverse signaling pathways. Additionally, levels of Ca^{2+} can be regulated by Cam and FKBP13 and abnormal Ca^{2+} homeostasis leads to oxidative stress (Bellinger et al., 2009; Chakkalakal et al., 2006). The DGC interactors, Pgk and Vimar have been implicated in cellular homeostasis, and Rack1 modulates response to energetic stress (Qiu et al., 2010).

Since muscle is a highly sensitive tissue that responds to environmental stresses in its pattern of metabolic activity and tissue integrity, we decided to test first how *Drosophila* normal muscles respond to stress: suboptimal ambient temperatures, oxidative and energetic deficiency stress.

To begin with we evaluated the frequency of muscle degeneration in two control laboratory lines (*OregonR* and w^{1118}) kept at different temperatures. Muscle maintenance was not affected in flies residing at 18 °C and 25 °C and any significant difference was detected between these two groups. However, staying at higher temperature (33 °C) led to muscle maintenance defects. Not only was the frequency of muscle degeneration significantly increased (~4 times in comparison to 18 °C and 25 °C, Figs. 5A–D, Supplementary Table 5), extreme muscle degeneration was also observed (Fig. 5A, black bars).

It has been shown that hyperthermia-induced muscle degeneration is linked with oxidative stress (Mujahid et al., 2005). There is also increasing evidence that oxidative stress, due to reactive oxygen species (ROS) production overpowering the intracellular antioxidant systems, causes muscle wasting both during ageing and in chronic pathological states (Vercherat et al., 2009). Therefore we next attempted to amplify oxidative stress by culturing flies on food containing Paraquat, a superoxide radical generating agent. The occurrence of degenerated muscles was significantly higher than under normal conditions including extreme muscle degeneration (Figs. 5A, E–F, Supplementary Table 5).

Unexpectedly, in flies the frequency of abnormally maintained muscles did not increase with age, implying that healthy muscles did not show any dependence on animal's age (Fig. 5A, Supplementary Table 5).

Table 1
Components implicated in muscle maintenance.

Drosophila protein	Vertebrate homologs						*Drosophila* mutants					
							Muscle degeneration in 3 weeks old animals			Temperature-sensitive mobility defects in 1–5 day old animals		
	Human homolog	Identity, %	Positive, %	Gaps, %	Function	Involvement in disorders	Genotype	% [a]	n	Allele/+	Index [b]	n
Control	–	–	–	–	–	–	*Oregon R* *tub-Gal4/+* *MHC-Gal4/+* *D42-Gal4/+*	3.0 ± 3.0 0.8 2.4 4.0	n = 98 n = 81 n = 42 n = 97	*Oregon R*	1.00 ± 0.14	n = 118
βv-Integrin	ITGB5	31	48	7	Cell adhesion, signaling	Muscular dystrophy, cardiomyopathy, cancer	$βv\text{-}Integrin^{BG01037}$	0.0	n = 104	$βv\text{-}Integrin^{BG01037}$	0.68 ± 0.29	n = 65
Cam	CAM2	97	98	0	Ca^{2+} -dependant pathways regulation, interaction with DGC components	Enhances muscular dystrophy in mice	Cam^{RNAi}; *tub-Gal4*	7.8	n = 129	Cam^{n339}	1.31 ± 0.21	n = 46
capt	CAP1 CAP2	49 48	66 64	4 4	Actin polymerization, signaling, cell polarity, cell motility, CAP2 found in developing striated muscles	Cancer, metastasis	$capt^{RNAi}$; *tub-Gal4*	4.8	n = 84	$capt^{E636}$	0.86 ± 0.21	n = 42
CG34400	DFNB31	36	56	18	Actin cytoskeleton organization	Deafness	$CG34400^{c07121/c05107}$	32.0**	n = 50	$CG34400^{c05107}$	0.74 ± 0.52	n = 106
CG7845	WDR74	31	50	4	Unknown	Unknown	$CG34400^{RNAi}$; *tub-Gal4* $CG7845^{RNAi}$; *MHC-Gal4*	23.1** 20.0**	n = 65 n = 70	$CG7845^{EMS\text{-}Mod4}$	0.65 ± 0.10*	n = 61
chif	DBF4	25	42	23	Regulatory subunit of Cdc 7 kinase, DNA replication, cell cycle, integrin signaling	Cancer	$chif^{EY05746/A507}$ $chif^{EY05746/BG02820}$ $chif^{BG02820/A507}$	31.8** 22.6** 18.3**	n = 157 n = 53 n = 104	$chif^{BG02820}$	0.51 ± 0.03**	n = 41
Fhos	FHOD3	46	61	10	Actin polymerization, MTs organization, signaling, muscle function regulation	Unknown	$Fhos^{A055}$ $Fhos^{EY09842}$ $Fhos^{A055/EY09842}$	46.7** 17.1** 24.3**	n = 30 n = 117 n = 140	$Fhos^{A055}$	0.56 ± 0.04**	n = 57
Fkbp13	FKBP14	44	64	4	Unknown	Unknown	$Fkbp13^{RNAi}$; *tub-Gal4*	26.0**	n = 58	$Fkbp13^{P962}$	0.96 ± 0.12	n = 57
Lis-1	LIS1	70	87	0	Actin polymerization, dynein binding, cellular macromolecule localization, microtubule-based movement	Lissencephaly	$Lis\text{-}1^{RNAi}$; *MHC-Gal4*	34.0**	n = 94	NA	–	–
mbl	MBNL1	43	54	12	Regulation of splicing, muscle differentiation, recruitment of integrin to focal adhesions	Myotonic dystrophy	mbl^{RNAi}; *MHC-Gal4*	12.0*	n = 109	mbl^{E27}	0.57 ± 0.04**	n = 50
nAcRalph a-30D	CHRNA7	–	–	–	Acetylcholine receptor, Ca^{2+} transport, activation of MAPK	Schizophrenia, cognitive defects	$nAcR\alpha\text{-}30D^{EY13897}$ $nAcR\alpha\text{-}30D^{EY13897/KG05852}$	27.3** 16.1**	n = 44 n = 62	NA	–	–
Nrk	MUSK	60	75	5	Receptor for Agrin, MAPK signaling, transcription, protein phosphorylation, muscle development, function in NMJs	Congenital myasthenic syndrome	Nrk^{RNAi}; *MHC-Gal4* Nrk^{RNAi}; *D42-Gal4*	3.0 27.0**	n = 150 n = 18	Nrk^{k14302}	0.57 ± 0.04**	n = 51
Pgk	PGK1 PGK2	70 68	82 83	0 0	Glycolytic enzyme, electron carrier activity, transferase activity, functions in glycolysis, function in NMJs	Mental retardation, Menkes disease	Pgk^{RNAi}; *MHC-Gal4*	8.6	n = 85	$Pgk^{KG07478}$	1.23 ± 0.76	n = 52
Rack1	RACK1	77	87	0	Signaling	Cancer	$Rack1^{RNAi}$; *MHC-Gal4*	4.4	n = 90	$Rack1^{EY00128}$	0.66 ± 0.05*	n = 58
robo	ROBO2	38	55	4	Cytoskeleton rearrangement, axon guidance receptor, ureteric bud development	Multiple congenital abnormalities, vesicoureteral reflux	$robo^{RNAi}$; *tub-Gal4*	10.3	n = 58	$robo^{2}$	0.61 ± 0.06*	n = 40
SP1070	NOTCH1	38	51	7	Cell fate specification, aortic valve specification	Aortic valve disease	$SP1070^{Uif[E(br)155}/+$ $SP1070^{Uif2B7}/+$	18.1** 21.1**	n = 105 n = 90	NA	–	–
SP2353	AGRNL AGRN	32	49	5	Dg ligand, photoreceptor ribbon synapse formation	Congenital muscular dystrophy (AGRN)	$SP2353^{RNAi}$; *tub-Gal4* $SP2353^{f01290/c05961}$	19.0** 30.7**	n = 21 n = 179	$SP2353^{MB00605}$	0.67 ± 0.05*	n = 37
vimar	RAP1	30	50	10	GTP–GDP dissociation stimulator , regulation of mitochondrial function	Cancer	$vimar^{RNAi}$; *MHC-Gal4*	81.0**	n = 32	$vimar^{EY09646}$	0.48 ± 0.01**	n = 37

[a] Muscle degeneration frequency results were statistically compared using χ^2 test with one degree of freedom and Yates's correction.

[b] Relative mobility results were statistically compared using t –test, *$p \leq 0.05$; **$p \leq 0.01$.

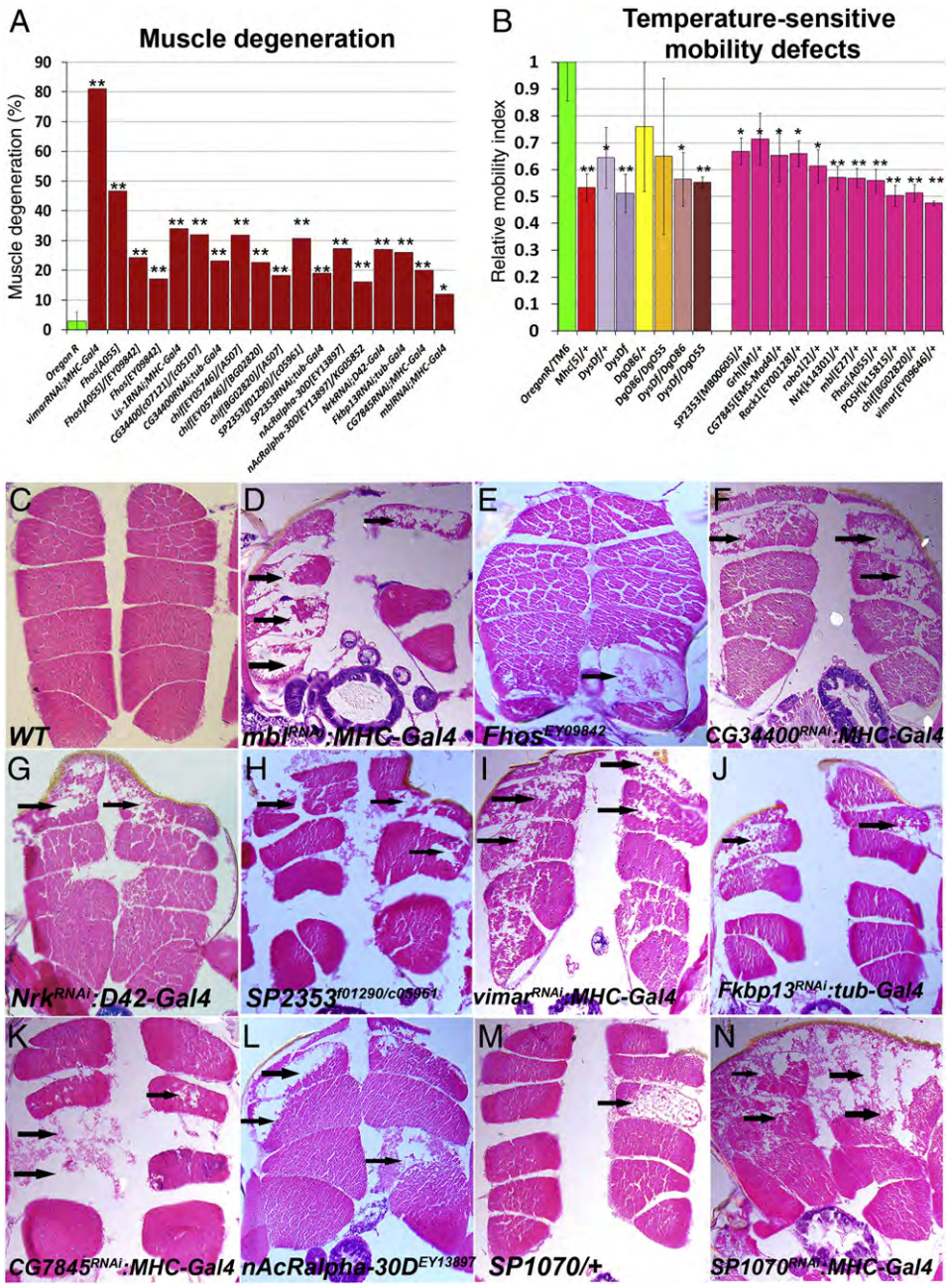

Fig. 4. Mutations in DGC modifiers result in muscle phenotypes. (A) Frequency of muscle degeneration in 3 week old mutant animals. Statistics were done using the χ^2-test with one degree of freedom and Yates`s correction. (B) Mutants exhibit dominant temperature-sensitive mobility defects. Statistics were done using the *t*-test. $^{*}p \leq 0.05$; $^{**}p \leq 0.01$. (C–N) H&E-stained paraffin sections of exemplary IFMs, arrows indicate muscle degeneration.

Interestingly, sugar deprivation also had no effect on muscle welfare (Fig. 5A, Supplementary Table 5). Normally when flies are glucose-deprived, they adapt by changing their metabolism from glycolysis and glycogenolysis to lipolysis, which results in lower CO_2 production. Control flies lower their metabolic rate approximately 5 times as a reaction to change in food conditions measured here by the amount of produced CO_2 (Fig. 5G, Supplementary Table 6).

Adult Drosophila dystrophic muscles are more sensitive to stress

Now we showed that suboptimal conditions have an effect on normal muscle maintenance in *Drosophila*. Dystrophic muscles, however, may have a somewhat different response to stresses depending on the structural differences of muscle cells as well as changes in metabolic processes. To study the specificity of stress response in dystrophic muscles we applied different stresses to *Dys* and *Dg* mutants. Because of higher lethality of *Dys* and *Dg* mutants under the stress in comparison to control (*OregonR*) line, less amount of time was used to keep animals under experimental conditions (Supplementary Table 5, experimental groups 2 and 3).

As expected, high temperature and oxidative stress affected muscle welfare in all tested animals, wild type and mutants (Fig. 6A, Supplementary Table 5). Elevation of environmental temperature from 25 °C to 33 °C about two times increased the incidence of degenerated muscles in mutant animals, similarly to non-mutant. In all analyzed lines, the calculated phenotype included 20–30% of cases with extreme muscle degeneration (Fig. 6A, black bars, E–F, Supplementary Table 5). Also on Paraquat-containing food the ratio or degree of muscle degeneration was not increased in *Dys* and *Dg* mutants in comparison to control (Fig. 6A, Supplementary Table 5), suggesting

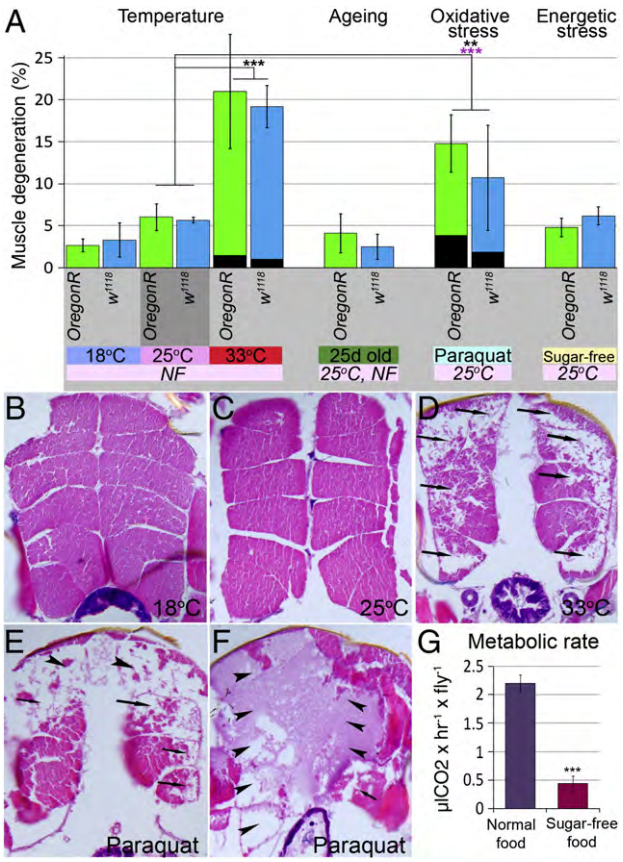

Fig. 5. Oxidative and temperature stress cause muscle degeneration in wild type *Drosophila*. (A) A bar graph shows frequency of muscle degeneration in *OregonR* and w^{1118} flies under influence of different conditions (temperature—18 °C, 25 °C, and 33 °C, ageing, oxidative stress induced by feeding Paraquat and energetic stress induced by sugar deficit, NF - normal food). Frequency of severe muscle degeneration is represented as black bars. Statistics were done using one-way ANOVA with post Dunnett's tests, where data from different "experimental conditions" groups (light grey box) were compared with control group (dark grey box). ** $p \leq 0.01$; *** $p \leq 0.001$. Black stars show comparison of total muscle degeneration, while pink stars represent comparison of extreme muscle degeneration. (B–F) Examples of *OregonR* IFMs at different conditions. Arrows indicate degenerated muscles and arrowheads point to muscles scored as extremely deteriorated. The metabolism response of wild type animals to loss of energy source is shown in (G). Statistics were done using the *t*-test. *** $p \leq 0.001$.

that oxidative stress is not the specific cause for dystrophic muscle degeneration in *Drosophila,* but muscle tissue in general is sensitive to oxidative stress.

Unlike in wild type animals, exposure of *Dys* and *Dg* mutants to lower temperature (18 °C) caused the appearance of severe progressive degeneration, followed by focal muscle loss (Fig. 6A, C–D, Supplementary Table 5). The muscle metabolism is temperature dependent and requires a coordinated system of metabolic control. Since *Dys* and *Dg* mutant muscles already are compromised, lowering the temperature in addition would accelerate degenerative processes. At 25 °C the frequency of muscle degeneration was the lowest, suggesting that 25 °C is an optimal temperature regime for dystrophic animals.

Interestingly, ageing appeared to cause muscle degeneration exclusively in dystrophic animals. Even though *Dys* and *Dg* mutant ageing animals both showed an increased number of myofibrils with moderately and extremely abnormal tissue structure, only mutation in *Dys* gene significantly amplified the amount of degenerated muscles (Fig. 6A, Supplementary Fig. 2, and Supplementary Table 5).

Sugar-free food conditions promoted severe muscle loss only in *Dg* mutants (Fig. 6A, black bar, G, Supplementary Table 5). Under normal conditions *OregonR* flies and *Dys* and *Dg* mutant animals showed similar metabolic rates (2.20 ± 0.15, 2.41 ± 0.09, 2.36 ± 0.18 respectively). Under glucose deprivation control flies produced five times less CO_2 indicating that their metabolic activity went down as expected (Fig. 6B). *Dys* mutants also significantly slowed down their metabolism; on sugar-free food they produced 2. 3 times less CO_2 than on normal food (Fig. 6B, Supplementary Table 6), while *Dg* flies continued to produce a fair amount of CO_2 (only 1. 6 times reduction, Fig. 6B, Supplementary Table 6) implying that the protective system required for lowering the metabolism in response to energetic stress is malfunctioning when Dg is absent. The *Dys* phenotype can be explained due to the fact that Dg localization is diminished in the absence of Dys (data not shown). These data suggest that Dg, but probably not Dys, plays a role in the pathway required to maintain muscle integrity under energetic stress and may be involved in the process of metabolic switch as an adaptive response to sugar shortfall.

Dg is implicated in control of muscle cell metabolism

One of the newly found DGC interactors involved in control of cellular metabolism is a phosphoglycerate kinase, PGK, an enzyme required for ATP generation in the terminal stage of the glycolytic pathway. Similar to the DGC, PGK has been localized in the *Drosophila* flight muscle cells to M-lines and Z-disks (Sullivan et al., 2003). *Drosophila Pgk* mutants display reduced lifespan, abnormal mobility, blocked synaptic transmission and heat-induced seizures (Wang et al., 2004). Our data also show strong genetic interaction of PGK with Dg, but not with Dys (Figs. 7A, C–D), suggesting that Dg together with PGK may have a role in regulation of cellular metabolism. To test this we analyzed the frequency of muscle degeneration in double trans-heterozygous mutants on sugar-free conditions. If PGK is involved in the control of glycolysis, then upon sugar deficit when animals transit their metabolism from glycolysis to fatty acids oxidation, the Dg and Pgk interaction should not be manifested. Indeed, on sugar-free food *Dg/Pgk* trans-heterozygous mutants did not display a muscle degeneration phenotype (Figs. 7A, E) showing that Dg has a role in regulation of the glycolytic pathway. The function of glycolysis and glycogenolysis in muscle is to provide ATP for myosin ATPase to enable contraction. Decrease in ATP levels should lead to the lowering of muscle contraction subsequently leading to abnormal motor behavior. Neither *Dg/+* nor *Pgk/+* mutants showed significantly decreased mobility upon heating (Table 1 for *Pgk/+*, Fig. 4B for *Dg/+*); however, *Dg/Pgk* heterozygotes significantly lessened their ability to move (Fig. 7B). Taken together these data show that Dg interacts with Pgk, a component of the glycolytic pathway that is essential to sustain energy for proper muscle functioning. This implies that Dg has a role in cellular response to energetic crisis.

Discussion

The DGC deficiencies lead to muscle degeneration and malfunction

Within the past couple of years different animal models for DGC-associated muscular dystrophy have significantly contributed to understanding the disease pathogenesis, but many questions about the mechanisms of these disorders remain unanswered. *Drosophila* has been shown to be an appropriate model to study the DGC since nearly all its known components are present and are evolutionarily conserved (Greener and Roberts, 2000), furthermore, mutations in its components, *Dystrophin*, *Dystroglycan* and *sarcoglycan* cause age-dependent progression of muscular dystrophy (Allikian et al., 2007; Shcherbata et al., 2007; Taghli-Lamallem et al., 2008).

We first show that like in vertebrates, *Drosophila* homologues of Dys and Dg are expressed in muscles. In multinucleated muscle cells Dg is present in the sarcolemma and is enriched around Z-bands that

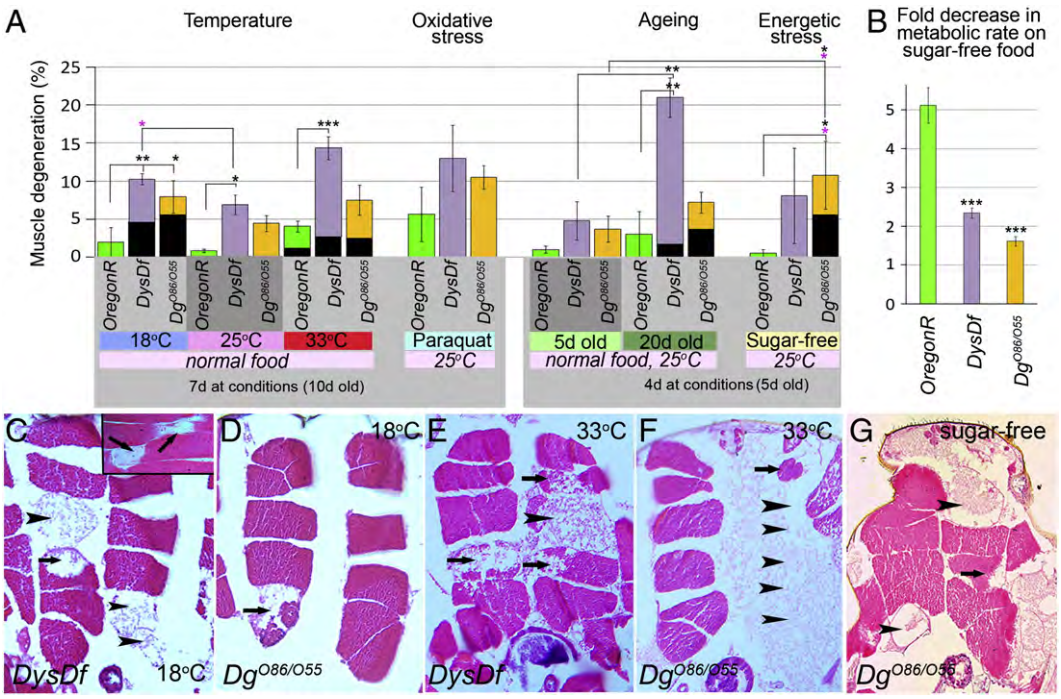

Fig. 6. Dystrophic muscles respond differently than wild type to stress. (A) A bar graph shows frequency of muscle degeneration in *OregonR* flies and *Dys* and *Dg* mutants under influence of different conditions (temperature—18 °C, 25 °C, and 33 °C, oxidative and energetic stress, ageing). Black bars represent the frequency of extreme muscle degeneration. Statistics were done using one-way ANOVA with post Dunnett's tests. First, data for *Dys* and *Dg* mutants were compared to *OregonR* within each "experimental conditions" group and then data from different groups (light grey box) were compared with control group (dark grey box). $^{*}p \leq 0.05$; $^{**}p \leq 0.01$; $^{***}p \leq 0.001$. Black stars show comparison of total muscle degeneration, while pink stars represent comparison of extreme muscle degeneration. (B) Bar graph shows fold decrease in metabolic rate in dystrophic animals and *OregonR* line in response to loss of energy source. To determine the fold reduction in CO_2 production the amount of CO_2 generated under normal food conditions was divided by the amount of CO_2 generated under sugar-free food conditions for each genotype tested. The average value is reported with the error bars representing the standard error. Statistics were determined using a two-tailed Student's *t*-test, $^{***}p \leq 0.001$. (C–G) Exemplary *Dys* and *Dg* mutant IFMs at different conditions. Arrows indicate degenerated muscles and arrowheads point to muscles scored as extremely deteriorated.

correspond to costameres in vertebrates, while Dg's binding partner Dys is enriched in the muscle cytoplasm adjacent to the sarcolemma. Dys and Dg are also located postsynaptically in the larval NMJ, and both are believed to be involved in retrograde signaling to the presynapse (Bogdanik et al., 2008; van der Plas et al., 2006). Therefore the DGC controls not only cellular homeostasis of the muscle cell but also its ability to communicate with the motoneuron. Mutations in the DGC affect both, muscle tissue maintenance leading to myodegeneration and functioning causing heat-induced immobility.

Dys and Dg have different partners implying their involvement in different signalling

Even though Dys and Dg are biochemically linked, mutations in each of them cause partially distinct phenotypes, suggesting that they may act with various components regulating diverse processes required for maintaining muscle integrity. Dys mutants differ from Dg mutants in their behavior; while the first are not able to move, the second jump chaotically (based on observations). It has been noted in studies of the *Drosophila* larval NMJ that *Dys* and *Dg* mutants have opposite phenotypes, *Dg* mutants have shown a decrease in quantal content (Bogdanik et al., 2008), while *Dys* mutants have shown an increase in quantal content with an increase in spontaneous neurotransmitter release (van der Plas et al., 2006). When Dg was down regulated at the larval NMJ Dys expression was no longer localized (Bogdanik et al., 2008); however, when Dys was down regulated, Dg was still localized but to a lesser extent. The absence of Dg causes laminin to not be localized to the larval NMJ leading to disorganization of active zones (Bogdanik et al., 2008; Jacobson et al., 2001; Taniguchi et al., 2006; Tremblay and Carbonetto, 2006; van der Plas et al., 2006). This could lead to a severely mis-functioning NMJ that is not capable of transmitting a signal to the muscle to lead to a temperature-sensitive phenotype. Conversely, when Dys is absent, there is still the organization of the NMJ to lead to neurotransmission, but ultimately causing a failure of the contractile apparatus of the muscle possibly due to over excitation of neurotransmitter release. Therefore, we can propose that heat-induced immobility in *Dys* mutants is caused by improper retrograde signaling from muscle to the neuron, which causes constant muscle hypercontraction and subsequent degeneration of flight muscles. In *Dg* mutants shortage in NMJ functioning may cause faulty neurotransmission to the muscle leading to a loss of insufficiently innervated muscle fibers (manuscript in preparation).

Ageing also differentially affects muscle morphology: *Dys* mutants significantly increased the number of degenerated muscles, while *Dg* deficiency mainly promotes the severity of muscle deterioration. The similarity of phenotypes in *Dys* and *Dg* mutants is likely explained by the secondary destabilization of the entire DGC that results from deficiency of only one member. The differences in phenotypes are probably due to distinct roles of each protein, Dys being a cytosolic scaffold protein connecting the actin cytoskeleton to the plasmalemma, and a transmembrane Dg providing the link to the ECM.

Since both proteins may have different binding partners and be involved in different signaling pathways, we screened for unknown components that can influence Dys and Dg-dependent MD phenotypes. Our *in vivo* genetic screen in ageing dystrophic muscles revealed that the process of dystrophic muscle pathogenesis is multifunctional by nature, as is the DGC function. Dys and Dg genetically interact with multiple proteins that are involved in regulation of cell signalling, calcium homeostasis, cytoskeleton rearrangements, sarcolemma stability, energetic and oxidative stress, and cell polarity. Almost half of identified genes showed interaction with both proteins, and about one quarter specifically interacted with Dys or Dg (Fig. 3B). In general, all found interactors could be divided into three subgroups: genes that

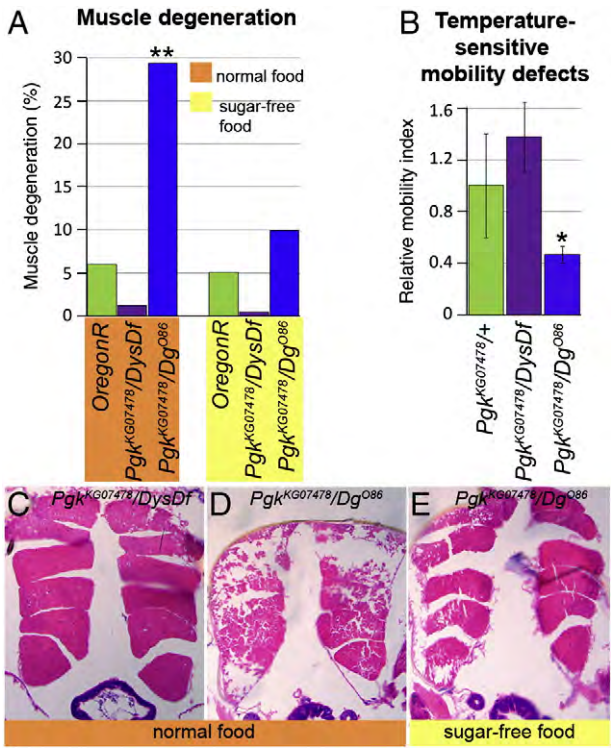

Fig. 7. Dg interacts with the glycolytic enzyme Pgk. (A) A bar graph shows frequency of muscle degeneration from genetic interaction of *Pgk* with *Dys* and *Dg* in 13-15d old animals kept for 10 days at normal or sugar-free food conditions in comparison with *OregonR*. Statistics were done using the χ^2-test with one degree of freedom and Yates`s correction. Percentage of degenerated muscles for $Pgk^{KG07478}/DysDf$ on normal food was 1% (n=72), sugar-free 0.5% (n=56) and $Pgk^{KG07478}/Dg^{O86}$ on normal food 33.8% (n=59), sugar-free food 10% (n=70), for *OregonR* control see Supplementary Fig. 5. (B) A bar graph represents temperature-sensitive mobility defects in *Pgk/Dys* and *Pgk/Dg* heterozygotes. Indexes for temperature-sensitive mobility in 1–5 day old animals is 1.23 ± 0.76 (n=52) for $Pgk^{KG07478}/+$, 1.68 ± 0.38 (n=58) $p=0.236$ for $Pgk^{KG07478}/DysDf$ and 0.57 ± 0.08 (n=58) $p=0.029$ for $Pgk^{KG07478}/Dg^{O86}$. Statistics were done using the *t*-test. $^*p\leq0.05$. (C–E) Exemplary IFMs showing muscle degeneration from 13–15 day old animals of the genotypes $Pgk^{KG07478}/DysDf$ and $Pgk^{KG07478}/Dg^{O86}$ kept at normal (C–D) and sugar-free (E) food.

are involved in mechanosignaling, cellular stress response factors, and genes that control neuron–muscle communication.

Muscle homeostasis depends not only on the cell autonomous DGC function, but also on neuron–muscle communication

Interestingly 4 out of 16 interactors (Nrk, Pgk, FKBP13 and SP2353) that have been found in our screen in ageing dystrophic muscles are supposedly involved in NMJ function and all of them, except for Nrk, genetically interact with Dg only. Disrupted glycosylation of α-DG in humans results in congenital muscular dystrophies that are associated with both progressive muscle degeneration and abnormal neuronal migration in the brain (Collins and Bonnemann, 2010). Disorders with the defects in NMJ transmission (congenital myasthenic syndromes, CMSs) also lead to muscle weakness (Massoulie and Millard, 2009). *Drosophila* Nrk (neurospecific receptor kinase) is highly homologous (60% identity) to human MuSK (muscle receptor kinase), which is essential for establishment and maintenance of the NMJs (Meriggioli and Sanders, 2009). Activation of MuSK by binding to agrin leads to clustering of acetylcholine receptors on the postsynaptic side of the NMJ (Stiegler et al., 2009). Furthermore, it is known that agrin and Laminin B can directly interact with dystroglycan and both of these ligands have been shown to be involved in CMS development (Huze et al., 2009). We also found in the screen *Drosophila* SP2353, a novel agrin-like protein that contains a Laminin G domain, which makes it a potential new extracellular binding partner for Dystroglycan. The human ortholog for SP2353 (AGRN) is involved in congenital MD development and the mouse homolog, pikachurin has been shown to bind Dg in photoreceptor ribbon synapses (Huze et al., 2009; Sato et al., 2008). Supposedly, dystroglycan and MuSK (Nrk) could be two receptors and SP2353 a ligand important for transferring signals necessary for normal NMJ function. However, whether these pathways share the same ligand components to provide neuron–muscle communication has to be studied further.

FKBP13 is not extensively analyzed, however another member of the FK506 binding protein family, FKBP12 is believed to be important in regulating Ca^{2+} release through all ryanodine-receptor isoforms and the 1,4,5-inositoltriphosphate receptors. Recently it has been reported that FKBP12 is part of a macromolecular complex with RyR1 in mouse skeletal muscle. In *mdx* mice the associate of FKBP12 with RyR1 is reduced leading to sarcoplasmic calcium leakage (Bellinger et al., 2009). This dissociation is caused by increased RyR1 S-nitrosylation via inducible NOS (iNOS), which is up-regulated in dystrophic mouse (Bellinger et al., 2009). The DGC binds to neuronal NOS (nNOS) via α-syntrophin, where nNOS is the principle source of nitric oxide in skeletal muscle. When the DGC is disrupted via loss of dystrophin nNOS is downregulated and a compensatory mechanism causes the upregulation of iNOS, and consequently destabilization of RyR1 due to nitrosative stress.

The DGC may act as a sensor in the mechanical stress response pathway

Muscle mechanosensitivity modulates diverse cellular functions that ensure structural stability of muscle tissue in response to mechanical stresses. There is an interesting group of the genes, identified from our screen that play an important role in the assembly of the actin cytoskeleton architecture and signal transfer to cause cytoskeleton reconstruction. Dystrophic muscle stability is jeopardized upon mechanical stress (Petrof, 1998), which suggests misregulation of proteins that control cellular response to extracellular mechanics. This implies that the DGC can act as a mechanosensoring unit that transduces physical forces into biochemical information.

Actin cytoskeleton reorganization in response to mechanical tension is controlled via different signaling pathways and, interestingly Dys interactors Capt and Lis-1 are involved in this process (Moriyama and Yahara, 2002; Wynshaw-Boris, 2007). Capt (cyclase-associated protein) is a *Drosophila* homologue of human CAP1 (Table 1), which has been shown to play a key role in speeding up the turnover of actin filaments by effectively recycling cofilin and actin through its effect on both ends of actin filaments (Moriyama and Yahara, 2002). CAP1 has cofilin- and actin-binding domains, which makes it an attractive component to be involved in signal transduction and thereby links the cell signaling with actin polymerization. LIS1 is associated with Miller–Dieker (classical lissencephaly) syndrome; it interacts with the actin cytoskeleton and dynein activity (Gil-Krzewska et al., 2010; Wynshaw-Boris, 2007).

Found DGC interactor, RACK1 binds activated protein kinase C (aPKC) and anchors it to the cytoskeleton. It has not been shown yet that the *Drosophila* Rack1 gene can bind to aPKC, but it is 76% homologues to the mammalian Rack1 proteins (Table 1). In mouse skeletal muscle aPKC α associates with Annexin VI (Schmitz-Peiffer et al., 1998), which provides a possible structural link for Rack1 to the DGC through the hypothesized binding of Annexins to the TRPC channels TRPC1 and TRPC4 that bind with α-syntrophin (Sabourin et al., 2009). Rack1 also has a pro-apoptotic function by blocking Src activation of the Akt cell survival pathway (Mamidipudi and Cartwright, 2009). There has also been suggested a role for the DGC in inhibiting apoptosis by laminin binding to αDg which in turn activates the PI3K/Akt pathway (Langenbach and Rando, 2002).

An additional cytoskeleton-controlling mutant identified from the screen that exhibits muscle degeneration and temperature-sensitive mobility defects is *Fhos*. A microarray screen identified an up-

regulated Fhos transcript in *Drosophila Mhc* mutants and further *in situ* analysis revealed strong expression of Fhos in somatic muscles and putative midline mesodermal cell (Montana and Littleton, 2006). *Fhos* encodes for the protein homologues to human FHOD1 (a formin homology containing protein). Formins are conserved in eukaryotes from yeasts to mammals; they control cell polarity during processes such as motility, cytokinesis, and differentiation by organizing the actin cytoskeleton and microtubules (MTs) (Gasteier et al., 2005). Recently a direct interaction between dystrophin and MTs has been identified (Prins et al., 2009). This proposes that the DGC and Fhos may act as a team in the MT organizing procedure.

Since skeletal muscle basal lamina is linked to the sarcolemma through transmembrane receptors, including integrins and dystroglycan, it is plausible that their function may be somewhat redundant. It had previously been shown that upregulation of integrin α_7 in the *mdx* background could ameliorate aspects of muscular dystrophy (Burkin et al., 2001). However, when functional dystrophin is absent, upregulation of integrin α_7 could only compensate in mediating cell-extracellular matrix attachment but cannot rescue the dystrophic phenotype (Cote et al., 2002). In addition, in *Drosophila,* integrin-mediated adhesion maintains sarcomeric integrity (Perkins et al., 2010). Our finding that one of the *Drosophila* integrins interacts with both Dys and Dg implies that the DGC is linked to the integrin signaling pathway and further studies of different components of the pathway may help to find a way how to strengthen the plasma membrane in dystrophic muscles. Additionally, mammalian homologs for *mbl* and *chif*, MBNL1 and DBF4 found in our screen have been implicated in integrin signaling (Chen et al., 2009; Vicente et al., 2007).

Since defects in mechanotransduction are linked with the development of various diseases, ranging from muscular dystrophies to cancer progression and metastasis, understanding the roles of the DGC and its interacting proteins in mechanical stress response is very important.

Stress influences the speed and the onset of muscle degeneration as dystrophic muscles have abnormal cellular metabolism

Although the genetic basis of many dystrophies is known, the exact processes by which muscles become progressively nonfunctional remain a mystery. Since genes found in our screen have been previously associated with cellular adaptive responses to stress, we first analyzed and compared the normal and dystrophic muscle stress responsiveness using different stress conditions. Our data show that muscle degeneration can be induced by stress. Furthermore, stress accelerates the onset and severity of age-dependent muscular dystrophy in *Dys* and *Dg* mutants. Normal and dystrophic muscles are similarly sensitive to elevated temperature and oxidative stress. Remarkably, cooler temperature amplified dystrophic muscle damage comparable to what was seen in aged mutant animals. Energetic stress had a large impact on the muscle structure of *Dg* mutants with severe muscle degeneration far exceeding that observed in *Dys* mutants. This finding is supported by previous studies, which also showed association of Dg with energy homeostasis (Mirouse et al., 2009; Takeuchi et al., 2009).

The muscle is the largest organ in the body that is required not only for movement, but also for heat production and cold tolerance, playing a crucial role in the overall energy balance. Calmodulin that plays a role in the oxidative stress response pathway, is an expected DGC interactor, since it binds to syntrophin (a component of the DGC) and CaM dependent kinase is involved in phosphorylation of dystrophin and syntrophin (Madhavan and Jarrett, 1999). In addition, the selective oxidation or nitration of CaM that occurs *in vivo* during ageing and under conditions of oxidative stress modulates signal transduction processes and intracellular energy metabolism (Squier, 2001). Additionally, the Ca^{2+}-buffering capacity of dystrophic muscles by Calmodulin and Calsequestrin also seems to be impaired due to a decrease in the levels of these proteins (Pertille et al., 2010); and targeted inhibition of CAM signaling worsens the dystrophic phenotype in *mdx* mouse muscle (Chakkalakal et al., 2006). Importantly, reduction of *Cam* by one copy, found as a Dys interactor in our screen rescues the Dys hypercontraction phenotype (manuscript in preparation).

Also we have determined here that in muscles Dg, but not Dys is required under conditions of energetic stress and both proteins involved in metabolic processes, PGK and Vimar, showed interactions with Dg only. Based on prior screen data, Vimar has been shown to regulate mitochondrial function via an increase in citrate synthase activity (Chen et al., 2008). Citrate synthase deficiency leads to a decrease in ATP levels consistent with disruption of mitochondrial energy production (Fergestad et al., 2006). Possibly, the involvement Vimar has with the muscular dystrophy phenotype could be due to its role in mitochondrial regulation. PGK is essential for the breakdown of glycogen, resulting in the release of energy (Das et al., 2010; Wang et al., 2004). In order to contract muscle cells needs ATP for myosin ATPase, which can be provided either via the glycolytic pathway or by mitochondrial oxidative phosphorylation. In *Drosophila*, a substantial fraction of the ATP for flight muscle contraction is provided through the glycolytic pathway (Leopold and Perrimon, 2007; Sullivan et al., 2003). In IFMs, glycolytic enzymes, including Pgk, are co-localized along sarcomeres at M-lines and Z-discs and this co-localization is required for normal muscle function (Sullivan et al., 2003; Wojtas et al., 1997). Similarly to *Dg* mutants, *Drosophila Pgk* mutants display reduced lifespan, abnormal motor behavior, altered synaptic structure, defective neurotransmitter release, and temperature-sensitive seizures (Wang et al., 2004). *Pgk* deficiency in humans is a rare inherited metabolic disorder sometimes associated with myopathies (Das et al., 2010) and it would be thought-provoking to study in more detail the effect of energy metabolism on dystrophic muscles.

Taken together our data demonstrate that the DGC is involved in the muscle stress response pathway. Understanding the differences between healthy and dystrophic adaptive reactions can lead to new approaches for dystrophic muscle metabolism manipulation to prevent progressive muscle loss. Further analysis of found Dys and Dg specific interactions will allow for new opportunities for easier drug targets in muscular dystrophy therapeutics and a better understanding of muscular dystrophy dynamics.

Acknowledgments

We thank Hannele Ruohola-Baker, Robert Ray, Robert Ward, Lee Fradkin and Andreas Wodarz for fly stocks and antibodies, members of the Eichele Department for help with cryosections, Herbert Jaeckle, Gregor Eichele and Martin Goepfert for suggestions on the manuscript, Hugo Bellen, Mary Hatten, members of the Jaeckle Department and H. R. S. 's lab for helpful discussion. V. R. was supported by a DAAD fellowship. Work in H. R. S.'s lab is funded by Max-Planck-Gesselschaft.

Appendix A. Supplementary data

Supplementary data to this article can be found online at doi:10.1016/j.ydbio.2011.01.013.

References

Adams, M.E., Tesch, Y., Percival, J.M., Albrecht, D.E., Conhaim, J.I., Anderson, K., Froehner, S.C., 2008. Differential targeting of nNOS and AQP4 to dystrophin-deficient sarcolemma by membrane-directed alpha-dystrobrevin. J. Cell Sci. 121, 48–54.

Allikian, M.J., Bhabha, G., Dospoy, P., Heydemann, A., Ryder, P., Earley, J.U., Wolf, M.J., Rockman, H.A., McNally, E.M., 2007. Reduced life span with heart and muscle dysfunction in Drosophila sarcoglycan mutants. Hum. Mol. Genet. 16, 2933–2943.

Batchelor, C.L., Winder, S.J., 2006. Sparks, signals and shock absorbers: how dystrophin loss causes muscular dystrophy. Trends Cell Biol. 16, 198–205.

Bellinger, A.M., Reiken, S., Carlson, C., Mongillo, M., Liu, X., Rothman, L., Matecki, S., Lacampagne, A., Marks, A.R., 2009. Hypernitrosylated ryanodine receptor calcium release channels are leaky in dystrophic muscle. Nat. Med. 15, 325–330.

Benshalom, G., Dagan, D., 1981. Transient and long-term effects of temperature on electrogenic activity of Drosophila nerves and muscles. Brain Res. 213, 117–182.

Boehm, M.B., Milius, T.J., Zhou, Y., Westendorf, J.J., Koka, S., 2005. The mammalian formin FHOD1 interacts with the ERK MAP kinase pathway. Biochem. Biophys. Res. Commun. 335, 1090–1094.

Bogdanik, L., Framery, B., Frolich, A., Franco, B., Mornet, D., Bockaert, J., Sigrist, S.J., Grau, Y., Parmentier, M.L., 2008. Muscle dystroglycan organizes the postsynapse and regulates presynaptic neurotransmitter release at the Drosophila neuromuscular junction. PLoS ONE 3, e2084.

Burkin, D.J., Wallace, G.Q., Nicol, K.J., Kaufman, D.J., Kaufman, S.J., 2001. Enhanced expression of the alpha 7 beta 1 integrin reduces muscular dystrophy and restores viability in dystrophic mice. J. Cell Biol. 152, 1207–1218.

Bus, J.S., Gibson, J.E., 1984. Paraquat: model for oxidant-initiated toxicity. Environ. Health Perspect. 55, 37–46.

Cacchiarelli, D., Martone, J., Girardi, E., Cesana, M., Incitti, T., Morlando, M., Nicoletti, C., Santini, T., Sthandier, O., Barberi, L., Auricchio, A., Musaro, A., Bozzoni, I., 2010. MicroRNAs involved in molecular circuitries relevant for the Duchenne muscular dystrophy pathogenesis are controlled by the dystrophin/nNOS pathway. Cell Metab. 12, 341–351.

Chakkalakal, J.V., Michel, S.A., Chin, E.R., Michel, R.N., Jasmin, B.J., 2006. Targeted inhibition of Ca2+/calmodulin signaling exacerbates the dystrophic phenotype in mdx mouse muscle. Hum. Mol. Genet. 15, 1423–1435.

Chen, J., Shi, X., Padmanabhan, R., Wang, Q., Wu, Z., Stevenson, S.C., Hild, M., Garza, D., Li, H., 2008. Identification of novel modulators of mitochondrial function by a genome-wide RNAi screen in Drosophila melanogaster. Genome Res. 18, 123–136.

Chen, Y., Lu, B., Yang, Q., Fearns, C., Yates III, J.R., Lee, J.D., 2009. Combined integrin phosphoproteomic analyses and small interfering RNA-based functional screening identify key regulators for cancer cell adhesion and migration. Cancer Res. 69, 3713–3720.

Christoforou, C.P., Greer, C.E., Challoner, B.R., Charizanos, D., Ray, R.P., 2008. The detached locus encodes Drosophila Dystrophin, which acts with other components of the Dystrophin Associated Protein Complex to influence intercellular signalling in developing wing veins. Dev. Biol. 313, 519–532.

Collins, J., Bonnemann, C.G., 2010. Congenital muscular dystrophies: toward molecular therapeutic interventions. Curr. Neurol. Neurosci. Rep. 10, 83–91.

Constantin, B., Sebille, S., Cognard, C., 2006. New insights in the regulation of calcium transfers by muscle dystrophin-based cytoskeleton: implications in DMD. J. Muscle Res. Cell Motil. 27, 375–386.

Cote, P.D., Moukhles, H., Carbonetto, S., 2002. Dystroglycan is not required for localization of dystrophin, syntrophin, and neuronal nitric-oxide synthase at the sarcolemma but regulates integrin alpha 7B expression and caveolin-3 distribution. J. Biol. Chem. 277, 4672–4679.

Das, A.M., Steuerwald, U., Illsinger, S., 2010. Inborn errors of energy metabolism associated with myopathies. J. Biomed. Biotechnol. 2010, 340849.

Davies, K.E., Nowak, K.J., 2006. Molecular mechanisms of muscular dystrophies: old and new players. Nat. Rev. Mol. Cell Biol. 7, 762–773.

Deng, W.M., Schneider, M., Frock, R., Castillejo-Lopez, C., Gaman, E.A., Baumgartner, S., Ruohola-Baker, H., 2003. Dystroglycan is required for polarizing the epithelial cells and the oocyte in Drosophila. Development (Cambridge, England) 130, 173–184.

Durbeej, M., Campbell, K.P., 2002. Muscular dystrophies involving the dystrophin–glycoprotein complex: an overview of current mouse models. Curr. Opin. Genet. Dev. 12, 349–361.

Ervasti, J.M., 2003. Costameres: the Achilles' heel of Herculean muscle. J. Biol. Chem. 278, 13591–13594.

Fergestad, T., Bostwick, B., Ganetzky, B., 2006. Metabolic disruption in Drosophila bang-sensitive seizure mutants. Genetics 173, 1357–1364.

Fuentes-Mera, L., Rodriguez-Munoz, R., Gonzalez-Ramirez, R., Garcia-Sierra, F., Gonzalez, E., Mornet, D., Cisneros, B., 2006. Characterization of a novel Dp71 dystrophin-associated protein complex (DAPC) present in the nucleus of HeLa cells: members of the nuclear DAPC associate with the nuclear matrix. Exp. Cell Res. 312, 3023–3035.

Gasteier, J.E., Schroeder, S., Muranyi, W., Madrid, R., Benichou, S., Fackler, O.T., 2005. FHOD1 coordinates actin filament and microtubule alignment to mediate cell elongation. Exp. Cell Res. 306, 192–202.

Gil-Krzewska, A.J., Farber, E., Buttner, E.A., Hunter, C.P., 2010. Regulators of the actin cytoskeleton mediate lethality in a *Caenorhabditis elegans* dhc-1 mutant. Mol. Biol. Cell 21, 2707–2720.

Greener, M.J., Roberts, R.G., 2000. Conservation of components of the dystrophin complex in Drosophila. FEBS Lett. 482, 13–18.

Huze, C., Bauche, S., Richard, P., Chevessier, F., Goillot, E., Gaudon, K., Ben Ammar, A., Chaboud, A., Grosjean, I., Lecuyer, H.A., Bernard, V., Rouche, A., Alexandri, N., Kuntzer, T., Fardeau, M., Fournier, E., Brancaccio, A., Ruegg, M.A., Koenig, J., Eymard, B., Schaeffer, L., Hantai, D., 2009. Identification of an agrin mutation that causes congenital myasthenia and affects synapse function. Am. J. Hum. Genet. 85, 155–167.

Jaalouk, D.E., Lammerding, J., 2009. Mechanotransduction gone awry. Nat. Rev. Mol. Cell Biol. 10, 63–73.

Jacobson, C., Cote, P.D., Rossi, S.G., Rotundo, R.L., Carbonetto, S., 2001. The dystroglycan complex is necessary for stabilization of acetylcholine receptor clusters at neuromuscular junctions and formation of the synaptic basement membrane. J. Cell Biol. 152, 435–450.

Kucherenko, M.M., Pantoja, M., Yatsenko, A.S., Shcherbata, H.R., Fischer, K.A., Maksymiv, D.V., Chernyk, Y.I., Ruohola-Baker, H., 2008. Genetic modifier screens reveal new components that interact with the Drosophila dystroglycan–dystrophin complex. PLoS ONE 3, e2418.

Kucherenko, M.M., Marrone, A.K., Rishko, V.M., Yatsenko, A.S., Klepzig, A., Shcherbata, H.R., 2010. Paraffin-embedded and frozen sections of drosophila adult muscles. J. Vis. Exp. pii: 2438.

Langenbach, K.J., Rando, T.A., 2002. Inhibition of dystroglycan binding to laminin disrupts the PI3K/AKT pathway and survival signaling in muscle cells. Muscle Nerve 26, 644–653.

Leopold, P., Perrimon, N., 2007. Drosophila and the genetics of the internal milieu. Nature 450, 186–188.

Liu, J., Burkin, D.J., Kaufman, S.J., 2008. Increasing alpha 7 beta 1-integrin promotes muscle cell proliferation, adhesion, and resistance to apoptosis without changing gene expression. Am. J. Physiol. Cell Physiol. 294, C627–C640.

Madhavan, R., Jarrett, H.W., 1999. Phosphorylation of dystrophin and alpha-syntrophin by Ca(2+)-calmodulin dependent protein kinase II. Biochim. Biophys. Acta 1434, 260–274.

Mamidipudi, V., Cartwright, C.A., 2009. A novel pro-apoptotic function of RACK1: suppression of Src activity in the intrinsic and Akt pathways. Oncogene 28, 4421–4433.

Massoulie, J., Millard, C.B., 2009. Cholinesterases and the basal lamina at vertebrate neuromuscular junctions. Curr. Opin. Pharmacol. 9, 316–325.

Mburu, P., Mustapha, M., Varela, A., Weil, D., El-Amraoui, A., Holme, R.H., Rump, A., Hardisty, R.E., Blanchard, S., Coimbra, R.S., Perfettini, I., Parkinson, N., Mallon, A.M., Glenister, P., Rogers, M.J., Paige, A.J., Moir, L., Clay, J., Rosenthal, A., Liu, X.Z., Blanco, G., Steel, K.P., Petit, C., Brown, S.D., 2003. Defects in whirlin, a PDZ domain molecule involved in stereocilia elongation, cause deafness in the whirler mouse and families with DFNB31. Nat. Genet. 34, 421–428.

Medina, P.M., Worthen, R.J., Forsberg, L.J., Brenman, J.E., 2008. The actin-binding protein capulet genetically interacts with the microtubule motor kinesin to maintain neuronal dendrite homeostasis. PLoS ONE 3, e3054.

Medioni, C., Astier, M., Zmojdzian, M., Jagla, K., Semeriva, M., 2008. Genetic control of cell morphogenesis during *Drosophila melanogaster* cardiac tube formation. J. Cell Biol. 182, 249–261.

Meriggioli, M.N., Sanders, D.B., 2009. Autoimmune myasthenia gravis: emerging clinical and biological heterogeneity. Lancet Neurol. 8, 475–490.

Miller, A., 1950. The internal anatomy and histology of the imago of *Drosophila melanogaster*. CSHL Press.

Mirouse, V., Christoforou, C.P., Fritsch, C., St Johnston, D., Ray, R.P., 2009. Dystroglycan and perlecan provide a basal cue required for epithelial polarity during energetic stress. Dev. Cell 16, 83–92.

Montana, E.S., Littleton, J.T., 2004. Characterization of a hypercontraction-induced myopathy in Drosophila caused by mutations in Mhc. J. Cell Biol. 164, 1045–1054.

Montana, E.S., Littleton, J.T., 2006. Expression profiling of a hypercontraction-induced myopathy in Drosophila suggests a compensatory cytoskeletal remodeling response. J. Biol. Chem. 281, 8100–8109.

Moore, C.J., Winder, S.J., 2010. Dystroglycan versatility in cell adhesion: a tale of multiple motifs. Cell Commun. Signal. 8, 3.

Moriyama, K., Yahara, I., 2002. Human CAP1 is a key factor in the recycling of cofilin and actin for rapid actin turnover. J. Cell Sci. 115, 1591–1601.

Mujahid, A., Yoshiki, Y., Akiba, Y., Toyomizu, M., 2005. Superoxide radical production in chicken skeletal muscle induced by acute heat stress. Poult. Sci. 84, 307–314.

Muschler, J., Levy, D., Boudreau, R., Henry, M., Campbell, K., Bissell, M.J., 2002. A role for dystroglycan in epithelial polarization: loss of function in breast tumor cells. Cancer Res. 62, 7102–7109.

Oishi, I., Sugiyama, S., Liu, Z.J., Yamamura, H., Nishida, Y., Minami, Y., 1997. A novel Drosophila receptor tyrosine kinase expressed specifically in the nervous system. Unique structural features and implication in developmental signaling. J. Biol. Chem. 272, 11916–11923.

Palomero, J., Jackson, M.J., 2010. Redox regulation in skeletal muscle during contractile activity and aging. J. Anim. Sci. 88, 1307–1313.

Perkins, A.D., Ellis, S.J., Asghari, P., Shamsian, A., Moore, E.D., Tanentzapf, G., 2010. Integrin-mediated adhesion maintains sarcomeric integrity. Dev. Biol. 338, 15–27.

Pertille, A., de Carvalho, C.L., Matsumura, C.Y., Neto, H.S., Marques, M.J., 2010. Calcium-binding proteins in skeletal muscles of the mdx mice: potential role in the pathogenesis of Duchenne muscular dystrophy. Int. J. Exp. Pathol. 91, 63–71.

Petrof, B.J., 1998. The molecular basis of activity-induced muscle injury in Duchenne muscular dystrophy. Mol. Cell. Biochem. 179, 111–123.

Pilgram, G.S., Potikanond, S., Baines, R.A., Fradkin, L.G., Noordermeer, J.N., 2010. The roles of the dystrophin-associated glycoprotein complex at the synapse. Mol. Neurobiol. 41, 1–21.

Prins, K.W., Humston, J.L., Mehta, A., Tate, V., Ralston, E., Ervasti, J.M., 2009. Dystrophin is a microtubule-associated protein. J. Cell Biol. 186, 363–369.

Qiu, Y., Mao, T., Zhang, Y., Shao, M., You, J., Ding, Q., Chen, Y., Wu, D., Xie, D., Lin, X., Gao, X., Kaufman, R.J., Li, W., Liu, Y., 2010. A crucial role for RACK1 in the regulation of glucose-stimulated IRE1alpha activation in pancreatic beta cells. Sci. Signal. 3, ra7.

Sabourin, J., Lamiche, C., Vandebrouck, A., Magaud, C., Rivet, J., Cognard, C., Bourmeyster, N., Constantin, B., 2009. Regulation of TRPC1 and TRPC4 cation channels requires an alpha1-syntrophin-dependent complex in skeletal mouse myotubes. J. Biol. Chem. 284, 36248–36261.

Sato, S., Omori, Y., Katoh, K., Kondo, M., Kanagawa, M., Miyata, K., Funabiki, K., Koyasu, T., Kajimura, N., Miyoshi, T., Sawai, H., Kobayashi, K., Tani, A., Toda, T., Usukura, J., Tano, Y., Fujikado, T., Furukawa, T., 2008. Pikachurin, a dystroglycan ligand, is essential for photoreceptor ribbon synapse formation. Nat. Neurosci. 11, 923–931.

Schmitz-Peiffer, C., Browne, C.L., Walker, J.H., Biden, T.J., 1998. Activated protein kinase C alpha associates with annexin VI from skeletal muscle. Biochem. J. 330 (Pt 2), 675–681.

Schneider, M., Khalil, A.A., Poulton, J., Castillejo-Lopez, C., Egger-Adam, D., Wodarz, A., Deng, W.M., Baumgartner, S., 2006. Perlecan and Dystroglycan act at the basal side of the Drosophila follicular epithelium to maintain epithelial organization. Development (Cambridge, England) 133, 3805–3815.

Shcherbata, H.R., Yatsenko, A.S., Patterson, L., Sood, V.D., Nudel, U., Yaffe, D., Baker, D., Ruohola-Baker, H., 2007. Dissecting muscle and neuronal disorders in a Drosophila model of muscular dystrophy. EMBO J. 26, 481–493.

Spence, H.J., Dhillon, A.S., James, M., Winder, S.J., 2004. Dystroglycan, a scaffold for the ERK-MAP kinase cascade. EMBO Rep. 5, 484–489.

Squier, T.C., 2001. Oxidative stress and protein aggregation during biological aging. Exp. Gerontol. 36, 1539–1550.

Stiegler, A.L., Burden, S.J., Hubbard, S.R., 2009. Crystal structure of the frizzled-like cysteine-rich domain of the receptor tyrosine kinase MuSK. J. Mol. Biol.

Sullivan, D.T., MacIntyre, R., Fuda, N., Fiori, J., Barrilla, J., Ramizel, L., 2003. Analysis of glycolytic enzyme co-localization in Drosophila flight muscle. J. Exp. Biol. 206, 2031–2038.

Taghli-Lamallem, O., Akasaka, T., Hogg, G., Nudel, U., Yaffe, D., Chamberlain, J.S., Ocorr, K., Bodmer, R., 2008. Dystrophin deficiency in Drosophila reduces lifespan and causes a dilated cardiomyopathy phenotype. Aging Cell 7, 237–249.

Takeuchi, K., Nakano, Y., Kato, U., Kaneda, M., Aizu, M., Awano, W., Yonemura, S., Kiyonaka, S., Mori, Y., Yamamoto, D., Umeda, M., 2009. Changes in temperature preferences and energy homeostasis in dystroglycan mutants. Science 323, 1740–1743.

Taniguchi, M., Kurahashi, H., Noguchi, S., Fukudome, T., Okinaga, T., Tsukahara, T., Tajima, Y., Ozono, K., Nishino, I., Nonaka, I., Toda, T., 2006. Aberrant neuromuscular junctions and delayed terminal muscle fiber maturation in alpha-dystroglycanopathies. Hum. Mol. Genet. 15, 1279–1289.

Tremblay, M.R., Carbonetto, S., 2006. An extracellular pathway for dystroglycan function in acetylcholine receptor aggregation and laminin deposition in skeletal myotubes. J. Biol. Chem. 281, 13365–13373.

van der Plas, M.C., Pilgram, G.S., Plomp, J.J., de Jong, A., Fradkin, L.G., Noordermeer, J.N., 2006. Dystrophin is required for appropriate retrograde control of neurotransmitter release at the Drosophila neuromuscular junction. J. Neurosci. 26, 333–344.

Vercherat, C., Chung, T.K., Yalcin, S., Gulbagci, N., Gopinadhan, S., Ghaffari, S., Taneja, R., 2009. Stra13 regulates oxidative stress mediated skeletal muscle degeneration. Hum. Mol. Genet. 18, 4304–4316.

Vicente, M., Monferrer, L., Poulos, M.G., Houseley, J., Monckton, D.G., O'Dell, K.M., Swanson, M.S., Artero, R.D., 2007. Muscleblind isoforms are functionally distinct and regulate alpha-actinin splicing. Differentiation 75, 427–440.

Wallace, G.Q., McNally, E.M., 2009. Mechanisms of muscle degeneration, regeneration, and repair in the muscular dystrophies. Annu. Rev. Physiol. 71, 37–57.

Wang, P., Saraswati, S., Guan, Z., Watkins, C.J., Wurtman, R.J., Littleton, J.T., 2004. A Drosophila temperature-sensitive seizure mutant in phosphoglycerate kinase disrupts ATP generation and alters synaptic function. J. Neurosci. 24, 4518–4529.

Wojtas, K., Slepecky, N., von Kalm, L., Sullivan, D., 1997. Flight muscle function in Drosophila requires colocalization of glycolytic enzymes. Mol. Biol. Cell 8, 1665–1675.

Wynshaw-Boris, A., 2007. Lissencephaly and LIS1: insights into the molecular mechanisms of neuronal migration and development. Clin. Genet. 72, 296–304.

Yatsenko, A.S., Kucherenko, M.M., Pantoja, M., Fischer, K.A., Madeoy, J., Deng, W.M., Schneider, M., Baumgartner, S., Akey, J., Shcherbata, H.R., Ruohola-Baker, H., 2009. The conserved WW-domain binding sites in Dystroglycan C-terminus are essential but partially redundant for Dystroglycan function. BMC Dev. Biol. 9, 18.

Zhang, L., Ward, R.E.T., 2009. Uninflatable encodes a novel ectodermal apical surface protein required for tracheal inflation in Drosophila. Dev. Biol. 336, 201–212.

Zhou, Y., Jiang, D., Thomason, D.B., Jarrett, H.W., 2007. Laminin-induced activation of Rac1 and JNKp46 is initiated by Src family kinases and mimics the effects of skeletal muscle contraction. Biochemistry 46, 14907–14916.

Table S1. Decrease in Dystroglycan mRNA level in *Dg^{RNAi}:tub-Gal4* mutant

Genotype	Dg Average C_T	RpL32 Average C_T	ΔC_T Dg-RpL32[1]	$\Delta\Delta C_T$ ΔC_T-$\Delta C_{T,control}$[2]	Average Dg relative to control[3]	Dg mRNA fold reduction relative to control[4]
tub-Gal4/+	23.33±0.07	18.35±0.20	4.98±0.21	0.00±0.30	1.00±0.21	1.00±0.21
Dg^{RNAi}:tub-Gal4/+	25.94±0.13	18.37±0.11	7.57±0.18	2.59±0.28	0.17±0.03	6.02±1.16

Table S2. Decrease in Dystrophin mRNA level in *Dys$^{N\text{-}RNAi}$:act-Gal4* mutant

Genotype	Dys Average C_T	RpL32 Average C_T	ΔC_T Dys-RpL32[1]	$\Delta\Delta C_T$ ΔC_T-$\Delta C_{T,\ control}$[2]	Average Dys relative to control[3]	Dys mRNA fold reduction relative to control[4]
act-Gal4/+	21.25±0.11	15.60±0.03	5.65±0.11	0.00±0.16	1.00±0.11	1.00±0.11
Dys$^{N\text{-}RNAi}$:act-Gal4/+	23.47±0.06	16.49±0.03	6.96±0.07	1.33±0.13	0.40±0.04	2.51±0.23

[1] the ΔC_T value is determined by subtracting the average RpL32 C_T value from the average Dg (Dys) C_T value. The standard deviation of the difference is calculated from the standard deviations of the Dg (Dys) and RpL32 values using the following formula" $s=\sqrt{s_1^2 + s_2^2}$, where s=std dev;

[2] the calculation of the $\Delta\Delta C_T$ involves subtraction by the ΔC_T calibrator value. This standard deviation is determined the same as in 'a';

[3] the range given for Dg (Dys) relative to Control is determined by evaluating the expression: $2^{-\Delta\Delta CT}$ where the error is determined using regressional analysis;

[4] the fold reduction given for Dg (Dys) relative to Control is determined by evaluating the expression: $2^{\Delta\Delta CT}$ where the error is determined using regressional analysis.

Table S3. Frequency of muscle degeneration caused by reduction by one copy of screened genes in *Dys* and *Dg* mutant background

Gene name	Allele	Loss-of-function mutants									RNAi mutants						Control		
		DysDf x			*Dg^{O86}* x			*Dg^{323}* x			*$Dys^{N\text{-}RNAi}$:act-Gal4* x			*Dg^{RNAi}:tub-Gal4* x			*w^{1118}* x		
		degenerated muscles, %	n, analyzed muscles	χ^2-value	degenerated muscles, %	n, analyzed muscles	χ^2-value	degenerated muscles, %	n, analyzed muscles	χ^2-value	degenerated muscles, %	n, analyzed muscles	χ^2-value	degenerated muscles, %	n, analyzed muscles	χ^2-value	degenerated muscles, %	n, analyzed muscles	χ^2-value
w	*[1118]*	3.3±3.3	n=227	-	1.0±1.0	n=90	-	5.0	n=112	-	19.2±4.5	n=292	-	9.7±2.2	n=129	-	4.2±2.0	n=98	-
βv-Integrin	*[BG01037]*	27.2	n=258	17.19**	62.6	n=179	57.74**	NA	-	-	NA	-	-	NA	-	-	4.0	n=198	0.07
Cam	*[n339]*	21.8	n=55	12.20 **	6.7	n=75	2.86	0.0	n=20	3.20	74.3	n=35	31.30**	20.2	n=104	3.06	3.7	n=27	0.03
capt	*[E593]*	31.4	n=35	21.16**	0.0	n=60	0.50	0.0	n=22	3.20	45.3	n=137	9.76**	7.5	n=67	0.08	14.5	n=69	4.62*
	[E636]	44.0	n=50	33.32**	5.1	n=78	1.57	13.2	n=106	2.84	63.5	n=107	22.67**	21.9	n=96	3.90	0.0	n=7	2.40
CG34400	*[c03838]*	15.2	n=33	6.42*	32.1	n=28	27.37**	41.7	n=12	27.29**	37.5	n=16	5.27*	73.9	n=23	47.78**	9.1	n=11	0.14
CG7845	*[EMS-Mod4]* [1]	25.0	n=36	15.14**	37.0	n=54	32.24**	31.4	n=51	17.72**	16.7	n=12	0.06	28.6	n=35	8.36**	4.8	n=147	0.02
chif	*[BG02820]* [2]	41.9	n=105	31.27**	9.2	n=54	5.08*	18.5	n=91	6.64**	16.3	n=92	0.10	12.4	n=265	0.13	7.6	n=131	0.49
	[EY05746]	26.2	n=42	16.25**	8.8	n=114	4.71*	11.4	n=70	1.78	10.9	n=78	1.77	40.3	n=134	17.52**	10.9	n=82	2.15
	[A507], CyO	21.4	n=42	11.83**	NA	-	-	NA	-	-	NA	-	-	19.5	n=87	2.65	0.0	n=31	2.43
del	*[3]*	NA	-	-	NA	-	-	14.0	n=50	3.36	12.8	n=47	0.91	2.5	n=39	3.15	NA	-	-
	[KG10262]	0.0	n=50	2.72	2.6	n=38	0.10	5.9	n=17	0.001	16.8	n=113	0.05	6.0	n=17	0.46	NA	-	-
Dmn	*[k16109]* [2]	3.0	n=33	0.07	NA	-	-	3.0	n=33	0.12	20.0	n=20	0.001	6.5	n=123	0.29	NA	-	-
Fhos	*[EY09842]*	17.5	n=57	8.37**	9.0	n=155	4.90*	5.2	n=116	0.06	31.1	n=122	2.36	28.6	n=14	8.36*	0.0	n=36	2.43
	[A055]	32.0	n=25	21.73**	15.5	n=71	11.04**	21.3	n=47	8.90**	12.8	n=47	0.91	24.0	n=154	5.24*	2.3	n=44	0.12
Fkbp13	*[P962]*	2.9	n=34	1.60	16.6	n=28	12.20**	30.5	n=74	16.9**	15.4	n=13	0.22	5.9	n=41	0.50	3.4	n=29	0.01
gcm	*[KG01117]* [2]	13.3	n=160	4.87*	0.0	n=116	0.50	4.3	n=70	0.01	15.7	n=184	0.18	19.0	n=84	2.40	NA	-	-
	[rA87]	0.0	n=85	1.60	NA	-	-	12.2	n=41	2.23	13.1	n=61	0.80	8.0	n=26	0.03	NA	-	-
Grh	*[IM]*	0.0	n=21	1.60	2.8	n=72	0.17	3.4	n=58	0.04	8.7	n=52	3.22	5.4	n=56	0.72	7.5	n=53	0.45
Lis-1	*[k13209]* [2]	19.8	n=111	10.40**	9.0	n=109	4.90*	12.2	n=24	2.24	26.5	n=68	0.87	14.8	n=195	0.68	13	n=117	3.53
	[k11702]	31.8	n=22	21.54**	12.1	n=58	7.78**	0.0	n=41	3.20	9.6	n=48	2.56	14.5	n=62	0.59	8.7	n=103	0.94
	[G10.14]	37.5	n=16	27.01**	0.0	n=24	0.50	NA	-	-	19.1	n=68	0.02	9.9	n=81	0.03	0.0	n=72	2.43
mbl	*[E27]*	23.8	n=42	14.03**	12.0	n=25	7.69**	28.3	n=60	14.93**	40.0	n=70	6.63**	22.8	n=149	4.50*	1.0	n=98	0.93
nAcRa-30D	*[EY13897]* [2]	29.4	n=68	19.26**	4.5	n=176	1.13	6.5	n=93	0.02	8.9	n=146	3.07	8.8	n=90	0.001	NA	-	-
	[KG05852]	9.4	n=53	2.05	7.5	n=187	3.33	1.5	n=67	0.96	14.3	n=91	0.45	5.5	n=72	0.67	NA	-	-
Nrk	*[k14301]* [2]	37.5	n=48	27.02**	19.9	n=58	15.33**	47.0	n=34	32.33**	15.0	n=40	0.29	16.9	n=230	1.44	7.0	n=185	0.29
Pgk	*[KG07478]*	10.1	n=99	2.51	30.0	n=80	25.29**	NA	-	-	NA	-	-	NA	-	-	9.5	n=105	1.34
POSH	*[k15815]* [2]	1.1	n=90	0.32	0.0	n=82	0.50	0.0	n=75	3.20	10.8	n=37	1.82	18.2	n=33	2.02	6.6	n=61	0.18
Rack1	*[EY00128]* [2]	18.1	n=83	8.89**	5.6	n=107	1.96	33.3	n=15	19.45**	11.6	n=112	1.41	11.3	n=133	0.02	3.8	n=105	0.05
	[1.8]	11.1	n=27	3.21	10.3	n=68	6.09*	8.9	n=45	0.60	9.5	n=42	2.63	12.3	n=122	0.12	0.0	n=127	2.44
	[EE]	13.8	n=36	5.27*	19.7	n=132	15.13**	7.4	n=27	0.16	76.9	n=39	33.45**	19.0	n=216	2.40	7.3	n=82	0.38
robo	*[2]*	0.0	n=27	1.60	0.9	n=110	0.42	0.0	n=20	3.20	4.4	n=45	8.06**	0.9	n=107	5.73*	3.6	n=84	0.02
SP1070	*[UifE(br)155]* [3]	5.4	n=74	0.13	16.4	n=91	11.41**	4.0	n=20	0.05	30.7	n=88	2.20	13.8	n=94	0.41	18.1	n=105	7.46**
	[Uif2B7] [3]	14.1	n=142	5.52*	12.3	n=81	7.97**	4.4	n=91	0.02	37.6	n=117	5.33*	44.4	n=9	20.99*	21.1	n=90	9.99**
SP2353	*[MB00605]*	0.0	n=59	1.60	12.0	n=52	7.69**	18.5	n=40	6.64**	11.1	n=27	1.66	16.5	n=121	1.28	1.6	n=62	0.44
vimar	*[k16722]* [2]	4.3	n=46	0.06	4.6	n=55	1.20	54.8	n=73	39.82**	12.7	n=71	0.94	33.8	n=65	12.27**	11.2	n=89	2.33
	[09]	0.0	n=84	1.60	9.4	n=32	5.26*	16.4	n=110	5.05*	12.9	n=70	0.87	32.7	n=49	11.41**	0.7	n=142	0.93

All mutant alleles obtained from BDSC, except [1] – described previously (Kucherenko et al., 2008), [2] – obtained from DGRC, [3] – described previously (Zhang and Ward, 2009)

NA – not analyzed

The results were statistically compared using χ^2 test with one degree of freedom and Yates`s correction, *p≤0.05; **p≤0.01

Table S4. Other tested genes that did not show genetic interaction with DGC in muscles

Gene name	Allele	Loss-of-function mutants								
		DysDf x			Dg^{O86} x			w^{1118} x		
		degenerated muscles, %	n, analyzed muscles	χ^2-value	degenerated muscles, %	n, analyzed muscles	χ^2-value	degenerated muscles, %	n, analyzed muscles	χ^2-value
w	*[1118]*	3.3±3.3	n=227	-	1.0±1.0	n=90	-	4.2±2.0	n=98	-
argos	*[Delta7]*	4.6	n=131	0.01	2.9	n=173	0.21	10.1	n=158	1.69
Dl	*[RevF10]*	12.3	n=112	4.10*	5.0	n=159	1.50	12.0	n=125	2.85
dpp	*[KG08191]*	1.8	n=111	0.05	3.7	n=54	0.61	0.0	n=126	2.43
fra	*[3]*	10.7	n=178	2.90	7.7	n=52	3.73	11.6	n=69	2.59
hipk	*[BG00855]*	1.6	n=127	0.10	2.7	n=73	0.13	6.3	n=176	0.11
kek1	*[k07332]*	10.5	n=143	2.80	6.7	n=84	2.86	8.7	n=92	0.95
kis	*[BG01657]*	3.9	n=204	0.02	5.4	n=56	1.80	4.6	n=109	0.04
msk	*[5]*	NA	-	-	3.6	n=139	0.55	10.4	n=134	1.88
Sdc	*[10608]*	2.1	n=143	0.01	6.4	n=110	2.61	7.6	n=159	0.47
Sema-1a	*[k13702]*	10.7	n=56	2.93	3.5	n=116	0.50	12.1	n=99	2.93
Sema-2a	*[k11240]*	1.2	n=168	0.27	5.4	n=112	1.80	2.4	n=166	0.09
slit	*[1118]*	14.4	n=167	5.76*	8.9	n=112	4.80*	15.6	n=186	5.46*
stan	*[19alpha]*	0.8	n=122	0.52	7.7	n=91	3.73	1.6	n=63	0.44
wg	*[Sp-1]*	0.0	n=147	1.60	4.7	n=146	1.28	10.5	n=76	1.92

all mutant alleles obtained from BDSC;

NA – not analyzed;

the results were statistically compared using χ^2 test with one degree of freedom and Yates`s correction,

*p≤0.05

Table S5. Muscle degeneration in wild type and dystrophic animals in response to stress

[§]TMD - total muscle degeneration, EMD - extreme muscle degeneration,
[Ø]Statistics were calculated with one-way ANOVA and post Dannett's tests; the mean difference is significant at the 0.05 level,

	Experimental conditions	Genotype	Analyzed muscles, n	% of TMD (EMD)[§], Mean±SE	Statistical analysis[Ø], *p*			
					Within "experimental conditions"		Within "experimental group"	
					TMD	EMD	TMD	EMD
Experimental group 1	25°C, normal food, 13-15d old	*OregonR*	743	6.03±1.58 (0)	control		control[◊]	
		w^{1118}	461	6.01±0.34 (0)	*p*=1.000	-		
	18°C, normal food, 13-15d old (10d)*	*OregonR*	1091	2.65±0.78 (0)	control		*p*=0.843	-
		w^{1118}	426	3.28±2.03 (0)	*p*=1.000	-		
	33°C, normal food, 13-15d old (10d)*	*OregonR*	510	21.00±6.80 (1.50)	control		***p*=2x10^{-6}**	*p*=0.450
		w^{1118}	955	19.17±2.50 (1.02)	*p*=1.000	*p*=1.000		
	25°C, normal food, 25 d old	*OregonR*	1213	4.10±2.29 (0)	control		*p*=0.832	-
		w^{1118}	395	2.50±1.51 (0)	*p*=0.716	-		
	25°C, Paraquat, 13-15d old (10d)*	*OregonR*	633	14.79±6.26 (10.95)	control		***p*=0.01**	***p*=0.008**
		w^{1118}	75	11.92±6.26 (10.07)	*p*=1.000	*p*=1.000		
	25°C, sugar-free food, 13-15d old (10d)*	*OregonR*	279	4.80±1.10 (0)	control		*p*=0.656	*p*=1.000
		w^{1118}	685	6.17±1.07 (0)	*p*=0.999	*p*=0.978		
Experimental group 2	25°C, normal food, 8-10d old	*OregonR*	518	0.90±0.20 (0)	control		control for *OregonR*	
		DysDf	244	6.90±1.30 (0)	***p*=0.036**	-	control for *DysDf*	
		$Dg^{O86/O55}$	101	4.50±1.10 (0)	*p*=0.129	-	control for $Dg^{O86/O55}$	
	18°C, normal food, 8-10d old	*OregonR*	303	1.90±1.90 (0)	control		*p*=0.524	-
		DysDf	852	10.30±0.70 (4.63)	***p*=0.004**	*p*=0.166	*p*=0.348	***p*=0.050**
		$Dg^{O86/O55}$	256	7.90±2.20 (5.60)	***p*=0.049**	*p*=0.172	*p*=0.179	*p*=0.076
	33°C, normal food, 8-10d old (7d)*	*OregonR*	1309	4.10±0.70 (1.20)	control		*p*=0.127	*p*=0.232
		DysDf	711	13.80±1.50 (2.70)	***p*=1x10^{-4}**	*p*=0.762	*p*=0.125	*p*=0.310
		$Dg^{O86/O55}$	421	7.50±1.90 (2.50)	*p*=0.211	*p*=0.726	*p*=0.225	*p*=0.322
	25°C, Paraquat, 8-10d old (7d)*	*OregonR*	201	5.70±1.90 (0)	control		*p*=0.093	-
		DysDf	218	13.00±4.40 (0)	*p*=0.163	-	*p*=0.162	-
		$Dg^{O86/O55}$	186	10.50±1.60 (0)	*p*=0.485	-	*p*=0.051	-
Experimental group 3	25°C, normal food, 5d old	*OregonR*	166	1.00±1.00 (0)	control		control for *OregonR*	
		DysDf	174	4.80±2.50 (0)	*p*=0.087	-	control for *DysDf*	
		$Dg^{O86/O55}$	82	3.70±1.70 (0)	*p*=0.314	-	control for $Dg^{O86/O55}$	
	25°C, sugar-free food, 5d old (4d)*	*OregonR*	501	0.50±0.50 (0)	control		*p*=0.466	-
		DysDf	173	8.10±6.30 (0)	*p*=0.167	-	*p*=0.393	-
		$Dg^{O86/O55}$	541	10.80±4.40 (5.60)	***p*=0.050**	***p*=0.011**	***p*=0.044**	***p*=0.032**
	25°C, normal food 20d old	*OregonR*	98	3.00±3.00 (0)	control		*p*=0.881	-
		DysDf	131	21.00±2.60 (1.70)	***p*=0.004**	*p*=0.433	***p*=0.024**	*p*=0.317
		$Dg^{O86/O55}$	214	7.20±1.40 (3.65)	*p*=0.224	*p*=0.258	*p*=0.209	*p*=0.200

[◊]since there is no a statistically significant difference between the two control lines (*OregonR* and w^{1118}) within "experimental conditions" groups these two genotypes were treated as one data set in further analysis,
*in parenthesis is shown the time flies were kept at the experimental conditions

Table S6. Metabolic rate of DGC mutants and *OregonR* line under the normal and sugar-free food conditions

Genotype	CO_2 production under the normal food conditions[1] ($\mu lCO_2 \times hr^{-1} \times fly^{-1}$)	Number of measure-ments	CO_2 production under the sugar-free food conditions[1] ($\mu lCO_2 \times hr^{-1} \times fly^{-1}$)	Number of measure-ments	Fold decrease in metabolic rate on sugar-free food[1,2]
OregonR	2.20±0.15	n=10	0.43±0.14	n=3	5.12±0.46
DysDf	2.41±0.09	n=13	1.03±0.09	n=7	2.34±0.13
$Dg^{O86/O55}$	2.36±0.18	n=6	1.46±0.19	n=7	1.60±0.12

[1]Mean±SE

[2]to determine the fold reduction in CO_2 production the amount of CO_2 generated under normal food conditions was divided by the amount of CO_2 generated under sugar-free food conditions for each genotype tested.

Supplementary Figure Legends

Supplementary Fig. 1. DGC is localized in the sarcolemma of different *Drosophila* muscle types. Schematic view of *Drosophila* reproductive system (A) and intestinal tract morphology (B). Squares show part of the organ analyzed for presence of DGC in muscle tissue. (C-R, T-W) Detection of Dg and Dys (red in C-R, T-W and white in C'-R', T'-W') in oviduct (C-F), uterus (G-J), midgut (K-N), hindgut (O-R) and rectal ampulla (T-W) muscles. Both Dg and Dys are localized to the sarcolemma. Dystroglycan can also be seen to a lesser extent in regions correlated with Z-discs as indicated by Kettin (green in C-D, G-H, K-l, O-P and T-U) localization in uterus muscles. Neither Dg nor Dys staining is detected in Dg^{O86}/Dg^{O55} (D, H, L, P, U) or *DysDf* (F, J, N, R, W) loss-of-function mutants. (S, S') The Dystroglycan antibody localization was seen in heart muscles. Nuclei are visualized with DAPI.

Supplementary Fig. 2. DGC mutants have age-dependant muscle degeneration and climbing defects. (A-J) H&E-stained transverse (A-F, J) and longitudinal (G-I) IFM sections from 10 day old (A-C) and 20 day old (G-J) *DysDf*, Dg^{O86}/Dg^{O55} and $DysDf/Dg^{O86}$ mutants and wild type flies. Ten day old mutant flies exhibit mild changes in muscle tissue morphology, while 20 day old flies have more deteriorated muscles (arrows) and exhibit cases with severe loss of muscle tissue (arrowheads). Muscle degeneration is seen more often from the muscle termini (H); on transverse sections degenerated muscles are pale and form vacuoles indicating necrosis (I). Dystrophin homozygous viable (*DysDf*) flies and Dystroglycan semi-lethal transheterozygotes Dg^{O86}/Dg^{O55} show reduced ability to climb (K). Statistics were done using Student's t-test, **p≤0.01, *** p≤0.001. Oil red O-stained IFMs of *WT* (L) and *DysDf* (M) flies. Intramuscular lipid droplets are indicated with arrows. In addition, the different behavior in *Dys* and *Dg* mutants was noticed: while *Dys* deficient flies were shaking and not able to climb, the *Dg* mutant animals performed uncoordinated movements and jumped randomly.

Supplementary Figure 1

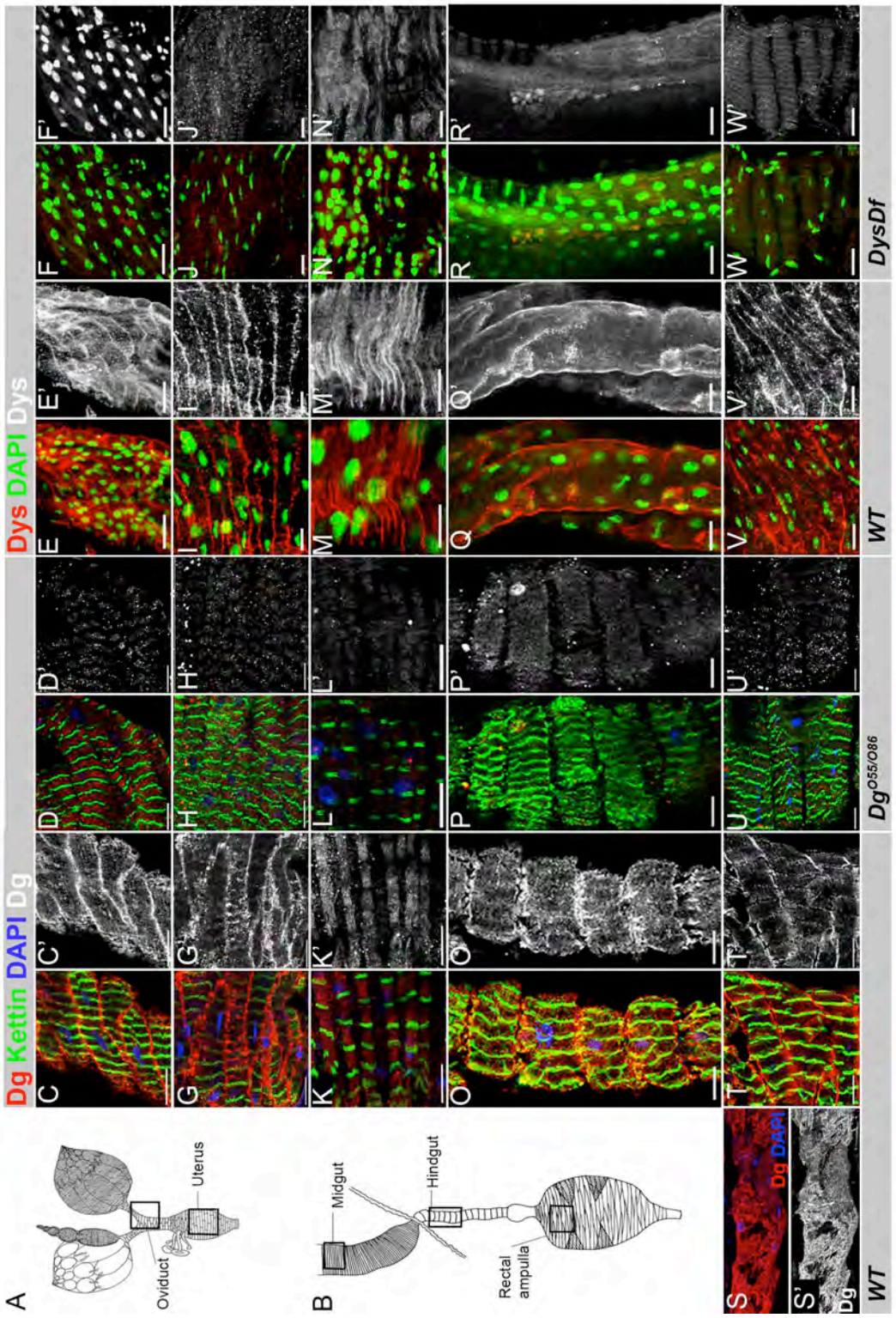

Supplementary Figure 2

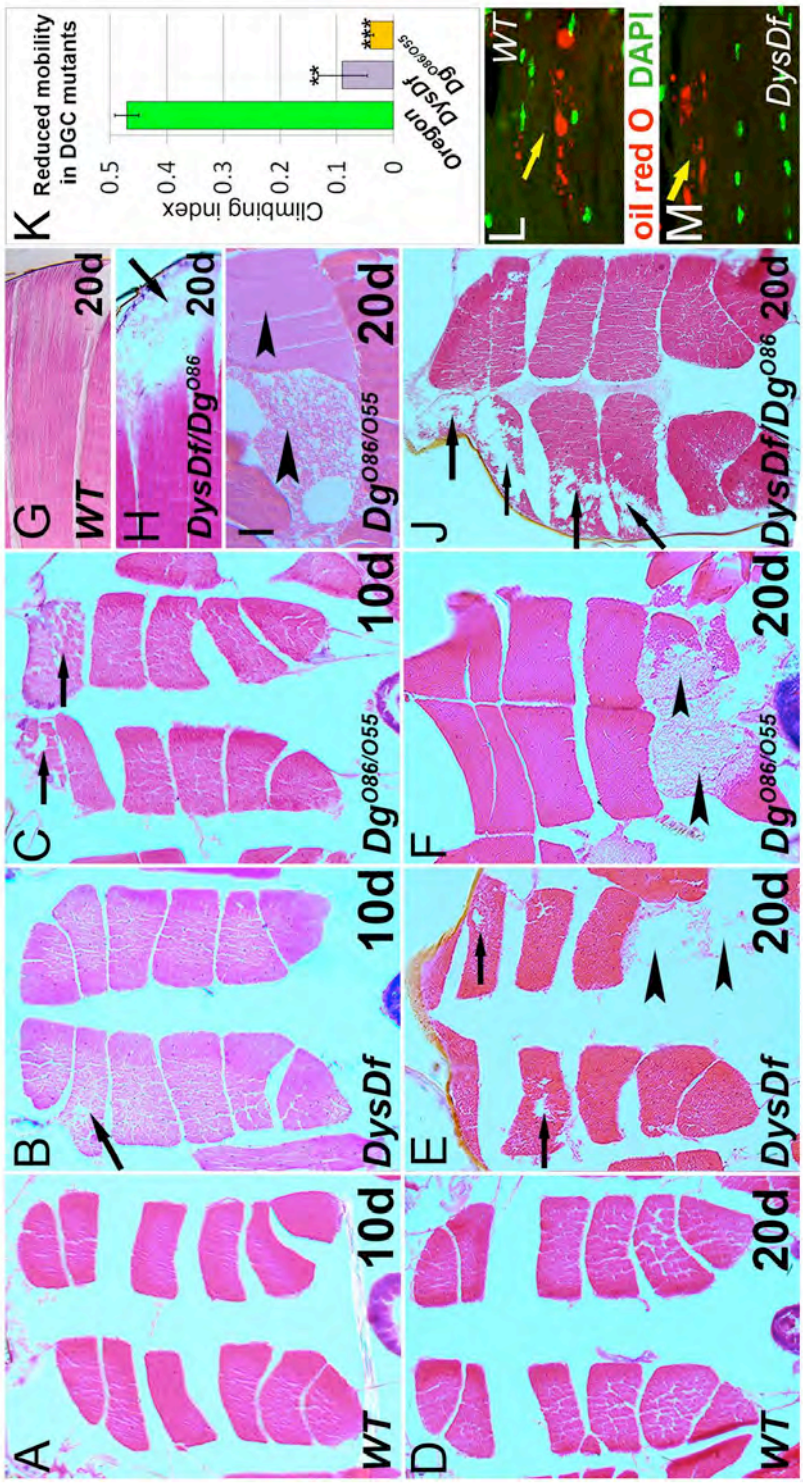

SCIENTIFIC REPORTS

94

OPEN

SUBJECT AREAS:
SYNAPTIC TRANSMISSION
MODEL ORGANISMS
DROSOPHILA
DEVELOPMENTAL BIOLOGY

Received
20 June 2011

Accepted
14 July 2011

Published
28 July 2011

Correspondence and requests for materials should be addressed to H.R.S. (halyna.shcherbata@mpibpc.mpg.de)

Hyperthermic seizures and aberrant cellular homeostasis in *Drosophila* dystrophic muscles

April K. Marrone[1], Mariya M. Kucherenko[1], Robert Wiek[2], Martin C. Göpfert[2] & Halyna R. Shcherbata[1]

[1]Max Planck Gene Expression and Signaling Group, Max Planck Institute for Biophysical Chemistry, Am Fassberg 11, 37077, Göttingen, Germany, [2]Department of Cellular Neurobiology, Georg August University, Max Planck Institute for Experimental Medicine, Hermann Rein 3, 37075 Göttingen, Germany.

In humans, mutations in the Dystrophin Glycoprotein Complex (DGC) cause muscular dystrophies (MDs) that are associated with muscle loss, seizures and brain abnormalities leading to early death. Using *Drosophila* as a model to study MD we have found that loss of Dystrophin (Dys) during development leads to heat-sensitive abnormal muscle contractions that are repressed by mutations in Dys's binding partner, Dystroglycan (Dg). Hyperthermic seizures are independent from dystrophic muscle degeneration and rely on neurotransmission, which suggests involvement of the DGC in muscle-neuron communication. Additionally, reduction of the Ca^{2+} regulator, Calmodulin or Ca^{2+} channel blockage rescues the seizing phenotype, pointing to Ca^{2+} mis-regulation in dystrophic muscles. Also, Dys and Dg mutants have antagonistically abnormal cellular levels of ROS, suggesting that the DGC has a function in regulation of muscle cell homeostasis. These data show that muscles deficient for Dys are predisposed to hypercontraction that may result from abnormal neuromuscular junction signaling.

Muscular dystrophy (MD) patients have progressive muscle weakening and loss and so far no cure exists to treat these fatal disorders. Many forms of MDs are associated with abnormalities in the evolutionary conserved Dystrophin Glycoprotein Complex (DGC) that links the extracellular matrix (ECM) to the cytoskeleton[1]. Dystrophin (Dys) is the main component of the DGC required for muscle stability and is found at extrasynaptic and synaptic regions of muscle fibers where it is required for neuromuscular junction (NMJ) development[2]. Dys structurally links cytoskeletal actin to the ECM via the glycoprotein Dystroglycan (Dg), where Dys also binds several other proteins (two syntrophins, two dystrobrevins, and four sarcoglycans)[3–4]. Improper association between muscle and the surrounding basal lamina is found in a variety of MDs and cardiomyopathies[5–7].

The DGC has been also shown to play a role in cellular signaling processes that require Dg extracellular binding to Laminin. For example, G-protein binding to Syntrophin activates PI3K/Akt signaling in a manner that is dependent upon Laminin-Dg interaction[8], as well Syntrophin phosphorylation has been shown to be dependent upon this interaction resulting in Syntrophin-Grb2-Sos1-Rac1-Pak1-JNK signaling[9]. Additionally, the DGC is involved in TRPC channel activation at the muscle sarcolemma where Syntrophin regulates cation influx via anchoring the store-operated channels that are critical for normal calcium homeostasis in muscle cells[10–11].

Recently *Drosophila* has been shown to be a suitable genetic model to study the DGC[12]. Initial characterization of the DGC in *Drosophila* has portrayed that components studied so far are evolutionary conserved[13] and DGC deficiencies lead to age dependent muscle degeneration, reduced mobility, dilated cardiomyopathy and a shorter life span[12,14–15]. Using this *Drosophila* MD model we previously performed *in vivo* genetic screens in ageing dystrophic muscles to find novel DGC interactors[16]. These interactors were divided into three main functional groups: mechanosignaling, cellular stress response, and neuron-muscle communication. While the role of the DGC in providing muscle integrity has been extensively studied, its function in muscle-neuron communication has not been fully defined.

Since our previous data showed that the DGC mutants and the interactors found in the screen show mobility defects that are intensified by higher temperatures, we decided to analyze the reason for this behavioral defect. Temperature induced walking disability can originate from muscle or neuron malfunction. Here we measured the muscle activity on live dystrophic animals and showed that *Drosophila Dys* mutants have muscle defects resulting in seizures. These seizures robustly occur at elevated temperatures that seem to enhance an underlying

physiological defect. On further inspection we have determined that this phenotype is only displayed when Dys is downregulated during development of muscles, implying a developmental requirement for Dys. Surprisingly, the seizure phenotype is not shared by, and repressed by mutations in, the binding partner of Dys, Dg, possibly due to malfunctioning of the NMJ. In addition, we show that a deficiency in the Ca^{2+} regulator Calmodulin (Cam) and calcium channel blockers rescue the *Dys* phenotype, suggesting that Ca^{2+} plays a role in dystrophic seizures. Under stress *Dys* and *Dg* mutants have altered levels of ROS suggesting that these proteins play a role in maintaining cellular homeostasis. These results reveal novel dynamics between two components of the DGC and their interaction.

Results

In a previous report we showed that the DGC is involved in the stress response pathway and that energetic stress and changes in the ambient temperature accelerate dystrophic muscle degeneration[16]. Therefore we decided to test if dystrophic animals show abnormal cellular homeostasis. Since elevated temperatures enhance cellular responses[17–18], we measured the amount of lipid peroxidation products which are the result of reactive oxygen species (ROS) of animals kept for three days at 29°C (higher than ambient, but not heat shock temperature). *Dys* mutants had a strikingly larger amount of lipid peroxidation products than did *wt* animals (Fig. 1a). Inversely, *Dg* mutants have significantly decreased ROS levels relative to control. Though heterozygous single mutants (*Dys*/+ and *Dg*/+) do not have

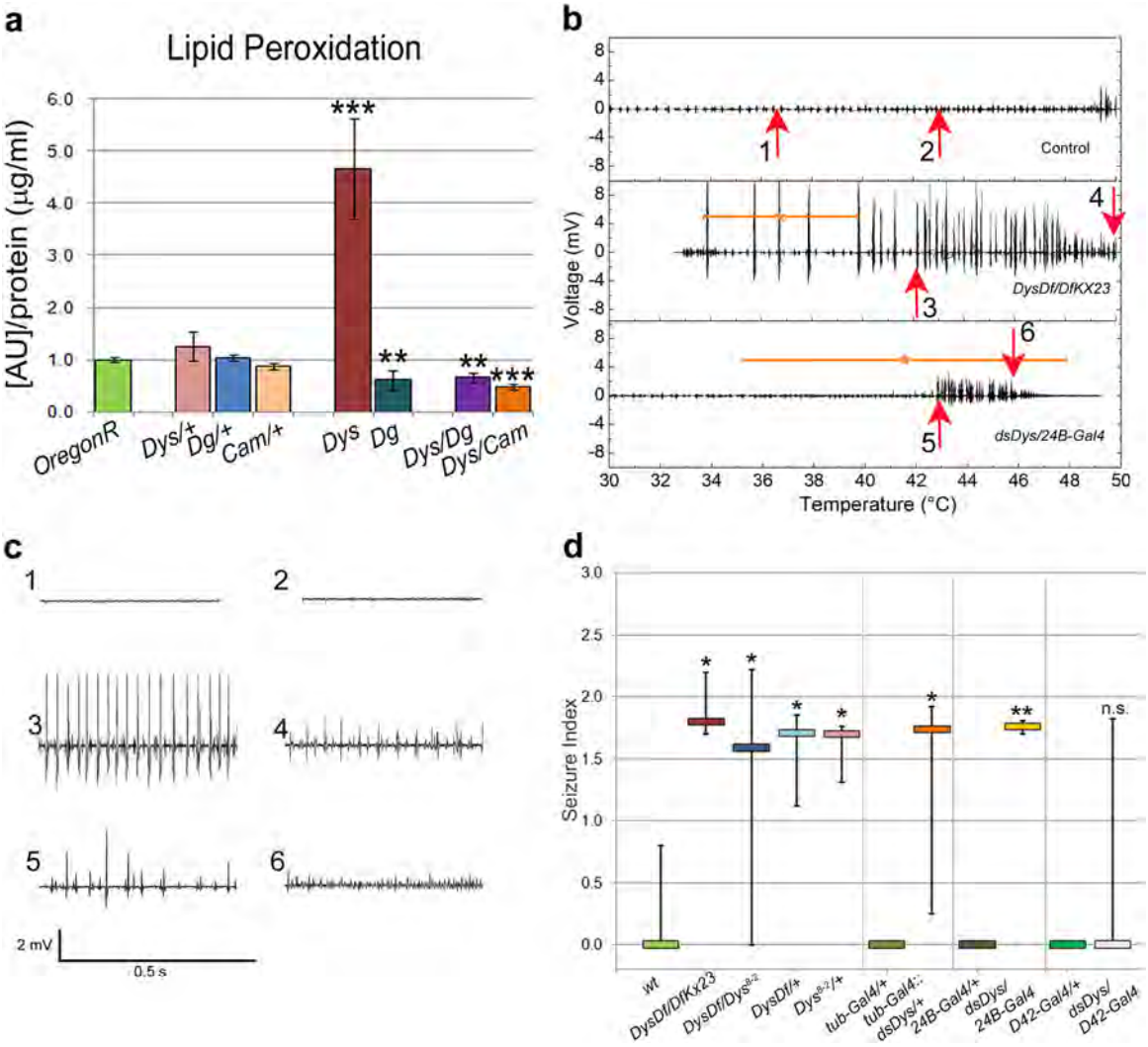

Figure 1 | *Dystrophin* mutants have elevated ROS and hyperthermic seizures. (a) Assessment of cellular lipid peroxidation products normalized to protein content in animals housed at 29°C for three days. The axis represents the raw molar absorption after blank subtraction and normalization to protein content. Statistical analysis was done using a one-tailed Student's t-test and the error bars represent the standard deviation. All comparisons are made against *OregonR*. Exact experimental values and P-values are given in Supplementary Table 1. (b) Electrical output from IFM vs. temperature during seizures of *DysDf/DfKX23* and *dsDys/24B-Gal4* mutants compared to Control. Stars indicate the average start temperature where the error bar indicates the standard deviation. Arrows indicate where plots in panel c are taken from. (c) Electrical output relative to time where the region examined correlates with the numbered arrows in panel b. Output is displayed over a 0.5 s time period emphasizing the increase in frequency and decrease in amplitude as the seizure progresses. (d) All tested *Dys* classical and *RNAi* alleles (levels of *Dys* mRNA downregulation are shown in Supplementary Table 2) had hyperthermic seizures with similar seizure indices tested in a two-tailed Kruskal-Wallis test where P=0.316 excluding data from *dsDys/D42-Gal4* animals (Supplementary Figure 1, Table 1). Seizure indices of dystrophic mutants are significantly higher when compared to the appropriate control (separated by vertical lines). One to one comparative statistics were done using a one-tailed Mann-Whitney U-test. Error bars indicate the 25th and 75th percentiles of the data spread considering that if an animal does not seize then the index is 0. The S_i range of some controls have zero values in the 25th and 75th percentile range, thus it appears that there is no error bar.*P ≤ 0.05, **P ≤ 0.01, ***P ≤ 0.001.

changed ROS levels, the levels are significantly decreased in double heterozygous mutants (*Dg*/+; *Dys*/+) indicating that these two proteins interact in maintaining proper ROS cellular levels (Fig. 1a).

Cellular homeostasis depends on Ca^{2+} levels and a protein regulating proper calcium levels, Calmodulin (Cam) was found to interact with Dys leading to muscle degeneration[16]. We analyzed ROS levels of animals heterozygous for both *Cam* and *Dys* (*Cam*/+; *Dys*/+) and observed a significant decrease in ROS levels indicating that these two proteins genetically interact (Fig. 1a), suggesting that Dys-dependent cellular stress depends on Ca^{2+} levels.

Next, we applied higher than ambient temperatures to *Dys* classical and *RNAi* mutants to examine *in vivo* dystrophic muscle function in increased temperature conditions. This revealed a complex physiological defect that can be measured by electrophysiological recordings from indirect flight muscles (IFMs). All *Dys* mutant animals at temperatures ranging anywhere from 30–46°C started to have abnormal muscle contractions (seizures) (Fig. 1b–d, Supplementary Fig. 1). These seizures slowly decreased in amplitude while increasing in frequency. When a seizure occurred a seizure index (S_i) was calculated taking into consideration the amplitude and duration of the seizure as well as the temperature seizing started at. If an animal did not have a seizure then the S_i was assigned a value of zero (Table 1). Using different *Dys* allelic combinations we observed that 60–100% of dystrophic animals had seizures with the median S_i ranging from 1.6 to 2.4, while the median S_i for control animals was 0 (Table 1).

To understand the origin of this phenotype, we downregulated *Dys* in different tissues using specific *Gal4* drivers and *Dys RNAi*. Animals with ubiquitous and mesodermal *Dys* downregulation showed a strikingly similar phenotype to that seen with the allelic mutations (Fig. 1b,d). Contrarily, the indices were not significantly greater compared to control when *Dys RNAi* was expressed using a

Table 1 | Seizure Indices (S_i)

Genotype	n	% seized[Ŧ]	Avg. $T_s \pm$sd (°C)*	Avg. $A_{max} \pm$sd (mV)*	Avg. Area $\pm$sd (pixel $\times 10^{-3}$)*	Median S_i** ($25^{th}/75^{th}$ percentiles)	[+]P-value
OregonR	7	29	40.7±6.1	12.2±13.4	2.9 ± 2.4	0.0 (0.0/0.9)	0.944
w^{1118};*CyO*/+; *TM6*/+	4	25	46.4	2.6	1.3	0.0 (0.0/0.4)	($\chi^2 = 0.115$)
w^{1118};*CyO*/*Pin*	4	25	38.3	14.3	6.9	0.0 (0.0/0.6)	
*wt****	15	24	42.1±4.1	14.0±13.8	4.5±2.9	0.0 (0.0/0.8)	-
DysDf/*DfKX23*	5	80	37.0±3.1	6.0±5.2	2.4 ± 2.0	**1.8 (1.7/2.2)**	**0.028***
DfKX23/+	4	100	43.0±3.3	11±6.8	4.9 ± 5.4	**1.8 (1.5/2.2)**	**0.011***
DysDf/$Dys^{8\text{-}2}$	10	60	40.8±6.4	13±6.4	4.2 ± 2.9	**1.6 (0.0/2.2)**	**0.045***
$Dys^{8\text{-}2}$/+	5	80	40.2±8.2	3.3±1.7	1.4 ± 0.8	**1.7 (1.3/1.8)**	**0.045***
DysDf	9	89	35.2±4.7	7.7±6.4	4.9 ± 3.7	**2.4 (2.2/2.4)**	**2.6×10^{-4}*****
DysDf/+	8	75	39.6±3.5	8.7±5.3	2.4 ± 2.5	**1.7 (1.1/1.8)**	**0.050***
[◇]$Dg^{-/-}$	9	11	45.3	5.6	1.3	0.0 (0.0/0.0)	0.19
Dg^{O86}/+;*DysDf*/+	10	20	38.0±7.6	5.2±2.9	2.8 ± 0.3	0.0 (0.0/0.0)	0.50
[•]$para^{ts1}$/+; *DysDf*/+	5	0	0	0	-	-	0.28
$cora^{k08713}$	8	0	-	-	-	-	0.15
$cora^{k08713}$/+; *DysDf*/+	8	12.5	36.0°C	5.2	5.6	0.0 (0.0/0.0)	0.41
[•]Cam^{n339}/+; *DysDf*/+	7	0	-	-	-	-	0.19
tub-Gal4/+	10	20	42.5±5.5	2.6±0.1	1.6±0.4	0.0 (0.0/0.0)	-
tub-Gal4::dsDys/+	10	70	40.1±5.8	4.5±2.1	2.3 ±1.8	**1.7 (0.2/1.9)**	**0.020***
tub-Gal4::dsDg/+	8	50	43.6±2.6	4.1±2.1	1.2 ±0.7	0.7 (0.0/1.6)	0.19
tub-Gal4::dsDys/dsDg [£]	6	50	44.2±5.3	12±13.4	0.8 ±0.2	0.7 (0.0/1.4)	0.29
tub-Gal80^{ts}/+, *tub-Gal4::dsDys*/+ – Put to 29°C after eclosion	14	29	45.7±2.4	10±5.8	2.1 ± 1.2	0.0 (0.0/0.9)	0.47
tub-Gal80^{ts}/+, *tub-Gal4::dsDys*/+ – Put to 29°C as L3 larvae	13	77	40.1±4.9	7.9±5.2	4.2 ± 4.2	**2.0 (1.7/2.2)**	**3.7×10^{-4}*****
tub-Gal80^{ts}/+, *tub-Gal4::dsDg*/+ – Put to 29°C after eclosion	5	0	-	-	-	-	0.40
tub-Gal80^{ts}/+, *tub-Gal4::dsDys/dsDg* – Put to 29°C after eclosion	6	17	48.2	5.1	0.4	0.0 (0.0/0.0)	0.34
$para^{ts1}$/+; *tub-Gal4::dsDys*/+	5	0	0	0	-	-	0.40
CyO(Pin)/+;*24B-Gal4*/+	4	0	-	-	-	-	-
dsDys/*24B-Gal4*	5	100	41.5±6.3	5.8±4.1	3.1 ± 2.7	**1.8 (1.7/1.8)**	**0.0079****
dsDg/*24B-Gal4*	5	0	-	-	-	-	1.0
D42-Gal4/+	4	0	-	-	-	-	-
dsDys/*D42-Gal4*	5	40	37.8±8.2	5.7±5.2	2.3 ± 0.8	0.0 (0.0/1.8)	0.28
dsDg/*D42-Gal4*	5	0	-	-	-	-	1.0

n = number of animals measured for the specified genotype
[Ŧ]percent of animals measured that had a seizure
*Calculated using data from animals that seized only
**Index calculated by integrating the area of the graph of voltage vs. temperature during a seizure, taking the natural logarithm of this number, dividing by the temperature that the seizure started, and then multiplying times ten. A S_i of zero was assigned to animals that did not seize
***There is no difference between animals of genotypes *OregonR*, w^{1118};*CyO*/+;*TM6*/+ or w^{1118};*CyO*/*Pin* as assessed using a Kruskal-Wallis test. These animals were pooled and termed *WT*.
[+]P-values are relative to the control animals at the beginning of each shaded section, *P ≤ 0.05, **P ≤ 0.01, ***P ≤ 0.001
[◇]Five animals were of genotype $Dg^{O86/O55}$, two were of genotype Dg^{O86} and two were of genotype Dg^{O86}/+ where one animal of genotype $Dg^{O86/O55}$ had a seizure
[£]Four animals were of genotype *tub-Gal4::dsDg/dsDys* and two animals were of genotype *tub-Gal4::dsDys/dsDg*
[•]Animals of genotype $para^{ts1}$/*Y* and Cam^{n339}/+ did not have seizures (n=2)

motoneuron driver (Fig. 1d). From these data we conclude that seizures are a result of the lack of Dys in muscle tissue, but not in motoneurons.

The occurrence of temperature-sensitive seizures could be due to a problem arising upon Dys deficiency during muscle establishment or maintenance. To allow for developmental stage-specific downregulation of Dys, *RNAi* transgenic constructs were combined with the *Gal80* temperature-sensitive system that suppresses expression of constructs until the animals are transferred to 29°C. When *Dys RNAi* animals were shifted to 29°C after muscle development and synapse maturation is completed, a significant decrease in seizure indices took place compared to a Dys deficit in development (Fig. 2a,b). This evidence shows that Dys is required during development to prevent heat induced seizures.

Animals expressing *Dys RNAi* during development have properly developed muscles, which degenerate only as the animal ages[12]. To determine if previously shown age-dependent muscle degeneration is a result of the seizure activity described here, *Dys RNAi* animals were allowed to develop at a permissive temperature (no *RNAi* expression) and aged at the restrictive temperature after adult muscle and NMJ formation. Although the animals no longer had seizures, they exhibited muscle degeneration similar to animals with temporally unrestricted *Dys* downregulation (Fig. 2c,d, Supplementary Table 4). Importantly, seizing is not the result of aging since *wt* older animals still do not seize and older *Dys* mutants have a reduced occurrence of seizures (~50%). Perhaps, degenerating muscle is unable to respond in the same manner as young intact muscle. This result implies that the absence of Dys influences muscle degeneration and seizures independently.

The seizures in *Dys* mutants could be due to either muscle autonomous mis-regulation or inability to properly respond to synaptic input. To test if a neuronal contribution is required we used a previously described temperature-sensitive mutation in the *paralytic* gene that abolishes neuronal action potentials at temperatures above 29°C in adults (Fig. 2e)[19–20]. Opposite to *Dys* heterozygous and *RNAi* mutants, the introduction of the $para^{ts1}$ allele into a dystrophic background prevented seizures suggesting that neuronal transmission is required to trigger contractions in dystrophic muscles.

We initially believed that mutations in Dys's binding partner, *Dg* would phenocopy the dystrophic seizure phenotype. Surprisingly, *Dg* loss-of-function mutants exhibit no seizing activity (Fig. 3a,b, Table 1). Ubiquitous *Dg RNAi* expression produced some small low occurrence seizures, but specific expression in the mesoderm and motoneurons caused no seizures (Supplementary Fig. 3). Even more, *Dg/+;Dys/+* transheterozygous animals did not have heat-induced contractions (Fig. 3a,b, Table 1). This reveals that seizure susceptibility at high temperatures can be reduced by loss of one copy of *Dg*.

It has been shown that at *Drosophila* larval NMJs Dys is not localized in the absence of Dg, while Dg localization is only partially dependent upon Dys[20]. Accordingly, we found that at adult dystrophic NMJs Dg is reduced (Fig. 3c,d), while in transheterozygous mutants (*Dg/+;Dys/+*) Dg is missing from the NMJ similar to *Dg* loss-of-function mutants (Fig. 3c,d, Supplementary Table 5). Based on this evidence, we propose that the presence of Dg at the NMJ is necessary for *Dys* mutants to have temperature-induced seizures. This conclusion is further supported by the fact that animals expressing both *Dg* and *Dys RNAi* (causing Dys and Dg levels to be reduced but not abolished, Supplementary Table 1,6) have lower seizure occurrence than *Dys RNAi* mutants (Table 1).

Since Dys and Dg are the key components of the DGC, integrity of which is crucial for proper muscle function and maintenance, we

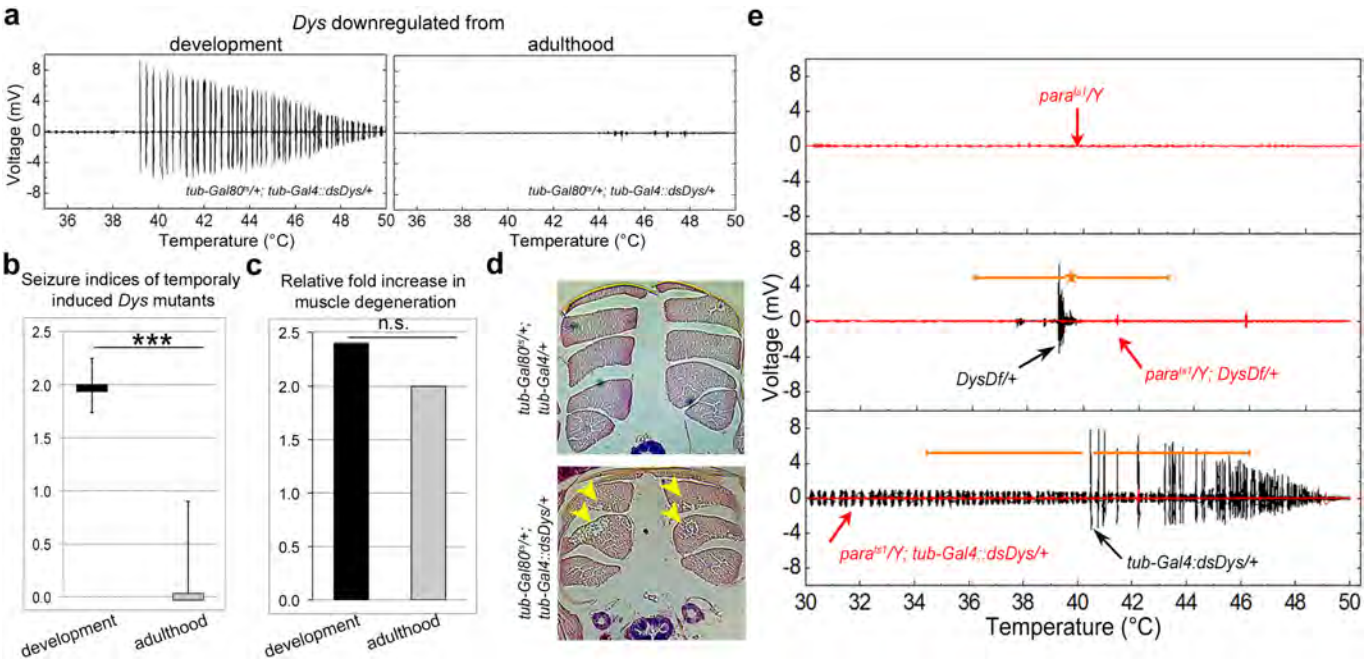

Figure 2 | Dystrophic seizures are dependent upon neuronal input that require Dys during development. (a) Electrical output of animals shifted to the restrictive temperature as late L3 larvae (left) and as adults (right). Dys protein reduction levels using the *Gal80* temperature sensitive system are given in Supplementary Table 3 and Supplementary Figure 2. (b) Seizure indices for *RNAi* mutants after being shifted to the restrictive temperature at different life stages. A Mann-Whitney U-test was used to compare seizure indices upon *Dys* downregulation in adulthood to *Dys* downregulation in development ($P = 0.007$). *Dys* downregulation in adulthood resulted in a S_i that is not significantly different from control (*tub-Gal4/+*, $P = 0.47$, Table 1). In addition, animals of the genotype *tub-Gal80^{ts}/+;tub-Gal4/+* shifted as adults did not have seizures ($n = 2$). (c) Bar graphs showing relative fold increase in the frequency of muscle degeneration of *Dys RNAi* mutants targeting *Dys* throughout the lifetime or shifted to the restrictive temperature as adult. The percent of muscle degeneration has been normalized to that in control animals under the same conditions (Supplementary Table 4). Statistics for muscle degeneration were done using a one-tailed chi-square test ($\chi^2=2.62$, $P = 0.11$). (d) Histological sections of thoracic muscles. Arrows indicate areas of degeneration. (e) The $para^{ts1}$ allele abolishes seizures in *DysDf/+* and *tub-Gal4::dsDys/+* animals (red plot). *P ≤ 0.05, **P ≤ 0.01, ***P ≤ 0.001.

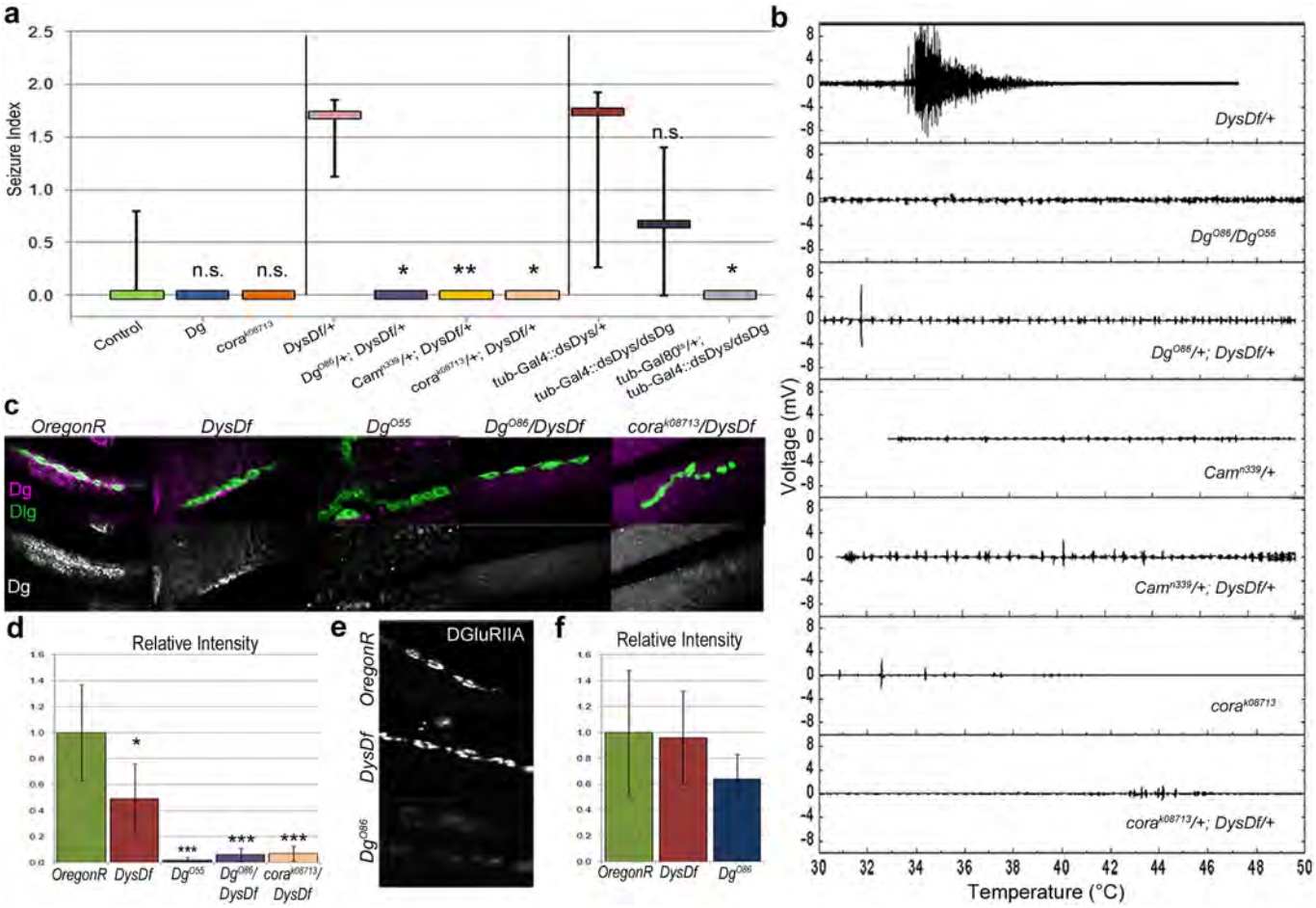

Figure 3 | Loss of Dystroglycan, Coracle or Calmoduline represses the seizure phenotype of *Dystrophin* mutants. (a) Seizure indices show that *Dg* and *cora* mutants do not have seizures (Table 1) and mutations in *Dg*, *Cam* or *cora* suppress the seizure phenotype in *Dys* transheterozygous animals ($P = 0.032$, 0.006 and 0.017 respectively when compared to *Dys*/+ animals). Animals carrying *RNAi* constructs against both *Dys* and *Dg* also showed a 50% decrease in seizure activity when downregulated during development and 17% when downregulated after development indicating a repression of the phenotype by downregulation of Dg ($P = 0.072$ and 0.017 respectively compared to *Dys RNAi* mutant, Table 1). Statistics were done using a one-tailed Mann-Whitney U-test. (b) Electrical output from IFM vs. temperature. (c) In control animals Dg (magenta) is localized to the NMJ. *Dys* mutants have a decreased amount of Dg at the NMJ, but some Dg localization is still observed. *Dg* mutants have no Dg localized to the NMJ. Transheterozygous animals (*Dg*/+;*Dys*/+, *cora*/+;*Dys*/+) show a significant decrease in Dg staining at the NMJ as well. The overall structure and presence of NMJs does not appear to be altered in the mutants as can be seen via Dlg staining (green). (d) In adult abdominal NMJs DGluRIIA is localized similarly in *Dys* mutants as in the wild type (*OregonR*) animals; however, *Dg* loss-of-function mutants have a decreased amount of the receptor. Statistics on relative intensities were done using a Student's t-test compared to *OregonR* where the error bars represent the average deviation from the mean. *$P \leq 0.05$, **$P \leq 0.01$, ***$P \leq 0.001$.

wanted to understand why *Dg* mutants do not have seizures while *Dys* mutants do. First, we considered that *Dg* mutants do not have temperature-sensitive seizures due to compensatory mechanisms. Integrins are likely candidates, as alpha (7B) integrin has been shown to compensate for Dg absence in mediating cell-extracellular matrix attachment[21]. If integrins are making up for loss of Dg, then trans-heterozygous animals might have enhanced seizures. However, the reduction of both *integrin* and *Dg* (mys^1/+;*Dg*/+) leads to a similar phenotype as mys^1/+ heterozygous animals, indicating that there is no genetic interaction between these two proteins in seizure occurrence (Supplementary Fig. 4).

Drosophila NMJs are glutamatergic, and previously it has been shown that Dg is required for proper localization of postsynaptic glutamate receptors at larval NMJs[20,22]. Since the amount of glutamate receptors influences muscle-neuron communications, we next analyzed the localization of glutamate receptor type II A (DGlulRIIA) at the adult NMJ. We found that *Dg* mutants have an approximately 40% decrease in the levels of the glutamate receptor at the NMJ (Fig. 3e,f). Conversely, this receptor in *Dys* mutants is localized like in *wt* animals (Fig. 3e,f) which is in accordance with previous reports on larvae[20,23]. This indicates that the seizing phenotype observed in *Dys* mutants is not due to mislocalization of DGlulRIIA.

Next, in order to analyze if the rescue of the seizing phenotype observed in *Dys*/+;*Dg*/+ transheterozygous mutants is due to interaction of Dys and Dg at the NMJ we used mutants of Coracle (Cora), a protein that is localized to the NMJ. Cora is the *Drosophila* homologue of mammalian brain 4.1 proteins[20] and it has been shown that Cora and Dg protein concentration at the NMJ are co-dependent[20]. Since in *cora*/+;*Dys*/+ mutants Dg is not properly localized to the adult NMJ (Fig. 3c,d), it would be expected that *cora* mutants should behave the same as *Dg* mutants and rescue dystrophic hyperthermic seizures, if they depend on DGC function at NMJs. Hypomorphic *cora* mutant animals exhibit a mild heat-induced muscle contraction phenotype of their own (Fig. 4a,b), but this activity is not of the nature described here, therefore no seizure indices were calculated for these animals. Data derived from *Dys* and *cora* transheterozygous animals (*cora*/+;*Dys*/+) mimicked that of the *cora* mutants and, similar to Dg reduction, rescued dystrophic seizures (Fig. 3a,b). Based on these data and previous reports of increased neurotransmitter release at dystrophic larval NMJs[23–24],

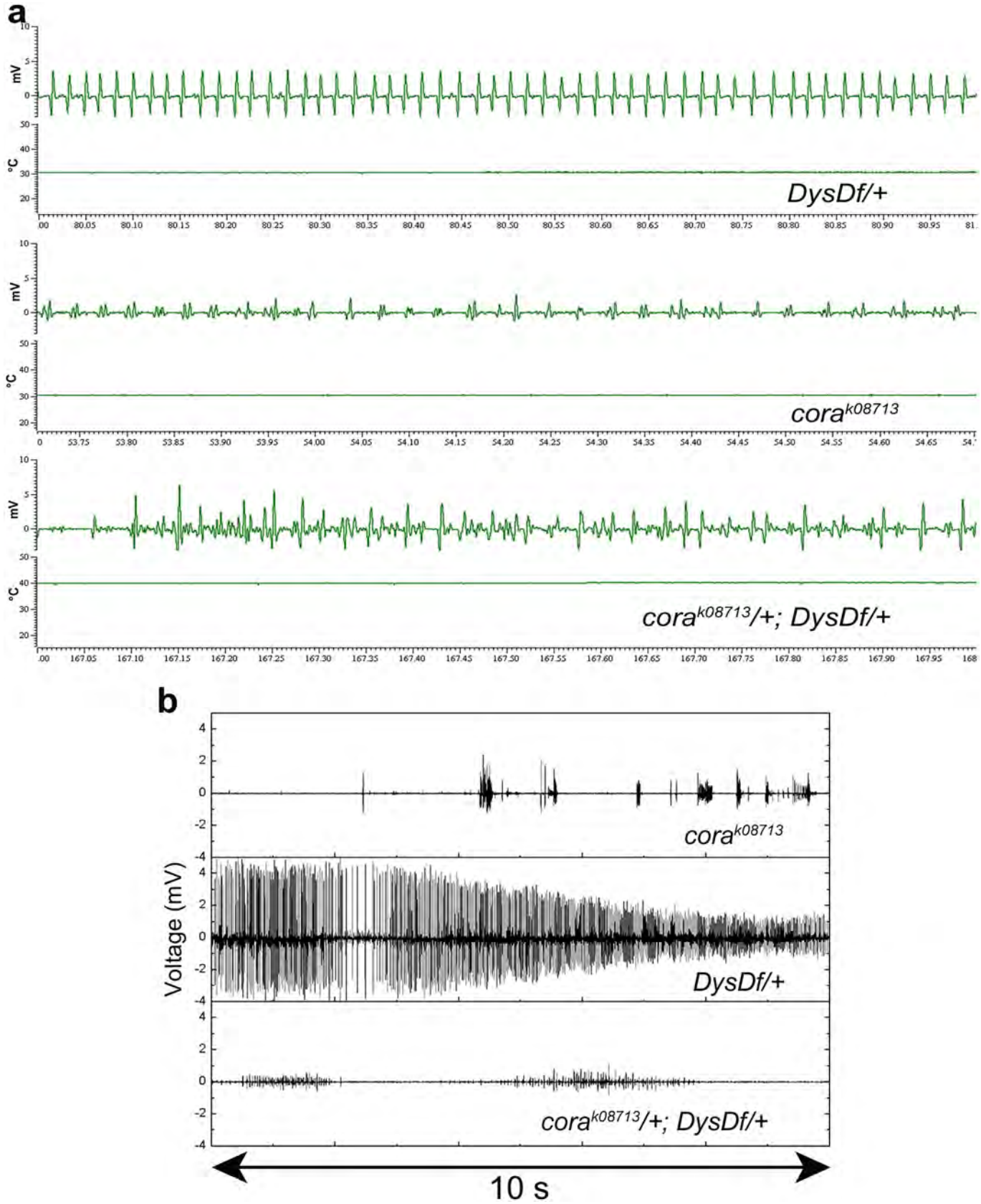

Figure 4 | ***Cora*** **mutants have a mild seizure phenotype that does not look like and overrides the dystrophic phenotype.** Mutation in the *cora* gene results in a distinctive electrophysiological phenotype from that seen with *Dys* heterozygous mutations. (a) *cora*^{k08713} mutants have electrical output that is not of a consistent frequency. Animals of genotype *cora*^{k08713}/+; *DysDf*/+ have a phenotype similar to the *cora* mutant. The output is recorded over 1 second. (b) Examples of the two types of electrical activity measured in *cora*^{k08713}, *DysDf*/+ and *cora*^{k08713}/+; *DysDf*/+ animals. The output is recorded over 10 seconds.

we suggest that hyperthermic seizures are derived from the improper function of the DGC at the NMJ.

Release of neurotransmitter at the NMJ results in depolarization of the muscle membrane causing release of Ca^{2+} from the SR required for muscle contraction. Thus, we examined how the Ca^{2+} binding protein, Calmodulin, which binds to DGC components dystrophin and syntrophins in mammals[25], affects the dystrophic seizure phenotype. In *Drosophila* there is only one gene encoding Cam that is homologous to the human CAM2 gene with 97% identity[26]. Introduction of a *Cam* null mutation into a *Dys* mutant background (*Cam*/+;*Dys*/+) rescued hyperthermic seizures (Fig. 3a,b). Since Cam regulates levels of Ca^{2+}, our data implies that Ca^{2+} levels are important for the dystrophic seizure activity.

Previous work has demonstrated that there is an increase in Ca^{2+} release from the sarcoplasmic reticulum (SR) in DMD human myotubes[27]. To assess by which mechanism Ca^{2+} plays a role in the observed seizures, *Dys* mutants were fed overnight various Ca^{2+} channel blockers [Nifedipine (dihydropyridine channel), 2-APB (inositol 1,4,5-triphosphate receptors, IP_3R) and Ryanodine (Ryanodine receptors, RyR)] and assayed for temperature induced seizures. To prevent total inhibition of muscle contraction a low drug concentration was used to block individual channels at one time. Animals fed Nifedipine did not show less seizure activity than controls, but both 2-APB and Ryanodine treated flies showed a decrease in seizure activity, with Ryanodine having the most dramatic effect (Fig. 5a,b, Supplementary Table 7). This shows that Ca^{2+} released via IP_3R and RyR activated channels plays a role in hyperthermic seizures.

Discussion

Muscle seizures accompany multiple human neurological and muscular disorders. Seizures can occur when a group of neurons becomes hyperexcited and discharge action potentials irregularly without suppression, which causes muscle fibers to contract inappropriately. The uncontrolled action potential is dependent upon K^+ and Na^+ channel permeability or Ca^{2+} mis-regulation[28]. Ryanodine receptors that are regulators of fast Ca^{2+} release from the sarcoplasmic reticulum have been found to play a role in the disease pathology of seizures[29]. Additionally, inositol 1,4,5-triphosphate receptors (IP_3Rs) which regulate slow Ca^{2+} release from the SR are necessary in the central nervous system, causing epilepsy when mutated[30]. Seizures can be alleviated by manipulation of ion channels or by blocking neurotransmission.

It has been shown that Laminin binds directly to voltage gated Ca^{2+} channels (Ca_V) at the presynapse in mice, specifically P/Q- and N-type channels, and this binding induces vesicle clustering[31]. Laminin also binds the transmembrane protein Dg providing a direct link between Dys and the presynaptic motoneuron in mammals. Importantly, not only does the motoneuron send signals to the muscle, but also retrograde signaling exists, where a signal travels from the muscle back to the presynaptic neuron. The current pathway by which synaptic retrograde signaling communicates is not known, however Dys has been implicated previously to play a role in the process[23–24]. If we assume that hyperthermic seizures reported here are related to the role of Dys in retrograde signaling, then the Ca_V-Laminin-Dg signaling cascade could explain why the P/Q- and N-type, but not the L-type Ca^{2+} channel blocker affected *Dys* seizures. Similarly, the reduction of Dg or Cora reduced the seizure occurrence possibly by preventing propagation of signaling via loss of communication with Laminin. Another pathway that plays a role in retrograde signaling at the NMJ[32] is TGF-β and interestingly, mutants of the TGF-β pathway have a hyperthermic seizure phenotype similar to *Dys* mutants (Supplementary Fig. 5). However, we did not observe a genetic interaction between the DGC and TGF-β pathway components suggesting that they might act in parallel.

Dys and Dg have been reported to have opposing functions in control of neurotransmitter release at the NMJ. *Dg* mutants show a decrease and *Dys* loss of function and heterozygous mutants an increase in release of neurotransmitter, however both mutants do not show a change in response to altered neurotransmitter levels[20,22–24].

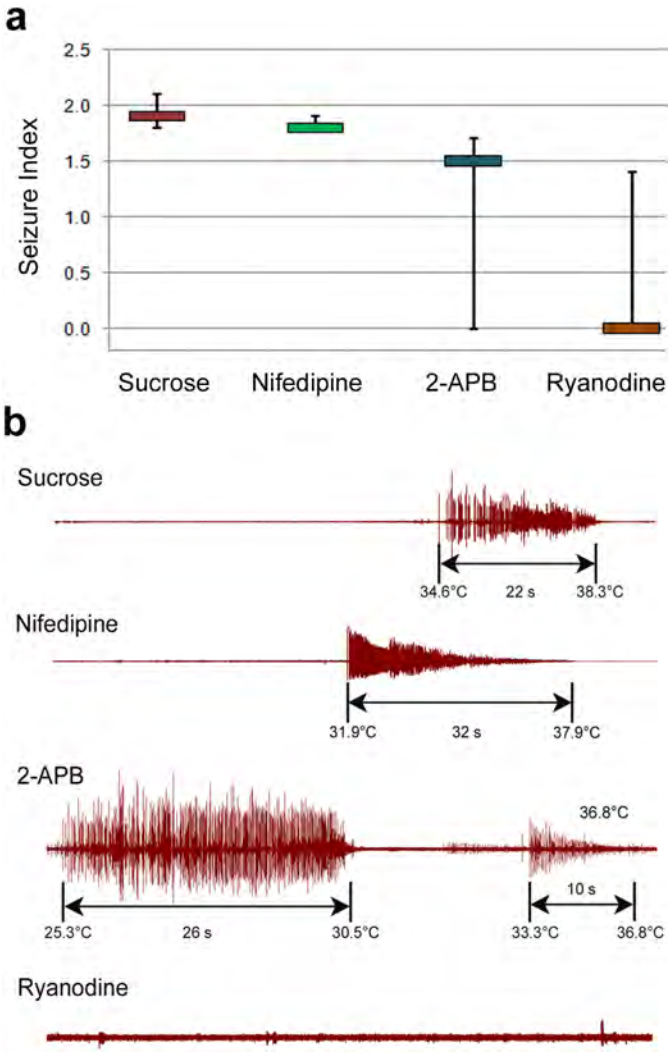

Figure 5 | Elevated Ca^{2+} from the SR leads to hyperthermic seizures. (a) Seizure indices of *DysDf* mutants after being fed various Ca^{2+} channel blockers. The control animals were only fed 5% sucrose and the other drugs were given in a 5% sucrose solution. Statistics were calculated using a one-tailed Mann-Whitney U-test where the following P-values were obtained by comparing to sucrose fed animals: Nifedipine: $P = 0.421$, 2-APB: $P = 0.107$ and Ryanodine: $P = 0.078$. (b) Electrical output from dystrophic heated muscles after being fed overnight with sucrose (control), L-type calcium channel blocker (Nifedipine), Ryanodine SR fast calcium channel blocker or IP_3R SR slow calcium channel blocker (2-APB). 5–6 animals were measured per condition. Seizure onset and subsiding temperatures are noted as well as seizure duration. Animals fed Nifedipine did not show a decrease in seizure activity. Animals fed 2-APB had additional seizure activity that was occurring spontaneously before heating began that was different in its electrical pattern that would be consistent with the observed phenotype of typical *Dys* mutants. This is shown here where output occurs for almost 30 s. This is later followed by a seizure at a reasonable temperature that looks like what would be expected for a dystrophic mutant. This extra output was only seen with animals fed this channel blocker, and in general the occurrence of seizures was less than controls (Supplementary Table 5). Animals fed Ryanodine still had seizures 33% of the time, but in general there was a decrease in the seizure indices associated with these animals, therefore we considered this reagent to have a therapeutic effect. *$P \leq 0.05$, **$P \leq 0.01$, ***$P \leq 0.001$.

These opposing phenotypes are similar to what we report here, where *Dys* mutants have seizures and *Dg* mutants do not. Additionally, *Dys* mutants have an increase in synaptic vesicle docking sites (T-bars) at larval NMJs[23], which could explain our data showing the developmental requirement for Dys. Once the NMJ is established with a normal number of active sites, animals would not be prone to seizures.

Our data also show that Dys and Dg mutants have altered cellular homeostasis. In vertebrates, multiple metabolic disorders have been implicated in seizure activity; for example, mitochondrial encephalopathy, the most common neurometabolic disorder, presents various symptoms including seizures[33] and mice that are partially deficient for mitochondrial superoxide dismutase have an increased incidence of spontaneous seizures[34]. Additionally, *mdx* mice, a model for MD has sustained oxidative stress in skeletal muscle[35–37]. In *Drosophila*, it has been shown that *Dg* mutant larvae have an altered state of cellular homeostasis and are sensitive to ambient temperature. A constant increase in mitochondrial oxidative metabolism, caused by a *Dg* hypomorphic mutation, results in a change in thermoregulatory behavior[38]. In addition, it was reported that suboptimal temperatures and energetic stress accelerate age-dependent muscular dystrophy in both, *Dys* and *Dg* mutants[16]. Now we show that *Dys* and *Dg* mutants have antagonistically abnormal cellular levels of ROS.

ROS are derived from elemental oxygen (O_2), and ROS cascades begin with the superoxide anion radical. Sources for superoxide anion radicals include xanthine oxidase, prostanoid metabolism, catecholamine autooxidation, NAD(P)H oxidase activity and NO synthase. These radicals are generated in normal muscle, and the rate of generation is increased by muscle contraction[39]. In Duchenne MD the absence of dystrophin at the sarcolemma delocalizes and downregulates neuronal nitric oxide synthase (nNOS), which in turn leads to increase in inducible nitric oxide synthase (nNOS) that generates excessive $NO^{\bullet}$[40]. This mechanism can explain extremely high ROS levels in *Dys* mutants. This high level of ROS in dystrophic *Drosophila* can be alleviated by transheterozygous interaction with *Dg* and *Cam,* which indicates a genetic interaction between *Dys* and these two genes in control of cellular homeostasis.

Our study provides the first *in vivo* measurements on dystrophic animals showing that they have hyperthermic seizures that are dependent upon neurotransmission. Dystrophin is required during development, since *Dys* downregulation in adulthood, after muscles and NMJs are already established precludes hyperthermic seizures. Our data suggest that the DGC has a role in signaling at the NMJ: reduction of Dg, a protein that binds Dys[12] and regulates localization of the NMJ specific proteins, prevents dystrophic seizure occurrence. Seizures are associated with abnormal Ca^{2+} release from the SR; introduction of a mutation of Ca^{2+} mediator *Calmodulin* and supply of calcium channel blockers reduce seizures. Taken together, our data show that the DGC acts at the muscle side of the NMJ to regulate muscle cell homeostasis in response to neuronal signaling and implies that Dys is involved in muscle-neuron communication.

Methods

Fly strains and genetics. Fly stocks were maintained at 25°C on a standard cornmeal-agar diet unless otherwise stated. Fly strains used in this study are: *UAS-Dys$^{C\text{-}RNAi}$ (dsDys), tub-Gal4::dsDys/TM6, UAS-Dg^{RNAi} (dsDg), tub-Gal4::dsDg/TM3* (described previously[12] and recombined onto chromosomes with the *tub-Gal4* driver where indicated), loss of function (lof) mutants *DysDf* (deletion of the *Dys* gene generated by outcrossing the deficiency *Df(3R)Exel6184*[41]), *Dg^{O86}/CyO, Dg^{O55}/CyO*[42], *DfKX23/Ser,TM3* (Df(3R)Dl-KX23 - partial deletion of *Dys* gene, Bloomington ID: 2411), *Dys$^{8\text{-}2}$/TM6* (deletion of N-terminal region causing a loss of at least one long isoform[12]), *tub-Gal4/TM3, 24B-Gal4, D42-Gal4, act-Gal4, tub-Gal80^{ts}, OregonR.* Alleles used in this study are: *para^{ts1}* (temperature sensitive, lof), *Cam^{n339}* (lof), *mys^{1}* (lof), *cora^{k08713}* (hypomorph), *tkv^{1}* (hypomorph) and *Mad^{12}* (lof). The *RNAi* line directed against *tkv* (*tkv^{RNAi}*) was obtained from the Vienna *Drosophila* RNAi Center. Unless otherwise stated, lines were obtained from Bloomington Stock Center.

Immunohistochemistry. Adult flies were immobilized on a tissue culture dish using Vaseline. The thorax and head were removed and the abdomen was opened in saline buffer (115 mM NaCl, 5 mM KCl, 6 mM $CaCl_2{\bullet}2H_2O$, 1 mM $MgCl_2{\bullet}6H_2O$, 4 mM $NaHCO_3$, 1 mM $NaH_2PO_4{\bullet}1H_2O$, 5 mM trehalose, 75 mM sucrose, and 5 mM N-Tris [hydroxymethyl] methyl-2-aminoethane sulfonic acid). The tissue was then fixed without agitation for 10 minutes at room temperature in 4% formaldehyde. Tissue was fixed for 5 minutes in methanol for the anit-DGluRIIA antibody. Antibody staining was performed as described before[17] except with the use of saline buffer. The following antibodies were used: rabbit anti-Dg[42] (1 : 1000), mouse anti-Dlg (1 : 50; Developmental Studies Hybridoma Bank), mouse anti-DGluRIIA (1 : 50; Developmental Studies Hybridoma Bank), Alexa 488 goat anti-mouse and Alexa 568 goat anti-rabbit (Invitrogen). Samples were then mounted on slides in 70% glycerol, 2% NPG, 1× PBS and analyzed using a confocal microscope (Leica TCS SP5). Quantification of staining intensities was done using Leica software (LAS AF version 2.1.1). The mean pixel value in the area of interest (NMJ) and in the same size area of the background was calculated. The background level was subtracted from the value found in the area of interest. Reported intensities were normalized to control and the Student's t-test was performed for statistical analysis.

Electrophysiology. IFM recordings were done on adult flies raised at 25°C. Flies were 3–5 days old unless otherwise indicated. Platinum electrodes were fashioned via KOH etching. The recording electrode was inserted into the lateral thorax with the ground electrode inserted into the abdomen. Temperature was shifted from room temperature (~25°C) up to ~50°C using an infrared lamp. Signals generated from the IFMs were amplified and digitized with the Micro 1401 data acquisition unit (Cambridge Electronic Design) and analyzed with Spike 2 software (Cambridge Electronic Devices). Temperature was monitored using an analogue thermometer (DKT200, 0–5 V, −20°C−80°C, ±0.3°C, Driesen Kern GmbH) where approximately every ten seconds resulted in a 1°C T increase. Plots were made of voltage output vs. temperature. All plots were scaled the same and converted into binary JPEG images. A macro was written using ImageJ software (NIH) to count the number of pixels of the voltage on the graph during the seizure. When a seizure occurred, a seizure index (S_i) was calculated to reflect the temperature that the seizure started at (T_s), the amplitude of the seizure, and the duration of the seizure. Since the T_s was deemed to be more informative than the size of the seizure, a S_i was calculated by taking the natural logarithm of the pixel count and dividing by the seizure start temperature. This number was then multiplied by 10.

$$\mathbf{S_i} = (\boldsymbol{ln}(\text{pixel number})/\mathbf{T_s}) * \mathbf{10}$$

If no seizure occurred then the index was set to zero because the T_s could not be determined if there was no seizure. Only seizures that occurred at lower than 49°C were considered because at very high temperatures even control animals start having contractions (Fig. 1b).

Statistics. Since our seizure electrophysiological data are not normally distributed, we used non-parametric methods for statistical analysis. Values are reported as M (x/y) where M = median, y = 25th percentile rank and x = 75th percentile rank. For determination of agreement between groups of data, the Kruskal-Wallis test was applied resulting in a chi-squared statistic. For comparison between two data sets a one-tailed Mann-Whitney U-test was used. Graphical representations of data show the median value of the data spread and error bars correspond to the 25th and 75th percentiles. Statistical analysis of muscle degeneration was done using a one-tailed chi-squared test. Statistical analysis of biochemical assays and immunohistochemical signal intensity was done using a one-tailed Student's t-test.

Histology. For analysis of indirect flight muscle (IFM) morphology, 10 µm paraffin-embedded sections were cut from fly thoraxes. In order to prepare *Drosophila* muscle sections, the fly bodies were immobilized in collars in the required orientation and fixed in Carnoy fixative solution (6 : 3 : 1 = Ethanol : Chloroform : Acetic acid) at 4°C overnight. Tissue dehydration and embedding in paraffin was performed as described previously[43]. Histological sections were prepared using a Hyrax M25 (Zeiss) microtome and stained with hematoxylin and eosin. All chemicals for these procedures were obtained from Sigma Aldrich. Muscle analysis was done using a light microscope (Zeiss). The frequency of muscle degeneration was quantified as a ratio of degenerated muscles to the total number of analyzed muscles.

Lipid peroxidation detection. Flies were kept at 29°C for three days after eclosion and emersed in liquid N_2. Cellular extracts were prepared via homogenization of 20–25 whole flies in cell lysis buffer and then boiling the homogenates for 5 min at 100°C followed by centrifuging on high for 5 min. Protein levels in the extracts were determined via the BCA protein assay (Pierce Chemical). 100 µl of fly extract was combined with 300 µl acetic acid (20%, pH 3.5), 300 µl TBA (0.8% w/v in 0.5 M NaOH) and 40 µl SDS (8% w/v). The mixture was heated for 45 min at 100°C to allow for adduct formation. Adducts were then extracted into 1-butanol and the absorption was measured at 540 nm along with appropriate blanks. The raw absorption values minus any absorbance from the blank samples were then normalized to protein content (µg/ml). Three replicates were measured from four or more independent extracts. Data was compared using a one-tailed Student's t-test. Heterozygous animals were the result of crossing mutant stocks to *OregonR.*

Drug assays. Flies (*DysDf* genotype) raised at 25°C that were 3–7 days old were put overnight in vials containing filter paper soaked in 5% sucrose and either 500 µM 2-APB, 20 µM Ryanodine or 3.6 mM Nifedipine. Controls were only kept on sucrose. Electrophysiological measurements of IFMs were done the following day. When testing for drug lethality, *OregonR* wild type flies were used with lethality rates as follows: sucrose (1/10 dead), 2-APB (3/10 dead), Ryanodine (0/10 dead), Nifedipine

(0/10 dead). When testing was conducted on *Dys* mutants there was a much higher lethality rate with both 2-APB and Ryanodine as follows: sucrose (4/15 dead), 2-APB (10/15 dead), Ryanodine (9/15 dead), Nifedipine (1/15 dead).

Reverse transcription quantitative PCR. Quantitative reverse transcription (RT-qPCR) was performed on total RNA derived from whole adult animals. RNAs were extracted from flies with the RNeasy Mini kit (Qiagen), followed by reverse transcription using the High Capacity cDNA Reverse Transcription kit (Applied Biosystems) following the manufacturer's protocols. mRNA amounts were tested with RpL32 as an endogenous control for q-PCR using the Fast SYBR® Green master mix on a Step One Plus 96 well system (Applied Systems). The reactions were incubated at 95°C for 10 min, followed by 40 cycles of 95°C for 15 s and 54°C for 30 s. All reactions were run in triplicate with appropriate blank controls. The threshold cycle (CT) is defined as the fractional cycle number at which the fluorescence passes the fixed threshold. Primers were used as follows: RpL32 forward - AAGATGACCA-TCCGCCCAGC; RpL32 reverse – GTCGATACCCTTGGGCTTGC; Dg forward – ACTCAAGGACGAGAAGCCGC; Dg reverse – ATGGTGGTGGCACATAATCG; Dys forward – GTTGCAGACACTGACCGACG; Dys reverse - CGAGGGCTC-TATGTTGGAGC. The ΔC_T value is determined by subtracting the average RpL32 C_T value from the average Dys/Dg C_T value. The $\Delta\Delta C_T$ value is calculated by subtracting the ΔC_T of the control sample from the ΔC_T of the suspect sample. The relative amount of mRNA is then determined using the expression $2^{-\Delta\Delta CT}$ and the fold reduction is determined using the expression $2^{\Delta\Delta CT}$. Errors for *RNAi* transgenes were determined starting with the standard deviation of the raw C_T values and performing appropriate regression analysis.

1. Barresi, R. & Campbell, K. P. Dystroglycan: from biosynthesis to pathogenesis of human disease. *J Cell Sci* **119**, 199–207 (2006).
2. Grady, R. M. *et al.* Maturation and maintenance of the neuromuscular synapse: genetic evidence for roles of the dystrophin–glycoprotein complex. *Neuron* **25**, 279–293, doi:S0896-6273(00)80894-6 [pii] (2000).
3. Kanagawa, M. & Toda, T. The genetic and molecular basis of muscular dystrophy: roles of cell-matrix linkage in the pathogenesis. *J Hum Genet* **51**, 915–926, doi:10.1007/s10038-006-0056-7 (2006).
4. Sciandra, F. *et al.* Dystroglycan and muscular dystrophies related to the dystrophin-glycoprotein complex. *Ann Ist Super Sanita* **39**, 173–181 (2003).
5. Lim, L. E. & Campbell, K. P. The sarcoglycan complex in limb-girdle muscular dystrophy. *Curr.Opin.Neurol.* **11**, 443–452 (1998).
6. Matsumura, K. & Campbell, K. P. Dystrophin-glycoprotein complex: its role in the molecular pathogenesis of muscular dystrophies. *Muscle Nerve* **17**, 2–15 (1994).
7. Hayashi, Y. K. *et al.* Mutations in the integrin alpha7 gene cause congenital myopathy. *Nat Genet* **19**, 94–97, doi:10.1038/ng0598-94 (1998).
8. Xiong, Y., Zhou, Y. & Jarrett, H. W. Dystrophin glycoprotein complex-associated Gbetagamma subunits activate phosphatidylinositol-3-kinase/Akt signaling in skeletal muscle in a laminin-dependent manner. *J Cell Physiol* **219**, 402–414, doi:10.1002/jcp.21684 (2009).
9. Zhou, Y. W., Thomason, D. B., Gullberg, D. & Jarrett, H. W. Binding of laminin alpha1-chain LG4-5 domain to alpha-dystroglycan causes tyrosine phosphorylation of syntrophin to initiate Rac1 signaling. *Biochemistry* **45**, 2042–2052 (2006).
10. Vandebrouck, A. *et al.* Regulation of capacitative calcium entries by alpha1-syntrophin: association of TRPC1 with dystrophin complex and the PDZ domain of alpha1-syntrophin. *Faseb J* **21**, 608–617 (2007).
11. Sabourin, J. *et al.* Regulation of TRPC1 and TRPC4 cation channels requires an alpha1-syntrophin-dependent complex in skeletal mouse myotubes. *J Biol Chem* **284**, 36248–36261 (2009).
12. Shcherbata, H. R. *et al.* Dissecting muscle and neuronal disorders in a Drosophila model of muscular dystrophy. *EMBO J.* **26**, 481–493 (2007).
13. Greener, M. J. & Roberts, R. G. Conservation of components of the dystrophin complex in Drosophila. *FEBS Lett* **482**, 13–18 (2000).
14. Taghli-Lamallem, O. *et al.* Dystrophin deficiency in Drosophila reduces lifespan and causes a dilated cardiomyopathy phenotype. *Aging Cell* **7**, 237–249 (2008).
15. Allikian, M. J. *et al.* Reduced life span with heart and muscle dysfunction in Drosophila sarcoglycan mutants. *Hum.Mol.Genet.* **16**, 2933–2943 (2007).
16. Kucherenko, M. M., Marrone, A. K., Rishko, V. M., Magliarelli Hde, F. & Shcherbata, H. R. Stress and muscular dystrophy: a genetic screen for dystroglycan and dystrophin interactors in Drosophila identifies cellular stress response components. *Dev Biol* **352**, 228–242 (2011).
17. Klose, M. K., Atwood, H. L. & Robertson, R. M. Hyperthermic preconditioning of presynaptic calcium regulation in Drosophila. *J.Neurophysiol.* **99**, 2420–2430 (2008).
18. Montana, E. S. & Littleton, J. T. Characterization of a hypercontraction-induced myopathy in Drosophila caused by mutations in Mhc. *J.Cell Biol.* **164**, 1045–1054 (2004).
19. Wu, C. F. & Ganetzky, B. Genetic alteration of nerve membrane excitability in temperature-sensitive paralytic mutants of Drosophila melanogaster. *Nature* **286**, 814–816 (1980).
20. Bogdanik, L. *et al.* Muscle dystroglycan organizes the postsynapse and regulates presynaptic neurotransmitter release at the Drosophila neuromuscular junction. *PLoS.One.* **3**, e2084 (2008).
21. Cote, P. D., Moukhles, H. & Carbonetto, S. Dystroglycan is not required for localization of dystrophin, syntrophin, and neuronal nitric-oxide synthase at the sarcolemma but regulates integrin alpha 7B expression and caveolin-3 distribution. *J Biol Chem* **277**, 4672–4679 (2002).
22. Wairkar, Y. P., Fradkin, L. G., Noordermeer, J. N. & DiAntonio, A. Synaptic defects in a Drosophila model of congenital muscular dystrophy. *J Neurosci* **28**, 3781–3789 (2008).
23. van der Plas, M. C. *et al.* Dystrophin is required for appropriate retrograde control of neurotransmitter release at the Drosophila neuromuscular junction. *J.Neurosci.* **26**, 333–344 (2006).
24. Pilgram, G. S., Potikanond, S., van der Plas, M. C., Fradkin, L. G. & Noordermeer, J. N. The RhoGAP crossveinless-c interacts with Dystrophin and is required for synaptic homeostasis at the Drosophila neuromuscular junction. *J Neurosci* **31**, 492–500 (2011).
25. Madhavan, R., Massom, L. R. & Jarrett, H. W. Calmodulin specifically binds three proteins of the dystrophin-glycoprotein complex. *Biochem.Biophys.Res.Commun.* **185**, 753–759 (1992).
26. Heiman, R. G. *et al.* Spontaneous avoidance behavior in Drosophila null for calmodulin expression. *Proc.Natl.Acad.Sci.U.S.A* **93**, 2420–2425 (1996).
27. Deval, E. *et al.* Na(+)/Ca(2+) exchange in human myotubes: intracellular calcium rises in response to external sodium depletion are enhanced in DMD. *Neuromuscul.Disord.* **12**, 665–673 (2002).
28. Surtees, R. Inherited ion channel disorders. *Eur J Pediatr* **159 Suppl 3**, S199–203 (2000).
29. Kushnir, A., Betzenhauser, M. J. & Marks, A. R. Ryanodine receptor studies using genetically engineered mice. *FEBS Lett* **584**, 1956–1965 (2010).
30. Matsumoto, M. *et al.* Ataxia and epileptic seizures in mice lacking type 1 inositol 1,4,5-trisphosphate receptor. *Nature* **379**, 168–171 (1996).
31. Nishimune, H., Sanes, J. R. & Carlson, S. S. A synaptic laminin-calcium channel interaction organizes active zones in motor nerve terminals. *Nature* **432**, 580–587 (2004).
32. Keshishian, H. & Kim, Y. S. Orchestrating development and function: retrograde BMP signaling in the Drosophila nervous system. *Trends Neurosci* **27**, 143–147 (2004).
33. Tucker, E. J., Compton, A. G. & Thorburn, D. R. Recent advances in the genetics of mitochondrial encephalopathies. *Curr Neurol Neurosci Rep* **10**, 277–285 (2010).
34. Liang, L. P. & Patel, M. Mitochondrial oxidative stress and increased seizure susceptibility in Sod2(−/+) mice. *Free Radic Biol Med* **36**, 542–554 (2004).
35. Dudley, R. W. *et al.* Dynamic responses of the glutathione system to acute oxidative stress in dystrophic mouse (mdx) muscles. *Am J Physiol Regul Integr Comp Physiol* **291**, R704–710 (2006).
36. Tidball, J. G. & Wehling-Henricks, M. The role of free radicals in the pathophysiology of muscular dystrophy. *J Appl Physiol* **102**, 1677–1686 (2007).
37. Whitehead, N. P., Pham, C., Gervasio, O. L. & Allen, D. G. N-Acetylcysteine ameliorates skeletal muscle pathophysiology in mdx mice. *J Physiol* **586**, 2003–2014 (2008).
38. Takeuchi, K. *et al.* Changes in temperature preferences and energy homeostasis in dystroglycan mutants. *Science* **323**, 1740–1743 (2009).
39. Reid, M. B. Invited Review: redox modulation of skeletal muscle contraction: what we know and what we don't. *J Appl Physiol* **90**, 724–731 (2001).
40. Bellinger, A. M. *et al.* Hypernitrosylated ryanodine receptor calcium release channels are leaky in dystrophic muscle. *Nat Med* **15**, 325–330 (2009).
41. Christoforou, C. P., Greer, C. E., Challoner, B. R., Charizanos, D. & Ray, R. P. The detached locus encodes Drosophila Dystrophin, which acts with other components of the Dystrophin Associated Protein Complex to influence intercellular signalling in developing wing veins. *Dev Biol* **313**, 519–532 (2008).
42. Deng, W. M. *et al.* Dystroglycan is required for polarizing the epithelial cells and the oocyte in Drosophila. *Development* **130**, 173–184 (2003).
43. Kucherenko, M. M. *et al.* Paraffin-embedded and frozen sections of Drosophila adult muscles. *J Vis Exp*, doi:2438 [pii]10.3791/2438 (2010).

Acknowledgements

We would like to thank H. Ruohola-Baker and R. Ray for fly stocks and reagents, N. Glyvuk, Y. Tsytsyura, G. Vorbrüggen, A. Yatsenko and A. König for comments on the manuscript. This work was funded by Max Planck Society.

Author contributions

AKM designed and performed experiments, analyzed data, wrote the manuscript, MMK performed experiments, analyzed data, RW and MCG helped with electrophysiology and discussed data, HRS designed experiments, analyzed data, wrote the manuscript.

Additional information

Supplementary Information accompanies this paper at http://www.nature.com/scientificreports

Competing financial interests: Authors declare no competing financial interests.

How to cite this article: Marrone, A.K., Kucherenko, M.M., Wiek, R., Göpfert, M.C. & Shcherbata, H.R. Hyperthermic seizures and aberrant cellular homeostasis in *Drosophila* dystrophic muscles. *Sci. Rep.* **1**, 47; DOI:10.1038/srep00047 (2011).

Supplementary Information

Supplementary Table 1: ROS levels seen in *Dys*, *Dg* and *Cam* mutants

Genotype	ROS ([AU]/µg/ml protein)	P-Value
OregonR [2]	1.00 ± 0.26	-
DysDf/+	1.25 ± 0.83	0.091
Dg^{O86}/+	1.04 ± 0.14	0.37
Cam^{n339}/+	0.88 ± 0.10	0.22
DysDf	4.66 ± 2.54	$3.0X10^{-8}$***
$Dg^{O86/O55}$	0.61 ± 0.37	0.0074**
Dg^{O86}/+; *DysDf/+*	0.66 ± 0.22	0.0034**
Cam^{n339}/+; *DysDf/+*	0.49 ± 0.17	$2.0X10^{-5}$***
$cora^{k08713}$/+; *DysDf/+*	0.86 ± 0.07	0.18

[1] P-Values are relative to control animals of genotype *OregonR*,
*P ≤ 0.05, **P ≤ 0.01, ***P ≤ 0.001
[2] All values are normalized relative to *OregonR*
[3] errors reported represent the standard deviation

Supplementary Table 2: Decrease in *Dystrophin* mRNA level

Genotype	*Dys* Average C_T	*RpL32* Average C_T	ΔC_T *Dys* – *RpL32*[1]	$\Delta\Delta C_T$ (ΔC_T-$\Delta C_{T,control}$[2])	Average *Dys* relative to control[3]	*Dys* mRNA fold reduction relative to control[4]
tub-Gal4/+	22.40±0.09	18.35±0.20	4.05±0.22	0.00±0.32	1.00±0.22	1.00±0.22
tub-Gal4::dsDys/+	22.26±0.06	16.35±0.04	5.91±0.08	1.86±0.24	0.28±0.05	3.63±0.60

[1] the ΔC_T value is determined by subtracting the average *RpL32* C_T value from the average *Dys* C_T value. The standard deviation of the difference is calculated from the standard deviation of the *Dys* and *RpL32* values using the formula "$s=\sqrt{(s_1^2+s_2^2)}$, where s=stdev

[2] the calculation of the $\Delta\Delta C_T$ involves subtraction by the ΔC_T calibrator value. This standard deviation is determined the same as in '1'

[3] the range given for *Dys* relative to Control is determined by evaluating the expression: $2^{-\Delta\Delta CT}$ where the error is determined using regressional analysis

[4] the fold reduction given for *Dys* relative to Control is determined by evaluating the expression: $2^{\Delta\Delta CT}$ where the error is determined using regressional analysis

Supplementary Table 3: Decrease in *Dystrophin* mRNA level using *tub-Gal80^{ts}* system

Genotype	*Dys* Average C_T	*RpL32* Average C_T	ΔC_T *Dys* – *RpL32*[1]	$\Delta\Delta C_T$ (ΔC_T-$\Delta C_{T,cont}$[2])	T Index[3]	T corrected *Dys* mRNA fold reduction relative to control[4]
tub-Gal80^{ts}/+; tub-Gal4/+ pupae at 18˚C	24.46±0.16	16.61±0.03	7.86±0.17	0.00±0.24	-	1.00±0.16
tub-Gal80^{ts}/+; tub-Gal4/+ pupae 3d. at 29˚C	21.87±0.02	16.53±0.27	5.34±0.27	-2.52±0.32	5.72	1.00±0.31
tub-Gal80^{ts}/+; tub-Gal4::dsDys/+ pupae at 18˚C	23.47±0.17	16.20±0.06	7.27±0.17	0.00±0.25	-	1.00±0.17
tub-Gal80^{ts}/+; tub-Gal4::dsDys/+ pupae 3d. at 29˚C	22.60±0.12	16.28±0.13	6.32±0.17	-0.95±0.25	5.72	2.97±0.27
tub-Gal80^{ts}/+; tub-Gal4::dsDys/+ flies at 18˚C	23.88±0.17	18.19±0.29	5.70±0.34	0.00±0.48	-	1.00±0.33
tub-Gal80^{ts}/+; tub-Gal4::dsDys/+ flies 3d. at 29˚C	24.76±0.23	17.28±0.03	7.48±0.24	1.78±0.41	-	3.44±0.99

[1] the ΔCT value is determined by subtracting the average *RpL32* CT value from the average *Dys* C_T value. The standard deviation of the difference is calculated from the standard deviation of the *Dys* and *RpL32* values using the formula "$s=\sqrt{(s_1^2+s_2^2)}$, where s=stdev

[2] the calculation of the $\Delta\Delta C_T$ involves subtraction by the ΔC_T calibrator value. This standard deviation is determined the same as in '1'

[3] the temperature dependent scaling factor was determined because expression levels of *Dys* in control pupae varied greatly depending on the temperature. Where applicable this value is calculated as $2^{-\Delta\Delta CT}$. This scaling factor is then used to determine the relative expression levels in mutant animals of the same life stage at 29˚C relative to the same animals at 18˚C (Supplementary Figure 2)

[4] the fold reduction given for *Dys* relative to Control is determined by evaluating the expression: $2^{\Delta\Delta CT}$ where the error is determined using regressional analysis. The temperature related scaling index has been multiplied by this value where applicable

Supplementary Table 4: Frequency of muscle degeneration in *Dys RNAi* mutants with and without developmentally restricted expression of *RNAi*

Genotype	*Dys* down regulated	Condition[1]	Age, days	n	% of muscle degeneration	P-Value[2]	Normalized[3] % of muscle degeneratio	P-Value[2]
tub-Gal4/+	Throughout lifetime	25˚C	16	121	9.1	0.021*	2.4	0.11
tub-Gal4:dsDys				73	21.9			
tub-Gal80^{ts}/+; tub-Gal4/+	As adult	18˚C development 29˚C adulthood	19	84	21.4	0.0081 **	2.0	
tub-Gal80^{ts}/+; tub-Gal4:dsDys/+				108	42.6			

[1] Note that higher temperature (29˚C) accelerates aging and muscle degeneration.

[2] P-value determined from the χ^2 statistic

[3] Normalized to the control value under the same conditions

Supplementary Table 5: Relative Dg immunofluorescence intensities

Genotype	Relative Intensity	P-Value[1]
OregonR [2]	1.00 ± 0.37[3]	-
DysDf	0.49 ± 0.27	0.042*
Dg^{O55}	0.02 ± 0.02	1.2×10^{-4}***
$cora^{k08713}$	0.11 ± 0.11	1.4×10^{-3}**
Dg^{O86}/+; *DysDf*/+	0.06 ± 0.05	1.9×10^{-5}***
$cora^{k08713}$/+; *DysDf*/+	0.07 ± 0.06	1.1×10^{-4}***
$cora^{k08713}/Dg^{O86}$	0.10±0.12	$9{,}9 \times 10^{-5}$***

[1] P-Values are relative to control animals of genotype *OregonR*,
*P ≤ 0.05, **P ≤ 0.01, ***P ≤ 0.001
[2] All values are normalized relative to *OregonR*
[3] errors reported represent the average deviation

Supplementary Table 6: Decrease in *Dystroglycan* mRNA level

Genotype	*Dg* Average C_T	*RpL32* Average C_T	ΔC_T *Dg* – *RpL32*[1]	$\Delta\Delta C_T$ (ΔC_T-$\Delta C_{T,control}$[2])	Average *Dg* relative to control[3]	*Dg* mRNA fold reduction relative to control[4]
tub-Gal4/+	23.33±0.07	18.35±0.20	4.98±0.21	0.00±0.30	1.00±0.21	1.00±0.21
tub-Gal4::dsDg/+	25.94±0.13	18.37±0.11	7.57±0.18	2.59±0.28	0.17±0.03	6.02±1.16
tub-Gal80^{ts}/+; tub-Gal4::dsDg/+ flies at 18˚C	20.97±0.05	16.09±0.05	4.87±0.07	0.00±0.10	1.00±0.07	1.00±0.07
tub-Gal80^{ts}/+; tub-Gal4::dsDg/+ flies 3d. at 29˚C	25.26±0.07	19.09±0.03	6.17±0.08	1.29±0.11	0.41±0.03	2.45±0.18

[1] the ΔC_T value is determined by subtracting the average *RpL32* C_T value from the average *Dg* C_T value. The standard deviation of the difference is calculated from the standard deviation of the *Dg* and *RpL32* values using the formula "$s=\sqrt{(s_1^2+s_2^2)}$, where s=stdev

[2] the calculation of the $\Delta\Delta C_T$ involves subtraction by the ΔC_T calibrator value. This standard deviation is determined the same as in '1'

[3] the range given for *Dg* relative to Control is determined by evaluating the expression: $2^{-\Delta\Delta CT}$ where the error is determined using regressional analysis

[4] the fold reduction given for *Dg* relative to Control is determined by evaluating the expression: $2^{\Delta\Delta CT}$ where the error is determined using regressional analysis

Supplementary Table 7: Impact of Ca^{2+} channel blockers on seizure activity of dystrophic animals (*DysDf*)

Drug	n	%Seized^{T}	Avg. T_s±sd (˚C)*	Avg. A_{max}±sd (mV)*	Avg. Area±sd (pixel x 10^{-3})*	Median S_i** (25^{th}/75^{th} percentiles)	P-Value
Sucrose	5	80	37.8±2.1	6.6±5.7	2.4 ±1.9	1.9 (1.8/2.1)	-
3.6 mM Nifedipine	5	100	37.8±3.3	3.1±2.2	1.2 ± 0.5	1.8 (1.8/1.9)	0.50
0.5 mM 2-APB	5	60	35.7±5.7	2.8±1.2	0.8 ± 0.4	1.5 (0.0/1.7)	0.21
20 µM Ryanodine	6	33	34.4±0.6	2.8±0.6	0.9 ±0.2	0.0 (0.0/1.4)	0.078

n = number of animals fed the indicated drug

Ŧ percent of animals measured that had a seizure

* Calculated using data from animals that seized only

** Index calculated by integrating the area of the graph of voltage vs. temperature during a seizure, taking the natural logarithm of this number, dividing by the temperature that the seizure started, and then multiplying times ten.

Supplementary Figure Legends

Supplementary Figure 1:

Control animals do not have temperature-sensitive seizures as can be seen by monitoring the output voltage from the IFMs as the temperature increases. b) All tested *Dys* mutant alleles exhibit hyperthermic seizures.

Supplementary Figure 2:

Average *Dys* expression relative to appropriate controls in *RNAi* knock-down mutants that are under the control of the *tub-Gal80^{ts}* driver. a) Control pupae showed a vast increase in *Dys* expression upon being shifted from 18˚C to 29˚C indicating a natural increase in protein expression with temperature increase. Thus, to determine adequately the effectiveness of *RNAi* down-regulation this change in expression had to be taken into consideration using a temperature index (Supplementary Table 5). b) Average *Dys* expression levels relative to control in pupae (after the temperature index was considered) and in adults after being shifted to 29˚C for four days.

Supplementary Figure 3:

Seizure indices showing that animals with *RNAi* directed against muscle (*24B-Gal4*) and mononeuron (*D42-Gal4*) *Dg* mRNA do not have temperature-sensitive seizures. Endogenous (*tub-Gal4*) expression results in a reduced amount of seizures that are not significant over controls, but this is reversed when *Dg* is down-regulated after development. Refer to Table 1 for exact P-values compared to control animals.

Supplementary Figure 4:

a) β_{PS} integrin subunit loss of function allele heterozygouts (*mys*^{1}*/+)* had seizures when heated, most likely due to compromised stability of the sarcolemma and/or NMJ. Introducing a mutant copy of *Dg* into the genome of these animals does not alter the seizure character. b) Seizure indices of *mys*^{1}/+ heterozygous and *mys*^{1}*/+; Dg/*+ trans-heterozygous animals where a Kruskal-Wallis test show that there are no significances in the indices (χ^2 = 2.93, P = 0.231). The following P-values were determined upon comparison to wild type animals: *mys*^{1}/+ (***P = 2.0X10^{-4}), *mys*^{1}*/+; Dg*^{O86}/+ (*P = 0.013), *mys*^{1}*/+; Dg*^{O55}/+ (*P = 0.082) using a one-tailed Mann-Whitney U-test. 100% of *mys*^{1}/+ animals tested had seizures (n=8) with T_s = 39.2 ± 2.6, A_{max} = 3.6 ± 1.7 and Avg. Area = 1.5 ± 1.1 x 10^3. 80% of *mys*^{1}*/+;Dg*^{O86}/+ animals tested had seizures (n=5) with T_s = 36.0 ± 0.7, A_{max} = 3.8 ± 2.4 and Avg. Area =1.2 ± 0.5 x 10^3. 83% of *mys*^{1}*/+;Dg*^{O55}/+ animals tested had seizures (n=6) with T_s = 40.3 ± 3.7, A_{max} = 4.3 ± 3.0 and Avg. Area =1.2 ± 1.0 x 10^3.

Supplementary Figure 5:

a) TGF-β pathway mutants, *tkv* (type-I receptor) and *Mad* (receptor-regulated Smad) have seizures similar to what is seen in *Dys* mutants, however; when animals are missing one copy of *Dys* and one copy of each of these genes there is no significant increase in seizures over what is seen in *Dys.* Down-regulation of *tkv* after NMJ development *(tub-Gal80*^{ts}*)* does not alleviate seizures implying that there is an additional need for *tkv* after development is complete. Animals that express *RNAi* against *tkv* prior to pupae formation die supporting an important role for TGF-β signaling during pupation. Transheterozygous animals when compared to *Dys* heterozygous

animals using a Mann-Whitney U-test had P-values of 0.25 and 0.46 for *tkv/Dys* and *Mad/Dys* respectively and P-values of 0.099 and 0.040 when compared to control animals respectively. Animals of genotypes tkv^{1}, $tub\text{-}Gal80^{ts}/act\text{-}Gal4;tkv^{RNAi}$ and $Mad^{12}/+$ have P-values of 1.9×10^{-3}, 0.012 and 0.072 when compared to controls respectively. 100% of tkv^{1} animals tested had seizures (n=9) with $T_s = 39.4 \pm 4.7$, $A_{max} = 4.8 \pm 3.6$ and Avg. Area = $1.3 \pm 0.8 \times 10^{3}$. 60% of $tkv^{1}/+;DysDf/+$ animals tested had seizures (n=5) with $T_s = 44.2 \pm 2.1$, $A_{max} = 7.4 \pm 1.3$ and Avg. Area = $1.9 \pm 1.3 \times 10^{3}$. 67% of $Mad^{12}/+;DysDf/+$ animals tested had seizures (n=6) with $T_s = 42.2 \pm 4.0$, $A_{max} = 15 \pm 8.7$ and Avg. Area = $2.0 \pm 1.0 \times 10^{3}$. 80% of $Mad^{12}/+$ animals tested had seizures (n=5) with $T_s = 42.8 \pm 3.2$, $A_{max} = 8.8 \pm 6.3$ and Avg. Area = $1.7 \pm 1.4 \times 10^{3}$. 100% of $tub\text{-}Gal80^{ts}/act\text{-}Gal4;\ tkv^{RNAi}/+$ animals tested had seizures (n=5) with $T_s = 40.0 \pm 3.4$, $A_{max} = 7.3 \pm 2.8$ and Avg. Area = $4.4 \pm 2.8 \times 10^{3}$. b) Electrical output from IFM vs. temperature of TGF-β pathway mutants exhibiting seizures. *P ≤ 0.05, **P ≤ 0.01 and ***P ≤ 0.001

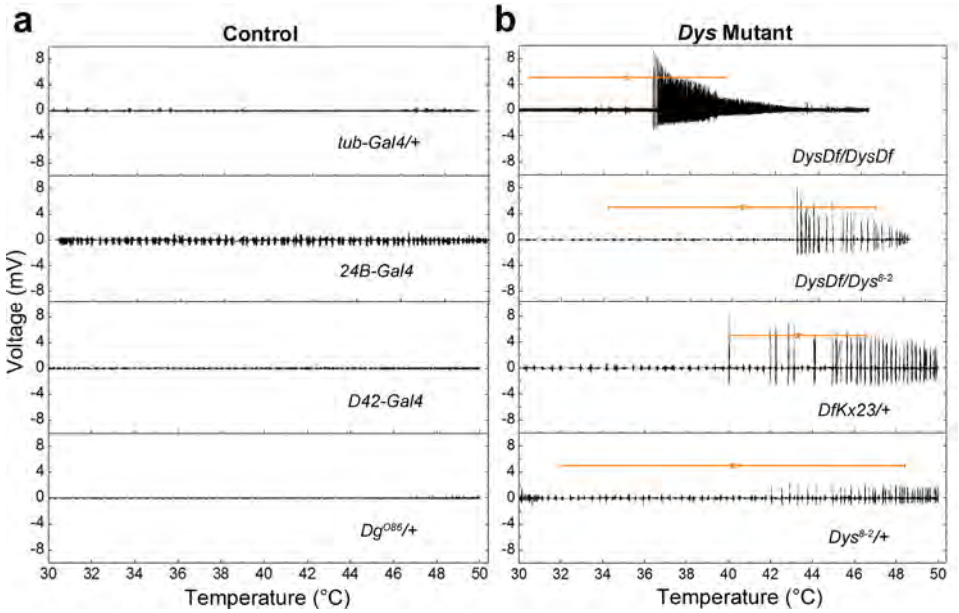

Supplementary Figure 1

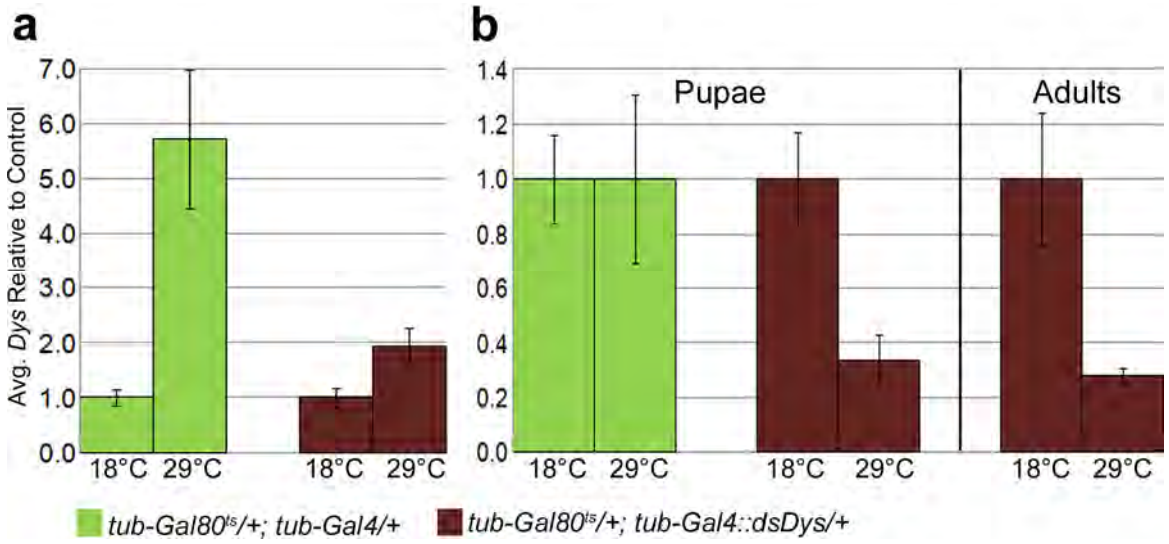

Supplementary Figure 2

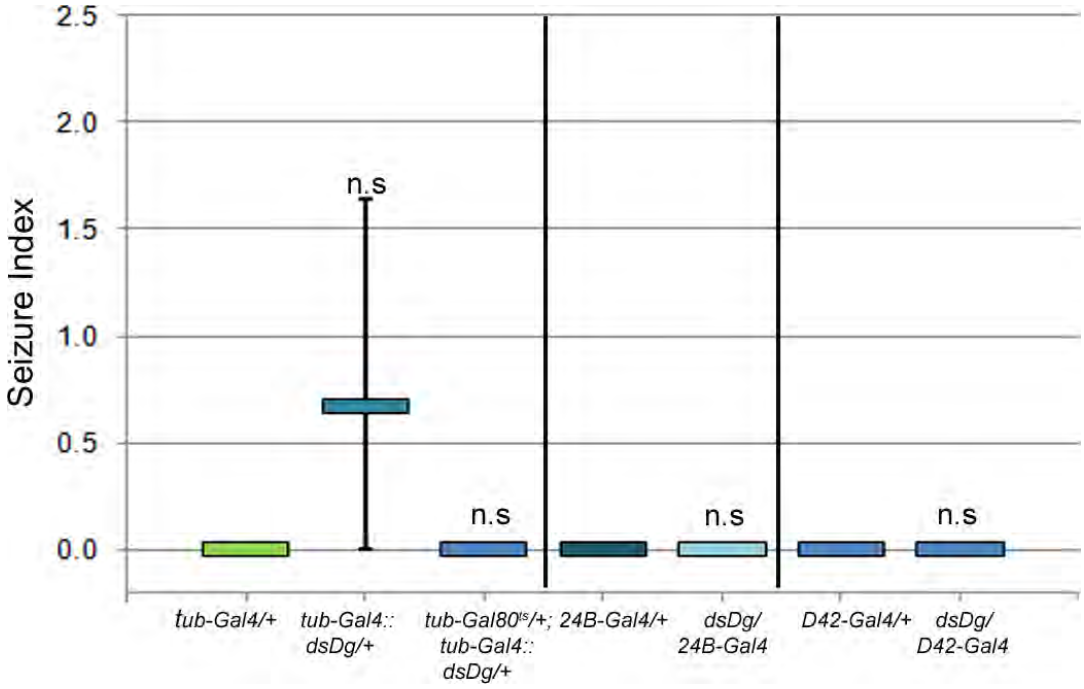

Supplementary Figure 3

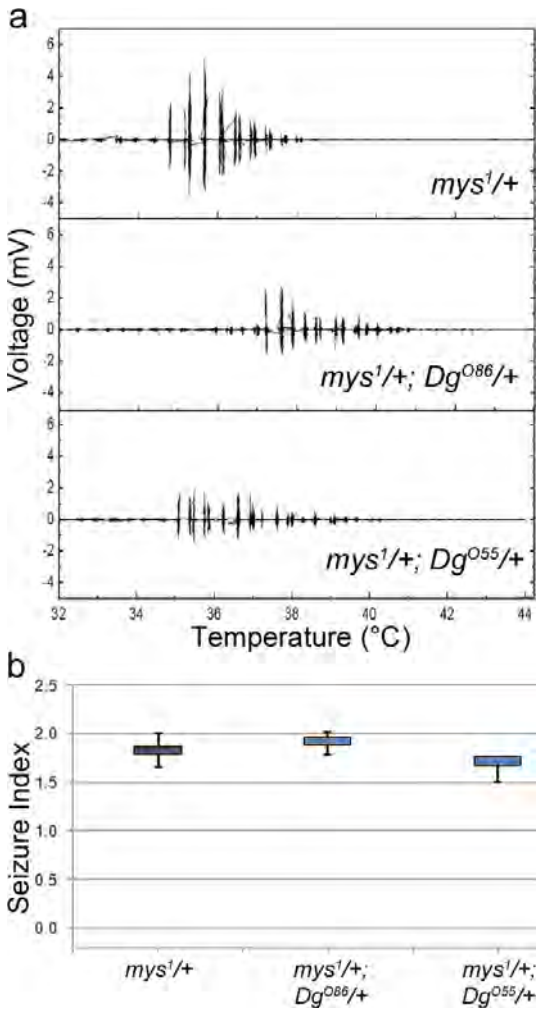

Supplementary Figure 4

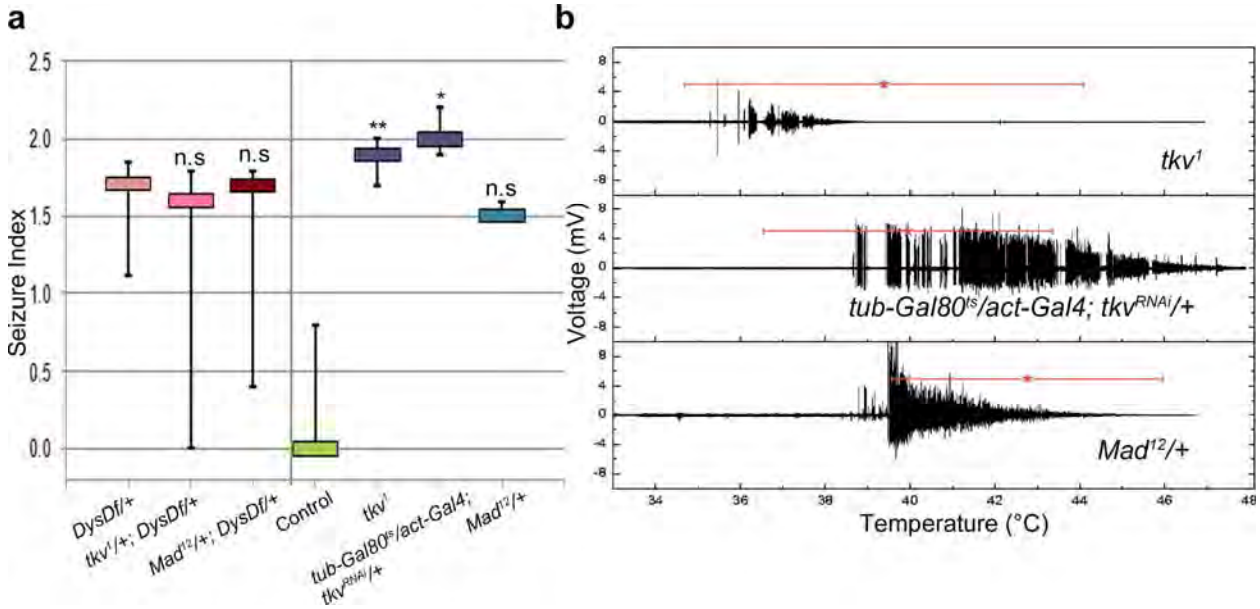

Supplementary Figure 5

Marrone et al. BMC Neuroscience 2011, 12:93
http://www.biomedcentral.com/1471-2202/12/93

BMC Neuroscience

RESEARCH ARTICLE Open Access

New Dystrophin/Dystroglycan interactors control neuron behavior in *Drosophila* eye

April K Marrone[1†], Mariya M Kucherenko[1†], Valentyna M Rishko[1,2†] and Halyna R Shcherbata[1*]

Abstract

Background: The Dystrophin Glycoprotein Complex (DGC) is a large multi-component complex that is well known for its function in muscle tissue. When the main components of the DGC, Dystrophin (Dys) and Dystroglycan (Dg) are affected cognitive impairment and mental retardation in addition to muscle degeneration can occur. Previously we performed an array of genetic screens using a *Drosophila* model for muscular dystrophy in order to find novel DGC interactors aiming to elucidate the signaling role(s) in which the complex is involved. Since the function of the DGC in the brain and nervous system has not been fully defined, we have here continued to analyze the DGC modifiers' function in the developing *Drosophila* brain and eye.

Results: Given that disruption of *Dys* and *Dg* leads to improper photoreceptor axon projections into the lamina and eye neuron elongation defects during development, we have determined the function of previously screened components and their genetic interaction with the DGC in this tissue. Our study first found that mutations in *chif, CG34400, Nrk, Lis1, capt* and *Cam* cause improper axon path-finding and loss of *SP2353, Grh, Nrk, capt, CG34400, vimar, Lis1* and *Cam* cause shortened rhabdomere lengths. We determined that *Nrk, mbl, capt* and *Cam* genetically interact with *Dys* and/or *Dg* in these processes. It is notable that most of the neuronal DGC interacting components encountered are involved in regulation of actin dynamics.

Conclusions: Our data indicate possible DGC involvement in the process of cytoskeletal remodeling in neurons. The identification of new components that interact with the DGC not only helps to dissect the mechanism of axon guidance and eye neuron differentiation but also provides a great opportunity for understanding the signaling mechanisms by which the cell surface receptor Dg communicates via Dys with the actin cytoskeleton.

Background

Muscular dystrophies (MDs) are a group of diseases that are characterized by progressive muscular degeneration and concomitant loss of muscular strength ultimately leading to skeletal muscle deterioration and cardiac and/or respiratory failure [1-3]. In addition, MDs are often associated with brain defects. Based upon the clinical symptoms of MDs they are categorized into various subtypes and currently no cures or preventions exist for these diseases, making them a worthwhile field of research. The most severe form of MD is Duchenne MD (DMD), an X-linked fatal disorder that afflicts approximately 1 out of every 3,500 males worldwide. The DMD pathology contains a subset of individuals (about 1 in 3) that suffer from cognitive impairment and mental retardation, and these attributes of the disease appear to be independent from the muscular handicap [4,5].

DMD arises from the loss of the Dystrophin (Dys) protein product, which provides a link between cytoskeletal actin and the ECM via the glycoprotein Dystroglycan (Dg). Dys binds Dg along with several other transmembrane proteins (two syntrophins, two dystrobrevins, and four sarcoglycans) [6,7] to assemble the Dystrophin Glycoprotein Complex (DGC).

Mutations of Dystroglycan, the key transmembrane component of the DGC, lead to discontinuities in the basement membrane surrounding the cerebral cortex and disorganized cortical layering (for review see [8]). In addition, Dg hypoglycosylation leads to congenital muscular dystrophies (CMDs), of which some feature brain

* Correspondence: halyna.shcherbata@mpibpc.mpg.de
† Contributed equally
[1]Max Planck Institute for biophysical chemistry, Research group of Gene Expression and Signaling, Am Fassberg 11, 37077, Goettingen, Germany
Full list of author information is available at the end of the article

defects including cobblestone (type II) lissencephaly. This type of lissencephaly is characterized by heterotopic glia and neurons that disrupt the laminar organization of the cerebral cortex [9], and mutations in glycosyltransferases that act upon α-Dg have been linked to these disorders [10-18].

Disruption of the DGC not only affects cerebral cortex layering and lamina organization but also leads to physiological defects in neuron function. DMD patients and *mdx*^{Cv3} (DMD mouse model missing the 427 and 70 kD isoforms of Dys) and Dystroglycan knockout mice have reduced b-wave amplitudes in electroretinograms [19-22] supporting its specific role in the nervous system establishment and function. While the role of the DGC in muscle has been intensively studied, its function in the brain and nervous system has not been completely defined.

Drosophila has been demonstrated to serve as a useful model for studying the DGC *in vivo* since DGC mutants develop symptoms similar to MD patients [23-25]. Key human and *Drosophila* DGC components are evolutionarily conserved and interact in a similar manner [24,26,27]. As in mammals, in *Drosophila* proteins of the DGC are not only found at the muscle sarcolemma but also at the neuromuscular junction and in the PNS and CNS [23-25,28-32]. In the *Drosophila* brain Dg is expressed in R cells, glia and neurons, indicating that this protein has an important role in nervous system function [24,33,34]. *Drosophila* R cells provide an excellent system in which to study axon guidance, growth and elongation, negative and attractive guidance cues and neuron polarity establishment that later results in cell shape rearrangement. Both Dys and Dg affect photoreceptor cell elongation and are required in neurons and glia for proper photoreceptor axon migration [24,33]. Based on these phenotypes we performed a genetic interaction screen in order to find novel neuronal DGC components. We analyzed potential interactors that were identified in a previous screen to interact with Dys and/or Dg in muscle degeneration [35] and have found new components that interact with primarily Dys and to a lesser extent Dg in developing eye neurons. Among them are the calcium binding protein Calmodulin (Cam), Neurospecific receptor kinase (Nrk), a splicing factor Muscleblind (Mbl) and the actin recycling protein Capulet (Capt). Since most of these proteins have been shown to affect actin organization, polymerization and recycling, these results suggest that in neurons the DGC is involved in the processes of actin cytoskeleton regulation.

Results

Dys and Dg are expressed in Drosophila larval and adult nervous system

In this study we used antibodies that specifically recognize Dys and Dg proteins in order to detect the expression pattern of the main DGC components in the larval and adult nervous system. Previously it has been shown that Dg is expressed in neurons and glia in the larval *Drosophila* brain; high levels of Dg were detected in axons of photoreceptor sensory neurons, in the optic stalk, and in glial cells in the optic lobes [24]. Now we show that Dg is also expressed in the neuropile of 3rd instar larval CNS and in three symmetric clusters at the lateral sides of the neuropile (Figure 1A). As expected, we observed a similar expression pattern for Dg's binding partner Dys (Figure 1C-D). The carboxy terminal specific Dys antibody that recognizes all isoforms [28], localizes in the neuropile, the optic lobes and in the axons of photoreceptor sensory neurons (Figure 1C). In accord with previously reported data [30], a strong Dys signal was detected in the neuropile and in the optic lobes when using an antibody that recognizes the CNS-specific Dp186 isoform (Figure 1D). In the adult *Drosophila* brain Dg is detected in the medulla and the lamina (Figure 1F-G) and a strong Dg signal is also seen in the retina (Figure 1F-). Dys expression in the adult brain appears to be localized to the lamina (Figure 1I). Dys and Dg are not only expressed in the CNS, but also the PNS (Figure 1K-L): Dg staining was seen in and around the motoneurons (Figure 1K), while the Dys signal was overlaid with neuronal 22C10 staining (Figure 1L). In *Dg* and *Dys* loss-of-function homozygous mutants (*Dg*^{O86} and *DysDf*) Dg and Dys signals were diminished (Figure 1B, E, J) implying that the detected expression pattern was specific in accord with previous reports for these antibodies [24,28,35]. A definite expression pattern for Dys and Dg in the *Drosophila* nervous system implies that the DGC is involved in nervous system development. As has been shown previously, disruption of Dys or Dg gives rise to a disorganized lamina plexus, and these two components genetically interact [24]. This abnormal photoreceptor guidance can result from growth cone malfunction, compromised cell polarity, malformed actin cytoskeleton or disrupted glia-neuron communication. During *Drosophila* development, eye discs contain ommatidia and photoreceptor neurons that project axons down the optic stalk to innervate the brain. For each ommatidia there are eight photoreceptors (R-cells), where six of the eight cells stop at the superficial lamina forming the lamina plexus, and the other two photoreceptors project further into the medulla. Later, during pupation photoreceptors differentiate and undergo morphological changes including elongation and Dys and Dg both affect this process [24,33]. Since recently we identified genes that interact with Dys and/or Dg in age related muscle degeneration [35], in the present work we analyzed these gene candidates for their involvement together with the DGC in neuron behavior during *Drosophila* visual system development.

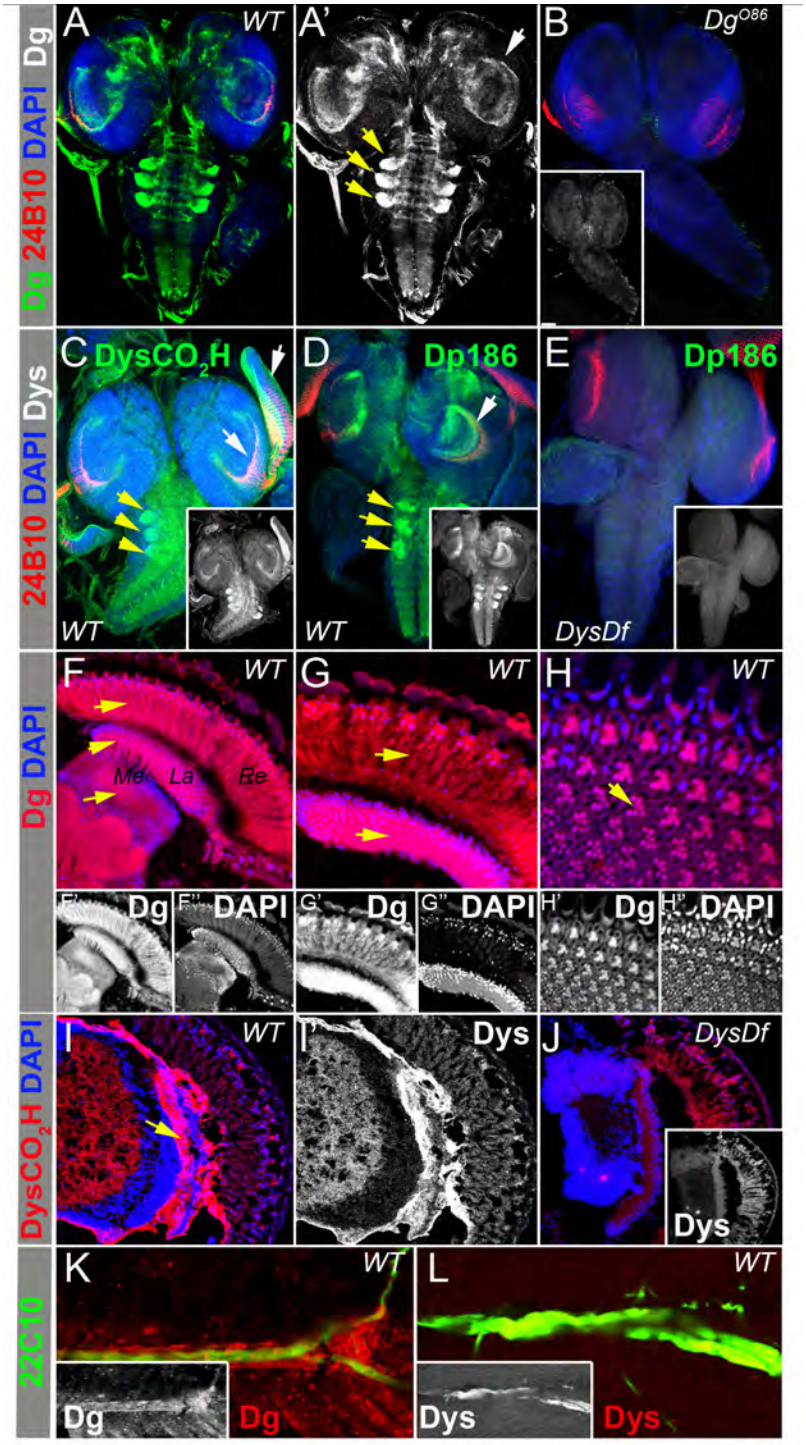

Figure 1 Dys and Dg are expressed in Drosophila larval and adult nervous systems. Expression pattern for Dg (A-B) and Dys (C-E) in *Drosophila* 3rd instar larval brains. Photoreceptor neurons are marked with the 24B10 antibody (red). The Dys antibody that recognizes all Dys isoforms by targeting the carboxy terminus shows localization in the brain and the eye discs (C) whereas an antibody that recognizes the Dp186 isoform is present only in the brain (D). Dg (B) and Dys (E) staining is absent in *Dg* and *Dys* loss-of-function homozygous mutants respectively. White arrows indicate Dys and Dg signal in the optic lobes and yellow arrows show staining in clusters at the lateral sides of the neuropile. The expression pattern for Dg (F-H) and Dys (I) in the adult brain. Arrows show strong Dg and Dys signals detected in the lamina *(La)* and medulla *(Me)* and Dg expression is also seen in the retina *(Re)*. Dys staining is diminished from the brain of *Dys* loss-of-function homozygous mutant (J). Expression pattern for Dg (K) and Dys (L) in *Drosophila* motorneurons marked with the 22C10 antibody (green).

Muscle DGC-interacting components also affect photoreceptor axon guidance and rhabdomere length

First, we questioned if previously identified DGC-interacting components have a role in neuronal architecture. Analysis of the 24B10 staining pattern in 3rd instar larvae found a significantly increased frequency of axon migration abnormalities in the brains of seven of the sixteen analyzed mutants (Calmodulin (*Cam*), Capulet (*capt*), Neurospecefic receptor kinase (*Nrk*), Chiffon (*chif*), *CG34400*, Lissencephaly-1 (*Lis1*) and Roundabout (*robo*)) - 22-47% in comparison to less than 10% observed in control animals (Figure 2A, Table 1), resulting in lamina plexus breaks or overgrown axons (Figure 2D-E). Next we asked if the DGC interactors are required to provide proper photoreceptor differentiation via analysis of adult brain histological sections. We used *RNAi* transgenic mutants crossed to *GMR-Gal4* to target gene expression specifically in the visual system and identified shorter rhabdomeres in *Cam, capt, Nrk, mbl, CG34400, Lis1*, Visceral mesodermal armadillo repeats (*vimar*), *SP2353* and Grainyhead (*Grh*) (Figure 2B, F-K, Table 1). Interestingly, we also noticed vacuoles in the retinas of Mbl^{RNAi}/*GMR-Gal4* and $Lis1^{RNAi}$/*GMR-Gal4* mutants (Figure 2G-H).

Mutations in many of the DGC-interacting genes cause visual system defects; therefore, we analyzed the expression of these genes in the *Drosophila* nervous system via examination of published data and available GFP expression lines. *Lis1* mRNA was found in the brain hemispheres and eye imaginal discs of 3rd instar larvae [36]. Mbl is also expressed in larval eye discs and is required for photoreceptor differentiation and *mbl* deficiency results in shortened rhabdomeres [37]. In addition, expression in the central and peripheral nervous system has been shown for Grh [38], Nrk [39], Vimar [40] and Robo [41]. Interestingly, Robo is a transmembrane receptor for the extracellular matrix protein Slit, and previous reports showed that *robo* mutation results in improper axon crossing in the embryo and defects in compartmentalization of visual centers in the larval and adult brain [42-44].

We used modENCODE temporal expression data [45] to determine the expression of *chif, CG34400* and *SP2353*. Expression of *SP2353* is enriched in the adult brain and thoracic-abdominal ganglion. *CG34400* and *chif* are expressed during development and adulthood and a previous report showed that *chif* mutants have a rough eye phenotype [46].

We also used GFP trap lines to recognize the expression pattern for Cam and Capt in the larval brain. We identified that Capt is expressed ubiquitously in the central and ventral brain and its expression is enriched in optic lobes and eye discs (Figure 2L-M). Cam has a more defined expression pattern in the neuropile and central brain and is also enhanced in optic lobes and eye discs (Figure 2N-O). Capt and Cam are expressed in R cells of the eye disc (Figure 2M,O) and enriched in the area where R1-6 axons terminate, similarly to Dys and Dg suggesting that they may act in the same cell types (Figure 1A,C). Since many of the proteins that interact with the DGC in muscle are expressed in the nervous system and have comparable phenotypes in the visual system to *Dys* and *Dg* mutants, we determined if they genetically interact with *Dys* and *Dg* in this tissue as well.

Search for Dys and/or Dg interacting partners in photoreceptor axon pathfinding

First we looked at photoreceptor axon pathfinding to assess the genetic interaction of *Dys* and *Dg* with components shown to be required in visual system neurons. For genetic analysis we used loss-of-function mutants for *Dys* and *Dg* that in homozygous and heterozygous state demonstrate breaks in the lamina plexus (Figure 3A-B). Since reduction of one copy of *Dys* or *Dg* has a mild phenotype (Figure 3C-D), they can be used for a transheterozygous genetic interaction analysis in photoreceptor cell projections. Deleting one copy of an interacting gene in the heterozygous *Dg* or *Dys* mutant background will increase the frequency of abnormal lamina plexuses if there is a genetic interaction. Seven genes were found to increase the appearance of abnormal lamina plexuses in a *Dys* heterozygous background and three in a *Dg* heterozygous background (Figure 3C-D, Table 2). To avoid an additive effect, we tested the found interactors for a dominant phenotype. Three genes, *Lis1, CG34400* and *Grh* have abnormal lamina plexuses while reduced by one copy (37.5%, 14.3% and 10.0% respectively) and were therefore not considered to interac. In summary, in this screen we have identified Nrk - a protein with tyrosine kinase activity, Cam - a main player in calcium-mediated signaling, Mbl - a DNA binding protein implicated in mRNA splicing, and Capt - a factor required to prevent actin filament polymerization.

Genetic interaction with Dys and Dg in controlling rhabdomere elongation

To complement the data derived from analysis of 3rd instar larval brains, we have performed a separate assay to evaluate the genetic interaction with the DGC in the process of rhabdomere (photoreceptor cell) elongation. First, we analyzed histological sections of *Drosophila* adult eyes and showed that *Dys* and *Dg* loss-of-function mutants also have shortened rhabdomeres, and reduction by one copy of both *Dys* and *Dg* results in a genetic interaction (Figure 4A). Next we found that *Cam* and *capt* genetically interact with *Dys*

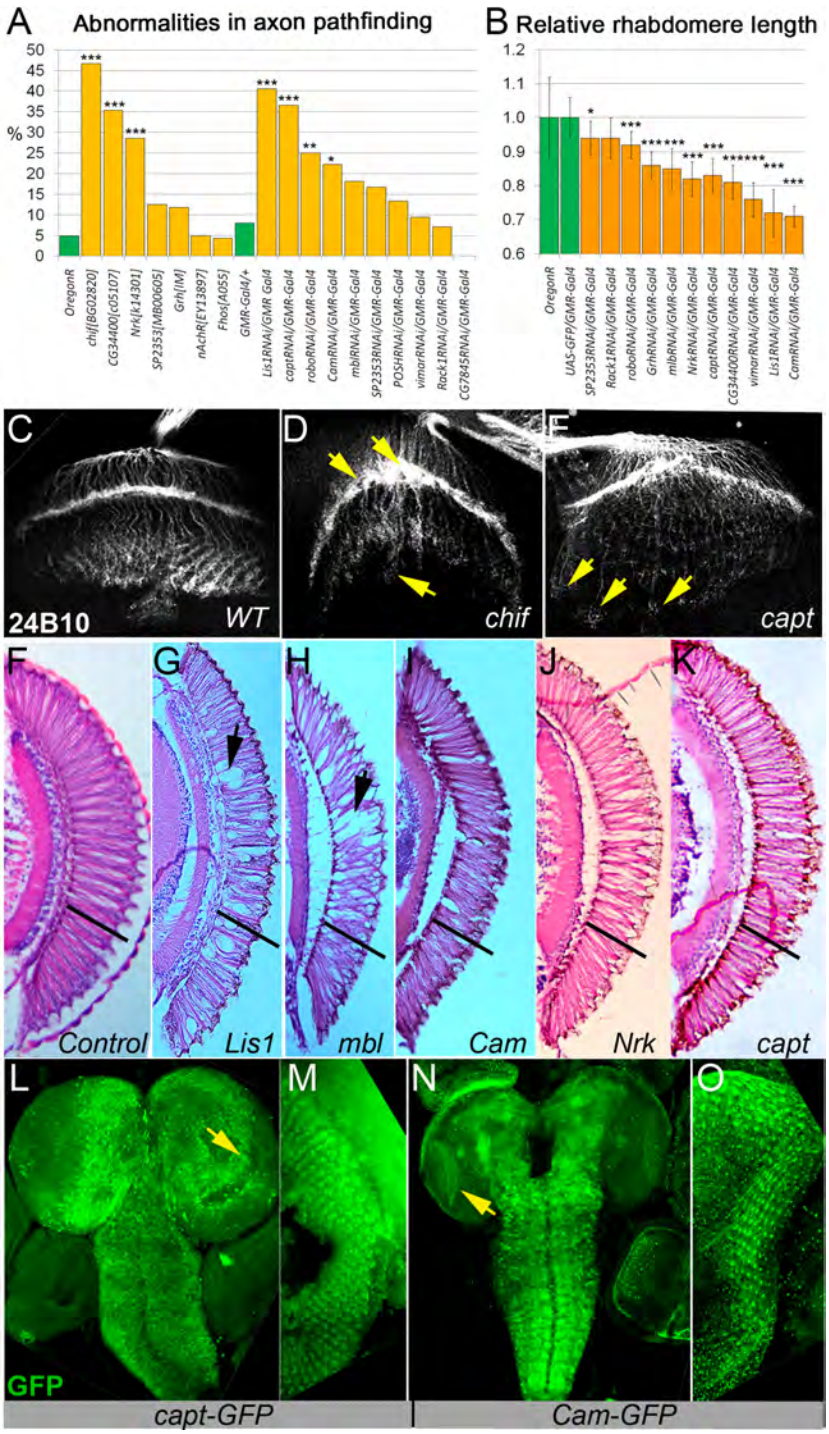

Figure 2 Requirement of screened components for photoreceptor cell development. (A) Bar graph represents frequency of defective photoreceptor axon projections in 3rd instar larval brain. Statistics were determined using the χ^2-test with Yate's correction where ***p ≤ 0.001, **p ≤ 0.01, *p ≤ 0.05. (B) Bar graph shows relative rhabdomere length in adult flies with down regulation of tested components. Statistics were determined using a one-tailed Student's t-test where ***p ≤ 0.001, **p ≤ 0.01, *p ≤ 0.05. (C) Photoreceptor axons projection in wild type 3rd instar larval brain visualized with the 24B10 antibody. (D-E) Abnormal R cells growth and termination in 3rd instar larvae with down regulated Chif and Capt (*chif*^{BG02820}, *capt*^{RNAi}/*GMR-Gal4*). Arrows indicate irregular axon termination in the lamina plexus, lamina plexus breaks and sites of overgrown axons. (F-K) Exemplary brain sections represent rhabdomere length and morphology in tested mutants in comparison to control (F). Arrows show vacuoles in retina and black bars indicate *wt* rhabdomere length. (L-O) *capt* and *Cam* GFP trap lines show expression patterns for Cam and Capt in the larval brain. (M, O) Enlarged view of eye discs. Arrows indicate expression pattern in optic lobes.

Table 1 Genetic interactors of *Dys* and *Dg* in muscle have photoreceptor axon pathfinding defects and shortened rhabdomeres

Genotype	Defective lamina plexuses (%)	n, analyzed optic lobes	χ^2-value	Relative rhabdomere length	n, analyzed eyes	p-value
OregonR (Control)	4.9	41		1.0 ± 0.12	8	-
CG34400[c05107]	**35.3**	**17**	**21.7 *****	-	-	-
chif[BG02820]	**46.7**	**15**	**28.4 *****	-	-	-
Fhos[A055]	4.3	23	3.3×10^{-2}	-	-	-
Grh[IM]	11.8	17	2.1	-	-	-
nAcRα-30D[EY13897]	5.0	40	6.5×10^{-2}	-	-	-
Nrk[k14301][1]	**28.6**	**14**	**15.5 *****	-	-	-
SP2353[MB00605]	12.5	32	2.6	-	-	-
eyeFlpFRT/Lis1FRT	-	-	-	0.94 ± 0.08	10	0.20
GMR-Gal4/+	8.0	25	-	1.00 ± 0.06	32	-
Cam^{RNAi}*/GMR-Gal4*	**22.2**	**18**	**5.8***	**0.71 ± 0.03**	**6**	**1.3×10^{-12}*****
[2]$capt^{RNAi}$*/GMR-Gal4*	**36.6**	**71**	**17.1 *****	**0.81 ± 0.03**	**18**	**2.9×10^{-11}*****
[3]$capt^{RNAi}$*/GMR-Gal4*	**42.9**	**49**	**22.6*****	**0.76 ± 0.07**	**18**	**1.0×10^{-14}*****
$CG7845^{RNAi}$*/GMR-Gal4*	0.0	13	6.1	-	-	-
$Fkbp13^{RNAi}$*/GMR-Gal4*	4.7	21	6.1	-	-	-
$Lis1^{RNAi}$*/GMR-Gal4*	**40.6**	**32**	**20.5 *****	**0.72 ± 0.07**	**18**	**1.8×10^{-11}*****
mbl^{RNAi}*/GMR-Gal4*	18.2	22	3.2	**0.85 ± 0.06**	**10**	**1.4×10^{-7}*****
$POSH^{RNAi}$*/GMR-Gal4*	13.3	15	0.9	-	-	-
$Rack1^{RNAi}$*/GMR-Gal4*	7.1	14	6.6×10^{-4}	0.94 ± 0.06	11	0.13
$robo^{RNAi}$*/GMR-Gal4*	**25.0**	**20**	**7.8 ****	0.92 ± 0.04	6	0.14
$SP2353^{RNAi}$*/GMR-Gal4*	16.7	12	2.4	**0.94 ± 0.05**		**0.014***
Nrk^{RNAi}*/GMR-Gal4*	-	-	-	**0.82 ± 0.05**	**14**	**3.8×10^{-11}*****
$CG34400^{RNAi}$*/GMR-Gal4*	-	-	-	**0.81 ± 0.05**	**17**	**2.0×10^{-9}*****
Grh^{RNAi}*/GMR-Gal4*	-	-	-	**0.86 ± 0.04**	**6**	**1.1×10^{-4}*****
$vimar^{RNAi}$*/GMR-Gal4*	9.5	21	1.0	**0.76 ± 0.05**	**13**	**2.2×10^{-15}*****
Pgk^{RNAi}*/GMR-Gal4*	-	-	-	**0.77 ± 0.04**	**18**	**4.2×10^{-6}*****

all mutant alleles were obtained from BDSC, all RNAi mutants - from VDRC, [1] - from DGRC

[2] Vienna stock number v21995

[3] Vienna stock number v101588

(Figure 4B, E-F, Table 3) and *Cam*, *capt* and *mbl* with *Dg* (Figure 4C, Table 3) displaying significantly shortened rhabdomeres. None of the tested mutants in a heterozygous state showed a significant phenotype (1.04 ± 0.05, 0.97 ± 0.02, 1.03 ± 0.06, 1.00 ± 0.02 and 1.04 ± 0.04 for *capt*, *Nrk*, *mbl*, *Lis1* and *Cam* respectively when normalized to *wt* control).

Here we have found genes that interact with *Dys* and/or *Dg* in axon pathfinding and in the process of photoreceptor cell elongation. Shortened rhabdomeres can result from actin cytoskeletal defects, but also from improper photoreceptor cell fate specification, retinal degeneration or abnormal innervations. Dynamic changes in actin filaments provide cell shape and control photoreceptor cell differentiation in developing *Drosophila* pupae. Therefore disruption of these processes may also affect the rhabdomere elongation in the *Drosophila* adult eye.

The DGC coordinates actin cytoskeleton remodeling

In our screen we identified Cam, Capt and Mbl as DGC-interacting partners that have roles in actin dynamics (Figure 5A), which implies that the phenotypes observed in the DGC mutants might at least partially result from improper actin cytoskeleton organization. To explore this hypothesis we generated clones in developing *Drosophila* eye discs homozygous for *Dg* loss-of-function alleles using the FLP/FRT system. These clones resulted in irregular ommatidia in adult animals (Figure 5B-C). For detailed characterization of this phenotype we performed immunohistochemical analysis of clonal pupal retinas using multiple cell markers including actin (Figure 5D-F). First we noticed that clones (marked by absence of GFP) have shortened ommatidia (Figure 5D-F, yellow bars). Further analysis revealed that there was also disrupted

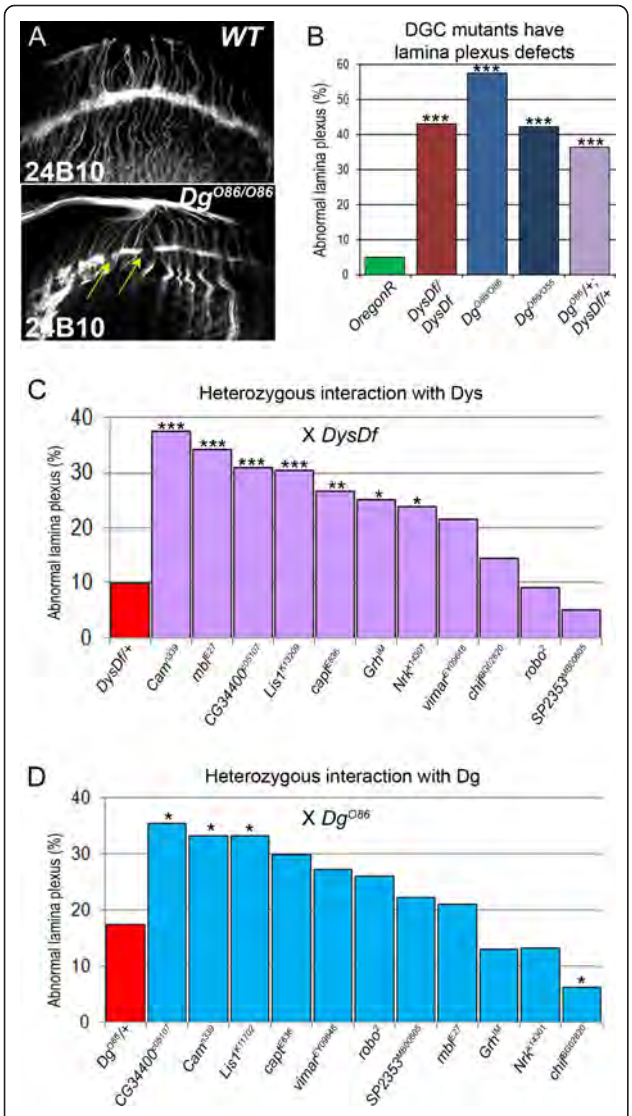

Figure 3 Genetic interactors were found to cause lamina plexus defects with Dys and Dg. (A) Wild type properly formed lamina plexus and defects found in Dg (and Dys) mutants showing gaps in the axon projections (arrows). 24B10 antibody was used to visualize photoreceptor axons. (B) Dys and Dg homozygous mutants have a significantly higher percentage of these defects from control and genetically interact. (C) Genetic interactions found with *Dys*, and with *Dg* (D). Statistics were determined using the χ^2-test with Yate's correction where ***p ≤ 0.001, **p ≤ 0.01, *p ≤ 0.05.

layering of nuclei. DAPI staining made clear that nuclear migration during development does not occur properly, resulting in disorganized layers (Figure 5 E-F). We also observed a different pattern of β-catenin (Arm) in clonal areas compared to wild type (Figure 5E-F) suggesting that during development cells lacking Dg cannot change their shape and elongate properly. In addition, irregular Actin was seen in *Dg* mutant clones indicating DGC involvement in actin dynamics in photoreceptor cells. This result suggests that the DGC cell autonomously coordinates actin cytoskeleton remodeling, the process required for proper photoreceptor cell growth and elongation, as well as axon migration during *Drosophila* eye development; it further indicates that photoreceptor axon pathfinding and R-cell elongation defects observed in DGC mutants might be a result of improper actin reorganization during development.

Discussion

The roles that Dys and Dg play in disease have been apparent for some time since their disruption or misregulation has been closely linked to various MDs. Dg depletion results in CMD-like brain malformations associated with layering defects and aberrant neuron migration [34]. These defects arise due to extracellular matrix protein affinity problems that influence neuronal communication and result in learning and memory defects. Similar to brain layer formation, the migration of R1-R6 growth cones into the lamina occurs in a similar manner where glia cells that migrate from progenitor regions into the lamina provide a termination cue to innervating axons. In *Drosophila* Dys and Dg are expressed in the CNS, PNS and visual system and both proteins are required for proper photoreceptor axon guidance and rhabdomere elongation [24,33]. In this work we identified novel components implicated in the process of eye-neuron development. Moreover, we found that Nrk, Mbl, Cam and Capt genetically interact with Dys and/or Dg in visual system establishment.

The proteins Mbl, Capt, Cam, Robo, Lis1 and Nrk have been shown previously to be associated with the nervous system, and now we have additionally found that mutations in *chif, SP2353, CG34400* and *vimar* cause abnormal photoreceptor axon pathfinding and/or differentiation phenotypes. Lis1 has been shown to bind microtubules in the growth cone [47], and the human Lis1 homologue is important for neuronal migration and when mutated causes Lissencephaly, a severe neuronal migration defect characterized by a smooth cerebral surface, mental retardation and seizures [48]. Now we have found that $Lis1^{RNAi}$/*GMR-Gal4* mutants have abnormally formed lamina plexuses, shortened rhabdomeres, and retinal vacuoles. Chif has been shown to regulate gene expression during egg shell development and is related to a DNA replication protein in yeast [46]. The human ortholog for SP2353 (AGRN) is involved in congenital MD development [49,50]. *Drosophila* SP2353 is a novel agrin-like protein that contains Laminin G domains, which makes it a potential new extracellular binding partner for Dg. *CG34400* encodes for a protein homologues to human DFNB31 (Deafness, autosomal recessive 31) that causes congenital hearing impairment

Table 2 Genetic interaction with *Dys* and *Dg* in photoreceptor axon path finding

Gene name	Defective lamina plexuses (%)	n, analyzed optic lobes	χ^2-value	Defective lamina plexuses (%)	n, analyzed optic lobes	χ^2-value	Defective lamina plexuses (%)	n, analyzed optic lobes	χ^2-value
	***DysDf* x**	***DysDf* x**	***DysDf* x**	***Dg^{O86}* x**	***Dg^{O86}* x**	***Dg^{O86}* x**	***OregonR* x**	***OregonR* x**	***OregonR* x**
OregonR	9.8	61	1.1°	17.5	40	6.0° *	4.9	41	-
DysDf	**42.9**	**49**	**28.8° *** **	**36.4**	**55**	**22.5° *** **	9.8	61	1.1°
Dg[O86]	**36.4**	**55**	**22.5° *** **	**57.5**	**40**	**42.7° *** **	17.5	40	6.0° *
Dg[O55]	-	-	-	**42.1**	**19**	**27.9° *** **	-	-	-
Cam[n339]	**37.5**	**48**	**15.0 *** **	**33.3**	**39**	**4.3 ***	0.0	9	3.0
Capt[E636]	**26.7**	**45**	**6.9 ** **	29.8	47	2.7	2.9	35	0.1
CG34400 [c05107]	**30.9**	**42**	**9.9 ** **	**35.5**	**31**	**5.4 ***	14.3	35	3.7
CG7845 [EMS-Mod4][1]	11.1	9	4.0×10^{-3}	**5.6**	**18**	**5.2 ***	-	-	-
chif [BG02820]	14.3	14	0.5	**6.3**	**16**	**4.4 ***	-	-	-
Fhos[A055]	19.0	21	2.3	8.3	12	2.6	-	-	-
Fkbp13 [P962]	21.4	14	3.6	11.1	9	1.0	-	-	-
Grh[IM]	**25.0**	**24**	**5.8 ***	13.0	23	0.4	10.0	20	1.2
Lis1[k11702]	17.8	28	1.8	31.2	16	3.3	7.7	13	0.3
Lis1[k13209][2]	**30.3**	**33**	**9.5****	**33.3**	**12**	**4.3***	**37.5**	**16**	**23.7*****
Lis1[k13209]	**33.3**	**12**	**11.8*****	11.1	9	1.0	**28.6**	**14**	**15.5*****
mbl[E27]	**34.3**	**35**	**12.5 *** **	21.0	38	0.2	0.0	7	3.0
nAcRα-30D [EY13897]	**0.0**	**9**	**7.9 ***	12.5	8	0.5	-	-	-
Nrk[k14301][2]	**23.7**	**38**	**4.9 ***	13.3	15	0.3	0.0	7	3.0
POSH [k15815][2]	9.1	22	5.0×10^{-3}	21.7	23	0.3	-	-	-
Rack1 [EY00128][2]	**0.0**	**13**	**7.9 ***	21.7	23	0.3	-	-	-
robo[2]	9.1	11	4.0×10^{-3}	26.1	23	1.3	-	-	-
SP2353 [MB00605]	5.0	20	1.0	22.2	18	0.3	-	-	-
vimar [EY09646]	21.4	42	3.6	27.3	22	1.7	-	-	-

all mutant alleles were obtained from BDSC, all RNAi mutants - from VDRC, [1] - described previously [70], [2] - from DGRC

° - compares to *Oregon R*

in DFNB31 deficient people and mouse whirlin, that causes deafness in the whirler mouse [51]. Hearing loss has been as well demonstrated in association with various forms of muscular dystrophy [51]. Vimar has been shown to regulate mitochondrial function via an increase in citrate synthase activity [52].

Mbl is a *Drosophila* homologue of the human gene MBNL1. Mutations of this gene cause myotonic dystrophy and are associated with the RNA toxicity of CUG expansion diseases protein [53]. Here we show that Mbl deficiency results in similar phenotypes to Dys and Dg loss of function, and to specifically interact with *Dys* in axon projections which is in accord with the *Dys* specific interaction seen in muscle [35]. Dys has multiple isoforms, and the variability of DMD patients to have mental impairment has been linked in part to small Dys isoform mutations, which leads to speculation that Dys is a target for Mbl mediated splicing.

Interestingly, Mbl isoforms have been demonstrated to regulate splicing of α-actinin [54], which belongs to the spectrin gene superfamily that also includes dystrophins. α-actinin and Capt, the *Drosophila* homologue of

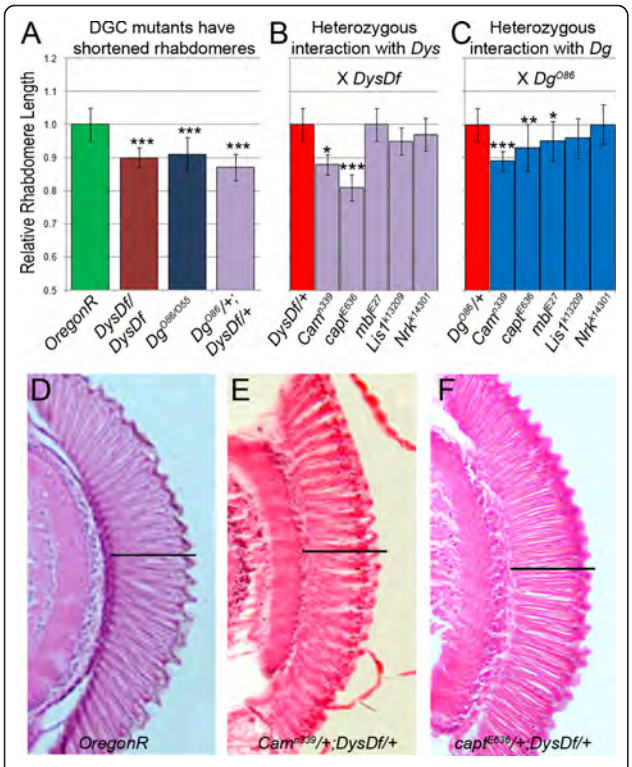

Figure 4 Genetic interactors were found to cause shortened rhabdomeres with Dys and Dg. (A) *Dys* and *Dg* homozygous mutants have significantly shorter rhabdomeres in the developed adult eye and interact in this process. Measurements have been normalized to control. (B) Genetic interactions found with *Dys*, and with *Dg* normalized to *Dys*/+ or *Dg*/+ appropriately (C). Rhabdomere examples from *OregonR* (WT,D), Cam^{n339}/+;*DysDf*/+ (E) and $capt^{E636}$/+;*DysDf*/+ (F). Scale bare represents *wt* rhabdomere length. Statistics were determined using a one-tailed Student's t-test where ***p ≤ 0.001, **p ≤ 0.01, *p ≤ 0.05.

Cyclase-associated protein (CAP) are actin-binding proteins in the growth cone. Capt was first identified in yeast and is highly conserved throughout eukaryotic evolution [55]. The main known function of Capt is to act in the process of actin recycling by working in conjunction with Actin Depolymerization Factor (ADF a.k.a. Cofilin) to help displace Cofilin from G-actin during depolymerization [56,57]. It has already been reported that ADF/Cofilin has a role in retinal elongation [58]. The actin cytoskeleton is a major internal structure that defines the morphology of neurons, and Capt has already been shown to be required to maintain PNS neuronal dendrite homeostasis in *Drosophila* via kinesin-mediated transport [59]. Additionally, Capt has been found to lead to excessive actin filament polymerization in the eye disc and to cause premature differentiation of photoreceptors [60]. The rate of axon projection is much slower than the rate of microtubule polymerization during axonal growth [61], implying that depolymerization/polymerization of actin is important during pathfinding. We have also shown that Capt interacts with Dys and is necessary for proper projection of photoreceptor axons in the developing brain, and when absent, eyes develop with abnormal rhabdomeres. Furthermore, we have demonstrated that $capt^{RNAi}$ mutants exhibit overgrowth of photoreceptor axons, and we believe a possible explanation for this is improper turnover of actin (Figure 5A).

Importantly, proteins that can be regulated by Ca^{2+} to organize actin filament bundles and to promote filament turnover include α-actinin and (ADF)/Cofilin, respectively [62-64]. Cam functions as an intracellular Ca^{2+} sensor, and when Ca^{2+}-Cam was selectively disrupted in a subset of neurons in *Drosophila* embryos, stalls in axon extension and errors in growth cone guidance resulted [65]. Actin turnover is highly regulated by Ca^{2+} levels, and many proteins are Ca^{2+}-mediated to regulate motility and axon guidance. Our results and those from prior studies suggest that Cam is a major functional player of Ca^{2+} regulation in growth cones. Since we show here that mutations in *Cam* and *capt* have similar phenotypes in photoreceptor axon pathfinding and rhabdomere development, we postulate that actin dynamics is the link between these two proteins and the

Table 3 Genetic interaction with *Dys* and *Dg* in rhabdomere elongation

Gene name	Relative rhabdomere length	n, analyzed eyes	p-value	Relative rhabdomere length	n, analyzed eyes	p-value
	***DysDf* x**	***DysDf* x**	***DysDf* x**	***Dg^{O86}***	***Dg^{O86}***	***Dg^{O86}***
OregonR	1.00 ± 0.05	6	-	1.00 ± 0.05	20	-
DysDf	**0.89 ± 0.03**	**15**	**4.6×10^{-5}**	**0.80 ± 0.04**	**12**	**3.5×10^{-10}**
Dg[O86]	**0.85 ± 0.04**	**12**	**4.0×10^{-5}**	-	-	-
Dg[O55]	-	-	-	**0.83 ± 0.05**	**15**	**3.7×10^{-9}**
Cam[n339]	**0.88 ± 0.03**	**3**	**1.4×10^{-2}**	**0.89 ± 0.03**	**6**	**3.7×10^{-4}**
Capt[E636]	**0.81 ± 0.04**	**6**	**5.0×10^{-5}**	**0.93 ± 0.07**	**12**	**1.0×10^{-2}**
Mbl[E27]	1.00 ± 0.05	6	0.5	**0.95 ± 0.06**	**14**	**2.8×10^{-2}**
Nrk[k14301]	0.97 ± 0.05	12	0.2	1.00 ± 0.06	12	0.5
Lis1[k13209]	0.95 ± 0.04	7	0.087	0.96 ± 0.06	13	0.084

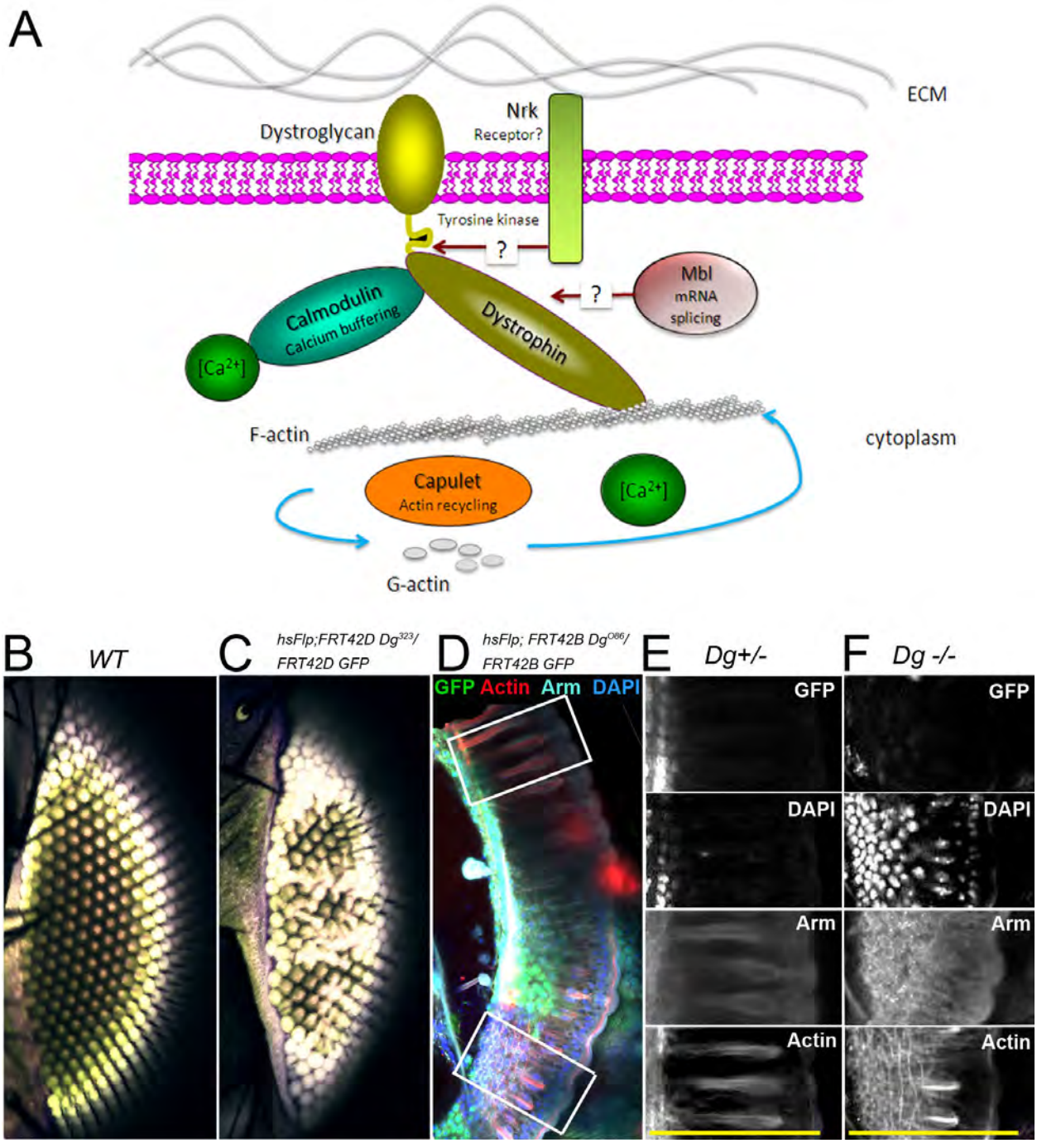

Figure 5 The DGC coordinates actin cytoskeleton remodeling. (A) Scheme showing a cell with the DGC and found Dys/Dg-interacting components. Autofluorescence image shows a regular ommatidia pattern (B) which is disrupted by Dg^{323} clone induction (C). (D) Dg^{O86} mutant clones (marked by the absence of nuclear GFP) in a *Drosophila* pupal eye stained with anti-phalloidin (Actin) and the nuclear marker DAPI. Rectangles indicate *wt* (upper) and mutant (lower) areas. An enlarged view of *wt* (E) and mutant (F) zones (indicated with rectangles in D) with GFP, DAPI, Arm and Actin cell markers in different channels. $Dg^{-/-}$ cells (GFP negative) have disorganized nuclei, improper Arm and Actin localization and shorter rhabdomeres when compared to sister *wt* cells (GFP positive). Yellow bars in lower panel indicate normal rhabdomere length.

phenotypes described here. Due to the importance of Cam for actin dynamics, its interaction with both Dg and Dys suggests that the DGC coordinates the actin cytoskeleton in the developing eye.

The last gene that we have identified in this work is Nrk. Recently various kinases, channels and other enzymes have been shown to associate with the DGC, although only a few of these interactions have been confirmed *in vivo* [66,67]. Since Nrk is a component found to interact with *Dys* in photoreceptor axon pathfinding, it is most likely that it functions as a receptor to sense guidance cues rather than as a molecule affecting actin cytoskeletal rearrangement. Our data here hint that Dg and Nrk could be two receptors integral to transferring signals important for neuronal layering.

Conclusions

Dynamic rearrangement of the actin cytoskeleton is crucial for the central and peripheral nervous system establishment, which depends on proper neuron migration and differentiation. This process requires not only the cell autonomous regulation of neuron motility, but also the interaction between the migrating cell and its underlying substrate. This interaction is often dependent on the signaling transduced via the ECM. The DGC and other factors are believed to be mediators of actin dynamics in growing axons and during neuronal cell morphogenesis, and our study found components that interact with Dys and/or Dg in both of these activities (Figure 5A). Additionally, disruption in gene expression of these components results in the same phenotypes seen with *Dys* and *Dg* mutants in the developing and adult eye. Our data allows us to conclude that the DGC is involved in signaling to cause cytoskeletal rearrangement and actin turnover in growth cones (Figure 5A). Since many cases of muscular dystrophies are associated with mental retardation, we believe that it is important to understand the role of the DGC in axon migration because understanding of this process could aid in finding an adequate therapy for this aspect of the disease's physiology. Since the human brain continues to develop well after gestation, and evidence shows that nerves maintain plasticity throughout an individual's lifespan, therapies could be devised that reverse these defects after birth.

Methods

Fly Strains and Genetics

Fly stocks were maintained at 25°C on a standard cornmeal-agar diet. Fly strains used in this study are: loss of function mutants *DysDf*, Dg^{O86}, Dg^{O55} [68], Dg^{323} [69] *GMR-Gal4* and *OregonR* (wild type). Lines carrying screened mutations include the following alleles: Cam^{n339}, Grh^{IM}, mbl^{E27}, $CG34400^{c05107}$, $Capt^{E636}$, Nrk^{k14301}, $Fkbp13^{P962}$, $vimar^{EY09646}$, $Fhos^{A055}$, $Lis1^{k11702}$, $Lis1^{k13209}$, $FRT42D\text{-}Lis1^{k13209}$ (Kyoto DGRC), $chif^{BG02820}$, $CG7845^{EMS\text{-}MOD4}$ [70], $POSH^{k15815}$, $robo^{2}$, $SP2353^{MB00605}$, $nAcR\alpha\text{-}30D^{Ey13897}$, $Rack1^{EY00128}$. Unless otherwise stated, lines were obtained from BDRC. *RNAi* lines were obtained from the VDRC and line numbers are as follows: *Cam (v28242), capt (v21995 and v101588), CG34400 (v28945), Fkbp13 (v12863), Lis1 (v106777), mbl (v28731), Nrk (v36282), Rack1 (v104470), robo (v4329), vimar (v21686), POSH (v26655)* and *Grh (v33679)*. To determine protein expression of Capt and Cam we obtained GFP protein trap lines from the FlyTrap project [71] that generates a fused GFP protein (Cam^{P00695}) or GFP expression is controlled by enhancer elements ($capt^{YB0070}$).

Homozygous lethal lines were balanced over the *CyO* balancer chromosome marked with Kruppel-GFP to make it possible to determine the genotypes of larvae. Third chromosome alleles were balanced with the *TM6, Tb* balancer chromosome which results in shorter and thicker larvae allowing for its detection. Non-GFP and non-Tb progeny (F1) were collected from crosses at the L3 larval stage of development for axon path-finding analysis and as adult flies for retina length determination.

Dg mutant clonal cells were generated by crossing females of genotype *hsFlp; FRT 42B GFP/CyO* with males of genotype *FRT 42B* Dg^{O86}*/CyO*. Vials were exposed to 2 hrs of 37°C heat shocks per day starting 1 day AEL until pupae formation. Dissection of eyes was done approximately 70 hrs APF.

Immunohistochemistry

Dissections were done in PBS, fixed in 4% formaldehyde and antibodies were applied as described previously [24]. The following antibodies were used: mouse anti-24B10 (1:50, Development Studies Hybridoma Bank), rabbit anti-Dg [69] (1:1000), anti-Dp186 and anti-Dys-CO_2H [28] (1:600), anti-Arm, Alexa 488 and 568 goat anti-mouse, Alexa 488 goat anti-rabbit (1:500, Molecular probes) and Alexa 568 conjugated phalloidin (1:40, Invitrogen). DAPI was used to visualize nuclei. Samples were mounted on slides in 70% glycerol, 2% NPG, 1X PBS and analyzed using a confocal microscopes (Leica TCS SP5, Zeiss Axio Imager).

Histology

For analysis of eye and head morphology, 10 μm paraffin-embedded sections were cut of fly heads. In order to prepare *Drosophila* sections, fly heads were immobilized in collars in the required orientation and fixed in Carnoy fixative solution (6:3:1 Ethanol:Chloroform:Acetic acid) at 4°C overnight. Tissue dehydration and embedding in paraffin was performed as described previously

[72]. Histological sections were prepared using a Hyrax M25 (Zeiss) microtome and stained with hematoxylin and eosin. All chemicals for these procedures were obtained from Sigma Aldrich. Analysis was done using a light microscope (Zeiss). To prepare *Drosophila* adult brain cryosections the protocol adapted from [72] was used. First flies were located in collars and immediately frozen in TissueTek® O.C.T. (Tissue-Tek) at ≈ -40°C. Then frozen heads were sectioned on a cryo-microtom Leica CM3050S with a section thickness of 10 μm. Fixation was carried out in 4% formaldehyde (Polyscience, Inc.) for 10 min at room temperature.

Data Analysis

The percentage of larval brain lobes with abnormalities in the lamina plexus were quantified as the percentage of defective lobes divided by the total lobes examined. Adult ommatidia lengths were measured and normalized to the appropriate control.

Statistics

Statistical analysis of abnormal lamina plexus formation was done using a one-tailed χ^2 test. Statistical analysis of ommatidia length was done using a one-tailed Student's t-test where error bars represent the average deviation. For transheterozygous interation of screened genes with *Dys* and *Dg* comparisons were made to *Dys/+* or *Dg/+* as appropriate.

Abbreviations

DGC: Dystrophin Glycoprotein Complex; Dys: Dystrophin; Dg: Dystroglycan; MD: muscular Dystrophy

Author details

[1]Max Planck Institute for biophysical chemistry, Research group of Gene Expression and Signaling, Am Fassberg 11, 37077, Goettingen, Germany. [2]Ivan Franko National University of Lviv, Department of Genetics and Biotechnology, Hrushevsky 4, 79005, Ukraine.

Authors' contributions

AKM, MMK and VMR carried out all immunohistochemistry and histological experiments. AKM, MMK and HRS participated in the design of the study and drafted the manuscript. All authors read and approved the final manuscript.

Received: 19 April 2011 Accepted: 26 September 2011
Published: 26 September 2011

References

1. Lim LE, Campbell KP: **The sarcoglycan complex in limb-girdle muscular dystrophy.** *Curr Opin Neurol* 1998, **11(5)**:443-452.
2. Matsumura K, Campbell KP: **Dystrophin-glycoprotein complex: its role in the molecular pathogenesis of muscular dystrophies.** *Muscle Nerve* 1994, **17(1)**:2-15.
3. Hayashi YK, Chou FL, Engvall E, Ogawa M, Matsuda C, Hirabayashi S, Yokochi K, Ziober BL, Kramer RH, Kaufman SJ, Ozawa E, Goto Y, Nonaka I, Tsukahara T, Wang JZ, Hoffman EP, Arahata K: **Mutations in the integrin alpha7 gene cause congenital myopathy.** *Nat Genet* 1998, **19(1)**:94-97.
4. Billard C, Gillet P, Signoret JL, Uicaut E, Bertrand P, Fardeau M, Barthez-Carpentier MA, Santini JJ: **Cognitive functions in Duchenne muscular dystrophy: a reappraisal and comparison with spinal muscular atrophy.** *Neuromuscul Disord* 1992, **2(5-6)**:371-378.
5. Perronnet C, Vaillend C: **Dystrophins, utrophins, and associated scaffolding complexes: role in mammalian brain and implications for therapeutic strategies.** *J Biomed Biotechnol* 2010, **2010**:849426.
6. Kanagawa M, Toda T: **The genetic and molecular basis of muscular dystrophy: roles of cell-matrix linkage in the pathogenesis.** *J Hum Genet* 2006, **51(11)**:915-926.
7. Sciandra F, Bozzi M, Bianchi M, Pavoni E, Giardina B, Brancaccio A: **Dystroglycan and muscular dystrophies related to the dystrophin-glycoprotein complex.** *Ann Ist Super Sanita* 2003, **39(2)**:173-181.
8. Montanaro F, Carbonetto S: **Targeting dystroglycan in the brain.** *Neuron* 2003, **37(2)**:193-196.
9. Olson EC, Walsh CA: **Smooth, rough and upside-down neocortical development.** *Curr Opin Genet Dev* 2002, **12(3)**:320-327.
10. Kobayashi K, Nakahori Y, Miyake M, Matsumura K, Kondo-Iida E, Nomura Y, Segawa M, Yoshioka M, Saito K, Osawa M, Hamano K, Sakakihara Y, Nonaka I, Nakagome Y, Kanazawa I, Nakamura Y, Tokunaga K, Toda T: **An ancient retrotransposal insertion causes Fukuyama-type congenital muscular dystrophy.** *Nature* 1998, **394(6691)**:388-392.
11. Yoshida A, Kobayashi K, Manya H, Taniguchi K, Kano H, Mizuno M, Inazu T, Mitsuhashi H, Takahashi S, Takeuchi M, Herrmann R, Straub V, Talim B, Voit T, Topaloglu H, Toda T, Endo T: **Muscular dystrophy and neuronal migration disorder caused by mutations in a glycosyltransferase, POMGnT1.** *Dev Cell* 2001, **1(5)**:717-724.
12. Beltran-Valero de Bernabe D, Currier S, Steinbrecher A, Celli J, van Beusekom E, van der Zwaag B, Kayserili H, Merlini L, Chitayat D, Dobyns WB, Cormand B, Lehesjoki AE, Cruces J, Voit T, Walsh CA, van Bokhoven H, Brunner HG: **Mutations in the O-mannosyltransferase gene POMT1 give rise to the severe neuronal migration disorder Walker-Warburg syndrome.** *Am J Hum Genet* 2002, **71(5)**:1033-1043.
13. Beltran-Valero de Bernabe D, Voit T, Longman C, Steinbrecher A, Straub V, Yuva Y, Herrmann R, Sperner J, Korenke C, Diesen C, Dobyns WB, Brunner HG, van Bokhoven H, Brockington M, Muntoni F: **Mutations in the FKRP gene can cause muscle-eye-brain disease and Walker-Warburg syndrome.** *J Med Genet* 2004, **41(5)**:e61.
14. Barresi R, Michele DE, Kanagawa M, Harper HA, Dovico SA, Satz JS, Moore SA, Zhang W, Schachter H, Dumanski JP, Cohn RD, Nishino I, Campbell KP: **LARGE can functionally bypass alpha-dystroglycan glycosylation defects in distinct congenital muscular dystrophies.** *Nat Med* 2004, **10(7)**:696-703.
15. van Reeuwijk J, Brunner HG, van Bokhoven H: **Glyc-O-genetics of Walker-Warburg syndrome.** *Clin Genet* 2005, **67(4)**:281-289.
16. van Reeuwijk J, Grewal PK, Salih MA, Beltran-Valero de Bernabe D, McLaughlan JM, Michielse CB, Herrmann R, Hewitt JE, Steinbrecher A, Seidahmed MZ, Shaheed MM, Abomelha A, Brunner HG, van Bokhoven H, Voit T: **Intragenic deletion in the LARGE gene causes Walker-Warburg syndrome.** *Hum Genet* 2007, **121(6)**:685-690.
17. Clement E, Mercuri E, Godfrey C, Smith J, Robb S, Kinali M, Straub V, Bushby K, Manzur A, Talim B, Cowan F, Quinlivan R, Klein A, Longman C, McWilliam R, Topaloglu H, Mein R, Abbs S, North K, Barkovich AJ, Rutherford M, Muntoni F: **Brain involvement in muscular dystrophies with defective dystroglycan glycosylation.** *Ann Neurol* 2008, **64(5)**:573-582.
18. Godfrey C, Clement E, Mein R, Brockington M, Smith J, Talim B, Straub V, Robb S, Quinlivan R, Feng L, Jimenez-Mallebrera C, Mercuri E, Manzur AY, Kinali M, Torelli S, Brown SC, Sewry CA, Bushby K, Topaloglu H, North K, Abbs S, Muntoni F: **Refining genotype phenotype correlations in muscular dystrophies with defective glycosylation of dystroglycan.** *Brain* 2007, **130(Pt 10)**:2725-2735.
19. Pillers DA, Weleber RG, Woodward WR, Green DG, Chapman VM, Ray PN: **mdxCv3 mouse is a model for electroretinography of Duchenne/Becker muscular dystrophy.** *Invest Ophthalmol Vis Sci* 1995, **36(2)**:462-466.
20. Cibis GW, Fitzgerald KM, Harris DJ, Rothberg PG, Rupani M: **The effects of dystrophin gene mutations on the ERG in mice and humans.** *Invest Ophthalmol Vis Sci* 1993, **34(13)**:3646-3652.
21. Pillers DA, Bulman DE, Weleber RG, Sigesmund DA, Musarella MA, Powell BR, Murphey WH, Westall C, Panton C, Becker LE, *et al*: **Dystrophin**

expression in the human retina is required for normal function as defined by electroretinography. *Nat Genet* 1993, **4(1)**:82-86.
22. Cox GA, Phelps SF, Chapman VM, Chamberlain JS: **New mdx mutation disrupts expression of muscle and nonmuscle isoforms of dystrophin.** *Nat Genet* 1993, **4(1)**:87-93.
23. van der Plas MC, Pilgram GS, de Jong AW, Bansraj MR, Fradkin LG, Noordermeer JN: **Drosophila Dystrophin is required for integrity of the musculature.** *Mech Dev* 2007, **124(7-8)**:617-630.
24. Shcherbata HR, Yatsenko AS, Patterson L, Sood VD, Nudel U, Yaffe D, Baker D, Ruohola-Baker H: **Dissecting muscle and neuronal disorders in a Drosophila model of muscular dystrophy.** *EMBO J* 2007, **26(2)**:481-493.
25. Taghli-Lamallem O, Akasaka T, Hogg G, Nudel U, Yaffe D, Chamberlain JS, Ocorr K, Bodmer R: **Dystrophin deficiency in Drosophila reduces lifespan and causes a dilated cardiomyopathy phenotype.** *Aging Cell* 2008, **7(2)**:237-249.
26. Campbell KP: **Three muscular dystrophies: loss of cytoskeleton-extracellular matrix linkage.** *Cell* 1995, **80(5)**:675-679.
27. Greener MJ, Roberts RG: **Conservation of components of the dystrophin complex in Drosophila.** *FEBS Lett* 2000, **482(1-2)**:13-18.
28. van der Plas MC, Pilgram GS, Plomp JJ, de JA, Fradkin LG, Noordermeer JN: **Dystrophin is required for appropriate retrograde control of neurotransmitter release at the Drosophila neuromuscular junction.** *J Neurosci* 2006, **26(1)**:333-344.
29. Wairkar YP, Fradkin LG, Noordermeer JN, DiAntonio A: **Synaptic defects in a Drosophila model of congenital muscular dystrophy.** *J Neurosci* 2008, **28(14)**:3781-3789.
30. Fradkin LG, Baines RA, van der Plas MC, Noordermeer JN: **The dystrophin Dp186 isoform regulates neurotransmitter release at a central synapse in Drosophila.** *J Neurosci* 2008, **28(19)**:5105-5114.
31. Bogdanik L, Framery B, Frolich A, Franco B, Mornet D, Bockaert J, Sigrist SJ, Grau Y, Parmentier ML: **Muscle dystroglycan organizes the postsynapse and regulates presynaptic neurotransmitter release at the Drosophila neuromuscular junction.** *PLoS One* 2008, **3(4)**:e2084.
32. Marrone AK, Kucherenko MM, Wiek R, Gopfert MC, Shcherbata HR: **Hyperthermic seizures and aberrant cellular homeostasis in Drosophila dystrophic muscles.** *Sci Rep* 2011, **1**.
33. Zhan Y, Melian NY, Pantoja M, Haines N, Ruohola-Baker H, Bourque CW, Rao Y, Carbonetto S: **Dystroglycan and mitochondrial ribosomal protein l34 regulate differentiation in the Drosophila eye.** *PLoS One* 2010, **5(5)**: e10488.
34. Moore SA, Saito F, Chen J, Michele DE, Henry MD, Messing A, Cohn RD, Ross-Barta SE, Westra S, Williamson RA, Hoshi T, Campbell KP: **Deletion of brain dystroglycan recapitulates aspects of congenital muscular dystrophy.** *Nature* 2002, **418(6896)**:422-425.
35. Kucherenko MM, Marrone AK, Rishko VM, Magliarelli Hde F, Shcherbata HR: **Stress and muscular dystrophy: a genetic screen for dystroglycan and dystrophin interactors in Drosophila identifies cellular stress response components.** *Dev Biol* 2011, **352(2)**:228-242.
36. Lei Y, Warrior R: **The Drosophila Lissencephaly1 (DLis1) gene is required for nuclear migration.** *Dev Biol* 2000, **226(1)**:57-72.
37. Begemann G, Paricio N, Artero R, Kiss I, Perez-Alonso M, Mlodzik M: **muscleblind, a gene required for photoreceptor differentiation in Drosophila, encodes novel nuclear Cys3His-type zinc-finger-containing proteins.** *Development* 1997, **124(21)**:4321-4331.
38. Uv AE, Harrison EJ, Bray SJ: **Tissue-specific splicing and functions of the Drosophila transcription factor Grainyhead.** *Mol Cell Biol* 1997, **17(11)**:6727-6735.
39. Oishi I, Sugiyama S, Liu ZJ, Yamamura H, Nishida Y, Minami Y: **A novel Drosophila receptor tyrosine kinase expressed specifically in the nervous system. Unique structural features and implication in developmental signaling.** *J Biol Chem* 1997, **272(18)**:11916-11923.
40. Lo PC, Frasch M: **bagpipe-Dependent expression of vimar, a novel Armadillo-repeats gene, in Drosophila visceral mesoderm.** *Mech Dev* 1998, **72(1-2)**:65-75.
41. Kidd T, Brose K, Mitchell KJ, Fetter RD, Tessier-Lavigne M, Goodman CS, Tear G: **Roundabout controls axon crossing of the CNS midline and defines a novel subfamily of evolutionarily conserved guidance receptors.** *Cell* 1998, **92(2)**:205-215.
42. Pappu KS, Morey M, Nern A, Spitzweck B, Dickson BJ, Zipursky SL: **Robo-3–mediated repulsive interactions guide R8 axons during Drosophila visual system development.** *Proc Natl Acad Sci USA* 2011, **108(18)**:7571-7576.
43. Seeger M, Tear G, Ferres-Marco D, Goodman CS: **Mutations affecting growth cone guidance in Drosophila: genes necessary for guidance toward or away from the midline.** *Neuron* 1993, **10(3)**:409-426.
44. Tayler TD, Robichaux MB, Garrity PA: **Compartmentalization of visual centers in the Drosophila brain requires Slit and Robo proteins.** *Development* 2004, **131(23)**:5935-5945.
45. Daines B, Wang H, Wang L, Li Y, Han Y, Emmert D, Gelbart W, Wang X, Li W, Gibbs R, Chen R: **The Drosophila melanogaster transcriptome by paired-end RNA sequencing.** *Genome Res* 2011, **21(2)**:315-324.
46. Landis G, Tower J: **The Drosophila chiffon gene is required for chorion gene amplification, and is related to the yeast Dbf4 regulator of DNA replication and cell cycle.** *Development* 1999, **126(19)**:4281-4293.
47. Sasaki S, Shionoya A, Ishida M, Gambello MJ, Yingling J, Wynshaw-Boris A, Hirotsune S: **A LIS1/NUDEL/cytoplasmic dynein heavy chain complex in the developing and adult nervous system.** *Neuron* 2000, **28(3)**:681-696.
48. Wynshaw-Boris A: **Lissencephaly and LIS1: insights into the molecular mechanisms of neuronal migration and development.** *Clin Genet* 2007, **72(4)**:296-304.
49. Huze C, Bauche S, Richard P, Chevessier F, Goillot E, Gaudon K, Ben Ammar A, Chaboud A, Grosjean I, Lecuyer HA, Bernard V, Rouche A, Alexandri N, Kuntzer T, Fardeau M, Fournier E, Brancaccio A, Ruegg MA, Koenig J, Eymard B, Schaeffer L, Hantai D: **Identification of an agrin mutation that causes congenital myasthenia and affects synapse function.** *Am J Hum Genet* 2009, **85(2)**:155-167.
50. Sato S, Omori Y, Katoh K, Kondo M, Kanagawa M, Miyata K, Funabiki K, Koyasu T, Kajimura N, Miyoshi T, Sawai H, Kobayashi K, Tani A, Toda T, Usukura J, Tano Y, Fujikado T, Furukawa T: **Pikachurin, a dystroglycan ligand, is essential for photoreceptor ribbon synapse formation.** *Nat Neurosci* 2008, **11(8)**:923-931.
51. Mburu P, Mustapha M, Varela A, Weil D, El-Amraoui A, Holme RH, Rump A, Hardisty RE, Blanchard S, Coimbra RS, Perfettini I, Parkinson N, Mallon AM, Glenister P, Rogers MJ, Paige AJ, Moir L, Clay J, Rosenthal A, Liu XZ, Blanco G, Steel KP, Petit C, Brown SD: **Defects in whirlin, a PDZ domain molecule involved in stereocilia elongation, cause deafness in the whirler mouse and families with DFNB31.** *Nat Genet* 2003, **34(4)**:421-428.
52. Chen J, Shi X, Padmanabhan R, Wang Q, Wu Z, Stevenson SC, Hild M, Garza D, Li H: **Identification of novel modulators of mitochondrial function by a genome-wide RNAi screen in Drosophila melanogaster.** *Genome Res* 2008, **18(1)**:123-136.
53. Paul S, Dansithong W, Kim D, Rossi J, Webster NJ, Comai L, Reddy S: **Interaction of muscleblind, CUG-BP1 and hnRNP H proteins in DM1-associated aberrant IR splicing.** *Embo J* 2006, **25(18)**:4271-4283.
54. Vicente M, Monferrer L, Poulos MG, Houseley J, Monckton DG, O'Dell KM, Swanson MS, Artero RD: **Muscleblind isoforms are functionally distinct and regulate alpha-actinin splicing.** *Differentiation* 2007, **75(5)**:427-440.
55. Hubberstey AV, Mottillo EP: **Cyclase-associated proteins: CAPacity for linking signal transduction and actin polymerization.** *Faseb J* 2002, **16(6)**:487-499.
56. Balcer HI, Goodman AL, Rodal AA, Smith E, Kugler J, Heuser JE, Goode BL: **Coordinated regulation of actin filament turnover by a high-molecular-weight Srv2/CAP complex, cofilin, profilin, and Aip1.** *Curr Biol* 2003, **13(24)**:2159-2169.
57. Moriyama K, Yahara I: **Human CAP1 is a key factor in the recycling of cofilin and actin for rapid actin turnover.** *J Cell Sci* 2002, **115(Pt 8)**:1591-1601.
58. Pham H, Yu H, Laski FA: **Cofilin/ADF is required for retinal elongation and morphogenesis of the Drosophila rhabdomere.** *Dev Biol* 2008, **318(1)**:82-91.
59. Medina PM, Worthen RJ, Forsberg LJ, Brenman JE: **The actin-binding protein capulet genetically interacts with the microtubule motor kinesin to maintain neuronal dendrite homeostasis.** *PLoS One* 2008, **3(8)**:e3054.
60. Benlali A, Draskovic I, Hazelett DJ, Treisman JE: **act up controls actin polymerization to alter cell shape and restrict Hedgehog signaling in the Drosophila eye disc.** *Cell* 2000, **101(3)**:271-281.
61. Schulze E, Kirschner M: **New features of microtubule behaviour observed in vivo.** *Nature* 1988, **334(6180)**:356-359.
62. Fukushima N, Ishii I, Habara Y, Allen CB, Chun J: **Dual regulation of actin rearrangement through lysophosphatidic acid receptor in neuroblast cell lines: actin depolymerization by Ca(2+)-alpha-actinin and polymerization by rho.** *Mol Biol Cell* 2002, **13(8)**:2692-2705.

63. Lu M, Witke W, Kwiatkowski DJ, Kosik KS: **Delayed retraction of filopodia in gelsolin null mice.** *J Cell Biol* 1997, **138(6)**:1279-1287.
64. Sarmiere PD, Bamburg JR: **Regulation of the neuronal actin cytoskeleton by ADF/cofilin.** *J Neurobiol* 2004, **58(1)**:103-117.
65. VanBerkum MF, Goodman CS: **Targeted disruption of Ca(2+)-calmodulin signaling in Drosophila growth cones leads to stalls in axon extension and errors in axon guidance.** *Neuron* 1995, **14(1)**:43-56.
66. Pilgram GS, Potikanond S, Baines RA, Fradkin LG, Noordermeer JN: **The roles of the dystrophin-associated glycoprotein complex at the synapse.** *Mol Neurobiol* 2010, **41(1)**:1-21.
67. Adams ME, Tesch Y, Percival JM, Albrecht DE, Conhaim JI, Anderson K, Froehner SC: **Differential targeting of nNOS and AQP4 to dystrophin-deficient sarcolemma by membrane-directed alpha-dystrobrevin.** *J Cell Sci* 2008, **121(Pt 1)**:48-54.
68. Christoforou CP, Greer CE, Challoner BR, Charizanos D, Ray RP: **The detached locus encodes Drosophila Dystrophin, which acts with other components of the Dystrophin Associated Protein Complex to influence intercellular signalling in developing wing veins.** *Dev Biol* 2008, **313(2)**:519-532.
69. Deng WM, Schneider M, Frock R, Castillejo-Lopez C, Gaman EA, Baumgartner S, Ruohola-Baker H: **Dystroglycan is required for polarizing the epithelial cells and the oocyte in Drosophila.** *Development* 2003, **130(1)**:173-184.
70. Kucherenko MM, Pantoja M, Yatsenko AS, Shcherbata HR, Fischer KA, Maksymiv DV, Chernyk YI, Ruohola-Baker H: **Genetic modifier screens reveal new components that interact with the Drosophila dystroglycan-dystrophin complex.** *PLoS One* 2008, **3(6)**:e2418.
71. Quinones-Coello AT, Petrella LN, Ayers K, Melillo A, Mazzalupo S, Hudson AM, Wang S, Castiblanco C, Buszczak M, Hoskins RA, Cooley L: **Exploring strategies for protein trapping in Drosophila.** *Genetics* 2007, **175(3)**:1089-1104.
72. Kucherenko M, Marrone A, Rishko V, Yatsenko A, Klepzig A, Shcherbata H: **Paraffin-embedded and Frozen Sections of Drosophila Adult Muscles.** *JoVE* 2010.

doi:10.1186/1471-2202-12-93
Cite this article as: Marrone *et al.*: New Dystrophin/Dystroglycan interactors control neuron behavior in *Drosophila* eye. *BMC Neuroscience* 2011 **12**:93.

BMC Developmental Biology

BioMed Central

Research article

Open Access

The conserved WW-domain binding sites in Dystroglycan C-terminus are essential but partially redundant for Dystroglycan function

AS Yatsenko†[1,2,3], MM Kucherenko†[1,2,3], M Pantoja[1], KA Fischer[1], J Madeoy[4], W-M Deng[5], M Schneider[6], S Baumgartner[7], J Akey[4], HR Shcherbata*[1,3] and H Ruohola-Baker*[1,4]

Address: [1]Department of Biochemistry, Institute for Stem Cell and Regenerative Medicine, Program in Neurobiology and Behaviour, University of Washington, Seattle, WA 98195, USA, [2]Department of Genetics and Biotechnology, Ivan Franko Lviv National University, Lviv, 79005 Ukraine, [3]Max Planck Institute for biophysical chemistry, Goettingen, 37077, Germany, [4]Department of Genome Sciences, University of Washington, Seattle, WA 98195, USA, [5]Department of Biological Science, Florida State University, Tallahassee, FL 32306, USA, [6]Department of Biology, University of Copenhagen, 2100 Copenhagen, Denmark and [7]Department of Experimental Medical Sciences, Lund University, BMC B13, 22184 Lund, Sweden

Email: AS Yatsenko - anubius81@gmail.com; MM Kucherenko - kucherenkomari@gmail.com; M Pantoja - mpantoja@u.washington.edu; KA Fischer - fischera@u.washington.edu; J Madeoy - akeyj@u.washington.edu ; W-M Deng - wumin@bio.fsu.edu; M Schneider - maschneider@bio.ku.dk; S Baumgartner - Stefan.Baumgartner@med.lu.se; J Akey - akeyj@u.washington.edu; HR Shcherbata* - hshcher@gwdg.de; H Ruohola-Baker* - hannele@u.washington.edu

* Corresponding authors †Equal contributors

Published: 27 February 2009

BMC Developmental Biology 2009, **9**:18 doi:10.1186/1471-213X-9-18

Received: 19 September 2008
Accepted: 27 February 2009

This article is available from: http://www.biomedcentral.com/1471-213X/9/18

Abstract

Background: Dystroglycan (Dg) is a transmembrane protein that is a part of the Dystrophin Glycoprotein Complex (DGC) which connects the extracellular matrix to the actin cytoskeleton. The C-terminal end of Dg contains a number of putative SH3, SH2 and WW domain binding sites. The most C-terminal PPXY motif has been established as a binding site for Dystrophin (Dys) WW-domain. However, our previous studies indicate that both Dystroglycan PPXY motives, WWbsI and WWbsII can bind Dystrophin protein *in vitro*.

Results: We now find that both WW binding sites are important for maintaining full Dg function in the establishment of oocyte polarity in *Drosophila*. If either WW binding site is mutated, the Dg protein can still be active. However, simultaneous mutations in both WW binding sites abolish the Dg activities in both overexpression and loss-of-function oocyte polarity assays *in vivo*. Additionally, sequence comparisons of WW binding sites in 12 species of *Drosophila*, as well as in humans, reveal a high level of conservation. This preservation throughout evolution supports the idea that both WW binding sites are functionally required.

Conclusion: Based on the obtained results we propose that the presence of the two WW binding sites in Dystroglycan secures the essential interaction between Dg and Dys and might further provide additional regulation for the cytoskeletal interactions of this complex.

Background

The Dystroglycan-Dystrophin (Dg-Dys) complex has been shown to provide cells with structural integrity by forming a conduit between the extracellular matrix and the cytoskeletal network and there are lines of evidence that implicate an additional signaling role for the complex [1,2] Dystroglycan binds to extracellular matrix components, including Laminin at its N-terminus and the actin cytoskeleton via Dystrophin at its C-terminus [3,4] Defects in these interactions can result in muscular dystrophies (MD) and various epithelial cancers [5]

The characterization of the Dystrophin Glycoprotein Complex (DGC) in *Drosophila* has revealed that it possesses similar roles in muscle integrity and neuronal migration in flies as it does in humans [6] These abnormalities include age dependent muscle degeneration, reduced mobility, defects in eye development as manifested by altered photoreceptor axon path finding and photoreceptor morphology. Additionally, mutations in Dys and Dg affect cell polarity in *Drosophila* [6-8] Interestingly, some of these phenotypes are affected by the nutrition or energy metabolism in the animals [9] Recently, a reduced lifespan, as well as heart and muscle abnormalities, have been reported in *Drosophila* mutants of another component of the DGC, -sarcoglycan [10] and heart and further eye phenotypes have been observed in *Drosophila* Dys and Dg mutants [11,12]

Analogous defects observed when the Dg-Dys complex is disturbed in both flies and humans make *Drosophila* an attractive model for further studies on clarifying the cellular function of the DGC. Recent biochemical and *in vivo* structure-function analyses have revealed that a specific set of C-terminal domains are critical for the function of Dystroglycan. We have found that a putative SH3 domain binding motif but, surprisingly, not the most C-terminal Dystrophin WW domain binding motif is required for Dg function in cellular polarity in *Drosophila* [13]. However, since two potential WW binding sites exist near the Dg C-terminus it is possible that the second WW binding site can also bind Dystrophin *in vivo*, as has been shown *in vitro* [13]. In this study we dissect the roles of the two WW binding sites in the *Drosophila* Dystroglycan C-terminus *in vivo* and, interestingly, find that the sites are essential and their functions are partially overlapping.

Results

In order to understand the regulation of Dg and its role in signaling, we have analyzed the binding motifs that are required for the function of the Dg-Dys complex in cellular polarity in *Drosophila*. The proline-rich C-terminus of Dg has several potential protein binding motifs, which suggests that it may be involved in regulating the complex and potentially may have signaling role(s). Proline-rich sequences have been shown to be the targets of several protein interaction domains involved in signal transduction. The most C-terminal PPxY motif has been established as a binding site for the WW domain of Dystrophin in humans [14-16] and in *Drosophila* by *in vitro* binding studies [6]. However, this WW domain binding site at the very C-terminus of Dystroglycan, is not essential for the function of the Dg-Dys complex in cellular polarity in *Drosophila*. An internal region of the Dystroglycan C-terminus containing a second WW domain binding site and a putative SH3 domain binding site appear to be sufficient for function in this context. We have also shown that Dystrophin can bind both the C-terminal and the internal WW domain binding sites *in vitro* [13]. We now test whether the internal WW domain binding site is essential, whether the two WW domain binding sites are redundant or whether neither is required for Dg function in *Drosophila*. To distinguish between these possibilities we used both overexpression and loss-of-function rescue analyses.

Generation of transgenic lines expressing biochemically verified WWbs mutations

Previous results show that two mutations designed from computer predictions resulted in dramatic alterations in the affinity between Dg and Dys *in vitro* [13] These two mutations, predicted to abolish the WW but not the SH3 binding domain, resulted in very low binding affinities between the Dystroglycan C-terminal peptide and the Dystrophin WW domain with EF-hand region (DmWWbsI-W: Kd = 178 μM and DmWWbsII-G: Kd = 147 μM), as compared to wild type peptides (DmWWbsI: Kd = 16 μM and DmWWbsII: Kd = 46 μM). These values are comparable to the dissociation constant observed with a negative control for the assay (p53: Kd = 248 μM), suggesting that specific binding is abolished. We therefore generated transgenic lines expressing the following representative mutations: PPSG, which has a mismatch in WWbsII (PPSY → PPSG) and 2WW, which has mutations in both WW binding sites (WWbsI, PPPY → WAPY and WWbsII, PPSY → PPSG) (Figure 1). At least two independent transgenic *Drosophila* lines for each construct were obtained and analyzed. Similar results with two independent transgenic lines confirmed that the phenotype was due to the Dg mutation and not due to positional effects of the transgene inserts.

We first tested the ability of the transgenic constructs to produce functional forms of the Dg protein using the *Gal4/UAS* system. In order to overexpress the transgenic constructs in follicle cells we used the *hsFlp; actin-FRT<CD2>FRTGal4/UAS* system in which clonal cells that overexpress the gene of interest were marked with GFP. Dg, in the wild type follicular epithelium, is located at the basal membrane (Figure 2C; WT). Overexpression of the transgenes resulted in Dg localizing to both the apical and

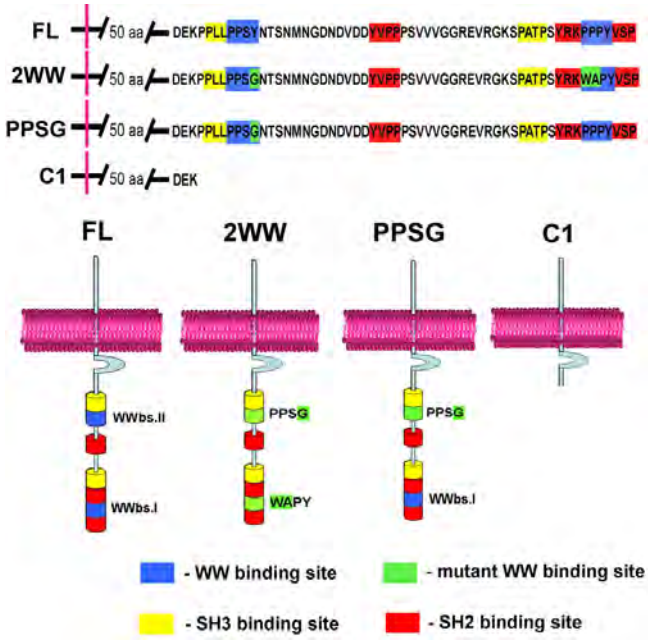

Figure 1
Transgenic constructs with mutations of WW binding sites at the Dystroglycan C-terminal end. Schematic drawing of pUASp constructs with mutations in different WW binding sites. FL – construct which encodes full length Dg, 2WW – constructs with mutations in both WW binding sites, PPSG – mutation in the N-terminal WW binding motif WWbsII PPSY → PPSG. C1 – deletion of the proline-rich C-terminus.

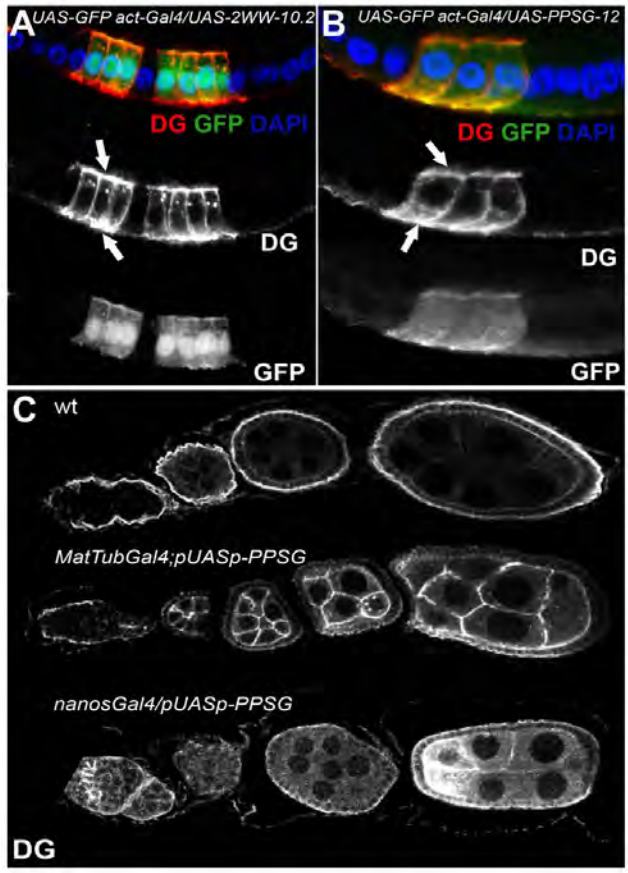

Figure 2
Overexpression of Dg constructs with mutation in WW binding sites in follicle and germline cells. **A, B**. Overexpression of 2WW (A) and PPSG (B) constructs in follicle cells marked by GFP. Dg in the wild type cells is expressed at the apical side of the follicle cell epithelium, in contrast to overexpression where Dg is localized in both apical and basal sides (indicated by arrows). C. Overexpression of the constructs in the germline cells.wt – Dg expression in wild type germline cells, MatTubGal4;pUASp-PPSG, nanosGal4/pUASp-PPSG – overexpression of transgenic constructs in germline cells. Both MatTub- and nanosGal4 have distinct expression patterns.

basal sides of the follicle cells (Figure 2A, B). We also tested the expression of the constructs in germline cells using the *MatTubGal4* and *nanosGal4* drivers. During oogenesis, Dg is expressed at low levels in the germline (Figure 2C; WT). At stage 2–3 of oogenesis overexpression with *MatTubGal4* shows Dg levels are substantially increased in germline cells (Figure 2C). Increased protein levels were also observed using the *nanosGAl4* driver which showed a distinct pattern starting with high levels in the germarium, lower levels during stages 3–6 and with higher levels during later stages (Figure 2C). Similar patterns and levels of the Dg constructs were observed with all the transgenic lines analyzed in these experiments (Figure 2, Additional Figure 1, Additional Figure 4).

WW binding site function as assayed by oocyte polarity

To analyze whether the Dg mutant forms are functional in oocyte polarity, we expressed mutant and wild type Dg constructs in germline cells using a germline specific driver (*MatTubGal4*), and examined oocyte polarity using Orb protein as a marker. Orb is a member of the cytoplasmic polyadenylation element binding (CPEB) family of RNA-binding proteins that are implicated in local protein synthesis [17]. In *Drosophila* oogenesis Orb co-localizes with the microtubule organizing center (MTOC), which is localized to the anterior of the oocyte during stage 1, and then moves to the posterior by stage 3. Between stages 3 and 6, Orb is clearly localized to the posterior of the oocyte, making it an excellent marker to analyze the polarity of the oocyte (Figure 3A, 4A). Absent or mislocalized Orb during these stages indicates a failure to establish early oocyte polarity.

We have previously shown that overexpression of the wild type form of *Drosophila* Dystroglycan (FL = full length) is sufficient to generate oocyte polarity defects [13] (Figure 3B). When FL is overexpressed in the germline, Orb

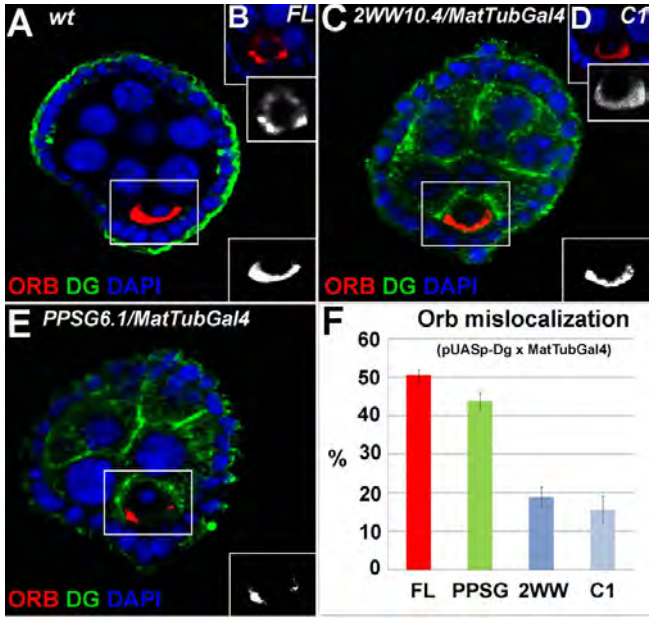

Figure 3
Overexpression of pUASp with MatTubGal4 in germline disrupts the polarity marker Orb. (Orb-red, Dg-green, DAPI – blue, separate channels for Orb are shown on the side of each corresponding picture). A. wild type (wt) stage 4 egg chamber shows normal Orb (red) localization at the posterior side of the oocyte. B. Overexpression of the pUASp-FL transgenic construct disrupts the normal Orb localization. C. Overexpression of the pUASp-2WW does not disrupt normal Orb (red) localization. Similar phenotype is seen with C1-construct that lacks the entire C-terminal region of Dg (D; Fig. 1). E. Overexpression of pUASp-PPSG constructs disrupts oocyte polarity indicated by mislocalization of Orb which has an abnormal side location, F. Percentage of Orb mislocalization as the result of overexpression of different pUASp-Dg constructs. (FL, 49 ± 2, PPSG 44 ± 2, 2WW 19 ± 2, C1 16 ± 3).

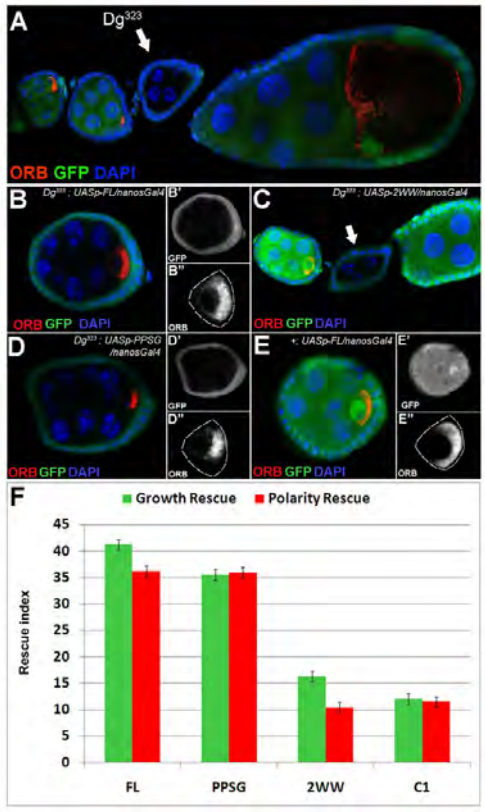

Figure 4
Rescue of Dg loss-of-function germline clones with expression of pUASp-Dg constructs. Orb (Red); GFP (Green), DAPI (Blue) A', B', D' GFP of the corresponding stages shown in a separate channel; A", B", D" Orb staining of the corresponding stages shown in a separate channel with dotted lines which indicates the border of the oocyte. A. Dg loss-of-function germline clones (black, white arrow; *hsFLP; FRT42D Dg*^{323}) are arrested prior to stage 6 and have disrupted oocyte polarity (absent or mislocalized Orb). B. Expression of *pUASp-FL* with the nanos-Gal4 driver in Dg clones partially rescues oocyte polarity in arrested clones stages 3–6 as indicated by proper localization of Orb to the posterior of 36% of the oocytes; (*hsFLP; FRT42D Dg*^{323}*; P(w+:nanosGal4:VP-16)Ab-2/pUASp-FL) C*. Expression of pUASp-2WW with the *nanos-Gal4* driver in *Dg* clones does not rescues oocyte polarity in arrested clones stages 3–6 (arrow) [as indicated by development arrest and absent Orb marker; (*hsFLP; FRT42D Dg*^{323}*; P(w+:nanosGal4:VP-16)Ab-2/pUASp-2WW*)] *D*. Expression of *pUASp-PPSG* with the *nanos-Gal4* driver in *Dg* clones rescues oocyte polarity in arrested clones stages 3–6 [as indicated by proper localization of Orb to the posterior of the oocyte; (*hsFLP; FRT42D Dg*^{323}*; P(w+:nanosGal4:VP-16)Ab-2/pUASp-PPSG*)]*E*. Wild type egg chamber with posterior Orb localization (+/+; *P(w+:nanosGal4:VP-16)Ab-2/pUASp-FL) F*. FL, PPSG are able to rescue Dg loss-of-function phenotypes, while 2WW and C1 do not (Red: rescued polarity index, Green: rescued growth index).

becomes mislocalized, surrounds the entire oocyte nucleus, or accumulates in a clump to one side of the oocyte instead of localizing to the posterior. Therefore, Dystroglycan, when expressed at elevated levels in germline cells, is sufficient to disrupt oocyte polarity. Overexpression of the full length form of Dg with the *tubGal4* driver causes semi-lethality (data not shown). Similarly, in vertebrates overexpression of Dg has been shown to cause defects in neuromuscular junctions [18,19]. We used the overexpression oocyte polarity assays to test whether either of the WW domain binding sites is essential for Dystroglycan function.

To test the function of WWbsI *in vivo* we overexpressed the PPSG mutant protein in germline cells using the *MatTubGal4* driver and determined the localization of the early oocyte polarity marker Orb. As discussed, in wild

type cells Orb marks the localization of the microtubule organizing center and is localized to the posterior side of the oocyte during stages 3–6 (Figure 3A). Overproduction of the PPSG protein results in the mislocalization of the usually posterior Orb marker. In mutants Orb surrounds the oocyte nucleus or localizes to the sides of the oocyte nucleus in 44 ± 2% of 3–6 stage oocytes (n = 147, Figure 3E–F). The level of this defect is similar to the one observed with the FL construct [6,13], which contains both WW binding sites (Figure 1; Figure 3B, D; 49 ± 2%, n = 80). These data suggest that disturbing the second WW binding site at the Dg C-terminus does not dramatically affect the functionality of the protein; similar to FL construct, when overexpressed it still is sufficient to disturb the oocyte polarity.

In contrast to the FL and PPSG constructs, overexpression of a 2WW mutant construct did not result in a high percentage of Orb mislocalization (Figure 3C, F, 19 ± 3%, n = 123). With 2WW overexpression, Orb, in most cases, was localized to the posterior of the oocyte (Figure 3C). The frequency of mislocalization with the 2WW construct, in which both WW binding sites were mutated was similar to that of the C1 construct which lacked all the C-terminal binding sites (Figure 1, Figure 3D, F, 16 ± 2%, n = 86).

These data, in combination with our previous data [13] show that a single mutation in WWbsII or the lack of WWbsI does not result in dramatic defects in Dg activity in this sufficiency assay measuring the oocyte polarity. However, simultaneous mutations in both WW binding sites dramatically reduce the function of Dystroglycan in this assay.

One WW binding site is required for Dystroglycan function

We also tested the function of the WW binding site mutants in rescue experiments by expressing the transgenes in a Dg loss-of-function background. Dg^{323} germline mutant clones are arrested prior to stage 3–4 and have mislocalized or missing Orb protein (Figure 4A). We have previously shown that these defects are partially rescued by wild type (full-length) Dg expression [13] (Figure 4, 36–40% rescue). Full rescue is not expected since the Dg^{323} deletion also affects a newly described neighboring gene mRpl34 (Additional Figure 3) and recent data implies that the level of nutrients and energy metabolism in the animal may affect cellular polarity [9]. To test if our mutant constructs were capable of rescuing the developmental arrest and the defects in oocyte polarity on the same level as the Dg full-length construct, we expressed them using the germline driver *nanosGal4* and calculated the percentage of loss-of-function clones with rescued growth and polarity. Using this assay we tested whether the Dg WWbs mutations were capable of a similar level of rescue as full-length Dg. If the Dg mutant with both WW binding sites mutated (2WW, Figure 1) could rescue the Dg^{323} phenotype in oocyte polarity at the same level as wild type Dg, we conclude that neither of the WW binding sites in *Drosophila* is required for Dg activity. On the other hand, if Dg with two WWbs mutations cannot rescue, we conclude that both or just the internal WW binding site is essential for Dg activity (we have already shown that the C-terminal WWbs is not essential [13]). As discussed above, to distinguish between these possibilities, we have generated a single mutation in WWbsII (PPSG, Figure 1) and will test whether this mutant still has the full length Dg activity in the loss-of-function rescue assays.

Similar to the full length Dg (FL, Figure 4B), the PPSG mutant constructs were capable of partially rescuing the Dg mutant phenotype (Figure 4D). Loss-of-function clones with expression of FL (Figure 4B-B") and PPSG (Figure 4D-D") had similar levels of posterior localization of the polarity marker, Orb (Figure 4F, FL: 36 ± 0.5% n = 52; PPSG: 41% n = 22). These mutants were also capable of restoring the developmental arrest phenotype by showing a higher percentage of loss-of-function clones that were older than stage 4–6 (Figure 4F, FL: 47 ± 8% n = 55; PPSG 38% n = 21). In contrast, 2WW was unable to rescue (2WW rescued at the level of the C1 mutant that lacks most of the Dg C-terminus; [13]; Figure 1.). Dg loss-of-function clones with expression of 2WW and C1 showed lower percentages of normal polarity (Figure 4F; 2WW: 12 ± 0.6% n = 66; C1: 9% n = 22) and growth rescue (Figure 4F; 2WW: 19 ± 2% n = 66; C1: 13%) than FL or PPSG constructs (Figure 4F). This result indicates that at least one WW binding site is required for normal function of Dg but a mutation in only one of the sites does not alter the functionality of Dg protein dramatically.

Since a single WWbsII mutation or a WWbsI deletion does not cause a severe loss of Dg activity but the double mutant does, we conclude that the two binding sites act, at least partially in a redundant manner in oocyte polarity and growth assays.

WW binding sites are highly conserved

Since both WW binding sites proved to be important in our *in vivo* experiments we wanted to know if the importance of these sites has been preserved among the interspecies population. To analyze the conservation of WW binding sites, we tested for variability in the sequence of those sites among all *Drosophila* species. For this purpose, using the ClustalW program, we aligned the *Dystroglycan* sequences of the 12 species of *Drosophila* obtained from the GBrowse database. The alignment analysis indicates that the two WW binding sites are fully conserved among all 12 *Drosophila* species (Figure 5A). Some variation in the nucleotide sequences of the WW binding sites were observed between the species, however these changes did

not lead to amino acid sequence changes (Additional Figure 2). Furthermore, both Dg WW binding sites were also conserved between *Drosophila* and humans (Figure 5B).

In order to better understand patterns of polymorphisms in human Dystroglycan (*DAG*), and, in particular, the WW domains, we sequenced a 348 bp fragment spanning the region of interest in 88 samples from six geographically diverse human populations. In total, only one segregating site was identified among the 176 chromosomes sequenced (table 1) and none were identified in either of the WW domains. The estimated nucleotide diversity (defined as the average number of pairwise differences between two randomly selected chromosomes per nucleotide) in the combined sample is 3.24×10^{-5}. In contrast, the average nucleotide diversity of 322 genetic regions that were sequenced in a panel of 23 European-Americans and 22 African-Americans is 8.53×10^{-4}, suggesting that the sequenced region of *DAG* is under significant functional constraint. These data suggest that during evolution both WW binding sites have been important and therefore are preserved among species.

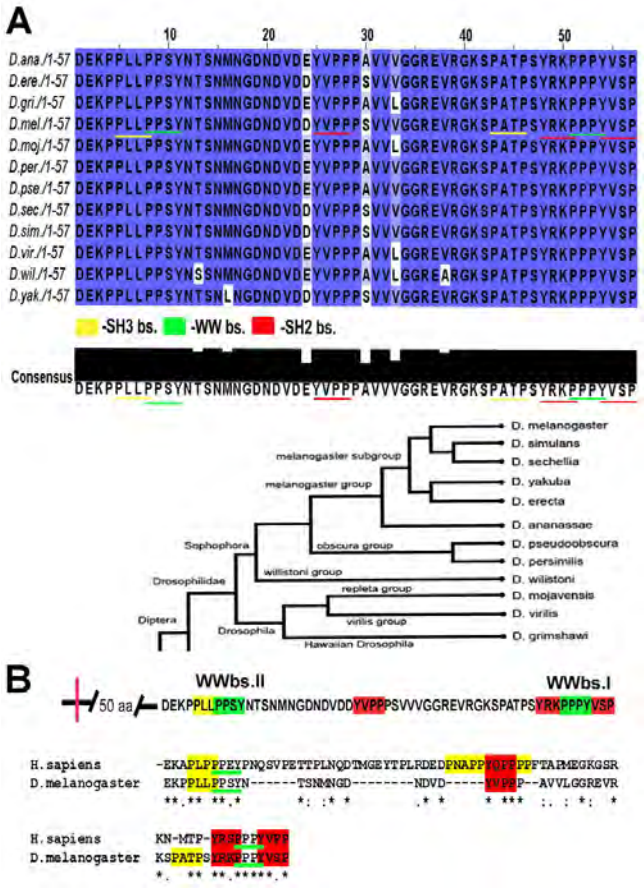

Figure 5
Both WW binding sites are conserved in all 12 species of *Drosophila*. A. Amino acid sequence alignment of the C-terminal end from 12 species of *Drosophila* using the computer program ClustalW shows absolutely no variation between both WW binding sites. B. Both WW binding sites are highly conserved between humans and *Drosophila*.

Table 1: Summary statistics of sequencing data.

Population	N[a]	S[b]	θ_W[c]	π[d]
CEPH	40	0	0	0
Han Chinese	40	0	0	0
Middle East	20	0	0	0
Pygmy	20	0	0	0
South Africa	16	0	0	0
South America	20	1	5.26×10^{-3}	2.73×10^{-4}
South East Asia	20	0	0	0
Total	176	1	6.49×10^{-5}	3.24×10^{-5}

[a] Number of chromosomes
[b] Number of segregating sites
[c] Watterston's theta per bp
[d] Nucleotide diversity per bp

Discussion

The functional redundancy of the WW binding sites poses interesting questions: have both binding sites survived through evolution to protect organisms from the mutations in an essential complex or does each binding site have a specific function in different tissues and/or developmental stages. Mutations in the DGC cause muscular dystrophies; however only mutations in Dystrophin, but not Dystroglycan per se, are associated with known types of muscular dystrophies in vertebrates. In mice, mutations in Dystroglycan are embryonic lethal, which suggests that Dg is an essential gene and, perhaps the redundant Dystrophin binding sites in Dystroglycan provide an additional means for DGC regulation.

The comparative sequence analysis of *Drosophila* and human WW binding motifs revealed very high conservation. However, each WWbs resides in a specific protein micro-environment, which may suggest that each site has specific binding partners. The previously performed genetic screens for modifiers [20] of Dg and Dys showed that the Dg-Dys complex interacts with components of different signaling pathways and components involved in cell/neuronal migration, cytoskeletal rearrangement and muscle development. This suggests that the Dg-Dys complex might be a major hub that regulates transfer of extracellular information to the cytoskeleton. Therefore it will be important in the future to test if WW binding sites have specific and independent biological functions in different tissues. This kind of analysis is likely to provide insights into the specific functions of the Dg-Dys complex and

serve as a basis for the development of novel therapeutic approaches for the treatment of muscular dystrophy.

Conclusion

We have investigated the role of the WW binding sites at the C-terminus of Dystroglycan protein and found that both sites may bind to the WW+EF hand domain of Dystrophin. Our previous studies [6,13], indicate that WWbsI and WWbsII both can bind Dystrophin protein *in vitro*. To test whether both WW binding sites can function and are required *in vivo* we generated two transgenic mutants: 2WW, which has mutations in both WW binding sites (WWbsI, PPPY → WAPY and WWbsII, PPSY → PPSG), and PPSG, which has a mismatch in WWbsII (PPSY → PPSG). We used the establishment of early oocyte polarity as an assay to verify the functionality of WWbsI and WWbsII. Importantly, the data show that while each WW binding site mutation yields to close to normal Dg function, the double WWbs mutation has lost Dg C-terminal activity. These data suggest that at least one WWbs is required for full Dg function *in vivo* and that the two sites may be partially redundant.

Methods

Fly Stocks

Drosophila melanogaster stocks were raised on standard cornmeal/yeast/agar medium at 25°C. For overproduction of pUASp-Dg in the germline, we used the following: *NGT40*; *P*(*w*$^{+}$:*nanosGal4*:*VP-16*)*Ab-2* [21,22] and *Mat-α4-TubGal4-VP16/CyO* [23]. For overproduction of pUASp-Dg in the follicle cells, we used *hsFlp; act < FRT-CD2-FRT < Gal4; UAS-GFP*[24]. For generation of *Dystroglycan* clones, we used *FRT42D-Dg*^{323}*/CyO* (*Dg*^{323} is a *Dystroglycan* loss-of-function mutant with a 3324 bp deletion between bp 32,345 and 35,669 of DS03910 [7] disrupting the Dg 5' region and the adjacent mRPL34 gene; Additional Figure 3) and *hsFLP;FRT42D Ubi-GFP/CyO*. For overproduction of pUASp-Dg in a *Dystroglycan* mutant background, we used *FRT42D-Dg*323*/CyO; P*(*w nosGal4*:*VP16*)*A4-2 III*, and *hsFLP; FRT42D Ubi-GFP/CyO; pUASp-Dg/TM3* (pUASp-Dg refers to all *Dystroglycan* constructs: FL, C1, 2WW, PPSG). Two deletions in the *Dystroglycan* region exist; *Dg*^{248} (11985709:11986494) whose breakpoints are 333 bp downstream of the *Dg* transcription start site (11986042) and 3 bp upstream of the mRpL34 start codon (11986498) and *Dg*^{323} (11983340:11986664) whose breakpoints are 2.7 kb downstream of the *Dg* transcription start site and 166 bp downstream of the mRpL34 start codon (Additional Figure 3). We also used: dg043 [25].

Generation of pUASp-Dg Transgenic Animal

Full length and modified *Dystroglycan* PCR products that can be expressed in the germline were synthesized from the template LD11619. pUASp-FL and pUASp-C1 constructs used in this work have been described previously [13]. To generate a construct with mutated WWbsII (pUASp-PPSG) LD11619 was used as a template with the following primers: 5'-GGGGTACCAACATGAGATTC-CAGTGGTTCT-3' 5'-GCTCTAGATTATGGCGACACA-CATA-TGGCGGT-3'. The PCR products were digested with KpnI and XbaI and cloned into the pUASp vector [26]. The constructs were injected into embryos to obtain at least two independent stable transformant lines. Injections were done by Rainbow Transgenic Flies, Inc. (California, USA).

Overproduction of Dystroglycan in the Germline and Follicle Cell

For overproduction in germline cells, balanced *pUASp-Dg/Mat-α4-TubGal4-UP16/CyO or P*(*w*$^{-}$: *nanosGal4*:*VP-16*)*Ab-2* animals were raised in yeasted vials at 25°C for 3 days before dissection and analysis. For overproduction in the follicle cells, *hsFlp; UAS-GFP act <FRTCD2FRT <Gal4/pUASp-Dg* animals were heat-shocked at 37°C for 1 h, raised in yeasted vials at 25°C for 3 days before dissection and analysis. All pUASp-Dg constructs used were crossed to these three Gal4 drivers to test for proper overproduction of protein and correct localization of protein to the membrane in the germline and somatic cells. The following pUASp-Dg lines were used for germline analysis: FL-1, 5; C1-1, -2; 2WW-10.2, -5.6, -13, 15.4; PPSG-11.1, -12.5, -6.3, -13.4. For the rescue experiments the following lines were used: FL-1, -2, -5; C1-1, -2; 2WW-10.4, -13, -15.6; PPSG-11.4, 11.1.

Antibody Staining Procedures

Drosophila ovaries were dissected rapidly in PBS and fixed in 4% paraformaldehyde for 10 minutes. The antibody staining procedure was the same as described previously [13]. The following primary antibodies were used at the following designated dilutions: rabbit anti-Dystroglycan (1:3000 [7]), mouse anti-Orb (1:20; Developmental Studies Hybridoma Bank), the following secondary antibodies were used at the designated dilutions: Alexa 488 anti-rabbit and Alexa 568 anti-mouse (1:500; Molecular Probes).

Western Blot and densitometry analyses

Sample preparation and SDS-PAGE have been described previously [13]. Bio-Rad ready-made 4–20% polyacrylamide gels were used for protein separation. Proteins were transferred to polyvinylidene difluoride (PDVF) membranes (Immobilon) using a semi-dry transfer apparatus (Bio-Rad). Primary affinity purified anti-Dg antibodies were used at 1:30,000 dilutions. Goat anti-rabbit HRP conjugated antibodies (Bio-Rad) were used as detection reagents at 1:10,000 dilutions. Proteins were visualized via enhanced chemiluminescence (Millipore). Densitometry analysis was performed with the public domain NIH IMAGEJ program (developed at the US National Institutes

of Health and available on the Web at http://rsb.info.nih.gov/ij/). Scans of immunoblots determined to be in the linear range (i.e. twice the amount of protein correlated with twice the signal seen on photographic film) were used as sources for analysis.

Sequence alignment

Sequences of 12 species of *Drosophila* were obtained from the FlyBase genome database. Sequence alignment was done using software ClustalW designed by the European Bioinformatics Institute http://www.ebi.ac.uk/Tools/clustalw/index.html.

DNA samples used for sequencing

We sequenced a 348 bp fragment of *DAG* that includes both WW domains in DNA samples from 88 humans representing six populations. Samples were obtained from the Coriell Institute for Medical Research Cell Repositories (Camden, NJ, USA). Coriell repository numbers for these samples are as follows: CEPH European-American (NA06990, NA07019, NA10830, NA10831, NA07348, NA07349, NA10842, NA10843, NA10844, NA10845, NA10848, NA10850, NA10851, NA10852, NA10853, NA10854, NA10857, NA10858, NA10860, NA10861, NA17201) Han Chinese of L.A. (NA17733 – NA17747, NA17749, NA17752 – NA17757, NA17759, and NA17761), Middle East (NA17041 – NA17050), Pygmy (NA10469 – NA10473, NA10492 – NA10496), South Africa (NA17319, NA17341 – NA17348), South America (NA17301 – NA17310) and South East Asia (NA17081 – NA17090). We compared patterns of polymorphism to 322 genes that were sequenced as part of the SeattleSNPs project [27].

DNA sequencing and statistical analysis

Sequencing primers were designed with primer3 (http://frodo.wi.mit.edu/cgi-bin/primer3/primer3_www.cgi; primer sequences available upon request). We used standard PCR-based sequencing reactions using Applied Biosystem's Big Dye sequencing protocol on an ABI 3130xl. Sequence data was assembled using Phred/Phrap [28,29] and the alignments were inspected for accuracy with Consed [30,31]. Polymorphisms were identified with PolyPhred 4.0 [32]. All polymorphic sites were manually verified and confirmed by sequencing the opposite strand. Standard measures of nucleotide diversity, including θ_W and π were calculated as previously described [27].

Authors' contributions

ASY conception, design, acquisition, analysis and interpretation of the data, drafting the manuscript. MMK conception, design, acquisition, analysis and interpretation of the data. HRS drafting the manuscript. MP conception, design, acquisition, analysis and interpretation of the data, revising the manuscript. KAF acquisition, analysis and interpretation of the data. JM acquisition, analysis and interpretation of the data. WMD conception and interpretation of the data. MS conception and interpretation of the data. SB conception and interpretation of the data. JA conception, design and interpretation of the data, drafting the manuscript. HRB conception, design and interpretation of the data, drafting the manuscript. All the authors have read the article and accepted the final manuscript.

Additional material

Additional file 1

***Figure 1**. Overexpression of Dg constructs with mutation in WW binding sites in follicle and germline cells. A, B. Overexpression of 2WW (A) and PPSG (B) constructs in follicle cells marked by GFP. Dg in the wild type cells is expressed at the apical side of the follicle cell epithelium, in contrast to overexpression where Dg is localized in both apical and basal sides (indicated by arrows). To compare the expression levels of different constructs and insertions the intensities of Dg expression was compared to the intensity of the GFP signal in the same cell. The observed mean intensity ratios are similar in the two constructs (2WW = 1.2, PPSG = 1.1), suggesting that the differences observed between these two conatructs in oocyte polarity assay are not due to dramatically different levels of expression. C. Overexpression of the constructs in the germline cells.wt – Dg expression in wild type germline cells, MatTubGal4; pUASp-WW, nanosGal4/pUASp-WW – overexpression of transgenic constructs in germline cells. Both MatTub- and nanosGal4 have distinct expression patterns.*

Click here for file
[http://www.biomedcentral.com/content/supplementary/1471-213X-9-18-S1.tiff]

Additional file 2

***Figure 2**. Comparative analysis of Dg C-terminus nucleic acid sequences in 12 species of* Drosophila.

Click here for file
[http://www.biomedcentral.com/content/supplementary/1471-213X-9-18-S2.tiff]

Additional file 3

***Figure 3**. The genomic region of the* Dystroglycan *gene. The genomic regions that are deleted in the* Dystroglycan *mutant alleles* Dg^{323} *and* Dg^{248} *are indicated as black bars.*

Click here for file
[http://www.biomedcentral.com/content/supplementary/1471-213X-9-18-S3.tiff]

Additional file 4

***Figure 4**. Western blot analysis of Dg protein in wild type, DgO43, 2WW and PPSG ovaries and whole animals show the following Dg intensities compared to OregonR (WT): DgO43 [25] = 0.4, 2WW = 1.3, PPSG = 1.2. The specific bands that correspond to different Dg forms can be seen at ~180 (two bands), 110 and faintly at 70 kD. A presumable degradation product can be seen below 25 kD. Increased band intensities can be seen with the 110 kD band and most notably with the higher 180 kD species. Band intensities were normalized to actin and samples were run on a gradient 4–20% gel.*

Click here for file
[http://www.biomedcentral.com/content/supplementary/1471-213X-9-18-S4.tiff]

Acknowledgements

We thank members of the Ruohola-Baker lab for useful discussions and Dr. R. Ray for fly lines. This work was supported by an AHA fellowship for H.R.S., CRDF for A.S.Y., K.M.M., H.R.S. and H.R-B. and by the grants from the National Institute of Health and Muscular Dystrophy Association for H.R-B.

References

1. Russo K, Di Stasio E, Macchia G, Rosa G, Brancaccio A, Petrucci TC: **Characterization of the beta-dystroglycan-growth factor receptor 2 (Grb2) interaction.** *Biochem Biophys Res Commun* 2000, **274:**93-8.
2. Zhou YW, Thomason DB, Gullberg D, Jarrett HW: **Binding of laminin alpha1-chain LG4-5 domain to alpha-dystroglycan causes tyrosine phosphorylation of syntrophin to initiate Rac1 signaling.** *Biochemistry* 2006, **45:**2042-52.
3. Davies KE, Nowak KJ: **Molecular mechanisms of muscular dystrophies: old and new players.** *Nat Rev Mol Cell Biol* 2006, **7:**762-73.
4. Haenggi T, Fritschy JM: **Role of dystrophin and utrophin for assembly and function of the dystrophin glycoprotein complex in non-muscle tissue.** *Cell Mol Life Sci* 2006, **63:**1614-31.
5. Barresi R, Campbell KP: **Dystroglycan: from biosynthesis to pathogenesis of human disease.** *J Cell Sci* 2006, **119:**199-207.
6. Shcherbata HR, Yatsenko AS, Patterson L, Sood VD, Nudel U, Yaffe D, Baker D, Ruohola-Baker H: **Dissecting muscle and neuronal disorders in a Drosophila model of muscular dystrophy.** *Embo J* 2007, **26:**481-93.
7. Deng WM, Schneider M, Frock R, Castillejo-Lopez C, Gaman EA, Baumgartner S, Ruohola-Baker H: **Dystroglycan is required for polarizing the epithelial cells and the oocyte in Drosophila.** *Development* 2003, **130:**173-84.
8. Poulton JS, Deng WM: **Cell-cell communication and axis specification in the Drosophila oocyte.** *Dev Biol* 2007, **311:**1-10.
9. Mirouse V, Christoforou CP, Fritsch C, St Johnston D, Ray RP: **Dystroglycan and perlecan provide a basal cue required for epithelial polarity during energetic stress.** *Dev Cell* 2009, **16:**83-92.
10. Allikian MJ, Bhabha G, Dospoy P, Heydemann A, Ryder P, Earley JU, Wolf MJ, Rockman HA, McNally EM: **Reduced life span with heart and muscle dysfunction in Drosophila sarcoglycan mutants.** *Hum Mol Genet* 2007, **16:**2933-43.
11. Taghli-Lamallem O, Akasaka T, Hogg G, Nudel U, Yaffe D, Chamberlain JS, Ocorr K, Bodmer R: **Dystrophin deficiency in Drosophila reduces lifespan and causes a dilated cardiomyopathy phenotype.** *Aging Cell* 2008, **7:**237-49.
12. Zhan M, Yamaza H, Sun Y, Sinclair J, Li H, Zou S: **Temporal and spatial transcriptional profiles of aging in Drosophila melanogaster.** *Genome Res* 2007, **17:**1236-43.
13. Yatsenko AS, Gray EE, Shcherbata HR, Patterson LB, Sood VD, Kucherenko MM, Baker D, Ruohola-Baker H: **A putative Src homology 3 domain binding motif but not the C-terminal dystrophin WW domain binding motif is required for dystroglycan function in cellular polarity in Drosophila.** *J Biol Chem* 2007, **282:**15159-69.
14. Jung D, Yang B, Meyer J, Chamberlain JS, Campbell KP: **Identification and characterization of the dystrophin anchoring site on beta-dystroglycan.** *J Biol Chem* 1995, **270:**27305-10.
15. Rentschler S, Linn H, Deininger K, Bedford MT, Espanel X, Sudol M: **The WW domain of dystrophin requires EF-hands region to interact with beta-dystroglycan.** *Biol Chem* 1999, **380:**431-42.
16. Huang X, Poy F, Zhang R, Joachimiak A, Sudol M, Eck MJ: **Structure of a WW domain containing fragment of dystrophin in complex with beta-dystroglycan.** *Nat Struct Biol* 2000, **7:**634-8.
17. Keleman K, Kruttner S, Alenius M, Dickson BJ: **Function of the Drosophila CPEB protein Orb2 in long-term courtship memory.** *Nat Neurosci* 2007, **10:**1587-93.
18. Heathcote RD, Ekman JM, Campbell KP, Godfrey EW: **Dystroglycan overexpression in vivo alters acetylcholine receptor aggregation at the neuromuscular junction.** *Dev Biol* 2000, **227:**595-605.
19. Kahl J, Campanelli JT: **A role for the juxtamembrane domain of beta-dystroglycan in agrin-induced acetylcholine receptor clustering.** *J Neurosci* 2003, **23:**392-402.
20. Kucherenko MM, Pantoja M, Yatsenko AS, Shcherbata HR, Fischer KA, Maksymiv DV, Chernyk YI, Ruohola-Baker H: **Genetic modifier screens reveal new components that interact with the Drosophila dystroglycan-dystrophin complex.** *PLoS ONE* 2008, **3:**e2418.
21. Jr WD Tracey, Ning X, Klingler M, Kramer SG, Gergen JP: **Quantitative analysis of gene function in the Drosophila embryo.** *Genetics* 2000, **154:**273-84.
22. Doren M Van, Williamson AL, Lehmann R: **Regulation of zygotic gene expression in Drosophila primordial germ cells.** *Curr Biol* 1998, **8:**243-6.
23. Hacker U, Perrimon N: **DRhoGEF2 encodes a member of the Dbl family of oncogenes and controls cell shape changes during gastrulation in Drosophila.** *Genes Dev* 1998, **12:**274-84.
24. Pignoni F, Zipursky SL: **Induction of Drosophila eye development by decapentaplegic.** *Development* 1997, **124:**271-8.
25. Christoforou CP, Greer CE, Challoner BR, Charizanos D, Ray RP: **The detached locus encodes Drosophila Dystrophin, which acts with other components of the Dystrophin Associated Protein Complex to influence intercellular signalling in developing wing veins.** *Dev Biol* 2008, **313:**519-32.
26. Rorth P: **Gal4 in the Drosophila female germline.** *Mech Dev* 1998, **78:**113-8.
27. Akey JM, Eberle MA, Rieder MJ, Carlson CS, Shriver MD, Nickerson DA, Kruglyak L: **Population history and natural selection shape patterns of genetic variation in 132 genes.** *PLoS Biol* 2004, **2:**e286.
28. Ewing B, Hillier L, Wendl MC, Green P: **Base-calling of automated sequencer traces using phred. I. Accuracy assessment.** *Genome Res* 1998, **8:**175-85.
29. Ewing B, Green P: **Base-calling of automated sequencer traces using phred. II. Error probabilities.** *Genome Res* 1998, **8:**186-94.
30. Gordon D, Abajian C, Green P: **Consed: a graphical tool for sequence finishing.** *Genome Res* 1998, **8:**195-202.
31. Gordon D, Desmarais C, Green P: **Automated finishing with autofinish.** *Genome Res* 2001, **11:**614-25.
32. Bhangale TR, Stephens M, Nickerson DA: **Automating resequencing-based detection of insertion-deletion polymorphisms.** *Nat Genet* 2006, **38:**1457-62.

Supplementary Information

Supplementary Figure 1. Overexpression of Dg constructs with mutation in WW binding sites in follicle and germline cells. A, B. Overexpression of 2WW (A) and PPSG (B) constructs in follicle cells marked by GFP. Dg in the wild type cells is expressed at the apical side of the follicle cell epithelium, in contrast to overexpression where Dg is localized in both apical and basal sides (indicated by arrows). To compare the expression levels of different constructs and insertions the intensities of Dg expression was compared to the intensity of the GFP signal in the same cell. The observed mean intensity ratios are similar in the two constructs (2WW = 1.2, PPSG = 1.1), suggesting that the differences observed between these two conatructs in oocyte polarity assay are not due to dramatically different levels of expression. C. Overexpression of the constructs in the germline cells.wt – Dg expression in wild type germline cells, MatTubGal4; pUASp-WW, nanosGal4/pUASp-WW – overexpression of transgenic constructs in germline cells. Both MatTub- and nanosGal4 have distinct expression patterns.

Supplementary Figure 2. Comparative analysis of Dg C-terminus nucleic acid sequences in 12 species of *Drosophila*.

Supplementary Figure 3. The genomic region of the *Dystroglycan* gene. The genomic regions that are deleted in the *Dystroglycan* mutant alleles Dg^{323} and Dg^{248} are indicated as black bars.

Supplementary Figure 4. Western blot analysis of Dg protein in wild type, DgO43, 2WW and PPSG ovaries and whole animals show the following Dg intensities compared to OregonR (WT): DgO43 [25] = 0.4, 2WW = 1.3, PPSG = 1.2. The specific bands that correspond to different Dg forms can be seen at ~180 (two bands), 110 and faintly at 70 kD. A presumable degradation product can be seen below 25 kD. Increased band intensities can be seen with the 110 kD band and most notably with the higher 180 kD species. Band intensities were normalized to actin and samples were run on a gradient 4–20% gel.

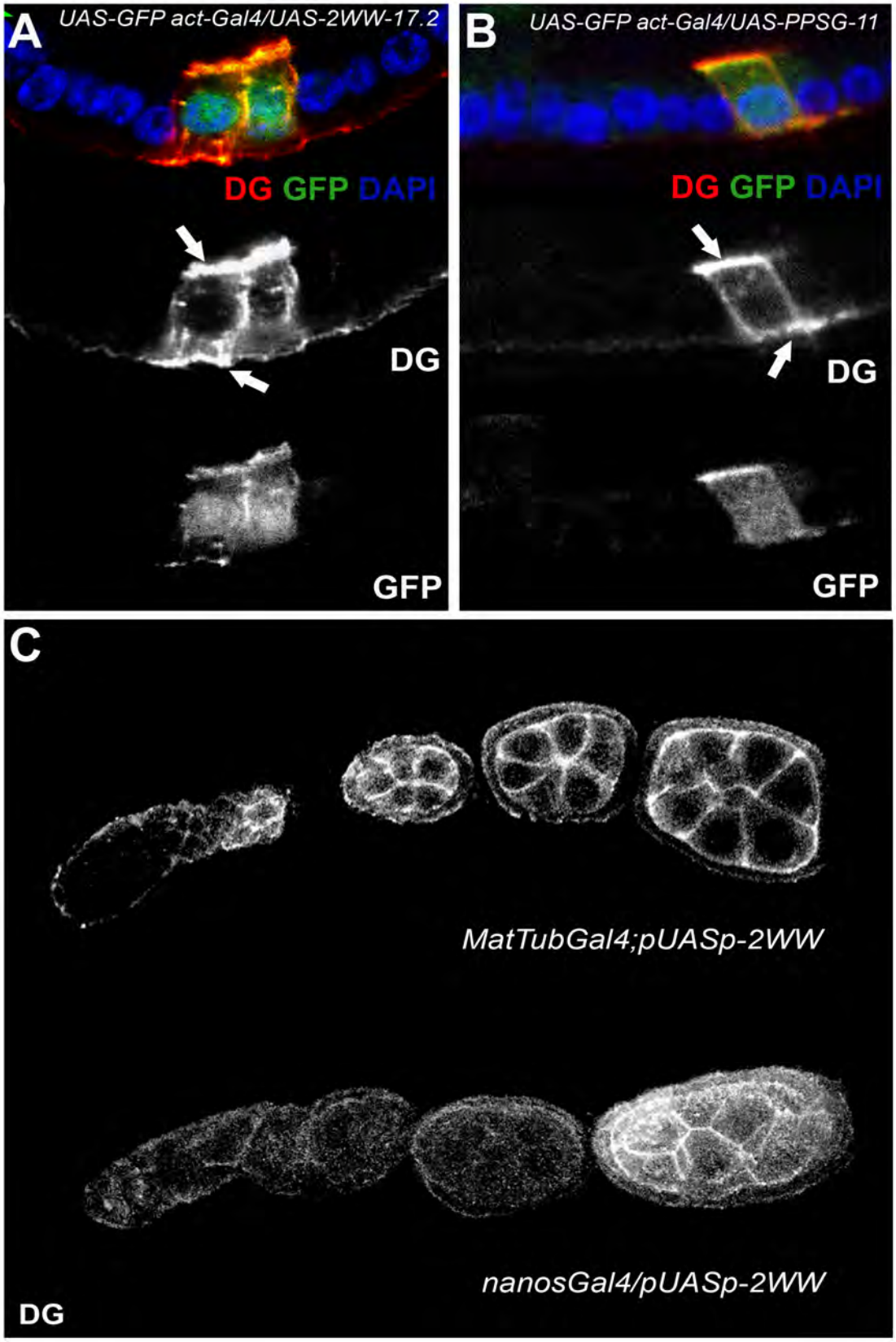

Supplementary Figure 1

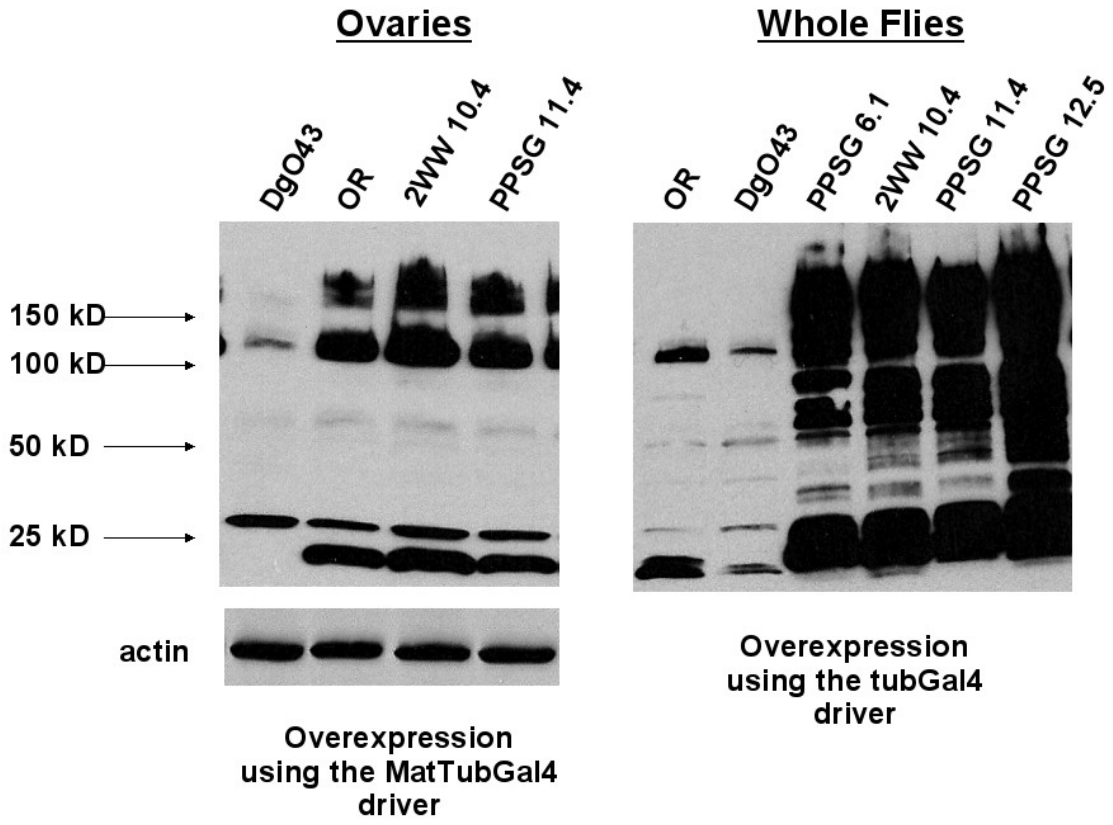

Supplementary Figure 2

16 June 2005 | www.nature.com/nature | $10

THE INTERNATIONAL WEEKLY JOURNAL OF SCIENCE

nature

SILICON-42
What shapes a 'magic' nucleus?

HUMAN RIGHTS IN MYANMAR
Coping with a military regime

TEACHING SCIENCE
US magnet schools examined

STEM CELL DIVISION

Regulatory role for microRNAs

NATUREJOBS
East Coast biomedicine

$10.00US $12.99CAN
24>
0 71486 03070 6

nature 435, 855-1002 16 June 2005 www.nature.com/nature
no.7044 npg

nature Vol 435|16 June 2005|doi:10.1038/nature03816

LETTERS

Stem cell division is regulated by the microRNA pathway

S. D. Hatfield[1]*, H. R. Shcherbata[1]*, K. A. Fischer[1], K. Nakahara[2], R. W. Carthew[2] & H. Ruohola-Baker[1]

One of the key characteristics of stem cells is their capacity to divide for long periods of time in an environment where most of the cells are quiescent. Therefore, a critical question in stem cell biology is how stem cells escape cell division stop signals. Here, we report the necessity of the microRNA (miRNA) pathway[1–4] for proper control of germline stem cell (GSC) division in *Drosophila melanogaster*. Analysis of GSCs mutant for *dicer-1* (*dcr-1*), the double-stranded RNaseIII essential for miRNA biogenesis, revealed a marked reduction in the rate of germline cyst production. These *dcr-1* mutant GSCs exhibit normal identity but are defective in cell cycle control. On the basis of cell cycle markers and genetic interactions, we conclude that *dcr-1* mutant GSCs are delayed in the G1 to S transition, which is dependent on the cyclin-dependent kinase inhibitor Dacapo, suggesting that miRNAs are required for stem cells to bypass the normal G1/S checkpoint. Hence, the miRNA pathway might be part of a mechanism that makes stem cells insensitive to environmental signals that normally stop the cell cycle at the G1/S transition.

MicroRNAs and short interfering RNAs (siRNAs), processed by the type III double-stranded RNase Dicer, function in an RNA-based mechanism of gene silencing[1–4]. Most characterized miRNAs from animals repress gene expression by blocking the translation of complementary messenger RNAs into protein; they interact with their targets by imperfect base-pairing to mRNA sequences within the 3′ untranslated region (3′ UTR)[1]. Experimental evidence has suggested that small RNAs regulate stem cell character in plants and animals[5–7]. Moreover, some miRNAs are differentially expressed in stem cells, suggesting a specialized role in stem cell regulation[8,9]. However, the molecular mechanisms underlying stem cell control by miRNAs are not understood.

To determine the role of miRNAs in the control of stem cell biology, we specifically eliminated processing of all miRNAs in stem cells. The *Drosophila* genome contains two Dicer isozymes: Dicer-1 and Dicer-2 (ref. 10). Dicer-1 (Dcr-1) is essential for processing miRNAs, whereas Dicer-2 (Dcr-2) is required for siRNAs; loss of Dcr-1 completely disrupts the miRNA pathway and only has a weak effect on the siRNA pathway. Using *Drosophila* GSCs as a model system, we impaired Dcr-1 activity with two *dcr-1* alleles: $dcr\text{-}1^{d102}$ and a null $dcr\text{-}1^{Q1147X}$ (ref. 10). *Drosophila* oogenesis depends on the presence of self-renewing GSCs in the adult ovary[11,12], as has recently been reported in a mammalian system[13]. The continuous division of GSCs generates an array of progressively developed egg chambers in wild-type ovarioles (Fig. 1).

Analysis of *dcr-1* mutant clones in the *Drosophila* ovary 12 days after clone induction revealed a marked depletion of developing egg chambers (see Fig. 1b–f for $dcr\text{-}1^{Q1147X}$ and Supplementary Fig. 1a

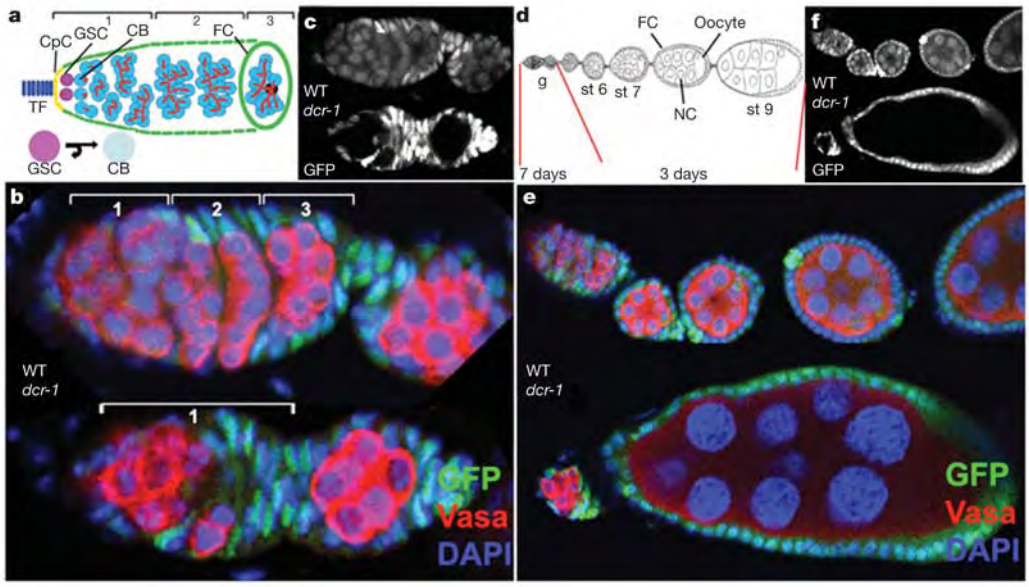

Figure 1 | Loss of Dcr-1 function in GSCs reduces the rate of egg chamber production. **a**, Schematic of a germarium divided into three regions. Region one contains GSCs and dividing cysts. **b**, **c**, All three regions are observed in a wild-type heterozygous $dcr\text{-}1^{Q1147X}/+$ germarium (WT, top), but not in a mosaic $dcr\text{-}1^{Q1147X}$ germarium 12 days after clone induction (no GFP, *dcr-1*, bottom). **d**, Oocyte development is divided into 14 stages. **e**, **f**, Many of the developmental stages are missing in ovarioles that are complete $dcr\text{-}1^{Q1147X}$ germline clones (no GFP, 12 days after clone induction; bottom of panels **e** and **f**). CpC, cap cells; CB, cystoblast; DAPI, 4,6-diamidino-2-phenylindole; FC, follicle cells; NC; nurse cells; TF, terminal filaments. Vasa marks the germ line. Absence of GFP marks *dcr-1* mutant cells.

[1]Department of Biochemistry, University of Washington, J591, HSB, Seattle, Washington 98195-7350, USA. [2]Department of Biochemistry, Molecular Biology and Cell Biology, Northwestern University, 2205 Tech Drive, Evanston, Illinois 60208, USA.
*These authors contributed equally to this work.

for *dcr-1*^{d102}). In contrast, *dcr-2* null mutant GSCs produced a normal progression of egg chambers. These data suggest that Dcr-1 is required for efficient germline production. Although *dcr-1* mutants showed reduced numbers of gametes, most developing gametes appeared morphologically normal (although they exhibit polarity defects; data not shown). We therefore analysed potential problems in GSC maintenance, identity and division. Clonal experiments revealed that the percentage of germaria with clonal stem cells at different time points after clone induction was similar in the *dcr-1*^{Q1147X} mutant and the wild-type control (Fig. 2b), suggesting that the loss of cysts in *dcr-1* mutants is not primarily due to problems in the maintenance of GSCs.

To determine whether reduced cyst production in *dcr-1* germaria was due to altered GSC fate, we analysed the identity of the *dcr-1* mutant GSCs. Female GSCs are identified by their location and the expression patterns of three markers (Fig. 2a): the presence of Adducin, a protein present in the spectrosome[14]; the presence of phosphorylated Mad protein (P-Mad), indicating TGF-β signalling[14,15]; and the absence of Bam, repressed by the TGF-β pathway[16]. The *dcr-1*^{Q1147X} GSCs showed normal spectrosome morphology and position (100%, $n = 53$), and normal TGF-β pathway activity (P-Mad: wild type 88%, $n = 114$; *dcr-1*^{Q1147X} 85%, $n = 47$; Fig. 2c, d). Furthermore, as with wild-type GSCs, *dcr-1*^{Q1147X} GSCs did not stain positively for the Bam protein (Fig. 2e). From these analyses, we conclude that decreased cyst production from *dcr-1*^{Q1147X} GSCs does not result from either a loss of GSCs or a change in their identity.

The frequency of cell division in *dcr-1*^{Q1147X} GSCs was impaired. Examination of individual germaria containing a single heterozygous GSC and a single *dcr-1*^{Q1147X} mutant GSC revealed that GSCs lacking Dcr-1 activity produced cysts at a frequency that was reduced to 18% of normal levels (41% for *dcr-1*^{d102}; Table 1 and Fig. 3a–c). In contrast, the frequency of division was not significantly reduced for GSCs that were homozygous for the *dcr-2* mutation or for the isogenized parental chromosome from which the *dcr-1* mutant alleles were generated (Table 1 and Fig. 3c). Thus, Dcr-1 is required cell autonomously in GSCs for the cell divisions that produce developing cystoblasts (no obvious defect in cyst division was observed; see Supplementary Fig. 2c, d).

To determine whether the reduced cyst formation reflected a block in the normal cell cycle programme, we analysed the distribution of cell cycle stages in mutant *dcr-1*^{Q1147X} GSCs by staining mosaic germaria with antibodies against different cell cycle markers (Fig. 3d).

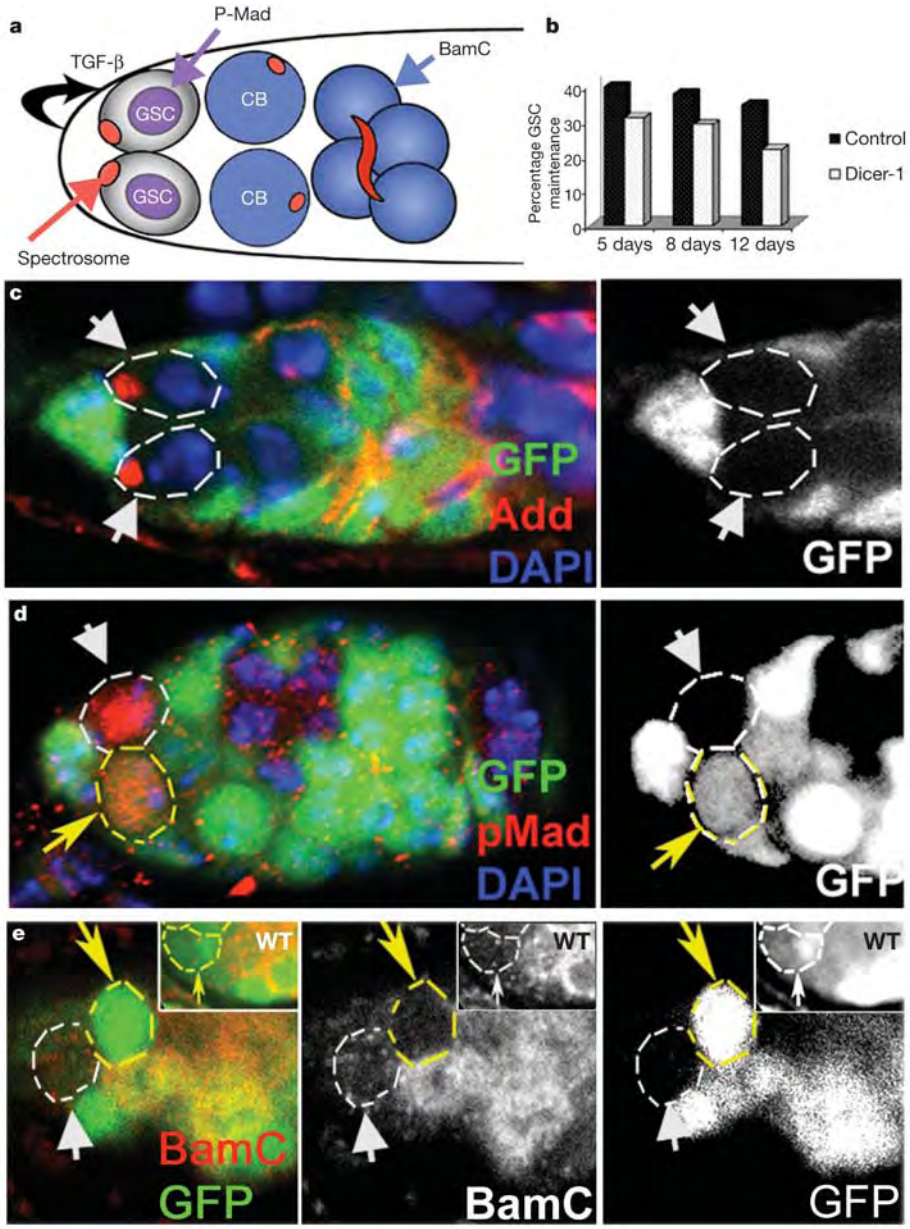

Figure 2 | *dcr-1* mutant GSCs remain in the stem cell niche and retain stem cell identity. **a**, GSC markers: P-Mad, spectrosome (Adducin, Add), lack of BamC. **b**, *dcr-1*^{Q1147X} mutant and wild-type GSCs are maintained in germaria. A low rate of GSC loss was observed for both backgrounds[30]. Bars represent the percentage of germaria with clonal stem cells at different time points after clone induction. **c**–**e**, *dcr-1*^{Q1147X} GSCs (no GFP, white arrows) possess a spectrosome (100%, $n = 53$; **c**) and respond to the TGF-β signal (anti-P-Mad staining: *dcr-1* mutant, 85%, $n = 47$; control, 88%, $n = 114$; **d**) but do not exhibit BamC expression ($n = 13$; **e**). Yellow arrows in **d**, **e** mark non-clonal, wild-type GSCs.

Table 1 | Effect of the miRNA pathway on GSC division frequency

Brief genotype	Genotype of GSC and cysts	Frequency of GSC division (±s.d.)*	Sample size (*n*)	Division index (±s.d.)†
Wild type	Non-clonal (GFP^+): *hsFlp; FRT82B hsNmyc/FRT82B Ubi-GFP*	4.53 ± 0.93	17	-
Wild type	Clonal (GFP^-): *hsFlp; FRT82B hsNmyc/FRT82B hsNmyc*	4.64 ± 0.87	17	1.03 ± 0.20
$dcr\text{-}1^{Q1147X}$	Non-clonal (GFP^+): *hsFlp; FRT82B* $dcr\text{-}1^{Q1147X}/$*FRT82B Ubi-GFP*	4.37 ± 0.74	27	-
$dcr\text{-}1^{Q1147X}$	Clonal (GFP^-): *hsFlp; FRT82B* $dcr\text{-}1^{Q1147X}/$*FRT82B* $dcr\text{-}1^{Q1147X}$ (8 days)	1.41 ± 0.69	27	0.32 ± 0.16
$dcr\text{-}1^{Q1147X}$	Clonal (GFP^-): *hsFlp; FRT82B* $dcr\text{-}1^{Q1147X}/$*FRT82B* $dcr\text{-}1^{Q1147X}$ (12 days)	0.77 ± 0.59	20	0.18 ± 0.13
$dcr\text{-}1^{d102}$	Non-clonal (GFP^+): *hsFlp; FRT82B* $dcr\text{-}1^{d102}/$*FRT82B Ubi-GFP*	4.64 ± 0.83	24	-
$dcr\text{-}1^{d102}$	Clonal (GFP^-): *hsFlp; FRT82B* $dcr\text{-}1^{d102}/$*FRT82B* $dcr\text{-}1^{d102}$ (8 days)	2.5 ± 0.65	24	0.53 ± 0.26
$dcr\text{-}1^{d102}$	Clonal (GFP^-): *hsFlp; FRT82B* $dcr\text{-}1^{d102}/$*FRT82B* $dcr\text{-}1^{d102}$ (12 days)	1.72 ± 0.56	39	0.41 ± 0.13
dcr-2	Non-clonal (GFP^+): *hsFlp; FRT42D dcr-2/FRT42D Ubi-GFP*	4.48 ± 1.31	24	-
dcr-2	Clonal (GFP^-): *hsFlp; FRT42D dcr-2/FRT42D dcr-2* (8 days)	4.01 ± 0.88	24	0.89 ± 0.19
dcr-2	Clonal (GFP^-): *hsFlp; FRT42D dcr-2/FRT42D dcr-2* (12 days)	4.20 ± 1.36	24	0.85 ± 0.28
Parental chromosome	Non-clonal (GFP^+): *hsFlp; FRT82B* (parental)*/FRT82B Ubi-GFP*	4.58 ± 0.97	23	-
Parental chromosome	Clonal (GFP^-): *hsFlp;* FRT82B (parental)/FRT82B (parental) (8 days)	4.80 ± 1.04	23	1.04 ± 0.17
Parental chromosome	Clonal (GFP^-): *hsFlp;* FRT82B (parental)/FRT82B (parental) (12 days)	5.77 ± 0.69	22	1.16 ± 0.14
dap	Non-clonal (GFP^+): *hsFlp; FRT42B* $dap^4/$*FRT42B Ubi-GFP*	4.44 ± 0.66	20	-
dap	Clonal (GFP^-): *hsFlp; FRT42B* $dap^4/$*FRT42B* dap^4	4.12 ± 0.79	20	0.93 ± 0.18
dap/+; dcr-1	Non-clonal (GFP^+): *hsFlp; FRT42B* $dap^4/+$*; FRT82B* $dcr\text{-}1^{Q1147X}/$*FRT82B Ubi-GFP*	4.25 ± 0.55	29	-
dap/+; dcr-1	Clonal (GFP^-): *hsFlp; FRT42B* $dap^4/+$*; FRT82B* $dcr\text{-}1^{Q1147X}/$*FRT82B* $dcr\text{-}1^{Q1147X}$	2.72 ± 0.75	19	0.64 ± 0.18

8 or 12 days indicate the number of days after clone induction (this is 8 days if not indicated).
*The number of cystoblasts and cysts divided by the number of GSCs.
†The frequency of clonal GFP^- GSC division divided by the frequency of control non-clonal GFP^+ GSC division.

We observed an increase in the number of *dcr-1* mutant GSCs staining positive for Cyclin E (CycE) using two independent *dcr-1* alleles (Fig. 3e, f; see also Supplementary Table 1 and Supplementary Fig. 1b). In contrast, GSCs that were homozygous for *dcr-2* or the parental chromosome expressed CycE with frequencies similar to that of wild-type GSCs (Supplementary Fig. 1b). Furthermore, pulse labelling of ovaries with the nucleotide analogue 5-bromodeoxyuridine (BrdU)[17,18] revealed that the number of $dcr\text{-}1^{Q1147X}$

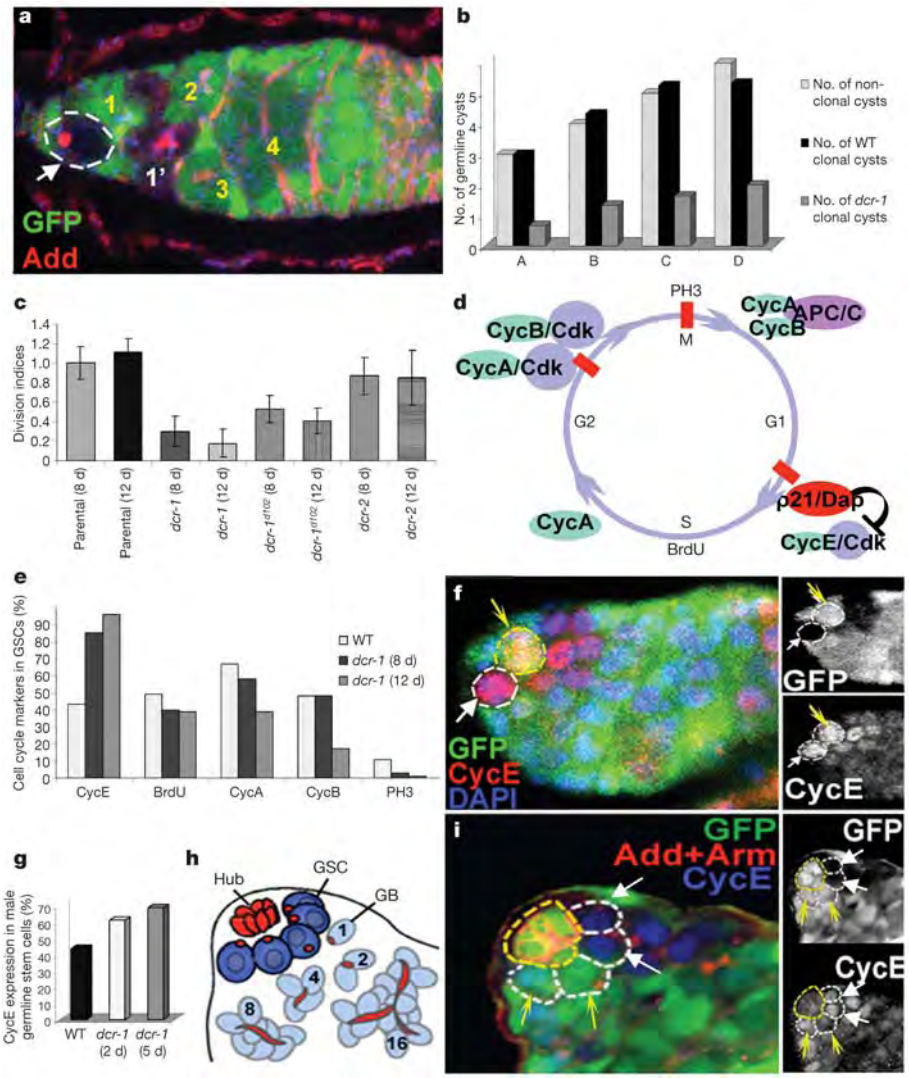

Figure 3 | *dcr-1* causes a cell cycle delay in GSCs. **a**, $dcr\text{-}1^{Q1147X}$ GSCs (white arrow) produce fewer cysts (white number) than wild-type GSCs (yellow numbers). **b**, $dcr\text{-}1^{Q1147X}$ cysts are produced at a lower frequency than wild-type and non-clonal cysts. Samples A–D are grouped according to the number of non-clonal cysts per germarium ($n = 27$). **c**, Division indices are decreased for *dcr-1* mutant GSCs compared with control and *dcr-2* mutant GSC clones. Error bars represent standard deviation. Times are days after the last clonal induction. **d**, Cell cycle markers. **e**, $dcr\text{-}1^{Q1147X}$ (*dcr-1*) GSCs are more frequently CycE-positive and less frequently positive for other cell cycle markers compared with wild-type $dcr\text{-}1^{Q1147X}/+$ GSCs. **f**, CycE-positive *dcr-1* mutant GSC (white arrow). **g**, Percentage of CycE-positive male GSCs that are $dcr\text{-}1^{Q1147X}$ or wild type. **h**, Male GSC niche. **i**, CycE in male *dcr-1* mutant GSCs (white arrow). Arm (Armadillo) marks somatic hub cells. Yellow arrows in **f**, **i** mark non-clonal, wild-type GSCs.

mutant GSCs in S phase was reduced (Fig. 3e; see also Supplementary Table 1). Similarly, the number of *dcr-1*^{Q1147X} mutant GSCs staining positive for Cyclin A (CycA), Cyclin B (CycB) and the mitotic marker Phosphohistone-3 (PH3) was reduced (Fig. 3e; see also Supplementary Table 1). These data indicate that perturbation of the miRNA pathway by mutant *dcr-1* in GSCs delays the cell cycle at the G1/S transition.

We tested whether loss of Dcr-1 function has similar consequences on the cell cycle in the GSCs of male flies. Each male testis contains approximately ten GSCs surrounding a somatic structure called the hub (Fig. 3h–i)[19,20]. Similar to female GSCs, the number of male GSCs staining positive for CycE was increased in *dcr-1* mutants (Fig. 3g–i). These data show that Dcr-1 also functions in the male GSC niche, and suggest that Dcr-1 has a conserved role in GSC division.

To test the possibility that the miRNA pathway might be a general cell cycle regulator, we examined other cell types to determine whether the G1/S delay and reduced cell division frequency are also observed in other mitotically dividing *dcr-1* mutant cells. *dcr-1*^{Q1147X} clones in imaginal discs revealed that the number of CycE-positive cells was not increased in mutant cells (Supplementary Fig. 2a). The number of *dcr-1*^{Q1147X} mutant cells in imaginal discs was approximately equal to the number of marked wild-type cells that descended from a common parent cell, indicating that the frequency of cell division in imaginal disc cells is not reduced in a *dcr-1* mutant (Supplementary Fig. 2a, b). *dcr-1*^{Q1147X} dividing germline cysts express CycE at a frequency comparable to that of wild-type dividing cysts, suggesting that the mitotic cystoblast cell divisions are not affected in *dcr-1* mutants (Supplementary Fig. 2c, d). Therefore, the reduction in cell division frequency observed in the *dcr-1* mutant germ line is specific to the GSC division. Together, these data suggest that the miRNA pathway has a specific role in regulating stem cell division.

We explored the potential cause for the G1/S arrest by examining the expression of Dacapo (Dap; a homologue of the p21/p27 family of cyclin-dependent kinase (CDK) inhibitors)[21,25] in *dcr-1*^{Q1147X} mutant GSCs. The transition between the G1 and S phases of the cell cycle is negatively regulated by Dap[21,25]. Dap protein traps the CycE/CDK2 complex in a stable but inactive form[22], and elevated levels of Dap lead to cell cycle arrest at the G1/S phase transition with prolonged expression of CycE protein[17]. Notably, the number of Dap-positive GSCs increased in the *dcr-1* mutant GSC population (Fig. 4b; see also Supplementary Table 1 and Supplementary Fig. 3a).

To determine whether Dap mediated the effect of *dcr-1* on the GSC cell cycle, we reduced the level of Dap by 50% in *dcr-1*^{Q1147X} mutant GSCs and observed a partial rescue in cyst production (Table 1 and Fig. 4c, e). Furthermore, the number of GSCs staining positive for CycE was reduced to normal levels (Fig. 4d), demonstrating that the CycE defect observed in *dcr-1* mutant GSCs is dependent on Dap. Consistent with this, overexpression of a Dap transgene resulted in some germaria resembling *dcr-1* germline mutants: the germaria were small, containing a few cysts, and had a high number of CycE-positive GSCs (Fig. 4d; see also Supplementary Fig. 3d). The fact that reduction of Dap levels led to a normal GSC CycE profile, but partial rescue of cyst generation, suggests that Dcr-1 might also regulate later cyst development.

These data suggest that miRNAs act on stem cell division by reducing the levels of Dap. How is this regulation achieved? We found

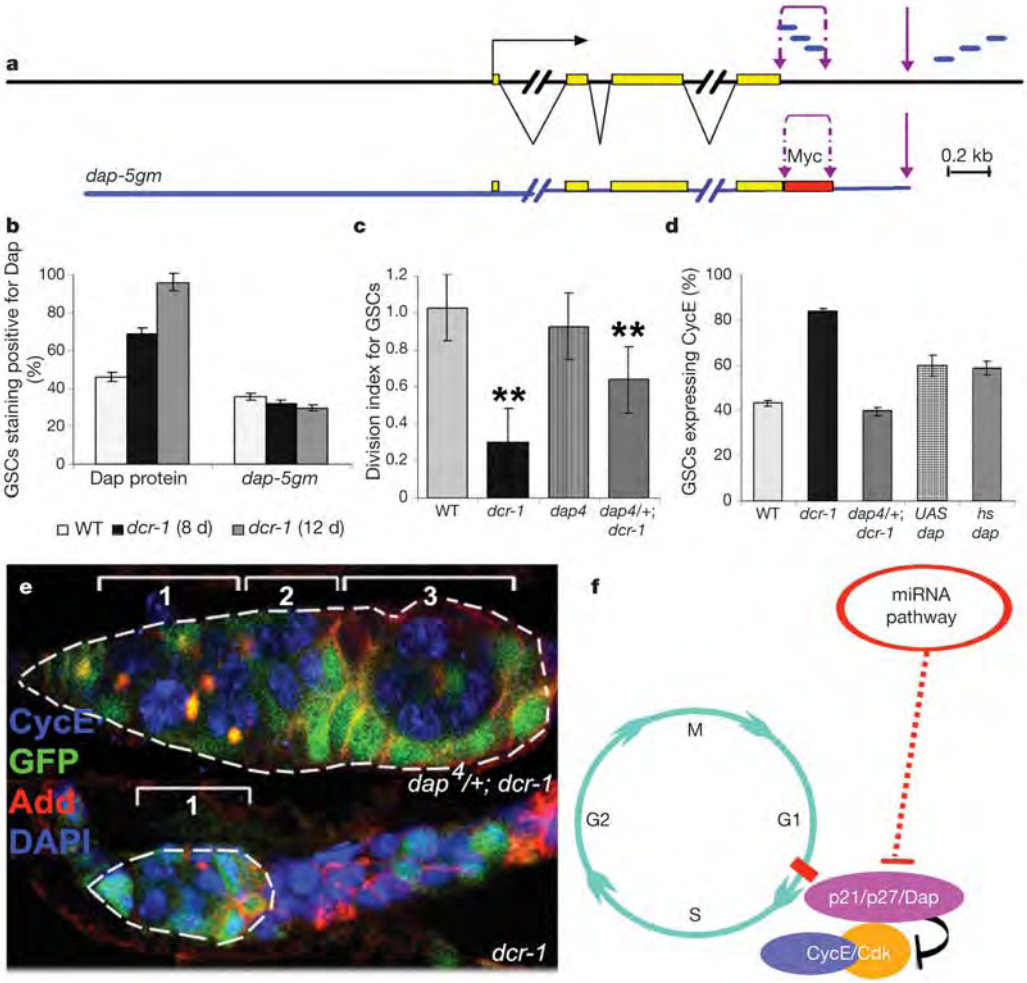

Figure 4 | The GSC division defect is dependent on Dap. **a**, The *dap-5gm* transgene compared to the endogenous *dap* locus. A 6 × Myc tag replaces a region of the 3′ UTR containing predicted miRNA-binding sites (blue bars). The UTR lacks the last 540 base pairs. **b**, Endogenous Dap is detected more frequently in *dcr-1* mutant than wild-type GSCs but Dap from *dap-5gm* is not detected more frequently in *dcr-1* GSCs. **c**, **e**, Germaria with *dap*^{4}/+;*dcr-1*^{Q1147X} GSCs produce more cysts than germaria with *dcr-1*^{Q1147X} GSCs. Double asterisk, $P \leq 10^{-3}$ (Student's *t*-test). **d**, Percentage of CycE-positive GSCs. Dap was overexpressed by *nos-Gal4/pUASp-dap* or *hs-dap*. Error bars represent standard deviations (**c**) or errors from the mean (**b**, **d**). **f**, miRNA pathway modulates the GSC cell cycle by affecting the G1/S transition through Dap (p21/p27).

that expression of a Dap transgene containing the Dap promoter and essentially all of the endogenous gene except some of the 3′ UTR (*dap-5gm*)[23] was similar in *dcr-1* mutant and wild-type GSCs (Fig. 4b; see also Supplementary Fig. 3b, c). These data suggest that the effect of Dcr-1 on Dap regulation in GSCs (Fig. 4b) is at a post-transcriptional level and might involve the 3′ UTR region that is missing in the *dap-5gm* transgene (Fig. 4a).

We propose that miRNAs are required for GSCs to transit the G1/S checkpoint by repressing directly or indirectly the G1/S inhibitor Dap (Fig. 4f). Because Dap is a key component of the G1/S transition[21–25], it is a plausible target for machinery that assures continuous cell division in a microenvironment in which most of the cells are quiescent. We propose that while the TGF-β pathway—which can upregulate p21/p27 (ref. 24)—is active in GSCs[16], miRNAs downregulate Dap to assure the continuous cell division essential for stem cells. This downregulation might be direct, because the Dap 3′ UTR contains several predicted miRNA-binding sites[26–28] (Supplementary Fig. 4). A Dap transgene lacking these sites showed no response to Dcr-1 levels (Fig. 4b; see also Supplementary Fig. 3b, c), suggesting that the potential binding sites are responsive to Dicer-1. However, it is also possible that the Dap misregulation in *dcr-1* mutant GSCs might be due to a secondary effect of Dcr-1 loss. Our finding that miRNAs are required for stem cell division suggests that miRNAs might be part of a mechanism that makes stem cells insensitive to environmental signals that normally stop the cell cycle. Because miRNAs are a novel class of genes involved in human tumorigenesis[29], it is tempting to speculate that miRNAs could have a similar role in cancer cells.

METHODS

We used the following stocks: *eyFLP;FRT82Bdcr-1^{Q1147X}/TM3Sb*, *eyFLP;FRT82Bdcr-1^{d102}/TM3Sb*, *eyFLP;FRT42Ddcr-2^{L811X}/CyO*, *eyFLP;FRT82B* parental[10], *w;FRT42Bdap^{4}/CyO* (ref. 25), *dap5gm* (ref. 23), *w;NGT40/SM6a; nosGal4VP16/TM3Sb*, *hsFlp;FRT82BUbi-GFP/TM3Sb*, *hsFlp;FRT42BUbi-GFP/CyO*, *hsFlp;FRT42DUbi-GFP/CyO*, *FRT82BhsNmyc*.

For female germline clones, Flp-FRT flies were heat shocked (third instar larvae for 1 h, pupae for 1 h at 37 °C) and dissected 5–12 days after the last heat shock. For male germline clones, adult flies were heat shocked for 40 min at 37 °C twice per day for 3 days and dissected 2–6 days after the last heat shock.

We used the following antibodies: mouse anti-CycA, anti-CycB, anti-Adducin (1:20) and anti-Armadillo (1:40) (Developmental Studies Hybridoma Bank), mouse anti-Dap (1:5, I. Hariharan), anti-BrdU (1:20, PharMingen) and anti-c-Myc (1:50, Calbiochem), rabbit anti-PH3 (1:200, Upstate Biotechnology), anti-GFP (1:1,000, Molecular Probes), anti-Vasa (1:10,000, P. Lasko) and anti-P-Mad (1:500, P. ten Dijke), guinea-pig anti-CycE (1:500, T. Orr-Weaver), rat anti-BamC (1:1,000, D. McKearin), Alexa 488, 568, or 633 goat anti-mouse, anti-rabbit and anti-guinea-pig (1:500, Molecular Probes), and goat-anti-rat Cy5 (1:250, Jackson Immunoresearch).

Received 23 March; accepted 16 May 2005.
Published online 8 June 2005.

1. He, L. & Hannon, G. J. MicroRNAs: small RNAs with a big role in gene regulation. *Nature Rev. Genet.* **5,** 522–531 (2004).
2. Nakahara, K. & Carthew, R. W. Expanding roles for miRNAs and siRNAs in cell regulation. *Curr. Opin. Cell Biol.* **16,** 127–133 (2004).
3. Bartel, B. & Bartel, D. P. MicroRNAs: at the root of plant development? *Plant Physiol.* **132,** 709–717 (2003).
4. Ambros, V. microRNAs: tiny regulators with great potential. *Cell* **107,** 823–826 (2001).
5. Bernstein, E. *et al.* Dicer is essential for mouse development. *Nature Genet.* **35,** 215–217 (2003).
6. Schauer, S. E., Jacobsen, S. E., Meinke, D. W. & Ray, A. DICER-LIKE1: blind men and elephants in *Arabidopsis* development. *Trends Plant Sci.* **7,** 487–491 (2002).
7. Carmell, M. A., Xuan, Z., Zhang, M. Q. & Hannon, G. J. The Argonaute family: tentacles that reach into RNAi, developmental control, stem cell maintenance, and tumorigenesis. *Genes Dev.* **16,** 2733–2742 (2002).
8. Suh, M. R. *et al.* Human embryonic stem cells express a unique set of microRNAs. *Dev. Biol.* **270,** 488–498 (2004).
9. Houbaviy, H. B., Murray, M. F. & Sharp, P. A. Embryonic stem cell-specific MicroRNAs. *Dev. Cell* **5,** 351–358 (2003).
10. Lee, Y. S. *et al.* Distinct roles for *Drosophila* Dicer-1 and Dicer-2 in the siRNA/miRNA silencing pathways. *Cell* **117,** 69–81 (2004).
11. Spradling, A., Drummond-Barbosa, D. & Kai, T. Stem cells find their niche. *Nature* **414,** 98–104 (2001).
12. Gilboa, L. & Lehmann, R. How different is Venus from Mars? The genetics of germ-line stem cells in *Drosophila* females and males. *Development* **131,** 4895–4905 (2004).
13. Johnson, J., Canning, J., Kaneko, T., Pru, J. K. & Tilly, J. L. Germline stem cells and follicular renewal in the postnatal mammalian ovary. *Nature* **428,** 145–150 (2004).
14. Kai, T. & Spradling, A. Differentiating germ cells can revert into functional stem cells in *Drosophila melanogaster* ovaries. *Nature* **428,** 564–569 (2004).
15. Newfeld, S. J. *et al.* Mothers against dpp participates in a DDP/TGF-β responsive serine-threonine kinase signal transduction cascade. *Development* **124,** 3167–3176 (1997).
16. Song, X. *et al.* Bmp signals from niche cells directly repress transcription of a differentiation-promoting gene, *bag of marbles*, in germline stem cells in the *Drosophila* ovary. *Development* **131,** 1353–1364 (2004).
17. Shcherbata, H. R., Althauser, C., Findley, S. D. & Ruohola-Baker, H. The mitotic-to-endocycle switch in *Drosophila* follicle cells is executed by Notch-dependent regulation of G1/S, G2/M and M/G1 cell-cycle transitions. *Development* **131,** 3169–3181 (2004).
18. Calvi, B. R. & Lilly, M. A. Fluorescent BrdU labeling and nuclear flow sorting of the *Drosophila* ovary. *Methods Mol. Biol.* **247,** 203–213 (2004).
19. Gonczy, P. & DiNardo, S. The germ line regulates somatic cyst cell proliferation and fate during *Drosophila* spermatogenesis. *Development* **122,** 2437–2447 (1996).
20. Kiger, A. A., Jones, D. L., Schulz, C., Rogers, M. B. & Fuller, M. T. Stem cell self-renewal specified by JAK-STAT activation in response to a support cell cue. *Science* **294,** 2542–2545 (2001).
21. de Nooij, J. C., Letendre, M. A. & Hariharan, I. K. A cyclin-dependent kinase inhibitor, Dacapo, is necessary for timely exit from the cell cycle during *Drosophila* embryogenesis. *Cell* **87,** 1237–1247 (1996).
22. Pavletich, N. P. Mechanisms of cyclin-dependent kinase regulation: structures of Cdks, their cyclin activators, and Cip and INK4 inhibitors. *J. Mol. Biol.* **287,** 821–828 (1999).
23. Meyer, C. A. *et al. Drosophila* p27Dacapo expression during embryogenesis is controlled by a complex regulatory region independent of cell cycle progression. *Development* **129,** 319–328 (2002).
24. Datto, M. B. *et al.* Transforming growth factor beta induces the cyclin-dependent kinase inhibitor p21 through a p53-independent mechanism. *Proc. Natl Acad. Sci. USA* **92,** 5545–5549 (1995).
25. Lane, M. E. *et al.* Dacapo, a cyclin-dependent kinase inhibitor, stops cell proliferation during *Drosophila* development. *Cell* **87,** 1225–1235 (1996).
26. Enright, A. J. *et al.* MicroRNA targets in *Drosophila*. *Genome Biol.* **5,** R1 (2003).
27. Stark, A., Brennecke, J., Russell, R. B. & Cohen, S. M. Identification of *Drosophila* MicroRNA targets. *PLoS Biol.* **1,** E60 (2003).
28. Lewis, B. P., Shih, I. H., Jones-Rhoades, M. W., Bartel, D. P. & Burge, C. B. Prediction of mammalian microRNA targets. *Cell* **115,** 787–798 (2003).
29. He, L. *et al.* A microRNA polycistron as a potential human oncogene. *Nature* doi:10.1038/nature03552 (in the press).
30. Margolis, J. & Spradling, A. Identification and behavior of epithelial stem cells in the *Drosophila* ovary. *Development* **121,** 3797–3807 (1995).

Supplementary Information is linked to the online version of the paper at www.nature.com/nature.

Acknowledgements We thank B. Calvi, B. Wakimoto and E. Ward for comments on the manuscript, and the members of the H.R.-B. laboratory for suggestions throughout the course of this study. We also thank E. Kerr for making *dacapo* constructs; V. Shcherbatyy for creating transgenic lines; B. Akiyashi for UAS-Dap experiments; K. Kim for the *dcr-1^{d102}* strain; and M. Lilly, C. Lehner, I. Hariharan, T. Orr-Weaver, D. McKearin, P. ten Dijke, A. Spradling and C.-H. Heldin for flies, antibodies and advice. This work was supported by the Schultz Fellowship for S.D.H., grants from the National Institutes of Health to R.W.C and H. R.-B., and the American Heart Association and the American Cancer Society to H.R.-B.

Author Information Reprints and permissions information is available at npg.nature.com/reprintsandpermissions. The authors declare no competing financial interests. Correspondence and requests for materials should be addressed to H.R.-B. (hannele@u.washington.edu) and R.W.C. (r-carthew@northwestern.edu).

Materials and Methods

dcr-1^{d102} results in a Q1948X mutation and therefore truncates the second RNAIII domain in Dcr-1.

Generation of Transgenic Lines

Full-length Dacapo PCR products were synthesized using the forward primer GCTCTAGATTAGTTGTTGTGGCGCGGCCGCTT and the reverse primer GCTTCAGAATGGTCAGTGCCCGAGTCCTG (Invitrogen) from the template pSK+ dap (a gift from Christian Lehner). PCR products were then digested with *XbaI* and cloned into p-hsCaSpeR and pUAS-P vectors (a gift from Pernille Rorth). This XbaI fragment contained only the coding region; the 5' and 3' untranslated regions were not included. Transformant lines were generated by germline transformation in a w^{1118} background. Four independent transformant lines were obtained for *UAS-Dap (UAS-Dap-18* was analysed in Fig4d, other independent insertions gave similar results) and one transformant line for *hs-Dap* (*hs-Dap-7*).

Dacapo Overexpression

Ectopic expression of Dacapo was achieved by two different ways: 1) heat-shock-induced expression by administering 3x50 min heat-shocks in 36 hours and dissected 3-6 days after the last heat-shock; and 2) Gal4/UAS-dependent overexpression with the germline driver *nanos (nos Gal4 VP16)*.

Generation of clones and kinetic- and statistical-analysis

Drosophila melanogaster stocks were raised on standard cornmeal-yeast-agar-medium at 25^{o}C. Clones were induced using the FLP-FRT system for mitotic recombination *(Supplementary Ref1)*. To obtain imaginal disc clones, we heat-shocked second-instar larvae for 120 minutes at 37° C and dissected them after 2 days. Transient cyst clones were induced by a single 50 minute heat-shock and the animals were dissected after 5 days at 21°C; cysts were counted only if they had not yet reached the 16-cell stage and if no stem cell clone was observed in the germarium.

Division frequencies were measured using germaria containing one *GFP*$^{+}$ GSC and one *GFP*$^{-}$ GSC. The total number of cysts from a GSC that are produced in a given time window provides a measurement of GSC division frequency. In our case, the time window spanned from the first heat-shock treatment to the time of harvesting the adults. Therefore, we limited our counts to the region of the germarium that was anterior to the easily-identifiable *GFP*$^{+/+}$ cyst. This cyst developed from the first daughter cell of the clonal GSC *(GFP*$^{-}$*)* after heat-shock induced mitotic recombination. Since *dcr-1* GSCs could have been induced by either of the two heat-shocks that were given, the total number of GSC progeny (cysts) found in the relevant region could vary (Fig3b). However, in all cases, the number of cysts produced from the *dcr-1* GSCs was lower than for control GSCs regardless of time. Cyst production from homozygous clonal GSCs was divided by the cyst production from heterozygous non-clonal GSCs in the same germarium to obtain the division index (Fig3c).

The student T-test was used to determine the statistical significance in Fig4c. The Dap 3'UTRs from D. melanogaster and D. pseudoobscura were analyzed for potential miRNA-binding sites. Four algorithms were independently applied: the program miRanda[24], an EMBL program[27], TargetScan[28] and a program devised by Nakahara and Carthew (*Supplementary Ref3*).

Staining Procedures

Antibody stainings, BrdU-labeling (90 minute pulse) and confocal microscopy was performed as described previously[17-18] (*Supplementary Ref2*). A two-photon laser-scanning microscope (Leica TCS SP/MP) was used in this study.

Supplementary References

1. K. G. Golic, *Science* **252**, 958 (Jun 17, 1991).
2. M. Keller Larkin *et al.*, *Dev Genes Evol* **209**, 301 (May, 1999).
3. K.Nakahara and R.Carthew, unpublished.

Supplementary Table 1. *Dcr-1* mutant GSCs are blocked in G1/S cell cycle transition

Genotype	**% GSCs that show positive staining for cell cycle markers**					
	CycE	**Dap**	**CycA**	**CycB**	**BrdU**	**PH3**
Control dcr-1/+ (GFP^{+}) *hsFlp; FRT82B dcr-1^{Q1147X}/FRT82B Ubi-GFP*	43.2% n=88	46.0% n=50	67.1% n=76	48.4% n=64	49.2% n=131	11% n=134
***Mutant dcr-1/dcr-1* (GFP^{-})** *hsFlp; FRT82B dcr-1^{Q1147X}/FRT82B dcr-1^{Q1147X}* *(8 days post induction)*	85.0% n=40	68.5% n=35	58.3% n=24	48.4% n=31	39.3% n=87	2.9% n=35
(12 days post induction)	96% n=25	96% n=24	33.0% n=24	17.0% n=47	23.8% n=61	0.0% n=10

n = number of GSCs counted

Supplementary Figure 1 Legend

The *dcr-1*^{d102} allele yields a phenotype identical to, albeit slightly milder than the *dcr-1*^{Q1147X} allele. (a) *dcr-1*^{d102} germaria are smaller then wild-type and exhibit a marked decrease in germline cyst number. (**b**) *dcr-1*^{d102} allele shows an increase in the frequency of CycE expression whereas GSCs that are homozygous for the parental chromosome express CycE with frequencies similar to what is observed for wild-type GSCs. No significant effect on CycE in *dcr-2* mutant clones was observed. Days indicate the timepoint after clonal induction.

Supplementary Figure 2 Legend

The *dcr1*-related reduction in cell division rate and cell cycle delay are germline stem cell-specific. (a-a'') *dcr-1* (*dcr-1*^{Q1147X}) clones in a leg imaginal disc. Clones are marked by dotted line in panels **a'** and **a''**. Legend refers to top clone and its sister clone, which are in the best orientation. The number of cells in the *dcr-1* clone (**a'**, black) is approximately equal to the number of cells in the adjacent sister clone (**a,** bright green). **a''** Only a small percentage of cells within the *dcr-1* clone are cyclin E-positive (while 96% of *dcr-1* GSCs are CycE positive; Fig3e). (**b**) The average number of cells in *dcr-1* imaginal disc clones is approximately equal to the number of cells in the sister (WT aka *GFP*$^{+/+}$) clones. Data is shown for 21 individual imaginal disc clones (n=21). (**c**) Loss of *dcr-1*^{Q1147X} does not cause transient germline cysts to express CycE with the high frequency observed in *dcr-1* GSCs. (**d**) CycE is expressed in transient *dcr-1*^{Q1147X} germline cysts with a frequency similar to that observed for wild-type transient cysts.

Supplementary Figure 3 Legend

Analysis of Dacapo expression in GSCs. (a) Dap protein is detected with high frequency in *dcr-1*^{Q1147X} GSCs (no GFP, arrow). **(b)** CycE and Dap-5gm co-expressed in a wild type GSC. **(c)** In *dcr-1* GSCs CycE expression is more frequent than in wild type (85% and 40% respectively). However, Dap-5gm frequency is similar in wild type and *dcr-1* GSCs. **(d)** Over-expression of Dacapo lacking the 3'UTR partially phenocopies *dcr-1* (37%, n=85). Quantitations with these assays are shown in Fig4b-d.

Supplementary Figure 4 Legend

Computational prediction of miRNA binding sites in the *dap* 3' UTR. (a) The complete 3' UTR of *D. melanogaster dap* mRNA with the predicted microRNA target sites (shown in blue type) and their corresponding microRNAs. The miR-7 is additionally underlined since it partially overlaps with one of the miR-289 sites. **(b)** These specific sites were each predicted by at least two of four independent algorithms listed [26,27,28, Supplementary Ref3] to be targets of the indicated miRNAs. Each algorithm only scored a site as positive if it was also found in the 3'UTR sequence of the *D. pseudoobscura dap* gene. Thus the sites are conserved in dap between different *Drosophila* species. The position of the 5' nucleotide of each target site in the *dap* 3'UTR sequence is indicated.

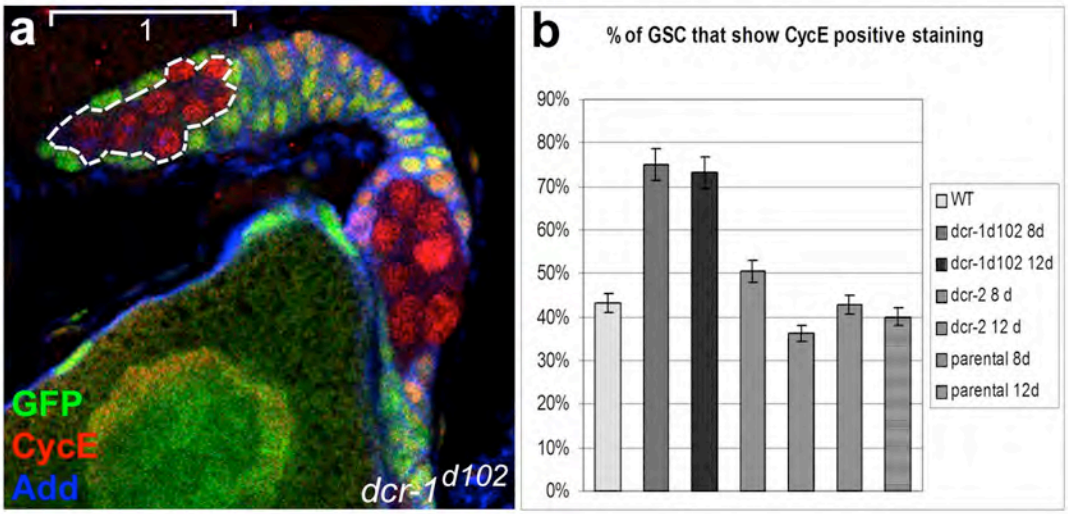

Supplementary Fig1 2005-03-03383

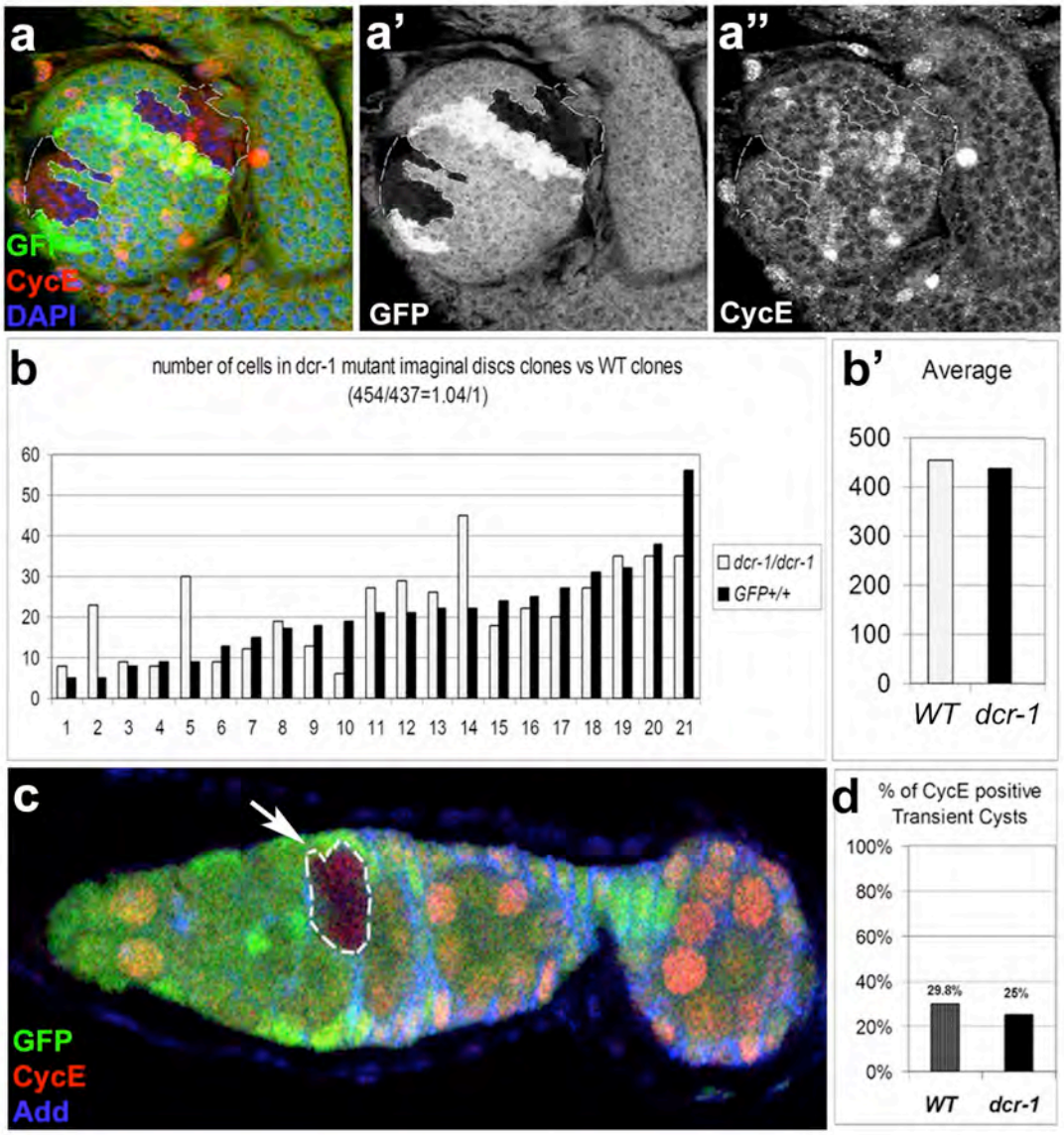

Supplementary Fig2 2005-03-03383

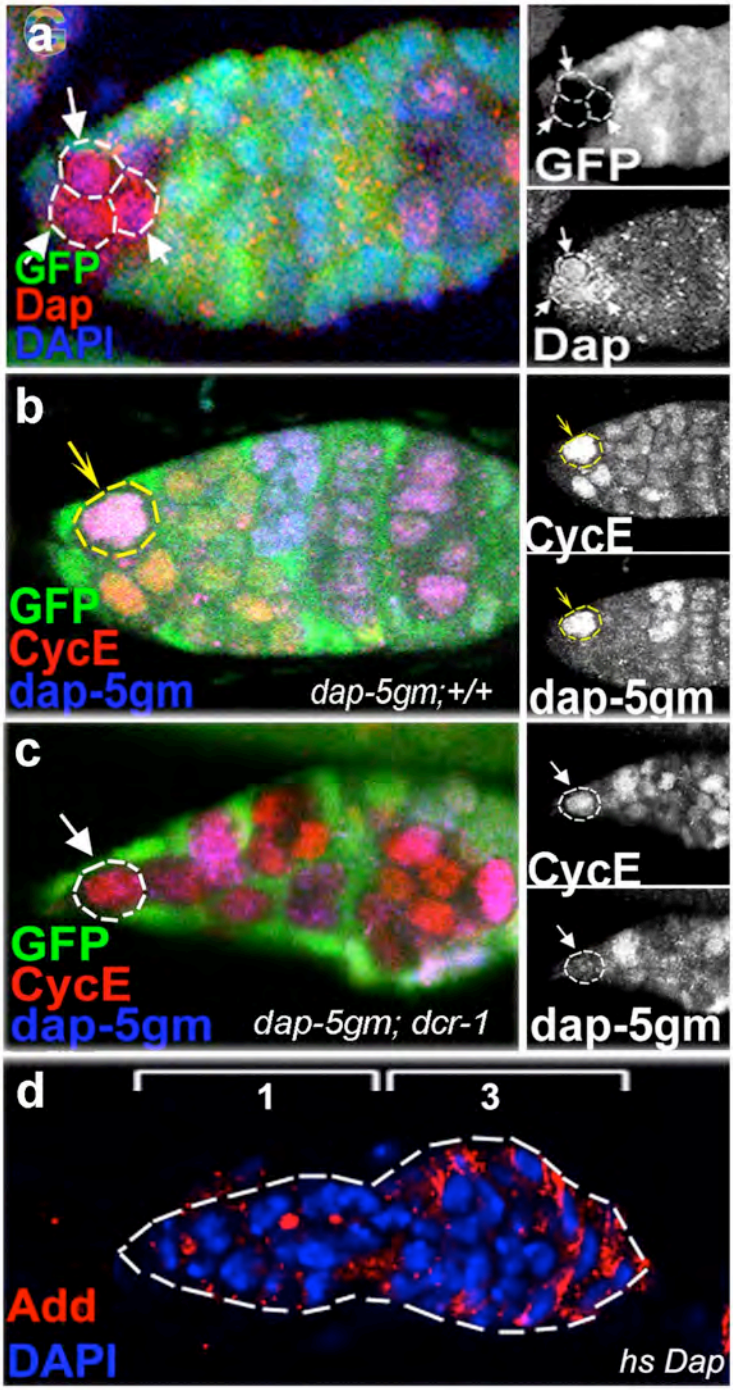

Supplementary Fig3 2005-03-03383

Cell Stem Cell
Article

Stage-Specific Differences in the Requirements for Germline Stem Cell Maintenance in the *Drosophila* Ovary

Halyna R. Shcherbata,[1] Ellen J. Ward,[1] Karin A. Fischer,[1] Jenn-Yah Yu,[1] Steven H. Reynolds,[1] Chun-Hong Chen,[2] Peizhang Xu,[2,3,4] Bruce A. Hay,[2] and Hannele Ruohola-Baker[1,*]
[1]Department of Biochemistry, Institute for Stem Cell and Regenerative Medicine, University of Washington, Seattle, WA 98195, USA
[2]Division of Biology, MC 156-29, California Institute of Technology, Pasadena, CA 91125, USA
[3]Howard Hughes Medical Institute
[4]Department of Physiology
University of California, San Francisco, San Francisco, CA 94158-0725, USA
*Correspondence: hannele@u.washington.edu
DOI 10.1016/j.stem.2007.11.007

SUMMARY

In this study, we uncover a role for microRNAs (miRNAs) in *Drosophila* germline stem cell (GSC) maintenance. Disruption of Dicer-1 function in GSCs during adult life results in GSC loss. Surprisingly, however, loss of Dicer-1 during development does not result in a GSC maintenance defect, although a defect is seen if both Dicer-1 and Dicer-2 function are disrupted. Loss of the *bantam* miRNA mimics the Dicer-1 maintenance defect when induced in adult GSCs, suggesting that *bantam* plays a key role in GSC self-renewal. Mad, a component of the TGF-β pathway, behaves similarly to Dicer-1: adult GSC maintenance requires Mad if it is lost during adult life, but not if it is lost during pupal development. Overall, these results show stage-specific differential sensitivity of GSC maintenance to certain perturbations and suggest that there may be a Dicer-2-dependent GSC maintenance mechanism during development that is lost in later life.

INTRODUCTION

The formation of embryonic tissues and the regeneration of adult tissues in the animal kingdom depend on stem cell populations. Embryonic stem cells are considered pluripotent due to their ability to differentiate into almost any cell type if placed in an appropriate context. Adult stem cells are undifferentiated cells that mainly reside in microenvironments known as niches, and they possess the ability to produce an undifferentiated stem cell and a daughter cell that can differentiate (Fuchs et al., 2004). Stem cell function has shown recently to be controlled by concerted actions of extrinsic signals from its respective regulatory niche and intrinsic factors, including hyper-dynamic plasticity of chromatin proteins (Li and Xie, 2005; Meshorer et al., 2006). However, not all stem cells remain in their niches continuously. For example, hematopoietic stem cells can relocate from their niche in adult animals (Li and Li, 2006). Yet, it is thought that many adult stem cells can only be fully functional in an appropriate niche. It is therefore important to understand how stem cell maintenance in the niche is regulated.

One of the most fundamental processes a developing animal needs to accomplish is to set aside and protect its precious stem cell population to replenish injured or lost tissues during adult life. At the moment, little is known about the processes involved in establishing stem cells during development, though communication between stem cells and their environment is suggested to be a key regulator of the homeostasis of the process (Gilboa and Lehmann, 2006; Ward et al., 2006). The *Drosophila* GSC niche has been extensively studied and has been an instructive model for understanding niche-stem cell communications. The GSC-niche interaction has shown to be reciprocal; stem cells communicate to niche through the Delta ligand, and the niche furthermore controls GSC maintenance via the TGF-β pathway (Chen and McKearin, 2003; Ward et al., 2006; Xie and Spradling, 1998).

Previous work has demonstrated that miRNAs, small (21–23 nt) RNA molecules that can regulate gene expression, are required for normal stem cell function in mouse, *Drosophila*, and plants (for reviews see Hatfield et al., 2007; Hatfield and Ruohola-Baker, 2007; Shcherbata et al., 2006). Detailed analysis in *Drosophila* GSCs using cell-cycle stage markers revealed that *dcr-1*-deficient GSCs were delayed in the p21/p27/Dacapo-dependent G_1/S transition concomitant with increased expression of CDK-inhibitor p21/27/Dacapo, suggesting that miRNAs are required for stem cells to bypass the normal G_1/S checkpoint. Hence, loss of the miRNA pathway might inactivate a mechanism that makes stem cells sensitive to environmental signals that normally control the cell cycle at the G_1/S transition (Hatfield et al., 2005; Shcherbata et al., 2006).

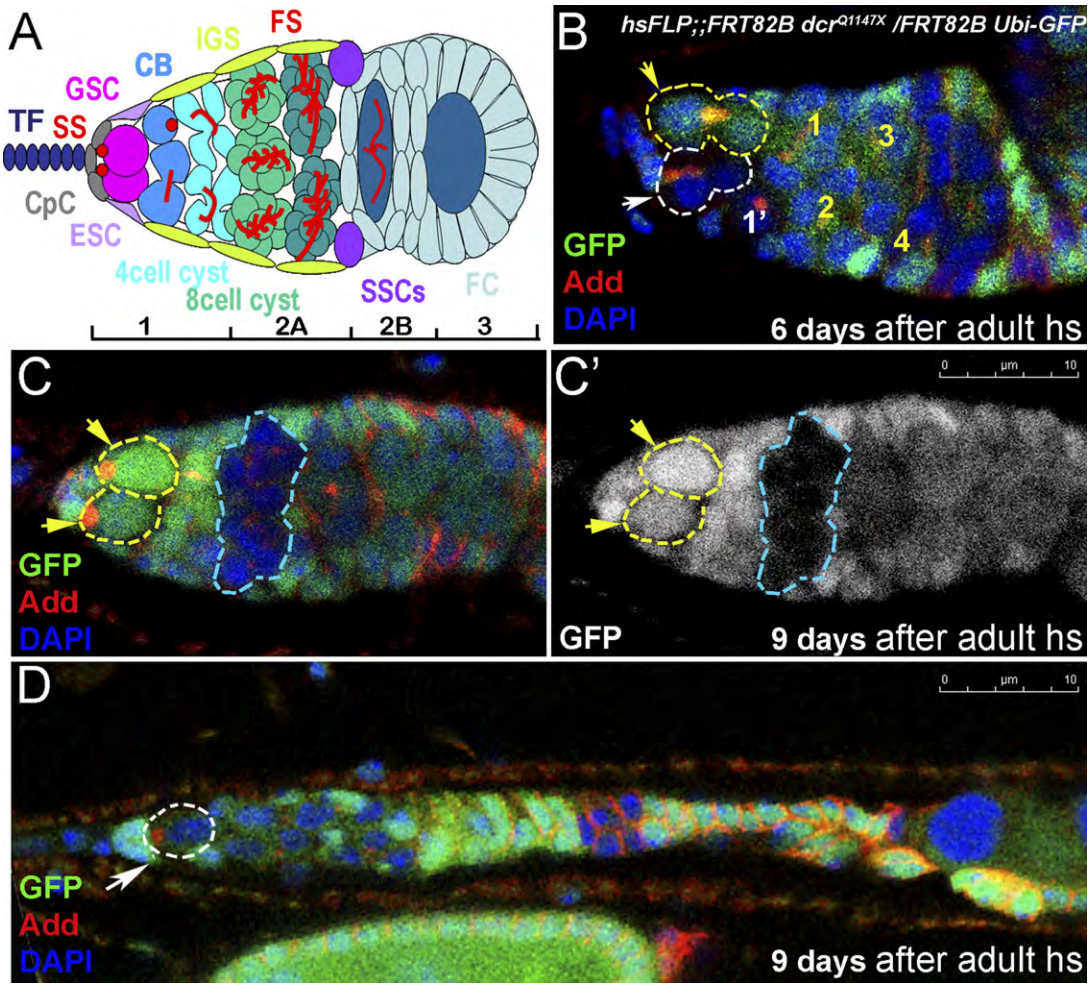

Figure 1. Adult-Induced *dicer-1* Mutant Germline Stem Cell Clones Are Lost from the Niche

(A) Diagram showing the germarium. Germline stem cells (GSC, pink) indicated by anterior spectrosomes (SS, red) are located at the anterior end of the germarium adjacent to the niche cap cells (CpC, gray). Terminal filament (TF; dark blue), escort stem cell (ESC, lavender), differentiated cystoblast (CB, blue), inner germarial sheath cell (IGS, lime), 4, 8, and 16 cell cysts (celadon, emerald, and green, respectively), marked by the presence of branched fusomes (FS, red), somatic stem cells (SSCs, violet), and follicle cells (FC, light blue) are as noted.

(B) Adult-induced *dicer-1*^{Q1147} mutant GSCs divide slower than control GSCs (the mutant produced one progeny, whereas the control produced four progeny) and leave the niche producing cysts that move posteriorly (C).

(D) GSC loss coupled with a reduction in germline stem cell division results in smaller germaria (a germarium shown with a single *dicer-1* mutant germline stem cell). Red, Adducin; blue, DAPI; and green, GFP. Mutant clones are outlined with white dashed lines, control clones with yellow.

Here, we show that, in addition to stem cell division, miRNAs are also required for stem cell maintenance. Furthermore, we identify *bantam* as a key miRNA required for germline stem cell maintenance in adults. Importantly, Dicer-1 activity is required for germline stem cell maintenance in adults, but surprisingly, its activity is dispensable for maintenance if lost during development. Interestingly, we find that Dicer-2 is required for this developmental resistance of GSCs to loss of Dicer-1 function; if both *dcr-1* and *dcr-2* are absent in preadult GSCs, the GSCs are not maintained. Similarly, we find that Mad activity is required for GSC maintenance if lost in the adult, but not if it is lost at a younger stage. Our data therefore suggest that *Drosophila* ovarian GSCs have differential and stage-specific requirements for maintenance during development and in adults and that at earlier stages Dcr-2-dependent adaptive mechanisms may exist that allow GSCs to withstand perturbations that are not tolerated in the adult.

RESULTS

miRNAs Are Required for Adult GSC Maintenance

To assess the requirement for miRNAs in stem cells during different stages of development, we generated germline stem cells (GSCs) that developed in normal conditions throughout larval and pupal stages but lacked Dicer-1 during adult stages. These *dicer-1* mutant germline stem cells (*hsFLP;; FRT82Bdcr-1*^{Q1147X}) generated during adult life showed a defect in germline stem cell division kinetics (Figure 1B and Table S4 and Figures S1A–S1C, available

online), similar to that shown previously for *dicer-1* GSCs generated during late larval/early pupal stages (Hatfield et al., 2005). To our surprise, these mutant GSCs showed an additional phenotype: a maintenance defect (Figure 1C and Figure S3A). Similar findings were described recently (Jin and Xie, 2007; Park et al., 2007). Adult-induced *dicer-1* mutant GSCs divide slowly and leave the niche. In many cases, a wild-type GSC replaces the departed mutant GSC (Figure 1C). In other cases when there are two mutant GSCs, both GSCs may leave the niche, resulting in an empty germarium (Figure S3B). On average, 12% of *dicer-1* mutant GSCs were lost per day, whereas only 2% were lost in the control group (Figure 6A and Figure S1D). This is in sharp contrast to *dicer-1* mutant preadult germline stem cells, which are not lost (Figure 6A; Hatfield et al., 2005).

bantam Is Required for Adult GSC Maintenance

Because Dicer-1 and, therefore, miRNA function are required for adult GSC maintenance, we analyzed which miRNA(s) is responsible for this phenotype. By using sensor constructs for *miR-8* and *bantam*, we found that these miRNAs are expressed in GSCs (Figure 2). Although the control sensor lacking miRNA binding sites shows uniform GFP expression, including the GSCs (Figure 2A), the GFP expression of *miR-8*- and *bantam-sensor* is highly reduced in the wild-type GSCs (Figures 2B and 2D) but is upregulated in *miR-8*$^{\Delta 1}$ and *dcr-1* mutant GSCs (Figures 2C and 2E). These data indicate that *miR-8* and *bantam* are expressed in adult GSCs.

Because *miR-8* and *bantam* are expressed in GSCs, we tested whether they are required for GSC maintenance. GSCs, mutant for *miR-8*, showed no obvious maintenance or cell division defects during preadult or adult stages (1.6 ± 0.5%, 1.3 ± 0.6% of *miR-8*$^{\Delta 1}$ mutant GSCs lost/day; Figures 3A and 3B and Table S1). However, adult-generated GSCs mutant for *bantam* showed maintenance and cell division defects (Figures 3C and 3D and Tables S1 and S4). On average, 14.1% ± 2.8% of *bantam* mutant GSCs (*hsFLP;;ban*$^{\Delta 1}$ *FRT80B/Ubi-GFP FRT80B*) were lost per day, whereas no loss was observed in the control group (*hsFLP;;FRT80B/arm lacZ FRT80B*; Table S1). When *bantam* clones were generated in preadult stages, the loss was not as dramatic (6.2% ± 0.4% per day; Table S1). However, given the existing evidence that all miRNA production in flies is strictly dependent on Dcr-1 function, it is surprising to note that the *bantam* larval/pupal clones appear to have a stronger phenotype than the *dcr-1* clones. This apparent difference in phenotypic severity may be attributable to differences in gene product perdurance and/or to the inherent variability in the GSC loss assay. Heteroallelic combinations of *bantam* mutants (*ban*^{L1170}/*ban*^{EP3622}, *ban*^{L1170}/*ban*$^{\Delta 1}$, and *ban*^{EP3622}/*ban*$^{\Delta 1}$) exhibit similar mutant phenotypes as the *ban*$^{\Delta 1}$ clones (but at a lower frequency), suggesting that the defects are due to the loss of *bantam* function and not due to second site mutations (Figures 3E–3G and Figures S4B–S4E). These data show that *bantam* and *dicer-1* mutant defects in GSC maintenance are similar and therefore suggest that *bantam* is a key miRNA in assuring the maintenance of adult GSCs.

Mad-Mutant GSCs Are Maintained if the Mutation Is Induced during Development

The results described above present an unexpected scenario in which a mutation causes a maintenance defect when the deficiency is introduced during adult stages, but not if it is introduced during late larval/pupal stages. To address the generality of the phenomenon, we tested whether a well-studied component of the GSC maintenance pathway, the transcription factor Mad, fits this paradigm. Similar to *dicer-1*, *Mad* was not essential for GSC maintenance if the defect was induced during late larval/early pupal stages (Figures 4A, 4B, and 6A) but was essential if the *Mad* mutation was introduced in GSCs during adulthood (Figures 4D and 6A; Xie and Spradling, 1998). In addition, as shown before (Xie and Spradling, 1998), these adult-induced *Mad*-mutant GSCs were defective not only in maintenance but also in normal cell-cycle kinetics (Figures 4C and 6B and Table S4). These data show a similarity between *Mad* and *dicer-1* mutants: both maintain the adult GSCs if the mutation is introduced during pupal development. However, if the mutations are introduced during adult life, Mad and Dicer-1 are essential for normal GSC maintenance.

TGF-β signaling within the GSC niche blocks germline stem cell differentiation by silencing *Bam*. In the absence of Mad, *Bam* is derepressed and the GSC differentiates (Chen and McKearin, 2003; Song et al., 2004; Xie and Spradling, 1998). Because GSCs lacking the transcription factor Mad, a key component of the TGF-β pathway, from late larval/pupal developmental stages onward were maintained in the niche, we decided to test whether the differentiation factor *Bam* was still repressed. Interestingly, we found *Bam* being repressed in this case (Figure 4F; n = 36 *Mad*^{12} GSCs and n = 42 *WT* GSCs). These data suggest that larval/pupal-induced *Mad*^{12}-mutant GSCs silence *Bam* by a mechanism other than transcriptional repression by Mad.

Period of Competence of Preadult Stem Cells Extends through Pupal Development and Ends at Adulthood

Our data suggest that the miRNA pathway and Mad activity are dispensable when they are lost in young GSCs, but they are essential when they are lost in older GSCs. To identify the latest stage of development at which GSCs are able to overcome the loss of Mad activity for GSC maintenance, we introduced *Mad*^{12} mutations in GSCs of 3rd instar larva/early pupae, late pupae, and 1- to 4-day-old adult flies (Figure 4E). Interestingly, *Mad*^{12} GSCs were lost only after adult clonal induction, suggesting that the period of competence of preadult GSC maintenance extends through late pupal stages, but not into adulthood. Previous studies have shown that GSCs already reside in a niche at the late pupal stage (Zhu and Xie, 2003), suggesting that this resilience is not a result of major differences in the morphological environment of GSCs during development and adulthood.

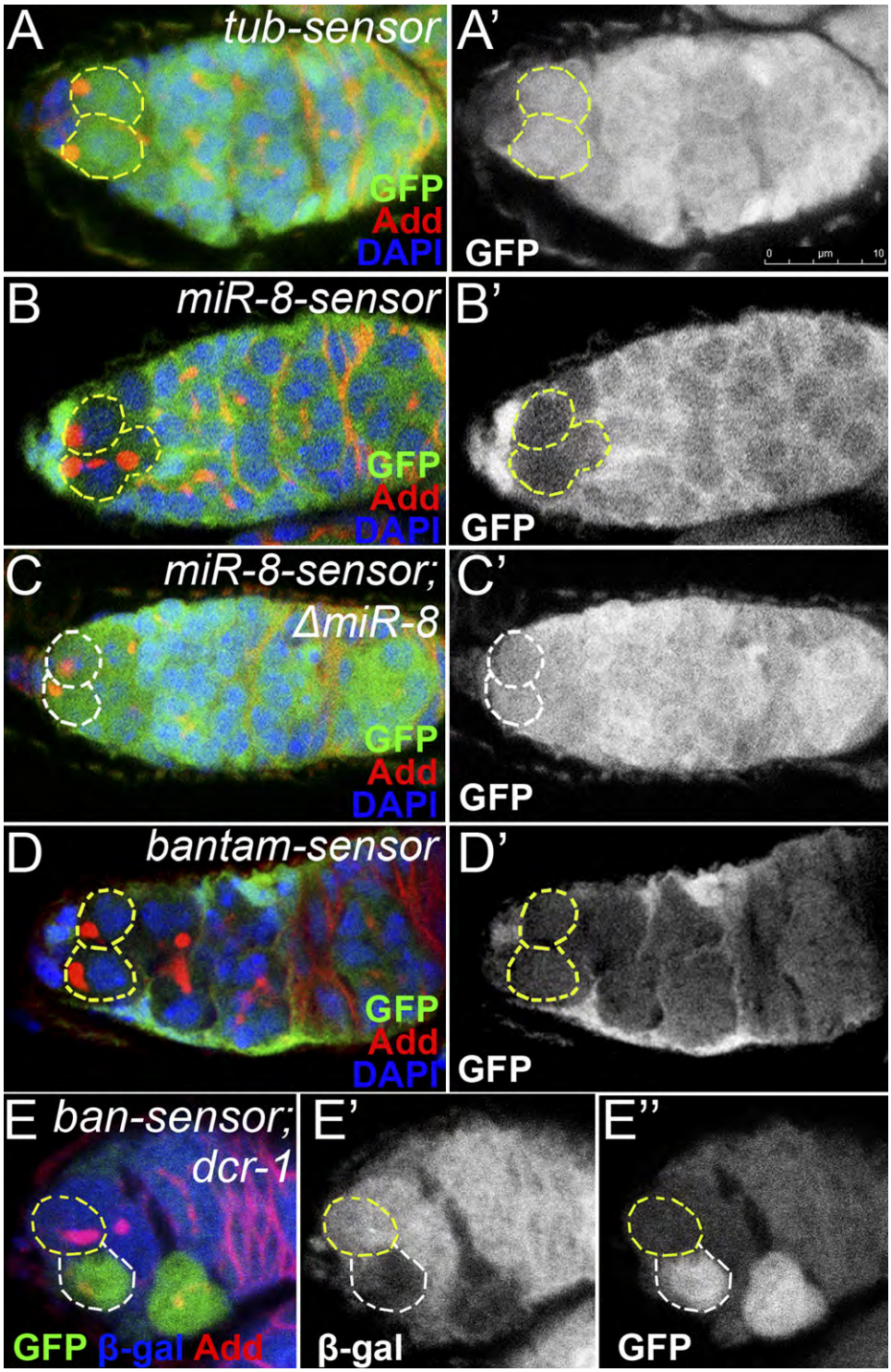

Figure 2. miRNA-GFP Sensors Are Expressed in Distinct Subsets of Cells in the Germarium

miRNA sensor expression patterns in (A, B, and D) wild-type, (C) *miR-8*$^{\Delta 1}$, and (E) *dcr-1* mutant germaria. Sensor expression patterns determined by staining homozygous lines with anti-GFP antibodies (A–D). High GFP levels are observed in control (A), but not in *miR-8*- (B) or *bantam-sensor* GSCs (D), suggesting that *miR-8* and *bantam* are expressed in GSCs. (C) Consistent with this, *miR-8-sensor* GFP levels increase substantially in homozygous *miR-8*$^{\Delta 1}$ mutant germaria. (E) *bantam-sensor* is responsive to Dicer; in *dcr-1* clones, marked by the absence of β-gal (E'), the level of GFP fluorescence is higher than that in a nonclonal neighbor (E''). In (E), native GFP expression by one copy of *bantam-sensor* is analyzed (*hs Flp; ban*$^{\alpha tub84BT:Avic/GFP\text{-}EGFP}$*/+; FRT82B dcr-1*^{Q1147X}*/FRT82B arm*-lacZ). Red, Adducin; blue, DAPI (A–D) or β-gal (E); green, GFP. GSCs are marked with dashed lines (white indicates mutant, yellow wild-type or control).

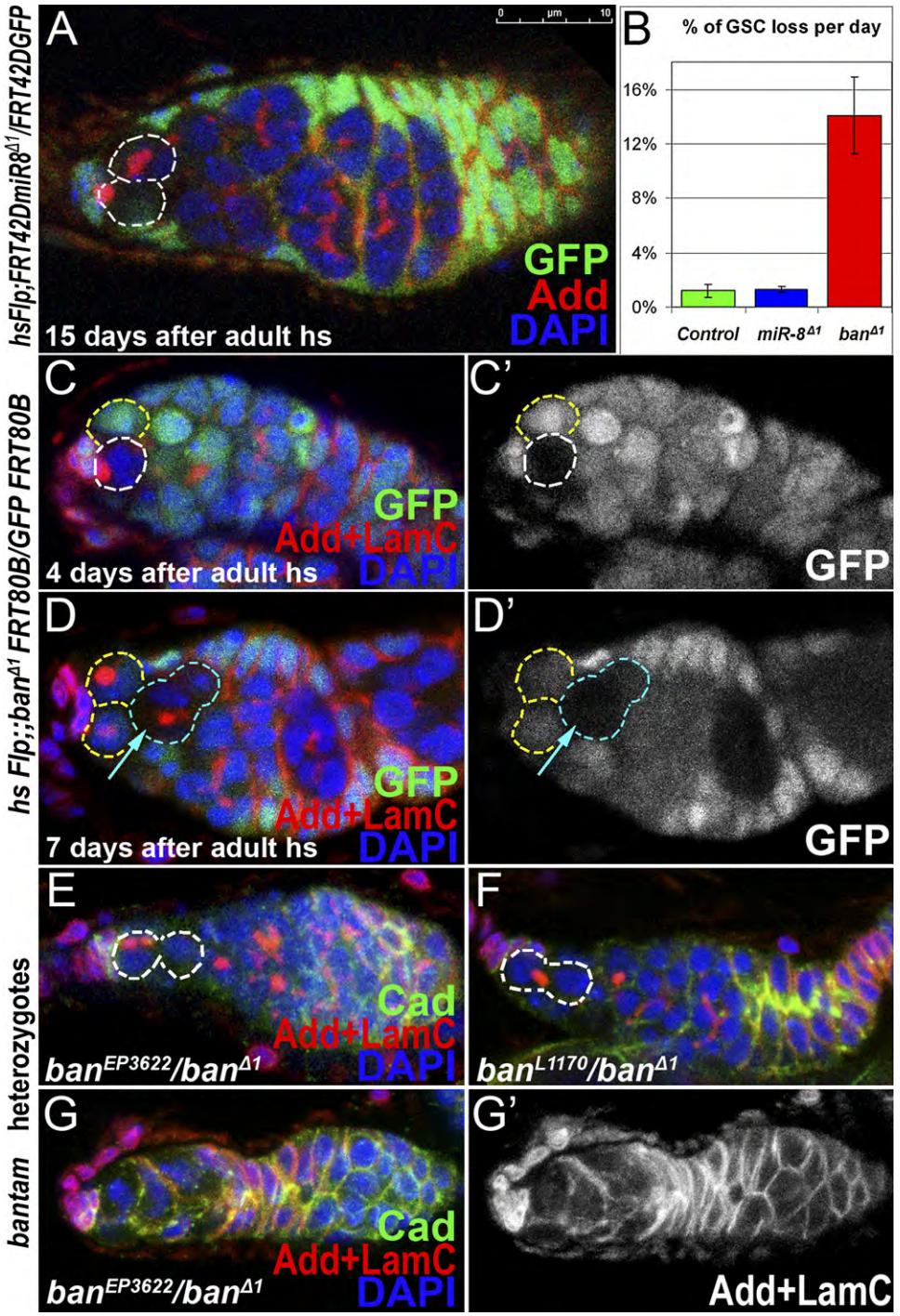

Figure 3. *bantam* miRNA Is Required for GSC Maintenance in the Niche

(A) *miR-8*$^{\Delta 1}$-mutant germline stem cells are maintained in the niche and divide properly 15 days after adult heat shock.

(B) Graph showing that the *bantam* mutant GSCs are lost 11 times faster from the niche compared to *miR-8* or control GSCs.

(C and D) *bantam*-mutant GSC clones ([C], 4 days after clonal induction) are not maintained in the niche ([D], 7 days after clonal induction).

(E–G) Germaria from *bantam* hetereoallelic mutants *ban*^{EP3622}/*ban*$^{\Delta 1}$ (E and G) and *ban*^{L1170}/*ban*$^{\Delta}$ (F) exhibit mutant phenotypes similar to *bantam* clones: germaria are reduced in size and have a single GSC (E and F) or no GSC (G).

Red, Adducin (A) or Adducin+LaminC (C–G); blue, DAPI; and green, GFP (A–D) or Cadherin (E–G); mutant GSCs or cysts are outlined with dashed lines, departed or differentiated stem cells with turquoise dashes (white indicates mutants, yellow controls).

Preadult Mad and Dicer-1 Interact in GSC Maintenance

Because both Mad and Dicer-1 are required during adult stages but are not required if the components are lost during preadult stages, we tested whether they interact during earlier development to maintain germline stem cells in the niche. Specifically, we reduced the level of Mad in a *dicer-1* clonal background or reduced the level of Dicer-1 in a *Mad* clonal background (*hsFLP; Mad*^{12} *FRT40A/+; FRT82B dcr-1*^{Q1147X}*/FRT82B GFP* and *hsFLP; Mad*^{12} *FRT40A/ GFP FRT40A; FRT82B dcr-1*^{Q1147X}*/+*). In both cases, the clones were induced during late larval/early pupal stages. Interestingly, when both Mad and Dicer-1 activities were reduced at the same time, a clear maintenance defect was observed after preadult clone induction (Figure 6A). These data show that Dicer-1 and Mad interact genetically during developmental stages (a synthetic GSC maintenance defect).

Preadult Germline Stem Cells Lacking Both Dicer-1 and Dicer-2 Activities Are Lost from the Niche

To investigate whether another short RNA producing enzyme contributes to GSC maintenance, we tested the role of small interfering RNAs (siRNAs) in preadult germline stem cells, we tested *dcr-2; dcr-1* double mutants and observed a strong maintenance defect when the double mutants were induced during larval/pupal development (Figures 5 and 6A). However, the Dicer-2 pathway alone is not required for larval/pupal or adult germline stem cell maintenance (Figure 6A and Table S3). These data indicate that *dicer-1* and *dicer-2* interact genetically in some manner to maintain preadult germline stem cells. The Dicer-2 contribution to the *dicer-2; dicer-1* germline stem cell maintenance phenotype is not likely to be due to defective miRNA processing, as previous biochemical studies showed that Dicer-2 does not appear to process miRNAs (Lee et al., 2004; Pham et al., 2004). Furthermore, we did not observe any reduction of mature *bantam* levels by QPCR analysis in *dcr-2* homozygous animals compared to the control animals, suggesting that Dicer-2 does not have a major role in *bantam* processing (data not shown). Interestingly Dicer-2 is known to act through the RNAi pathway to modify chromatin (Grimaud et al., 2006; Lee et al., 2004; Pal-Bhadra et al., 2002, 2004; Peng and Karpen, 2007; Verdel et al., 2004), raising the possibility that chromatin modification contributes to the robust maintenance behavior of preadult germline stem cells.

Notch Pathway Does Not Require Mad Activity during Development

In contrast to our observations with *Mad* and *dicer-1* clones, GSC maintenance requires Notch signaling from the GSCs to the niche throughout development. In the absence of Neuralized (required for proper processing of Delta or Serrate ligands), GSCs are not maintained in the niche. This Notch signaling requirement is observed in both late larval/early pupal and adult clones (Ward et al., 2006). Furthermore, an increase in Notch ligand production in the germline results in an enlarged niche, which in turn supports additional GSCs. This niche expansion can be induced after pupal development (Ward et al., 2006).

In order to determine whether Notch pathway function in GSC maintenance is Mad dependent during larval/pupal development, we analyzed whether the additional GSCs produced by increased Notch signaling during developmental stages require Mad signaling for their maintenance. We assayed whether ectopic GSCs induced by overexpression of Delta were maintained in the niche if they were also mutant for *Mad*. Our clonal analysis shows that the ectopic GSCs produced during development do not require Mad for their maintenance in the niche. Similar to the *Mad*-mutant GSCs described above, we find that the *Mad, pUASP-Delta*-mutant GSCs are not lost from the niche after larval/pupal clonal induction (*hsFLP; Mad*^{12} *FRT40A/Ubi-GFP FRT40A; pUASP-Delta/nano-sGAL4*, Figure 6A, 0.2% ± 1.8% loss/day); the number of germaria containing mutant GSCs remains the same in the two time points analyzed. However, unlike the *Mad*-mutant GSCs described above, in the Delta overexpression background, the number of *Mad* GSCs increases (approximately two mutant GSCs to approximately three mutant GSCs/7 days; Figures 6C and 6D), indicating that the *Mad*-mutant GSCs can divide and are recruited to and maintained in the enlarged niche. Thus, the extra GSCs produced by increased Notch signaling behave similarly to normal GSCs: they do not require Mad activity for maintenance in the niche if the *Mad* mutation is introduced during preadult stages. Therefore, ectopic GSCs as well as wild-type stem cells have a period of competence during preadult stages that ensures their maintenance within the niche even in the absence of Mad.

DISCUSSION

We draw two important conclusions from this work. First, Dicer-1 and, more specifically, *bantam* miRNA are required for adult stem cell maintenance (Figure 7A). Second, preadult stem cells have a youthful resilience that is lost at adulthood. Thus, if certain key components required for adult germline stem cell maintenance in developing animals are lost, the animal can overcome this loss and maintain the stem cells throughout life (Figure 7B).

bantam Function in GSCs

The miRNA *bantam* has been previously found to promote tissue growth in *Drosophila* imaginal discs (Brennecke et al., 2003). In addition, removing one copy of the endogenous *bantam* gene has shown to enhance, and overexpression of *bantam* suppress, the severity of Hid overexpression-induced apoptosis in the eye (Brennecke et al., 2003). Based on these results, a hypothesis was put forward that *bantam* simultaneously stimulates cell proliferation and inhibits apoptosis. Furthermore, recent studies have revealed that *bantam* overexpression mitigates degeneration induced by the pathogenic polyglytamine protein Ataxin-3, which is mutated in the human polyglutamine disease spinocerebellar ataxia type 3 (SCA3)

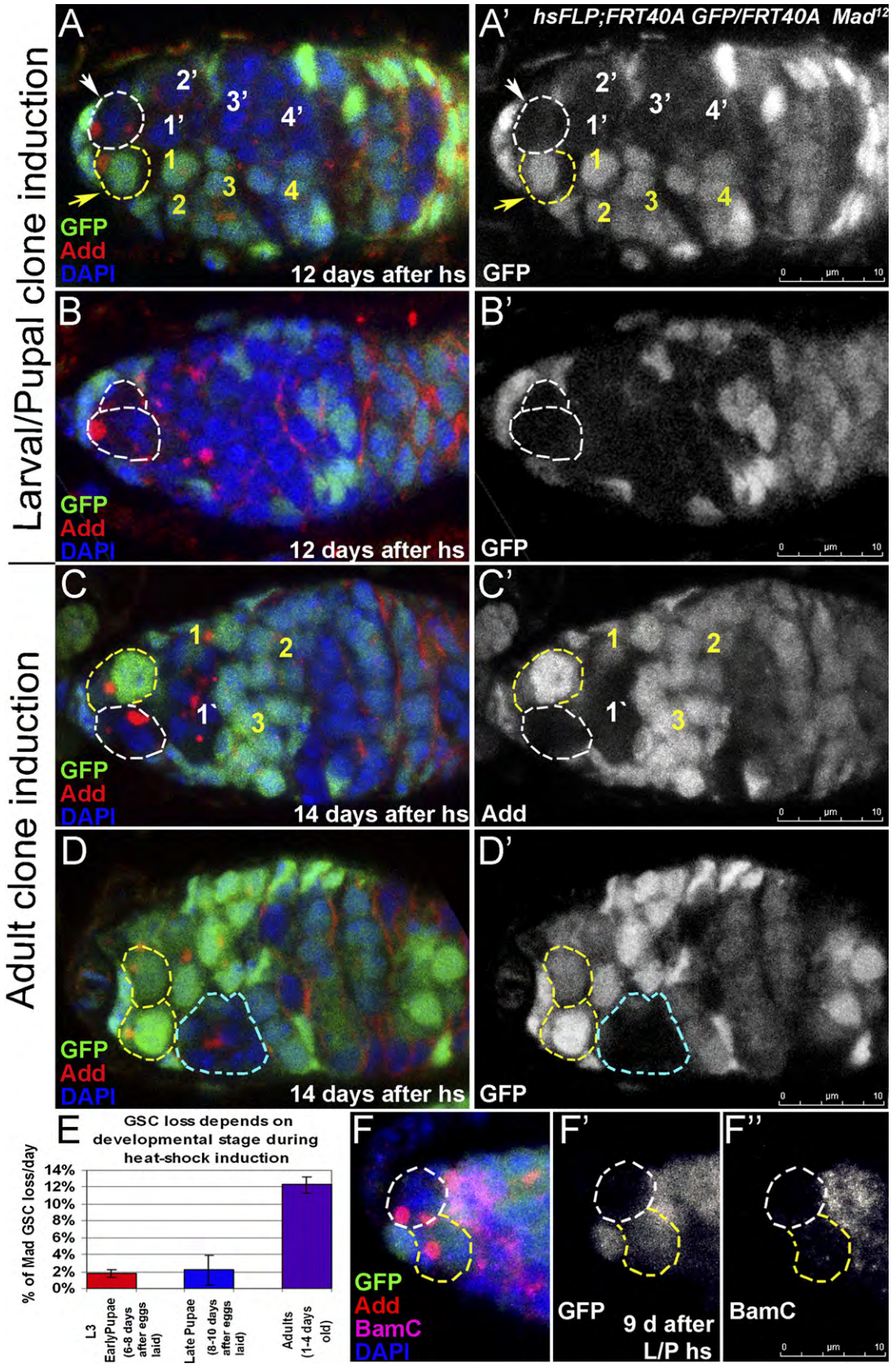
Larval/Pupal clone induction
Adult clone induction
A
A'
hsFLP;FRT40A GFP/FRT40A Mad12
2'
3'
4'
1'
1
2
3
4
GFP
Add
DAPI
12 days after hs
GFP
B
B'
12 days after hs
GFP
C
C'
1
2
1`
3
14 days after hs
Add
D
D'
14 days after hs
GFP
E
GSC loss depends on developmental stage during heat-shock induction
% of Mad GSC loss/day
14%
12%
10%
8%
6%
4%
2%
0%
L3 EarlyPupae (6-8 days after eggs laid)
Late Pupae (8-10 days after eggs laid)
Adults (1-4 days old)
F
F'
F''
GFP
Add
BamC
DAPI
GFP
9 d after L/P hs
BamC
0 µm 10

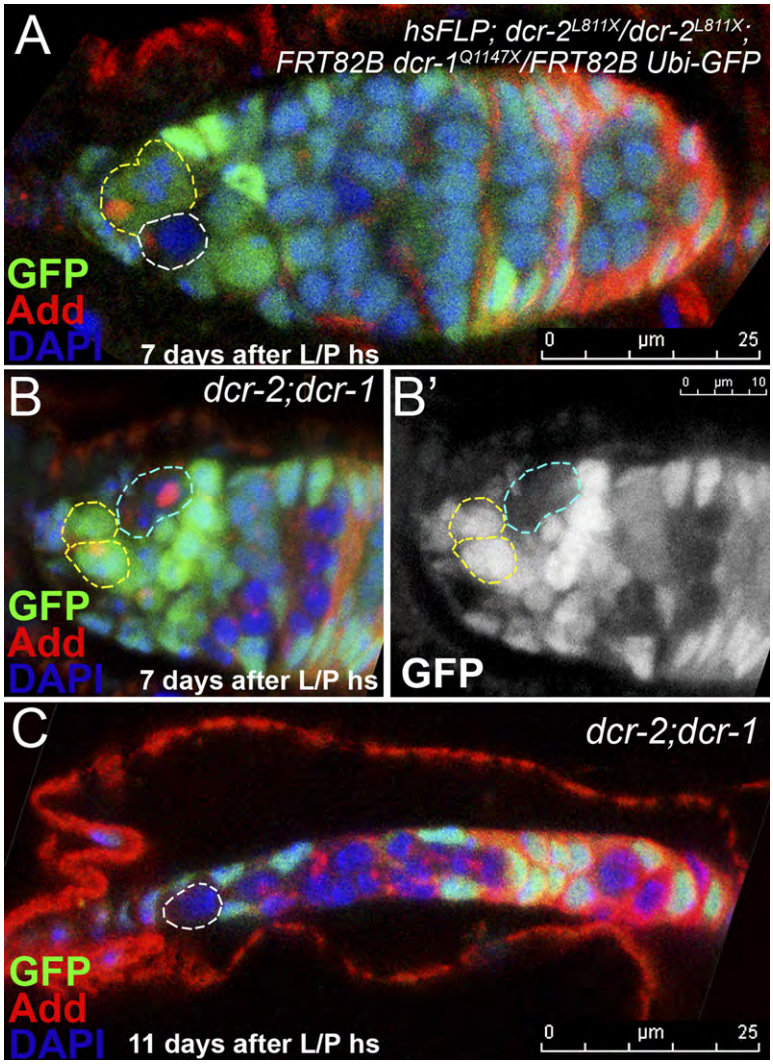

Figure 5. GSCs Lacking Dicer-1 Activity and Dicer-2 Activity from Pupal Stages onward Are Lost from the Niche

(A–C) Larval-induced *dicer-1* mutant GSCs in a *dicer-2*-mutant background (*hsFLP; dcr-2^{L811X}/dcr-2^{L811X}; FRT82B dcr-1^{Q1147X}/FRT82B Ubi-GFP*) do not divide normally and are readily lost from the niche (B). Recall, that when Dicer-2 activity is present, larval-induced *dicer-1* mutant GSCs are not lost from the niche. (C) Example of a severely reduced germarium with a single mutant GSC. GSCs are outlined with dashes: yellow, normal; white, mutant. GSCs departed from the niche are outlined with turquoise dashes. Red, Adducin; green, GFP; and blue, DAPI.

(Bilen et al., 2006). These studies suggest that *bantam* miRNA can also suppress neuronal degeneration. The Hippo-tumor-suppressor pathway has emerged as a key regulator for *bantam* expression in *Drosophila* imaginal discs in regulating cell division (Nolo et al., 2006; Thompson and Cohen, 2006).

The present work supports a different view of *bantam* action in *Drosophila* GSCs, adding new possibilities to the repertoire of *bantam*'s functions. In the adult stem cell population, *bantam* miRNA is essential for the stem cell maintenance in the niche (Figures 2 and 3 and Figure S4) and appears to be acting independently of the Hippo pathway as *yorkie* mutant GSCs are maintained in the niche (Table S1). Many questions remain about this new function of *bantam*. What biological process is defective in *bantam*-mutant GSCs that results in their loss from the niche? What are the targets of *bantam*, and what are the pathways that regulate *bantam* expression in GSCs? In theory, the biological process and the targets of *bantam* in GSCs might be the same as those involved with imaginal disc cell-cycle control. However, cell-cycle defects alone cannot account for the GSC loss as *dicer-1*-mutant GSCs that are generated during preadult stages show adult GSC division defects but are maintained normally

Figure 4. Larval/Pupal-Induced *Mad^{12}* Mutant GSCs Are Maintained in the Niche

Larval/pupal-induced *Mad^{12}* mutant GSCs divide at the same frequency as control GSCs ([A]; Table S4) and are maintained in the niche 12 days after clonal induction ([B]; Table S1). However, as described before (Xie and Spradling, 1998), *Mad^{12}*-mutant GSC clones induced during adulthood divide slower than nonclonal germline stem cells ([C]; Table S4) and are not maintained in the niche ([D]; 14 days after adult clonal induction, the *Mad*-mutant GSC has left the niche and become an 8 cell cyst). The bar graph shows that GSC maintenance has a development-dependent character: when *Mad^{12}* mutation was induced during late larval/early pupal or even late pupal developmental stages, mutant GSCs were maintained; however, a clear GSC loss was observed for adulthood-induced *Mad^{12}* GSCs (E). A differentiation factor, Bam, is not derepressed in mutant GSCs, showing that larval/pupal-induced *Mad^{12}*-mutant GSCs maintain their SC identity. Red, Adducin; blue, DAPI; green, GFP; and purple, BamC; mutant GSCs are outlined with white dashed lines, control GSCs with yellow dashes.

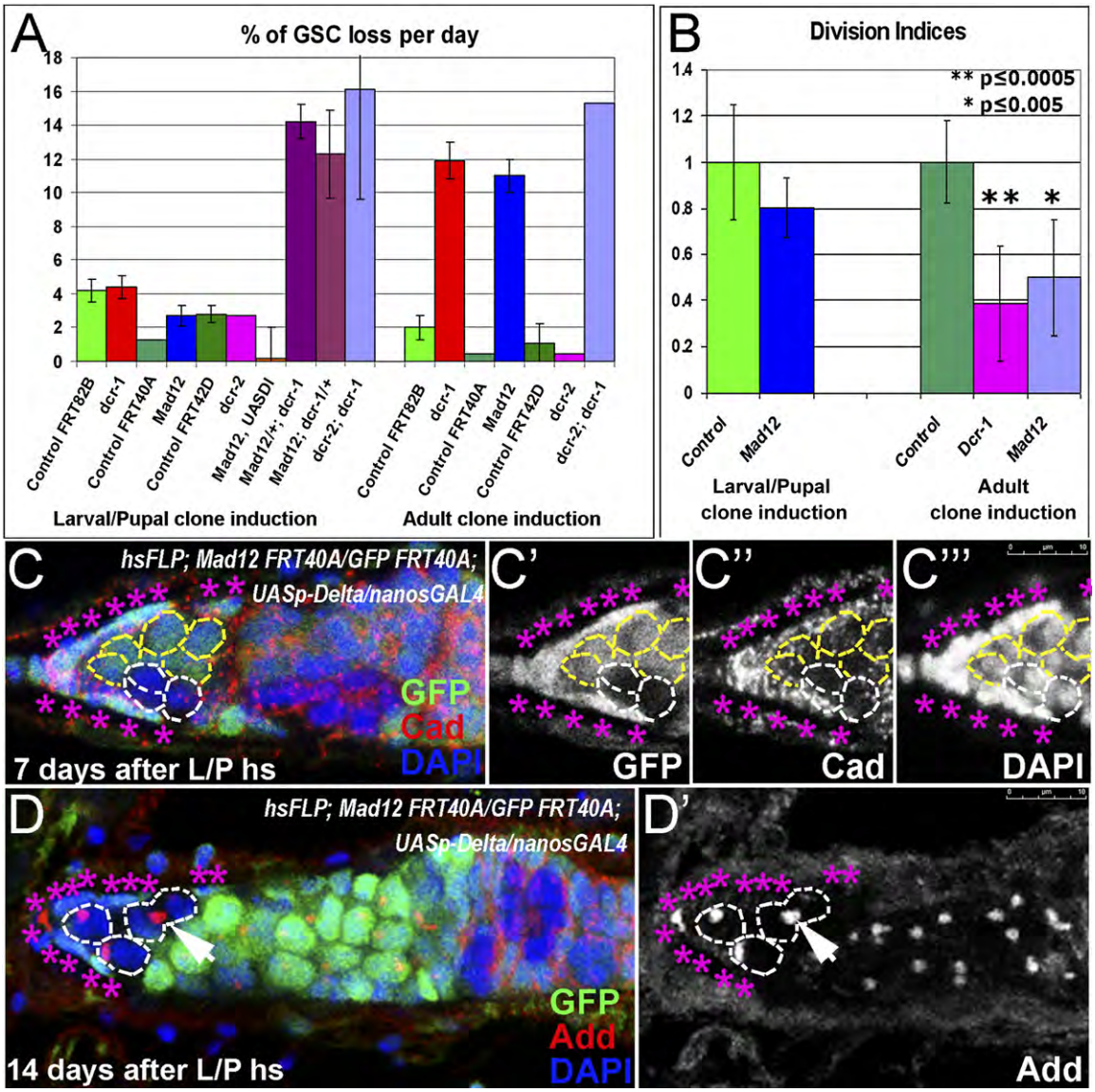

Figure 6. GSC Maintenance Is Governed by a Robust Redundant Mechanism during Development

(A) The percentage of GSC loss per day is similar to controls when either *dicer-1* or *Mad* is removed from GSCs during larval/pupal stages. In contrast, the GSCs are lost rapidly when either *dicer-1* or *Mad* is removed from the GSCs during adulthood. In addition, a synthetic maintenance defect is observed when both Dicer-1 and Mad levels are reduced simultaneously during larval/pupal stages (Mad^{12}/+; *dcr-1* or Mad^{12}; *dcr-1*/+). Error bars represent standard error of the mean.

(B) GSCs lacking Mad activity from larval/pupal stages onward divide relatively normally compared to controls, whereas GSCs lacking either Dicer-1 or Mad activity during adulthood divide significantly slower that controls. The bar graph shows the division indices at 14 days after larval/early pupal heat shock and 9 days after adult heat shock (see Table S4). Error bars represent average deviation.

(C and D) Mad^{12}-mutant GSCs in germaria overexpressing *UASp-Delta* in the germline (*hsFLP;* Mad^{12} *FRT40A/Ubi-GFP FRT40A; UASp-Delta/nanosGAL4*) are maintained in the enlarged niche. Furthermore, the number of *Mad*-mutant GSCs in the niche is increased from the 7 to 14 day time point after larval/pupal clonal induction ([C] and [D], respectively; a dividing *Mad* mutant GSC is marked with an arrow. *Mad*-mutant GSCs are outlined with white dashed lines, cap cells identified with pink asterisks. Red, Cadherin (C) or Adducin (D); blue, DAPI; and green, GFP.

in the niche (Hatfield et al., 2005; Figure 6A). Interestingly, the 3′UTR of *Mad* is a validated target of *bantam* miRNA in S2 cells (Robins et al., 2005). It is therefore possible that *bantam* miRNA may directly regulate *Mad* in GSCs. However, in this scenario, loss of *bantam* should result in *Mad* overexpression, yet the *bantam* mutant phenocopies *Mad* loss-of-function phenotypes. One potential explanation is that high levels of Mad are just as deleterious to germline stem cells as the lack of Mad activity. If this is the case, then Mad levels would need to be finely tuned by miRNAs in germline stem cells to ensure their maintenance in the niche. Similar fine-tuned regulation of Atrophin by *miR-8*

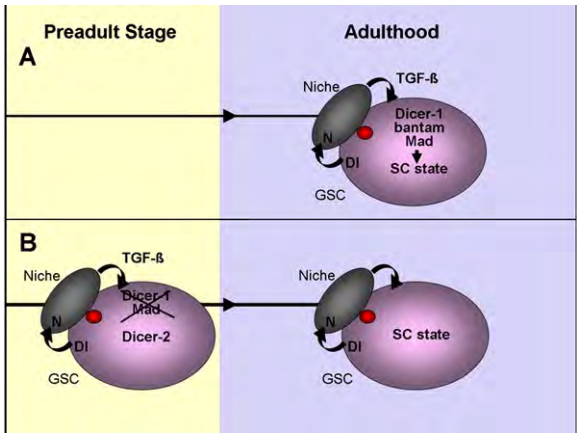

Figure 7. Model Showing Different Mechanisms for GSC Maintenance during Development and Adulthood

(A) TGF-β and Dicer-1 are required for GSC maintenance in adult *Drosophila* ovaries. We have identified *bantam* as the key miRNA in this process. *bantam* has previously been studied in cell cycle and cell death in *Drosophila* imaginal disc epithelial cells. However, in GSCs, the *bantam* target process that leads to GSC maintenance in the niche remains to be revealed.

(B) Surprisingly, we find that Mad and Dicer-1 are not required for GSC maintenance if these components are lost in GSCs during larval/pupal development. Preadult GSCs lacking Dicer-1 are no longer maintained if they also lack Dicer-2. We propose that the Dicer-2 pathway prevents GSC loss, possibly by chromatin remodeling during developmental stages, which as a consequence promotes stem cell fate during adulthood.

was recently reported (Karres et al., 2007). Further studies are required to test this hypothesis.

Robust Maintenance of Preadult GSCs

The presented work reveals the resilience of preadult stem cells to perturbations that cause GSC maintenance defects if introduced in adults. It seems logical that developing organisms would have a means of protecting their precious stem cells during the many intricate developmental processes that occur. We have shown that stem cells are still protected late in preadult development (during pupation), but not during adulthood. What protects the germline stem cells prior to adulthood in *Drosophila*? As the niche has already formed by pupal stage, we suggest that the period of competency does not reflect a morphological difference in the niche at different time points. Instead, however, we found that the preadult competence requires Dcr-2. Dcr-2 activity is shown to be required for the siRNA pathway. As RNA interference (RNAi) pathway-dependent chromatin modifications have been previously observed in *Drosophila* (Grimaud et al., 2006; Lee et al., 2004; Pal-Bhadra et al., 2002, 2004; Peng and Karpen, 2007; Verdel et al., 2004), one possibility is that Dcr-2 acts through stem cell chromatin remodeling in preadult GSCs. Further work will help to unravel the role of Dcr-2 in this process.

Overall, our study shows that in *Drosophila* young germline stem cells are better able to withstand perturbations that disrupt their maintenance than adult germline stem cells. Further analysis of these findings might ultimately lead to insights into cancer stem cell resilience and even help to reveal ways to rejuvenate failing and/or aging stem cells.

EXPERIMENTAL PROCEDURES

Fly Strains

We used the following mutant stocks: *eyFLP;;FRT82B dcr-1*^{Q1147X}*/TM3Sb*, *eyFLP;;FRT82B*, *eyFLP; FRT42D dcr-2*^{L811X}*/CyO* (Lee et al., 2004), *Mad*^{12} *FRT40A/CyO* (Xie and Spradling, 1998), *FRT42D yki*^{B5} (Huang et al., 2005), *FRT42B iswi*^{2} (a gift from J. Tamkun), *pUASP Delta* (Jordan et al., 2006), *w*$^{-}$*;;Df(3L)ban*$^{\Delta 1}$ *FRT80B/TM6*, *ban*^{L1170}, *ban*^{EP3622}, *w*$^{-}$*;ban*$^{Scer\UAS.T:Avic\GFP-EGFP}$ (*pUAST-bantam* [Brennecke et al., 2003]), *ban*$^{\alpha tub84BT:Avic/GFP-EGFP}$ (*bantam-sensor* [Brennecke et al., 2003]), *hsFLP;;FRT82B Ubi-GFP/TM3Sb*, *hsFLP; Ubi-GFP FRT40A/CyO*, *yw hsFLP;FRT42D Ubi-GFP/CyO*, *hsFLP;;Ubi-GFP FRT80B/TM3*, and *w;NGT40/SM6a;nanosGal4/TM3Sb* (Bloomington Stock Center). The *miR-8*$^{\Delta 1}$ deletion line was generated by imprecise *P* element excision of *EP(2)2269*. *EP(2)2269* flies were isogenized with *w*^{1118} and balanced. Standard *P* element imprecise excision was carried out, and 300 individual excision stocks were screened by primers 5′-ATCACACGTTAACGTAACGTAACGGCAG-3′ and 5′-AGATTCG AAAGCCCCACACGCACAATC-3′. The *miR-8*$^{\Delta 1}$ deletion removes 1316 bp of genomic DNA, including the 23 bp mature *miR-8* miRNA. The deletion spans from 1057 bp upstream of the mature *miR-8* sequence to 236 bp downstream of the mature sequence. The *miR-8*$^{\Delta 1}$ deletion was recombined onto the *FRT42D* chromosome by using standard meiotic recombination protocols (Xu and Rubin, 1993). The recombined *FRT42D miR-8*$^{\Delta 1}$ lines were screened by PCR with primers 5′-AAATCTTCACCGTCACCCAGTCGT-3′ and 5′-AGAAACC AGCAGAAAGCAGCATCC-3′.

Generation of *pUASP-bantam*, *pUASP-miR-8*, and *miR-8-sensor*

pUASP-bantam: A partial *bantam* precursor sequence (584 nt) was amplified from *pUAST-EGFP-bantam* construct (Brennecke et al., 2003) by using the following primers: *bantam* forward, 5′-ATAGCG GCCGCGTTAACTGGCAGCATATAATTTC-3′; *bantam* reverse, 5′-ATT CTAGATTATAGGCAGATTTAACATGTGG-3′. The amplified fragments were cloned into UASP plasmid using Not1 and Xba1.

pUASP-miR-8: A partial *miR-8* precursor sequence (729 nt) was amplified from adult fly genomic DNA with the following primers: *miR-8* forward, 5′-ATAGCGGCCGCCGCGGTCACACGCACATTTCAATA-3′; *miR-8* reverse, 5′-ATTCTAGAAATGGGAATTGGGAACGATCTCGC-3′. The amplified fragments were cloned into UASP plasmid with Not1 and Xba1.

miR-8-sensor: Two perfect complementary target sequences of *miR-8* separated by 16 nt were inserted downstream of *tub-GFP* plasmid into the 3′UTR of the *P* element in CaSpeR4 with Not1 and Xba1. The following oligonucleotides containing the target sequences of miR-8 were used: 5′- CCGCCCTTGACATCTTTACCTGACAGTATTAA CGCGAATATCCCTTTGACATCTTTACCTGACAGTATTATGAACCT-3′; 5′-TAGAGGTTCATAATACTGTCAGGTAAAGATGTCAAAGGGATATT CGCGTTAA TACTGTCAGGTAAAGATGTCAAGGGC-3′.

Transgenic flies were generated by injection of purified plasmid DNA into *w*^{1118} *Drosophila* embryos (Rainbow Transgenic Flies Inc., CA). These flies were crossed with *w*^{1118}, and transformants with germline insertion of plasmid DNA were selected based on eye color. For *pUASP-bantam*, 27 independent transgenic lines were generated and three analyzed. For *pUASP-miR-8*, 34 independent transgenic lines were generated, and three were screened and showed no defects in GSC maintenance and kinetics. For *miR-8-sensor*, 27 independent transgenic lines were generated. Six out of seven examined lines show similar GFP expression patterns in the germarium as shown in Figure 2.

Generation of Clones, Maintenance, and Kinetic and Statistical Analysis

Drosophila melanogaster stocks were raised on standard cornmeal-yeast-agar medium at 25°C. Clones were induced by using the *hsFLP-FRT* system for mitotic recombination.

Larval/early pupal germline clones were produced by heat shocking third instar larvae/early pupae (usually 6 and 7 days after crosses were set up) for 1 hr at 37°C 2 days in a row and dissected at different time points after the last heat shock. Late pupal germline clones were produced by heat shocking late pupae (9 and 10 days after crosses were set up) for 1 hr at 37°C 2 days in a row. The flies eclosed1–2 days after the last heat shock. Adult heat-shock germline clones were induced by heat shocking 2- to 4-day-old F_1 adult females in empty vials for 50 min 2 days in a row in a 37°C water bath. The time points were calculated from the last heat shock.

Adult-induced *bantam* clones were generated by heat shocking 2- to 4-day-old *hsFLP;;ban*$^{\Delta 1}$ *FRT80B/Ubi-GFP FRT80B* flies at 37°C for 50 min twice daily 2 days in a row, with a 5 hour recovery period between daily heat shocks. Flies for this were collected for 2 days after they began eclosing and then kept on wet yeast at 25°C until dissected. They were turned over into fresh vials with wet yeast every other day.

The germline stem cell loss per day (Tables S1–S3) was determined by comparison of the percentage of germaria with clonal GSCs between two different time points after clonal induction. GSC loss per day = (percentage of clonal GSC at time point 1 − percentage of clonal GSC at time point 2) × 100% / percentage of clonal GSC at time point 1 / elapsed time.

The relative division index (Table S4) for a marked GSC is determined by the number of cysts generated by a marked GSC divided by the number of unmarked cysts generated by an unmarked GSC in the same germaria (Hatfield et al., 2005). Division frequencies were measured with germaria containing one *GFP*-positive GSC and one clonal (GFP-negative) GSC. The total number of cysts from a GSC that are produced in a given time window provides a measurement of GSC division frequency. In our case, the time window spanned from the first heat-shock treatment to the time of harvesting the adults. Therefore, we limited our counts to the region of the germarium that was anterior to the easily identifiable *GFP*$^{+/+}$ cyst. This cyst developed from the first daughter cell of the clonal GSC *(GFP*$^{-}$*)* after heat-shock-induced mitotic recombination. Cyst production from homozygous clonal GSCs was divided by the cyst production from heterozygous nonclonal GSCs in the same germarium to obtain the division index. A Student's t test was used to determine the statistical significance.

Staining Procedures

Antibody stainings and confocal microscopy were performed as described previously (Shcherbata et al., 2004). GFP was detected either by analyzing the native GFP (Figures 1 and 4–6) or by using anti-GFP-directly conjugated with Alexa 488 (Figures 2 and 3). A confocal laser-scanning microscope (Leica SPE5) was used in this study. We used the following mouse monoclonal antibodies: Engrailed (1:20), Armadillo (1:40), Adducin (1:20), anti-DE-Cadherin (1:50), and Lamin C (1:20) from the Developmental Studies Hybridoma Bank and anti-p-Mad (1:500, P. ten Dijke), guinea pig anti-CycE (1:500, T. Orr-Weaver), rat anti-Bam-C (1:1000, D. McKearin), and rabbit anti-GFP-directly conjugated with Alexa 488 (1:3000, Invitrogen). Secondary antibodies were Alexa 488, 568, 633, or 647 goat anti-mouse, anti-rabbit, anti-guinea pig (1:500, Molecular Probes), and goat-anti-rat Cy5 (1:250, Jackson Immunoresearch).

Supplemental Data

Supplemental Data include Supplemental Results, Supplemental Experimental Procedures, five figures, and four tables and can be found with this article online at http://www.cellstemcell.com/cgi/content/full/1/6/698/DC1/.

ACKNOWLEDGMENTS

We thank Drs. A. Spradling, D. Pan, B. Calvi, S. Cohen, T.T. Su, T. Orr-Weaver, T. Xie, J. Tamkun, and R. Carthew for suggestions, flies, and reagents, Christian Nelson, Louise von Stechow, and Andriy Yatsenko for help with experiments, and Dr. Bradford Stadler for help with QPCR analysis. This work was supported by AHA fellowships for H.R.S. and S.H.R. and MOD and NIH grants and the Tietze Fellowship for H.R-B.

Received: April 24, 2007
Revised: September 11, 2007
Accepted: November 21, 2007
Published: December 12, 2007

REFERENCES

Bilen, J., Liu, N., Burnett, B.G., Pittman, R.N., and Bonini, N.M. (2006). MicroRNA pathways modulate polyglutamine-induced neurodegeneration. Mol. Cell *24*, 157–163.

Brennecke, J., Hipfner, D.R., Stark, A., Russell, R.B., and Cohen, S.M. (2003). bantam encodes a developmentally regulated microRNA that controls cell proliferation and regulates the proapoptotic gene hid in Drosophila. Cell *113*, 25–36.

Chen, D., and McKearin, D. (2003). Dpp signaling silences bam transcription directly to establish asymmetric divisions of germline stem cells. Curr. Biol. *13*, 1786–1791.

Fuchs, E., Tumbar, T., and Guasch, G. (2004). Socializing with the neighbors: stem cells and their niche. Cell *116*, 769–778.

Gilboa, L., and Lehmann, R. (2006). Soma-germline interactions coordinate homeostasis and growth in the Drosophila gonad. Nature *443*, 97–100.

Grimaud, C., Bantignies, F., Pal-Bhadra, M., Ghana, P., Bhadra, U., and Cavalli, G. (2006). RNAi components are required for nuclear clustering of Polycomb group response elements. Cell *124*, 957–971.

Hatfield, S.D., Shcherbata, H.R., Fischer, K.A., Nakahara, K., Carthew, R.W., and Ruohola-Baker, H. (2005). Stem cell division is regulated by the microRNA pathway. Nature *435*, 974–978.

Hatfield, S., and Ruohola-Baker, H. (2007). microRNA and stem cell function. Cell Tissue Res., in press Published online November 7, 2007. 10.1007/s00441-007-0530-3.

Hatfield, S., Shcherbata, H.R., Ward, E.J., Reynolds, S., and Ruohola-Baker, H. (2007). microRNAs and their involvement in stem cell division. In microRNAs; Biology, Function and Expression, N. Clarke and P. Sanseau, eds. (Eagleville, PA: DNA Press), pp. 221–250.

Huang, J., Wu, S., Barrera, J., Matthews, K., and Pan, D. (2005). The Hippo signaling pathway coordinately regulates cell proliferation and apoptosis by inactivating Yorkie, the Drosophila Homolog of YAP. Cell *122*, 421–434.

Jin, Z., and Xie, T. (2007). Dcr-1 maintains Drosophila ovarian stem cells. Curr. Biol. *17*, 539–544.

Jordan, K.C., Schaeffer, V., Fischer, K.A., Gray, E.E., and Ruohola-Baker, H. (2006). Notch signaling through tramtrack bypasses the mitosis promoting activity of the JNK pathway in the mitotic-to-endocycle transition of Drosophila follicle cells. BMC Dev. Biol. *6*, 16.

Karres, J.S., Hilgers, V., Carrera, I., Treisman, J., and Cohen, S.M. (2007). The conserved microRNA miR-8 tunes atrophin levels to prevent neurodegeneration in Drosophila. Cell *131*, 136–145.

Lee, Y.S., Nakahara, K., Pham, J.W., Kim, K., He, Z., Sontheimer, E.J., and Carthew, R.W. (2004). Distinct roles for Drosophila Dicer-1 and Dicer-2 in the siRNA/miRNA silencing pathways. Cell *117*, 69–81.

Li, L., and Xie, T. (2005). Stem cell niche: structure and function. Annu. Rev. Cell Dev. Biol. *21*, 605–631.

Li, Z., and Li, L. (2006). Understanding hematopoietic stem-cell microenvironments. Trends Biochem. Sci. *31*, 589–595.

Meshorer, E., Yellajoshula, D., George, E., Scambler, P.J., Brown, D.T., and Misteli, T. (2006). Hyperdynamic plasticity of chromatin proteins in pluripotent embryonic stem cells. Dev. Cell *10*, 105–116.

Nolo, R., Morrison, C.M., Tao, C., Zhang, X., and Halder, G. (2006). The bantam microRNA is a target of the hippo tumor-suppressor pathway. Curr. Biol. *16*, 1895–1904.

Pal-Bhadra, M., Bhadra, U., and Birchler, J.A. (2002). RNAi related mechanisms affect both transcriptional and posttranscriptional transgene silencing in Drosophila. Mol. Cell *9*, 315–327.

Pal-Bhadra, M., Leibovitch, B.A., Gandhi, S.G., Rao, M., Bhadra, U., Birchler, J.A., and Elgin, S.C. (2004). Heterochromatic silencing and HP1 localization in Drosophila are dependent on the RNAi machinery. Science *303*, 669–672.

Park, J.K., Liu, X., Strauss, T.J., McKearin, D.M., and Liu, Q. (2007). The miRNA pathway intrinsically controls self-renewal of Drosophila germline stem cells. Curr. Biol. *17*, 533–538.

Peng, J.C., and Karpen, G.H. (2007). H3K9 methylation and RNA interference regulate nucleolar organization and repeated DNA stability. Nat. Cell Biol. *9*, 25–35.

Pham, J.W., Pellino, J.L., Lee, Y.S., Carthew, R.W., and Sontheimer, E.J. (2004). A Dicer-2-dependent 80s complex cleaves targeted mRNAs during RNAi in Drosophila. Cell *117*, 83–94.

Robins, H., Li, Y., and Padgett, R.W. (2005). Incorporating structure to predict microRNA targets. Proc. Natl. Acad. Sci. USA *102*, 4006–4009.

Shcherbata, H.R., Althauser, C., Findley, S.D., and Ruohola-Baker, H. (2004). The mitotic-to-endocycle switch in Drosophila follicle cells is executed by Notch-dependent regulation of G1/S, G2/M and M/G1 cell-cycle transitions. Development *131*, 3169–3181.

Shcherbata, H.R., Hatfield, S., Ward, E.J., Reynolds, S., Fischer, K.A., and Ruohola-Baker, H. (2006). The MicroRNA pathway plays a regulatory role in stem cell division. Cell Cycle *5*, 172–175.

Song, X., Wong, M.D., Kawase, E., Xi, R., Ding, B.C., McCarthy, J.J., and Xie, T. (2004). Bmp signals from niche cells directly repress transcription of a differentiation-promoting gene, bag of marbles, in germline stem cells in the Drosophila ovary. Development *131*, 1353–1364.

Thompson, B.J., and Cohen, S.M. (2006). The Hippo pathway regulates the bantam microRNA to control cell proliferation and apoptosis in Drosophila. Cell *126*, 767–774.

Verdel, A., Jia, S., Gerber, S., Sugiyama, T., Gygi, S., Grewal, S.I., and Moazed, D. (2004). RNAi-mediated targeting of heterochromatin by the RITS complex. Science *303*, 672–676.

Ward, E.J., Shcherbata, H.R., Reynolds, S.H., Fischer, K.A., Hatfield, S.D., and Ruohola-Baker, H. (2006). Stem cells signal to the niche through the Notch pathway in the Drosophila ovary. Curr. Biol. *16*, 2352–2358.

Xie, T., and Spradling, A.C. (1998). decapentaplegic is essential for the maintenance and division of germline stem cells in the Drosophila ovary. Cell *94*, 251–260.

Xu, T., and Rubin, G.M. (1993). Analysis of genetic mosaics in developing and adult Drosophila tissues. Development *117*, 1223–1237.

Zhu, C.H., and Xie, T. (2003). Clonal expansion of ovarian germline stem cells during niche formation in Drosophila. Development *130*, 2579–2588.

Cell Stem Cell, Volume *1*

Supplemental Data

Stage-Specific Differences in the Requirements for Germline Stem Cell Maintenance in the *Drosophila* Ovary

Halyna R. Shcherbata, Ellen J. Ward, Karin A. Fischer, Jenn-Yah Yu, Steven H. Reynolds, Chun-Hong Chen, Peizhang Xu, Bruce A. Hay, and Hannele Ruohola-Baker

Supplemental Results

Loss of *dicer-1* and *Mad* mutant adult GSCs

Since both Dicer-1 and Mad are required for adult GSC maintenance, we analyzed the process of GSC loss in these two mutant backgrounds. Interestingly, the extreme phenotypes for *Mad* and *dcr-1* GSC clones observed in late timepoints (S 3B,D) are somewhat different for the two mutants. While the extreme *dicer-1* mutant phenotypes show germaria with either very few germline cells (Figure 1D, S 1A-1C) or no germline cells (S 3B), in the *Mad* extreme phenotypes, large cysts often develop in the niche (S 3C-E). To further dissect the cause of these differences, we analyzed the earliest events that take place in GSC loss in each mutant. The *dicer-1* mutant GSCs leave the niche moving posteriorly while undergoing a stereotypic division pattern (S 3A). While *Mad* GSCs also undergo a stereotypic division pattern, they can initiate this differentiation process in an abnormal location, while still in the niche (S 3C-E). For example, in SC a four cell *Mad* mutant cyst is observed in the niche five days after adult clonal induction. Therefore, while both *dicer-1* and *Mad* GSCs have a maintenance problem, the manifestation is different. *dicer-1* GSCs leave the niche and differentiate outside the niche. While *Mad* germline stem cells can also leave the niche, 40% of the time GSCs initiate the differentiation process while still in the niche.

The target for TGF-β pathway control in GSCs is the transcriptional repression of Bam. We tested whether Bam protein was upregulated in *dicer-1* mutant GSCs; a potential cause for the observed maintenance defect. However, no obvious upregulation of BamC was observed in adult *dicer-1* GSC clones (S 1B), again supporting the notion that *dicer-1* and *Mad* adult GSC maintenance defects manifest themselves somewhat differently.

Supplementary Materials and Methods

QPCR analysis of microRNA levels in *dcr-2* mutants

Total RNA was prepared from 10 to 20 female whole flies using TRIzol (Invitrogen) and treated with DNaseI (Fermentas). 0.5μg of the extracted RNA was reversed transcribed into cDNA with Omniscript reverse transcriptase (Qiagen) and oligo dT primer. mRNA levels of RP49, a ribosomal protein, were tested by QPCR with SyberGreen master mix (Applied Biosystems) on ABI 7300 Real-time PCR system to

evaluate the total RNA levels in the sample with the following primers: Forward, ATGACCATCCGCCCAGCA; Reverse, TTGGGGTTGGTGAGGCGGAC (PCR fragment=436bp). The reaction were incubated in a 96 well plate at 95^{o}C for 10 min, followed by 40 cycles of 95^{o}C for 15 sec and 60^{o}C for 60 sec. miRNA levels were quantified using TaqMan MicroRNA Assays (dme-miR-8 and dme-bantam, Applied Biosystems) according to the manufacturer's instruction using 10ng of total RNA on ABI 7300 Real-time PCR system.

We used following fly lines in the QPCR assays: *w-*, *+/+;Ly/TM3, FRT42Ddcr-2;Ly/TM3, +/+;FRT82Bdcr-1/TM3, FRT42Ddcr-2;FRT82Bdcr-1/TM3, FRT42D miR-8*$^{\Delta 1}$.

Table S1.
GSC maintenance depends on clonal induction stage in *dcr-1* and *Mad* mutants

Genotype	Clone induction stage		% germaria with clonal GSC			%GSC loss/day[1]
			Time point 1	Time point 2	Time point 3	
Control hsFLP;;FRT82B GFP/ FRT82B	Larval/Pupal	Exp.I	27.3%(5d) n=252	25.4%(8d) n=315	11.4%(14d) n=157	4.2±0.7
		Exp.II	24.4%(5d) n=41	18.8%(8d) n=32	15.0%(14d) n=40	
		Exp.III	23.1%(5d) n=117	22.0%(8d) n=83		
		Exp.IV	40.0%(5d) n=105	38.0%(8d) n=50	35.0%(21d) n=57	
dcr-1 hsFLP;;FRT82B GFP/ FRT82B dcr-1^{Q1147x}	Larval/Pupal	Exp.I	27.7%(5d) n=224	19.4%(8d) n=165	14.5%(14d) n=96	4.4±0.7
		Exp.II	27.0%(5d) n=48	24.2%(8d) n=33	20.0%(14d) n=54	
		Exp.III	19.6%(5d) n=112	19.0%(8d) n=57		
		Exp.IV	31.0%(5d) n=77	29.0%(8d) n=42	22.0%(21d) n=134	
Control hsFLP;GFP FRT40A/ FRT40A	Larval/Pupal	Exp.I	34.4%(7d) n=93		31.3%(14d) n=83	1.3
Mad^{12} hsFLP;GFP FRT40A/ Mad^{12} FRT40A	Larval/Pupal	Exp.I	32.7%(7d) n=107		24.8%(14d) n=129	2.7±0.6
		Exp.II	38.9%(7d) n=79		36.6%(14d) n=134	
		Exp.III	20.1%(7d) n=214		14.3%(14d) n=140	
		Exp.IV	17.4%(7d) n=132		14.4%(12d) n=178	
Mad^{12}; UASDl hsFLP;GFP FRT40A/FRT40A Mad^{12}; UASpDl/nanos Gal4	Larval/Pupal	Exp.I	19.1%(7d) n=68		14.6%(14d) n=41	0.2±1.8
		Exp.II	18.6%(7d) n=97		22.4%(14d) n=76	
Control *hsFLP;FRT42D GFP/ FRT42D*	Larval/Pupal	Exp.I		18.3%(8d) n=224	13.7%(15d) n=300	2.8±0.5
		Exp.II		19.2%(8d) n=245	16.4%(15d) n=329	
miR-8$^{\Delta 1}$ hsFLP;FRT42D GFP/ FRT42D miR-8$^{\Delta 1}$	Larval/Pupal	Exp.I		18.9%(8d) n=175	15.9%(15d) n=301	1.6±0.5
		Exp.II		20.2%(8d) n=233	18.8%(15d) n=425	
ban$^{\Delta 1}$ hsFLP;;GFP FRT80B / ban$^{\Delta 1}$ FRT80B	Larval/Pupal	Exp.I	11.3%(5d) n=115	8.7%(10d) n=126	6.5%(14d) n=170	6.1±0.3
		Exp.II		7.4%(10d) n=135	5.4%(14d) n=147	
		Exp.III		8.7%(8d) n=115	4.9%(15d) n=163	
		Exp.IV		11.1%(8d) n=99	5.6%(15d) n=107	
iswi hsFLP;FRT42B GFP/ FRT42D iswi[2]	Larval/Pupal	Exp.I	11.9%(7d) n=188		2.4%(14d) n=168	10.3±0.3
		Exp.II	17.0%(7d) n=182		4.7%(14d) n=170	

Control ***hsFLP;;FRT82B GFP/ FRT82B***	**Adult**	**Exp.I**	**23.1%(4d) n=248**	**21.2%(7d) n=170**	**20.9%(10d) n=144**	**2.0±0.7**
		Exp.II	**31.4%(3d) n=137**	**31.2%(5d) n=231**	**34.1%(10d) n=231**	
		Exp.III	**27.6%(5d) n=182**		**26.5%(10d) n=215**	
		Exp.IV	**32.5% (6d) n=123**		**26.3% (9d) n=156**	
dcr-1 hsFLP;;FRT82B GFP/ FRT82B dcr-1^{Q1147x}	**Adult**	**Exp.I**	**30.4%(4d) n=125**	**15.5%(7d) n=58**		**11.9±1.1**
		Exp.II	**23.2%(3d) n=289**	**16.8%(5d) n=190**	**12.7%(10d) n=189**	
		Exp.III	**22.8%(5d) n=281**		**8.3%(10d) n=319**	
		Exp.IV	**20.2%(3d) n=79**	**13.9%(6d) n=79**	**8.3%(9d) n=121**	
Control ***hsFLP;GFP FRT40A/ FRT40A***	**Adult**	**Exp.I**	**31.0%(7d) n=84**		**29.9%(14d) n=67**	**0.5**
Mad^{12} hsFLP;GFP FRT40A/ Mad^{12}FRT40A	**Adult**	**Exp.I**	**40.4%(5d) n=94**	**21.2%(9d) n=108**	**14.5%(14d) n=145**	**11±1.0**
		Exp.II	**21.9%(5d) n=155**		**1.6%(12d) n=62**	
		Exp.III	**32.4%(7d) n=102**		**6.8%(14d) n=29**	
Control hsFLP;;GFP FRT80B / **FRT80B or** ***hsFLP;;arm lacZ FRT80B/ GFP FRT80B***	**Adult**	**Exp.I**	**9.9%(4d) n=91**	**10.8%(9d) n=65**		**-1.6±2.3**
		Exp.II	**7.1%(4d) n=70**	**8.2%(6d) n=98**		
		Exp.III	**21.1%(5d) n=95**		**13.0%(14d) n=92**	
ban$^{\Delta 1}$ hsFLP;;GFP FRT80B / ban$^{\Delta 1}$ FRT80B	**Adult**	**Exp.I**	**17.1%(4d) n=88**	**3.0%(9d) n=66**		**14.1±2.8**
		Exp.II	**13.2%(4d) n=121**	**6.7%(6d) n=89**		
		Exp.III	**6.9%(5d) n=72**		**2.5%(14d) n=80**	
		Exp.IV		**5.5%(7d) n=128**	**1.9%(15d) n=162**	
Control ***hsFLP;FRT42D GFP/ FRT42D***	**Adult**	**Exp.I**		**18.1%(8d) n=198**	**18.6%(15d) n=313**	**1.1±1.1**
		Exp.II		**16.1%(8d) n=174**	**13.1%(15d) n=275**	
miR-8$^{\Delta 1}$ hsFLP;FRT42D GFP/ FRT42D miR-8$^{\Delta 1}$	**Adult**	**Exp.I**		**28.6%(8d) n=256**	**27.5%(15d) n=335**	**1.3±0.6**
		Exp.II		**27.8%(8d) n=266**	**23.7%(15d) n=354**	
yorkie hsFLP;FRT42D GFP/ FRT42D yki^{b5}	**Adult**	**Exp.I**	**33.0%(5d) n=297**	**33.6%(9d) n=345**	**31.9%(15d) n=345**	**0.2±0.5**

n = number of germaria analyzed

( ) - days after heat shock induction in parentheses

[1] – average germline stem cell loss per day ± standard error

GSC loss per day = (% of clonal GSC at timepoint 1 - % of clonal GSC at timepoint 2)^{x}100%
% of clonal GSC at timepoint 1/elapsed time

Table S2.
The microRNA and TGF-ß pathways interact to maintain GSCs during development

Genotype	Clonal induction stage		% germaria with clonal GSC			
			Time point 1	Time point 2	Time point 3	%GSC loss/day[1]
Control dcr-1 hsFLP;; FRT82B dcr-1^{Q1147X}/ FRT82B GFP	Larval/ Pupal	Exp.I	27.0%(5d) n=48	24.2%(8d) n=33	20.0%(14d) n=54	3.2±0.3
Control CyO/+;dcr-1 hsFLP; CyO/+; FRT82B dcr-1^{Q1147X}/ FRT82B GFP	Larval/ Pupal	Exp.I	25.8%(6d) n=116		22.6%(12d) n=106	2.5±0.4
		Exp.II	22.0%(6d) n=36	20.0%(9d) n=15		
Control iswi/+;dcr-1 hsFLP; iswi^{2}/+; FRT82B dcr-1^{Q1147X}/ FRT82B GFP	Larval/ Pupal	Exp.I	11.5%(7d) n=227		7.6%(14d) n=173	4.9
Mad/+;dcr-1 hsFLP; Mad^{12} FRT40A/+; FRT82B dcr-1^{Q1147X}/ FRT82B GFP	Larval/ Pupal	Exp.I	23.9%(6d) n=142		9.7%(12d) n=113	14.1±1.1
		Exp.II	28.8%(6d) n=118	31.3%(9d) n=76	0%(12d) n=15	
		Exp.III		6.5%(12d) n=31	1.1%(18d) n=89	
		Exp.IV		10.4%(9d) n=134	0.0%(15d) n=144	
Control Mad; TM6/+ hsFLP; Mad^{12} FRT40 / GFP FRT40A; TM6/+	Larval/ Pupal	Exp.I	16.9%(6d) n=77	16.7%(9d) n=24		0.2
Mad;dcr-1/+ hsFLP; Mad^{12}FRT40A/ GFP FRT40A; FRT82B dcr-1^{Q1147X}/+	Larval/ Pupal	Exp.I	17.4%(6d) n=167	11.1%(9d) n=89		12.3±2.6
		Exp.II	17.2%(5d) n=29		3.8%(14d) n=26	

Table S3.
Preadult GSC lacking Dicer-1 and Dicer-2 activities are lost

Genotype	Clonal induction stage		% germaria with clonal GSC			
			Time point 1	Time point 2	Time point 3	%GSC loss/day[1]
dcr-2 hsFLP; FRT42D dcr2^{L811X}/ FRT 42D Ubi-GFP	Larval/ Pupal	Exp.I	34.3%(7d) n=137		27.9%(14d) n=136	2.7
dcr-2;dcr-1 hsFLP; dcr-2^{L811X}; FRT82B dcr-1^{Q1147X}/ FRT82B GFP	Larval/ Pupal	Exp.I	15.4%(7d) n=117	15.6%(10d) n=90	1.01%(13d) n=99	16.1±6.5
		Exp.II	12.0%(7d) n=31		3.6%(11d) n=89	
dcr-2 hsFLP; FRT42D dcr2^{L811X}/ FRT 42D Ubi-GFP	Adult	Exp.I	22.2%(5d) n=180	21.8%(9d) n=55		1.8±0.9
		Exp.II	28.3%(5d) n=113		22.2%(12d) n=45	
dcr-2;dcr-1 hsFLP; dcr-2^{L811X}; FRT82B dcr-1^{Q1147X}/ FRT82B GFP	Adult	Exp.I	5.9%(5d) n=186	3.2%(8d) n=193		15.3

n = number of germaria analyzed
( ) - days after heat shock induction in parentheses
[1] – average germline stem cell loss per day ± standard error

GSC loss per day = $\frac{\text{(\% of clonal GSC at timepoint 1 - \% of clonal GSC at timepoint 2)} \times 100\%}{\text{\% of clonal GSC at timepoint 1/elapsed time}}$

Table S4.
GSCs require Dicer-1 for proper division during all developmental stages, whereas preadult GSCs lacking Mad activity divide normally

Genotype	Clonal induction stage	Time point	Average number of cysts generated heterozygous GSCs	Average number of cysts generated by mutant *GFP*$^{-}$ GSCs	Relative Division Index[1] ± AD
Mad*^{12} *hsFLP; GFP FRT40A / Mad*^{12} *FRT40A	**Larval/ Pupal**	**7d**	**4.73 n=11**	**4.55 n=11**	**0.96±0.22**
		12d	**3.82 n=17**	**3.17 n=23**	**0.87±0.25**
		14d	**4.57 n=7**	**3.67 n=18**	**0.80±0.13**
***dcr-1 hsFLP;;FRT82B GFP/ FRT82B dcr-1*^{Q1147x}**	**Adult**	**3d**	**3.50 n=4**	**2.16 n=6**	**0.61±0.07**
		6d	**4.60 n=15**	**2.20 n=10**	**0.48±0.21**
		7d	**4.75 n=12**	**1.55 n=17**	**0.34±0.14**
		9d	**4.83 n=6**	**1.75 n=28**	**0.39±0.25**
Mad*^{12} *hsFLP; GFP FRT40A/ Mad*^{12} *FRT40A	**Adult**	**5d**	**4.15 n=13**	**1.64 n=14**	**0.50±0.24**
		9d	**5.81 n=16**	**3.13 n=22**	**0.51±0.25**
		14d	**3.91 n=23**	**1.95 n=20**	**0.40±0.17**
ban*$^{\Delta 1}$ *hsFLP;;GFP FRT80B / ban*$^{\Delta 1}$ *FRT80B	**Adult**	**5d**	**3.0 n=6**	**1.3 n=4**	**0.43**
		9d*	**2.8 n=5**	**1.07 n=13**	**0.38**

[1] - The Relative Division Rate or Division Index for a mutant GSC is determined by the average number of GFP^{-} mutant cysts generated by a GFP^{-} GSC divided by the average number of GFP/+ mutant cysts generated by a GFP/+ GSC. n= the number of total GSC examined. * - few examples of *ban*$^{\Delta 1}$ GSCs analyzed 12 days after adult heat shock produced no progeny.

Figure S1. Adult induced *dicer-1* GSC clones

(A-C) show tissue from females with adult-induced *dicer-1* GSC clones, (D) shows a germarium with control clones. Germaria oriented anterior right, GSCs outlined with dashes, cap cells identified with pink asterisks

(A) Example of an extreme phenotype observed when both GSCs are mutant for *dicer-1*. This germarium contains only a single germline stem cell (white dashes). Due to reduced cell divisions, the germarium is smaller and adjacent to an older egg chamber.

(B) Although germline stem cells lacking *dicer-1* are lost from the niche at a high frequency (see Figure 3A), *dicer-1* mutant germline stem cells do not express BamC.

(C) GSCs lacking Dicer-1 activity from adulthood onwards divide slower which results in smaller germaria in comparison to control (D). (D) Germarium with two control (parental) clonal GSCs in the niche. Red=Adducin (A), BamC (B) or Adducin+Lamin C (C-D), Blue=DAPI, Green=GFP.

Figure S2. Larva/pupal induced GSC clones.

When GSCs lose Mad activity during larval/pupal development, the Mad^{12} mutant GSCs are maintained in the niche, divide normally and produce normal cysts (A,B). However, when Mad levels are reduced in *dcr-1* mutant background, GSC are lost even after larval/pupal clone induction (C,D).

(A) Upper ovariole shows larval/pupal-induced mutant GSCs in the niche producing normal cysts and egg chambers. Lower ovariole shows that larval/pupal-induced Mad^{12} mutant follicle cells are defective, leading to encapsulation defects (Jordan et al., 2000).

(B) A germarium with an all clonal germline showing that larval/pupal-induced Mad^{12} mutant germline stem cells divide normally and are maintained in the niche.

(C,D) When Mad levels are reduced in GSCs lacking Dicer-1 during larval/pupal stages (*hsFlp; Mad^{12} FRT40A/+; FRT82B dcr-1^{Q1147X}/FRT82B GFP)*, mutant GSCs leave the niche (C,C') and have division defects typical for *dcr-1* mutant GSCs, resulting in smaller germaria (D). Red=Adducin (A,C-D) or Cyclin E (B), Blue=DAPI, Green=GFP, mutant GSCs outlined with white dashed lines, control GSCs with yellow dashes.

Jordan, K.C., Clegg, N.J., Blasi, J.A., Morimoto, A.M., Sen, J., Stein, D., McNeill, H., Deng, W.M., Tworoger, M., and Ruohola-Baker, H. (2000). The homeobox gene mirror links EGF signalling to embryonic dorso-ventral axis formation through notch activation. Nat. Genet. 24, 429–433.

Figure S3. Different defects are observed when GSCs lack either *dicer-1* or *Mad*

dicer-1^{Q1147X} mutant germline stem cells generated during adulthood leave the niche by differentiation (A; 6 days after adult clone induction *dicer* GSC has left the niche and produced a 2-cell *dicer-1* cyst marked with turquoise dashes; Figure 6A). (B) Occasionally, when both germline stem cells lack *dicer-1* activity, both germline stem cells leave the niche, ultimately resulting in an empty niche. Mad^{12}

mutant GSCs are lost by two different mechanisms. Most *Mad* mutant GSCs leave the niche. However, 43% of *Mad* mutant GSCs stay in the niche and differentiate while still being in contact with the niche cells (C-E). Mad cysts outlined with turquoise dashes; the niche/cap cells marked with pink asterisks, Red=Adducin (A-C, E) or Adducin+Lamin C (D), Blue=DAPI, Green=GFP.

Figure S4. Germaria from *bantam* hetereoallelic mutants exhibit the same mutant characteristics associated with *bantam* clones

(A-E) Show tissue from (A) control and (B-E) listed bantam heteroallelic mutants.

(A) Normal size germarium from a control fly with two GSCs. (B) An example of abnormally small germarium from a *bantam* heteroallelic mutant (ban^{L1170}/ban^{EP3622}). The single GSC is dividing, but must be dividing very slowly since there are very few cysts and the overall size of the germarium is small. Note the *bantam* alleles were isolated independently. (C-D) Two examples from another *bantam* heteroallelic combination ($ban^{L1170}/ban^{\Delta 1}$) showing a germarium reduced in size with a single GSC (C) and an empty germarium (D). (E) Another example of a germarium reduced in size with a single GSC from a $ban^{EP3622}/ ban^{\Delta 1}$ heteroallelic fly. Germaria oriented anterior right, GSCs outlined with white dashes, Red=Adducin, Blue=DAPI.

Figure S5. Germline stem cell maintenance depends on developmental stage during mutation induction

Exponential curves are fitted to a time-course of germline stem cells maintenance, where the numbers of clonal germline SCs at 5 days after preadult heat shock or 3 days after adult heat shock are normalized to 1. (A) Larval-pupal induced *dcr-1, Mad,* and *Mad, UAS Dl* GSCs show no maintenance defects, suggesting that Dcr -1 and Mad are not required for GSC maintenance in developmental stages. However, chromatin remodeling factor ISWI is required for GSC maintenance regardless which stage of development it is lost. (B) In contrast GSCs are lost in exponential order when components of Dcr-1 and Mad *(dcr-1, bantam* miRNA and *Mad)* were mutated in GSC during adulthood, showing that Mad and miRNA pathway, and specifically *bantam* miRNA, are essential for adult germline stem cell maintenance.

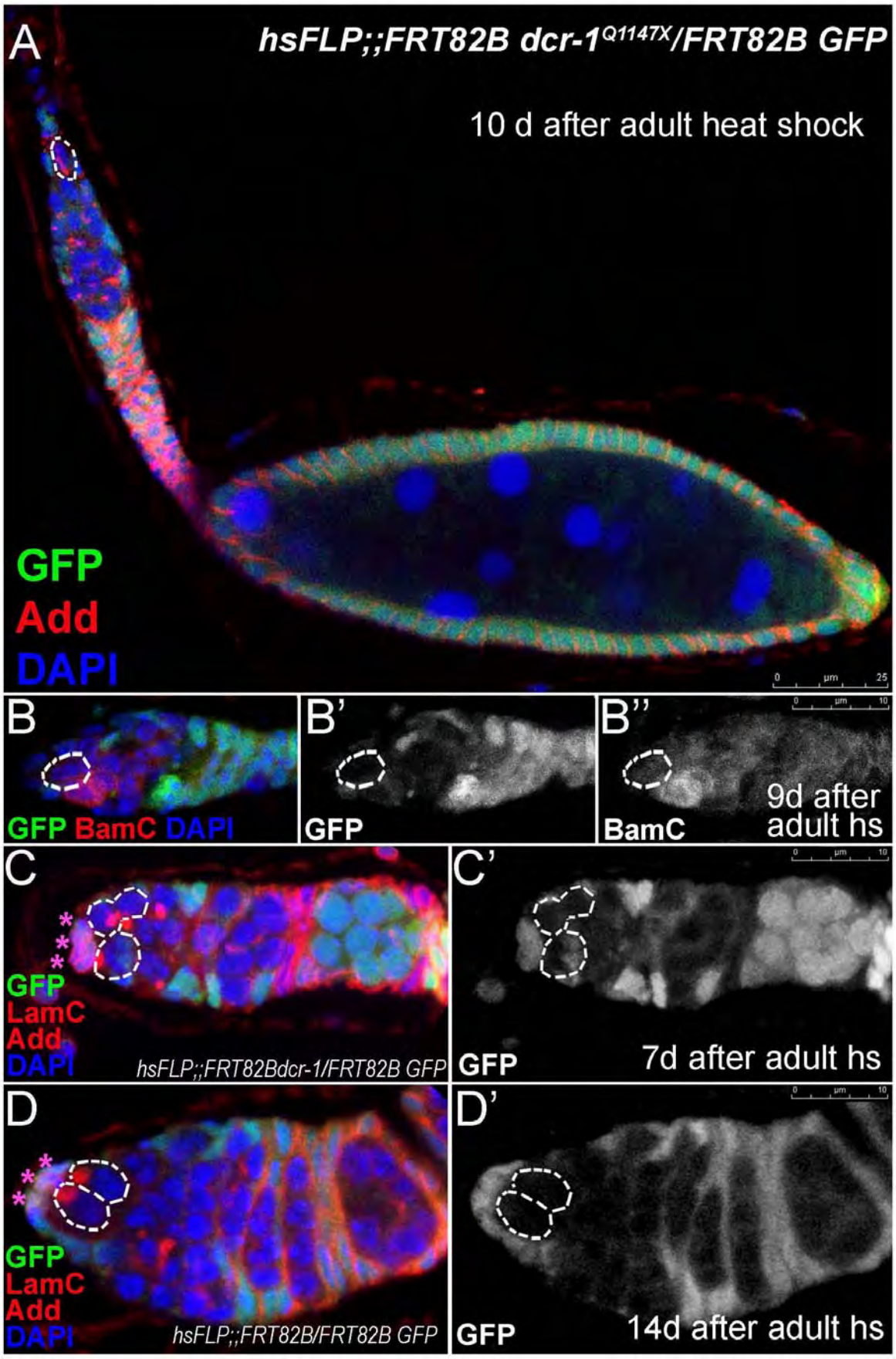
A
hsFLP;;FRT82B dcr-1Q1147X/FRT82B GFP
10 d after adult heat shock
GFP
Add
DAPI
B
GFP BamC DAPI
B'
GFP
B''
BamC
9d after adult hs
C
GFP
LamC
Add
DAPI
hsFLP;;FRT82Bdcr-1/FRT82B GFP
C'
GFP
7d after adult hs
D
GFP
LamC
Add
DAPI
hsFLP;;FRT82B/FRT82B GFP
D'
GFP
14d after adult hs

Figure S1

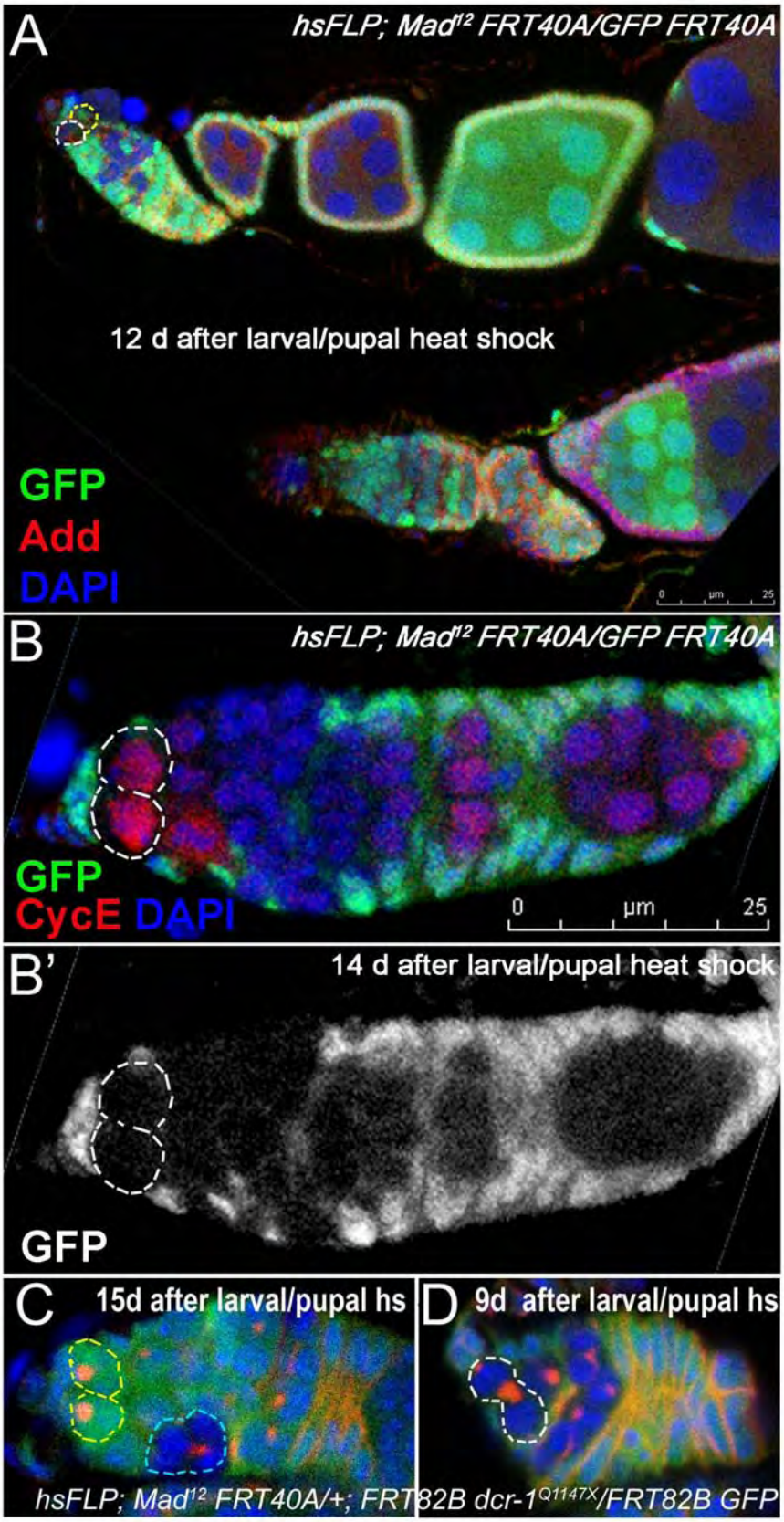
A
hsFLP; Mad12 FRT40A/GFP FRT40A
12 d after larval/pupal heat shock
GFP
Add
DAPI
0 µm 25
B
hsFLP; Mad12 FRT40A/GFP FRT40A
GFP
CycE DAPI
0 µm 25
B'
14 d after larval/pupal heat shock
GFP
C
15d after larval/pupal hs
D
9d after larval/pupal hs
hsFLP; Mad12 FRT40A/+; FRT82B dcr-1Q1147X/FRT82B GFP

Figure S2

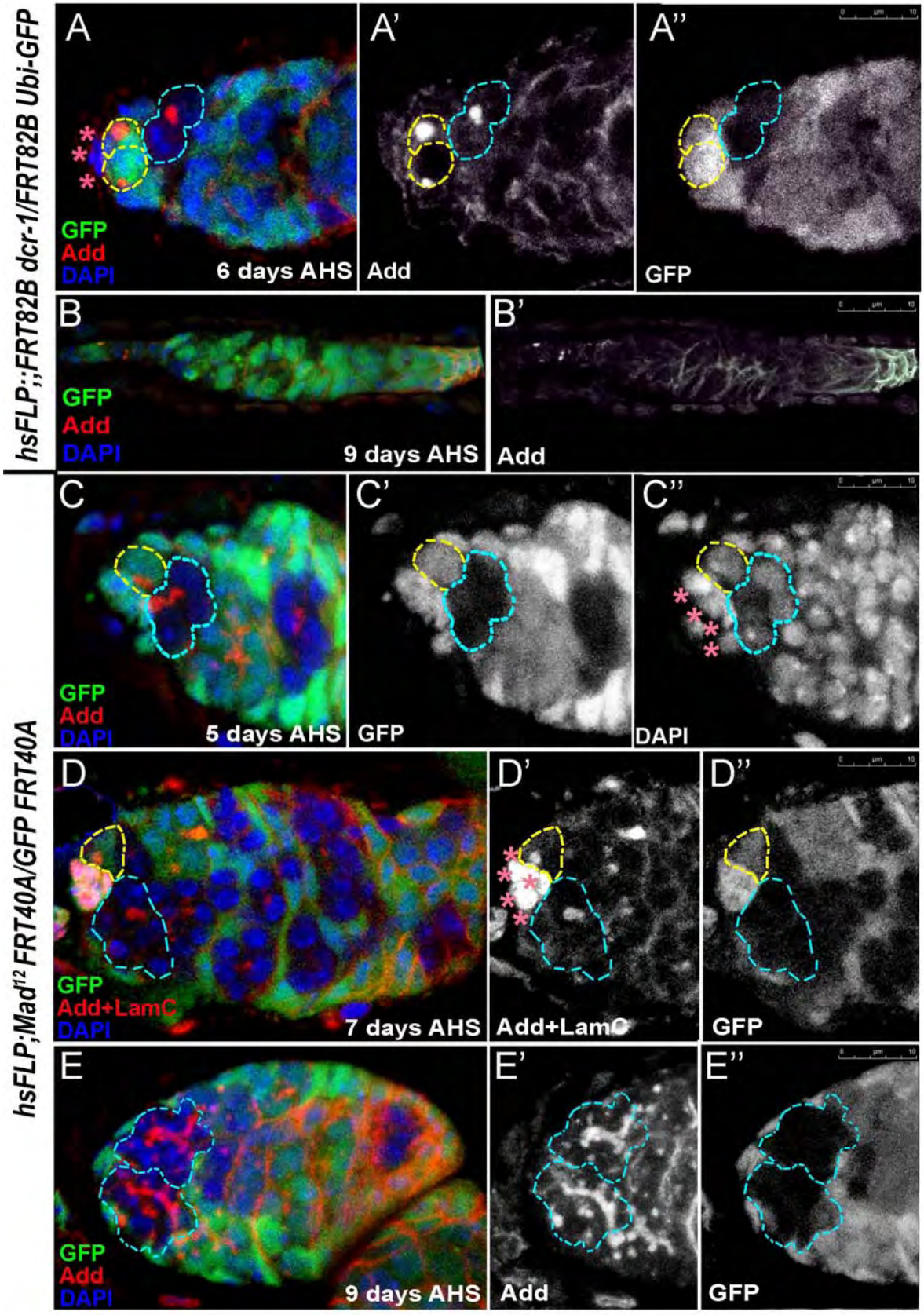
hsFLP;;FRT82B dcr-1/FRT82B Ubi-GFP
hsFLP;Mad12 FRT40A/GFP FRT40A
A
A'
A''
GFP
Add
DAPI
6 days AHS
Add
GFP
B
B'
GFP
Add
DAPI
9 days AHS
Add
C
C'
C''
GFP
Add
DAPI
5 days AHS
GFP
DAPI
D
D'
D''
GFP
Add+LamC
DAPI
7 days AHS
Add+LamC
GFP
E
E'
E''
GFP
Add
DAPI
9 days AHS
Add
GFP

Figure S3

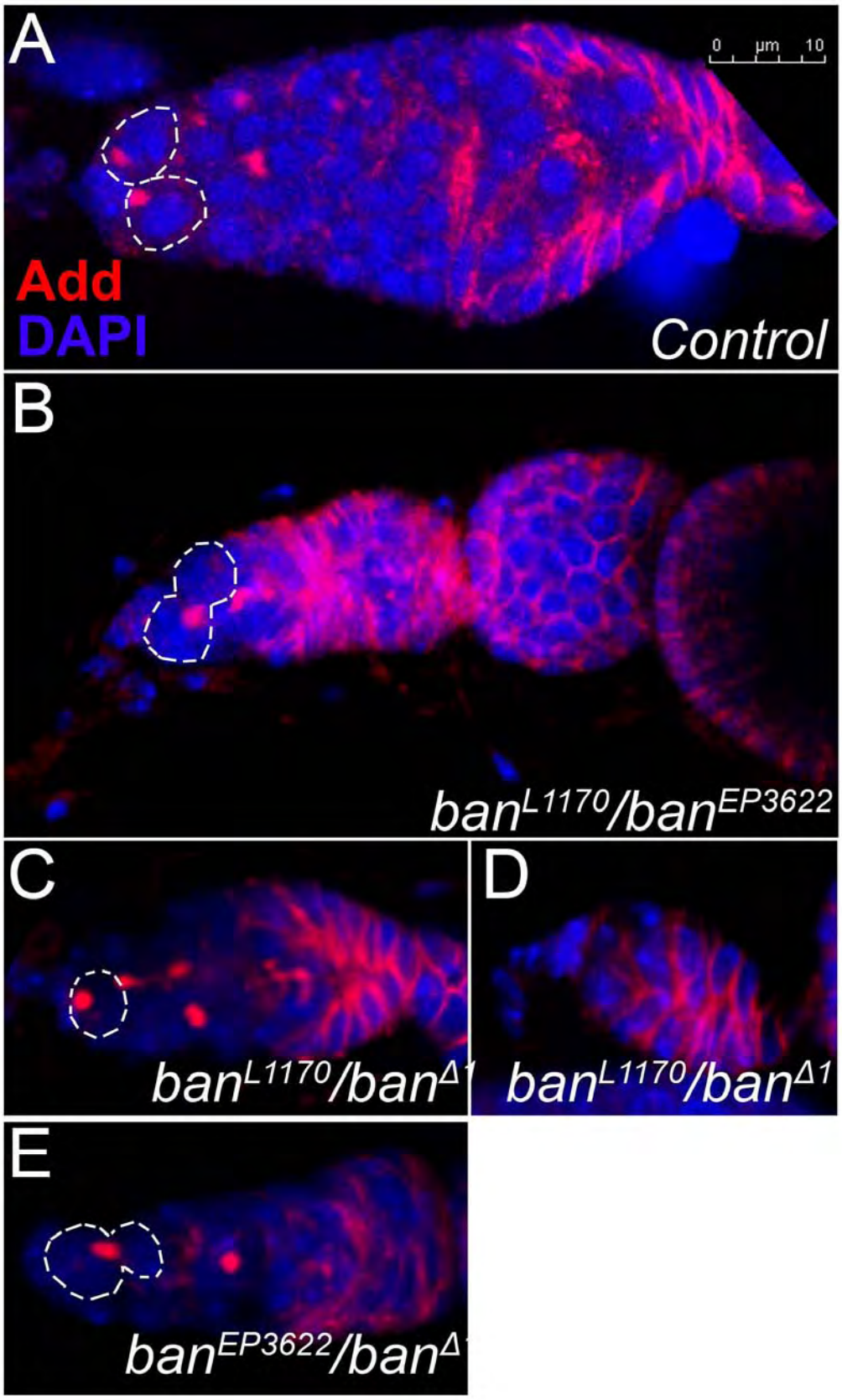
A
0 µm 10
Add
DAPI
Control
B
ban^L1170/ban^EP3622
C
ban^L1170/ban^Δ1
D
ban^L1170/ban^Δ1
E
ban^EP3622/ban^Δ

Figure S4

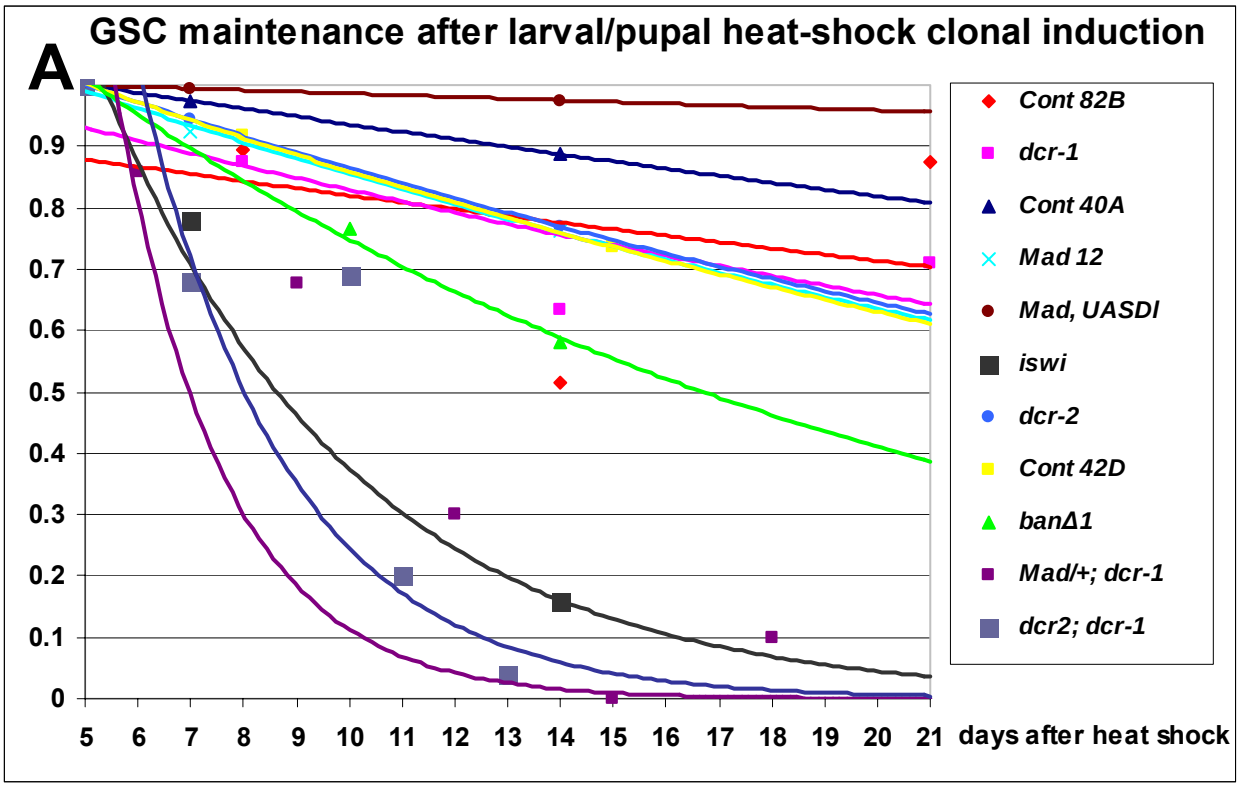
A
GSC maintenance after larval/pupal heat-shock clonal induction
0
0.1
0.2
0.3
0.4
0.5
0.6
0.7
0.8
0.9
5 6 7 8 9 10 11 12 13 14 15 16 17 18 19 20 21
days after heat shock
Cont 82B
dcr-1
Cont 40A
Mad 12
Mad, UASDl
iswi
dcr-2
Cont 42D
banΔ1
Mad/+; dcr-1
dcr2; dcr-1

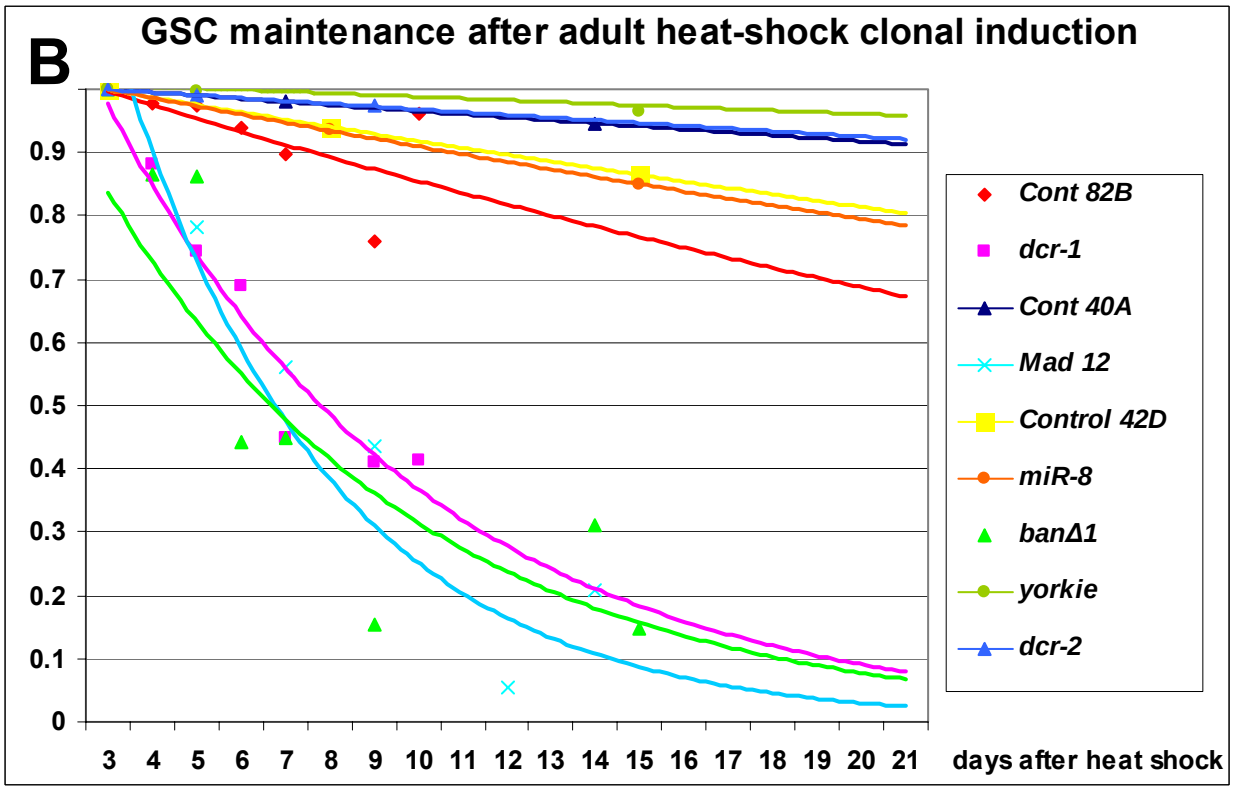
B
GSC maintenance after adult heat-shock clonal induction
0
0.1
0.2
0.3
0.4
0.5
0.6
0.7
0.8
0.9
3 4 5 6 7 8 9 10 11 12 13 14 15 16 17 18 19 20 21
days after heat shock
Cont 82B
dcr-1
Cont 40A
Mad 12
Control 42D
miR-8
banΔ1
yorkie
dcr-2

Figure S5

The EMBO Journal (2011) 30, 1549–1562 | © 2011 European Molecular Biology Organization | Some Rights Reserved 0261-4189/11
www.embojournal.org

THE EMBO JOURNAL

EMBO open

Ecdysteroids affect *Drosophila* ovarian stem cell niche formation and early germline differentiation

Annekatrin König, Andriy S Yatsenko, Miriam Weiss and Halyna R Shcherbata*

Max Planck Research Group of Gene Expression and Signaling, Max Planck Institute for Biophysical Chemistry, Göttingen, Germany

Previously, it has been shown that in *Drosophila* steroid hormones are required for progression of oogenesis during late stages of egg maturation. Here, we show that ecdysteroids regulate progression through the early steps of germ cell lineage. Upon ecdysone signalling deficit germline stem cell progeny delay to switch on a differentiation programme. This differentiation impediment is associated with reduced TGF-β signalling in the germline and increased levels of cell adhesion complexes and cytoskeletal proteins in somatic escort cells. A co-activator of the ecdysone receptor, Taiman is the spatially restricted regulator of the ecdysone signalling pathway in soma. Additionally, when ecdysone signalling is perturbed during the process of somatic stem cell niche establishment enlarged functional niches able to host additional stem cells are formed.

The EMBO Journal (2011) **30,** 1549–1562. doi:10.1038/emboj.2011.73; Published online 18 March 2011
Subject Categories: signal transduction; development
Keywords: *Drosophila*; ecdysone signalling; germline stem cell; stem cell niche

Introduction

One of the key characteristics of adult stem cells is their ability to divide for a long period of time in an environment where most other cells are quiescent. Typically, stem cells divide asymmetrically where a mother cell gives rise to two daughter cells with different fates, another stem cell and a differentiated progeny (Gonczy, 2008).

Adult stem cells also require niches. The niche itself is as significant as stem cell autonomous functions and its environment has the potential to reprogramme somatic cells and to transform them into stem cells (Brawley and Matunis, 2004; Kai and Spradling, 2004; Boulanger and Smith, 2009). The niche includes all cellular and non-cellular components that interact in order to control the adult stem cell. These interactions can be divided into one of two main mechanistic types—physical contacts and diffusible factors. Diffusible factors travel over varying distances from a cell source to instruct the stem cell, often affecting transcription (Walker *et al*, 2009). Stem cells must be anchored to the niche through cell-to-cell interactions so they will stay both close to niche factors that specify self-renewal and far from differentiation stimuli. While multiple studies focused on the aspects of how the niche regulates stem cells, the question of how the niche is established itself has not been addressed in depth.

The *Drosophila* ovarian stem cell niche model is an exemplary system where two different stem cell types, germline stem cells (GSCs) and somatic escort stem cells (ESCs) share the same niche and coordinate their development. Niche cells contact GSCs via E-cadherin and Integrin-mediated cell adhesion complexes that bind to the extracellular matrix and connect to the cytoskeleton and this physical docking of stem cells to the niche is essential for GSC maintenance (Xie and Spradling, 2000; Tanentzapf *et al*, 2007). In addition, the stem cell niche sends short-range signals that specify and regulate stem cell fate by maintaining the undifferentiated state of GSCs next to the niche. Not only does the niche have an effect on stem cells, but also the stem cells communicate with the niche. A feedback loop exists between the stem cells and niche cells: Delta from the GSC can activate Notch in the somatic cells that maintains a functional niche and in turn controls GSC maintenance (Ward *et al*, 2006). While the management of GSCs within the niche is relatively well understood, the control of the other present stem cell type, ESCs is not clear. An ESC, like a GSC divides asymmetrically producing another ESC and a daughter, escort cell (EC) that will differentiate into a squamous cell that envelops the GSC progeny once disconnected from the niche. It is believed that developing cyst encapsulation by ECs protects from TGF-β signalling that maintains GSC identity (Decotto and Spradling, 2005). The ESC and GSC cycles have to be tightly coordinated, so a sufficient number of ECs will be produced in response to GSC division. However, the pathway used for GSC and ESC communication is unknown.

Adult stem cell division mostly is activated locally in response to tissue demands to replace lost cells. In addition, stem cells can be regulated via more general stimuli in response to systemic needs of the whole organism. Hormones are systemic regulators that regulate a variety of processes in different organs in response to the body's status. Even though the effects of hormonal signalling have been extensively studied, the specific roles for hormones in stem cell biology remain complex, poorly defined and difficult to study *in vivo*.

Drosophila is a great system to study the role of endocrine signalling as it contains only one major steroid hormone, ecdysone (20-hydroxyecdysone, 20E) that synchronises the

*Correspondence: Gene Expression and Signalling Group, Max Planck Institute for Biophysical Chemistry, Am Fassberg 11, Göttingen 37077, Germany. Tel.: +49 551 201 1656; Fax: +49 551 201 1755; E-mail: halyna.shcherbata@mpibpc.mpg.de

Received: 9 November 2010; accepted: 22 February 2011; published online: 18 March 2011

behavioural, genetic and morphological changes associated with developmental transitions and the establishment of reproductive maturity (Shirras and Bownes, 1987; Riddiford, 1993; Buszczak *et al*, 1999; Kozlova and Thummel, 2003; Gaziova *et al*, 2004; Schubiger *et al*, 2005; Terashima and Bownes, 2005; McBrayer *et al*, 2007). Ecdysteroids act through the heterodimeric nuclear receptor complex consisting of the ecdysone receptor, EcR (Koelle *et al*, 1991) and its partner ultraspiracle (USP), the *Drosophila* retinoid X receptor homologue (Shea *et al*, 1990; Oro *et al*, 1992; Yao *et al*, 1992). The ecdysone/EcR/USP receptor/ligand complex binds to ecdysone response elements (EcREs) to coordinate gene expression in diverse tissues (Riddihough and Pelham, 1987; Cherbas *et al*, 1991; Dobens *et al*, 1991). Ecdysone signalling is patterned spatially as well as temporally; depending on the tissue type and the developmental stage, the EcR/USP complexes with different co-activators or co-repressors including Taiman, Alien, Rig, SMRTER, Bonus, Trithorax-related protein and DOR (Dressel *et al*, 1999; Tsai *et al*, 1999; Bai *et al*, 2000; Beckstead *et al*, 2001; Sedkov *et al*, 2003; Gates *et al*, 2004; Jang *et al*, 2009; Francis *et al*, 2010; Mauvezin *et al*, 2010). These co-factors can have other binding partners that are themselves regulated by different signalling pathways. For example, Abrupt controlled by JAK/STAT attenuates ecdysone signalling by binding to its co-activator Taiman (Jang *et al*, 2009). In addition, other signalling pathways (insulin, TGF-β) interact with ecdysone pathway components to further modulate cell type-specific responses (Zheng *et al*, 2003; Jang *et al*, 2009; Francis *et al*, 2010). This offers an additional level of combinatorial possibilities and suggests a model of gene expression regulation that is highly managed by this global endocrine signalling.

Data presented here show that ecdysone signalling is involved in control of early germline differentiation. When ecdysone signalling is perturbed, the strength of TGF-β signalling in GSCs and their progeny is modified resulting in a differentiation delay. Moreover, soma-specific disruption of ecdysone signalling affects germline differentiation cell non-autonomously. Ecdysteroids act in somatic ESCs and their daughters to regulate cell adhesion complexes and cytoskeletal proteins important for soma–germline communication. Misexpression of ecdysone signalling components during developmental stages leads to the formation of the enlarged GSC niche that can facilitate more stem cells.

Results

Taiman, a Drosophila homologue of a steroid receptor co-activator amplified in breast and ovarian cancer (AIB1) influences the size of the niche and GSC number

The *Drosophila* ovary contains distinct populations of stem cells: GSCs, which give rise to the gametes, and two types of somatic stem cells: ESCs and follicle stem cells (FSCs) (Figure 1A). These stem cells reside in stereotyped positions inside the germarium, a specialised structure at the anterior end of the *Drosophila* ovary. Both GSCs and ESCs are adjacent to somatic signalling centres or niches consisting of the terminal filament (TF) and cap cells (CpCs), which promote stem cell identity. ESCs produce squamous daughters with long processes that encase developing cysts to protect them from niche signalling and allow differentiation. These different cell types have distinct morphologies and molecular markers (Figure 1C and E).

We performed a pilot genetic screen where clonal germaria of *hsFlp;FRT40A* lethals (DGRC) were analysed in order to find novel genes that affect stem cell niche architecture. One of the genes found in our screen encoding a *Drosophila* homologue of a human steroid receptor co-activator amplified in breast cancer *taiman* (*tai*) was of a particular interest. Downregulation of Tai using different combinations of *tai* amorphic and hypomorphic mutant alleles resulted in increased GSC number and an enlarged niche (Figure 1D and F). The GSC average number ranged from 3.2 to 5.1 depending on the genotype, which was significantly higher than in heterozygous control flies (2.1–2.4, Figure 1D, F and H; Supplementary Table S1). This increase in GSC number coincided with stem cell niche enlargement. While control germaria contained on average 6 niche cells, *tai* mutant niches consisted of 7–10 CpCs (Figure 1D, F and G; Supplementary Table S1). These observations imply that Tai participates in niche formation and/or GSC maintenance or differentiation.

As it has been shown that in *Drosophila* Taiman is a co-activator of the ecdysone transcription-activating complex (Figure 1I; Bai *et al*, 2000), we tested if *tai* and ecdysone pathway components genetically interact in the process. Transheterozygous germaria (*tai/EcR* and *tai/usp*) also showed additional GSCs and enlarged niches (Figure 1J; Supplementary Table S1), suggesting that the ecdysone pathway regulates early germline progression and GSC niche assembly.

Figure 1 The ecdysone receptor co-activator Taiman controls the number of ovarian germline stem cell niche cells. (**A**) Schematic view of a wild-type germarium: germline stem cells (GSCs, pink) marked by anterior spectrosomes (SS, red dots) are located at the apex of the germarium next to the niche cap cells (CpCs, grey). Further noted are terminal filament (TF; dark blue), escort stem cells (ESCs, olive), differentiating cystoblasts (CBs, blue), escort cells (ECs, lime), 4, 8 (bright green) and 16 cell (green) cysts in region 2A, indicated by the presence of fusomes (FS, red branched structures), follicle stem cells (FSCs, violet) and follicle cells (FC, light grey) in regions 2B and 3. (**B**) Schematic view of a *tai* mutant germarium with an increased number of single spectrosome containing cells (SSCs, pink and blue), CpCs (grey) and additional somatic cells (plum). (**C**, **E**) In wild-type germaria, two GSCs marked by the presence of the stem cell marker pMad (**C**), spectrosomes (stained with Adducin) and the absence of the differentiation factor BamC (**E**) are directly attached to the niche (marked with LaminC, arrows). (**D**, **F**) In the $tai^{61G1}/tai^{BG02711}$ transheterozygous mutant germarium, the enlarged niche is coupled with an increased number of GSCs that are pMad positive (**D**) and BamC negative (**F**). In addition, extra somatic cells are present at the anterior (marked with brackets). CpC (**G**) and GSC (**H**) numbers are increased in *tai* mutant germaria. (**I**) Scheme illustrating that Tai is a co-activator of the EcR/USP nuclear receptor complex that is activated upon binding of its ligand ecdysone; Ab negatively regulates the ecdysone signalling by direct binding to Tai (based on Bai *et al* (2000) and Jang *et al* (2009)). (**J**) EcR^{Q50st}/tai^{61G1} transheterozygous germaria also contain an increased number of GSCs and CpCs, indicating that *tai* genetically interacts with *EcR* (see Supplementary Table S1). (**D**–**F**, **J**) Projections of optical sections assembled through the germarial tissue; GSCs are outlined with yellow dashed lines, niche cells are marked with white arrows; Red, Adducin + LaminC; blue, DAPI; and green, pMad (**C**, **D**), BamGFP (**E**), BamC (**F**) and Vasa (**J**); Error bars represent s.e.m. $*P<0.05$, $**P<0.005$, $***P<0.0005$.

The steroid hormone ecdysone controls GSC progeny differentiation

To further test the role of the endocrine pathway in the germline, we used the *ecdysoneless1* temperature-sensitive mutation ($ecd1^{ts}$) that blocks biosynthesis of the mature ecdysteroid hormone, 20-hydroxyecdysone. $ecd1^{ts}$ animals were allowed to develop normally at the permissive temperature and transferred to restrictive temperature conditions as 3-day-old adults. When ecdysone production was disrupted during adulthood, GSCs continued to divide increasing the germarium size, however, their progeny delayed progression through differentiation (Figure 2A and B). Similar phenotypes were obtained upon ecdysone signalling disruption using dominant-negative mutants for the

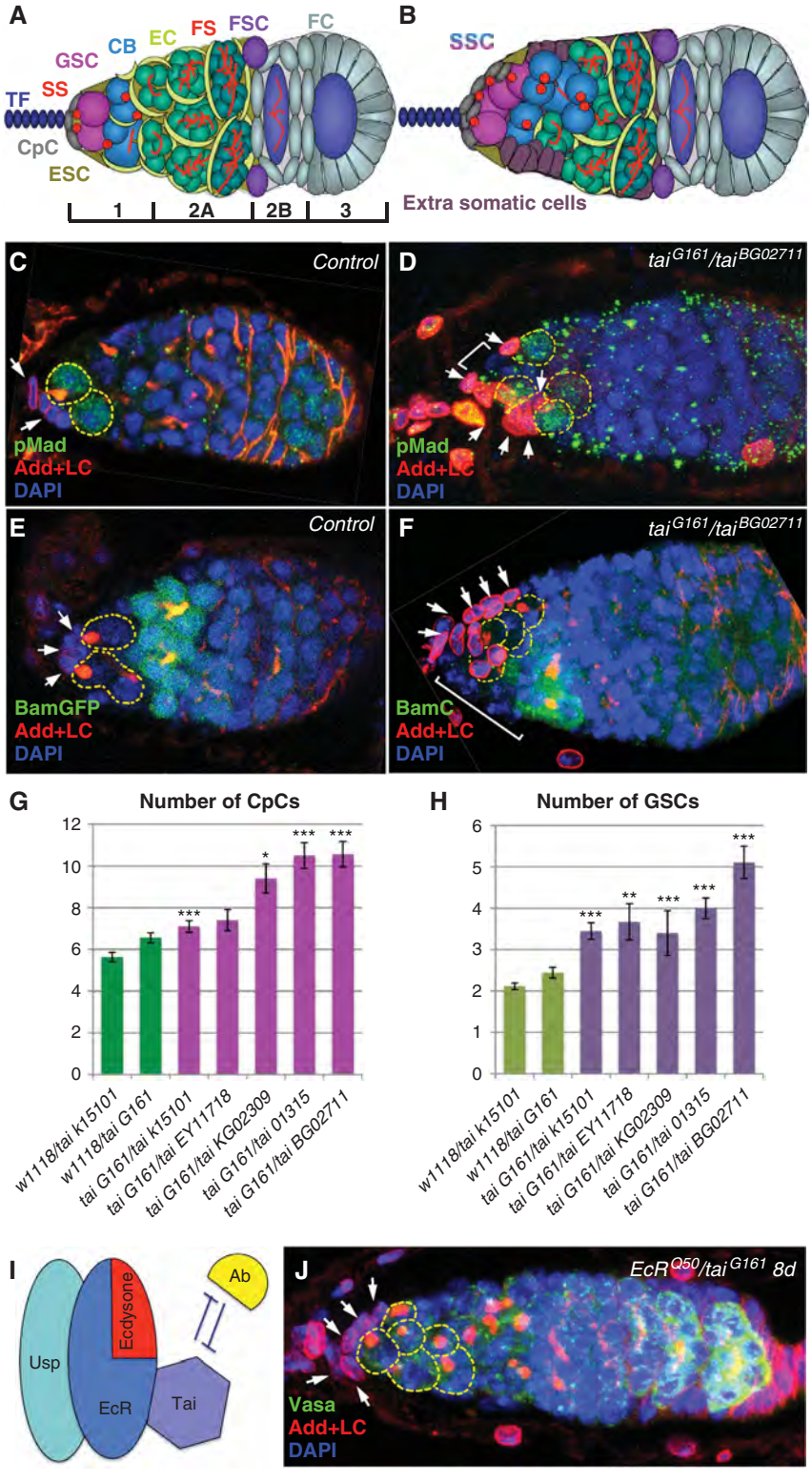

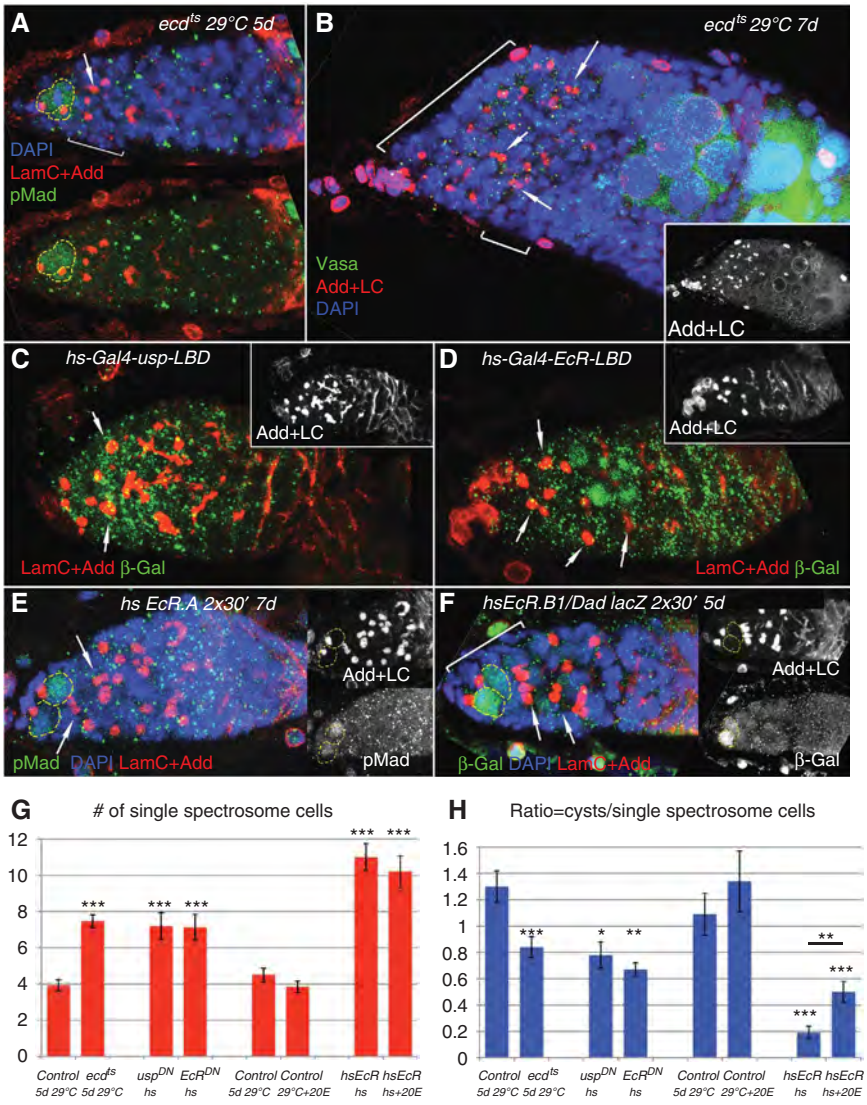

Figure 2 Disrupted ecdysone signalling during adulthood results in delayed germline differentiation. (**A**) At the restrictive temperature (29°C) *ecd1*^{ts} adult animals contain germaria filled with supernumerary SSCs. (**B**) Extended depletion of ecdysone furthermore increases the undifferentiated SSC number and causes somatic cell defects affecting cyst pinching off from the germarium. (**C**, **D**) Heat shock induced expression of USP and EcR dominant-negative forms (*usp*^{DN} (*hs-Gal-4-usp-LBD*) and *EcR*^{DN} (*hs-Gal-4-usp-LBD*)) also lead to the appearance of supernumerary SSCs. (**E**, **F**) Similarly to the effects that are caused by disturbing the ecdysone pathway via *ecd1*^{ts} or dominant-negative *EcR*^{DN} and *usp*^{DN} mutations, expression of the *EcR* isoforms *EcR.A* or *EcR.B1* induced by heat shock (twice per day for 30 min 4 days in a row) increases the number of SSCs, but not GSCs and influences CB differentiation. Note the presence of dumbbell-shaped fusomes in (**A**–**F**). (**G**) In control conditions around four SSCs per germarium are detected. Ecdysone withdrawal via *ecd1*^{ts} mutation as well as heat shock-induced expression of *usp*^{DN} or *EcR*^{DN} and overexpression of *EcR* led to a 2- or 2.5-fold increase in SSC number, whereas external supply of ecdysone does not change the amount of SSCs within the germarium. (**H**) The ratio of differentiating cysts to SSCs is about 1.5-fold decreased in *ecd1*^{ts}, *usp*^{DN} and *EcR*^{DN} mutant germaria. This decrease is even more pronounced (seven times) in *hsEcR* flies. Providing 20E externally can partially, but significantly alleviate this early germline differentiation delay. (**A**–**F**) Projections of optical sections assembled through the germarial tissue. GSCs are outlined with yellow dashed lines, dumbbell-shaped fusomes are marked with arrows and additional somatic cells are marked with brackets. Red, LaminC + Adducin; blue, DAPI; and green, pMad (**A**, **E**); Vasa (**B**) and β-galactosidase (**C**, **D**, **F**) Error bars represent s.e.m. $^{*}P<0.05$, $^{**}P<0.005$, $^{***}P<0.0005$.

ecdysone receptor, EcR and its dimerisation partner USP (*hs–Gal4-EcR-LBD* (*EcR*^{DN}) and *hs-Gal4-usp-LBD* (*usp*^{DN}); Kozlova and Thummel, 2002), (Figure 2C and D; Supplementary Table S2). Instead of progressively developed cysts, mutant germaria were filled with germline cells containing a single spectrosome (single spectrosome containing cells (SSCs)), on average seven SSCs per *ecd1*^{ts} or *EcR*^{DN} and *usp*^{DN} germarium were detected in comparison to four in control (Figure 2G; Supplementary Table S2). After longer ecdysone deprivation germaria look even more abnormal; a slightly decreased GSC number and additional follicle cell defects along with abnormal cyst pinching off from the germarium, not shared by *tai* mutants, were observed (Figure 2B; Supplementary Table S2). The differentiation index or the ratio between developing fusome-containing cells and SSCs in the region 1–2A was decreased 1.5–2-fold in ecdysone mutant germaria (Figure 2H; Supplementary Table S2). Disruption of ecdysone signalling via overexpression of EcR (*hsEcR.A* and *hsEcR.B1*) also resulted in the appearance of germaria filled with supernumerary SSCs

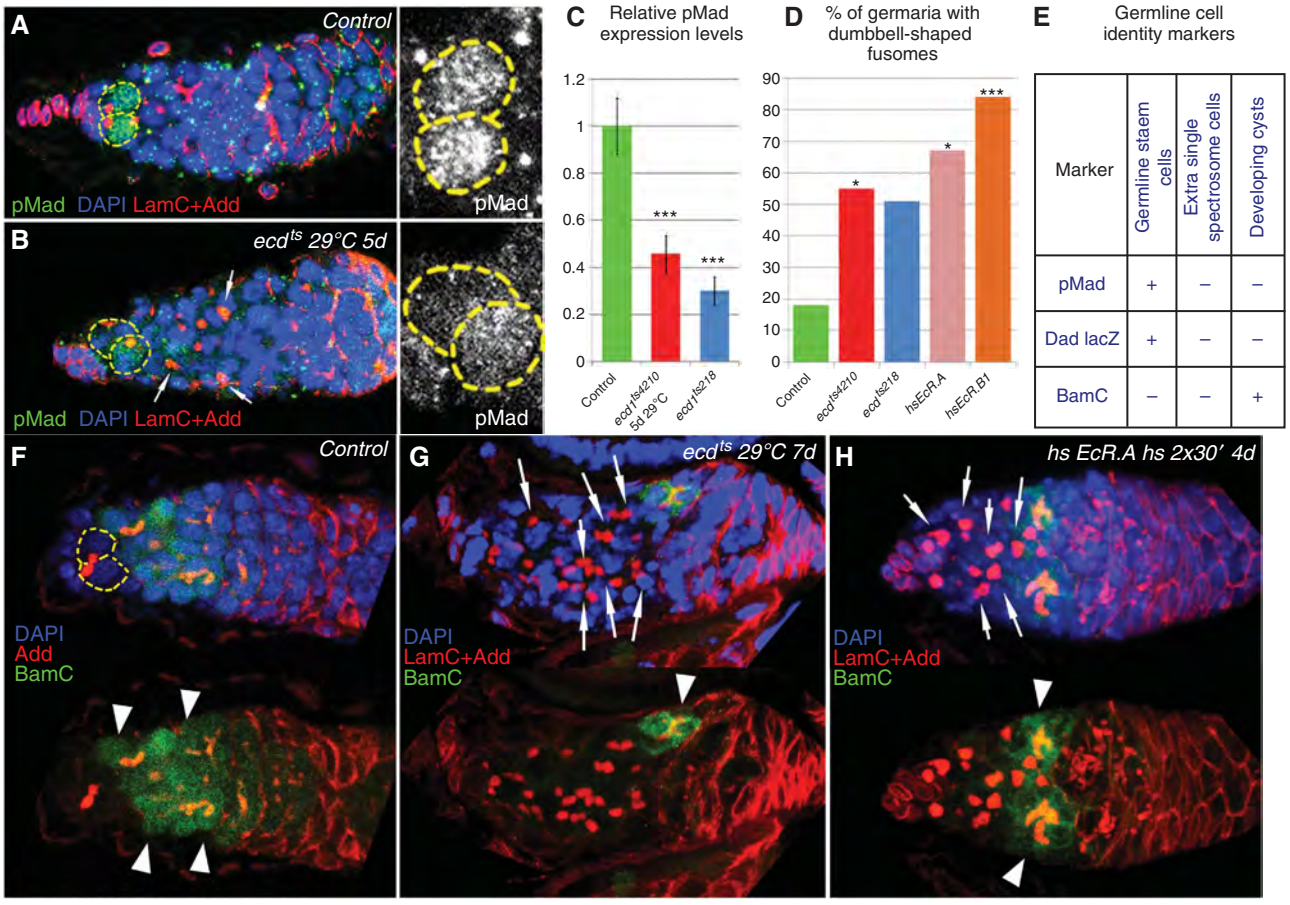

Figure 3 Ecdysone signalling affects the TGF-β pathway. (**A**) Wild-type germarium containing two GSCs, marked by pMad staining. (**B**) Upon blocked ecdysone production the relative pMad expression levels in GSCs are decreased (**C**, compare the pMad levels measured by grey value in **A** and **B**). (**D**) Disruption of ecdysone signalling results in the increase of dumbbell-shaped fusome quantity. In $ecd1^{ts4210}$ mutant flies that were at the restrictive temperature for up to 7 days, 55% ($n=33$) of the germaria have dumbbell-shaped fusomes ($ecd1^{ts218}$ 51%, $n=37$) whereas in equally treated w^{1118} germaria, only 18% ($n=11$) of the germaria contain dumbbell-shaped fusomes. After overexpression of *EcR.A* or *EcR.B1* for 7 days 67% or 84% ($n=15$, 19, respectively) of the analysed germaria contain dumbbell-shaped fusomes. (**E**) The characteristics of GSCs, SSCs and developing cysts are compared schematically. GSCs express the stem cell markers pMad and Dad lacZ and developing cysts the differentiation factor BamC, whereas additional SSCs in germaria deficient of ecdysone signalling are pMad, Dad lacZ and BamC negative, showing that they do not maintain stem cell identity and are delayed in development. (**F**) In wild-type germarium, BamC is present in developing CBs adjacent to GSCs, while in ecdysone pathway mutants, $ecd1^{ts}$ (**G**) and *hsEcR* (**H**), the anterior part of the germarium is filled with cells that do not express the differentiation marker BamC and contain a single spectrosome or a dumbbell-shaped fusome. (**A**, **B**, **F**–**H**) Projections of optical sections assembled through the germarial tissue. GSCs are outlined with yellow dashed lines, dumbbell-shaped fusomes are marked with arrows and BamC-positive differentiating cysts with arrowheads. Red, Adducin + LaminC; blue, DAPI; and green, pMad (**A**, **B**); BamC (**F**–**H**). Error bars represent s.e.m. Significance calculated using the *t*-test (**C**), χ^2-test (**D**). $^*P<0.05$, $^{***}P<0.0005$.

(on average 11 in comparison to 4 in control, Figure 2E–H; Supplementary Table S3).

The described phenotypes show that ecdysone signalling loss of function (by disruption of ecdysone biosynthesis or by expression of EcR and USP dominant-negative forms) and overexpression of the main receptor of the pathway, EcR cause similar abnormalities. Previously, it has been shown that the EcR can form homodimers in the absence of its binding partners *in vitro* (Elke *et al*, 1997), moreover the un-liganded receptor complex is repressive and this repression is relieved as the hormone titre increases (Schubiger and Truman, 2000; Schubiger *et al*, 2005).

To test if the latter can be the case in our system, we performed experiments where adult flies were fed with 20E. Feeding flies with ecdysone alone had no significant effect on the number of SSCs or germline differentiation measured by the ratio of differentiated cysts to SSCs within one germarium (Figure 2G and H; Supplementary Table S3). Interestingly, feeding of ecdysone to the animals that overexpressed EcR moderately, but significantly rescued the cyst/SSC ratio (Figure 2H; Supplementary Table S3), indicating that EcR overexpression when the ecdysone receptor is abundant and the ligand is limited is unfavourable for germline differentiation.

Ecdysone signalling disturbance affects the intensity of TGF-β signalling

Next, we attempted to analyse the identity of supernumerary SSCs. If they are GSCs, they should express appropriate markers. However, we found that additional SSCs are negative for the stem cell markers, phosphorylated Mad and Dad (Figures 2A, E, F, 3B and E). We also noticed that levels of pMad in GSCs were significantly reduced upon ecdysone deficit (Figure 3A–C), suggesting that ecdysone signalling can modulate pMad levels.

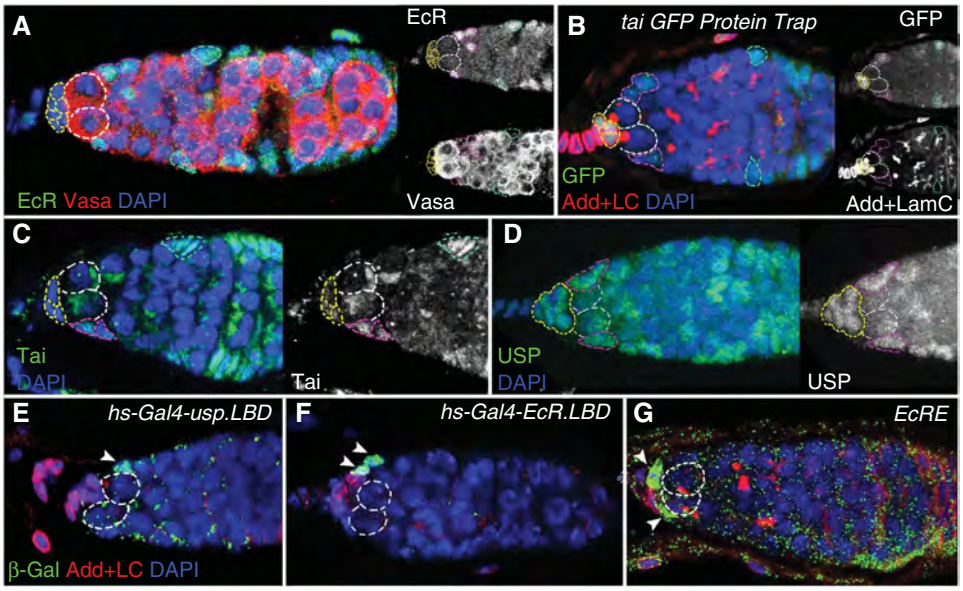

Figure 4 Expression pattern of the ecdysone pathway components in the *Drosophila* germarium. (**A**) The anti-EcR (common region) antibody detects high levels of EcR in ESCs and FCs. (**B**) In the *tai G00308* protein trap line where GFP is expressed under the control of the endogenous *tai* promoter, high GFP levels were detected in CpCs, ESCs and FSCs. (**C**) Comparable expression pattern is observed with the anti-Tai antibody. (**D**) The nuclear receptor USP detected by the anti-USP antibody shows identical expression pattern to its binding partner EcR. (**E**, **F**) Spatial patterns of ecdysone signalling activation identified via β-Gal staining of heat-treated *hs-Gal4-usp.LBD/+*; *UAS-lacZ/+* (**E**) and *hs-Gal4-EcR.LBD/+*; *UAS-lacZ/+* (**D**) germaria prove ecdysone signalling being mainly active in the ESCs (marked with arrowheads). (**E**) The ecdysone signalling reporter *EcRE-lacZ* shows the presence of active ecdysone transcription complex in ESCs as well (marked with arrowheads). Different cell types are marked as follows: GSCs, white dashed lines; CpCs, yellow dashed lines; ESCs/ECs, red dashed lines; FCs, green dashed lines. Red, Vasa (**A**), Adducin + LaminC (**B**, **E**–**G**); blue, DAPI; and green, anti-EcR (common region) (**A**); GFP (**B**); anti-Tai (**C**), anti-USP (**D**) and β-galactosidase (**E**–**G**).

As supernumerary SSCs did not express the stem cell markers, we next analysed if the increased number of SSCs can be explained by abnormal organisation of fusomes, the structures that connect daughter cells within one cyst. Cysts are formed by a process of mitosis with incomplete cytokinesis, and all cells forming one cyst divide simultaneously (de Cuevas and Spradling, 1998). If ecdysone signalling affects fusome stability leading to the appearance of dot-like instead of branched fusomes, then SSCs are really cells within a differentiating cyst and should have synchronised divisions. However, staining with a mitotic marker phosphohistone H3 (PH3) showed that the cell cycle was not coordinated in SSCs, which shows that single spectrosomes are not the result of fusome breakage in pursuit of cyst de-differentiation into single stem cell-like cells (Supplementary Figure S1).

We also noticed that many fusomes had a dumbbell shape, which is a characteristic of perturbed Bam, a TGF-β signalling target (McKearin and Ohlstein, 1995) (Figures 2B–F, 3B, G and H). The amount of germaria with dumbbell-shaped fusomes increased from 18% in control to 51–84% in animals with exogenous EcR expression and ecdysone deficit (Figure 3D). Interestingly, SSCs in germaria mutant for ecdysone signalling, unlike wild-type differentiating cystoblasts do not express Bam, a factor essential for germline differentiation (Figure 3F–H). Taken together, these analyses show that additional SSCs resulting from ecdysone signalling disruption are 'undecided' cells that express neither stem cell nor differentiation markers (Figure 3E).

These data suggest that ecdysone signalling affects early germline differentiation possibly by modulation of the TGF-β signalling strength causing a developmental delay. Eventually some germline differentiation takes place implying that ecdysone signalling is at least partially redundant with other pathways for germline progression.

Ecdysone signalling is predominantly active in ESCs and Taiman, an EcR/USP co-activator is spatially limited to the soma

Previous studies show that ecdysone signalling in *Drosophila* has a role in egg maturation and vitellogenesis (Shirras and Bownes, 1987; Riddiford, 1993; Buszczak *et al*, 1999; Kozlova and Thummel, 2003; Gaziova *et al*, 2004; Schubiger *et al*, 2005; Terashima and Bownes, 2005; McBrayer *et al*, 2007), now our data indicate that it is also required for differentiation of developing germline cysts. As germline differentiation can be regulated cell autonomously or cell non-autonomously, we decided to test what goes awry in the GSC niche community when the ecdysone pathway is perturbed. We began with analysing the expression pattern of ecdysone signalling pathway components to find out in which cell types ecdysone signalling is working. The EcR protein measured by a specific antibody was detected mostly in ESCs and ECs, thin cells which envelop the differentiating cystoblast to assist in differentiation by protecting it from the niche signals (Figure 4A). Next, we used a GFP protein trap line inserted in the *tai* gene and detected levels of GFP expression in CpCs that form the niche and also to a lesser amount in ESCs (Figure 4B). Similarly, staining with Tai and USP-specific antibodies (Figure 4C and D; Supplementary Figure S2) showed that these proteins are expressed predominantly in somatic cells, however, some low levels are also present in

the germline indicative of a possible dual role of this endocrine pathway in the germline and the soma.

After determining protein expression we wanted to confirm that the ecdysone signalling pathway was active. For this, we used reporters with a *Gal4* transcription factor fused to the ligand-binding domain of USP or EcR (*hs-Gal4-uspLBD*, *hs-Gal4-EcRLBD*; Kozlova and Thummel, 2002). The ecdysone pathway activity was detected mainly in ESCs and ECs analysed using a somatically expressed *UASt lacZ* transgene (Figure 4E and F). The *EcRE-lacZ* construct that senses the presence of the active ecdysone receptor transcription complex (Koelle *et al*, 1991) also validated the pathway activity in ESCs and random CpCs (Figure 4G).

Ecdysone signalling is required cell non-autonomously for progression through the early steps of germ cell lineage

Our expression data demonstrate that ecdysone signalling components are expressed in somatic cells within the GSC niche and the signalling is active predominantly in ESCs, leading to the hypothesis that ecdysone signalling controls germline cell differentiation extrinsically. This idea is further supported by the analysis of *tai* loss-of-function germline clones (Supplementary Figure S3) that show that Tai is not essential for germline progression: *tai* mutant GSCs were normally maintained (Supplementary Table S4; Supplementary Figure S3B) and in general germline differentiation was not affected (Supplementary Figure S3A). Together with spatially restricted somatic Tai expression this provides evidence that the ecdysone co-activator Taiman can act as a cell-specific co-activator of ecdysone signalling in niche and ECs.

To identify specific cellular processes regulated by the ecdysone pathway in somatic cells proximal to the ovarian stem cell niche, we downregulated ecdysone signalling using transgenic *UAS tai RNAi*, *UAS EcR RNAi* and *UAS ab* lines crossed to ovarian soma-specific drivers (*bab1Gal4* and *ptcGal4*, for expression patterns see Supplementary Figure S4) combined with the temperature-sensitive *Gal80* system to avoid the lethality caused by downregulation of ecdysone pathway components during developmental stages.

When the co-activator of ecdysone signalling Tai was downregulated or the co-repressor Abrupt overexpressed in soma, mutant germaria contained multiple SSCs (Figure 5A–C); this mutant phenotype became even more pronounced over time (Figure 5B and D) resembling older $ecd1^{ts}$ (Figure 2B) as well as JAK/STAT mutant germaria (Decotto and Spradling, 2005). Similar phenotypes were observed when *EcR RNAi* flies were kept at the restrictive temperature; the development of germline cysts was retarded (Figure 5E–G), and the ratio of fusome-containing cysts to SSCs was reduced 2–3 times (Figure 5I; Supplementary Table S5). Downregulation of EcR for longer periods (15, 21 days) led to an increase in the number of SSCs (from 5 to 9–11 SSCs per germarium, Figure 5H; compare 5F and 5G). In addition, in proximity to undeveloped cysts mutant germaria contained extra somatic cells, most likely improperly differentiated ECs (Figure 5, brackets).

These data provide evidence that the soma-specific disruption of the ecdysone pathway is causing germline differentiation defects, indicating a cell non-autonomous role of this steroid hormone signalling.

Ecdysone signalling regulates turnover of cell adhesion proteins

In order to analyse how mutant somatic cells cause a block in germline cyst maturation, we used an FRT recombination system to compare ecdysone pathway deficient and wild-type somatic cells within one germarium. Detailed analysis of *tai* mutant ESCs and their progeny showed that they lose their squamous shape, and form a layer resembling columnar epithelium (Figure 6A). Interestingly, these mutant cells expressed higher levels of the cell adhesion molecules β-Catenin/Armadillo, DE-Cadherin and a cytoskeleton component Adducin (Figure 6A, C and D). DE-Cadherin was also upregulated in abnormal somatic cells resulting from somatic overexpression of Abrupt or downregulation of EcR (*UAS ab* or *UAS EcR RNAi* crossed to $ptcGal4/tubGal80^{ts}$; Figure 6E and F) pointing towards possible defects in cell–cell contacts, shape rearrangement and signalling transduction processes. These data imply that in our system the ecdysone pathway has a specific role in EC differentiation via regulation of cell adhesion complexes that are required for establishment of correct germline–soma communications. Perhaps, when connections between germline cysts and surrounding soma are perturbed, signalling cascades that initiate germline differentiation are also perturbed causing a developmental delay.

Ecdysone signalling controls the stem cell niche formation

Another process in the germarium that should require a very accurate regulation of cell adhesion is the niche establishment. If ecdysone signalling is essential to control this process as well, we would expect to see abnormalities in niche formation in ecdysone pathway mutants. Recall that mutant *tai* animals indeed had enlarged niches and extra GSCs (Figure 1C and D), a phenotype not seen in other cases analysed here. This discrepancy can be explained by the time during the animal's development when the mutation was introduced. In the *tai* experiment, animals were *tai* deficient during all developmental stages, including the period of niche establishment. In other cases in this study the ecdysone pathway was misregulated during adulthood after the niche was already formed and CpCs had stopped division. Also, in *tai* heterozygouts both the soma and the germline were mutant and the germline can affect via Notch signalling the size of the niche (Ward *et al*, 2006). To prove that the niche expansion is a soma-originated phenotype, we knocked down *tai* in somatic pre-adult cells that contribute to niches using the *FRT/bab1Gal4/UASFlp* system that allows to induce mutant CpC clones during niche formation. As expected, germaria with *tai* clonal CpCs had substantially enlarged niches (Figure 7A and B), which provides evidence that the ecdysone pathway co-activator Tai is required during developmental stages specifically in the pre-niche cells to control the GSC niche assembly. Possibly in *tai* mutant somatic cells within the larval ovary, like in ECs in adults, increased levels of cell adhesion molecules allow them to adhere better to germline cells and receive more signalling (Notch for example) which makes them adopt the niche cell fate.

To confirm that the niche enlargement is an ecdysone signalling-reliant phenotype and is not associated with Tai-independent function, we introduced other ecdysone pathway component mutations during the period of niche

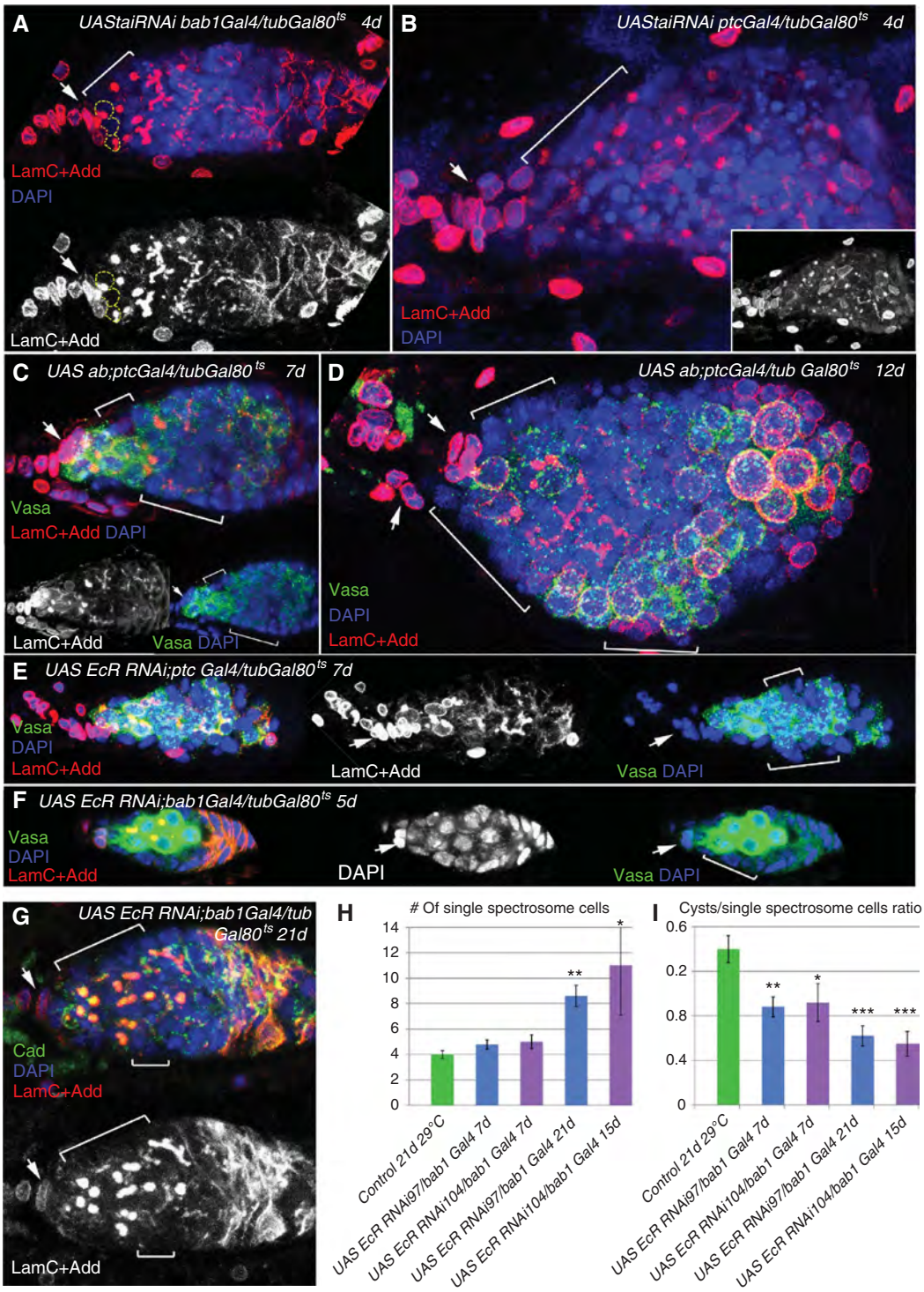

Figure 5 Ecdysteroids act from the soma to regulate the progression of germline development in the germarium. (**A**, **B**) The EcR co-activator Tai is downregulated specifically in the somatic cells of the germarium using *ptcGal4* and *bab1Gal4* in combination with *tubGal80^{ts}* system to avoid lethality. Upon downregulation of *tai* in the soma, the number of developmentally delayed SSCs increases dramatically. (**C**, **D**) Overexpression of the Tai repressor, Abrupt using *UAS ab* with the same drivers causes similar phenotypes as seen with downregulation of *tai*. (**B**, **D**) The *tai* and *ab* mutant germaria are filled with undifferentiated SSCs, cysts are not pinching off and additional somatic cells (brackets) are in the vicinity. Note the similarity of phenotypes caused by ecdysteriod deficit (*ecd1^{ts}*, Figure 2B) and disruption of ecdysone signalling pathway components just in germarial soma. (**E**–**G**) The downregulation of the EcR in the somatic cells of the germarium via expression of *UAS EcR RNAi^{97}* under control of *ptcGal4* (**E**) and *bab1Gal4* (**F**, **G**) leads to an increase of SSCs at the expense of developing cysts. Note the presence of dumbbell-shaped spectrosomes and additional somatic cells. (**H**) Bar graph showing extra quantities of SSCs upon EcR downregulation via expression of *UAS EcR RNAi^{97}* or *UAS EcR RNAi^{104}* with the somatic drivers *ptcGal4* or *bab1Gal4*. This phenotype gets more pronounced with longer duration of EcR abolition. (**I**) The ratio of differentiating cysts to SSCs is also decreased correspondingly to the increase in the SSC number. (**A**–**G**) Projections of optical sections assembled through the germarial tissue are shown. CpCs are marked with arrows, additional somatic cells with brackets. Red, Adducin + LaminC (**A**–**G**); blue, DAPI; and green, Vasa (**C**–**F**), Cadherin (**G**). Error bars represent s.e.m. $^{*}P<0.05$, $^{**}P<0.005$, $^{***}P<0.0005$.

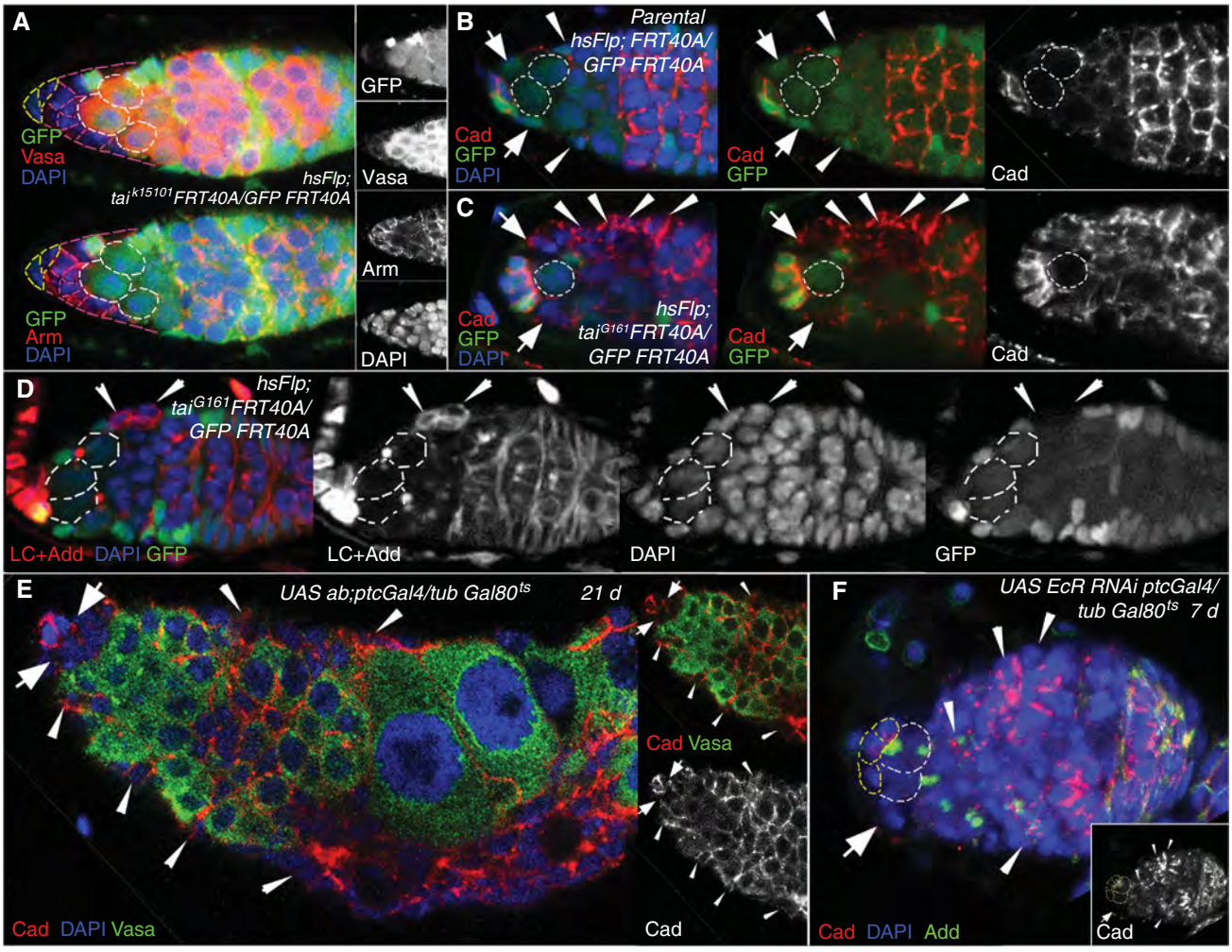

Figure 6 Cell adhesion and cytoskeleton proteins are misregulated in escort cells mutant for ecdysone signalling pathway components. (**A**) The progeny of *tai*^{k15101}-deficient ESCs marked by the absence of GFP (*hsFlp*; *tai*^{k15101}*FRT40A/UbiGFP FRT40A*) formed a columnar epithelium-like somatic tissue adjacent to the stem cell niche. These cells also express higher levels of β-catenin/Armadillo than normal. (**B**) In the control germarium (*hsFlp*; *FRT40A/UbiGFP FRT40A*) ESCs (marked by arrows) and EC (marked by arrowheads) show moderate levels of DE-Cadherin, while niche–GSC cell contacts have higher DE-Cadherin levels. (**C**) *tai*^{61G1} deficiency (*hsFlp*; *tai*^{G161}*FRT40A/UbiGFP FRT40A*) led to the upregulation of the cell adhesion protein DE-Cadherin in ECs (arrowheads) and ESCs (arrows). Note also that the number of abnormally shaped *tai* mutant escort cells is increased in (**A**, **C**). (**D**) *tai* mutant escort cells (arrowheads, *hsFlp*; *tai*^{G161}*FRT40A/UbiGFP FRT40A*) do not properly change their morphology and show higher levels of the cytoskeletal protein Adducin and nuclear envelope marker LaminC. (**E**) The overexpression of the ecdysone signalling inhibitor Abrupt leads to a strongly mutant germarial structure. Somatic cells (marked by the absence of the germline marker Vasa) are forming layers all along the germarium and show high DE-Cadherin levels. (**F**) Somatic abolition of EcR (*UAS EcR RNAi*; *ptcGal4/tubGal80*^{ts}) also increases levels of cell adhesion and cytoskeleton proteins, DE-Cadherin and Adducin. Wide arrows, ESCs; arrowheads, ECs; Red, Vasa, Armadillo (**A**), Cadherin (**B**, **C**, **E**, **F**), Adducin + LaminC (**D**); blue, DAPI; and green, GFP (**A**–**E**).

development. As most of the tested mutant combinations affected viability, we could disrupt ecdysone signalling during development only via induction of single cell clones using the *act*<*CD2*<*Gal4*, *hsFlp* system and via *EcR* overexpression. Mutant single somatic clonal cells expressing *UAS ab* or *UAS EcR RNAi* resembled niche cells by their shape and ability to hold SSCs (Figure 7C and D). On average, mutant germaria contained 7.5–8.5 germline SSCs oriented either towards *ab* or *EcR* mutant or niche cells. *UAS EcR.A* and *UAS EcR.B1* expressed by the niche cell-specific driver *bab1Gal4* also caused formation of an enlarged niche (on average 10 CpCs in comparison to 6 in control, Figure 7F, G and K; Supplementary Table S6) and appearance of supernumerary SSCs (Figure 7H and I; Supplementary Table S6). To test if these excessive niches were able to host extra stem cells, we analysed the number of GSCs per germarium by staining mutant germaria with specific markers. We observed that in *tai* and *EcR* mutants additional SSCs that are touching expanded niches are positive for the stem cell marker pMad and do not stain positively for the differentiation factor Bam (Figure 7H–K). The number of pMad-positive GSCs per germarium significantly increased in clonal *tai* mutants (4.47 ± 0.26 ($P = 4.29 \times 10^{-7}$, $n = 15$) in *tai*^{61G1}*FRT40A/UbiGFP FRT40A*;*bab1Gal4Flp* in comparison to 2.18 ± 0.26 ($n = 12$) in control) and ecdysone mutants (3.50 ± 0.43 ($P = 0.02$, $n = 6$) in *UAS EcR.A bab1Gal4* and 3.33 ± 0.29 ($P = 0.01$, $n = 9$) in *UAS EcR.B1 bab1Gal4* in comparison to 2.36 ± 0.20 ($n = 11$) in *UASlacZ*, *bab1Gal4* control). These observations infer that additional cells in enlarged niches are functional and can facilitate extra GSCs. We assume that during development the ecdysone signalling pathway has a role in the establishment of the stem cell niche.

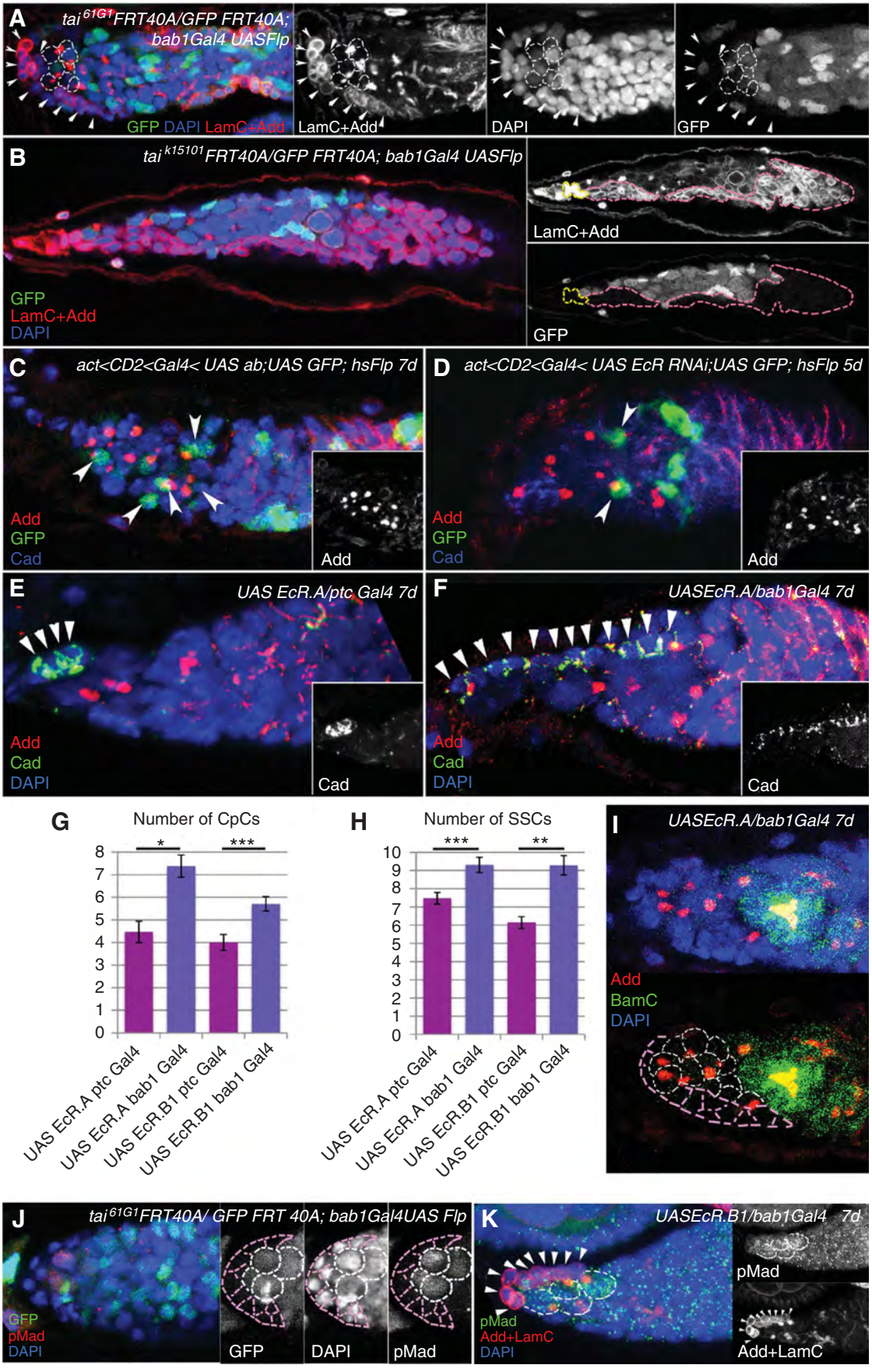

Discussion

Here, we show for the first time that in *Drosophila* ecdysone signalling regulates differentiation of a GSC daughter and modulates ovarian stem cell niche size (Figure 8). The delay in GSC progeny differentiation correlates with reduced expression levels of TGF-β pathway components. Based on expression patterns it appears that germarial somatic cells, niche and ECs are the critical sites of ecdysteroid action and a co-activator of ecdysone receptor, Taiman is the spatially restricted regulator of ecdysone signalling in soma. During adulthood the ecdysone pathway has a specific role in EC differentiation and soma–germline cell contact establishment. In addition, during development the ecdysone signalling pathway has a role in somatic niche formation (Figure 8).

Ecdysteroids in general control major developmental transformations such as metamorphosis and morphogenesis in *Drosophila*. Different tissues and even different cell types within the same tissue respond to this broad signalling in a specific fashion and in a timely manner. In the developing *Drosophila* ovary steroid hormone receptors are expressed in a well-timed mode, high levels coinciding with proliferative and immature stages and low levels preceding reduced DNA replication and differentiation (Hodin and Riddiford, 1998). Mutations in ecdysone pathway components affect ovarian morphogenesis, including heterochronic delay or acceleration in the onset of TF differentiation. During the niche establishment the levels of both ecdysone receptors, EcR and USP are greatly downregulated in anterior somatic cells that will contribute to the niche *per se* (Hodin and Riddiford, 1998). Now, we show that perturbation of ecdysone signalling in pre-adult ovarian soma leads to the formation of enlarged niches. The specific response to systemic hormonal signalling in niche precursors is achieved by a specific function of the ecdysone receptor co-activator Taiman. When timely regulation of ecdysone signalling does not occur, more cells are recruited to become niche cells resulting in enlarged niches that are capable to host more stem cells. These data first show that ecdysone steroid hormonal signalling regulates the formation of the adult stem cell niche and suggest that a developmental tuning of ecdysone signalling controls the number of anterior somatic cells that will differentiate into CpCs.

It is logical that stem cell division and germline differentiation are regulated by some systemic signalling depending on the general state of the organism, which depends on age, nutrition, environmental conditions and so on. Hormones are great candidates for this type of regulation as they act in a paracrine fashion and their levels are changing in response to ever-changing external and internal conditions. Steroid binding to nuclear receptors in vertebrates triggers a conformational switch accompanied by increased histone acetylation that permits transcriptional co-activators binding and the transcription initiation complex assembly (Collingwood *et al*, 1999; Privalsky, 2004). In *Drosophila*, the trithorax-related protein, a histone H3 methyltransferase that like Taiman belongs to the p160 class of co-activators, and an ISWI-containing ATP-dependent chromatin remodelling complex (NURF), that regulates transcription by catalysing nucleosome sliding, both bind EcR in an ecdysone-dependent manner (Sedkov *et al*, 2003; Badenhorst *et al*, 2005), showing that chromatin modifications can mediate response to this general signalling. Transcriptional regulation has a key role in GSC maintenance and differentiation, for example, the TGF-β ligand dpp secreted by niche cells induces phosphorylation of the transcription factor Mad in GSCs that in turn suppresses transcription of the differentiation factor Bam (McKearin and Ohlstein, 1995; Xie and Spradling, 1998; Chen and

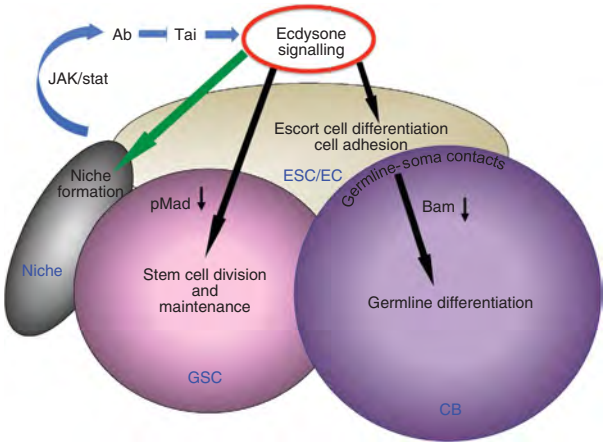

Figure 8 Model showing the role of the ecdysone signalling in *Drosophila* ovarian stem cell niche. During development (green arrow) ecdysone signalling participates in defining the stem cell niche size. During adulthood (black arrows) this hormonal pathway has a dual role in regulation of early germline differentiation: regulation of cell contacts and cell shape rearrangements via adjustment of adhesion complexes and cytoskeletal proteins in ESCs and their progeny and control of the potency of TGF-β signalling.

Figure 7 Ecdysone signalling is required for niche formation. (**A**) Downregulation of tai^{61G1} before the niche is established (tai^{G161}*FRT40A/UbiGFP FRT40A*; *bab1Gal4 UASFlp*) causes significant niche enlargement (CpCs marked with arrowheads) that allows to anchor more GSC-like cells (marked with white dashed lines). (**B**) In some extreme cases tai^{k15101} mutant somatic cells (marked with pink dashed lines) encapsulate the whole germarium that is filled with SSCs. CpCs are marked with yellow dashed lines. (**C**) Clonal overexpression of the Tai repressor Ab (*UAS<CD2<Gal4 UAS ab*; *UAS GFP*; *hsFlp*) in somatic cells results in the appearance of supernumerary SSCs that are anchored to *UAS ab* cells marked by GFP. (**D**) The same can be observed in somatic clonal *EcR* mutant cells (*UAS<CD2<Gal4 UAS EcR RNAi*; *UAS GFP*; *hsFlp*). (**E**, **F**) The pre-adult expression of exogenous EcR only in the niche progenitor cells (*bab1Gal4*, **F**), but not in other somatic cells (*ptcGal4*, **E**) results in the appearance of enlarged niches marked by DE-Cadherin (arrowheads). The average numbers of CpCs (**G**) and SSCs (**H**) are significantly increased when *UAS EcR.A* or *UAS EcR.B1* are overexpressed during the niche establishment in most anterior pre-niche somatic cells (*bab1Gal4*), but not in other intermingled somatic cells (*ptcGal4*) within the larval ovary. (**I**) The niche expansion increases the number of SSCs that are also negative for the differentiation marker BamC. Niche is outlined with pink and GSCs with white dashed lines. (**J**, **K**) The enlarged *tai* clonal niches (tai^{61G1}*FRT 40A/Ubi GFP FRT 40A*; *bab1 Gal4 Flp*) and niches overexpressing EcR bear a higher number of GSCs whose identity is confirmed by the stem cell marker pMad. Niche is outlined with pink dashed lines in (**J**) and arrowheads in (**K**), GSCs are marked with white dashed lines. (**A**–**F**, **I**–**K**) Projections of optical sections assembled through the germarial tissue are shown. Red, Adducin + LaminC (**A**, **B**, **K**), Adducin (**C**–**F**, **I**), pMad (**J**); blue, DAPI; and green, GFP (**A**–**D**, **J**), Cadherin (**E**, **F**), BamC (**I**), pMad (**K**). Error bars represent s.e.m. $*P<0.05$, $**P<0.005$, $***P<0.0005$.

McKearin, 2003; Song *et al*, 2004). In addition, it has been shown recently that in *Drosophila* adult GSC ecdysone modulates the strength of TGF-β signalling through a functional interaction with the chromatin remodelling factors ISWI and Nurf301, a subunit of the ISWI-containing NURF chromatin remodelling complex (Ables and Drummond-Barbosa, 2010). Therefore, it is plausible that ecdysone regulates Mad expression cell autonomously via chromatin modifications. As pMad directly suppresses a differentiation factor Bam, it is expected that Bam would be expressed in pMad-negative cells. Interestingly, our findings show that ecdysone deficit decreases amounts of phosphorylated Mad in GSCs and also cell non-autonomously suppresses Bam in SSCs. As SSCs that express neither pMad nor Bam are accumulated when the ecdysone pathway is perturbed it suggests that there should be an alternative mechanism of Bam regulation. Even though eventually this still can be done on the level of chromatin modification, our data suggest that the origin of this soma-generated signal may be associated with cell adhesion protein levels. Further understanding of the nature of this signalling is of a great interest.

The progression of oogenesis within the germarium requires cooperation between two stem cell types, germline and somatic (escort) stem cells. In *Drosophila*, reciprocal signals between germline and escort (in female) or somatic cyst (in male) cells can inhibit reversion to the stem cell state (Brawley and Matunis, 2004; Kai and Spradling, 2004) and restrict germ cell proliferation and cyst growth (Matunis *et al*, 1997). Therefore, the non-autonomous ecdysone effect can be explained by the necessity of two stem cell types that share the same niche (GSC and ESC) to coordinate their division and progeny differentiation. This coordination is most likely achieved via adhesive cues, as disruption of ecdysone signalling affects turnover of adhesion complexes and cytoskeletal proteins in somatic ECs: mutant cells exhibited abnormal accumulation of DE-Cadherin, β-catenin/Armadillo and Adducin.

Cell adhesion has a crucial role in *Drosophila* stem cells; GSCs are recruited to and maintained in their niches via cell adhesion (Song *et al*, 2002). Two major components of this adhesion process, DE-Cadherin and Armadillo/β-catenin, accumulate at high levels in the junctions between GSCs and niche cells, while in the developing CB and ECs levels of these proteins are strongly reduced. Levels of DE-Cadherin in GSCs are regulated by various signals, for example, nutrition activation of insulin signalling or chemokine activation of STAT (Hsu and Drummond-Barbosa, 2009; Leatherman and Dinardo, 2010), and here we show that in ESCs it is regulated by steroid hormone signalling. Possibly, these two stem cell types respond to different signals but then differentiation of their progeny is synchronised via cell contacts. While hormones, growth factors and cytokines certainly manage stem cell maintenance and differentiation, our evidence also reveals that the responses to hormonal stimuli are strongly modified by adhesive cues.

Specificity to endocrine signalling can be achieved via availability of co-factors in the targeted tissue. Tai is a spatially restricted co-factor that cooperates with the EcR/USP nuclear receptor complex to define appropriate responses to globally available hormonal signals. Tai-positive regulation of ecdysone signalling can be alleviated by Abrupt via direct binding of these two proteins that prevents Tai association with EcR/USP (Jang *et al*, 2009). Abrupt has been shown to be downregulated by JAK/STAT signalling (Jang *et al*, 2009). Interestingly, JAK/STAT signalling also has a critical role in ovarian niche function and controls the morphology and proliferation of ESCs as well as GSCs (Decotto and Spradling, 2005). JAK/STAT signalling may interact with ecdysone pathway components in ECs to further modulate cell type-specific responses to global endocrine signalling. A combination of regulated by different signalling pathway factors that are also spatially and timely restricted builds a network that ensures the specificity of systemic signalling.

Knowledge of how steroids regulate stem cells and their niche has a great potential for stem cell and regenerative medicine. Our findings open the way for a detailed analysis of a role for steroid hormones in niche development and regulation of germline differentiation via adjacent soma.

Materials and methods

Fly stocks

Drosophila melanogaster stocks were raised on standard cornmeal-yeast-agar-medium at 25°C unless otherwise stated. Clones were induced using the *hsFlp/FRT* system for mitotic recombination. The following stocks were used: $y^{d2}w^{1118}$;tai^{k15101} *FRT40A/CyO* (DGRC Kyoto), $dp^{ov}tai^{61G1}$*FRT40A/CyO*, $tai^{01351}cn^{1}$/*CyO*;ry^{506}, w^{1118}; $tai^{BG02711}$, $tai^{KG02309}$/*CyO*, w^{1118};$y^{1}w^{67c23}$;$tai^{EY11718}$/*CyO*, w^{1118};*pUASt tai*, EcR^{M554fs}/*SM6b*, EcR^{Q50st}/*SM6b*, w^{1118};*hs-GAL4-EcR.LBD*, w^{1118}; *hs-GAL4-usp.LBD*, w^{1118};*EcRE.lacZ*, w^{1118};*hs-EcR.B1*, w^{1118},*hs-EcR.A*, w^{1118};*UAS-EcR-RNAi*^{97}, w^{1118},*UAS-EcR-RNAi*^{104}, usp^{4}/*FM7a*, usp^{EP1193}, w^{1118};*UAS-EcR.A*, *w*[*];*UAS-EcR.B1*, w^{1118};*UAS-ab.B*, *UAS-lacZ*, $ecd1^{218}$, ecd^{4210} (Bloomington Stock Centre), *tai G00308/CyO* (Carnegie GFP trap line), *tai RNAi* (w^{1118}; P{GD4265}, VDRC), *BamGFP* (Dennis McKearin), w^{1118} was used for wild-type analysis.

Transheterozygous interaction

We used the amorph and hypomorph *tai* alleles and ecdysone pathway mutants EcR^{Q50st}/*SM6b* or usp^{4}/*FM7a*, usp^{EP1193}. Both the number of GSCs (single spectrosome cells that are touching the CpCs) and the number of CpCs itself were counted. As a control, $dp^{ov}tai^{61G1}$*FRT40A/CyO* and $y^{d2}w^{1118}$; tai^{k15101}*FRT40A/CyO* were crossed to w^{1118} flies.

Disruption of EcR in soma

To specifically disrupt the ecdysone signalling in the somatic cells of the germarium, w^{1118};*UAS EcR RNAi*^{97}, w^{1118},*UAS EcR RNAi*^{104}, w^{1118};*UAS ab.B* or *tai RNAi* (w^{1118}; P{*GD4265*}), females were crossed to *ptcGal4*; $tubGal80^{ts}$ or $tubGal80^{ts}$; *bab1Gal4/TM6* males at 18°C. The hatched flies were then transferred to 29°C and aged for 7, 14 and 21 days. Controls were treated the same.

Clonal analysis

Germline and somatic cell clones were done as described previously (Shcherbata *et al*, 2004, 2007) using *hsFlp/FRT* system for mitotic recombination. Early formation of clones in CpCs and ESCs were obtained via crossing $y^{d2}w^{1118}$; tai^{k15101}*FRT40A/CyO* and dp^{ov}-tai^{61G1}*FRT40A/CyO* to *Ubi-GFP FRT40A/CyO*; *bab1Gal4*:*UAS-Flp/TM2* flies (gift from A González-Reyes). Mutant clones were identified by the absence of GFP.

To induce adult clones $y^{d2}w^{1118}$; tai^{k15101}*FRT40A/CyO* and $dp^{ov}tai^{61G1}$*FRT40A/CyO* males were crossed to *hsFlp*; *FRT40A GFP/CyO* females. 2–4-day-old adult F1 females were heat shocked in empty vials for 60 min 2 days in a row in a 37°C water bath and analysed 5, 7, and 12, 14 days after heat shock. CpC and ESC clones were identified by the absence of GFP.

For generation of somatic ovarian clones we crossed *hsFlp*;; *UASt GFPact>FRT-CD2-FRT>Gal4/TM3* males to w^{1118};*UAS ab.B* or w^{1118},*UAS EcR RNAi* females. Third instar larvae were heat shocked 2 days in a row for 2 h. Clonal cells expressing *ab.B* or *EcR RNAi* were identified by GFP expression.

Overexpression analysis

For overexpression of EcR isoforms in adult flies, w^{1118};*hsEcR.A* flies were crossed to w^{1118} flies. The offspring with one copy of the transgene were heat shocked (37°C) twice per day for 30 min 4 or 7 days in a row. Controls were heat shocked as well. Furthermore, flies with a copy of the *hsEcR.A* transgene were kept at 25°C without heat treatment.

To overexpress the different EcR isoforms specifically in the soma w^{1118};*UAS EcR.A* and w^{1118};*UAS EcR.B1* (Bloomington Stock Center) were crossed to *bab1Gal4/TM6* or *ptcGal4*.

Alteration of ecdysone signalling

To supply more ecdysone hormone, 20-Hydroxyecdysone (20E, Sigma-Aldrich) was diluted in 5% ethanol to a 1 μM concentration and mixed with dry yeast to reach a dough-like consistency. The mixture was then placed on top of agar juice plates to culture flies. In all, 5% ethanol was used for controls.

The $ecd1^{ts}$ temperature-sensitive mutation is known to reduce ecdysone levels at the non-permissive temperature. Fly stocks were kept at the permissive temperature (18°C) and adult flies were shifted to the restrictive temperature (29°C) in order to block ecdysone synthesis. As a control, wild-type flies were kept at 29°C for the same time and $ecd1^{ts}$ flies that had not been shifted to 29°C were analysed.

w^{1118};*hs-GAL4-EcR.LBD* and w^{1118};*hs-GAL4-usp.LBD* (Kozlova and Thummel, 2002) animals were heat shocked 30 min/day, 1–3 days in a row.

Ecdysone signalling pattern

To analyse the ecdysone signalling in the germarium, w^{1118};*hs-GAL4-EcR.LBD* and w^{1118};*hs-GAL4-usp.LBD* (Kozlova and Thummel, 2002) females were crossed to *UAS-lacZ* males. Flies were heat shocked for 60 min in a water bath before they were fixed and stained. *EcRE-lacZ*, a homozygous viable stock with seven EcREs inserted into a *lacZ* promoter was used to determine the pattern of ecdysone signalling (Koelle *et al*, 1991). Adult flies were stained for β-galactosidase. Taiman expression was identified with the *tai G00308/CyO* enhancer-trap line (Morin *et al*, 2001).

Immunofluorescence and antibodies

Ovaries were fixed in 5% formaldehyde (Polysciences, Inc.) for 10 min and the staining procedure was performed as described (Shcherbata *et al*, 2004). We used the following mouse monoclonal antibodies: anti-Armadillo (1:40); anti-Adducin (1:50), anti-LaminC (1:50), anti-EcR Ag10.2 (1:20, EcR common region) (Developmental Studies Hybridoma Bank), anti-usp (1:50, RB Olano, F Kafatos), rat anti-DE-Cadherin (1:50, DSHB), anti-BamC (1:1000, D McKearin) and rat anti-Vasa (1:1000, P Lasko), rabbit anti-pMad (1:5000, D Vasiliauskas, S Morton, T Jessell and E Laufer), anti-β-Gal (1:1000), rabbit anti-tai (1:1000, D Montell), rabbit anti-PH3 (1:3000, Upstate Biotechnology) and anti-GFP-directly conjugated with AF488 (1:3000, Invitrogen), Alexa 488, 568 or 633 goat anti-mouse, anti-rabbit (1:500, Molecular Probes), goat anti-rat Cy5 (1:250, Jackson Immunoresearch). Images were obtained with a confocal laser-scanning microscope (Leica SPE5) and processed with Adobe Photoshop.

Analysis and statistics

To determine the number of CpCs, LaminC-positive cells on the tip of the germarium were counted. Single spectrosome cells that were touching the niche cells were counted as GSCs. Single spectrosome cells that were not touching the niche were counted separately. In addition, the number of fusomes (indicating the number of cysts) until region 2B, where follicle cells start cyst encapsulation, was counted. To describe the differentiation in a given germarium the number of cysts was divided by the number of SSCs (ratio = cysts/SSCs). The percentage of germaria-containing dumbbell-shaped fusomes (McKearin and Ohlstein, 1995) was counted. The intensity of the pMad-positive area was determined via measuring the grey value in at least 10 GSCs with Leica LAS AF Lite software, the background levels were measured by the intensity of the pMad-negative area in the germarium. Background levels were subtracted to normalise the levels of antibody staining in different germaria. Intensity levels relative to control were calculated. GSC maintenance was determined by comparison of the percentage of germaria with clonal GSCs between two different time points after clonal induction.

χ^2-test was used to determine if the percentage of dumbbell-shaped fusomes was significantly increased. For all other statistical analyses, the two-tailed Student's *t*-test was performed.

Supplementary data

Supplementary data are available at *The EMBO Journal* Online (http://www.embojournal.org).

Acknowledgements

We thank Hannele Ruohola-Baker, Acaimo González-Reyes, Dennis McKearin, Ed Laufer, Denise Montell, Rosa Barrio Olano and Fotis Kafatos for flies and reagents, Department of Stefan Hell for use of confocal microscope, April Marrone and Mariya Kucherenko for comments on the manuscript and Department of Herbert Jäckle for discussion. The Max Planck Society supported this work.

Conflict of interest

The authors declare that they have no conflict of interest.

References

Ables ET, Drummond-Barbosa D (2010) The steroid hormone ecdysone functions with intrinsic chromatin remodeling factors to control female germline stem cells in Drosophila. *Cell Stem Cell* **7:** 581–592

Badenhorst P, Xiao H, Cherbas L, Kwon SY, Voas M, Rebay I, Cherbas P, Wu C (2005) The Drosophila nucleosome remodeling factor NURF is required for ecdysteroid signaling and metamorphosis. *Genes Dev* **19:** 2540–2545

Bai J, Uehara Y, Montell DJ (2000) Regulation of invasive cell behavior by taiman, a Drosophila protein related to AIB1, a steroid receptor coactivator amplified in breast cancer. *Cell* **103:** 1047–1058

Beckstead R, Ortiz JA, Sanchez C, Prokopenko SN, Chambon P, Losson R, Bellen HJ (2001) Bonus, a Drosophila homolog of TIF1 proteins, interacts with nuclear receptors and can inhibit betaFTZ-F1-dependent transcription. *Mol Cell* **7:** 753–765

Boulanger CA, Smith GH (2009) Reprogramming cell fates in the mammary microenvironment. *Cell Cycle* **8:** 1127–1132

Brawley C, Matunis E (2004) Regeneration of male germline stem cells by spermatogonial dedifferentiation *in vivo*. *Science* **304:** 1331–1334

Buszczak M, Freeman MR, Carlson JR, Bender M, Cooley L, Segraves WA (1999) Ecdysone response genes govern egg chamber development during mid-oogenesis in Drosophila. *Development* **126:** 4581–4589

Chen D, McKearin DM (2003) A discrete transcriptional silencer in the bam gene determines asymmetric division of the Drosophila germline stem cell. *Development* **130:** 1159–1170

Cherbas L, Lee K, Cherbas P (1991) Identification of ecdysone response elements by analysis of the Drosophila Eip28/29 gene. *Genes Dev* **5:** 120–131

Collingwood TN, Urnov FD, Wolffe AP (1999) Nuclear receptors: coactivators, corepressors and chromatin remodeling in the control of transcription. *J Mol Endocrinol* **23:** 255–275

de Cuevas M, Spradling AC (1998) Morphogenesis of the Drosophila fusome and its implications for oocyte specification. *Development* **125:** 2781–2789

Decotto E, Spradling AC (2005) The Drosophila ovarian and testis stem cell niches: similar somatic stem cells and signals. *Dev Cell* **9:** 501–510

Dobens L, Rudolph K, Berger EM (1991) Ecdysterone regulatory elements function as both transcriptional activators and repressors. *Mol Cell Biol* **11:** 1846–1853

Dressel U, Thormeyer D, Altincicek B, Paululat A, Eggert M, Schneider S, Tenbaum SP, Renkawitz R, Baniahmad A (1999)

Alien, a highly conserved protein with characteristics of a corepressor for members of the nuclear hormone receptor superfamily. *Mol Cell Biol* **19:** 3383–3394
Elke C, Vogtli M, Rauch P, Spindler-Barth M, Lezzi M (1997) Expression of EcR and USP in Escherichia coli: purification and functional studies. *Arch Insect Biochem Physiol* **35:** 59–69
Francis VA, Zorzano A, Teleman AA (2010) dDOR is an EcR coactivator that forms a feed-forward loop connecting insulin and ecdysone signaling. *Curr Biol* **20:** 1799–1808
Gates J, Lam G, Ortiz JA, Losson R, Thummel CS (2004) Rigor mortis encodes a novel nuclear receptor interacting protein required for ecdysone signaling during Drosophila larval development. *Development* **131:** 25–36
Gaziova I, Bonnette PC, Henrich VC, Jindra M (2004) Cell-autonomous roles of the ecdysoneless gene in Drosophila development and oogenesis. *Development* **131:** 2715–2725
Gonczy P (2008) Mechanisms of asymmetric cell division: flies and worms pave the way. *Nat Rev Mol Cell Biol* **9:** 355–366
Hodin J, Riddiford LM (1998) The ecdysone receptor and ultraspiracle regulate the timing and progression of ovarian morphogenesis during Drosophila metamorphosis. *Dev Genes Evol* **208:** 304–317
Hsu HJ, Drummond-Barbosa D (2009) Insulin levels control female germline stem cell maintenance via the niche in Drosophila. *Proc Natl Acad Sci USA* **106:** 1117–1121
Jang AC, Chang YC, Bai J, Montell D (2009) Border-cell migration requires integration of spatial and temporal signals by the BTB protein Abrupt. *Nat Cell Biol* **11:** 569–579
Kai T, Spradling A (2004) Differentiating germ cells can revert into functional stem cells in Drosophila melanogaster ovaries. *Nature* **428:** 564–569
Koelle MR, Talbot WS, Segraves WA, Bender MT, Cherbas P, Hogness DS (1991) The Drosophila EcR gene encodes an ecdysone receptor, a new member of the steroid receptor superfamily. *Cell* **67:** 59–77
Kozlova T, Thummel CS (2002) Spatial patterns of ecdysteroid receptor activation during the onset of Drosophila metamorphosis. *Development* **129:** 1739–1750
Kozlova T, Thummel CS (2003) Essential roles for ecdysone signaling during Drosophila mid-embryonic development. *Science* **301:** 1911–1914
Leatherman JL, Dinardo S (2010) Germline self-renewal requires cyst stem cells and stat regulates niche adhesion in Drosophila testes. *Nat Cell Biol* **12:** 806–811
Matunis E, Tran J, Gonczy P, Caldwell K, DiNardo S (1997) punt and schnurri regulate a somatically derived signal that restricts proliferation of committed progenitors in the germline. *Development* **124:** 4383–4391
Mauvezin C, Orpinell M, Francis VA, Mansilla F, Duran J, Ribas V, Palacin M, Boya P, Teleman AA, Zorzano A (2010) The nuclear cofactor DOR regulates autophagy in mammalian and Drosophila cells. *EMBO Rep* **11:** 37–44
McBrayer Z, Ono H, Shimell M, Parvy JP, Beckstead RB, Warren JT, Thummel CS, Dauphin-Villemant C, Gilbert LI, O'Connor MB (2007) Prothoracicotropic hormone regulates developmental timing and body size in Drosophila. *Dev Cell* **13:** 857–871
McKearin D, Ohlstein B (1995) A role for the Drosophila bag-of-marbles protein in the differentiation of cystoblasts from germline stem cells. *Development* **121:** 2937–2947
Morin X, Daneman R, Zavortink M, Chia W (2001) A protein trap strategy to detect GFP-tagged proteins expressed from their endogenous loci in Drosophila. *Proc Natl Acad Sci USA* **98:** 15050–15055
Oro AE, McKeown M, Evans RM (1992) The Drosophila retinoid X receptor homolog ultraspiracle functions in both female reproduction and eye morphogenesis. *Development* **115:** 449–462
Privalsky ML (2004) The role of corepressors in transcriptional regulation by nuclear hormone receptors. *Annu Rev Physiol* **66:** 315–360
Riddiford LM (1993) Hormone receptors and the regulation of insect metamorphosis. *Receptor* **3:** 203–209
Riddihough G, Pelham HR (1987) An ecdysone response element in the Drosophila hsp27 promoter. *EMBO J* **6:** 3729–3734
Schubiger M, Carre C, Antoniewski C, Truman JW (2005) Ligand-dependent de-repression via EcR/USP acts as a gate to coordinate the differentiation of sensory neurons in the Drosophila wing. *Development* **132:** 5239–5248
Schubiger M, Truman JW (2000) The RXR ortholog USP suppresses early metamorphic processes in Drosophila in the absence of ecdysteroids. *Development* **127:** 1151–1159
Sedkov Y, Cho E, Petruk S, Cherbas L, Smith ST, Jones RS, Cherbas P, Canaani E, Jaynes JB, Mazo A (2003) Methylation at lysine 4 of histone H3 in ecdysone-dependent development of Drosophila. *Nature* **426:** 78–83
Shcherbata HR, Althauser C, Findley SD, Ruohola-Baker H (2004) The mitotic-to-endocycle switch in Drosophila follicle cells is executed by Notch-dependent regulation of G1/S, G2/M and M/G1 cell-cycle transitions. *Development* **131:** 3169–3181
Shcherbata HR, Ward EJ, Fischer KA, Yu JY, Reynolds SH, Chen CH, Xu P, Hay BA, Ruohola-Baker H (2007) Stage-specific differences in the requirements for germline stem cell maintenance in the Drosophila ovary. *Cell Stem Cell* **1:** 698–709
Shea MJ, King DL, Conboy MJ, Mariani BD, Kafatos FC (1990) Proteins that bind to Drosophila chorion cis-regulatory elements: a new C2H2 zinc finger protein and a C2C2 steroid receptor-like component. *Genes Dev* **4:** 1128–1140
Shirras AD, Bownes M (1987) Separate DNA sequences are required for normal female and ecdysone-induced male expression of Drosophila melanogaster yolk protein 1. *Mol Gen Genet* **210:** 153–155
Song X, Wong MD, Kawase E, Xi R, Ding BC, McCarthy JJ, Xie T (2004) Bmp signals from niche cells directly repress transcription of a differentiation-promoting gene, bag of marbles, in germline stem cells in the Drosophila ovary. *Development* **131:** 1353–1364
Song X, Zhu CH, Doan C, Xie T (2002) Germline stem cells anchored by adherens junctions in the Drosophila ovary niches. *Science* **296:** 1855–1857
Tanentzapf G, Devenport D, Godt D, Brown NH (2007) Integrin-dependent anchoring of a stem-cell niche. *Nat Cell Biol* **9:** 1413–1418
Terashima J, Bownes M (2005) A microarray analysis of genes involved in relating egg production to nutritional intake in Drosophila melanogaster. *Cell Death Differ* **12:** 429–440
Tsai CC, Kao HY, Yao TP, McKeown M, Evans RM (1999) SMRTER, a Drosophila nuclear receptor coregulator, reveals that EcR-mediated repression is critical for development. *Mol Cell* **4:** 175–186
Walker MR, Patel KK, Stappenbeck TS (2009) The stem cell niche. *J Pathol* **217:** 169–180
Ward EJ, Shcherbata HR, Reynolds SH, Fischer KA, Hatfield SD, Ruohola-Baker H (2006) Stem cells signal to the niche through the Notch pathway in the Drosophila ovary. *Curr Biol* **16:** 2352–2358
Xie T, Spradling AC (1998) Decapentaplegic is essential for the maintenance and division of germline stem cells in the Drosophila ovary. *Cell* **94:** 251–260
Xie T, Spradling AC (2000) A niche maintaining germ line stem cells in the Drosophila ovary. *Science* **290:** 328–330
Yao TP, Segraves WA, Oro AE, McKeown M, Evans RM (1992) Drosophila ultraspiracle modulates ecdysone receptor function via heterodimer formation. *Cell* **71:** 63–72
Zheng X, Wang J, Haerry TE, Wu AY, Martin J, O'Connor MB, Lee CH, Lee T (2003) TGF-beta signaling activates steroid hormone receptor expression during neuronal remodeling in the Drosophila brain. *Cell* **112:** 303–315

Supplementary Figure Legends

Supplementary Figure 1. PH3 staining reveals, that the high number of SSCs that is caused by EcR overexpression is not due to fusome breakdown.

(A) Cells in developing germline cysts that are connected via a fusome are dividing simultaneously as shown here by PH3 mitotic marker. **(B)** The SSCs that are observed upon exogenous *hsEcR.A* expression do not have their division synchronized. Red, Adducin+LaminC; blue, DAPI; and green PH3**.**

Supplementary Figure 2. Tai expression in escort cells.

(A-B) To confirm the specificity of Tai antibody staining in escort cells we generated *tai* loss of function somatic clones *(hs Flp*; tai^{61G1} *FRT40A/UbiGFP FRT40A)* and observed that Tai staining is diminished in *tai* mutant cells. Compare levels of antibody staining in *tai* mutant escort cell (white arrows) and sister clones (green arrows).

Red, Taiman; blue, DAPI; and green, GFP.

Supplementary Figure 3.

Tai is not required for progressive oocyte development and GSC maintenance.

(A) tai^{61G1} loss of function clones in the germarium do not affect the steady production of egg chambers, showing that loss of Tai does not affect GSC division or oocyte differentiation.

(B) tai^{61G1} or tai^{k15101} mutations do not affect the maintenance of GSC compared to parental GSC clones.

Red, Adducin+LaminC; blue, DAPI; and green, GFP.

Supplementary Figure 4. *ptcGal4* and *bab1Gal4*, the drivers used in this study drive *UAS lacZ* expression in the somatic cells of the germarium

Whereas *bab1Gal4* (*UAS lacZ/+; bab1Gal4/+***)** drives expression in CpCs (pink arrowheads), ECs and FCs **(A),** *ptcGal4* (*UAS lacZ/ptcGal4)* is only active in ECs and FCs, but not in the CpCs (pink arrowheads, **B)**.

(A, B) are projections of optical sections assembled through the germarial tissue. Red, Adducin+LaminC; blue, DAPI; and green, β-Galactosidase**.**

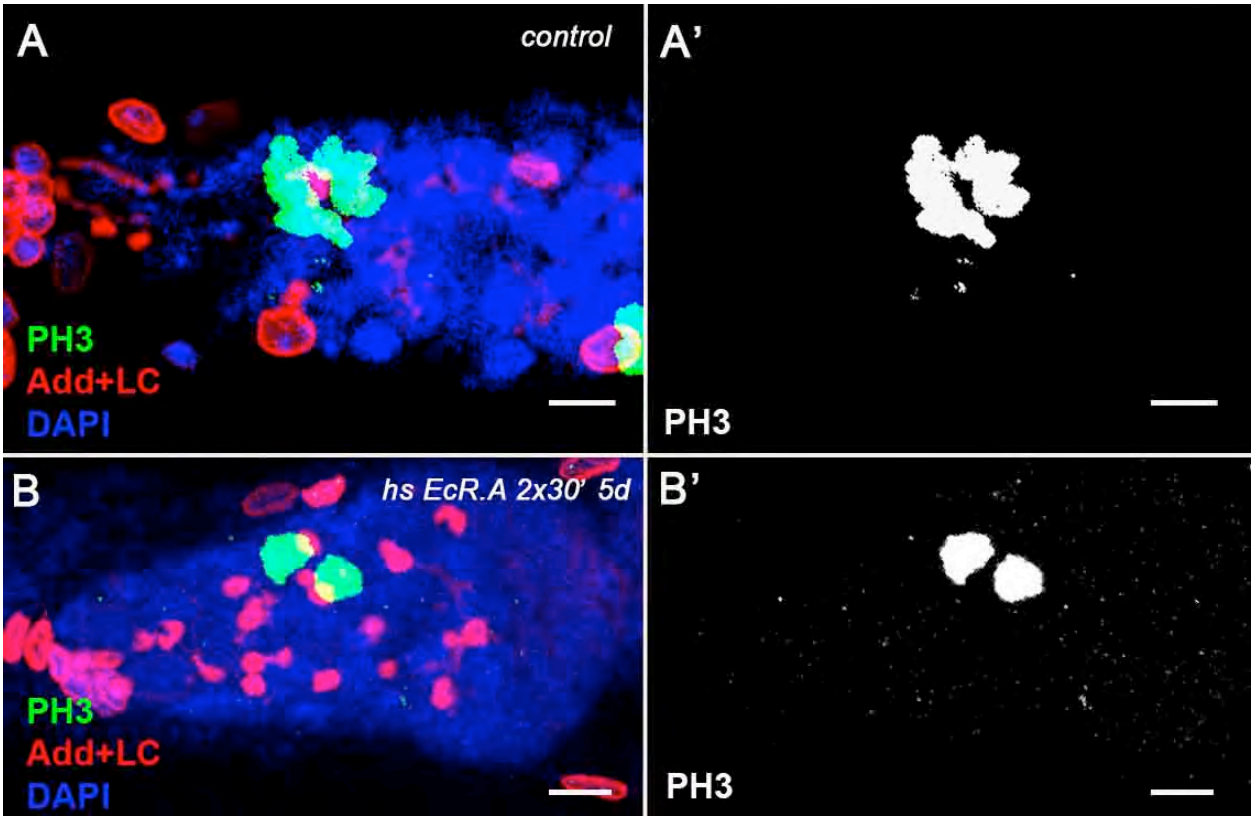

Supplementary Figure 1

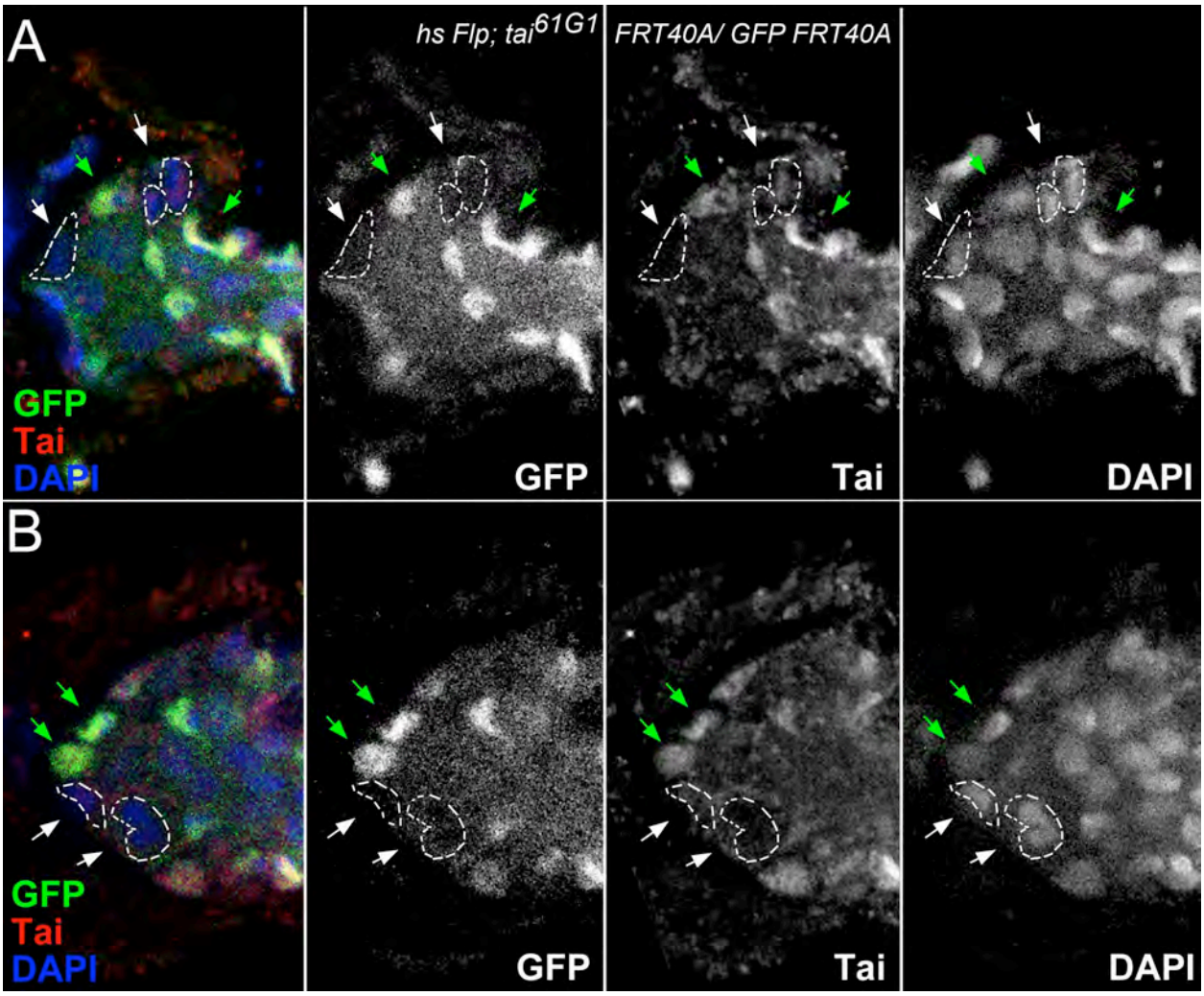

Supplementary Figure 2

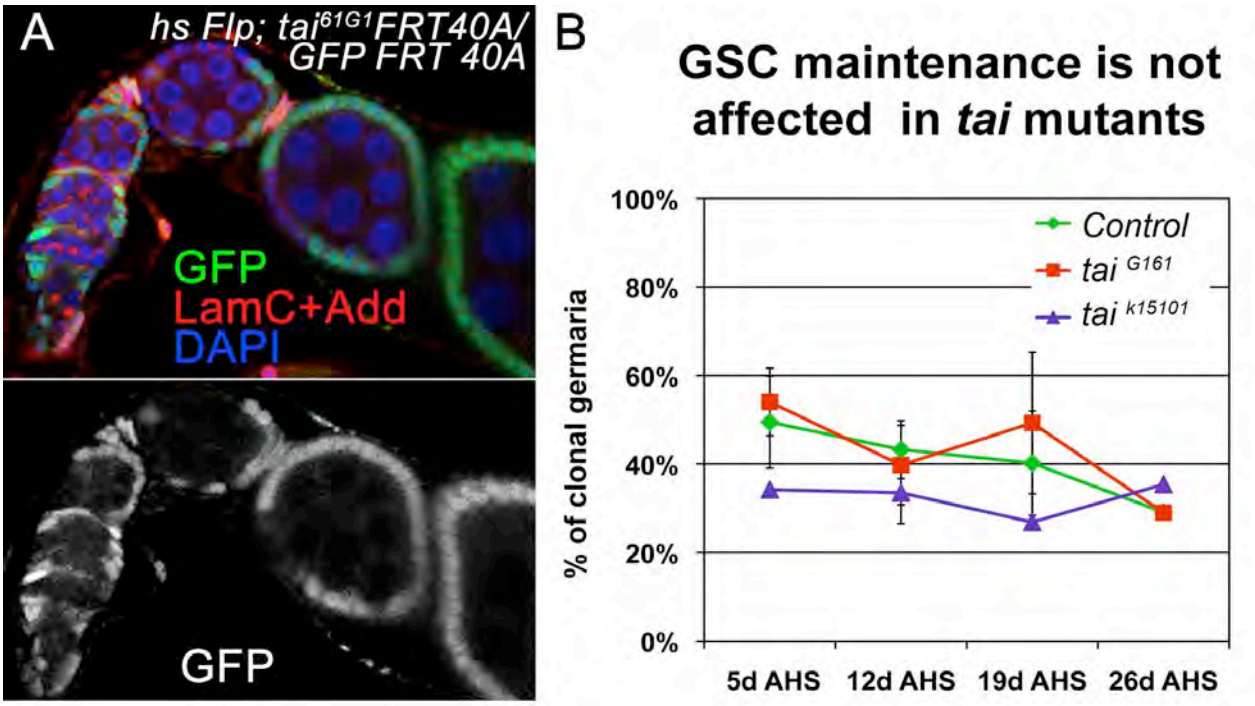

Supplementary Figure 3

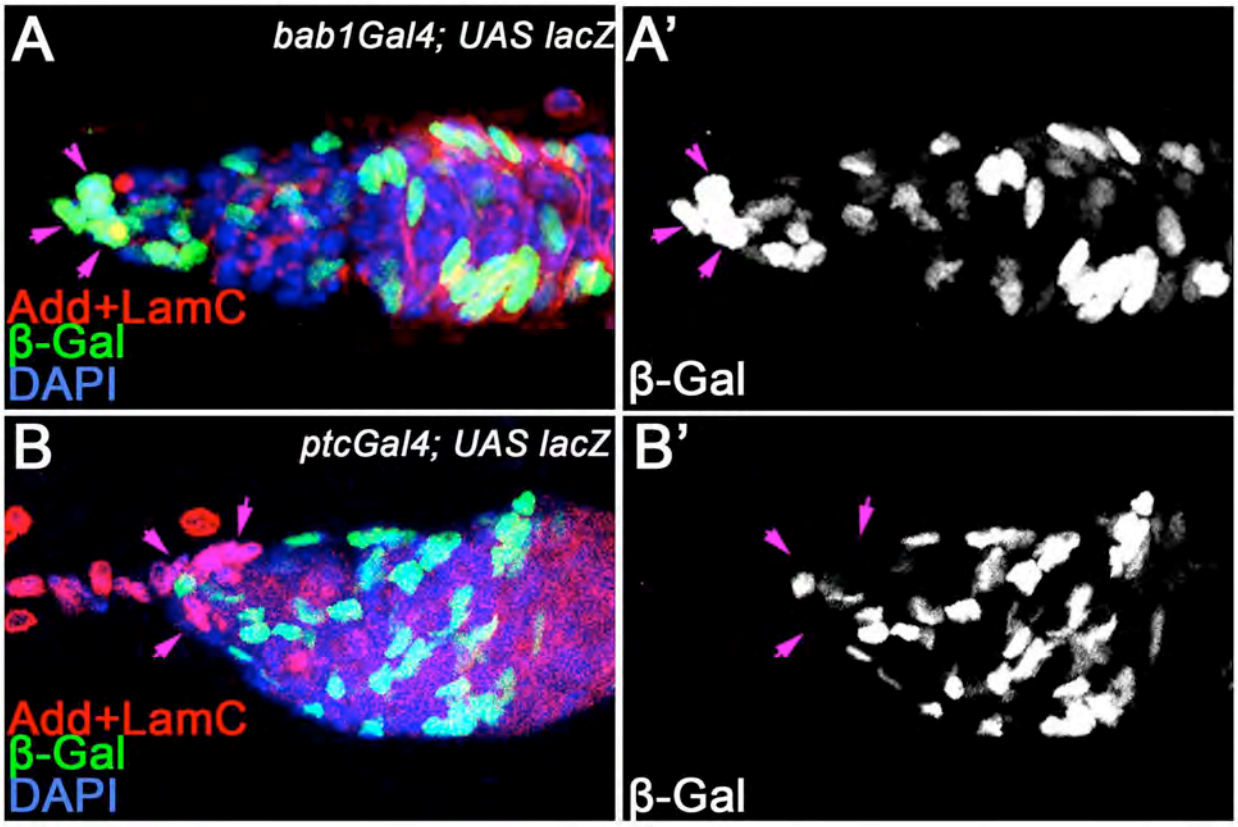

Supplementary Figure 4

Supplementary Table S1. Loss of function of ecdysone receptor co-activator *tai* increases number of niche and germline stem cells

Allele	*x tai^{G161}*			*x tai ^{k15101}*		
	# of CpCs AVE±SEM	# of GSCs AVE±SEM	# of germaria analyzed	# of CpCs AVE±SEM	# of GSCs AVE±SEM	# of germaria analyzed
	p (compared to *tai^{G161}/ w^{1118}*)			p (compared to *tai ^{k15101}/ w^{1118}*)		
Control, w^{1118}	6.56±0.24	2.44±0.13	25	5.63±0.22	2.11±0.08	27
tai ^{G161}	lethal			7.10±0.28 p=2.08x10^{-4}	3.45±0.20 p=1.52x10^{-7}	31
tai ^{01315}	10.50±0.61 p=6.20x10^{-11}	4.00±0.25 p=6.30x10^{-11}	11	6.33±0.53 p=0.16	3.22±0.32 p=2.55x10^{-6}	9
tai ^{EY11718}	7.40±0.51 p=0.16	3.67±0.26 p=4.49x10^{-3}	5	N/A		
tai ^{KG02309}	9.40±0.70 p=0.02	3.40±0.54 p=2.34x10^{-5}	10	N/A		
tai ^{BG02711}	10.56±0.60 p=1.11x10^{-9}	5.11±0.39 p=1.60x10^{-8}	10	N/A		
EcR^{Q50st}	8.40±0.78 p=5.08x10^{-3}	3.70±0.21 p=1.30x10^{-5}	10	7.86±0.93 p=1.31x10^{-3}	3.71±0.61 p=3.88x10^{-5}	7
usp^{4}	9.00±0.85 p=9.68x10^{-4}	3.67±0.27 p=3.30x10^{-5}	12	8.07±0.38 p=6.70x10^{-7}	2.79±0.19 p=0.10	14
usp ^{EP1193}	8.13±0.31 p=4.50x10^{-3}	3.50±0.51 p=1.05x10^{-3}	8	5.92±0.36 p=0.48	2.25±0.13 p=0.36	12

p-value was calculated using the two tailed Students t-test.

Supplementary Table S2. Reduction of ecdysone signaling via *ecd1^{ts}* mutation or dominant negative EcR forms increases the number of single spectrosome cells and delays cyst differentiation

Genotype	Number of CpCs Ave ± SEM	Number of GSCs Ave ± SEM	Number of SSCs Ave ± SEM	Number of Cysts Ave ± SEM	Ratio Cyst/SSC Ave ± SEM	# of analyzed germaria
w ^{1118} 5d at 29°C	5.78±0.25	2.18±0.12	3.91±0.31	4.82±0.38	1.30±0.12	11
ecd $^{4210\ ts}$ 1d at 29°C	5.71±0.30 (p=0.89)	2.19±0.19 (p=0.98)	9.81±1.12 ($p=2.38\times10^{-4}$)***	4.63±0.87 (p=0.86)	0.63±0.13 ($p=1.76\times10^{-3}$)**	16
ecd $^{4210\ ts}$ 3-5d at 29°C	5.77±0.17 (p=0.98)	1.80±0.19 (p=0.26)	7.47±0.36 ($p=1.58\times10^{-6}$)***	5.80±0.46 (p=0.23)	0.84±0.08 ($p=4.16\times10^{-3}$)**	30
ecd $^{4210\ ts}$ 7d at 29°C	6.00±0.22 (p=0.59)	1.62±0.20 (p=0.04)*	7.23±0.99 (p=0.01)*	3.85±0.47 (p=0.15)	0.66±0.10 ($p=6.61\times10^{-4}$)***	15
hs-Gal4-usp.LBD hs 30' 1-3d	6.20±0.30 (p=0.47)	3.20±0.37 ($p=4.73\times10^{-3}$)**	7.20±0.74 ($p=2.34\times10^{-4}$)***	5.40±0.51 (p=0.39)	0.78±0.10 (p=0.02)*	5
hs-Gal4-EcR.LBD hs 30' 1-3d	6.29±0.18 (p=0.23)	2.75±0.31 (p=0.08)	7.13±0.72 ($p=3.00\times10^{-4}$)***	4.86±0.38 (p=0.95)	0.67±0.05 ($p=1.30\times10^{-3}$)**	8

p-value was calculated using the two tailed Students t-test. *p<0.05, **p<0.005. ***p<0.0005

Supplementary Table S3. Adult EcR overexpression causes germline differentiation delay in the germarium that can be recovered by supplying 20E

Genotype	Condition	exp	Number of CpCs Ave ± SEM	Number of GSCs Ave ± SEM	Number of SSCs Ave ± SEM	Number of Cysts Ave ± SEM	Ratio Cyst/SSC Ave ± SEM	# of analyzed germaria
w^{1118}	control 25°C	I	6.33±0.20	2.88±0.23	4.5±0.38	4.63±0.46	1.09±0.16	8
	20E 25°C	I	5.78±0.19 [a](p=0.27)	2.26±0.24 [a](p=0.14)	3.84±0.32 [a](p=0.24)	4.16±0.24 [a](p=0.34)	1.34±0.23 [a](p=0.51)	19
hsEcR.A/+	control 25°C	I	6.00±0.22 [a](p=0.53)	2.67±0.19 [a](p=0.50)	4.80±0.31 [a](p=0.84)	5.31±0.27 [a](p=0.20)	1.13±0.16 [a](p=0.91)	15
		II	5.58±0.26	2.42±0.15	4.50±0.38	5.76±0.28	1.35±0.11	12
		III	5.67±0.24	2.22±0.22	4.00±0.33	5.44±0.44	1.44±0.16	9
	20E 25°C	I	6.40±0.31 [a](p=0.91)	2.50±0.17 [a](p=0.19)	4.50±0.65 [a](p=1.00)	5.40±0.40 [a](p=0.22)	1.57±0.33 [a](p=0.25)	10
		II	6.43±0.36	2.20±0.13	3.80±0.42	6.40±0.27	1.89±0.22	10
		III	5.67±0.27	2.44±0.18	5.44±0.73	5.33±0.33	1.27±0.29	9
w^{1118}	control heat shock	I	5.90±0.28 [a](p=0.44)	2.50±0.27 [a](p=0.32)	4.50±0.56 [a](p=1.00)	5.80±0.36 [a](p=0.06)	1.49± 0.22 [a](p=0.18)	10
		III	6.13±0.26	2.30±0.15	4.90±0.55	5.80±0.44	1.32±0.19	10
hsEcR.A/+	heat shock	I	5.70±0.21 [b](p=0.57) [c](p=0.36)	2.90±0.28 [b](p=0.31) [c](p=0.48)	11.0±0.75 [b]($p=1.68\times10^{-6}$)*** [c]($p=5.24\times10^{-9}$)***	2.30±0.67 [b]($p=2.14\times10^{-4}$)*** [c]($p=1.94\times10^{-4}$)***	0.19±0.05 [b]($p=1.95\times10^{-5}$)*** [c]($p=1.49\times10^{-4}$)***	10
		II	6.09±0.28 [c](p=0.20)	2.82±0.18 [c](p=0.10)	13.8±1.40 [c]($p=1.79\times10^{-6}$)***	2.6±0.29 [c]($p=4.33\times10^{-7}$)***	0.17±0.03 [c]($p=1.99\times10^{-9}$)***	11
		III	5.91±0.23 [c](p=0.48)	3.15±0.19 [c]($p=4.93\times10^{-3}$)**	13.46±1.26 [c]($p=5.72\times10^{-6}$)***	5.69±0.54 [c](p=0.74)	0.50±0.10 [c]($p=3.39\times10^{-5}$)***	13
	20E heat shock	I	5.9±0.35 [d](p=0.63)	3.6±0.22 [d](p=0.06)	10.2±0.87 [d](p=0.50)	4.70±0.50 [d](p=0.01)*	0.50±0.08 [d]($p=4.53\times10^{-3}$)**	10
		II	6.00±0.21 [d](p=0.80)	3.00±0.15 [d](p=0.44)	12.5±0.67 [d](p=0.44)	3.86±0.35 [d](p=0.02)*	0.33±0.04 [d](p=0.01)*	14
		III	5.92±0.22 [d](p=0.98)	2.46±0.14 [d]($p=7.96\times10^{-3}$)*	9.62±0.74 [d]($p=1.45\times10^{-2}$)*	7.15±0.30 [d]($p=2.52\times10^{-2}$)*	0.79±0.07 [d]($p=2.00\times10^{-2}$)*	13

Adult *hsEcR.A/+* or *w*^{1118} flies were treated as indicated. Heat shocks were performed twice per day for 30 min each. 1 µM Ecdysone (20E) was diluted in 5% Ethanol. For control 5% Ethanol was used.

p-value was calculated using the two tailed Students t-test. *p<0.05. **p<0.005. ***p<0.0005
a Compared to *w*^{1118} flies that were kept without heat shocks on 5% Ethanol for control.
b Compared to *w*^{1118} flies that were heat shocked for control.
c Compared to *hsEcR.A/+* flies of the respective experiment that were kept without heat shocks on 5% Ethanol for control.
d Compared to *hsEcR.A/+* flies of the respective experiment where overexpression of EcR.A was induced via daily heat shocks on 5% Ethanol.

Supplementary Table S4. Ecdysone receptor co-activator *tai* is not required for germline stem cell maintenance

Genotype	Experiment	% of germaria with clonal GSCs				Average GSC loss per day ±SD, %	GSCs half-life, days
		Time-point I (5d after hs)	Time-point II (12d after hs)	Time-point III (19d after hs)	Time-point IV (26d after hs)		
Control, parental hsFLP; FRT40A /FRT40A GFP	Exp I	56.8% n=44	35.7% n=28	28.3 % n=32	ND	1.74±2.82%	≥ 3 weeks
	Exp II	42.1% n=38	46.8% n=47	51.6% n=31	ND		
	Exp III	ND	47.3% n=55	40.9% n=66	29.1% n=86		
tai^{61G1} hsFLP; FRT40A tai^{61G1}/FRT40A GFP	Exp I	48.7% n=37	30.8% n=26	46.2% n=13	ND	1.83±2.08%	≥ 3 weeks
	Exp II	59.5% n=37	48.7% n=39	66.7% n=15	ND		
	Exp III	ND	39.8% n=103	35.1% n=57	29.0% n=100		
tai^{k15101} hsFLP; FRT40A tai^{k15101}/FRT40A GFP	Exp I	34.2% n=38	38.5% n=39	ND	ND	-1.07±1.68%	≥ 3 weeks
	Exp III	ND	28.6% n=77	26.9% n=67	35.4% n=48		

n=number of germaria analyzed

GSC loss per day=(% of clonal GSC at time-point 1 -% of clonal GSC at time-point 2)x100%/ % of clonal GSC at time-point 1/elapsed time

GSCs half-life=elapsed time x log[2]/log[% of clonal germaria at time-point1/% of clonal germaria at time-point2]

Supplementary Table S5. Ecdysone signaling alteration in soma causes germline differentiation delay

Genotype	days on 29°C	Number of CpCs Ave ± SEM	Number of GSCs Ave ± SEM	Number of SSCs Ave ± SEM	Number of Cysts Ave ± SEM	Ratio Cyst/SSC Ave ± SEM	# of analyzed germaria
Control*	*	6.19±0.19	2.15±0.15	4.00±0.31	4.82±0.27	1.40±0.12	33
tubGal80^{ts}/+; UAS EcR RNAi^{97}/ bab1Gal4	7d	6.16±0.29 (p=0.94)	2.42±0.26 (p=0.34)	4.79±0.36 (p=0.11)	3.89±0.25 (p=0.03)*	0.88±0.09 (p=5.18x10^{-3})**	19
tubGal80^{ts}/+; UAS EcR RNAi^{97}/ bab1Gal4	21d	6.93±0.32 (p=0.09)	2.21±0.21 (p=0.82)	8.57±0.83 (p=7.84x10^{-3})**	4.57±0.37 (p=0.60)	0.62±0.09 (p=3.41x10^{-4})***	14
tubGal80^{ts}/+; UAS EcR RNAi^{104} /bab1Gal4	7d	6.36±0.27 (p=0.67)	2.75±0.30 (p=0.06)	5.00±0.55 (p=0.11)	3.92±0.34 (p=0.07)	0.92±0.17 (p=0.04)*	12
tubGal80^{ts}/+; UAS EcR RNAi^{104}/ bab1Gal4	15d	5.86±0.44 (p=0.52)	2.07±0.16 (p=0.76)	11.0±3.90 (p=0.01)*	3.55±0.57 (p=0.04)*	0.55±0.11 (p=3.34x10$^{-4)}$***	14
ptcGal4/+; UAS EcR RNAi^{97}/ tubGal80^{ts}	14d	6.47±0.36 (p=0.54)	2.80±0.34 (p=0.05)	6.00±0.59 (p=2.30x10^{-3})*	NC	NC	14
ptcGal4/+; UAS EcR RNAi^{97}/ tubGal80^{ts}	21d	6.38±0.26 (p=0.671)	2.63±0.18 (p=0.150)	6.25±0.59 (p=1.86x10^{-3})*	NC	NC	8

Control*: *tubGal80^{ts}; UAS GFP/TM6, tubGal80^{ts}; UAS GFP/bab1Gal4, tubGal80^{ts}; UAS EcR RNAi ^{97}/TM6, tubGal80^{ts}; bab1Gal4/CyO;* analyzed at different time points

The expression of *EcR RNAi* during larval development is lethal. Therefore we used the *tubGal80^{ts}* system. Flies were raised at 18°C where *tubGal80^{ts}* suppresses the expression of Gal4. Transferring the adult flies to 29°C caused Gal4 and therefore *UAS EcR RNAi* expression in the soma. NC: Counting of cysts not possible due to strong morphological abnormalities. p-value was calculated using two tailed Students t-test. *p<0.05, **p<0.005. ***p<0.0005

Supplementary Table S6. Overexpression of *EcR* during niche development in larval somatic ovarian cells causes an increase in the number of CpCs

Genotype		Number of CpCs Ave ± SEM	Number of SSCs Ave ± SEM	# of analyzed germaria
ptcGal4 X	control *UAS lacZ*	5.70±0.34	4.20±0.25	10
	UAS EcR.A	7.47±0.32 [a]($p=1.63\times10^{-3}$)**	4.47±0.47 [a](p=0.68)	17
	UAS EcR.B1	6.14±0.32 [a](p=0.41)	4.00±0.35 [a](p=0.72)	22
bab1Gal4 X	control *UAS lacZ*	5.91±0.29	4.91±0.37	11
	UAS EcR.A	9.31±0.42 [a]($p=3.72\times10^{-5}$)*** [b]($p=7.08\times10^{-3}$)*	7.38±0.49 [a]($p=7.34^{-3}$)** [b]($p=3.91^{-4}$)***	32
	UAS EcR.B1	9.29±0.53 [a]($p=5.73\times10^{-5}$)*** [b]($p=7.10\times10^{-6}$)***	5.94±0.37 [a](p=0.07) [b]($p=5.99\times10^{-4}$)**	17
W^{1118} X	control *UAS EcR.A*	6.36±0.24	5.73±0.57	11
	control *UAS EcR.B1*	6.83±0.50	5.00±1.00	12

UAS EcR.A/bab1Gal4 and *UAS EcR.B1/bab1Gal4* express exogenous EcR in the CpCs. *ptcGal4/+; UAS EcR.A/+ and ptcGal4/+; UAS EcR.B1/+* express exogenous *EcR* in the other somatic ovarian cells, but not in CpCs (for expression patterns see Supplementary Figure S4). The stem cell marker pMad was used to confirm GSC identitiy if CpC number was increased. a *ptcGal4/+; UAS EcR/+* and *UAS EcR/bab1Gal4* were compared to *ptcGal4/+; UAS lacZ/+* or *bab1Gal4/UAS lacZ* respectively. b *UAS EcR.A* or *B1* driven by bab1Gal4 were compared to the *UAS EcR.A* or *B1* driven by *ptcGal4.* The p-value was calculated using two tailed Student´s t-test. *p<0.05, **p<0.005. ***p<0.0005.

CURRICULUM VITAE

Name: Halyna R. Shcherbata, PhD

Date of birth: January 16, 1971

Place of birth: Lemberg, Ukraine

Marital status: married

Children: 2 sons

Languages:

Ukrainian, English, Russian, Polish (fluent), German (functional)

Max Planck Research Group Leader
Gene Expression and Signaling Group
Max Planck Institute
for biophysical Chemistry
Am Faßberg 11
D-37077 Göttingen
Tel: ++49 551 201-1656
Fax: ++49 551 201-1755
e-mail: halyna.shcherbata@mpibpc.mpg.de

EDUCATION/TRAINING

INSTITUTION AND LOCATION	DEGREE	YEAR(s)	FIELD OF STUDY
University of Washington, Seattle, WA, USA	Postdoc	2001, 2003-2007	Biochemistry, Stem Cell Biology
Basel University, Switzerland	Postdoc	1996, 1998	Developmental Biology, Neurobiology
Lviv National University, Lemberg, Ukraine Institute of Gene Biology, Moscow, Russia Institute for Plant Genetics, Kiev, Ukraine	PhD	1992-1996	Genetics
Lviv National University Lemberg, Ukraine	MS	1987-1992	Biology and Chemistry

POSITIONS AND EMPLOYMENT

- July 2008- present **Max Planck Research Group Leader** at Max Planck Institute for biophysical chemistry, Goettingen, Germany
- Dec 2007 - July 2008 **Research Professor** (Acting Instructor) at the Department of Biochemistry, Institute for Stem Cell and Regenerative Medicine, University of Washington, Seattle, WA, USA
- Feb. 2003 – Dec 2007 **Postdoc** (Senior Fellow) at the Department of Biochemistry, University of Washington, Seattle, WA, USA
- 2000 -2003 **Assistant Professor** at the Department of Genetics and Biotechnology, Lviv National University, Lemberg, Ukraine
- 1996-2000 **Scientific Researcher** at the Department of Genetics and Biotechnology, Lviv National University, Lemberg, Ukraine
- 2001- 2002 **Visiting Scholar** in Prof. Ruohola-Baker Lab, University of Washington, Seattle, WA, USA
- 1996, 1998 **Visiting Scientist** in Prof. Heinrich Reichert Lab of Neurogenetics, Basel University, Switzerland
- 1993, 1994 **Visiting Student** at Institute of Gene Biology, Moscow, Russia
- 1992-1996 **Graduate Student** at the Department of Genetics and Biotechnology, Lviv National University, Lemberg , Ukraine
- 1987-1992 **Student** at the Biological Department, Lviv National University, Lemberg, Ukraine

HONORS

2005 –2008 American Heart Association Grant for Postdoctoral Fellows
2002 - WUBMR (West-Ukrainian Biomedical Research) Award for Postdocs
2000 - John Soros Award for Young Scientists

CONFERENCE ORGANIZER

Organizer of the "The Extracellular Matrix" workshop at the 48th and 49th Drosophila Research Conferences (2007, 2008, USA)
Co-organizer of XXIV International Congress of Entomology, (2012, Korea)

CONFERENCES

Neurobiology of *Drosophila*, CSHL Conference, New York, USA (2011)
European *Drosophila* Research Conference, Lisbon, Portugal (2011)
Drosophila Research Conference, San Diego, USA (2011)
The Non-Coding Genome, EMBL symposium, Heidelberg, Germany (2010)
European *Drosophila* Research Conference, Nice, France (2009)
Control and Regulation of Stem Cells, LXXIII CSHL Symposium on Quantitative Biology, New York, USA (2008)
Drosophila Research Conference, San Diego, USA (2008)
Drosophila Research Conference, Philadelphia, USA (2007)
European *Drosophila* Research Conference, Vienna, Austria (2007)
Drosophila Research Conference, Houston, USA (2006)
RNAi CSHL Conference, New York, USA (2005)
Drosophila Research Conference, San Diego, USA (2005)
Cell Cycle CSHL Conference, USA (2004)
Drosophila Research Conference, Washington DC, USA (2004)

EDITORIAL ACTIVITIES

Host Editor for the Research Topic "Genetic and Epigenetic Control of Stem Cell Fate" in **"**Frontiers in Genetics"
Reviewer for
Developmental Biology
PloS Biology
The International Journal of Neuroscience

TEACHING EXPERIENCE

CURRENT TEACHING

Since 2009 I am a Faculty member of the Master Program "Developmental, Neural and Behavioral Biology" at Georg-August-University and Master's/PhD Molecular Biology Program at Göttingen Graduate School for Neurosciences and Molecular Biosciences (GGNB).

Since 2011 I am also a Member of the Admission Committee of the IMPRS for Molecular Biology.

Lecture Courses, Seminars and Laboratory Lessons
for academic years 2009/10, 2010/11 and 2011/12

Winter Semester	**Lecture** ***"Cell cycle"***	**Lecture, seminar and practical course in the *"Cell Biology"* module for Master's students of the Master Developmental, Neural and Behavioral Biology Program, Georg-August-University**
	Seminar ***"The role for RNAi"***	
	Practical course ***"Drosophila germline stem cell niche model" (3 day course, 2 times per semester (2x3x8h))***	
Winter Semester	**Lecture** ***"RNA-based Regulation (Eukaryotes)"***	**Lectures, tutorials and method course for Master's students of the MSc/PhD Molecular Biology Program at Göttingen Graduate School for Neurosciences and Molecular Biosciences**
	Tutorial ***"RNAi"***	
Summer Semester	**Lecture** ***"Cell Adhesion"***	
	Tutorial ***"Cell Adhesion"***	
	Short methods course "*Introduction to basic histology techniques* (3 day course, 2 times per semester (2x3x8h))	

PREVIOUS TEACHING EXPERIENCE

Lecture Courses, Seminars and Laboratory Lessons

2001-2003	***"Special genetics", "Immunogenetics", "Molecular genetics" (one semester courses, one lecture per week)***	**lecture courses for 3rd and 5th year stationary students and 6th year correspondence course students of Genetics and Biotechnology Department, Lviv National University, Ukraine**
2002-2003	***"Genetics"***	**lecture course for students of the Small Academy of Science, Lviv National University, Ukraine**
2000-2003	***"General Genetics" (two semester course, 3-4 groups, one lab per week), "Biology of Individual Development" (one semester course, 3-4 groups, one lab per every two weeks)***	**laboratory lessons and scientific seminars for 2nd and 3rd year stationary students of the Biological Department, Lviv National University, Ukraine**
2003-2003	***"Genetic analysis", "Biochemical genetics", "Cytogenetics" (one semester courses)***	**laboratory and practical lessons for 3rd, 4th and 5th year stationary students of Genetics and Biotechnolody Department, Lviv National University, Ukraine**
2003-2004	***Journal Club, Literature Review Class* (graduate discussion)**	**helped in teaching for University of Washington graduate students, Seattle, USA**

TRAINING

• PhD students

Ibrahim Ömer Cicek since Oct 2011 (Molecular Biology Program at GGNB)

Annekatrin König since Oct 2009 (Molecular Biology Program at GGNB)

Mariya Kucherenko 2005-2009 (Lviv University, Georg-August-University)

Andriy Yatsenko 2003-2009 (Lviv University)

Valentyna Rishko 2010-2011 (DAAD student)

• Master/Diploma students

Helena Magliarelli 2009-2010 (Master, Mol Biology Program at GGNB)

Isabel Graft 2010 (Diploma, Tübingen University)

Andriy Yatsenko 2000-2003 (Diploma, Lviv University Undergrad)

Yura Rzhepetskyy 2001-2003 (Diploma, Lviv University, Honors Student)

Vira Radish 2002-2003 (Diploma, Lviv University, Honors Student)

Yulia Praded 1999-2002 (Diploma, Lviv University Undergrad)

Natalya Matijciv 1997-2001 (Diploma, Lviv University, Honors Student)

Anna Lukyanova 1996-2000 (Diploma, Lviv University, Honors Student)

• Master/PhD Lab Rotation Students

Lena Musiol (Molecular Biology Program at GGNB, 2012)

Evgeniia Samoiliuk(Molecular Biology Program at GGNB, 2012)

Ursula Budynjak (Erasmus Exchange Student, 2011)

Nasrin Sapour (Molecular Medicine at Georg-August-University, 2011)

Marina Samos (Molecular Medicine at Georg-August-University, 2011)

Sona Pirkulieva (Molecular Biology Program at GGNB, 2011)

Ewa Maj (Molecular Biology Program at GGNB, 2011)

Ibrahim Ömer Cicek (Molecular Biology Program at GGNB, 2011)

Bernard Freytag (Molecular Biology Program at GGNB, 2011)

Nesrin Tüysüz 2009 (Molecular Biology Program at GGNB, 2009)

- ## Bachelor students

Isabelle Everlien 2011 (Marburg University)

Naomi Latoraka 2011 (DAAD RISE, Pitsburg University)

Miriam Weiss 2009 (Medical Faculty, University of Rostock Bachelor)

Ben Drum 2007,2008 (UW Undergrad)

Krutika Shah 2008 (UW Undergrad)

Saman Tahir 2008 (UW Undergrad)

Melanie Stephens 2008 (UW Undergrad)

Ahmad Mohaedpardazi 2007 (UW Undergrad)

Katherine Tracy Liu 2006 (UW Undergrad)

Gary McLeary 2006 (Withman College)

Mike Brubaker 2005, 2006 (Withman College)

Betsy Gray 2003-2005 (NASA Fellow, Honors Student)

Aliya Hashemi 2003-2004 (UW Undergrad)

Kate Johnson 2003- 2004 (HHMI Scholar)

Merle Gilbert 2003-2004 (UW Undergrad)

Joicelyn Niimi 2001-2002 (Mary Gates Fellow)

Olena Hnativ 1992-1997 (Lviv University, Honors Student)

Iryna Yurasova 1992-1997 (Lviv University Undergrad)

Iryna Yarosh 1993-1996 (Lviv University Undergrad)

Natalya Melenchuk 1991-1994 (Lviv University Undergrad)

- ## High School students

Swenja Hirsch 2011 (Lubek)

LIST OF PUBLICATIONS

1. Konig, A., Yatsenko, A.S., Weiss, M., and Shcherbata, H.R. (2011). Ecdysteroids affect *Drosophila* ovarian stem cell niche formation and early germline differentiation. EMBO J *30*, 1549-1562.

2. Kucherenko, M.M., Marrone, A.K., Rishko, V.M., Magliarelli H., and Shcherbata, H.R. (2011). Stress and muscular dystrophy: a genetic screen for dystroglycan and dystrophin interactors in *Drosophila* identifies cellular stress response components. Dev Biol *352*, 228-242.

3. Marrone, A.K., and Shcherbata, H.R. (2011). Dystrophin orchestrates the epigenetic profile of muscle cells via miRNAs. Frontiers in Genetics *2*.

4. Marrone, A.K., Kucherenko, M.M., Wiek, R., Gopfert, M.C., and Shcherbata, H.R. (2011). Hyperthermic seizures and aberrant cellular homeostasis in *Drosophila* dystrophic muscles. Sci Rep *1*.

5. Marrone, A.K., Kucherenko, M.M., Rishko, V.M., and Shcherbata, H.R. (2011). New Dystrophin/Dystroglycan interactors control neuron behavior in *Drosophila* eye. BMC Neurosci *12*, 93.

6. Kucherenko, M.M., Marrone, A.K., Rishko, V.M., Yatsenko, A.S., Klepzig, A., and Shcherbata, H.R. (2010). Paraffin-embedded and frozen sections of *Drosophila* adult muscles. J Vis Exp.

7. Yu, J.Y., Reynolds, S.H., Hatfield, S.D., Shcherbata, H.R., Fischer, K.A., Ward, E.J., Long, D., Ding, Y., and Ruohola-Baker, H. (2009). Dicer-1-dependent Dacapo suppression acts downstream of Insulin receptor in regulating cell division of *Drosophila* germline stem cells. Development *136*, 1497-1507.

8. Yatsenko, A.S., Kucherenko, M.M., Pantoja, M., Fischer, K.A., Madeoy, J., Deng, W.M., Schneider, M., Baumgartner, S., Akey, J., Shcherbata, H.R., *et al.* (2009). The conserved WW-domain binding sites in Dystroglycan C-terminus are essential but partially redundant for Dystroglycan function. BMC Dev Biol *9*, 18.

9. Qi, J., Yu, J.Y., Shcherbata, H.R., Mathieu, J., Wang, A.J., Seal, S., Zhou, W., Stadler, B.M., Bourgin, D., Wang, L., *et al.* (2009). microRNAs regulate human embryonic stem cell division. Cell Cycle *8*, 3729-3741.

10. Kucherenko, M.M., Pantoja, M., Yatsenko, A.S., Shcherbata, H.R., Fischer, K.A., Maksymiv, D.V., Chernyk, Y.I., and Ruohola-Baker, H. (2008). Genetic modifier screens reveal new components that interact with the *Drosophila* dystroglycan-dystrophin complex. PLoS One *3*, e2418.

11. Yatsenko, A.S., Gray, E.E., Shcherbata, H.R., Patterson, L.B., Sood, V.D., Kucherenko, M.M., Baker, D., and Ruohola-Baker, H. (2007). A putative Src homology 3 domain binding motif but not the C-terminal dystrophin WW domain binding motif is required for dystroglycan function in cellular polarity in *Drosophila*. J Biol Chem *282*, 15159-15169.

12. Shcherbata, H.R., Yatsenko, A.S., Patterson, L., Sood, V.D., Nudel, U., Yaffe, D., Baker, D., and Ruohola-Baker, H. (2007). Dissecting muscle and neuronal disorders in a *Drosophila* model of muscular dystrophy. EMBO J *26*, 481-493.

13. Shcherbata, H.R., Ward, E.J., Fischer, K.A., Yu, J.Y., Reynolds, S.H., Chen, C.H., Xu, P., Hay, B.A., and Ruohola-Baker, H. (2007). Stage-specific differences in the requirements for germline stem cell maintenance in the *Drosophila* ovary. Cell Stem Cell *1*, 698-709.

14. Ward, E.J., Shcherbata, H.R., Reynolds, S.H., Fischer, K.A., Hatfield, S.D., and Ruohola-Baker, H. (2006). Stem cells signal to the niche through the Notch pathway in the *Drosophila* ovary. Curr Biol *16*, 2352-2358.

15. Shcherbata, H.R., Hatfield, S., Ward, E.J., Reynolds, S., Fischer, K.A., and Ruohola-Baker, H. (2006). The MicroRNA pathway plays a regulatory role in stem cell division. Cell Cycle *5*, 172-175.

16. Hatfield, S., Shcherbata, H.R., Ward, E.J., Reynolds, S., Fischer, K.A., and Ruohola-Baker, H. (2006). MicroRNAs and their involvement in Stem Cell division. In microRNAs; Biology, Function and Expression, N. Clarke, Sanseau, P., ed. (DNA Press).

17. Shcherbata, H.R*., Hatfield, S.D*., Fischer, K.A., Nakahara, K., Carthew, R.W., and Ruohola-Baker, H. (2005). Stem cell division is regulated by the microRNA pathway. Nature *435*, 974-978. *-equal contribution

18. Shcherbata, H.R., Althauser, C., Findley, S.D., and Ruohola-Baker, H. (2004). The mitotic-to-endocycle switch in *Drosophila* follicle cells is executed by Notch-dependent regulation of G1/S, G2/M and M/G1 cell-cycle

transitions. Development *131*, 3169-3181.

19. Shcherbata, G.R., Matiitsiv, N.P., Chernik Ia, I., and Maksimiv, D.V. (2004). [Chemically induced *Drosophila* melanogaster mutants with changes in brain structure]. Genetika *40*, 1280-1285.

20. Shcherbata, G.R., Matiitsiv, N.P., Chernik Ia, I., Iatsenko, A.S., Radysh, V.V., Kucherenko, M.M., and Maksimiv, D.V. (2004). [Genetic analysis of X-chromosome neurodegenerative mutants of *Drosophila* melanogaster induced by ethyl methansulfonate and nitrosoethylurea]. Genetika *40*, 1286-1292.

21. Schaeffer, V., Althauser, C., Shcherbata, H.R., Deng, W.M., and Ruohola-Baker, H. (2004). Notch-dependent Fizzy-related/Hec1/Cdh1 expression is required for the mitotic-to-endocycle transition in *Drosophila* follicle cells. Curr Biol *14*, 630-636.

22. Bobak Ia, P., Kimak, N., Maksymiv, D.V., Chernyk Ia, I., and Shcherbata, G.R. (2001). [Analysis of brain morphological changes induced by ethyl methanesulfonate in *Drosophila* melanogaster]. Tsitol Genet *35*, 34-37.

23. Shcherbata, H.R., Maksymiv, D.V., and Chernyk Ia, I. (1999). [Gene instability induced by mobile genetic elements in *Drosophila* melanogaster]. Tsitol Genet *33*, 54-70.

24. Shokhanov, S.O., Shcherbata, G.R., and Chernik Ia, I. (1997). [Genomic variation of laboratory strains and natural populations of *Drosophila* melanogaster exposed to X-irradiation]. Genetika *33*, 25-30.

25. Shcherbata, H.R., and Maksymiv, D.V. (1997). [A new system of prolonged genetic instability induced by N-ethyl-N-nitrosourea in *Drosophila* melanogaster]. Tsitol Genet *31*, 44-49.

26. Shcherbata, G.R., and Maksymiv, D.V. (1997). [Molecular genetic nature of mutations at the white locus, induced by chemical substances in *Drosophila* melanogaster]. Genetika *33*, 19-24.

27. Maksymiv, D.V., Shcherbata, H.R., and Chernyk Ia, I. (1995). [The detection and study of mitomycin C-induced mutational changes in stable lines of *Drosophila* melanogaster]. Tsitol Genet *29*, 62-68.